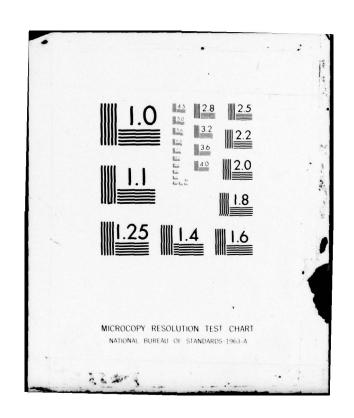
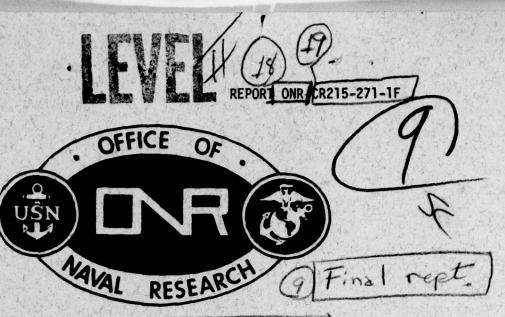
MASSACHUSETTS INST OF TECH CAMBRIDGE LAB FOR INFORMA--ETC F/G 12/1
RECENT DEVELOPMENTS IN THE ROBUSTNESS THEORY OF MULTIVARIABLE S--ETC(U)
AUG 79 N R SANDELL
N00014-79-C-0377 AD-A082 362 ONR-CR215-271-1F NL UNCLASSIFIED LIDS-R-954 1 OF 5 AD A 082362





RECENT DEVELOPMENTS IN THE BOBUSTNESS THEORY OF MULTIVARIABLE SYSTEMS

Proceedings of the ONR/MIT Workshop held April 25-27, 1979 at the Massachusetts Institute of Technology Cambridge, Massachusetts 02139

Edited by

Massachusetts Institute of Technology
Laboratory for Information and Decision Systems
Cambridge, Massachusetts 02139

Contract New 14-79-C-0377

31 August 1979

12 448

Approved for public release; distribution unlimited.

14 LIDS-R-954



PREPARED FOR THE Office of Naval Research 800 N. Quincy St. Arlington, VA. 22217

) 3

21 038

JOB

# Change of Address

Organizations receiving reports on the initial distribution list should confirm correct address. This list is located at the end of the report. Any change of address or distribution should be conveyed to the Office of Naval Research, Code 211, Arlington, VA. 22217.

## Disposition

When this report is no longer needed, it may be transmitted to other organizations. Do not return it to the organizator or the monitoring office.

## Disclaimer

The findings and conclusions contained in this report are not to be construed as an official Department of Defense or Military Department position unless so designated by other official documents.

# Reproduction

Reproduction in whole or in part is permitted for any purpose of the United States Government.

REPORT DOCUMENTATION PAGE		READ INSTRUCTIONS BEFORE COMPLETING FORM	
REPORT NUMBER	2. GOVT ACCESSION NO.	3. RECIPIENT'S CATALOG NUMBER	
ONR-CR-215-271-1F		The South and Alexander Tolk Indiana and Alberta	
. TITLE (and Subtitle)		5. TYPE OF REPORT & PERIOD COVERED	
Recent Developments in the Robus	stness Theory of	Final Report	
Multivariable Systems (Proceeding	ngs of the ONR/MIT	April 25-27, 1979	
Workshop, April 25-27, 1979, M.1 02139	I.T., Camb., MA.	6. PERFORMING ORG. REPORT NUMBER LIDS-R-954	
· AUTHOR(a)		8. CONTRACT OR GRANT NUMBER(s)	
Edited by - Nils R. Sandell, Ja	r.	N00014-79-C-0377 %	
PERFORMING ORGANIZATION NAME AND ADDR	ESS	10. PROGRAM ELEMENT, PROJECT, TASK AREA & WORK UNIT NUMBERS	
Massachusetts Institute of Technology		AREA & WORK UNIT NUMBERS	
Lab. for Information and Decision			
Cambridge, Massachusetts 02139			
1. CONTROLLING OFFICE NAME AND ADDRESS		12. REPORT DATE	
Office of Naval Research, Room	704	August 31, 1979	
800 N. Quincy Road		13. NUMBER OF PAGES	
Arlington, Virginia 22217		431	
4. MONITORING AGENCY NAME & ADDRESS(II dill	ferent from Controlling Office)	15. SECURITY CLASS. (of this report)	
		Unclassified	
		15a. DECLASSIFICATION/DOWNGRADING	
17. DISTRIBUTION STATEMENT (of the abstract ente	ered in Block 20, if different fro	m Report MAR 2 4 1080	
18. SUPPLEMENTARY NOTES		C	
Robustness Theory Multivariable Systems LQG Designs			
This report summarizes the Processor Developments in the Robustness for the workshop was the dissemple concerning the characterization fined here as systems that perform the mathematical model used for the design of such systems.	Theory of Multivarial ination and discuss of robust multivarial roma satisfactorily control synthesis	able Systems. The motivation ion of recent research result iable feedback systems, dedespite differences between	

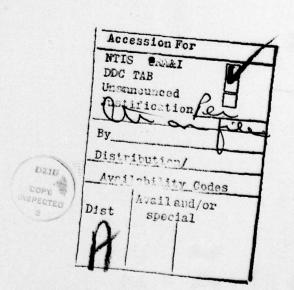
20. Abstract (contd.)

An introductory discussion of the papers presented at the workshop is provided; the papers themselves are included in an Appendix. Finally, the research directions indentified in a roundtable discussion held at the end of the workshop are summarized.

The methods leaf model west for convect synthemis and the actual dynomics, and the desirable that the motivation for the thee-

#### ABSTRACT

This report summarizes the proceedings of the ONR/MIT Workshop on Recent Developments in the Robustness Theory of Multivariable Systems. The motivation for the workshop was the dissemination and discussion of recent research results concerning the characterization of robust multivariable feedback systems, defined here as systems that perform satisfactorily despite differences between the mathematical model used for control synthesis and the actual dynamics, and the design of such systems. The report describes the motivation for the theoretical developments and the nature of the results that have been obtained. An introductory discussion of the papers presented at the workship is provided; the papers themselves are included in an Appendix. Finally, the research directions identified in a roundtable discussion held at the end of the workshop are summarized.



#### FOREWORD

This report summarizes the proceedings of a workshop, "Recent Developments in the Robustness Theory of Multivariable Systems", held at the Massachusetts Institute of Technology (MIT) on April 25-27. The workshop was the idea of Mr. D. Siegel of the Office of Naval Research (ONR). It was organized by Messrs. D. Siegel and R. Von Husen of ONR; and Profs. N.R. Sandell Jr., G. Stein, and M. Athans, Mr. R.A. Osborne, and Mrs. F. Frolik, all of M.I.T. To promote informal interaction, attendance was strictly limited to researchers actively working in the subject area of the workshop (narrowly defined) along with several research managers and a number of practicing engineers.

The tangible output of the conference is this final report. However, the editor firmly believes that the intangible benefits of the three days of intense discussion focused on the extremely important conference theme represent the most important output. Discussions with the workshop participants give some indication of the nature of these benefits. The practitioners seemed to gain an appreciation for the formal procedures described for the quantitative evaluation of robustness; the remarks of one engineer who indicated that he was going to go back and check the stability margins on an optimal linear-quadratic regulator design he was carrying out were typical. The research managers were exposed to several possible new directions for the programs they sponsor, and several indicated interest in pursuing those directions. The researchers in attendence gained a renewed appreciation for the robustness issue and a number of promising ideas were developed. The control engineering profession, and

the Navy as a major consumer of control technology, will benefit as researchers and engineers focus their attention on the long-neglected issue of multivariable system robustness.

# TABLE OF CONTENTS

			PAGE
ABSTRACT			ii
FOR	EWARD		iii
1.	INTR	ODUCTION	1
	1.1	Motivation	1
	1.2	Overview of Report	3
2.	2. BACKGROUND		4
	2.1	Robustness Characterization	4
	2.2	Robustness of LQG Designs	25
3.	3. WORKSHOP PROCEEDINGS		37
	3.1	Introduction to Papers	37
	3.2	Summary of Roundtable Discussion	41
REFERENCES		45	
DISTRIBUTION LIST			49
APPENDICES			52
	A.	Final Program	
	в.	List of Participants	
	c.	Papers Presented	

#### 1. INTRODUCTION

## 1.1 Motivation

The motivation for the ONR/MIT Workshop on Recent Developments in the Robustness Theory of Multivariable Systems was well-illustrated by the opening remarks of Mr. R. Von Husen of the Office of Naval Research (ONR). Mr. Von Husen noted that the Navy has in the past been delivered aircraft with unacceptable handling qualities in certain regions of their flight envelopes. This problem illustrates in a general way the conference theme of design of robust feedback control systems, i.e., systems that continue to satisfy their performance requirements dispite variations between the design model and the actual system dynamics.

The problems raised by Mr. Von Husen illustrate the conference theme in a much more specific sense as well. There are, of course, military specifications on the design of flight control systems for piloted aircraft [20]<sup>1</sup>. Among other requirements, a feedback control system must have certain gain and phase margins in order to be acceptable. To quote from [20],

"Stability margins are required for FCS to allow for variations in system dynamics. Three basic types of variations exist:

Math modeling and data errors in defining the nominal system and plant.

Variations in dynamic characteristics caused by changes in environmental conditions, manufacturing tolerances, aging, wear, noncritical material failures, and off-nominal power supplies.

Numbers in brackets refer to references listed at the end of the report. References 1-19 are included in Appendix C.

Maintenance induced errors in calibration, installation and adjustment."

It would seem from the above quotation that the robustness issue is well-understood from the viewpoint of classical frequency domain techniques, at least for flight control systems. Indeed, this is the case, for single-loop systems. However, the situation is quite different for multiple-loop systems. To quote again from [20],

"In multiple-loop systems, variations shall be made with all gain and phase values in the feedback paths held at nominal values except for the path under investigation."

The fundamental difficulty with this approach is that it fails to check for <u>simultaneous</u> gain and phase variations in several paths. Of course, real-world model uncertainty cannot be expected to nicely confine itself to a single loop of the system! In fact, for a flight control system, the dominant variation is due to the change in control surface effectiveness with dynamic pressure, which manifests itself as a change in the gains of the transfer functions from control surface deflections to the response variables of interest. The dynamic pressure variation is due to changes in aircraft altitude and speed, and clearly affects all loops simultaneously.

The recent conceptual breakthrough that provided the motivation for the Conference is the development of techniques that can satisfactorily test the robustness of multivariable systems. The breakthrough is not so much from the point of view of mathematical theory (although see [21]) since the basic ideas needed have been available in the literature for some time [22]. Rather the breakthrough has been the point of view of applications, where it is becoming clear that modern input-output stability theory can be used to develop what are essentially multivariable

stability margins. This development is clearly of considerable practical importance, for aircraft flight control systems as well as for other multivariable control systems.

## 1.2 Overview of Report

The remainder of this report is organized as follows.

In Section 2, we will give a brief description of the recent developments in the robustness theory of multivariable systems that motivated the workshop. We will begin by describing various characterizations of the robustness of multivariable linear systems that generalize classical stability margin definitions. Then we will describe the relationship of these characterizations to the robustness properties of linear-quadratic-Gaussian (LQG) optimal controllers.

In Section 3, we will briefly summarize the workshop proceedings.

We will attempt to indicate the nature of the presentations by the

participants, and to recapitulate the viewpoints expressed in the roundtable discussion at the end of the workshop.

The final workshop program is given in Appendix A, and a list of attendees is provided in Appendix B. Appendix C contains preprints and reprints of the papers presented.

#### 2. BACKGROUND

## 2.1 Robustness Characterizations

An important theme in system theory is the preservation of various system theoretic properties in the face of variations in the system model. It is possible to distinguish two variations on this theme.

In the first, attention is restricted to infinitesimal changes in the parameters of the nominal system model. Thus one may begin by assuming that the nominal system has a certain property and then ask if there exists an open set about the nominal model parameters such that all the systems with parameters in this set have the desired property. Alternatively, one may seek a relationship between an infinitesimal variation in a nominal system parameter and the corresponding change in some system property. We will refer to investigations of this first type as sensitivity theory. A second approach requires the explicit delineation of finite regions of models about the nominal model for which some given property is preserved. We will refer to investigations of this second type of robustness theory.

Within the context of sensitivity or robustness theory, there are several properties that have been investigated. For example, it is well known that the controllability property is insensitive to small parameter variations (see [23, p.43] for a precise statement). As another example, it is well known that type 1 servomechanisms have

There is an extensive literature on this subject, which will not be discussed further. See, e.g., [25] for a collection of many of the most important papers on sensitivity theory.

zero steady state step tracking error despite large (but not destabilizing) variations in their transfer function matrices [24]. The workshop proceedings described in this report were concerned with the robustness of the stability property of multivariable systems. This topic provided a coherent focus for the workshop, and moreover it was felt that

- stability is the most fundamental requirement of a feedback system, and
- ii) practical feedback systems must remain stable in the face of large parameter variations.

The importance of obtaining robustly stable feedback control systems has long been recognized by designers. Indeed, a principal reason for using feedback rather than open loop control is the presence of model uncertainties. Any model is at best an approximation of reality, and the relatively lower order, linear, time-invariant models most often used for controller synthesis are bound to be rather crude approximations.

More specifically, a given system model can usually be characterized as follows. There is a certain range of inputs typically bounded in amplitude and in rate of change for which the model gives a reasonable approximation to the system. Outside of this range, due to neglected nonlinearities and dynamic effects, the model and system may behave in grossly different ways. Unfortunately, this range of permissible inputs is rarely spelled out explicitly along with the model, but is rather implicit in the technology that the model came from - there is no "truth in modeling" law in systems theory. This situation has led to great fun - as practitioners examine the paper designs of theoreticians - as well as serious consequencies in which a spacecraft is unstable because of the

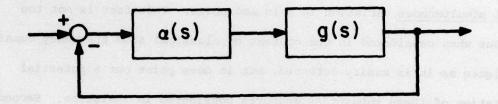
interaction of its flexure modes with a controller designed on the basis of a rigid body model.

In classical frequency domain techniques for single-input, single-output (SISO) control system design, the robustness issue is naturally handled. These techniques employ various graphical means (e.g., Bode, Nyquist, inverse-Nyquist, Nichols plots) of displaying the system model in terms of its frequency response. From these plots, it is automatic to determine by inspection the minimum change in the model frequency response that leads to instability.

Commonly used measures of the closeness of a SISO feedback system to instability are its gain and phase margins. The margins are defined with reference to Fig. 2.1-1. Here the nominal feedback system (with  $\alpha \equiv 1$ ) is assumed stable. The positive phase margin is the smallest value of  $\varphi$  greater than zero such that the system of Fig. 2.1-1 with  $\alpha(j\omega) = e^{j\varphi}$  is unstable. The negative phase margin is defined in an analogous fashion. The upward gain margin is the smallest value of  $\alpha = \text{constant} > 1$  for which the system is unstable (usually expressed in decibels with respect to  $\alpha = +1$ ), and the downward gain margin is similarly defined. The notions of gain and phase margins have gained such widespread acceptance that as described earlier, they have been incorporated into the military speci-

This phenomenon is by no means specific to aerospace applications. The subsynchronous resonance phenomenon in electric power system control is another excellent example.

See the fundamental work of Bode [26], and any good classical textbook, but especially [27].



below to be special and meaning the street of the second and the second second and the second second

as bend size id. i-; daing lasters and le appropriatione to rectmer and

Fig. 2.1-1 Feedback System For Stability Margin Definition

fications for aircraft flight control systems.

There are several considerations involved in gain and phase margins as characterizations of robustness. First, in theory these margins are not adequate measurements of robustness, since a system could conceivably have large gain and phase margins but be destabilized by an arbitrarily small <u>simultaneous</u> variation in gain and phase. This fact is not too serious when considered in the context of classical SISO frequency domain techiques as it is easily detected, but it does point out a potential limitation of these robustness measures considered in isolation. Second, the requirement for gain and phase margins depends on the degree of model uncertainty. This is often reflected in a frequency dependent requirement; for example, it is often specified that a flight control system should be "gain stable" (phase margins = + 180°) at frequencies in the vicinity of poorly damped, high frequency structural modes.

Gain and phase margins can be defined in terms of the various classical frequency domain stability plots. For the unit feedback system of Fig. 2.1-2, Fig. 2.1-3 illustrates the Nyquist stability criterion, and Fig. 2.1-4 shows how gain and phase margins can be determined from the Nyquist diagram. But more important that its role in determining gain and phase margins is the visual insight that a designer can obtain from such a diagram. Assuming that the diagram indicates that the nominal system is stable, a change in the loop transfer function that changes the number of encirclements of the critical point (-1,0) will lead to instability. Thus, nearness to the critical point indicates closeness

This statement assumes that the number of open-loop unstable roles remains constant.

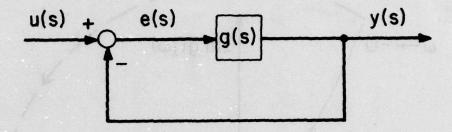


Fig. z.1-? Single-Input, Single-Output Unity Feedback System

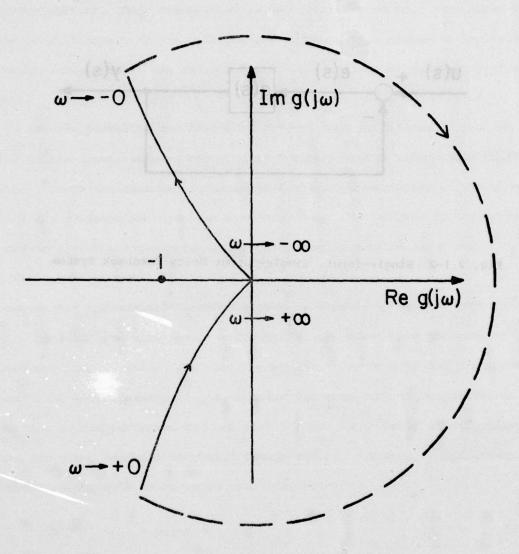


Fig. 2.1-3 Nyquist Diagram

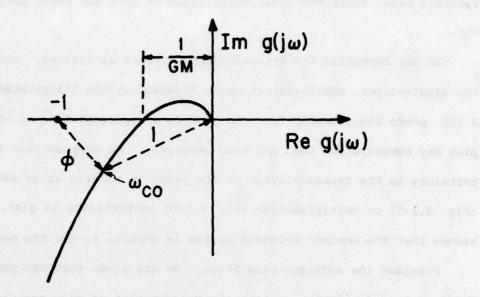


Fig. 2.1-4 Classical Robustness Measures

to instability. This observation is important, as we will see, since the notion of distance to the critical point generalizes nicely to the multivariable case, while the usual definitions of gain and phase margins do not.

We can formalize the foregoing observations as follows. Consider the single-input, single-output unity feedback system illustrated in Fig. 2.1-2, where the transfer function g(s) is a representation of the plant plus any compensation that has been employed. We suppose that the uncertainty in the representation of the plant is modeled as an additive (Fig. 2.1-5) or multiplicative (Fig. 2.1-6) perturbation to g(s). We assume that the nominal feedback system is stable, as are the perturbations.

Consider the additive case first. We are given that the nominal feedback loop is stable, so that the Nyquist plot of g(s) has the correct number of encirclements of the -l point for stability to be concluded.

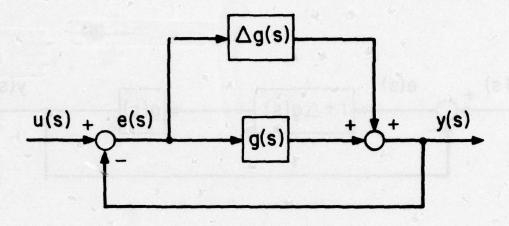
As long as the perturbed Nyquist plot has the same number of encirclements, the perturbed feedback loop will remain stable. Clearly, a sufficient condition for this to occur is that (Fig. 2.1-7)

$$|\Delta g(j\omega)| < |1 + g(j\omega)|$$
 (2.1-1)

for all  $\omega \geq 0$ . Notice that this condition is expressed in terms of the magnitude of the return difference transfer function of the nominal feedback loop, 1 + g(s).

The multiplicative version of this result is very similar, with  $\Delta g(s)$  replaced by g(s)  $\Delta g(s)$ . The sufficient condition is

$$|g(j\omega)| \Delta g(j\omega)| < |1 + g(j\omega)|$$
 (2.1-2)



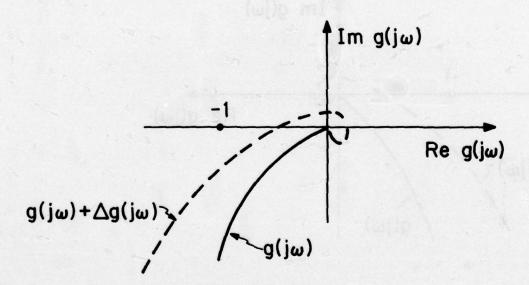
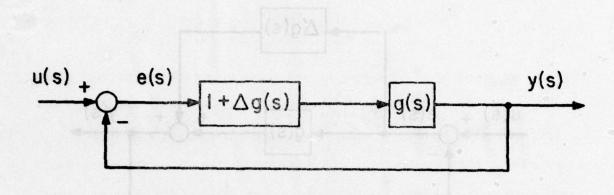


Fig. 2.1-5 Additive Perturbation



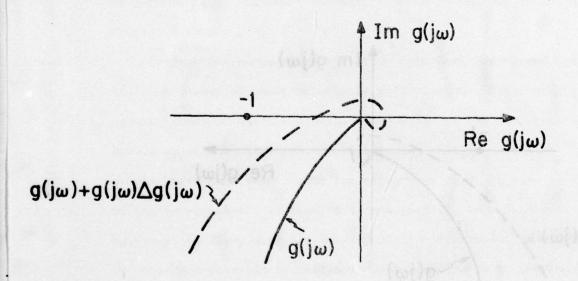


Fig. 2.1-6 Multiplicative Perturbation

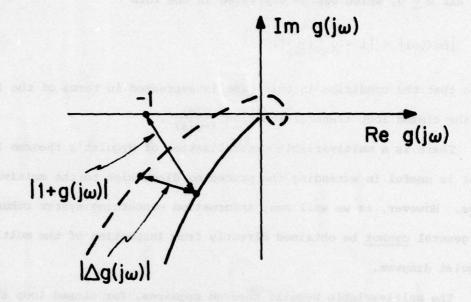


Fig. 2.1-7 Illustration of Condition (2.1-1)

for all  $\omega > 0$ , which can be expressed in the form

$$|\Delta g(j\omega)| < |1 + g^{-1}(j\omega)|.$$
 (2.1-3)

Note that the condition in this case is expressed in terms of the inverse of the closed loop transfer function  $\frac{g(s)}{1+g(s)}$ .

There is a multivariable generalization of Nyquist's theorem [28] that is useful in extending the preceding discussion to the multivariable case. However, as we will see, information concerning system robustness in general cannot be obtained directly from inspection of the multivariable Nyquist diagram.

The multivariable Nyquist theorem requires, for closed loop stability, that the number of counterclockwise encirclements of the origin by the Nyquist locus of  $\det(I+G(j\omega))$ , where  $G(j\omega)$  is the loop transfer matrix, should equal the number of open-loop poles that are unstable. The trouble with this result from the robustness point of view is the dependence on the determinent. Just as it is not possible to tell how close a matrix is to being singular by size of its determinent (see, e.g., [29]), so it is not possible to tell how close a system is to instability from its multivariable Nyquist plot. This comment applies also to closely

$$\det (I + G(j\omega)) = 1 + G(j\omega)$$

and the number of encirclements of the origin by  $1 + G(j\omega)$  is equal to the number of encirclements of the -1 point by  $G(j\omega)$ .

This result clearly generalizes the classical Nyquist theorem. For a scalar transfer function G(s),

There is a deep connection between these two facts, see, e.g., [2].

related multivariable stability plots such as the inverse Nyquist array [28] and characteristic loci method [30]. The nature of the difficulty is illustrated by the following example, from [31].

# Example:

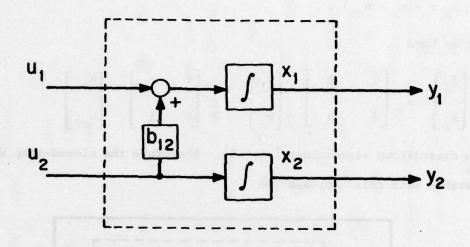


Fig. 2.1-8 Internal Structure of Example

$$\begin{bmatrix} \dot{\mathbf{x}}_1 \\ \dot{\mathbf{x}}_2 \end{bmatrix} = \begin{bmatrix} 1 & \mathbf{b}_{12} \\ 0 & 1 \end{bmatrix} \begin{bmatrix} \mathbf{u}_1 \\ \mathbf{u}_2 \end{bmatrix} \tag{2.1-4}$$

$$\begin{bmatrix} y_1 \\ y_2 \end{bmatrix} = \begin{bmatrix} 1 & 0 \\ 0 & 1 \end{bmatrix} \begin{bmatrix} x_1 \\ x_2 \end{bmatrix}$$
 (2.1-5)

$$G(s) = C(sI - A)^{-1}B = \begin{bmatrix} \frac{1}{s} & \frac{b_{12}}{s} \\ 0 & \frac{1}{s} \end{bmatrix}$$
 (2.1-6)

If we use the feedback compensation

$$u_1 = -(x_1 - u_{c1})$$
,  
 $u_2 = -(x_2 - u_{c2})$ , (2.1-7)

then we have

$$\begin{bmatrix} \dot{\mathbf{x}}_1 \\ \dot{\mathbf{x}}_2 \end{bmatrix} = \begin{bmatrix} -1 & -b_{12} \\ 0 & -1 \end{bmatrix} \begin{bmatrix} \mathbf{x}_1 \\ \mathbf{x}_2 \end{bmatrix} + \begin{bmatrix} 1 & b_{12} \\ 0 & 1 \end{bmatrix} \begin{bmatrix} \mathbf{u}_{c1} \\ \mathbf{u}_{c2} \end{bmatrix}$$
(2.1-8)

with closed-loop eigenvalues {-1, -1}. Therefore the closed-loop system is stable with this compensation.

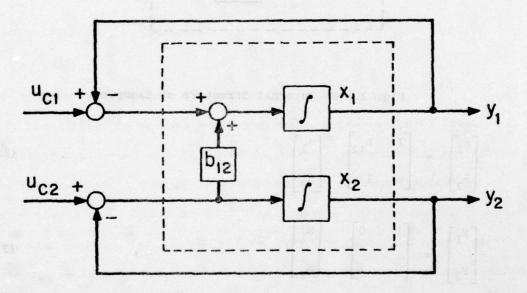
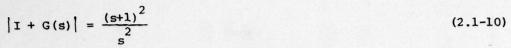


Fig. 2.1-9 System with Feedback

The multivariable Nyquist diagram is obtained as follows:

$$I + G(s) = \begin{bmatrix} \frac{s+1}{s} & \frac{b_{12}}{s} \\ 0 & \frac{s+1}{s} \end{bmatrix}$$
 (2.1-9)



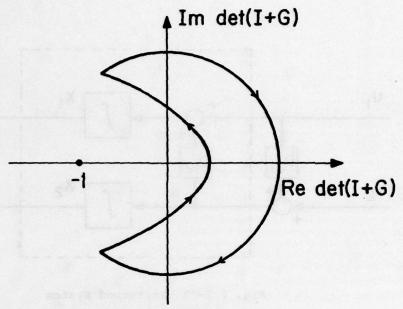


Fig. 2.1-10 Multivariable Nyquist Diagram Note that the diagram is completely independent of the value of  $b_{12}$ . However, as  $b_{12}$  becomes large, the system is nearly unstable in the following sense. If we perturb G(s) to obtain (Fig. 2.1-11)

$$\tilde{G}(s) = \begin{bmatrix} \frac{1}{s} & \frac{b_{12}}{s} \\ \frac{b_{21}}{s} & \frac{1}{s} \end{bmatrix}$$
(2.1-11)

then the closed-loop system is unstable for  $b_{21} > \frac{1}{b_{12}}$ . (This is readily seen from the state equations). If  $b_{12}$  is very large, then  $b_{21}$  can be very small so that a small change in the system dynamics results in an unstable system. This situation cannot be detected by examination of

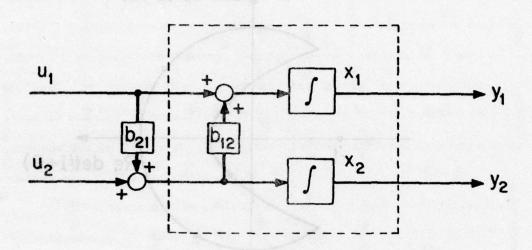


Fig. 2.1-11 Perturbed System

the multivariable Nyquist diagram for the nominal system.

The difficulty we have uncovered can be explained as follows: A multivariable system will be sensitive to modeling errors if its return difference matrix I +  $G(j\omega)$  is nearly singular at some frequency  $\omega_c$ , since then a small change in  $G(j\omega_c)$  will make I +  $G(j\omega_c)$  exactly singular. When this happens, det  $[I+G(j\omega_c)]=0$  and the number of encirclements changes. Unfortunately, near singularity of a matrix cannot be detected by the size of its determinant. A simple example is

$$A = \begin{bmatrix} 1 & 100 \\ 0 & 1 \end{bmatrix}$$
 (2.1-11)

which can be made singular with a small perturbation in its (2,1) element,

$$\widetilde{A} = \begin{bmatrix} 1 & 100 \\ & & \\ .01 & 1 \end{bmatrix}$$
 (2.1-12)

Reliable detection of near singularity of a matrix requires computations involving its norm, as we will see later on.

From the above example, we can see that the problem of determining a characterization of the robustness of a multivariable feedback system, i.e., its distance from instability, is of fundamental importance. Several authors [32] - [35], [12] have considered this issue in the context of characterizing the robustness properties of a linear-quadratic (LQ) optimal regulator with respect to nondynamical model variations (see the next section). However, the basic work is this area is due to Safonov [3], [36] - [37] who generalized an approach of Zames [38] - [39]. Safonov considers system models to be specified by relations between function spaces, as is now standard in the modern input-output formulation of stability theory. 1 He has developed a sector stability criterion that allows one to prove stability not just for a single feedback system, but a family of systems comprised of subsystems each of which lie within certain bounds about a nominal model. In the case of linear, time invariant subsystems, these bounds are characterized in terms of their transfer function matrices.

We will consider here a very special case of Safonov's characterization,

<sup>&</sup>lt;sup>1</sup>see, e.g., [40] or [41] .

derived in [1], [2], [7]<sup>1</sup>. We consider the multivariable unity feedback system illustrated in Fig. 2.1-12, where the transfer function matrix G(s) is a representation of the plant plus any compensation that has been employed. We suppose that the uncertainty in the representation of the plant is modeled as an additive (Fig. 2.1-13) or multiplicative (Fig. 2.1-14) perturbation to G(s). We assume that the nominal feedback system is stable, as are the perturbations.

Consider the additive case first. We are given that the nominal feedback system is stable so that the multivariable Nyquist plot of  $\det(I+G(j\omega))$  has the correct number of encirclements of the origin for stability to be concluded. As long as the perturbed multivariable Nyquist plot has the same number of encirclements, the perturbed feedback loop will remain stable. It turns out that a sufficient condition for this to occur is that

$$||\Delta G(j)|| < \frac{1}{||(x + G(j\omega))^{-1}||}$$
 (2.1-13)

for all  $\omega \geq 0$ , where  $||\cdot||$  is an appropriate matrix norm (see [7]). Since in the scalar case, the norm reduces to the absolute value, (2.1-13) is the multivariable generalization of (2.1-1). Notice that this condition is expressed in terms of the norm of the inverse return difference transfer function matrix,  $||(I+G(s))^{-1}||$ .

Doyle [1] considered the linear finite dimensional case and the spectral norm, while Sandell[2] gave a more general proof valid for infinite dimensional systems (e.g., systems with time delays) and nonlinear perturbations, and Laub [7] extended the result to more easily computed norms.

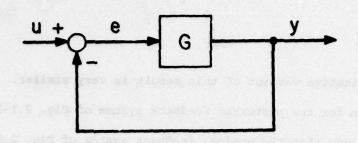


Fig. 2.1-12 Basic MIMO Linear Feedback System

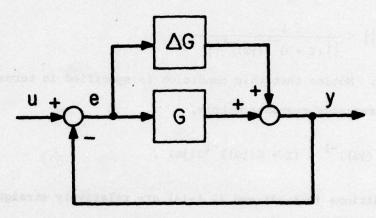


Fig. 2.1-13 System Subject to Additive Perturbations

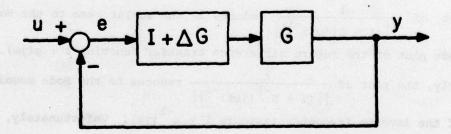


Fig. 2.1-14 System Subject to Multiplicative Perturbations

The multiplicative version of this result is very similar. A sufficient condition for the perturbed feedback system of Fig. 2.1-14 to remain stable, given that the nominal feedback system of Fig. 2.1-12 and the perturbation  $\Delta G(s)$  are stable, is

$$|\Delta G(j\omega)|| < \frac{1}{||(I+G^{-1}(j\omega))^{-1}||}$$
 (2.1-14)

for all  $\omega \geq 0$ . Notice that this condition is specified in terms of the closed-loop frequency response matrix,

$$(I + G^{-1}(j\omega))^{-1} = (I + G(j\omega))^{-1}G(j\omega)$$
.

The conditions (2.1-13) and (2.1-14) are relatively straightforward to test graphically. Computational details are discussed in [7]. Plots for several academic and physical examples are given in [1], [18], and [19]. In interpreting these plots, it is useful to keep in mind that the plot of  $\frac{1}{\left|\left|(\mathbf{I}+\mathbf{G}(\mathbf{j}\omega))^{-1}\right|\right|}$  reduces in the scalar case to the Bode magnitude plot of the return difference transfer function  $1+g(\mathbf{j}\omega)$ . Similarly, the plot of  $\frac{1}{\left|\left|\left(\mathbf{I}+\mathbf{G}^{-1}(\mathbf{j}\omega)\right)^{-1}\right|\right|}$  reduces to the Bode magnitude plot of the inverse frequency response  $1+g^{-1}(\mathbf{j}\omega)$ . Unfortunately, there is as yet no totally satisfactory notion of phase to go along with the magnitude plots - although see [1] for some ideas.

It is premature to state that the conditions (2.1-13) and (2.1-14) provide the sought after notion of multivariable stability margin. These are only sufficient conditions, and may prove overly conservative in practice. More experience is needed to verify that it is possible to spot

potential instabilities in physical systems that cannot be readily detected by other means. However, it is certainly true that the quantities

$$\frac{1}{\left|\left|\left(\mathbf{I}+\mathbf{G}(\mathbf{j}\omega)\right)^{-1}\right|\right|} \quad \text{and} \quad \frac{1}{\left|\left|\left(\mathbf{I}+\mathbf{G}^{-1}(\mathbf{j}\omega)\right)^{-1}\right|\right|} \quad \text{reduce in the scalar case to}$$

quantities that seem to capture the essence of the notion of robustness in classical control system design - namely, the distance as a function of frequency to the critical point of the Nyquist and inverse Nyquist Loci, respectively.

Another difficulty is that very little is known at present about how to shape the quantities  $\frac{1}{\left|\left|(I+G(j\omega))^{-1}\right|\right|} \text{ and } \frac{1}{\left|\left|(I+G^{-1}(j\omega))^{-1}\right|\right|}$  using established multivariable design methodologies such as pole placement or characteristic loci. An exception to this statement is the linear-quadratic-Gaussian (LQG) approach; the robustness properties of the LQG problem are our next topic of discussion.

## 2.2 Robustness of LQG Designs

In modern multivariable techniques for control system design, the robustness issue has been largely neglected, with interest picking up only recently. An exception to this statement is an early and basic paper of Kalman [42] on the properties of single-input steady-state linear-quadratic optimal regulators. Kalman established the fundamental inequality

$$|1 + g^{T}(j\omega I - A)^{-1}b| > 1$$
 (2.2-1)

for the return difference function of an LQ regulator. 1 This inequality

This equality is valid only when there are no crossterms between the state and control variables in the quadratic cost functional. In this equation  $g^T$  is the optimal feedback gain matrix.

proves that the Nyquist plot of the loop transfer function of an LQ regulation (see Fig. 2.2-1) avoids the unit disc about the critical point -1 + j0 (Fig. 2.2-2). Consequently, as pointed out in [43], every single-input LQ regulator has + 60° phase margin, infinite (positive) gain margin, and 50% gain reduction tolerance. The Nyquist plot for a typical example [44] is shown in Fig. 2.2-3.

Taken at face value, the guaranteed margins of an LQ controller are quite impressive. Indeed, the Military Specifications are almost 1 satisfied automatically! However, there are some limitations associated with this result. First, while the guarantees are adequate for model uncertainty within the basic frequency range for which the design model is valid, they may be grossly inadequate at higher frequencies. For example, common practice is to require gain stability (i.e., phase margin = + 180°) at frequencies higher than a specified cut-off frequency. Second, as we will see, the gain and phase margin guarantees do not apply if a Kalman filter or other state reconstructor is inserted in the loop. Third, the property is somewhat of an idealization of reality, since the Nyquist plot of a physical transfer function cannot avoid the unit circle at sufficiently high frequencies.

This last point requires elaboration, for it has been, in our opinion, the source of some confusion in the literature. It is possible to show, on very general theoretical grounds, that the loop transfer function of any physically realizable feedback system must have at least a two

The Military Specifications require ± 8 db gain margin at frequencies exceeding the first aeroelastic mode.

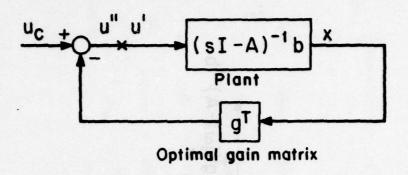


Fig. 2.2-1 The LQ Loop Transfer Function is Defined From u' to u"

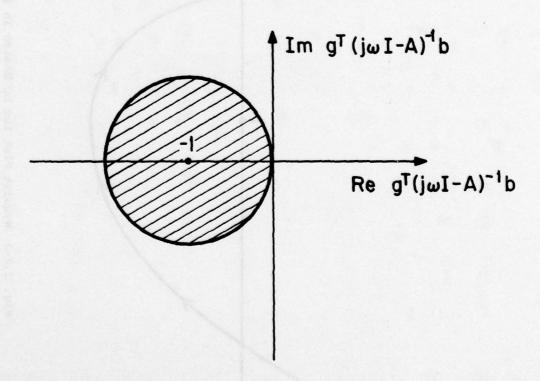


Fig. 2.2-2 Disk About Unit Circle Avoided by Optimal Nyquist Locus

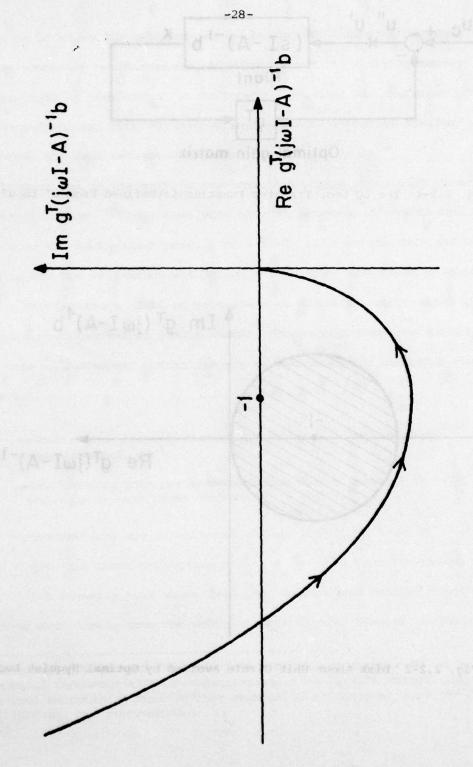


Fig. 2.2-3 Nyquist Plot for LQ Design in [44]

pole rolloff. Thus its asymptotic phase will be at least -180°, and its Nyquist plot must therefore penetrate the unit circle, in contradiction to Kalman's result.

The resolution of this contradiction is, of course, Kalman's assumption of full state feedback, which is a mathematical idealization that can never be exactly achieved in practice. There are always unmodeled dynamics in any physical system which at some sufficiently high frequency will contribute the additional phase and attentuation predicted by Bode's theorem.

This objection to Kalman's result is not too serious as long as the Nyquist locus of the real system penetrates the unit circle close to the origin, where the loop gain is low. Then the gain and phase margins predicted by (2.2-1) will be close to the actual margins. This will normally be the case when the unmodeled dynamics are well-separated in frequency from the dynamics given by the state space model used for design, and when the bandwidth of the loop transfer function is not too high.

The potential pitfall is that with modern design methods (including pole placement and characteristic loci as well as LQ methods), it is easy to achieve a very high speed of response (for the design model), but at the expense of obtaining an unrealistically high bandwidth. Comparison of closed-loop eigenvalue locations with the locations of poles of suspected unmodeled dynamics can help to avoid this situation, but there

<sup>1</sup> See [45] for an argument based on a theorem of Bode.

It may not be possible to always achieve this condition, as the example of a space structure with many flexure modes close to its rigid body modes shows.

seems to be no wholly satisfactory technique purely in the time domain.

To summarize our discussion of Kalman's result on the robustness of single-input LQ regulators, it suffices to say that the guaranteed properties are very good, but that the loop transfer function must be checked to insure that the gain crossover frequency is not too high.

Turning now to the multi-input case, the situation is less clear cut and still in flux. There have been several attempts at generalizing Kalman's result to the multi-input case, [32] - [35], [12] but the most definitive results are due to Safonov and Athans [13]. They have given a condition that characterizes a class of perturbations for which multi-input LQ regulators are guaranteed to remain stable. These perturbations include, for the case of a diagonal control weighting matrix in the quadratic cost function,

- •simultaneous phase perturbations of up to + 60° in each input channel, or
- •simultaneous gain perturbations from 50% of nominal to infinity in each input channel.

These perturbations are illustrated in Fig. 2.2-4, in which  $\alpha_i = e^{j\phi_i}$ ,  $|\phi_i| \leq 60^\circ$ , for phase variations or  $\frac{1}{2} \leq \alpha_i < \infty$  for gain variations.

It has recently been shown [46] that Savonov and Athans' result can be derived more simply from the multivariable Nyquist Theorem, using the

For example, Lehtomaki [46] has just obtained an example of a multiinput LQ regulator with an infinitesimally small gain margin. The control weighting matrix in this example is nondiagonal, so the results of [13] are not contradicted.

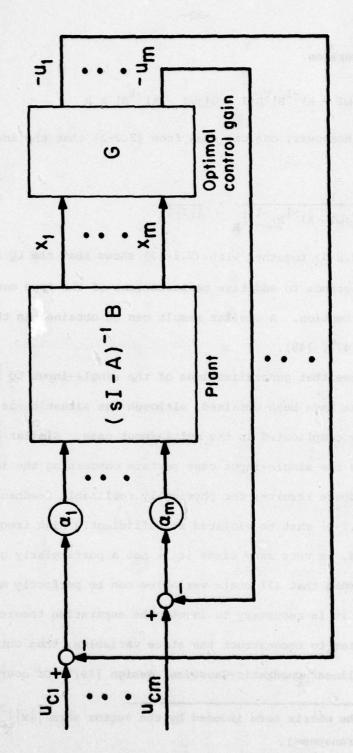


Fig. 2.2-4 Configuration for Definition of Multi-Input LQ Stability Margins

multi-input version

$$[I + G(-j\omega I - A)^{-1}B]^{T}R[I + G(j\omega I - A)^{-1}B] > R$$
 (2.2-2)

of (2.2-1). Moreover, one can show from (2.2-2) that the inequality 1

$$\frac{1}{||(I + G(j\omega I - A)^{-1}B)^{-1}||_{R}} \ge \frac{1}{||I||_{R}}$$
 (2.2-3)

holds, and (2.2-3) together with (2.1-13) shows that the LQ regulator has a degree of tolerance to additive perturbations of the type considered in the previous Section. A similar result can be obtained in the multiplicative case [47], [48].

Thus we see that generalizations of the single-input LQ stability margin results have been obtained, although the situation is naturally somewhat more complicated in the multi-input case. Similar comments to those made in the single-input case pertain concerning the idealizations implicit in these results; for physically realizable feedback systems the condition (2.2-2) must be violated at sufficiently high frequencies.

Of course, in very many cases it is not a particularly good approximation to assume that all state variables can be perfectly measured. In these cases, it is necessary to invoke the separation theorem and to use a Kalman filter to reconstruct the state variables, thus obtaining a so-called LQG (linear-quadratic-Gaussian) design [49]. Of course, the Kalman

 $<sup>|\</sup>cdot|_R$  is the matrix norm induced by the vector norm  $|\cdot|_R|_R^2 = x*Rx(* = conjugate transpose).$ 

filter explicitly incorporates a model of the system in its computations, and it might be expected that an LQG design would have much poorer robustness properties than the corresponding LQ design. This is indeed the case - there are no guaranteed margins for LQG feedback controllers, as has been shown by counter example [50]. The example in [50] is of course pathological, but poor stability margins can occur in actual LQG designs. Fig. 2.2-5 shows a design reported in the literature [44] that has less than 10° of phase margin.

Fortunately, there are two dual procedures<sup>2</sup> [14], [15] for "robustness recovery", i.e., for systematically adjusting an LQG design to asymptotically obtain the LQ stability margins. In one procedure [14], the state feedback gains are adjusted to take account of the fact that state estimate feedback is being used; in the other [15], the Kalman filter is adjusted to take account of the fact that it is being used in a feedback loop.

Thus the robustness issue can be fairly directly handled with the LQG approach.

Fig. 2.2-6, shows a robustified version of the LQG design in [44]. Stability margins are now quite satisfactory. However, it should be pointed out that more measurement noise is passed in this design than in the "optimal" design given by the separation theorem, so that there is

It can be shown that the LQG design is robust to errors in the model used to compute its Kalman filter gain - as distinct from the model used in the on-line filtering operations [51].

However, these procedures only apply to minimum phase plants, i.e., plants with no right half plane transmission zeroes.

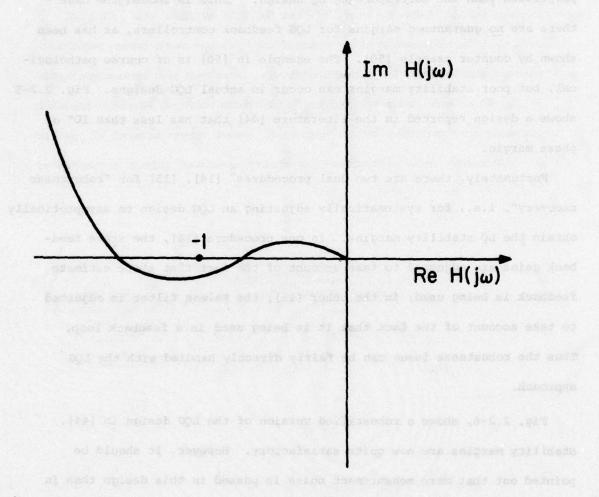


Fig. 2.2-5 Nyquist Plot for LQG Design in [44] (H(jw) = loop transfer function)

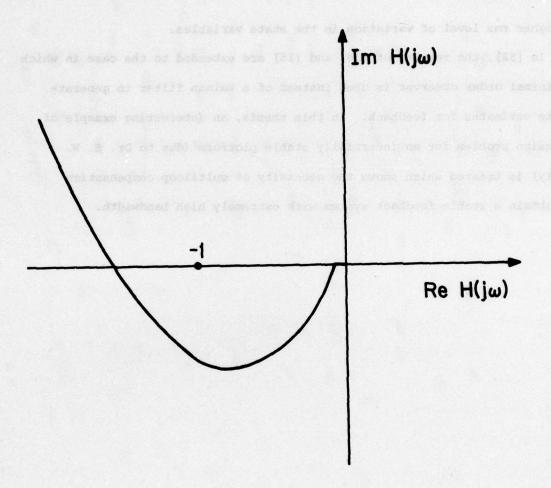


Fig. 2.2-6 Nyquist Plot for Robustified Version of LQG Design on [44]  $(\text{H}(j\omega) = loop \ transfer \ function)$ 

a higher rms level of variation in the state variables.

In [52], the results of [14] and [15] are extended to the case in which a minimal order observer is used instead of a Kalman filter to generate state estimates for feedback. In this thesis, an interesting example of a design problem for an intertially stable platform (due to Dr. S. W. Gully) is treated which shows the necessity of multiloop compensation to obtain a stable feedback system with extremely high bandwidth.

#### 3. WORKSHOP PROCEEDINGS

In the preceding section we described some recent results concerning the characterization of robustly stable multivariable feedback systems, and we discussed the relation of these results to the LQG design methodology. These results motivated the ONR/MIT Workshop on Recent Developments in the Robustness Theory of Multivariable Systems. The papers presented and the discussions held are very briefly summarized in this section; the papers are included in Appendix C.

#### 3.1 Introduction to Papers

The papers presented in the first day were concerned with characterizing the robustness of multivariable feedback systems with respect to model uncertainty.

The first paper was given by Mr. J.C. Doyle [1]. Mr. Doyle considered the case of a finite dimensional linear multivariable feedback system, with finite dimensional, linear model uncertainty. He derived a sufficient condition for stability in the presence of model uncertainty involving (in the case of additive model error) the minimum singular value of the return difference transfer function matrix. The derivation involved a relatively simple argument based on the multivariable Nyquist theorem. Mr. Doyle presented several interesting examples, and demonstrated various graphical means of evaluating multivariable feedback system robustness.

Prof. N.R. Sandell, Jr. considered a more general case of the basic problem considered by Mr. Doyle [2]. The nominal feedback system was linear but possibly infinite dimensional (so that time delays, for example,

could be considered), and the model perturbations were allowed to be nonlinear. A sufficient condition was obtained involving (for an additive model perturbation) the L<sub>2</sub> norm of the inverse return difference operator. The derivation was based on standard results in input-output stability theory. In the linear case, the condition obtained reduces to Doyle's condition. An application to singular perturbation theory was briefly mentioned.

Prof. M.G. Safonov consider a still more general case [3], in which the feedback system consisted of a set of interconnected nonlinear systems, with model uncertainty entering in a fairly general way. The analysis was based on some recent extensions of classical input-output stability-theoretic results [4], and the conditions derived included those of Doyle and Sandell when appropriately specialized.

Prof. C.A. Dosoer also considered a rather general case involving non-linear time-varying, multivariable, and distributed feedback systems [5].

Prof. Desoer did not confine himself to stabilization as the previous speakers largely did, but also considered the issues of desensitization, disturbance attenuation, linearizing effect, and asymptotic tracking and disturbance rejection. His results basically require that the linearized inverse return difference operator should be small for the nonlinear feedback system to possess advantages relative to the open-loop system.

Several of the previous speakers had discussed the notion of the singular value decomposition, and Prof. B.C. Moore gave a very interesting account of some preliminary results concerning the application of this decomposition to the on-line turning of multivariable proportional-integral controllers [6]. Prof. Moore explained that the basic ideas

of singular value analysis have long been known in the statistics literature where the terminology principal component analysis is used instead.

Dr. A.J. Laub's paper [7] was concerned with the basic problem formulation considered by 'ir. Doyle. Dr. Laub pointed out that the use of singular values is associated with a particular matrix norm (the  $\rm L_2$  norm). Other norms can be equally well used, and there is a very substantial computational advantage associated with some of them (the  $\rm L_1$  and  $\rm L_\infty$  norms).

After the focus on characterizing the robustness properties of multivariable feedback systems in the first day, attention turned in the second day to the issue of designing robust systems.

Prof. I. Horowitz has long been interested in the synthesis of feedback systems subject to model uncertainty, and he gave a presentation of his methods [8]. The basic objective of his technique is to achieve desired forms for the elements of the transfer function matrices between command and disturbance inputs and response outputs. Tolerances on these elements are necessitated by the presence of parameter uncertainty.

Dr. I. Postlethwaite represented Prof. MacFarlane's group at Cambridge University, and discussed their techniques for assessing the robustness properties of a linear multivariable feedback design [9], [10]. These techniques involve computing the singular values (termed principal gains) of certain transfer function matrices, as well as determinations of stability with respect to system parameters. The interested reader will want to carefully consider the discussion in Section 2 of [9] in light of the examples discussed in Section 2.1 of this report and Section 3 of [1].

Prof. J.E. Ackermann's paper [11] was also concerned with stability under parameter uncertainty. Prof. Ackermann's approach is a generalization of classical parameter plane techniques. The procedure was illustrated with an interesting example developing a feedback controller for a crane.

Prof. M. Athans presented an overview of what is known about the robustness properties of LQ regulators [12], [13]. He described how the motivation for the results obtained by himself and his students derived from a study supporting the design of the automatic depth-keeping controller for the TRIDENT submarine.

The guaranteed robustness properties of LQ regulators are not valid for LQG designs (i.e., with state estimate rather than state variable feedback). However, for minimum phase systems, these properties can be asymptotically recovered in a procedure described by Prof. H. Kwaakernaak [14]. The basic idea of this procedure is to modify the feedback gains to account for the fact that state estimate rather than state variable feedback is used. There is a dual approach involving adjustment of Kalman filter gains that was discussed by Mr. Doyle [15].

The robustness properties of LQ regulators can in certain cases be improved upon by other forms of state feedback. One result is that 100% gain reduction margins and 90° phase margins can be obtained for an open loop stable system when feedback obtained from solving a Lyapunov rather than a Riccati equation is considered. This result is implicit in [12], and was discussed, with related ideas, by Prof. J.C. Willems [16] and Dr. A. Harvey [17].

The final topic of discussion was design examples to illustrate the conference presentations during the previous days. Dr. G. Stein presented

an example involving some trial controller designs for the longitudinal degrees of freedom of the CH-47 helicopter, with model uncertainty due to rotor dynamics and rate limiting [18]. Messrs. N. Lehtomaki and S. Chan described control law development for a five terminal DC power distribution network with various sources of model uncertainty [19].

# 3.2 Research Directions

In the course of the workshop, and particularly during the roundtable discussion at its conclusion, numerous suggestions were advanced concerning directions for future research. In this section we will try to briefly recapitulate some of the suggestions; we will not attempt to identify specific suggestions with individuals.

There was widespread agreement on the need for work attempting to apply the concepts that have been developed to some specific design examples. This work is necessary to evaluate the results obtained so far and to compare the practical utility of the various approaches - for example, to compare the results obtained by computing  $||\mathbf{I}+\mathbf{G}^{+1}(\mathbf{j}\omega)||$  using the various matrix norms. In addition, working out some detailed examples is the best way to communicate the new approaches to designers. Finally, contact with applications usually suggests new theoretical problems. Indeed, it was the attempts to apply LQG theory, notably at MIT and Honeywell, that led to the work motivating the conference.

In the area of robustness analysis for multivariable systems, one of the basic needs is for more refined tests and measures of robustness. The present measures lead to overly conservative results in many instances, since they characterize model error simply by its norm. In

the single-input, single-output case this is equivalent to considering only the magnitude and not the phase error. It was pointed out that a generalization of the magnitude-phase representation of a transfer function is the singular value decomposition of a transfer function matrix. The singular values generalize the notion of gain and the orthogonal matrices of right and left singular vectors generalize the notion of phase. Thus it may be possible to use the singular value decomposition to develop robustness tests that give information concerning the nature of the perturbation that the system is most sensitive to.

The presentations at the workshop focused on the case of continuous time systems, but the discrete-time case is of great interest due to the trend toward digital implementation of sampled data controllers. Several phenomena occur in sampled data control that greatly complicate analysis. Most notable of these is aliasing, which implies that transfer functions need be considered that do not rolloff at high frequencies (in the idealized case of impulsive sampling). Some work has been done for the case of LQG sampled-data controllers [37], but the extension of the results discussed at the workshop to sampled-data systems represents an open area of research.

Similarly, the case of nonlinear multivariable systems needs more investigation. Some of the basic theoretical results [37], [2]-[5] are valid for nonlinear systems, but little has been accomplished in the practical exploitation of these results. By analogy with the single-input, single-output case, it might be conjectured that the present results are excessively conservative. One direction to mitigate this

difficulty would be to combine describing function and multivariable robustness analysis techniques, although the strict stability theoretic interpretation of the results would be lost.

In the area of techniques for synthesis of robust multivariable feedback systems, little is known except for the case of the LQG methodology, where the basic facts are in hand. In the LQ case, the robustness properties stem from the fundamental inequality of Kalman which implies that an LQ loop transfer matrix (at all frequencies) avoids the unit ball about the - I loop transfer matrix. It was pointed out that it would be desirable to have a more flexible property, in which one could chose a frequency dependent radius for the ball that is avoided. At present, this can be done in a somewhat ad hoc way by appending compensation to the plant's inputs and outputs. It was suggested that a more systematic approach might be possible utilizing frequency dependent weighting matrices in the quadratic cost function.<sup>2</sup>

For the LQG case, two dual methods for recovering the LQ robustness properties were described. The relation between these techniques, and more generally the tradeoff between robustness and performance implicit, needs to be explored. It is significant both techniques require a minimum phase condition. It is unclear what can be accomplished in the absence of this condition.

The implications of the results discussed at the workshop for other

In an appropriate norm.

Note that the usual practice of appending compensator dynamics to the plant amounts to using frequency dependent weighting matrices.

design methodologies are less obvious. The use of graphical frequency domain techniques for multivariable feedback system design has been most completely developed by MacFarlane and his colleagues, and incorporation of the robustness tests described herein into their software would be straightforward. However, the synthesis problem is more difficult to attack. The relationship between the singular values of  $I + G(j\omega)$  and any compensation imbedded in  $G(j\omega)$  is extremely complicated – even more so than for the eigenvalues of  $I + G(j\omega)$ . The basic problem is that, unlike the eigenvalues, the singular values of  $I + G(j\omega)$  bear no particular relationship to those of  $G(j\omega)$ . This is a particular problem in the important crossover region where I and  $G(j\omega)$  are of comparable magnitude.

MacFarlane and his colleagues have already consider the use of singular values, termed "principal gains", albeit in a slightly different context.

#### REFERENCES

Note: Refs. 1 - 18 are included in Appendix C.

- [1] J.C. Doyle, "Robustness of Multiloop Linear Feedback Systems," IEEE Conf. on Dec. and Control, San Diego, CA, Jan. 1979.
- [2] N.R. Sandell, Jr., Robust Stability of Linear Dynamic Systems with Application to Singular Perturbation Theory, Laboratory for Information and Decision Systems, MIT, ESL-P-837, Aug. 1978.
- [3] M.G. Safonov and M. Athans, "A Multiloop Generalization of the Circle Stability Criterion," <u>Twelfth Asilomar Conference on Circuits</u>, <u>Systems and Computers</u>, <u>Pacific Grove</u>, CA, Nov. 1978.
- [4] M.G. Safonov, "Tight Bounds on the Response of Multivariable Systems with Component Uncertainty," 16th Allerton Conference on Communication, Control, and Computing, Allerton, Ill., Oct. 1978.
- [5] C.A. Desoer and Y.T. Wang, "Foundations of Feedback Theory for Nonlinear Dynamical Systems," to appear in <u>IEEE Trans. Circuits and</u> Systems.
- [6] B.C. Moore, On-Line Tuning of Multivariable PI Controllers Using Principal Component Analysis: Preliminary Results, System Control Report No. 7905, Univ. of Toronto, Toronto, Canada, April 1979.
- [7] A.J. Laub, Robust Stability of Linear Systems Some Computational Considerations, Laboratory for Information and Decision Systems, MIT, LIDS-R-904, Feb. 1979.
- [8] I.M. Horowitz, "Quantitative Synthesis of Uncertain Multiple Input-Output Feedback System," to appear in Int. J. Control.
- [9] I. Postlethwaite, <u>Methods for Assessing the Robustness Properties</u> of a Linear <u>Multivariable Feedback Design</u>, <u>Cambridge Univ.</u>, <u>Cambridge</u>, <u>England</u>, 1979.
- [10] I. Postlethwaite, A Note on Parameteric Stability, Cambridge Univ., Cambridge, England, 1978.
- [11] J. Ackermann, "A Robust Control System Design," 1979 Joint Automatic Control Conference.
- [12] P.K. Wong and M. Athans, "Closed-Loop Structural Stability for Linear Quadratic Optimal Systems," IEEE Trans. on Automatic Control, Vol. AC-22, Feb. 1977.

- [13] M.G. Safonov and M. Athans, "Gain and Phase Margins of Multiloop LQG Regulators," IEEE Trans. Automatic Control, Vol. AC-22, April 1977.
- [14] H. Kwaakernaak, "Optimal Low-Sensitivity Linear Feedback Systems," Automatica, Vol. 5, May 1969.
- [15] J.C. Doyle and G. Stein, "Robustness with Observers", IEEE Trans.
  Automatic Control, Vol. AC-24, August 1979.
- [16] P. Molander and J.C. Willems, "Robustness Results for State Feedback Regulators," to be published.
- [17] C.A. Harvey, "On Feedback Systems Possessing Integrity with Respect to Actuator Outages," to be published.
- [18] G. Stein and J.C. Doyle, "Singular Values and Feedback: Design Examples," 16th Allerton Conference on Communication, Control and Computing, Allerton, Ill., Oct. 1978.
- [19] N.A. Lehtomaki, et. al., "Robust Control of Multiterminal DC/AC Systems," <u>IEEE Conf. on Dec. and Control</u>, Fort Lauderdale, Fla., Dec. 1979.
- [20] Background Information and User Guide for MIL-F-9490D, Flight Control Systems Design, Installation and Test of Piloted Aircraft, General Specification for, Air Force Flight Dynamics Laboratory, Technical Report AFFDL-TR-74-116, January 1975.
- [21] M.G. Safonov and M. Athans, "On Stability Theory," Proc. IEEE Conf. on Decision and Control, San Diego, Calif., Jan. 1979.
- [22] G. Zames, Nonlinear Operators for System Analysis, Research Laboratory of Electronics, M.I.T., TR-370, August, 1960.
- [23] W.M. Wonham, Linear Multivariable Control: A Geometric Approach. Springer-Verlag, New York, 1974.
- [24] N.R. Sandell, Jr. and M. Athans, "On Multivariable Type-L Systems," Automatica 9, pp. 131-136, 1973.
- [25] J.B. Cruz, Ed., System Sensitivity Analysis, Dowden, Hutchinson, and Ross, Stroudsburg, Pa., 1973.
- [26] H.W. Bode, <u>Network Analysis and Feedback Amplifier Design</u>, Van Nostrand, N.Y., 1945.
- [27] I.M. Horowitz, Snythesis of Feedback Systems, Academic Press, N.Y., 1963.

- [28] H.H. Rosenbrock, Computer Aided Control System Design, Academic Press, 1976.
- [29] G.W. Stewart, Introduction to Matrix Computations, Academic Press, N.Y., 1973.
- [30] I. Postlethwaite and A.G.J. MacFarlane, A Complex Variable Approach to the Analysis of Linear Multivariable Feedback Systems, Springer-Verlag, Berlin, 1979.
- [31] G. Stein and N.R. Sandell, Jr., <u>Classical and Modern Methods of</u>
  <u>Control System Design</u>, Notes for Subject 6.291, M.I.T., Cambridge,
  <u>Mass.</u>, 1979.
- [32] S. Barnett and C. Storey, "Insensitivity of Optimal Linear Control Systems," Int. J. Control, Vol. 4, 1966.
- [33] J.B. Moore and B.D.O. Anderson, "Applications of the Multivariable Popov Condition," Int. J. Control, Vol. 5, 1967.
- [34] P.J. Moylan and B.D.O. Anderson, "Nonlinear Regulator Theory and an Inverse Optimal Control Problem," <u>IEEE Trans.Automatic Control</u>, Vol. AC-18, Oct. 1973.
- [35] P.J. Moylan, "Implications of Positivity in Nonlinear Systems," IEEE Trans. Automatic Control, Vol. AC-19, Aug. 1974.
- [36] M.G. Safonov, Robustness and Stability Aspects of Stochastic Multivariable Feedback System Design, Ph.D. Thesis, M.I.T., Sept. 1977.
- [37] M.G. Safonov, Stability and Robustness of Multivariable Feedback Systems, M.I.T. Press, Cambridge, Mass., 1979.
- [38] G. Zames, "On the Input-Output Stability of Time-Varying Nonlinear Feedback Systems - Part I: Conditions Using Concepts of Loop Gain, Conicity, and Positivity," <u>IEEE Trans. Automatic Control</u>, Vol. AC-11, April 1966.
- [39] G. Zames, "On the Input-Output Stability of Time-Varying Nonlinear Feedback Systems Part II: Conditions Involving Circles in the Frequency Plane and Sector Nonlinearities," <u>IEEE Trans. Automatic</u> Control, Vol. AC-11, July 1966.
- [40] J.C. Willems, The Analysis of Feedback Systems, M.I.T. Press, Cambridge, Mass., 1971.
- [41] C.A. Desoer and M. Vidyasager, Feedback Systems: Input-Output Properties, Academic Press, N.Y., 1975.

- [42] R.E. Kalman, "When is a Linear System Optimal?", <u>Trans. ASME Ser. D:</u> J. Basic Eng., Vol. 86, 1964.
- [43] B.D.O. Anderson and J.B. Moore, Linear Optimal Control, Prentice-Hall, Englewood Cliffs, N.J. 1971.
- [44] A.E. Bryson, Random Problems in Control Theory, Stanford University, Report SUDAAR No. 447, Sept. 1972.
- [45] I.C. Horowitz and U. Shaked, "Superiority of Transfer Function Over State Variable Methods in Linear Time Invariant Feedback System Design," IEEE Trans. Auto. Control, AC-20, 1975.
- [46] N. Lehtomaki, personal communication.
- [47] S.W. Nuzman, and N.R. Sandell, Jr., "An Inequality Arising in the Robustness Analysis of Multivariable Systems," IEEE Trans. Automatic Control, Vol. AC-24, June 1979.
- [48] A.J. Laub, "An Inequality and Some Computations Related to the Robust Stability of Linear Dynamic Systems," IEEE Trans. Automatic Control, Vol. AC-24, April 1979.
- [49] M. Athans, "The Role and Use of the Stochastic Linear-Quadratic-Gaussian Problem in Control Systems Design," IEEE Trans. Automatic Control, Vol. AC-16, Dec. 1971.
- [50] J.C. Doyle, "Guaranteed Margins for LQG Regulators, "IEEE Trans. Automatic Control, Vol. AC-23, Aug. 1978.
- [51] M. Safonov and M. Athans, Robustness and Computational Aspects of Nonlinear Stochastic Estimators and Regulators, Laboratory for Information and Decision Systems, MIT, ESL-P-741, Cambridge, MA., 1977.
- [52] J.R. Dowdle, Robust Observer Based Compensators, Ph.D. Thesis, MIT, August 1979.

# DISTRIBUTION LIST

Office of Naval Research		Naval Coastal Systems Center	
800 N. Quincy St.		Hydromechanics Division	
Arlington, VA 22217		Panama City, FL 32407	
R. von Husen, Code 211		D. Humphreys, Code 794	a pe
S. L. Brodsky, Code 432	N 4 4 1 11	b. Humphreys, code 754	301112
5. L. Brousky, code 432		David Taulau Naual Chin Den Comton	
		David Taylor Naval Ship R&D Center	
Office of Naval Research		Bethesda, MD 20084	
Branch Office		Technical Library	1
495 Summer Street			
Boston, MA 02210	01891	Naval Post Graduate School	
1180		Monterey, CA 93940	
Office of Naval Research		Technical Reports Library	1
Branch Office		D. Kirk	
536 South Clark St.		U. NIIK	
			007
Chicago, IL 60605		Defense Technical Information Cent	er
		Building 5	
Office of Naval Research		Cameron Station	
Branch Office		Alexandria, VA 22314	12
1030 E. Green St.		unal and all the second and the	
이 보고 하는 것이 가게 하는 것이 되었다면 하는 것이 되었다면 보고 있는데 그리고 있다면 하는데 하는데 되었다.	mmoU 1	Air Force Office of Scientific Res	earch
Contraction is the contract to be a	hns	Building 410	
Naval Research Laboratory			
		Bolling Air Force Base	
Washington, DC 20375		Washington, DC 20332	. 60
Code 2627	3	C. L. Nefzger	1
Naval Air Systems Command		Air Force Flight Dynamics Laborato	rv
Washington, DC 20361		Wright-Patterson Air Force Base	, ,
	1		
G. Tsaparas, AIR 340D	1100	Dayton, OH 45433	THESE !
	090 1	R. Anderson, Control Dyn. Br.	
J. M. Rebel, AIR 53352	1	F. George, Control Dyn. Br.	
		S. J. Larimer, FGC	1
Naval Air Development Center			
Warminster, PA 18974		Air Force Institute of Technology	
C. R. Abrams, Code 6072		Wright-Patterson Air Force Base	
O. W. Maraina, Code Core	nu i	Dayton, OH 45433	
Naval Material Command			moN.
		P. Maybeck	
Washington, DC 20360		J. G. Reid	•
Code 08T23	1	ABOUT PERSON OF THE PERSON	
A STATE OF THE PARTY OF THE PAR		Army Armament R&D Command	
Naval Weapons Center		Building #18	
China Lake, CA 93555		Dover, NJ 07801	
B. Hardy, Code 3914	997 1	N. Coleman, DRDAR-SCFCC	1
0. 8ox 217			
Naval Surface Weapons Center	780	NASA Langley Research Center	
Silver Spring, MD 20910		Hampton, VA 23665	
J. Wingate, Code R44	1	E. Armstrong	SEA 1
panerty at Taranta	and a	Technical Library	1
		iccinical Library	all the same of

Scientific Systems, Inc.		Carspan corp.	
Suite No. 309-310		P. O. Box 400	
186 Alewife Brook Parkway		Buffalo, NY 14225	
Cambridge, MA 02138		E. G. Rynaski	1
	31	Manage and Committee and an	
K. K. Menra		Systems Control Inc.	
Systems Technology, Inc.		1801 Page Mill Road	
13766 South Hawthorne Blvd.		Palo Alto, CA 94306	
Hawthorne, CA 90250		E. Hall	1
R. Whitbeck	1		
The Militabeek		Flight Research Laboratory	
The Annal Ada Cadamana Caus		Dept. of Mechanical & Aerospace	
The Analytic Sciences Corp.			
6 Jacob Way		Engineering Addition of the Person of	
Reading, MA 01867		Princeton University	
C. Price		Princeton, NJ 08544	
Agrandia the 22314		R. F. Stengel	1
Massachusetts Institute of Technology			
		Coordinated Science Laboratory	
Lab. for INformation and Decision			
Systems		and Dept. of Electrical Engineering	
Cambridge, MA 02139		Decision and Control Laboratory	
M. Athans	1	4-111 CSL	
A. J. Laub	1	Urbana, IL 61801	
M. Triantafyllon	1	J. Ackermann	1
m. Iriancalytion		O, Mekerimann	
		University of California at Berkeley	
University of Michigan			
Dept. of Naval Architecture & Marine		College of Engineering	
Engr.		Dept. of Electrical Engineering and	
Ann Arbor, MI 48109		Computer Science	
M. G. Parsons	1	Berkeley, CA 94720	
11. 4. 14. 56.6		C. A. Desoer	1
Nielsen Engineering & Research, Inc.			
		Lockheed Missile and Space Corporation	n
510 Clyde Ave.			
Mountainview, CA 94043			,
J. N. Nielsen		M. Fong analysis of the product of aver-	1
		ONE ON LINE OF CHARLES AND ADDRESS OF THE AND ADDRESS OF THE ADDRE	
University of Notre Dame		Weizmann Institute of Science	
Dept. of Electrical Engineering		Rehovot, Israel	
Notre Dame, IN 46556		I. Horowitz	1
M. K. Sain	1	The state of the s	
M. N. Jaili		Twente University of Technology	
The C. S. Draper Laboratory, Inc.		P. O. Box 217	
555 Technology Square		7500 AE Enschede, The Netherland	
Cambridge, MA 02139		H. Kwakernaak	1
R. V. Ramnath	1		
Technolis I factories		University of Toronto	
Hanning 11 Inc		Dept. of Electrical Engineering	
Honeywell, Inc.		Toronto, Ont. Canada M5S 1A4	
Systems and Research Center			,
2600 Ridgway Parkway		B. C. Moore	1
Minneapolis, MN 55413			
C. A. Harvey	1		
J. Doyle	1		
G. Stein			

University Engineering Department
Congrol and Management Systems Division Mill Lane
Cambridge, England CB2 1RX I. Postlethwaite
Dept. of Electrical Eng Systems
University of Southern California Los Angeles, CA 90007
M. Safonov
Technion - Israel Institute of Technolog
Technion City, Haifa 32000
R. Sivan
Dept. of Computing and Control
Science and Technology
Imperial College
London, England
R. B. Vinter
University of Groningen
Math. Institute
P. O. Box 800
Groningen, Netherlands
J. C. Willems

# APPENDICES

- A. Final Program
- B. List of Participants
- C. Papers Presents

Appendix A - Final Program

ONR/M.I.T. - LIDS Workshop on Recent Developments in the Robustness Theory of Multivariable Systems

#### FINAL PROGRAM

Wednesday, April 25

9:30 AM - 5:00 PM

# Opening Remarks

N.R. Sandell, Jr., M.I.T.

Mr. R. Von Husen, ONR

#### Robustness Characterization

- 1. "Robustness of Multiloop Linear Feedback Systems", J.C. Doyle, Honeywell and University of California at Berkeley
- "Multivariable Systems Robustness: Theory, Applications, Connections", N.R. Sandell, Jr., M.I.T.
- "Frequency-Domain Analysis of Multivariable Feedback System Robustness",
   M.G. Safonov, University of Southern California
- 4. "Robustness in Nonlinear Systems", C.A. Desoer, Univ. of California at Berkeley

# Singular Value Analysis

- 1. "Singular Value Analysis of Linear Systems", B.C. Moore, Univ. of Toronto
- "Robust Stability of Linear Systems Some Computational Considerations",
   A.J. Laub, M.I.T.

#### Thursday, April 26

9:00 AM - 5:00 P.M.

## Robustness in Design - Frequency Domain Approaches

- "Quantitative Synthesis of Uncertain Multivariable Feedback Systems",
   I.M. Horowitz, Weizman Institute, Israel
- "Stability in the Face of Pertubations and Uncertainty", I. Postlethwaite, Cambridge University, England

# Robustness in Design - Pole Placement

 "A Robust Control System Design", J.A. Ackermann, Univ. of Illinois (Visiting Professor)

# Robustness in Design - The LQG Approach

- 1. "Robustness and the LQG Problem", M. Athans, M.I.T.
- 2. "Robustness Recovery", H. Kwakernaak, Twente University, The Netherlands
- 3. "Robustness with Observers", J.C. Doyle, Honeywell and University of California at Berkeley, and G. Stein, Honeywell and M.I.T.

Friday, April 27

9:00 AM - 3:00 PM

#### Robustness in Design - State Feedback

- "Robustness Designs by State Feedback, by P. Molander and J.C. Willems, presented by J.C. Willems, University of Groningen, The Netherlands
- "On Feedback Systems Possessing Integrity with Respect to Actuator Outages", A. Harvey, Honeywell

#### Design Examples

- "Singular Values and Feedback: Design Examples, G.Stein, Honeywell and M.I.T., and J.C.Doyle, Honeywell and University of California at Berkeley
- "Design Example: Control of a Power Network with Multiterminal DC Transmission", N.Lehtomaki, S.Chan, N.R.Sandell, Jr., and M.Athans, M.I.T.

#### Roundtable Discussion

Participants to be announced .

# INFORMATION

The conference will be held in Room 407 of the M.I.T. Student Center on Massachusetts Avenue on all days except for Thursday morning. The Thursday morning meeting will be held in the Bush Room, 10-105.

There will be a cocktail party hosted by the M.I.T. Laboratory for Information and Decision Systems at 5:00 PM on Wednesday in Room 26-414.

Appendix B - List of Attendees

# The ONR/M.I.T. - L.I.D.S. Workshop was attended by the following

ACKERMANN, Juergen, Visiting Professor, Coordinated Science Laboratory and Dept. of Electrical Engineering Decision and Control Laboratory 4-111 CSL Urbana, Ill. 61801

ARMSTRONG, Ernest, Aero-Space Technologist

NASA - Langley Research Center
Hampton, Virginia 23665

ATHANS, Michael, Director
Laboratory for Information and Decision Systems
Massachusetts Institute of Technology
Bldg. 35-304
77 Massachusetts Ave.
Cambridge, Mass. 02139

CASTANON, David, Research Staff
Laboratory for Information and Decision Systems
Massachusetts Institute of Technology
Bldg. 35-316
77 Massachusetts Ave.
Cambridge, Mass. 02139

CHAN, Sherman M., Student

Massachusetts Institute of Technology - Laboratory for

Information and Decision Systems

77 Massachusetts Ave.

Cambridge, Mass. 02139

COLEMAN, Norman, Mathematician
Army Armament R&D Command
AHN: DRDAR-SCFCC (Dr.N.Coleman)
Bldg. #18
Dover, N.J. 07801

DESOER, C.A., Professor
University of California at Berkeley
College of Engineering
Dept. of Electrical Engineering and Computer Science
Berkeley, CA 94720

DOWDLE, John, Student
Massachusetts Institute of Technology
77 Massachusetts Ave.
Cambridge, MA 02139

DOYLE, John, Consultant - Student
Honeywell - University of California at Berkeley
2600 Ridgway Parkway
Minneapolis, MN 55413

FONG, Mike, Lead Engineer
Lockheed Missile and Space Corporation
Sunnyvale, CA

HARDY, Bruce, Naval Weapons Center Code 3914 China Lake, CA 93555

HARVEY, Arthur C., Research Staff Engineer
Honeywell, Inc.
Systems and Research Center, MN 17-2367
2600 Ridgway Parkway
Minneapolis, MN 55413

HOROWITZ, Isaac, Professor

Weizmann Institute of Science
Rehovot, Israel

KWAKERNAAK, H., Professor
Twente University of Technology
P.O. Box 217
7500 AE Enschede, The Netherland

LARIMER, Stanley J. Lt. USAF,
Stability and Control Engineer
AFFDL/FGC
Wright-Patterson AFB
Ohio 45433

LAUB, Alan J., Research Associate

Massachusetts Institute of Technology - Laboratory for
Information and Decision Systems
77 Massachusetts Ave.
Cambridge, MA 02139

LEHTOMAKI, Norman, Student
Massachusetts Institute of Technology
77 Massachusetts Ave.
Cambridge, Mass. 02139

LEVY, Bernard C., Research Scientist

Massachusetts Institute of Technology - Laboratory for
Information and Decision Systems
77 Massachusetts Ave.
Cambridge, Mass. 02139

MAYBECK, Peter, Assoc. Professor of E.E., AFIT
Air Force Institute of Technology (AFIT/ENG)
Wright Patterson AFB, Ohio 45432

MOORE, B.C., Assistant Professor
University of Toronto
Dept. of Electrical Engineering
Toronto, Ont. Canada M5S 1A4

NEFZGER, Charles L., Program Manager

AFOSR/NM

Billing AFB, Washington D.C. 20332

POSTLETHWAITE, Ian,
University Engineering Department
Control and Management Systems Division
Mill Lane
Cambridge, England CB2 1RX

REID, J. Gary, Assistant Professor
Air Force Institute of Technology (AFIT/ENG)
Wright-Patterson AFB , Ohio 45433

ROHRS, Charles E., Student

Massachusetts Institute of Technology
77 Massachusetts Ave.
Cambridge, Mass. 02139

ROUHANI, Ramine, Research Engineer Scientific Systems, Inc. 186 Ailewife-Brook Parkway Cambridge, Mass. 02138

SAFONOV, Mike, Assistant Professor of EE

Dept. of Electrical Eng.- Systems
University of Southern California
Los Angeles, CA 90007

SANDELL, Nils R., Associate Professor

Massachusetts Institute of Technology - Laboratory for

Information and Decision Systems

77 Massachusetts Ave.

Cambridge, Mass. 02139

SIVAN, Raphael, Professor
Technion - Israel Institute of Technology
Technion City, Haifa 32000

Massachusetts Institute of Technology
Rm 37-215
77 Massachusetts Ave.
Cambridge, Mass. 02139

STEIN, Gunter, Adjunct Professor
Honeywell, Inc. - Massachusetts Institute of Technology
Laboratory for Information and Decision Systems
77 Massachusetts Ave.
Cambridge, Mass. 02139

TAN, Han-Ngee, Graduate Student
Laboratory for Information and Decision Systems Massachusetts Institute of Technology
77 Massachusetts Ave.
Cambridge, Mass. 02139

TRIANTAFYLLON, Michael, Assistant Professor (Ocean Engineering)
Massachusetts Institute of Technology
77 Massachusetts Ave.
Cambridge, Mass. 02139

VINTER, R. B., Lecturer

Dept. of Computing and Control

Science and Technology

Imperial College

London, England

Von HUSEN, Robert, Engineer
Office of Naval Research
800 North Quincy Rd.
Arlington, VA 22217

WILLEMS, Jan C., Professor
University of Groningen
Math. Institute
P.O. Box 800
Groningen, The Netherlands

# Appendix C - Papers Presented

- 1. J.C. Doyle, "Robustness of Multiloop Linear Feedback Systems."
- 2. N.R. Sandell, Jr., "Robust Stability of Linear Dynamic Systems with Application to Singular Perturbation Theory."
- 3. M.G. Safonov and M. Athans, "A Multiloop Generalization of the Circle Stability Criterion."
- 4. M.G. Safonov, "Tight Bounds on the Response of Multivariable Systems with Component Uncertainties."
- 5. C.A. Desoer and Y.T. Wang, "Foundations of Feedback Theory for Nonlinear Dynamical Systems."
- 6. B.C. Moore, "On-Line Tuning of Multivariable DI Controllers Using Principle Component Analysis: Preliminary Results."
- 7. A.J. Laub, "Robust Stability of Linear Systems Some Computational Considerations."
- 8. I.M. Horowitz, "Quantitative Synthesis of Uncertain Multiple Input-Output Feedback System."
- I. Postlethwaite, "Methods for Assessing the Robustness Properties of a Linear Multivariable Feedback System."
- 10. I. Postlethwaite, "A Note on Parametric Stability."
- 11. J.E. Ackermann, "A Robust Control System Design."
- 12. P.K. Wong and M. Athans, "Closed-Loop Structural Stability for Linear Quadratic Optimal Systems."
- 13. M.G. Safonov and M. Athans, "Gain and Phase Margins of Multiloop LQG Regulators."
- 14. H. Kwaakernaak, "Optimal Low Sensitivity Linear Feedback Systems."
- 15. J.C. Doyle and G. Stein, "Robustness with Observers."
- 16. P. Molander and J.C. Willems, "Robustness Results for State Feedback Regulators."
- 17. C.A. Harvey, "On Feedback Systems Possessing Integrity with Respect to Actuator Outages."

#### Appendix C (Cont'd)

- 18. G. Stein and J.C. Doyle, "Singular Values and Feedback: Design Examples."
- 19. N.A. Lehtomaki, et.al., "Robust Control of Multiterminal DC/AC Systems."

#### ROBUSTNESS OF MULTILOOP LINEAR FEEDBACK SYSTEMS\*

J. C. Doyle

Consultant

Honeywell Systems and Research Center

Minneapolis, Minnesota

# ABSTRACT

This paper presents a new approach to the analysis of robustness or sensitivity of multiloop linear feedback systems. The properties of the return difference equation are examined using the concepts of singular values, singular vectors and the spectral norm of a matrix. A number of new tools for multiloop systems are developed which are analogous to those for scalar Nyquist and Bode analysis, providing a generalization of the scalar frequency-domain notions such as stability margins and M-circles.

<sup>\*</sup> This work was performed for Honeywell Systems and Research Center, Minneapolis, MN, with partial support from the Office of Naval Research contract N-00014-75-C-0144

Mailing Address: M.S. MN17-2367, Honeywell Systems & Research Center,

<sup>2600</sup> Ridgway Parkway, Minneapolis, MN. 55413

Telephone No: (612)378-4254

## I. INTRODUCTION

A critical property of feedback systems is their robustness; that is, their ability to maintain performance in the face of uncertainties. In particular, it is important that a closed-loop system remain stable despite differences between the model used for design and the actual plant. These differences result from variations in modelled parameters as well as plant elements which are either approximated, aggregated, or ignored in the design model. The robustness requirements of a linear feedback design are often specified in terms of desired gain and phase margins and bandwidth limitations associated with loops broken at the input to the plant actuators (1, 2). These specifications reflect in part the classical notion of designing controllers which are adequate for a set of plants constituting a frequency-domain envelope of transfer functions [3]. The bandwidth limitation provides insurance against the uncertainty which grows with frequency due to unmodeled or aggregated high frequency dynamics.

The Nyquist or Inverse Nyquist diagram (polar plots of the loop transfer function) provides a means of assessing stability and robustness at a glance. For multiloop systems, scalar Nyquist diagrams may be constructed for each loop individually providing some measure of robustness. Unfortunately, the method may ignore variations which simultaneously affect multiple loops.

There are a number of other possible ways to extend the classical frequency-domain techniques. One involves using compensation or feedback to decouple (or approximately decouple) a multiloop system into a set of scalar systems which may be treated with scalar techniques (i.e., "Diagonal Dominance", Rosenbock  $\begin{bmatrix} 4 \end{bmatrix}$ ). Another method uses the eigenvalues of the loop transfer matrix (G(s) in Figure 1) as a function of frequency (i.e., "Characteristic Loci", MacFarlane, et. al.  $\begin{bmatrix} 5 \end{bmatrix}$ ,  $\begin{bmatrix} 6 \end{bmatrix}$ ). While these methods provide legitimate tools for dealing with multivariable systems, they can lead to highly optimistic conclusions about the robustness of multiloop feedback designs. Examples in Section III will demonstrate this.

This paper develops an alternative view of multiloop feedback systems which exploits the concepts of singular values, singular vectors, and the spectral norm of a matrix. ( $\begin{bmatrix} 7 \end{bmatrix} - \begin{bmatrix} 10 \end{bmatrix}$ ). This approach leads to a reliable method for analyzing the robustness of multivariable systems.

Section II presents a basic theorem on robustness and sensitivity properties of linear multiloop feedback systems. Multivariable generalizations of the scalar Nyquist, Inverse Nyquist and Bode analysis methods are then developed from this same result.

Two simple examples are analyzed in Section III using the tools of Section II. As promised, the inadequacies of the existing approaches outlined earlier will be made clear.

Section IV contains a discussion of some of the implications of this work.

The goal of this paper is to focus on the analysis of robustness and sensitivity aspects of linear multiloop feedback systems. Some new approaches emerge which yield important insignts into their behavior. The mathematical aspects of these topics are fairly mundane at best, so rigor and generality are almost always sacrificed for simplicity.

# Preliminaries and Definitions

A brief discussion of singular values and vectors follows. Although the concepts apply more generally, only square matrices will be considered in this paper. A more thorough discussion of these topics may be found in  $\begin{bmatrix} 7 \end{bmatrix} - \begin{bmatrix} 10 \end{bmatrix}$ .

The singular values  $\sigma_i$  of a complex n x n matrix A are the non-negative square roots of the eigenvalues of A\*A where A\* is the conjugate transpose of A. Since A\*A is Hermitian, its eigenvalues are real. The (right) eigenvectors  $v_i$  of A\*A and  $r_i$  of AA\* are the right and left singular vectors, respectively, of A. These may be chosen such that

$$\sigma_{\mathbf{i}} r_{\mathbf{i}} = A v_{\mathbf{i}} , \qquad \mathbf{i} = 1, \dots n$$

$$\sigma_{1} \leq \sigma_{2} \leq \dots \leq \sigma_{n}$$

$$(1)$$

and the  $\{r_i\}$  and  $\{v_i\}$  form orthonormal sets of vectors.

It is well known that

$$A = R \Sigma V^*$$
 (2)

where R and V consist of the left and right singular vectors, respectively, and  $\Sigma$  = diag.  $(\sigma_1, \ldots, \sigma_n)$ . The decomposition in (2) is called the singular value decomposition.

Denote

$$\frac{\sigma}{|X|} (A) = \min_{|X|=1} |AX| = \sigma_1$$
 (3)

and

$$\bar{\sigma}(A) = \max_{||x||=1}^{\max} ||Ax|| = ||A||_2 = \sigma_n$$
 (4)

where  $||x|| = (x^*x)^{\frac{1}{2}}$  and  $||\cdot||_2$  is the spectral norm.

The singular values are important in that they characterize the effect that A has as a mapping on the magnitude of the vectors x. The singular values also give a measure of how "close" A is to being singular (in a parametric sense). In fact, the quantity

is known as the condition number with respect to inversion  $\begin{bmatrix} 9 \end{bmatrix}$ . The eigenvalues of A do not in general give such information. If  $\lambda$  is an eigenvalue of A, then

$$\sigma < |\lambda| < \overline{\sigma}$$

and it is possible for the smallest eigenvalue to be much larger than  $\underline{\sigma}$ .

## 11. BASIC RESULTS

Consider identity the feedback system in Fig. 2 where G(s) is the rational loop transfer matrix and L(s) is a perturbation matrix, nominally zero, which represents the deviation of G(s) from the true plant. While this deviation is unknown, there is usually some knowledge as to its size. A reasonable measure of robustness for a feedback system is the magnitude of the otherwise arbitrary perturbation which may be tolerated without instability. The following theorem characterizes robustness in this way. The "magnitude" of L(s) is taken to be the spectral norm. Only stable perturbations are considered since no feedback design may be made robust with respect to arbitrary unmodeled unstable poles.

Robustness theorem: Consider the perturbed system in Fig. 2 with the following assumptions

- i) G(s) and L(s) are nxn rational square matrices,
- ii) det (G(s)) # 0
- iii) L(s) is stable
- iv) the nominal closed loop system  $H = G(I+G)^{-1}$ is stable.

Under these assumptions the perturbed system is stable if

$$\underline{\sigma} (I + G(s)^{-1}) > \overline{\sigma} (L(s))$$
 (5)

for all s in the classical Nyquist D-contour (defined below)

Proof:

It is well known [4] that since G is invertible

$$\det(H(s)^{-1}) = \det(I + G(s)^{-1}) = \frac{\psi_1(s)}{\phi_1(s)}$$
 (6)

where  $\psi_1(s)$  is the nominal closed-loop characteristic polynomial and  $\phi_1(s)$  is the transmission zero polynomial of G [11] .

For the perturbed system

$$\det (I + G(s)^{-1} + L(s)) = \frac{\psi_2(s)}{\phi_1(s)\psi_3(s)}$$
 (7)

where  $\psi_2(s)$  is the perturbed closed-loop characteristic polynomial and  $\psi_3(s)$  is the characteristic polynomial of L(s).

Let D be a large contour in the s-plane consisting of the imaginary axis from -jR to +jR, together with a semicircle of radius R in the right half-plane. The radius R is chosen large enough so that all finite roots of  $\psi_2(s)$  have magnitude less than R.

Let the contour  $\Gamma_0$  be the image of D under the map  $\psi_1(s)$  det  $(I + G(s)^{-1})$ . Since H is stable, it follows from the principle of the argument that  $\Gamma_0$  will not encircle the origin.

Define the map

$$\gamma(q,s) = \phi_1(s) \det (I + G(s)^{-1} + qL(s)), q real$$
 (8)

and let  $\gamma(q,s)$  map D into the Contour  $\Gamma(q)$  for fixed q,  $0 \le q \le 1$ . The map  $\gamma(q,s)$  may be written as

$$\gamma(q,s) = \frac{\psi_1(s)\psi_3(s) + q\theta_1(s) + ... + q^n \theta_n(s)}{\psi_3(s)}$$

$$= \frac{\psi_4(q,s)}{\psi_3(s)} . \tag{9}$$

Clearly, since  $\Gamma(0) = \Gamma_0$ , it does not encircle the origin. Since the roots of  $\psi_4$  are algebraic functions of q, they are continuous in  $\sigma \left\{12\right\}$ . Thus the only way that the perturbed contour  $\Gamma(1)$  can encircle the origin is for

$$\det (I + G(s)^{-1} + qL(s)) = 0$$
 (10)

for some s in D and some q on the interval o $\leq$ q $\leq$ 1. (Recall that  $\psi_3$ (s) has no right half-plane roots). When (10) is satisfied then  $\underline{\sigma}$  (I + G<sup>-1</sup> + qL) must also be zero. However, as a consequence of (5)

$$\underline{\sigma} (I + G^{-1} + qL) \ge \underline{\sigma} (I + G^{-1}) - q \overline{\sigma}(L)$$

$$\ge \underline{\sigma} (I + G^{-1}) - \overline{\sigma}(L)$$

$$> 0 \qquad . \tag{11}$$

Thus  $\Gamma(q)$  does not encircle the origin for o<q<1. In particular, the perturbed contour  $\Gamma(1)$  does not encircle the origin, and the perturbed closed-loop system is stable.

Similar theorems hold for additive rather than multiplicative perturbations (with I + G substituted for I +  $\mathrm{G}^{-1}$ ) as well as a number of other configurations.

This theorem points out the importance of singular values. In particular, the smallest singular value  $\underline{\sigma}(I+G(j_\omega)^{-1})$  gives a reliable frequency-dependent measure of robustness. Stability is guaranteed for all perturbations whose spectral norm is less than  $\underline{\sigma}$ . As will be seen in the examples, eigenvalues do not give a similarly reliable measure.

The singular values also have useful graphical interpretations. Consider the dyadic expansion

$$H^{-1} = I + G^{-1} = \sum_{i=1}^{n} \sigma_{i} r_{i} v_{i}^{*}$$

$$\sigma_{1} \leq \sigma_{2} \leq \cdots \leq \sigma_{n}$$
(12)

where the  $\sigma_i$ ,  $r_i$  and  $v_i$  are the singular values, and left and right singular vectors, respectively of I +  $G^{-1}$ . This is an alternative form of the singular value decomposition in equation (2).

It has been shown [5] that the eigenvalues and eigenvectors of a rational matrix are continuous (through generally not rational) functions of frequency. Since singular values and vectors are just special cases,  $\sigma_{\mathbf{j}}(\mathbf{j}\omega)$ ,  $\mathbf{r_{j}}(\mathbf{j}\omega)$  and  $\mathbf{v_{j}}(\mathbf{j}\omega)$  are also continuous functions of  $\omega$ .

Since

$$H = (I + G^{-1})^{-1} = \Sigma \frac{1}{\sigma_i} v_i r_i^*$$
 (13)

the values  $1/\sigma_1(j\omega)$  and  $1/\sigma_n(j\omega)$  give the maximum and minimum possible magnitude responses to an input sinusoid at frequency  $\omega$ . Eigenvalues give no such information. In this sense, a plot of these singular values vs. frequency may be thought of as a multivariable generalization of the Bode gain plot. Plots of this type will be referred to as  $\sigma$ -plots.

Another useful graphical interpretation analogous to the scalar Inverse Nyquist diagram may be constructed by noting that

$$G^{-1} = \Sigma \sigma_{i} r_{i} v_{i}^{*} - I$$

$$= \Sigma \sigma_{i} r_{i} v_{i}^{*} - \Sigma v_{i} v_{i}^{*}$$

$$= \Sigma (\sigma_{i} r_{i} - v_{i}) v_{i}^{*}$$

$$= \Sigma \beta_{i} g_{i} v_{i}^{*}$$
(14)

where  $\beta_i g_i = \sigma_i r_i - v_i$  with  $\beta_i$  real and  $||g_i|| = 1$  for all i. (The  $g_i$ 's do not necessarily form an orthonormal set.)

The quantities in (14) at some frequency  $\omega_0$  are related as in diagram in Fig. 3a. Since  $v_i$  is of unit length a complex plane may be constructed as

in Fig. 3b, to lie in the plane formed by the triangle of  $v_i$ ,  $\sigma_i r_i$  and  $\beta_i g_i$ .

Define  $z_i$  to be the complex number at the point of the triangle as in Fig. 3c. Then, by rotating the complex plane with the triangle as a function of frequency, a  $z_i(j\omega)$  may be obtained which is a continuous function of  $\omega$  (Fig. 3d). This allows the important quantities in (13) and (14), that is, the  $\sigma_i$  and  $\beta_i$  to be represented in convenient graphical form. As noted in Fig. 3d, there is an ambiguity to  $z_i$  depending on which side the plane is viewed. (To be more precise, the  $z_i$  represent a multivalued function of s which could be defined on appropriate Riemann sheets. However, this will be ignored.) The  $z_i$  may be calculated by finding the roots of the quadratic equation

$$z_i^2 + (1 + \beta_i^2 - \sigma_i^2)z_i + \beta_i^2 = 0$$
 (15)

By plotting the  $z_i(j_\omega)$   $c_i = 1,...m$ ) for frequencies of interest a plot analogous to the scalar Inverse Nyquist plot is generated. While phase does not have the conventional meaning on these plots, the more important notion of distance from the critical point preserves its importance. These plots will be referred to as z-plots.

Concepts such as M-circles are also obvious in this context. The minimum value of M is given by

$$M_{m} = \max_{\omega} (1/\sigma_{1}(j_{\omega}))$$

Similar results may be for obtained additive perturbations by working with I+G rather than  $I+G^{-1}$ . In this case a diagram is generated which is analogous to the scalar Nyquist diagram. A number of other configurations may be handled as well.

Note that singular values offer no encirclement condition to test for right half-plane poles. Another test must be made for absolute stability but this presents no obstacle as many simple techniques exist for doing this. Once stability is determined the various approaches presented in this Section may be used to reliably analyze robustness.

the detroit of those breaking a feet a section of the appropriate and

margin in each loop (with the other closed). This is wery misleading,

#### III. EXAMPLES

Two simple examples are presented and analyzed using the approaches developed in the previous section. For the purpose of comparison, the methods of loop-breaking, direct eigenvalue analysis of G, and diagonalization by compensation are also used. The advantage of the interpretation of robustness given in this paper is clearly illustrated.

The first example is an oscillator with open loop poles at  $\pm 10j$  and both closed loop poles at  $\pm 1.$  There are no transmission zeros. The loop transfer function is

$$G(s) = \frac{1}{s^2 + 100}$$

$$(16)$$

$$-10(s+1)$$

$$S-100$$

By closing either loop (the system is symmetric) as in Figure 4, the transfer function for the other loop is

$$g(s) = \frac{1}{s}$$

which indicates ∞ db gain margin in both directions and 90° phase margin in each loop (with the other closed). This is very misleading, however.

The z-plot for this example is shown in Figure 5. It may appear somewhat peculiar, since it is not a plot of a rational function.

The important feature is the proximity of the plot to the critical point, indicating a lack of robustness.

The apparent discrepency between these two robustness indications can be easily understood by considering a diagonal perturbation

$$L =$$

$$0 k_2 (17)$$

where  $k_1$  and  $k_2$  are constants.

Then regions of stability and instability may be plotted in the  $(k_1,\ k_2)$  plane as has been done in Figure 6. The open loop point corresponds to  $k_1=k_2=-1$  and nominal closed loop point corresponds to  $k_1=k_2=0$ . Breaking each loop individually examines stability along the  $k_1$ ,  $k_2$  axes where robustness is good, but misses the close unstable regions caused by simultaneous changes in  $k_1$  and  $k_2$ . Thus, single loop analysis is not a reliable way of testing robustness.

The second example is a two dimensional feedback system with openloop poles at -1 and -2 and no transmission zeroes.

The loop transfer matrix is

$$G(s) = \frac{1}{(s+1)(s+2)} \begin{bmatrix} -47s + 2 & 56s \\ \\ -42s & 50s + 2 \end{bmatrix}$$
 (18)

Assume that identity feedback is used, with closed-loop poles at -2 and -4. This system may be diagonalized by introducing constant compensation. Let

the important feature is the proximity of the plot to the critical

$$U = \begin{bmatrix} 7 & 8 \\ 6 & 7 \end{bmatrix}$$
 (19)

and

$$V = V^{-1} = . (20)$$

Then letting

$$\hat{\mathbf{G}} = VGU = 0$$

$$0 \quad \frac{2}{s+2}$$

$$(21)$$

the system may be rearranged so that

$$H = G(I + G)^{-1}$$

$$= U\hat{G}V(I + U\hat{G}V)^{-1}$$

$$= U\hat{G}(I + \hat{G})^{-1}V$$

$$= U[\hat{G}(I + \hat{G})^{-1}]V.$$
(22)

This yields a diagonal system that may be analyzed by scalar methods. In particular under the assumption of identity feedback

 $\hat{G}$  represents the new loop transfer matrix. Because U and V represent a similarity transformation, the diagonal elements of  $\hat{G}$  are also the eigenvalues of G so that the decoupling or dominance approach and eigenvalue or characteristic loci approach would generate the same Nyquist or Inverse Nyquist plot shown in Figure 7. Only a single locus is shown since the contours of 1/(s+1) and 2/(s+2) are identical. The tempting conclusion that might be reached from these plots is that the feedback system is emminently robust with apparent margins of  $\pm \infty$  db in gain and  $90^{\circ}$ + in phase. The closed-loop pole locations would seem to support this.

This conclusion, however, would be wrong. The z-plot for  $I+G^{-1}$  is shown in Figure 8 and there is clearly a serious lack of robustness. The  $(k_1, k_2)$  - plane stability plot for this example is shown in Figure 9. Neither the diagonal dominance nor eigenvalue approaches indicate the close proximity of an unstable region. This failure can be attributed to two causes.

First, the eigenvalues of a matrix do not, in general, give a reliable measure of its distance (in a parametric sense) from singularity, and so computing the eigenvalues of G(s) (or I+G(s)) does not give an indication of robustness. Using eigenvalues rather than singular values will always detect unstable regions that lie along the  $k_1=k_2$  diagonal, but may miss regions such as the one in Figure 9.

Second, when compensation and/or feedback is used to achieve dominance, the "new plant" includes this compensation and feedback. Because of this, no reliable conclusions may be drawn from this "new plant" concerning the robustness of the final design with respect to variations in the actual plant. It is important to

evaluate robustness where there is uncertainty.

Another important property of multiloop feedback is that, unlike scalar feedback, pole locations alone are not reliable indicators of robustness. This was demonstrated in the last example and may be explained as follows. Consider a state feedback problem where the plant is controllable from each of two inputs. One input may be used to place the poles far into the right half plane and the other used to bring them back to the desired location. Such a high-gain control design of "opposing" loops will be extremely sensitive to parameter variations regardless of the nominal pole locations.

It is interesting to examine the  $\sigma$ -plot of  $H = G(I+G)^{-1}$  for the second example shown in Figure 10. Recall that the singular values of H are equal to the inverses of the singular values of  $I+G^{-1}$ . There is a rather large peak in the frequency response at approximately 3 radians. This could not occur in scalar unity feedback systems without there being a pole relatively near the imaginary axis. It can happen in multiloop systems because of the high gains possible without correspondingly large pole movement.

this "new plant" concerating the robustness of the final des

## IV. FURTHER COMMENTS AND CONCLUSIONS

The approach to the analysis of robustness presented here appears to yield useful insight into the properties of multiloop feedback systems which may provide the basis for a multivariable stability specification analogous to gain and phase margines for scalar systems. One possible difficulty with the approach is that it can lead to overly pessimistic views of robustness because it considers perturbations which may not be physically possible. This problem exists as well with gain and phase margin evaluations. Of course, some of this difficulty can be alleviated by examining the specific perturbations leading to instability. These may be easily computed from equation (12). On the other hand, it might be argued that some healthy pessimism would be refreshing in the field of multivariable linear control research.

Although for simplicity's sake only rational transfer functions were considered the results in this paper should extend to nonrational transfer functions. In practical application it should be possible to use frequency response data directly.

The results may also be extended to include nonlinear perturbations by exploiting the general stability theory developed by Safonov [13]. In this setting, nonlinearities may be loosely viewed as linear time-invariant elements with time-varying parameters. A mathematically more rigorous treatment of these issues may be found in Zames ([14], [15]), as well as in [13].

The results in this paper concerning dominance methods and use of characteristic loci of the loop transfer matrix are not meant to imply that design procedures employing these methods are useless. However, simply designing "in the frequency domain" is no guarantee that resulting controllers will have no undesirable properties.

Multivariable diagrams such as the • and z- plots appear to be amenable to implementation on a computer with graphic and plotting capability. Singular

values and vectors are particularly easy quantities to compute [16]. This should facilitate their active use in multiloop feedback design procedures. The question naturally arises concerning the implications of the singular value approach for robust synthesis. Certainly, this appears to be a promising area for research.

#### ACKNOWLEDGEMENTS

I would like to thank all those whose criticisms and comments helped to mold this paper. I would particularly like to thank Drs. G. Stein, M. G. Safonov, and C. A. Harvey for their continued technical input.

I would also like to thank the Math Lab Group, Laboratory for Computer Sciences, MIT for use of their invaluable tool, MACSYMA, a large symbolic manipulation language. The Math Lab Group is supported by NASA under grant NSG 1323 and DOE under contract #E(11-1)-3070.

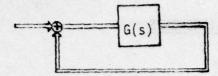


Fig. 1 Multiloop Feedback System

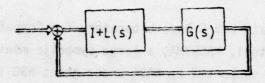


Fig. 2 Perturbed System

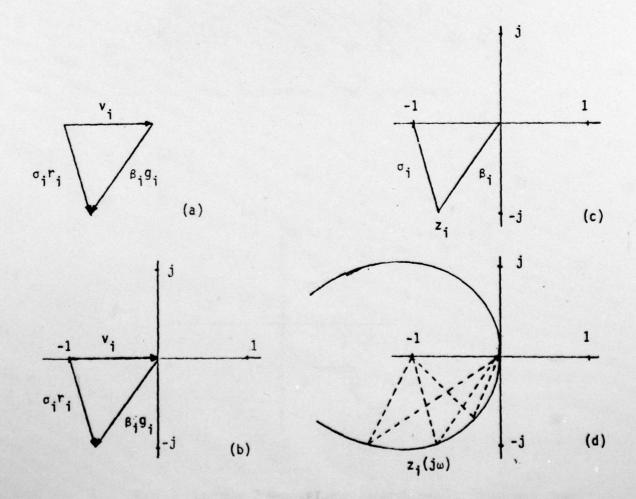


Fig. 3 Construction of z-plot

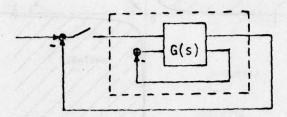


Fig. 4 Analysis by Loop-Breaking

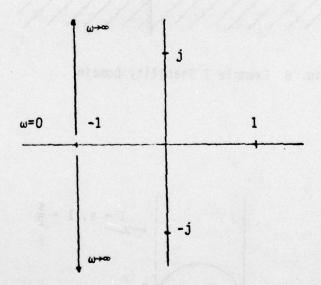


Fig. 5 Example 1 z-plot

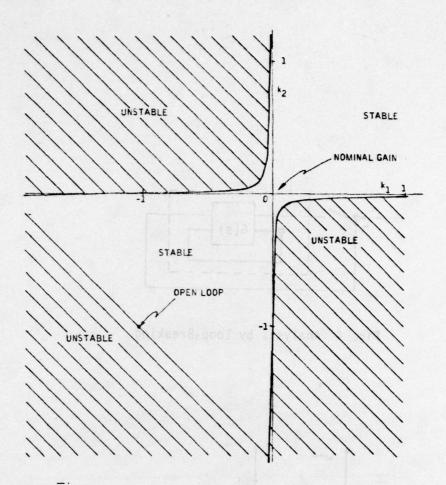


Fig. 6 Example 1 Stability Domain

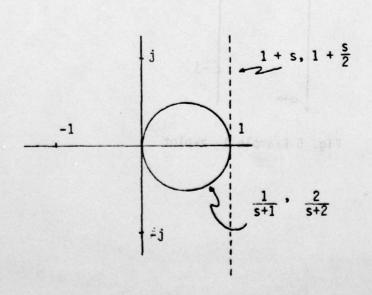


Fig. 7 Example 2 Nyquist and Inverse Nyquist Diagram

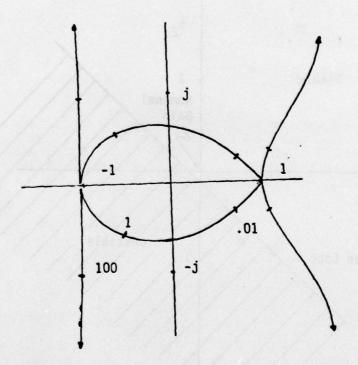


Fig. 8 Example 2 z-plot

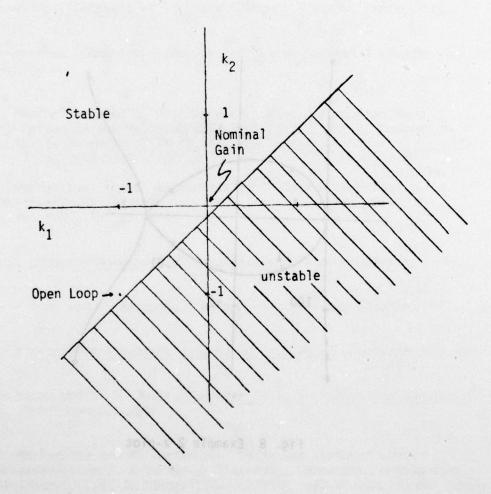
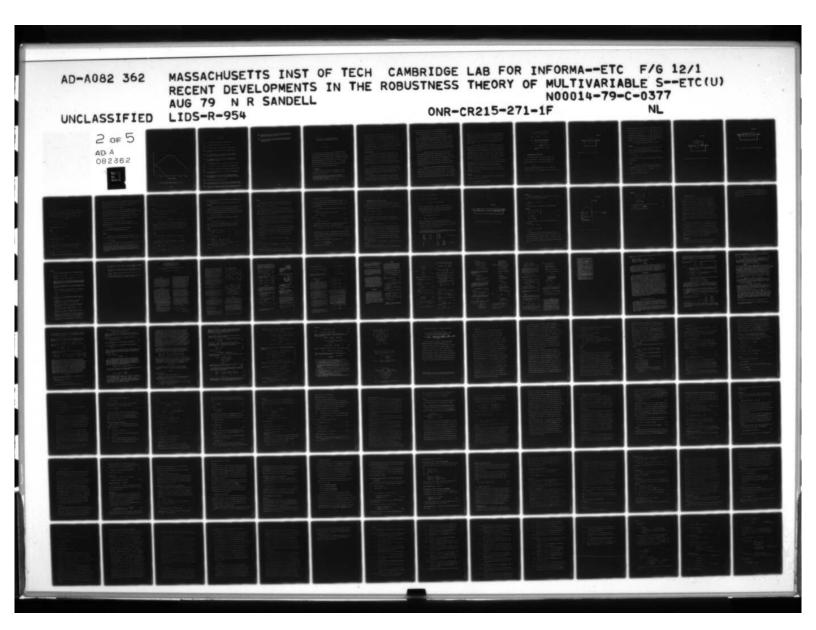
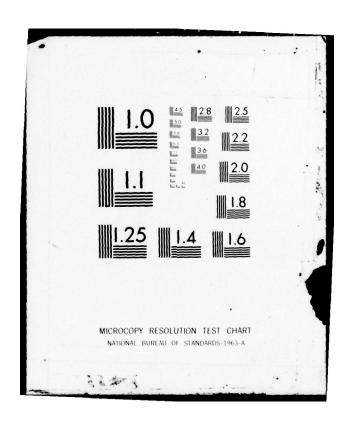


Fig. 9 Example 2 Stability Domain

#### REFERENCES

- 1 B. C. Kuo, Automatic Control Systems, Prentice-Hall, 1967.
- [2] J. W. Brewer, Control Systems, Prentice-Hall, 1974.
- [3] I. M. Horowitz, Synthesis of Feedback Systems, Academic Press, 1963.
- [4] H. H. Rosenbrock, <u>Computer-Aided Control System Design</u>, Academic Press, 1974.
- A. G. J. MacFarlane and I. Postlethwaite, "The Generalized Nyquist Stability Criterion and Multivariable Root Loci", Int. J. Control, Vol. 23, No. 1, January, 1977, pp. 81-128.
- [6] A. G. J. MacFarlane and B. Kouvaritakis, "A Design Technique for Linear Multivariable Feedback Systems", Int. J. Control, Vol. 23, No. 6, June, 1977, pp. 837-874.
- [7] G. Strang, Linear Algebra and It's Applications, Academic Press, 1976.
- [8] J. H. Wilkinson and C. Reinsch, Linear Algebra, Springer-Verlag, 1971.
- [9] J. H. Wilkinson, The Algebraic Eigenvalue Problem, Clarendon Press, 1965.
- [10] G. E. Forsythe and C. B. Moler, Computer Solutions of Linear Algebraic Systems, Prentice-Hall, 1967.
- A. G. J. MacFarlane and M. Karcanias, "Poles and Zeros of Linear Multivariable Systems: A Survey of Algebraic, Geometric, and Complex Variable Theory", Int. J. Control, July, 1976, Vol. 24, No. 1, pp. 33-74.
- [12] K. Knopp, Theory of Functions, Dover, 1947.
- M. G. Safonov, "Robustness and Stability Aspects of Stochastic Multivarible Feedback System Design", Ph.D. dissertation, Mass. Inst. Tech., Sept. 1977.
- G. Zames, "On the Input-Output Stability of Time-Varying Nonlinear Feedback Systems Part I", IEEE Trans. on Automatic Control, Vol. AC-11, No. 2,





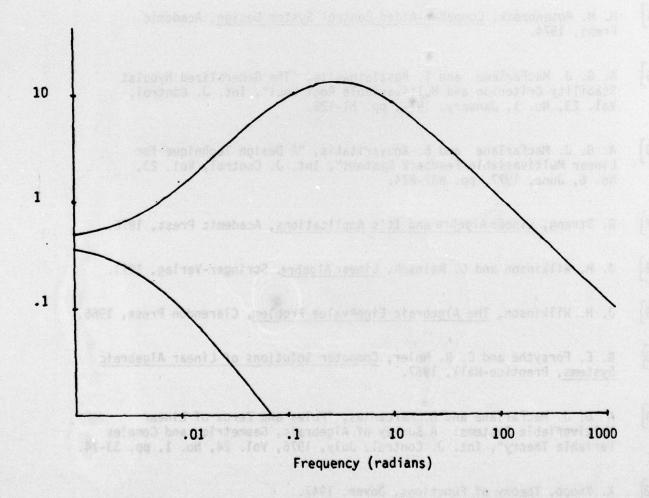


Fig. 10 Closed-Loop Frequency Response -  $1/\sigma(I + G^{-1})$ 

## REFERENCES

- B. C. Kuo, Automatic Control Systems, Prentice-Hall, 1967.
- [2] J. W. Brewer, Control Systems, Prentice-Hall, 1974.
- [3] I. M. Horowitz, Synthesis of Feedback Systems, Academic Press, 1963.
- [4] H. H. Rosenbrock, <u>Computer-Aided Control System Design</u>, Academic Press, 1974.
- A. G. J. MacFarlane and I. Postlethwaite, "The Generalized Nyquist Stability Criterion and Multivariable Root Loci", Int. J. Control, Vol. 23, No. 1, January, 1977, pp. 81-128.
- [6] A. G. J. MacFarlane and B. Kouvaritakis, "A Design Technique for Linear Multivariable Feedback Systems", Int. J. Control, Vol. 23, No. 6, June, 1977, pp. 837-874.
- [7] G. Strang, Linear Algebra and It's Applications, Academic Press, 1976.
- [8] J. H. Wilkinson and C. Reinsch, Linear Algebra, Springer-Verlag, 1971.
- [9] J. H. Wilkinson, The Algebraic Eigenvalue Problem, Clarendon Press, 1965.
- [10] G. E. Forsythe and C. B. Moler, <u>Computer Solutions of Linear Algebraic</u> Systems, Prentice-Hall, 1967.
- A. G. J. MacFarlane and M. Karcanias, "Poles and Zeros of Linear Multivariable Systems: A Survey of Algebraic, Geometric, and Complex Variable Theory", Int. J. Control, July, 1976, Vol. 24, No. 1, pp. 33-74.
- [12] K. Knopp, Theory of Functions, Dover, 1947.
- [13] M. G. Safonov, "Robustness and Stability Aspects of Stochastic Multivarible Feedback System Design", Ph.D. dissertation, Mass. Inst. Tech., Sept. 1977.
- G. Zames, "On the Input-Output Stability of Time-Varying Nonlinear Feedback Systems Part I", IEEE Trans. on Automatic Control, Vol. AC-11, No. 2,

- [15] G. Zames, "On the Input-Output Stability of Time-Varying Nonlinear Feedback Systems Part II", IEEE Trans. On Automatic Control, Vol. AC-11, No. 3, pp. 465-476, July, 1966.
- B. S. Garbo, et al, Matrix Eigensystems Routine EISPACK Guide Extension, Lecture Notes in Computer Science, Volume 51, Springer-Verlag, Berlin, 1977.

# ROBUST STABILITY OF LINEAR DYNAMIC SYSTEMS WITH APPLICATION TO SINGULAR PERTURBATION THEORY\*

by

Nils R. Sandell, Jr. \*\*

In this paper we will give a simple approach to determining conditions for stability of linear feedback systems subject to additive and multiplicative perturbations in the operators describing these systems. The approach is based on technic ies used in functional analysis, and provides an alternative development and generalization of some conditions for the time - invariant case that have appeared in the literature very recent. As an example of the application of the conditions, we consider the determination of finite regions of stability for singularly perturbed systems.

#### 1. Introduction

An important theme in system theory is the preservation of various system theoretic properties in the face of variations in the system model.

<sup>\*</sup> This research was supported by the Department of Energy under grant ERDA-E (49-18)-2087 and by ONR under contract N00014-76-C-0346. A preliminary version of the paper was presented at the IFAC Workshop on Singular Pertubations, June 1978.

<sup>\*\*</sup> Room 35-213, M.I.T., Cambridge, Massachusetts, 02139.

It is possible to distinguish two variations on this theme. In the first, attention is restricted to infinitesimal changes in the parameters of the nominal system model. Thus one begins by assuming that the nominal system has a certain property, and then asks if there exists an open set about the nominal system parameters such that all the systems with parameters in this set have the desired property. We will refer to investigations of this first type as sensitivity theory. A second approach requires the explicit delineation of finite regions of models about the nominal model for which the given property is preserved. We will refer to investigations of this second type as robustness theory.

Within the context of sensitivity or robustness theory, there are several properties that have been investigated. For example, it is well known that the controllability property is insensitive to small parameter variations [1,p. 43]. As another example, it is well known that type-1 servomechanisms have zero steady state step tracking error despite large (but not destabilizing) variations in their transfer function matrices [2].

In this paper we will focus on the robustness of the stability property of linear multivariable feedback systems. This subject is of special interest, since stability is the most basic system theoretic issue and since practical feedback systems must remain stable in the face of large parameter variations.

The importance of obtaining robustly stable feedback control systems has long been recognized by designers [3]. Indeed, a principal reason for using feedback rather than open-loop control is the presence of

model uncertainties. Any model is at best an approximation of reality, and the relatively low order, linear time-invariant models most often used for controller synthesis are bound to be rather crude approximations.

In classical frequency domain techniques for single-input, single-out-put (SISO) control system design, the robustness issue is naturally handled [3]. These techniques employ various graphical means (e.g., Bode, Nyquist, inverse-Nyquist, Nichols plots) of displaying the system model in terms of its frequency response. From these plots, one can determine by inspection the minimum charge in the model frequency response that leads to instability. These changes are often quantified by the gain and phase margins of the feedback system; sometimes the design is required to have certain minimal margins in order to be acceptable [4, p. 43].

In modern time domain techniques (such as the pole placement or linear-quadratic-Gaussian approaches) for multiple-input, multiple-output (MIMO) systems, the robustness issue is not directly dealt with. Instead, it is necessary to transform the resulting design to the frequency domain to examine its robustness properties. For SISO systems, this is accomplished as for classical designs, but the situation is less clear in the MIMO case, where it is necessary to consider simultaneous variations in the frequency responses of all the loops.

Very recently, there has been some important work addressing the multivariable robustness issue. In his thesis [5,6] Safonov gives a powerful approach, based on a multivariable sector stability theorem, that can characterize robustness for very general nonlinear MIMO feedback systems. In a recent paper [7], Doyle develops a robustness characterization for the linear time invariant MIMO case (It can be shown that Doyle's result can also be obtained by Safonov's

approach [8].) Doyle's characterization involves computing the minimum singular value of a certain transfer function matrix, and this computation essentially determines the minimum simultaneous variation of the system frequency responses that leads to instability. Since there is sophisticated and widely accessible software to compute singular values [9], this characterization is of great practical value.

The present paper is prompted by two observations. First, the use of singular values to characterize robustness is suggestive of connections with numerical analysis, but these connections are not clear from Doyle's approach utilizing the multivariable Nyquist theorem. Second, a specific instance of the robustness question arises when a system is approximated by making a singular perturbation to reduce its order. A related motivation, although only briefly discussed in this paper, arises from the desire to use multi-model techniques in the design of decentralized controllers for large scale systems [10,11].

The structure of this paper is as follows. In Section 2 we consider the robust stability of MIMO linear feedback systems using a generalized numerical-analytic approach. When specialized to the time invariant case, with rational transfer function matrix perturbations, Doyle's characterization results. In Section 3 we will apply the results of Section 2 to a specific robustness question arising in singular perturbation theory. Section 4 contains the summary and conclusions.

#### Notation

We will use the standard notation of input-output stability theory: see [12, pp. 13-14], or [13, pp. 38-39].

X = some Banach space of functions  $x:T \rightarrow X$ 

T = subset of the real numbers

X = finite dimensional vector space

$$X_e = \{x : P_T \times \epsilon X \text{ for all } \tau \epsilon T\}$$

$$(P_{\tau}x)(t) = \begin{cases} x(t) & t \leq \tau \\ 0 & t > \tau \end{cases}$$

 $\mathscr{Q}_2^{m}$  = space of m-vector functions on T with integrable Euclidean norm

$$I : X_e \rightarrow X_e = identity operator$$

$$G : X_e \rightarrow X_e$$
 is causal if  $P_T GP_T = P_T G$ 

A\* = conjugate transpose of a complex
matrix A.

#### Robust Stability of Linear Systems

We consider the feedback system depicted in Figure 1. Here the causal linear operator  $G:\mathscr{Q}_{2e}^{m}\to\mathscr{Q}_{2e}^{m}$  represents the plant plus any compensation that is used. The basic feedback equation is

$$(I + G)e = u (2.1)$$

and the basic stability question is whether  $(I+G)^{-1}:\mathscr{L}_{2e}^{m}\to\mathscr{L}_{2e}^{m}$  exists, is causal, and is a bounded linear operator when restricted to the

83702AW'065

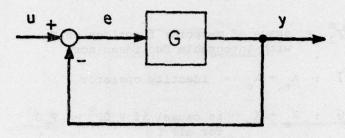


Figure 1. Basic MIMO Linear Feedback System

exists, in cassal, and it a bounded transf. Werehow when restricted Mg the

subspace  $\mathscr{Q}_2^m$  of  $\mathscr{Q}_{2e}^m$ . We will assume that the nominal system is stable in this sense throughout this section, i.e. for  $u \in \mathscr{Q}_{2e}^m$  there exists a unique causally related  $e \in \mathscr{Q}_{2e}^m$  satisfying (2.1), and that  $u \in \mathscr{Q}_2^m$  implies that the corresponding  $e \in \mathscr{Q}_2^m$  and consequently  $y = u - e \in \mathscr{Q}_2^m$ . We are interested in whether the closed loop system retains these properties when subject to additive (Figure 2) or multiplicative (Figure 3) perturbations representing uncertainty in the dynamical behavior of the system.

The following theorem provides the basis for our analysis.

# THEOREM 1

Let  $A: X_e \to X_e$  be a causal linear operator, and suppose  $A^{-1}$  exists, is causal, and is bounded when restricted to X. Then, if  $\Delta A: X_e \to X_e$  is a causal linear operator that is bounded when restricted to X, and if

$$||A^{-1}\Delta A||_{X}$$
 < 1, (2.2)

it follows that  $(A + \Delta A)^{-1} : X_e \to X_e$  exists, is causal and is bounded when restricted to X.

## Proof

The operator  $A^{-1}\Delta A$  is well defined, causal, and bounded on X by assumption. Since  $||A^{-1}\Delta A||_X < 1$ , the contraction mapping theorem implies that the sequence  $x_k$ , k = 0,1..., defined by

$$x_{k+1} = -A^{-1} \Delta A x_k + b; \quad x_0 \equiv 0$$
 (2.3)

converges to a unique solution xeX of

# 83702AV 066

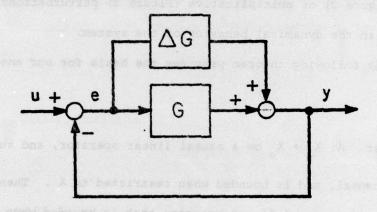


Figure 2. System Subject to Additive Perturbations

# 83702AV-067

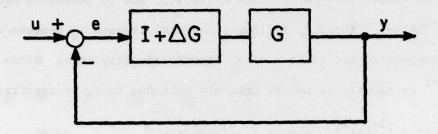


Figure 3. System Subject to Multiplicative Perturbations

$$(I + A^{-1}\Delta A)x = b (2.4)$$

for any b  $\epsilon$  X. Thus  $(I + A^{-1}\Delta A)^{-1}$ : X + X exists, and is therefore bounded since  $I + A^{-1}\Delta A$  is. Causality follows since each iterate  $\mathbf{x}_k$  depends causally on b and consequently the limit x of  $\mathbf{x}_k$  depends causally on b. Since  $(I + A^{-1}\Delta A)^{-1}$  is causal, it can be uniquely extended to  $X_e$  by requiring

$$P_{T}(I + A^{-1}\Delta A)^{-1}x = P_{T}(I + A^{-1}\Delta A)^{-1}P_{T}x$$
 (2.5)

for  $x \in X_e$ . Finally, defining

$$(A + \Delta A)^{-1} = (I + A^{-1} \Delta A)^{-1} A^{-1}, \qquad (2.6)$$

gives the required inverse of A + AA. Q.E.D.

# Remarks

1. Since

$$||A^{-1}\Delta A||_{X} \leq ||A^{-1}||_{X} ||\Delta A||_{X}$$
 (2.7)

a sufficient condition for (2.1) is

$$||A^{-1}||_{X} ||\Delta A||_{X} < 1.$$
 (2.8)

2. A basic result in numerical analysis is that if an nxm matrix A is invertible, then A +  $\Delta A$  is invertible for all  $\Delta A$  satisfying

$$\overline{\sigma}(\Delta A) < \underline{\sigma}(A)$$
 (2.9)

where 
$$\overline{\sigma}(\Delta A) = ||\Delta A||_2$$
,  $\underline{\sigma}(A) = (||A^{-1}||_2)^{-1}$ 

are respectively the smallest and largest singular values of the matrix A.

Theorem 1 is thus a generalization of this classical finite dimensional result where, of course, boundedness and causality are not at issue. In the finite dimensional case there exists  $\Delta A$  such that  $\overline{\sigma}(\Delta A) = \underline{\sigma}(A)$  and  $A + \Delta A$  is singular; this is easily proved by the singular value decomposition.

- 3. The contraction mapping argument in Theorem 1 is a standard technique of applied mathematics; the fact that  $X_{e}$  is not a Banach space complicates the argument. The causality argument has been used by Willems [12, p. 98] in a slightly different context. The linearity of the perturbation operator is not essential.
- 4. Theorem 1 can be used to give  $\mathscr{L}_p$  robust stability results, but we will confine ouselves to the case p=2 in the sequel.
- 5. Theorem 1 can be used to obtain robust stability results for both continuous and discrete time, but in the sequel we will confine our attention to the case  $T = [0,\infty]$ .

The robust stability questions posed at the beginning of this section are now answered in terms of Theorem 2.

# THEOREM 2

Assume that the basic feedback system of Figure 1 is stable. Then

(i) the system remains stable for additive pertubations G (Figure 2) provided

$$||(I+G)^{-1}\Delta G||_{\mathcal{Z}_{2}^{m}} < 1$$
 (2.10)

and (ii) the system remains stable for multiplicative perturbations  $\Delta G$  (Figure 3)

The singular value decomposition of an nxn nonsingular complex matrix A is  $A=U\Sigma V^*$ , where U and V are unitary nxn matrices,  $\Sigma=\mathrm{diag}\;(\sigma_1,\ldots,\sigma_n)$  and the singular values  $\sigma_i$  are the non-negative square roots of the eigenvalues of A\*A. See [14] for references, a more general definition, and an excellent discussion of the fundamental role of the singular value decomposition in linear systems theory.

provided

$$||[I - (I + G)^{-1}]\Delta G||_{\mathscr{L}_{2}^{m}} < 1$$
 (2.11)

Proof

For case (i), we apply Theorem 1 to the equation

$$(I + G + \Delta G)e = u \qquad (2.12)$$

while for case (ii) we consider

$$[I+G(I+\Delta G)]_e = (I+G+(I+G)\Delta G-\Delta G)_e = u.$$
 Q.E.D. (2.13)

The practical importance of Theorem 2 stems from the fact that the  $\mathscr{Q}_2^{\mathfrak{m}}$  norm of a linear convolution operator can be computed from its transfer function matrix. This fact, which is a consequence of Parseval's Theorem, is well known in the input-output stability theoretic literature; see, e.g., [13, p. 26].

# Lemma 1

Let the operator  $G: \mathscr{L}_2^{\mathbb{m}} \to \mathscr{L}_2^{\mathbb{m}}$  for  $T = [0,\infty]$  be defined by

$$(G_{\mathbf{x}})(t) = \int_{0}^{\infty} G(t-\tau) \mathbf{x}(\tau) d\tau \qquad (2.14)$$

where the elements of the impulse response matrix G(t) are assumed absolutely integrable on T. Then

$$||G||_{\mathscr{L}_{2}^{m}} = \sigma_{\max} \tag{2.15}$$

where

$$\sigma_{\text{max}} = \max_{\omega \ge 0} \max_{1 \le i \le m} \sigma_i(G(j\omega))$$
 (2.16)

and where  $\sigma_{\underline{i}}(G(j\omega))$  denotes the ith singular value of the transfer function matrix corresponding to G .

Combining Theorem 2 and Lemma 1, we obtain the following result. THEOREM 3

Assume that the nominal system in Figure 1 is time invariant, stable, and that the operators  $(I+G)^{-1}$ ,  $\Delta G$  can be represented as convolution operators with impulse response matrices with absolutely integrable elements. Then (i) the system remains stable for additive perturbations  $\Delta G$  satisfying

$$\overline{\sigma}(\Delta G(j\omega)) \le \underline{\sigma}(I+G(j\omega)), \quad \omega > 0$$
 (2.17)

and (ii) the system remains stable for multiplicative perturbations satisfying

$$\overline{\sigma}(\Delta G(j\omega)) < \underline{\sigma}(I+G^{-1}(j\omega)), \quad \omega > 0.$$
 (2.18)

Here  $G(j\omega)$  and  $\Delta G(j\omega)$  are the transfer functions of G and  $\Delta G$ , and  $\overline{G}(A)$  and  $\underline{G}(A)$  denote the maximum and minimum singular values of A.

## Proof

(i) From Lemma 1 and (2.17) we have

$$|\Delta G|$$
 <  $||(I+G)^{-1}||^{-1}$  (2.19)

so that

$$||(I+G)^{-1}|||\Delta G|| < 1.$$
 (2.20)

(ii) Note that

$$\underline{\sigma}(I+G^{-1}(j\omega)) = \left\{\overline{\sigma}\{(I+G^{-1}(j\omega))^{-1}\}\right\}^{-1}$$

$$= \left\{\overline{\sigma}\{(I+G(j\omega))^{-1} | G(j\omega)\}\right\}^{-1} = \overline{\sigma}\{I-(I+G(j\omega))^{-1}\} \quad (2.21)$$

Therefore Lemma 1 and (2.18) imply that

$$||I - (I+G)^{-1}|| ||\Delta G|| < 1.$$
 (2.22)

Q.E.D.

# Remarks

- Notice the analogy between Theorem 3 concerning robust stability of linear systems and the classical result quoted previously concerning robust inversion of matrices (or bounded operators).
- 2. Theorem 3 for the case of rational transfer function matrices is the result of Doyle alluded to previously. Doyle's proof is completely different, however, depending on the multivariable Nyquist Theorem, so that the connections with the inversion issue are only implicit.
- 3. The quantity  $\underline{\sigma}(I+G(j\omega))$  or  $\underline{\sigma}(I+G^{-1}(j\omega))$  is easily computed and plotted as a function of  $\omega$ . Doyle has made great use of this technique in the analysis of multivariable feedback systems. Such a plot plays much the same role for determining MIMO robustness properties as the more classical Bode, etc. plots in SISO design.
- 4. The quantity  $\underline{\sigma}^{-1}$  (I+G(j $\omega$ )) is the generalization of the classical Bode SISO sensitivity function of changes in the closed-loop transfer function with respect to changes in the open-loop transfer function in the following sense. Let  $y_1$  denote the output of the system of Figure 1 for a given input and  $y_2$  the corresponding output of the system of Figure 2 for the same input. Then one can show

$$y_1(j\omega) - y_2(j\omega) = (I+G(j\omega)^{-1}\Delta G(j\omega)(G(j\omega) + \Delta G(j\omega))^{-1}y_2(j\omega)$$
(2.23)

so that

$$||y_{1}(j\omega) - y_{2}(j\omega)|| \leq \frac{1}{\underline{\sigma}(I+G(j\omega))} ||\Delta G(j\omega)(I+G(j\omega) + \Delta G(j\omega))^{-1}||x$$

$$||y_{2}(j\omega)||. \qquad (2.24)$$

Consequently, the percentage change in the closed-loop transfer function matrix is attenuated from the percentage change in the open loop transfer

function matrix by the factor  $\underline{\sigma}^{-1}(I + G(j\omega))$ 

- 5. On the other hand, the perturbations defining the SISO gain and phase margins are multiplicative rather than additive, so that  $\underline{\sigma}(I + G^{-1}(j\omega))$  is more appropriate as a measure of the tolerance of the feedback system to model uncertainty.
- 6. It is in general impossible to express  $\underline{\sigma}(I + G^{-1}(j\omega))$  in terms of  $\sigma(I + G(j\omega))$ .
  - 7. Consider the feedback system in Figure 1 with

$$G(s) = -G(sI - A)^{-1}B$$
 (2.25)

where

$$G = B'K \tag{2.26}$$

$$O = A'K + KA + C'C - KBB'K$$
 (2.27)

(We assume [A,B] controllable and [A,C] observable so that a unique positive definite solution of (2.27) exists.) The well known equality [15]

$$[I + G(-sI - A)^{-1}B]' [I + G(sI - A)^{-1}B] = I + [C(-sI-A)^{-1}B]' [C(sI - A)^{-1}B],$$
(2.28)

which follows from (2.27) after a little manipulation, shows that the system is robust to additive pertubations. Safonov and Athans [6] have shown that the system of Figure 3 with G(s) defined by (2.25) is stable for  $\Delta G(j\omega)$  satisfying

$$\overline{\sigma}(\Delta G(j\omega)) \leq 1/2 \text{ for all } \omega \geq 0;$$

this can also be inferred directly using the inequality [19]

$$\underline{\sigma}(I + G^{-1}(j\omega)) \ge \frac{\underline{\sigma}(I + G(j\omega))}{1 + \underline{\sigma}(I + G(j\omega))}$$
 (2.29)

together with (2.28) and Theorem 3.

# 3. Application to Singular Perturbation Theory

In the previous section we have discussed the robustness of the stability property of a linear dynamic system to model variations. In this section we will consider a particular form of model variation due to a singular perturbation.

We consider systems of the form

$$\dot{x}_{1}(t) = A_{11}x_{1}(t) + A_{12}x_{2}(t)$$

$$\dot{\varepsilon}x_{2}(t) = A_{21}x_{1}(t) + A_{22}x_{2}(t)$$
(3.1)

where  $\epsilon>0$  is a small parameter, and it is assume that the matrix  $A_{22}$  is stable (has eigenvalues with negative real parts). We define the so called degenerate system

$$\dot{x}_{1d}(t) = (A_{11} - A_{12}A_{22}^{-1} A_{21})x_{1d}(t)$$
 (3.2)

associated with (3.1). This system is a reduced order system that neglects certain high-frequency or parasitic effects incorporated in the model (3.1). It has been shown that the stability of (3.2) (in the sense that the eigenvalues of the system matrix have negative real parts) is insensitive to these effects in the sense that there exists  $\varepsilon > 0$  such that (3.1) is stable for all  $0 < \varepsilon < \varepsilon_0$  if (3.2) is [17]. We propose to examine the robustness of the stability (in the input-output sense of Section 2) of (3.2) to the parasitic effects present in (3.1).

We begin by Laplace - transforming equations (3.1) (assuming zero initial condition).

See [16] for an excellent survey of results in singular perturbation theory.

$$x_1(s) = (sI - A_{11})^{-1} A_{12} x_2(s)$$
 (3.3)

$$x_2(s) = (\epsilon sI - A_{22})^{-1} A_{21} x_1(s)$$

= 
$$[I - \epsilon s (\epsilon s I - A_{22})^{-1}] (-A_{22}^{-1} A_{21}) x_1(s)$$
 (3.4)

To apply the input-output stability results of the previous section it is necessary to apply a test input to the system. This is most conveniently done as illustrated in Figure 4, although other locations are possible.

Figure 4 closely resembles Figure 3 with

$$G(s) = A_{22}^{-1} A_{21} (sI - A_{11})^{-1} A_{12}$$
 (3.5)

$$\Delta G(s,\epsilon) = -\epsilon s (\epsilon s I - A_{22})^{-1}$$
 (3.6)

except that the perturbation is post-multiplicative rather than premultiplicative. However, assuming G(s) has full rank as a rational matrix, it is easily verified that the analysis of the preceding section is essentially unaffected. Thus we have the following result.

$$\left\{ \begin{bmatrix} A_{11} & A_{12} \\ A_{21} & A_{22} \\ \overline{\epsilon} & \overline{\epsilon} \end{bmatrix} , \begin{bmatrix} A_{12} \\ 0 \end{bmatrix} \right\} controllable,$$

$$\left\{ \begin{bmatrix} 0 & I \end{bmatrix} , \begin{bmatrix} A_{11} & A_{12} \\ A_{21} & A_{22} \\ \overline{\epsilon} & \overline{\epsilon} \end{bmatrix} \right\} observable.$$

To insure the equivalence of the input-output stability analysis with the condition that the system matrix of (3.1) has eigenvalues with negative real parts, it is necessary to have the conditions

# 83702AW068

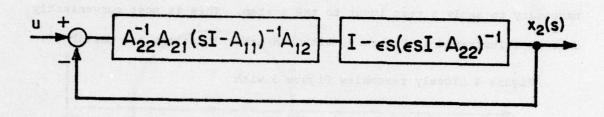


Figure 4. Singular Perturbation in the Frequency Domain.

# THEOREM 4

Assume that the system of Figure 4 is stable for  $\varepsilon$  = 0. Then it remains stable for all  $\varepsilon$  > 0 satisfying the inequality

$$\overline{\sigma}(\Delta G(j\omega, \varepsilon)) \leq \underline{\sigma}(I + G^{-1}(j\omega))$$
 (3.7)

for all  $\omega > 0$ .

The use of Theorem 4 is illustrated by the following examples.

# Example 1

$$G(s) = \frac{2}{s-1}$$
 (3.9)

$$\Delta G(s, \varepsilon) = \frac{\varepsilon s}{\varepsilon s + 1}$$
 (3.10)

In this case for which G and  $\Delta G$  are scalars, the condition (3.7) is equivalent to

$$\left|1+G^{-1}(j\omega)\right| > \left|G(j\omega,\varepsilon)\right| \tag{3.11}$$

or

$$|1 + G(j\omega)| > |G(j\omega)\Delta G(j\omega, \varepsilon)|$$
 (3.12)

for all  $\omega > 0$ .

The condition (3.12) has an interesting graphical interpretation. Specifically the Nyquist locus of  $G(j\omega)$  must avoid the critical point -1 by at least the distance  $|G(j\omega)\Delta G(j\omega)|$  (Figure 5). It is easily verified that for  $\varepsilon$  =+1 and  $\omega$  =  $\sqrt{2}$ , we have  $|1+G(j\omega)|=|G(j\omega)\Delta G(j\omega)|$  so that  $\varepsilon_0$  = 1. It can be directly verified that the system (3.8) becomes unstable for  $\varepsilon$  = 1.

83702AV 069

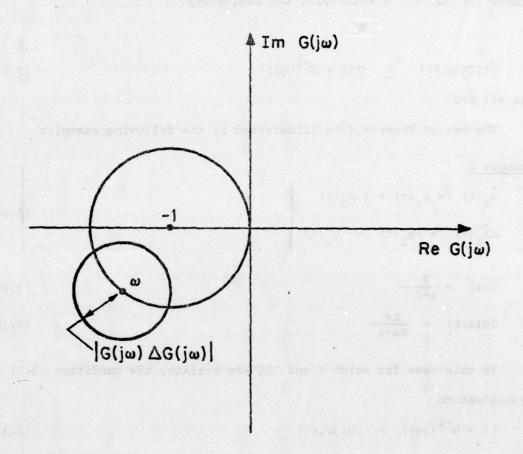


Figure 5. Illustrating the Condition (3.12).

Example 2

$$G(s) = \frac{1}{s+1}$$
 (3.14)

$$\Delta G(s,\varepsilon) = \frac{\varepsilon s}{1+\varepsilon s} \tag{3.15}$$

As in the previous example, we will check (3.12). We have

$$\sqrt{2+\omega^2} \ge 2 > 1 \ge \frac{\varepsilon\omega}{\sqrt{1+\varepsilon^2\omega^2}} \tag{3.16}$$

so that the system is stable for all  $\epsilon \geq 0$ :

# 4. Summary and Conclusions

In this paper we have considered the robustness of the stability property of a linear feedback system to variations in the system model. The approach was to generalize a fundamental result in numerical linear algebra concerning robust inversion of matrices to linear operators of the type arising in input-output stability theory. In the time-invariant case, this approach specializes to give sufficient conditions for stability under additive and multiplicative perturbations that are easily verified by computing the singular values of certain transfer function matrices. We then applied the robustness condition to the analysis of singularly perturbed systems. We were able to give an explicit, readily computable bound on the magnitude of the perturbation parameter  $\varepsilon$  that can be tolerated and still have a stability analysis of the reduced system valid for the full system.

The results of this paper are felt to be of interest for two reasons.

First, as Doyle has previously pointed out in the time invariant case [7],
the characterization and design of robustly stable MIMO feedback systems
is a fundamental problem in control theory that has yet to be completely
resolved. Second, as has been previously emphasized by Zames [18] and Safonov
[5], a fundamental problem in large scale system theory is to give conditions
for the success of designs based on multiple, aggregate models of a single
large system - this is essentially a robustness problem.

## Acknowledgement

M. Athans, J.C. Doyle, A. J. Laub, P. Kokotovic and M. Safonov.

Part of the work for this paper was accomplished during a visit to the Centro di Studio dei Sistemi di Controllo e Calcolo Automatica of the University of Rome; the author gratefully acknowledges the hospitality of Prof. F. Nicolò.

makers with the state and the state average that trans. On and the tale. (1819).

# References

- W.M. Wonham: <u>Linear Multivariable Control</u>: A <u>Geometric Approach</u>. Springer-Verlag, New York (1974).
- N.R. Sandell, Jr. and M. Athans: On multivariable type-L systems, Automatica 9, pp. 131-136 (1973).
- 3. I.M. Horowitz: Synthesis of Feedback Systems, Academic Press, New York (1963).
- 4. BACKGROUND INFORMATION AND USER GUIDE FOR MIL-F-9490D, Flight Control Systems Design, Installation and Test of Piloted Aircraft, General Specification for, Air Force Flight Dynamics Laboratory, Technical Report AFFDL-TR-74-116, January 1975.
- 5. M.G. Safonov: Robustness and Stability Aspects of Stochastic Multivariable Feedback System Design, Ph.D. Thesis, Massachusetts Institute of Technology (1977).
- M. Safonov and M. Athans: Gain and phase margins for multiloop LQG regulators. IEEE Trans. on Aut. Control AC-22, pp. 173-179 (1977).
- J.C. Doyle: Robustness of multiloop linear feedback systems.
   To appear.
- 8. M.G. Safonov, personal communication.
- 9. B.S. Garbow et.al.: Matrix Eigensystem Routines EISPACK Guide Extension. Lecture Notes in Computer Science, Vol. 51, Springer-Verlag, New York (1977).
- 10. N.R. Sandell, Jr., P. Variaya, M. Athans, and M.G. Safonov: Survey of decentralized control methods for large scale systems. IEEE Trans. on Aut. Control AC-23, pp. 108-128 (1978).
- 11. H.K. Khalil and P.V. Kokotovic: Control strategies for decision makers using different models of the same system. IEEE Trans. on Aut. Control, AC-23, pp. 289-298, (1978).
- 12. J.C. Willems, The Analysis of Feedback Systems. M.I.T. Press, Cambridge, Mass. (1971).
- 13. C.A. Desoer and M. Vidyasagar: Feedback Systems: Input-Output Properties. Academic Press, N.Y., (1975).
- 14. A.J. Laub: Linear multivariable control.Numerical considerations.
  Invited paper, American Mathematical Society Short Course on
  Control Theory, Providence, R.I., (1978). Also ESL-P-833 Electronic
  Systems Laboratory, Massachusetts Institute of Technology.
- 15. R.E. Kalman: When is a Linear System Optimal? Trans. ASME Ser.D: J. Basic Eng., Vol. 86, pp. 51-60 (1964).

- 16. P.V. Kokotovic, R.E. O'Malley, Jr., and P. Sannuti: Singular perturbations and order reduction in control theory an overview. <u>Automatic</u> 12, 123-132 (1976).
- 17. C.A. Desoer and M.J. Shensa: Networks with very small and very large parasitics: natural frequencies and stability. <a href="Proc. IEEE">Proc. IEEE</a>, 12, 1933-1938, Dec. 1970.
- 18. G. Zames: On feedback hierarchies and complexity (or information) 1976 CDC, Clearwater, Florida, (1976).
- 19. D. W. Nuzman and N.R. Sandell, Jr., "An Inequality Arising in Robustness Analysis of Multivariable Systems", submitted for publication.

#### at the I wellth Annual Astrollias Comes ----

## Circuits, Systems, and Computers, Pacific Grove,

California, November 6-8, 1978

## A MULTILOOP GENERALIZATION OF THE CIRCLE STABILITY CRITERION \*

Michael G. Safonov\* and Michael Athans \*\*

## Abstract

A frequency-domain stability criterion is presented, generalizing the well-known circle stability criterion to multiloop feedback systems having bounded nonlinearity, parameter variations, and/or frequency-dependent ignorance of component dynamics. Unlike previous generalizations, the theory is not restricted to weakly-coupled, diagonally dominant or nearly normal systems. Potential applications include the analysis of feedback system integrity and multiloop feedback system stability margins.

## 1. Introduction

A key step in the synthesis of robustly stable feedback systems is the characterization of a set of feedback laws that are stabilizing for every element of the set of possible plant dynamics. This type of information is precisely what is provided for single-loop feedback systems by such input-output stability criteria as the Nyquist, Popov, and circle theorems. Indeed, the practical merit of classical feedback design procedures involving Nyquist loci, Bode plots, and Nichols charts is in a large measure directly attributable to the fact that these design procedures provide the designer with an easily interpretable charcterization of such sets of robustly stable feedback laws. Available multivariable input-output stability criteria such as Rosenbrock's multivariable Nyquist theorem [1]

- Research supported in part by NASA/Ames grant NGL-22-009-124, by NASA/Langley grant NSG-1312, by Joint Services Electronics Program contract F44620-76C-006l monitored by AFOSR, and by NSF grant ENG78-05628.
- M. G. Safonov is with the Department of Electrical Engineering, University of Southern California, Los Angeles, CA 90007.
- M. Athans is with the Electronic Systems
  Laboratory, Massachusetts Institute of
  Technology, Cambridge, MA 02139.

and Zames' conic-relation and positivity stability theorems [2] have led to useful characterizations of sets of robustly stable feedback laws for only a limited class of problems, viz. interconnections of dissipative systems [3], weakly coupled interconnections of systems [4] (including socalled "diagonally dominant" systems [5] - [7]) and "nearly normal" systems [8] (which can be viewed as vector-space isomorphisms of weakly coupled systems). It has been argued convincingly by Rosenbrock and Cook [9] that an especially useful feedback design tool would be a more general multiloop frequency-domain stability criterion that includes diagonal dominance and normality results as special cases.

The main result of the present paper is a stability result that may serve this purpose: Theorem I is a multiloop generalization of the circle stability criterion which does not require diagonal-dominance, weak-coupling, normality, or near normality. The result allows the frequency-domain testing of the stability of multiloop feedback systems with time-varying nonlinearities, unknown-but-bounded parameter variations, and even singular perturbations.

The following notation is used:  $A^T$  and  $x^T$  denote respectively the transpose of the matrix A and the vector x; A and x denote the complex conjugate of the matrix  $A^T$  and the vector  $x^T$  respectively; the determinant of a matrix A is denoted  $\det(A)$ ; the Euclidian norm of a vector x is  $\|x\| = \sqrt{x} \|x\|$ ;  $\|x\|$  denotes nonnegative real numbers; the functional norm  $\|x\|_{T}$  and inner product  $\|x\|_{T} > 1$  are defined for functions  $\|x\|_{T} > 1$  as

where for any 
$$x_1$$
 and  $x_2$ 

$$< x_1, x_2 >_+ \stackrel{\searrow}{=} \int_0^- x_1^T (t) x_2 (t) dt.$$
The space  $L_{2e}(R_+, R^n)$  is defined as
$$L_{2e}(R_+, R^n) = \begin{cases} x: R_+ \rightarrow R^n |_{\mathbb{R}^N} x_1 < \infty \\ \text{for each } \exists R_+ \end{cases}.$$

Given any matrix A, the square-roots of the eigenvalues of A' A are called the singular values of A [10. pp. 5-11]. For any non-zero Matrix A, we use the notation  $\sigma_{\max}(A)$  to denote the largest singular value of A and  $\sigma_{\min}(A)$  to denote the smallest singular value of A; singular values are always nonnegative real numbers since  $A^n$  A is always positive semidefinite. For hermitian A (i. e., A = A \*), the notation  $\lambda_{\max}(A)$  and  $\lambda_{\min}(A)$  to denote respectively the greatest and least eigenvalues of A hermitian matrices have only real eigenvalues, so ordering of eigenvalues is always possible via the usual ordering of real numbers.

An operator is a mapping of functions into functions; for example, a dynamical system mapping inputs  $x \in L_{2e}(R_+, R^n)$  into outputs  $y \in L_{2e}(R_+, R^m)$  defines an operator. All operators considered in this paper are implicitly assumed to be mappings of  $L_{2e}(R_+, R^{nl})$  into  $L_{2e}(R_+, R^{nl})$  for some positive integers  $n_1$  and  $n_2$ , an operator H is said to be nonanticipative if

$$(H x_1)(t_0) = (H x_2)(t_0)$$

for any  $t_0$  and any pair of functions  $x_1$  and  $x_2$  having the property that for all  $t \le t_0$ .

$$x_1(t) = x_2(t);$$

i. e., a non anticipative operator  $\mbox{$\mathcal{H}$}$  is one having the property that its instantaneous output  $\mbox{$\mathcal{H}$} x$  at any time to is independent of the values assumed by the input x(t) at future times to the values assumed by the input x(t) at future times to the values assumed by the input x(t) at future times to the values assumed by the input x(t) at future times to the values assumed by the input x(t) at future times to the values assumed by the input x(t) at future times to the values assumed by the values as th

# II. Problem Formulation

Our results concern the input-output stability of systems consisting of a dynamical LTI negative-feedback interconnection of m memoryless time-varying nonlinear components and n dynamical LTI components. The system's equations thus take the following form (see Fig. 1):

Memoryless nonlinear components

$$y_1(t) = h_1(x_1(t), t)$$
  
 $y_m(t) = h_m(x_m(t), t)$  (2.1)

Dynamical LTI components

$$Y_{m+1}(s) = H_{m-1}(s) X_{m+n}(s)$$
  
 $Y_{m+1}(s) = H_{m-1}(s) X_{m+n}(s)$  (2.2)

Y (s) = H (s) X (s)

1 A form of global input-output stability, our definition of L<sub>2e</sub> - stable is equivalent to

L stable '[11] and to finite gain stable'

(with respect to the L<sub>2</sub> norm) [12] when H
is a nonanticipative operator.

# Dynamical LTI interconnection

$$\underline{X}(s) = -\underline{G}(s) \left( \underline{Y}(s) + \underline{Y}(s) \right) + \underline{U}(s) \qquad (2.3)$$

$$\underline{Y}(s) \stackrel{\triangle}{=} \begin{bmatrix} Y_1(s) \\ \vdots \\ Y_{n+m}(s) \end{bmatrix} : \underline{X}(s) \stackrel{\triangle}{=} \begin{bmatrix} X_1(s) \\ \vdots \\ X_{n+m}(s) \end{bmatrix} : \underline{U}(s) \stackrel{\triangle}{=} \begin{bmatrix} U_1(s) \\ \vdots \\ U_{n+m}(s) \end{bmatrix}$$

$$\underline{V}(s) \stackrel{\triangle}{=} \begin{bmatrix} V_1(s) \\ \vdots \\ V_{n+m}(s) \end{bmatrix} = \begin{bmatrix} G_{1,1}(s) \cdots G_{1,(n+m)}(s) \\ \vdots \\ G_{(n+m),1}(s) \cdots G_{(n+m),(n+m)}(s) \end{bmatrix}$$

$$\underline{G}(s) \stackrel{\triangle}{=} \begin{bmatrix} G_{1,1}(s) \cdots G_{n+m}(s) \\ \vdots \\ G_{n+m}(s) \end{bmatrix}$$

$$\underline{G}(s) \stackrel{\triangle}{=} \begin{bmatrix} G_{1,1}(s) \cdots G_{n+m}(s) \\ \vdots \\ G_{n+m}(s) \end{bmatrix}$$

$$\underline{G}(s) \stackrel{\triangle}{=} \begin{bmatrix} G_{1,1}(s) \cdots G_{n+m}(s) \\ \vdots \\ G_{n+m}(s) \end{bmatrix}$$

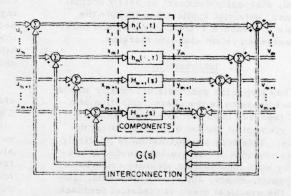


Fig. 1 The System

The indogenous variables  $y_i(t)$  and  $x_i(t)$  are the system 'outputs' and the exogenous variables  $u_i(t)$  and  $v_i(t)$  are the system 'inputs'. Each of the 'components'  $(h_1(\cdot), \ldots, h_m, H_{m+1}, \ldots, H_{m+n})$  may itself be a MIMO system in general, though our results seem to be most easily used and interpreted when the components are SISO.

Our stability results do <u>not</u> require that we have available an exact mathematical description of the components. For each of the nonlinear nondynamical elements, we assume only that matrices  $C_i$ ,  $R_i$ , and  $S_i$  can be found such that  $R_i$ ,  $R_i$  and  $S_i^TS_i$  are positive definite and such that  $S_i$   $\begin{pmatrix} h_i(x_i(t), t) - C_ix_i(t) \end{pmatrix}_i \leq |R_ix_i(t)|_i - \epsilon |k_i(t)|_i$  for some  $\epsilon > 0$ , all  $x_i(t)$ , and all t

for some 
$$\epsilon > 0$$
, all  $x_i(t)$ , and all  $t$ 

$$(i = 1, ..., m).$$

For each of the n dynamical LTI components  $H_i(s)$  ( $i = m+1, \ldots, m-n$ ) we assume only

that  $H_i(s)$  has a proper rational transfer function matrix and that proper rational transfer function matrices  $C_i(s)$ ,  $R_i(s)$ , and  $S_i(s)$  can be found such that  $R_i(-jw)$   $R_i(jw)$  and  $S_i^T(jw)$   $S_i(jw)$  are positive definite and have no poles on the s=jw axis and such that  $H_i(s)-C_i(s)$  has no poles in  $\{s \mid Re(s) \ge 0\}$ 

$$\left\| S_{i}(jw) \left( H_{i}(jw) X_{i}(jw) - C_{i}(jw) X_{i}(jw) \right) \right\|^{2}$$

$$\leq \left\| R_{i}(jw) X_{i}(jw) \right\|^{2} - \epsilon \left\| X_{i}(jw) \right\|^{2}$$
for some  $\epsilon > 0$ , all  $X_{i}(jw)$  and all  $w$ 

$$(i = m+1, \ldots, m+n).$$

For notational convenience, we define the following block-diagonal matrices

ing block-diagonal matrices
$$C(s) \stackrel{!}{=} diag(C_1, ..., C_m, C_{m+1}(s), ..., C_{m+n}(s))$$

$$(2.7)$$

$$R(s) \stackrel{!}{=} diag(R_1, ..., R_m, R_{m+1}(s), ..., R_{m+n}(s))$$

$$(2.8)$$

$$S(s) \stackrel{!}{=} diag(S_1, ..., S_m, S_{m+1}(s), ..., S_{m+n}(s))$$

## Comments:

The conditions (2.5) - (2.6) can be interpreted as saying that we are assuming knowledge about each of the components is limited to an approximate LTI model (viz. C<sub>1</sub>) and bounds (determined by (R<sub>1</sub>, S<sub>1</sub>)) on the coarseness of the approximation.

For the case of SISO components, the conditions (2.5) and (2.6) can be replaced respectively by the simpler conditions

$$\frac{\left| h_{i}(x_{i}(t), t) - c_{i}x_{i}(t) \right|^{2}}{\left| x_{i}(t) \right|^{2}} \leq r_{i}^{2} - \epsilon$$
for some  $\epsilon > 0$ , all  $x_{i}(t) \neq 0$ , and all  $t$ 

$$\left| H_{i}(j, u) - c_{i}(j, u) \right|^{2} \leq \left| r_{i}(j, u) \right|^{2} - \epsilon$$
for some  $\epsilon > 0$  and all  $\cdot u$ 

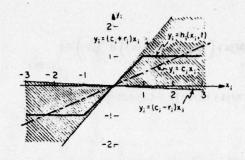
$$(2.5')$$

where for all i = 1,..., n+m

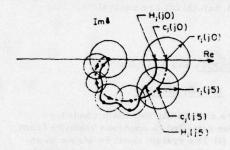
$$c_{i} = C_{i} \tag{2.10}$$

$$r_i = R_i S_i^{-1}$$
 (2.11)

These SISO conditions are readily interpreted graphically as shown in Fig. 2.



# (a) Nonlinear component satisfying (2.5')



# (b) Nyquist locus of LTI component satisfying (2.6')

Fig. 2 SISO Components

## III. Main Result

Our main result is now stated.

Theorem I (Multiloop Circle Stability
Criterion):

Suppose that the system (2,1)-(2,4) is  $L_2$ -stable for the case when

$$h_i(x_i,t) = C_i x_i \quad (i = 1,...,m)$$
 $H_i(s) = C_i(s) \quad (i=m+1,...,m).$  (3.1)

Then, a sufficient condition for the system (2.1) - (2.4) to be  $L_{2e}$  -stable for every collection of  $h_i(\cdot,t)$  (i=1,...,m) and  $H_i(s)$  (i=m+1,...,n) satisfying (2.5) and (2.6) respectively is that any one of the following conditions hold for all real  $\omega$ 

i) 
$$\lambda \min \left( (\mathbf{I} + C(\mathbf{j}u) G(\mathbf{j}u))^{\Gamma} \mathbf{S}^{\Gamma}(-\mathbf{j}u) \mathbf{S}(\mathbf{j}u) (\mathbf{I} + C(\mathbf{j}u) G(\mathbf{j}u)) - \mathbf{G}^{\Gamma}(-\mathbf{j}u) \mathbf{R}^{\Gamma}(-\mathbf{j}u) \mathbf{R}(\mathbf{j}u) \mathbf{G}(\mathbf{j}u) \right) \ge 0$$

$$(3.43)$$

ii) 
$$\lambda_{\min} \left( \left( C(-jw) + G^{-1}(-jw) \right)^{T} S^{T}(-jw) S(jw) \left( C(jw) + G^{-1}(jw) \right) - R^{T}(-jw) R(jw) \right) \ge 0$$

(3. 26)

iii) 
$$\sigma_{\min} \left( S(jw) \left( C(jw) + G^{-1}(jw) \right) R^{-1}(jw) \right) \ge 1$$
(3.2c)

iv) 
$$\sigma_{\max}\left(R(j\omega) G(j\omega)\left(I + C(j\omega)G(j\omega)\right)^{-1}S^{-1}(j\omega)\right) \le 1$$
(3.2d)

Condition (3. 2a) is implied by (3. 2b)-(3. 2d) and, when the inverses  $G^{-1}$ ,  $R^{-1}$ ,  $S^{-1}$  are defined, conditions (3, 2a)-(3, 2d) are equivalent.

# PROOF: See Appendix

### IV. Discussion

There are essentially two main conditions which must be satisfied to conclude stability from Theorem 1: (i) The system must be stable when the uncertain nonlinear components h; (., t) and LTI components H.(s) are all replaced by the respective LTI approximations C; and C;(s); and, (ii) the frequency-domain condition (3.2) must be satisfied. The former condition can be verified a variety of ways: for example, one may check that the roots of the characteristic equation

$$\det \left( \mathbf{I} + \mathbf{C}(\mathbf{s}) \mathbf{G}(\mathbf{s}) \right) = 0 \qquad (4.1)$$
all have negative real parts; alternatively, one may apply the multivariable Nyquist criterion, checking that the polar plot of the locus of det  $\left( \mathbf{C}(\mathbf{j} \mathbf{w}) \mathbf{G}(\mathbf{j} \mathbf{w}) \right)$  encircles the point  $-1 + \mathbf{j} \mathbf{0}$  exactly once counterclockwise for each unstable open-loop pole of  $\mathbf{C}(\mathbf{s}) \mathbf{G}(\mathbf{s})$  (multiplicities counted) [1], [21]. The latter condition (3.2) requires that one plot the variable  $\sigma_{\min}(\cdot)$  or  $\sigma_{\max}(\cdot)$ 

[1], [21]. The latter condition (3.2) requires that one plot the variable  $\sigma_{\min}(\cdot)$  or  $\sigma_{\max}(\cdot)$  verses z and verify that the appropriate inequality holds for all & .

In the special case in which there is a single scalar nonlinearity h, (x, t) (so that m = 1 and n = 0), both of the conditions of Theorem i can be verified by inspection of the polar plot of G(jw) vs . Stability for the special case  $h_1(x_1, t) = c_1x_1$ is assured by the Nyquist stability criterion if and only if G(ju) encircles -1 + j0 once for each unstable pole of G(s) as w increases from - " to + = . Condition (3.2) becomes

$$|c_{1}| + \frac{1}{|G(ju)|} | > |r_{1}|$$
 (4.2)  
where  $|c_{1}| = |R_{1}| |S_{1}^{-1}|$   $|c_{2}| = |C_{1}|$ 

or, equivalently (assuming c, > 0),

i) if 
$$c_1^2 - r_1^2 \ge 0$$
  

$$|G(jw) + \frac{c_1}{c_1^2 - r_1^2}| \ge |\frac{r_1}{c_1^2 - r_1^2}| \qquad (4.3a)$$
ii) if  $c_1^2 - r_1^2 < 0$   

$$|G(jw) + \frac{c_1}{c_1^2 - r_1^2} < 0$$

$$|G(jw) + \frac{c_1}{c_1^2 - r_1^2} < 0$$

$$|G(jw) + \frac{c_1}{c_1^2 - r_1^2} < 0$$

$$|Re(G(jw)) \ge \frac{-1}{c_1 + |r_1|} \qquad (4.3c)$$

These conditions on G(ju) are precisely the conditions of the well-known circle stability criterion (cf. [15]). It is this which motivates us to refer to Theorem 1 as a 'multiloop circle stability criterion' --- despite the fact that in general no circles are employed in verifying its conditions.

One can interpret the uncertainty bounds (R, S,) as specifications for the gain margins and phase margins of the system (2.1)-(2.4). If m=0, if  $H_i(s) \equiv C_i(s)$  (i=1,...,n) and if the components are SISO, then under the conditions of Theorem 1, the system will remain stable despite variations in the individual component gains of magnitudes as great as |ri(ju) | = Ri (ja)/Si (ja) |, even when the variations occur simultaneously in all components. So, for exampie, the system can tolerate simultaneous gain variations or phase variations of at least

$$G_{M_i} \stackrel{\Delta}{=} \inf_{w} 20 \log \left| \frac{r_i(jw)}{C_i(jw)} \right|, db$$
 (4.4)

 $\Theta_{M_i} \stackrel{\triangle}{=} \inf_{w} \arcsin \left| \frac{\mathbf{r}_i(jw)}{C_i(jw)} \right|$ 

<sup>2</sup> if C(s) G(s) has any 'decoupling zeroes' (i.e., uncontrollable or unobservable poles), then these will not be roots of (4.1) and one must check separately that these poles have negative real parts - cf. [14]

in each of the respective component input channel's  $(i=1,\ldots,n)$ ; i. e., the system has gain margins of at least  $G_{M_i}$  and phase margins of at least  $\partial_{M_i}$  at the inputs to the respective components  $C_i(s)$   $(i=1,\ldots,n)$ . The quantity

$$k_{\mathbf{m}} \stackrel{\Delta}{=} \sigma_{\mathbf{min}} \left( S(jw) \left( C(jw) + G^{-1}(jw) \right) R^{-1}(jw) \right)_{(4,6)}$$

is the amount by which the uncertainty bounding matrices  $R_i$  can be simultaneously increased without violating the stability conditions of Theorem i—the scalar  $k_m$  can be viewed as a lower bound on the amount by which the system (2.1)-(2.4) exceeds the stability margin specifications (2,5)-(2.6).

In general, the stability conditions—and the estimate (4.6) of excess stability margin  $k_m$ — of Theorem 1 will be conservative. The conservativeness can usually be reduced by multiplying equations (2.5)-(2.6) by appropriately chosen positive scalars  $|\alpha_i|^2$  and  $|\alpha_i(j\omega)|^2$  respectively before applying Theorem 1. This has the net effect of substituting 'weighted' uncertainty bounding matrices  $(\alpha_i R_i, \alpha_i S_i)$  for the original matrices  $(R_i, S_i)$ . Further study is required to determine the extent to which it will be practical to exploit such weighting to reduce the conservativeness of Theorem 1.

## V. Conclusions

The practical importance of our multiloop circle theorem is that it provides verifiable sufficient conditions for the stability of multiloop feedback systems using only crude bounds on system parameters, component frequency responses, and nonlinearities. Fotential applications include the testing of system integrity in the presence of actuator and/or sensor failures (cf. [16]) and the characterization of the stability margins (e.g., gain & phase margin) of multiloop feedback designs subject to simultaneous perturbations in gain and phase in the feedback loops. Theorem 1 also plays a key role in bounding the response of systems with uncertain dynamics [22].

## Appendix

In this appendix, Theorem 1 is proved using the sector stability criterion of [17], [18], [19]. We begin by introducing some additional terminology, and a relevant special case of the sector stability criterion, viz Theorem Al. We then establish via several lemmas that the conditions of Theorem 1 are sufficient to ensure that the conditions of Theorem Al are satisfied.

Definition(L2e-Cond(.,.,.); strictly inside, outside):

Given any three operators C, R, S, we define

$$L_{2e} - \text{Cone} (C, R, S) \stackrel{\Delta}{=} \left\{ (x, y) \middle| F(x, y, \tau) \le 0 \right\}$$
for all  $\tau \in R_+$  (A1)

 $F(x, y, 7) \stackrel{\triangle}{=} || S(y - Cx ||^2 - || Rx ||^2$  (A2)

and for all z, z, z

$$\|z\|_{T} \stackrel{\Delta}{=} \sqrt{\langle z, z \rangle} \tag{A3}$$

$$< z_1, z_2 >_{\tau} \stackrel{\triangle}{=} \int_0^{\tau} z_1^T(t) z_2(t) dt(A4)$$

Given an operator H mapping signals x into signals y, we say

if there exists an  $\epsilon > 0$  such that for every pair (x, y) satisfying  $y = H_X$ 

$$\| \underbrace{S} (y - \underbrace{C} x) \|_{T}^{2} \le \| \underbrace{R} x \|_{T}^{2} - \epsilon \left( \| x \|_{T}^{2} + \| y \|_{T}^{2} \right)$$
 (A6)

Given an operator -G mapping signals y into signals x, we say

$$(-G)^{I}$$
 outside  $L_{2e}$  - Cone  $(C, R, S)$  (A7)

if for every pair (x, y) satisfying x =-Gy we have

$$\| \underset{\sim}{\mathbb{S}} (\mathbf{y} - \mathbf{C} \mathbf{x}) \|_{\tau}^{2} \ge \| \underset{\sim}{\mathbb{R}} \mathbf{x} \|_{\tau}^{2}$$
(A8)

Theorem Al Let p be a positive integer; let H<sub>i</sub> (i=1,..., p) be operators mapping x into y<sub>i</sub>; let H be the operator

$$\underbrace{\mathbb{H}\underline{y}}_{\underline{y}} = \begin{bmatrix} \underbrace{\mathbb{H}_{1}y_{1}}_{1} \\ \vdots \\ \underbrace{\mathbb{H}_{p}y_{p}}_{p} \end{bmatrix}$$
(A9)

where

$$\underline{\mathbf{y}} = \begin{bmatrix} \mathbf{y}_1 \\ \vdots \\ \mathbf{y}_p \end{bmatrix} . \tag{A10}$$

If there exist operators  $C_i$ ,  $R_i$ ,  $S_i$  (i=1,..., p)

$$\underbrace{H}_{i} \quad \underline{\text{strictly inside}}_{2e} \quad L_{2e} \quad \text{Cone} (\underbrace{C}_{i}, \underbrace{R}_{i}, \underbrace{S}_{i})$$
for all  $i = 1, ..., p$  (All)

$$(-\underline{\varsigma})^{I}$$
 outside  $L_{2e}$  - Cone  $(\underline{\varsigma}_{i}, \underline{\varsigma}_{i}, \underline{\varsigma}_{i})$ , (A12)

then the system

$$\frac{\mathbf{y}}{\mathbf{x}} = \frac{\mathbf{H}}{\mathbf{x}} \mathbf{x}$$

$$= -\mathbf{G} (\mathbf{y} + \mathbf{v}) + \mathbf{u}$$
(A13)

is L2 stable.

Proof: The expression (A2) can be written equivalently,

$$\mathbf{E}(\mathbf{x}, \mathbf{y}, \tau) = \langle \mathbf{E}_{11} \mathbf{y} + \mathbf{E}_{12} \mathbf{x}, \mathbf{E}_{21} \mathbf{y} + \mathbf{E}_{22} \mathbf{x} \rangle_{\tau}$$
(A14)

where

$$\mathbf{\tilde{E}}_{11} = \mathbf{\tilde{E}}_{21} = \mathbf{\tilde{S}}$$
(A15)
$$\mathbf{\tilde{E}}_{12} = -\mathbf{\tilde{C}} + \mathbf{\tilde{R}}$$
(A16)

$$F_{12} = -C + R$$
 (A16)

$$F_{22} = -C - R$$
 (A17)

Thus

Cone 
$$(C_i, R_i, S_i) = Sector \begin{pmatrix} S_i & -C_i - R_i \\ S_i & -C_i + R_i \end{pmatrix}$$
; (A18)

(i = 1,..., m+n)

Cone (C, R, S) = Sector 
$$\begin{pmatrix} S & -C - R \\ S & -C + R \end{pmatrix}$$
. (A19)

By the composite system property of sectors (cf., Lemma 6.1 (vi) of [18]) and (All), it follows

$$\underbrace{H \text{ strictly inside Sector}}_{S \text{ ector}} \begin{pmatrix} S & -C - R \\ S & -C + R \end{pmatrix}. (A20)$$

By (A12),

$$\underbrace{\text{S outside Sector}}_{\text{S outside Sector}} \left( \underbrace{\text{S -C-R}}_{\text{S o-C+R}} \right).$$
(A21)

Theorem Al follows from Theorem 6.1 of [18] (the sector stability criterion).

Theorem Al together with the following three Lemmas, establish Theorem 1.

Lemma A2: Let h(x(t),t) be any function of x(t) and t and let H be given by

$$(\underbrace{H} x)(t) = h(x(t), t). \qquad (A22)$$

Let C, R, and S be matrices and let C, R, S be the operators defined by

$$(Cx)(t) = Cx(t) + x$$
 (A23)

$$(Rx)(t) = Rx(t) + x$$
 (A24)

$$(Sy)(t) = Sy(t). + y.$$
 (A25)

Suppose S-1 exists, then

H strictly inside L2e - Cone (C, R, S) (A26)

if and only if

$$\|S(h(x(t), t) - Cx(t))\|^2 \le \|Rx(t)\|^2 - \epsilon \|x(t)\|^2$$
 $\forall x(t).$ 
(A27)

Proof: Let y(t) = h(x(t), t). Suppose (A27)

$$||y(t)|| \le \alpha ||x(t)||$$
 (A28)

where
$$\alpha = \left(\frac{\sigma_{\max}(R)}{\sigma_{\min}(S)} + \sigma_{\max}(C)\right). \quad (A29)$$
Thus, taking

$$\mathcal{E}' = \frac{\mathcal{E}}{1+\alpha^2} \tag{A30}$$

we have that when (A27) holds, then

$$\| \underbrace{S} (y - \underbrace{C} x) \|_{T}^{2}$$

$$= \int_{0}^{T} \| S (h(x(t), t) - C x(t) \|^{2} dt$$

$$\leq \int_{0}^{T} \| R x(t) \|^{2} - \varepsilon \| x(t) \|^{2} dt$$

$$\leq \int_{0}^{T} \| R x(t) \|^{2} - \varepsilon (\| x(t) \|^{2}) dt$$

$$+ \| y(t) \|^{2} dt$$

$$= \| R x \|_{T}^{2} - \varepsilon (\| x \|_{T}^{2} + \| y \|_{T}^{2}).$$
(A31)

Conversely, when (A27) holds, then taking x(t) to be the constant function  $x(t) = x_0$  we have that for some  $\delta > 0$ 

$$\|\mathbf{S} \left(\mathbf{h} \left(\mathbf{x}_{0}, \mathbf{t}_{0}\right) - \mathbf{C}\right)\|^{2}$$

$$= \frac{1}{\tau} \cdot \|\mathbf{S} \left(\mathbf{H} \mathbf{x} - \mathbf{C} \mathbf{x}\right)\|_{\tau}^{2}$$

$$\leq \frac{1}{\tau} \left(\|\mathbf{R} \mathbf{x}\|_{\tau}^{2} - \delta \left(\|\mathbf{x}\|_{\tau}^{2} + \|\mathbf{y}\|_{\tau}^{2}\right)\right)$$

$$\leq \frac{1}{\tau} \left(\|\mathbf{R} \mathbf{x}\|_{\tau}^{2} - \delta \|\mathbf{x}\|_{\tau}^{2}\right)$$

$$= \|\mathbf{R} \mathbf{x}_{0}\|^{2} - \delta \|\mathbf{x}_{0}\|^{2}. \quad (A32)$$

Lemma A3: Let H, C, R, S be nonanticipative  $L_{2e}$ -stable linear-time-invariant operators with respective rational transfer function matrices H(s), C(s), R(s), S(s). Suppose that  $R^{-1}(s)$  exists and has no poles in  $Re(s) \ge 0$ .

Then

$$\| S(j\omega) (H(j\omega) - C(j\omega)) X(j\omega) \|^2 \le \| R(j\omega) X(j\omega) \|^2$$

$$-\varepsilon \| X(j\omega) \|^2 \qquad (A34)$$
for all X(j\omega) all \omega, and some \(\epsilon > 0\)

<u>Proof:</u> Let R<sup>-1</sup> denote the stable nonanticipative LTI operator having transfer function matrix R<sup>-1</sup>(s). Suppose that (A34) holds and let

$$\mathbf{z}_{\tau}(t) = \begin{cases} (\mathbb{R}^{\mathbf{x}})(t), & \text{if } t \leq \tau \\ 0, & \text{if } t > \tau \end{cases}$$
 (A35)

and let  $Z_{ij}(y)$  denote the Fourier transform of  $z_{ij}(t)$ . Then, for all  $y = H \times w$  we have

$$\| \underbrace{S}(y - \underbrace{C}x) \|_{T}^{2} = \| \underbrace{S}(\underbrace{H}x - \underbrace{C}x) \|_{T}^{2}$$

$$= \| \underbrace{S}(\underbrace{H} - \underbrace{C}) x \|_{T}^{2}$$
(by linearity)
$$= \| \underbrace{S}(\underbrace{H} - \underbrace{C}) \underbrace{R}^{-1} \underbrace{R}x \|_{T}^{2}$$
(since  $R^{-1}$  exists)

$$= \| \underbrace{S} (\underbrace{H} - \underbrace{C}) \underbrace{R}^{-1} z_{\tau} \|_{\tau}^{2}$$
(by nonanticipativeness)
$$\leq \int_{0}^{\infty} \| (\underbrace{S}(\underbrace{H} - \underbrace{C}) \underbrace{R}^{-1} z_{\tau}) (t) \|^{2} dt$$
(the integral exists since  $\underbrace{S}$ ,  $\underbrace{H}$ ,  $\underbrace{C}$ , and  $\underbrace{R}^{-1}$  are stable)
$$= \int_{-\infty}^{\infty} \| \underbrace{S}(\underbrace{H}) (\underbrace{H}(\underbrace{J}(\underbrace{U}) - C(\underbrace{J}(\underbrace{U})) R^{-1}(\underbrace{J}(\underbrace{U})) \\ \underbrace{Z}(\underbrace{J}(\underbrace{U})) \|^{2} du$$
(by Parseval's Theorem)
$$\leq \int_{0}^{\infty} \| \underbrace{Z}(\underbrace{J}(\underbrace{U}) \|^{2} dt \\ (\underbrace{D} + \underbrace{E}) \| (\underbrace{R}^{-1} z_{\tau})(t) \|^{2} dt$$
(by Parseval's Theorem)
$$\leq \int_{0}^{\infty} \| \underbrace{Z}(\underbrace{U}) \|^{2} dt \\ - \underbrace{E} \int_{0}^{\infty} \| (\underbrace{R}^{-1} z_{\tau})(t) \|^{2} dt$$

$$= \| \underbrace{Z}_{\tau} \|_{\tau}^{2} - \underbrace{E} \| \underbrace{R}^{-1} z_{\tau} \|_{\tau}^{2} \\ (\underbrace{D} + \underbrace{E}) \| \underbrace{R}^{-1} \underbrace{R} \times \|_{\tau}^{2} \\ (\underbrace{D} + \underbrace{E}) \| \underbrace{R}^{-1} \underbrace{R} \times \|_{\tau}^{2} \\ (\underbrace{D} + \underbrace{E}) \| \underbrace{R}^{-1} \underbrace{R} \times \|_{\tau}^{2} \\ (\underbrace{D} + \underbrace{E}) \| \underbrace{R} \times \|_{\tau}^{2} - \underbrace{E} \| \underbrace{R}^{-1} \underbrace{R} \times \|_{\tau}^{2} \\ (\underbrace{D} + \underbrace{E}) \| \underbrace{R} \times \|_{\tau}^{2} - \underbrace{E} \| \underbrace{R}^{-1} \underbrace{R} \times \|_{\tau}^{2} \\ (\underbrace{R} \times \|_{\tau}^{2} - \underbrace{E} \| \underbrace{R}^{-1} \underbrace{R} \times \|_{\tau}^{2} \\ (\underbrace{R} \times \|_{\tau}^{2} - \underbrace{E} \| \underbrace{R} \| \underbrace{R} \times \|_{\tau}^{2} \\ (\underbrace{R} \times \|_{\tau}^{2} - \underbrace{E} \| \underbrace{R} \| \underbrace{R} \times \|_{\tau}^{2} \\ (\underbrace{R} \times \|_{\tau}^{2} - \underbrace{E} \| \underbrace{R} \| \underbrace{R} \times \|_{\tau}^{2} \\ (\underbrace{R} \times \|_{\tau}^{2} - \underbrace{E} \| \underbrace{R} \| \underbrace{R} \times \|_{\tau}^{2} + \underbrace{R} \| \underbrace{R} \times \|_{\tau}^{2} \\ (\underbrace{R} \times \|_{\tau}^{2} - \underbrace{E} \| \underbrace{R} \| \underbrace{R} \times \|_{\tau}^{2} + \underbrace{R} \| \underbrace{R} \times \|_{\tau}^{2} \\ (\underbrace{R} \times \|_{\tau}^{2} - \underbrace{E} \| \underbrace{R} \| \underbrace{R} \times \|_{\tau}^{2} + \underbrace{R} \| \underbrace{R} \times \|_{\tau}^{2} \\ (\underbrace{R} \times \|_{\tau}^{2} - \underbrace{E} \| \underbrace{R} \| \underbrace{R} \times \|_{\tau}^{2} + \underbrace{R} \| \underbrace{R} \times \|_{\tau}^{2} \\ (\underbrace{R} \times \|_{\tau}^{2} - \underbrace{E} \| \underbrace{R} \| \underbrace{R} \times \|_{\tau}^{2} + \underbrace{R} \| \underbrace{R} \times \|_{\tau}^{2} + \underbrace{R} \| \underbrace{R} \times \|_{\tau}^{2} \\ (\underbrace{R} \times \|_{\tau}^{2} - \underbrace{E} \| \underbrace{R} \| \underbrace{R} \times \|_{\tau}^{2} + \underbrace{R} \| \underbrace{R}$$

where

$$\varepsilon' = \frac{\varepsilon}{1 + \alpha^2} \tag{A37}$$

and

$$\sigma = \sup_{\mathbf{x}, \tau} \left( \frac{\| \mathbf{H} \mathbf{x} \|_{\tau}}{\| \mathbf{x} \|_{\tau}} \right) < \sigma$$
(A38)
(since H is stable)

Conversely suppose (A33) holds. Let  $X_0$  and  $w_0$  be arbitrary. Then, letting  $x(t) \rightarrow 0$ 

$$X_0 = and \tau \rightarrow a$$
, we have trivially from

Parseval's Theorem that

$$||S(j\omega_{0}) (H(j\omega_{0}) - C(j\omega_{0}))X_{0}||$$

$$\leq ||R(j\omega_{0}) X_{0}||^{2} - \epsilon (||X_{0}||^{2} + ||H(j\omega_{0}) X_{0}||^{2})$$

$$\leq ||R(j\omega_{0}) X_{0}||^{2} - \epsilon ||X_{0}||^{2}.$$
(A39)

Lemma A4: Let G, C, R, S be linear-time-invariant operators with respective proper rational transfer functions H(s), C(s), R(s), S(s). Suppose that  $S^{-}(s)$  exists and has a proper rational transfer function matrix with no poles in  $Re(s) \ge 0$ . Suppose that R,  $G(I + CG)^{-}$ , and  $S^{-}$  are  $L_{2e}$  stable and nonanticipative. Then,

if and only if any one of the following conditions hold for all real 9

$$\begin{split} i) \quad & \lambda_{\min} \bigg( [I + C(-j\omega) \ G(-j\omega)]^T \ S^T(-j\omega) \ S(j\omega) \left( [I + C(j\omega) (G(j\omega)]^{-1} \right) \\ & - G^T(-j\omega) \ R^T(-j\omega) \ R(j\omega) \ G(j\omega) \bigg) \geq 0 \end{split} \tag{A41a}$$

ii) 
$$\lambda_{\min} \left( \left( C(-j\omega) + G^{-1}(j\omega) \right)^T S^T_{(-j\omega)} S(j\omega) \left( C(j\omega) + G^{-1}(j\omega) \right) - R^T_{(-j\omega)} R(j\omega) \right) \ge 0$$
 (A41b)

iii) 
$$\sigma_{\min}\left(S(j\omega)\left(C(j\omega) + G^{-1}j\omega\right)R^{-1}(j\omega)\right) \ge 1$$
 (A4lc)  
iv)  $\sigma_{\max}\left(R(j\omega)G(j\omega)\left(I + C(j\omega)G(j\omega)\right)^{-1}S^{-1}(j\omega)\right) \le 1$ . (A4ld)

When  $G^{-1}(jw)$  and  $R^{-1}(jw)$  exist, conditions (A41a)-(A41d) are equivalent.

## Proof:

It is trivial to show that (A4la) is always implied by (A4lb) - (A4ld) and that, when G (jw) and R (jw) exist, (A4la) - (A4ld) are equivalent.

Suppose that (A41a) holds. Let (x,y) by any input-output pair satisfying x = -Gy; let

$$\mathbf{v} = \mathbf{S}(\mathbf{y} - \mathbf{C} \times \mathbf{x}) \tag{A42}$$

and let

$$v_{\tau} = \begin{cases} v(t) & \text{if } 0 \le t \le \tau \\ 0 & \text{otherwise} \end{cases}$$
 (A43)

Let V (ju) denote the Fourier transform of v. Note that from (A4la), it follows that for all V (ju)

$$\|V(jw)\|^2 - \|R(jw)G(jw)(\underline{I} + \underline{G}jw)G(jw))^{-1} \underline{S}^{-1}(jw)$$

$$V_{-1}(jw)\|^2 \ge 0. \quad (A44)$$

Now,

$$\|\mathbf{R}\mathbf{y}\|_{\mathsf{T}}^{2} = \|\mathbf{R}\mathbf{G}(\mathbf{I} + \mathbf{C}\mathbf{G})^{-1}\mathbf{S}^{-1}\mathbf{v}\|_{\mathsf{T}}^{2}$$

$$= \|\mathbf{R}\mathbf{G}(\mathbf{I} + \mathbf{C}\mathbf{G})^{-1}\mathbf{S}^{-1}\mathbf{v}_{\mathsf{T}}\|_{\mathsf{T}}^{2}$$
(by the nonanticipativeness of B.  $\mathbf{G}(\mathbf{I} + \mathbf{C}\mathbf{G})^{-1}\mathbf{S}^{-1}\mathbf{v}_{\mathsf{T}}\|_{\mathsf{T}}^{2}$ 

$$\leq \int_{0}^{\infty} \|\left(\mathbf{R}\mathbf{G}(\mathbf{I} + \mathbf{C}\mathbf{G})^{-1}\mathbf{S}^{-1}\mathbf{v}_{\mathsf{T}}\right)(t)\|_{\mathsf{T}}^{2}dt$$

$$= \int_{-\infty}^{\infty} \|\mathbf{R}(\mathbf{j}\mathbf{u})\mathbf{G}(\mathbf{j}\mathbf{u})\left(\mathbf{I} + \mathbf{C}(\mathbf{j}\mathbf{u})\mathbf{G}(\mathbf{j}\mathbf{u})\right)^{-1}\mathbf{S}^{-1}\mathbf{j}\mathbf{u}$$

$$\mathbf{V}(\mathbf{j}\mathbf{u})\|_{\mathsf{T}}^{2}d\mathbf{u}$$

by Parseval's Theorem and the hypotheses that 
$$(R, G(I+CG)^T, and S^T)$$
 are  $L_{2e}$  stable.

$$\leq \int_{-\infty}^{\infty} \|V_{T}(j\omega)\|^2 d\omega$$

$$= \|v_{T}\|_{T}^2 = \|v\|_{T}^2$$

$$= \|S(y-Cx)\|_{T}^2. \quad (A45)^2$$

Conversely, suppose that (A40) holds. Let  $Y_0$  and  $y_0$  be arbitrary. The letting  $y \rightarrow Y_0 e^{j w_0 t}$  and  $\tau \rightarrow \infty$  we have from (A40) and Parseval's Theorem that

$$||R(jw_0)G(jw_0)Y_0||^2 \le ||S(jw_0)(I+C(jw_0)G(jw_0))Y_0|^2$$
  
and hence (A41a) holds.

This completes the proof of Theorem 1.

#### References

- H. H. Rosenbrock, "Design of Multivariable Control Systems Using Inverse Nyquist Array", Proc. IEE, v. U6, 1969, pp. 1929-1936.
- [2] G. Zames, "On the laput-Output Stability of Time-Varying Nonlinear Feedback Systems --- Part I: Conditions Using Concepts of Loop Gain, Conicity, and Positivity; IEEE Trans, on Automatic Control. v. AC-II, no. 2, pp. 223-233, Apr. 1966.
- [3] M. K. Sundaresnan and M. Vidyasagar, "L<sub>2</sub> Stability of Large-Scale Dynamical Systems --- Criteria Via Positive Operator Theory", IEEE Trans. on Automatic Control, AC-22, 3, Jun. 1977, pp. 196-199.
- [4] M. Araki, "Input-Output Stability of Composite Feedback Systems", IEEE Trans. on Automatic Control, v. AC-21, Apr. 1976, pp. 254-258.
- [5] H. H. Rosenbrock, "Progress in the Design of Multivariable Control Systems". <u>Trans. Inst. Measure. Control</u>. v. 4, 1971, pp. 9-11.
- [6] H. H. Rosenbrock, Multivariable Circle Theorems", in <u>Recent Mathematical Developments in Control</u>, ed. by D. J. Bell, Academic Press, 1973.
- [7] P. A. Cook, "Modified Multivariable Circle Theorems", in <u>Recent Mathematical Developments in Control</u>, ed. by D. J. Bell, Academic Press, 1973, pp. 357-373.

- [8] A. I. Mees and P. E. Rapp, "Stability Criteria for Multiple-Loop Nonlinear Feedback Systems", in Proc. IFAC MVTS Symposium, New Brunewick, Canada, Jul. 1977.
- [9] H. H. Rosenbrock and P. A. Cook, "Stability and the Eigenvalues of G(s)", Int. J. Control, v. 21, no. 1, 1975, pp. 99-104.
- [10] G. Forsythe and C. B. Moler, Computer Solution of Linear Algebraic Systems, Englewood Chiffs, N. J. Pantice-Hall, 1957.
- [11] C. A. Descer and M. Vidyasagar, Feedback Systems: Input-Output Properties. New York: Academic Press, 1975.
- [12] J. C. Willems, The Analysis of Feedback Systems, Cambridge, MA: The MIT Press, 1971.
- [13] D. C. Youla, "On the Factorization of Rational Matrices", IRE Trans. on Information Theory, v. IT-7, pp. 172-189, Jul, 1961.
- [14] A. G. J. MacFarlane and N. Karcanias, "Poles and Zeroes of Linear Multivariable Systems: A Survey of the Algebraic, Geometric and Complex-Variable Theory", 12t. J. Control. v. 24, 1976, pp. 33-74.
- [15] G. Zames, "On the Input-Output Stability of Time-Varying Nonlinear Feedback Systems --- Part II: Conditions Involving Circles in the Frequency Plane and Sector Nonlinearities", IEEE Trans. on Automatic Control. v. AC-il. no. 3, pp. 463-476, Jul. 1960.
- [16] A. G.J. MacFarlane and J. J. Belletrutti, "The Characteristic Locus Design Method", <u>Automatica</u>, v. 9, pp. 575-588, 1973.
- [17] M. G. Safonov, "Robustness and Stability Aspects of Stochastic Multi-Variable Feedback System Design", Rpt. no. ESt.-R-763, Electronic Systems Laboratory, MIT. Cambridge, MA., Sept. 1977.
- [18] M. G. Safonov and M. Athans. "On Stability Theory", Rpt. no. ESL-P-316, Electronic Systems Laboratory, MIT, Cambridge, MA; also to appear in Proc. IEEE Conf., on Decision and Control. Jan. 1979.
- [19] M. G. Safonov, Stability and Robustness of Multivariable Feedback Systems. Cambridge, MA: The MIT Fress, to be published 1979.
- [20] F. C. Schweppe, Uncertain Dynamic Systems. Prentice-Hall, Englewood Cliffs, N. J., 1973.
- [21] P. D. McMorran, "Extension of the Inverse Nyquist Method", Electronics Letters, v. o., pp. 800-801, 1970.
- [22] M. G. Safonov, "Tight Sounds on the Response of Multivariable Systems with Component Uncertainty", in Proc. Allerton Conf. on Communication, Control and Community, Manuscello, IL, Get. 4-5, 1978.

TIGHT BOUNDS ON THE RESPONSE OF MULTIVARIABLE SYSTEMS WITH COMPONENT UNCERTAINTY

MICHAEL G. SAFONOV

Department of Electrical Engineering - Systems
University of Southern California
Los Angeles, California 90007

# ABSTRACT

For Multi-Input-Multi-Output (MIMO) feedback systems having internal components that are subject to parameter variations, nonlinearity, or unmodeled dynamics within given 'conic sector' bounds, tight bounds (which also turn out to take the form of 'conic sector' bounds) are derived for the input-output relation of the closed-loop system. In the case of linear-time invariant systems, the 'conic sector' bounds are interpretable in terms of the maximal singular values of certain frequency-response matrices.

# INTRODUCTION

One of the main motivations for the use of feedback in control system design is to reduce the effects of plant ignorance on system response. In the case of single-input-single-output (SISO) feedback systems in which plant ignorance limited to a few (typically, 1 or 2) uncertain parameters known to lie within specified bounds, the Evans root-locus method [1] and Nichols chart frequency-response method [2, p. 197] are very useful (cf. [3, Ch. 6],[4]). In both cases, one graphically constructs 'regions of uncertainty' containing (for all possible parameter values) the corresponding representation of the system response. In the case of root Tocus approach, these 'regions' are the set of values assumed by each of the system poles as system parameters vary over specified ranges. Similarly, in the Nichol's chart approach the 'regions of uncertainty' are the sets of values assumed by the systems open-loop log magnitude versus phase plot at various frequencies as system parameters vary over specified ranges. Because the 'regions of uncertainty' used in these approaches are difficult to construct for systems with more than one or two uncertain parameters and because these approaches are incompatible with MIMO systems or with systems having nonlinear or time-varying plant ignorance, there is a need for an alternative approach to the problem of bounding the effects of plant uncertainty on closed-loop system response. The results of this paper establish that 'conic sector conditions' provide such an alternative approach. For, linear time-invarisnt systems, these conditions can be expressed in terms of the 'singular values' of certain frequency response matrices.

## NOTATION AND PROBLEM FORMULATION

We consider the class of systems which can be represented as a linear time-invariant (LTI) interconnection of N uncertain multi-input-multi-output components. It is assumed that an 'approximate' LTI model  $C_i$  (i = 1,...,N) and associated transfer function matrix  $C_i$  (s) is available for each of the N uncertain components, but that the actual system components

Research supported in part by NSF Grant ENG 78-05628, in part by Joint Services Electronics Program contract F-44620-76C-0061 monitored by AFOSR, and in part by the Honeywell Systems and Research Center, Minneapolis, MN 55413 with support from the Office of Naval Research under contract N00014-75-C-0144.

have 'perturbed' input-output relations which may in general include unmodeled 'cross-couplings' between components as well as uncertainty in the input-output relations of the individual components. Thus, we are considering the class of systems having an overall input-output relation

where the operator T is defined by feedback equations of the general form (See Figure 1) [Y] [U]

$$\begin{bmatrix} \underline{y} \\ \underline{e} \end{bmatrix} = \underbrace{H}_{\mathcal{N}} \begin{bmatrix} \underline{u} \\ \underline{f} \end{bmatrix}$$
 (1a)

 $\underline{\mathbf{f}} = (\mathcal{C} + \delta \mathcal{C}) \underline{\mathbf{e}} \tag{1b}$ 

where

 H is an LTI operator (having transfer function matrix H(s))
 representing the internal and external interconnections of the system's components;

• 
$$\mathcal{L} = \operatorname{diag}(\mathcal{L}_1, \ldots, \mathcal{L}_N);$$
 (2)

- 6C represents the uncertain perturbations and may in general be nonlinear, dynamical, and time-varying;
- $\underline{e} = \operatorname{col}(\underline{e}_1, \dots, \underline{e}_N)$  and  $\underline{f} = \operatorname{col}(\underline{f}_1, \dots, \underline{f}_N)$ ;

 $\underline{e_i}$  and  $\underline{f_i}$  represent the input and output signals respectively of the i-th 'perturbed' component;

- <u>u</u> is the exogenous input to the system;
- y is the observed output of the system.

To keep the mathematics tractable, it is assumed that  $\underline{H}(s)$  and  $\underline{C}(s)$  are rational transfer function matrices — this is not a serious restriction since most systems of interest with non-rational transfer functions can be approximated arbitrarily closely with respect to the  $\underline{L}_2$ -norm by systems with rational transfer functions.

Our ignorance regarding the accuracy of the 'approximate' models of the system components is assumed to be bounded by an L<sub>2</sub>-conic sector. Conic sectors are defined as follows:

For any collection of operators  $A_i$  (i = 1, ..., n), the notation diag( $A_1, ..., A_n$ ) is defined by  $\begin{array}{c} e_1 \\ \vdots \\ e_n \end{array}$  for all  $e_i$  (i = 1, ..., n).

We use the notation  $L_2$  to denote the normed space of  $c^n$ -valued signals  $\underline{z}: R \to c^n$  for some integer n for which the norm  $||\underline{z}||_L \triangleq \langle \underline{z}, \underline{z} \rangle$  exists and is finite;  $\underline{\tau}^{\langle \underline{z}_1}, \underline{z}_2 \rangle = \int_{-\infty}^{\infty} \underline{z}_1^T (t) \underline{z}_2(t) dt$  [5];  $\underline{z}_1$  is the congular congular of  $\underline{z}_1$ .

Laurus K, and output radius S. If H is an operator with the property that H-C is  $L_2$ -stable and if for all  $(\underline{x},\underline{y}) \in L_2 \times L_2$  with  $\underline{y} = \underline{H} \times \underline{x}$  we have

 $\left|\left| \sum_{x} (\underline{y} - \underline{c} \underline{x}) \right|\right|_{\underline{L}_{2}}^{2} \leq \left|\left| \sum_{x} \underline{x} \right|\right|_{\underline{L}_{2}}^{2} \tag{3}$ 

then we say

H inside  $L_2$ -Cone (C, R, S). (End of Definition) (4)

It is a trivial consequence of Parseval's theorem (cf. [5, p. 236]) that, in the case of L<sub>2</sub>-stable LTI operators S, R, and  $\delta C \stackrel{\triangle}{=} H-C$  having respective transfer functions S(s), R(s) and H(s)-C(s), the condition (4) is equivalent to the frequency-domain condition

 $\sigma_{\text{MAX}}\left(\underline{S}(j\omega)\left(\underline{H}(j\omega)-\underline{C}(j\omega)\right)\underline{R}^{-1}(j\omega)\right)\leq 1 \tag{5}$ 

(where  $\sigma_{MAX}(\underline{A})$  denotes the largest singular value of the complex matrix  $\underline{A}$  i.e., the square root of the largest eigenvalue of A\*A (or equivalently, of  $\underline{A}A*$ ) --cf. [7, Ch. 1]). The motivation for the designation of  $\underline{C}$ ,  $\underline{R}$ , and  $\underline{S}$  as the center, input radius, and output radius respectively of  $\underline{L}$ -Cone( $\underline{C}$ ,  $\underline{R}$ ,  $\underline{S}$ ) is that in the special case where  $\underline{H}$ ,  $\underline{C}$ ,  $\underline{R}$  and  $\underline{S}$  are SISO and LTI, then the statement  $\underline{H}$  inside  $\underline{L}$ -Cone ( $\underline{C}$ ,  $\underline{R}$ ,  $\underline{S}$ ) implies that the  $\underline{\omega}$ -dependent function  $\underline{H}(\underline{j}\underline{\omega})$  :  $\underline{C}$   $\rightarrow$   $\underline{C}$  given by  $\underline{Y}(\underline{j}\underline{\omega})$  =  $\underline{H}(\underline{j}\underline{\omega})$   $\underline{U}(\underline{j}\underline{\omega})$  maps inputs  $\underline{U}(\underline{j}\underline{\omega})$  lying inside the circle of radius  $\underline{R}(\underline{j}\underline{\omega})$  in the complex plane  $\underline{C}$  into outputs  $\underline{Y}(\underline{j}\underline{\omega})$  lying inside the circle of center  $\underline{C}(\underline{j}\underline{\omega})$  and radius  $\underline{S}(\underline{j}\underline{\omega})$  in the complex plane  $\underline{C}$ .

For memoryless operators  $(\underbrace{H} \underline{x})(t) = \underline{h}(\underline{x}(t), t), (\underbrace{C} \underline{x})(t) = \underline{C} \underline{x}(t),$   $(\underbrace{R} \underline{x})(t) = \underline{R} \underline{x}(t), \text{ and } (\underbrace{S} \underline{y})(t) = \underline{S} \underline{y}(t), \text{ the condition } (4) \text{ is equivalent to the condition}$ 

 $\frac{\left|\left|\underline{s}\right|\left(\underline{h}(\underline{x},\ t)\right.=C.\underline{x}\right)\right|\right|_{R^{n}}}{\left(\underline{w}\right)^{T}} \leq \frac{\left|\left|\underline{R}\right|\underline{x}\right|}{R^{n}}} \leq \frac{\left|\left|\underline{R}\right|\underline{x}\right|}{R^{n}} \qquad (6)$ (where  $\left|\left|\underline{z}\right|\right|_{R^{n}} \leq \left|\left|\underline{z}\right|^{T}\underline{z}\right|$  for all  $\underline{z} \in \mathbb{R}^{n}$ ). The motivation for using the term 'conic sector' comes from the fact that in the special case where S, h(·), C, and R are scalar, condition (6) implies that for each t the graph of h(x, t) vs. x is in a cone shaped subset of the real plane -- cf. [13].

Our results assume that  $C + \delta C = \frac{\text{inside}}{\text{lnside}} \quad C_2 - \text{Cone}(C, R_c, S_c)$ 

where C is as in equation (1) and (R, S) are given. It is further assumed that (R, S) are L<sub>2</sub>-stable LTI operators with square, rational transfer function matrices (R<sub>2</sub>(s), S<sub>2</sub>(s)) having the property that  $R_2^*(j\omega)R_2(j\omega)$  and  $R_2^*(j\omega)S_2(j\omega)$  are uniformly positive definite for all  $\omega$ .

An operator H is said to be L<sub>2</sub>-stable if H x L<sub>2</sub> whenever  $x \in L_2$  and further, for some constant  $k < \infty$ ,  $\left| \frac{H}{K} \times \frac{1}{L_2} \right|_{L_2} \le k \cdot \left| \frac{1}{|X|} \right|_{L_2}$  [5].

In the multivariable generalization of the circle stability criterion in [6], a set called L<sub>2</sub>-Cone(C, R, S) is employed which is closely related, but different, from the set L<sub>2</sub>-Cone(C, R, S). In general neither set is a proper subset of the other, but if H, C, S, and R<sup>-1</sup> are stable nonanticipative operators, then it can be shown (using the definition in [6] of L<sub>2</sub>-Cone(C, R, S). that H inside L<sub>2</sub>-Cone(C, R, S) if and only if H inside L<sub>2</sub>-Cone(C, R, S).

Of course  $\underline{R}^{-1}(j\omega)$  must exist for (5) to be equivalent to (4).

For any matrix  $\underline{A}$ , the transpose of  $\underline{A}$  is denoted  $\underline{A}^T$  and the complex congugate of  $\underline{A}^T$  is denoted  $\underline{A}^R$ .

In the special case when there is no ignorance regarding the interconnection structure of the system (i.e., when the perturbation  $\delta \mathcal{C}$  contains no 'cross-coupling' between components), then  $\delta \mathcal{C}$  takes the special form

$$\delta \xi = \text{diag} (\delta \xi_1, \ldots, \delta \xi_N)$$

where  $\delta C_i$  represents the ignorance regarding the dynamics of the i-th component (i = 1, ..., N). If there are conic sector bounds available for the uncertainty in the individual components' input-output relations

$$C_{ij} + \delta C_{ij} = \frac{\text{inside}}{\text{lnside}} L_{2} - \text{Cone} (C_{ij}, R_{ij}, S_{ij}), (i = 1, ..., N)$$
 (8)

then it follows (cf. [9, Lemma 6.2 (vi)], [10, Lemma 4.2 (vi)]) that (5) holds with

$$R_{C} = \operatorname{diag}(R_{1}, \ldots, R_{N})$$
 (9)

$$S_{C} = \operatorname{diag}(S_{1}, \ldots, S_{N})$$
 (10)

We denote by L the LTI operator whose transfer function matrix is (suppressing the argument 's')

$$\underline{L} \equiv \begin{bmatrix} \underline{L}_{yu} & \underline{L}_{yv} \\ \underline{L}_{eu} & \underline{L}_{ev} \end{bmatrix} = \begin{bmatrix} \underline{H}_{yu} & + & \underline{H}_{yf} & \underline{C}(\underline{I} - \underline{H}_{ef} & \underline{C})^{-1} \underline{H}_{eu} & \underline{H}_{yf}(\underline{I} - \underline{C} & \underline{H}_{ef})^{-1} \\ & (\underline{I} - \underline{H}_{ef} & \underline{C})^{-1} & \underline{H}_{eu} & \underline{H}_{ef}(\underline{I} - \underline{C} & \underline{H}_{ef})^{-1} \end{bmatrix}$$
(11)

For any full rank rational para-hermitian matrix  $\underline{A}(s)$  for which  $\underline{A}(j\omega)$  positive definite for all  $\omega$ , we denote by  $A^{1/2}(s)$  the rational spectral factor of  $\underline{A}(s)$  (unique to within a constant unitary left multiplier) having the properties that  $\underline{A}(s) = (\underline{A}^{1/2}(-s))^T \underline{A}^{1/2}(s)$ , that  $(\underline{A}^{1/2}(s))^{-1}$  exists, and that  $\underline{A}^{1/2}(s)$  and its inverse have no poles in  $Re(s) \geq 0$ ;  $\underline{A}^{1/2}(s)$  always exists [8, Theorem 2]. If  $\underline{A}$  is an operator, not necessarily nonanticipative, whose bilateral Laplace transform transfer function matrix is proper, rational, para-hermitian and has the property that  $\underline{A}(j\omega)$  is uniformly positive-definite for all  $\omega$ , then  $\underline{A}^{1/2}$  denotes the nonanticipative minimum phase LTI operator having transfer function  $\underline{A}^{1/2}(s)$ . Given any  $\underline{L}_2$ -stable LTI operator  $\underline{A}$ , we denote by  $\underline{A}^*$  the  $\underline{L}_2$  adjoint operator; i.e., denoting by  $\underline{A}_3(t)$  the impulse response matrix of  $\underline{A}$ ,  $\underline{A}^*$  is the LTI operator with impulse response matrix  $\underline{A}_3^T(-t)$ . Note that if  $\underline{A}(s)$  is the bilateral Laplace transform transfer function matrix of  $\underline{A}$ , then  $\underline{A}^T(-s)$  is the transfer function matrix of  $\underline{A}^*$  and further  $\underline{A}^T(-j\omega) = \underline{A}^*(j\omega)$ .

## MAIN RESULT

Our main result is the following theorem giving tight bounds on the overall systems input-output relation T.

Theorem 1: Suppose that (7) holds. If

(a) uniformly for all w

$$\sigma_{\min} \left( \underline{S}_{\mathbf{C}}(j\omega) \ \underline{L}_{\mathbf{e}\mathbf{V}}^{-1}(j\omega) \ \underline{R}_{\mathbf{C}}^{-1}(j\omega) \right) > 1$$
 (12)

(where  $\sigma_{\min}(\underline{A})$  denotes the smallest singular value of  $\underline{A}$ ), and

then, provided L (Jw) Lyv (Jw) is full fair for all w,

$$T_{\text{inside}} L_2\text{-Cone} (T_{\text{nom}}, P_T^{1/2}, Q_T^{1/2})$$
 (13)

where  $T_{\text{nom}}$ ,  $Q_{\text{T}}$ , and  $Q_{\text{T}}$  are the (not necessarily causal)  $L_2$ -stable LTI operators specified in terms of their bilateral Laplace transform transfer matrices by

$$\underline{\underline{T}}_{nom}(s) \stackrel{\Delta}{=} \underline{\underline{L}}_{yu}(s) + \underline{\underline{L}}_{yv}(s) \left(\underline{\underline{s}}_{c}^{T}(-s)\underline{\underline{s}}_{c}(s) - \underline{\underline{L}}_{ev}^{T}(-s)\underline{\underline{R}}_{c}^{T}(-s)\underline{\underline{R}}_{c}(s)\underline{\underline{L}}_{ev}(s)\right)^{-1}$$

$$\cdot \underline{\underline{L}}_{ev}^{T}(-s)\underline{\underline{R}}_{c}^{T}(-s)\underline{\underline{R}}_{c}(s)\underline{\underline{L}}_{eu}(s) \tag{14}$$

$$\underline{Q}_{T}(s) \stackrel{\Delta}{=} \left(\underline{L}_{yy}(s)\left(\underline{S}_{C}^{T}(-s)\underline{S}_{C}(s) - \underline{L}_{ev}^{T}(-s)\underline{R}_{C}^{T}(-s)\underline{R}_{C}(s)\underline{L}_{ev}(s)\right)^{-1}\underline{L}_{yv}^{T}(-s)\right)^{-1}$$
(15)

$$\underline{\underline{P}}_{T}(s) \stackrel{\Delta}{=} \underline{\underline{L}}_{eu}^{T}(-s)\underline{\underline{R}}_{c}^{T}(-s)\left(\underline{\underline{I}} - \underline{\underline{R}}_{c}(s)\underline{\underline{L}}_{ev}(s)\left(\underline{\underline{S}}_{c}^{T}(-s)\underline{\underline{S}}_{c}(s)\right)^{-1}\underline{\underline{L}}_{ev}(-s)\underline{\underline{R}}_{c}^{T}(-s)\right)^{-1}$$

$$\underline{\underline{R}}_{c}(s)\underline{\underline{L}}_{eu}(s). \tag{16}$$

Moreover, the set L<sub>2</sub>-Cone ( $T_{nom}$ ,  $p_T^{1/2}$ ,  $p_T^{1/2}$ ) is the tightest possible bound on T in the sense that for every pair of signals ( $\underline{u}$ ,  $\underline{y}$ )  $\in$  L<sub>2</sub>-Cone ( $T_{nom}$ ,  $p_T^{1/2}$ ,  $p_T^{1/2}$ ), there exists at least one 'perturbation' f satisfying (7) such that  $\underline{y} = T_{\underline{u}}$ .

Proof. See Appendix

### DISCUSSION

The uncertainty bound provided by Theorem 1, like the uncertainty bound on the plant ignorance  $\delta \mathcal{C}$ , takes the form of an  $L_2$ -conic sector condition. Consequently, in the special case in which the perturbation  $\delta \mathcal{C}$  is linear-time-invariant, Parseval's theorem [5, p. 236] implies that the  $L_2$ -conic sector bound on the overall system input-output relation provided by Theorem 1 can be expressed using singular values giving the bound on the system's frequency response matrix

$$\sigma_{\max}(Q_T^{1/2}(j\omega)(T(j\omega) - T_{nom}(j\omega)) P_T^{-1/2}(j\omega)) \leq 1$$
,

cf. equation (5). In particular for single-input-single-output LTI systems having uncertain LTI components, this bound becomes

$$|T(j\omega) - T_{nom}(j\omega)|^2 \le \frac{P_T(j\omega)}{Q_T(j\omega)}$$

For nonanticipative systems,  $L_2$ -stability is implied by  $L_2$ e-stability (which is defined in [6]). It can be shown that if the system (1) is nonanticipative and is  $L_2$ e-stable when  $\delta C \equiv 0$ , then (12) is sufficient to guarantee that (1) is  $L_2$ e-stable for all  $\delta C$  satisfying (7) [6]. Consequently, at least for nonanticipative systems, condition (b) of Theorem 1 is not very restrictive and may be easily verified by checking that L is  $L_2$ e-stable.

Theorem 1 gives the tightest possible bound on the overall system input-output relation T only when all available information about the perturbation & C is contained in condition (7). This is an important limitation, since in general this will not be the case. For example, if bounds on system uncertainty are given in the form of (8) then, although condition (7) holds with R and S specified by (9)-(10), condition (7) does not retain the 'structural' information that &C is diagonal (i.e., that δ C has no 'cross-couplings' between components). Consequently, in such situations one may in general expect the bound provided by Theorem 1 to be conservative. In contrast, the classical root-locus and frequencyresponse methods (cf. [3, Ch. 6] and [4]) for generating 'regions of uncertainty' (viz., root loci and frequency response 'templates') to bound system response need not be conservative. Thus, the response bounds provided by Theorem 1 are the most useful in the case of systems for which these classical approaches are impractical or inapplicable. Such systems include multiloop feedback systems, multi-input-multi-output systems, systems with more than a very few uncertain parameters, and systems with nonlinear components.

The problem formulation used in this paper is sufficiently general to accommodate multiloop 'two degree of freedom' (cf. [12, § 6.1], [4]) feedback structures with plant parameter ignorance such as depicted in Figure 2. For this configuration, one finds that the transfer function matrix L(s) of (11) is given by (suppressing the argument 's')

$$\begin{bmatrix} \underline{L}_{yu} & \underline{L}_{yv} \\ \underline{L}_{eu} & \underline{L}_{ev} \end{bmatrix} = \begin{bmatrix} \underline{G}_{0} & \underline{C}(\underline{I} + \underline{F} & \underline{C})^{-1}\underline{P} & \underline{G}_{0}(\underline{I} + \underline{C} & \underline{F})^{-1} \\ \underline{(\underline{I} + \underline{F} & \underline{C})^{-1}}\underline{P} & \underline{-\underline{F}}(\underline{I} + \underline{C} & \underline{F})^{-1} \end{bmatrix}$$

where  $\underline{F} = \underline{G}_F + \underline{G}_I \underline{G}_C \underline{G}_{FC}$  and  $P = \underline{G}_{IC} \underline{G}_C \underline{G}_{PC}$ . As one might expect

based on the work of Horowitz et al.(e.g., [4], [12]), it can be shown using Theorem 1 that the 'two degree of freedom' structure of Figure 2 permits one to adjust the amount of system uncertainty and the nominal value Too of the closed-loop system input-output relation independently to a certain extent -- this is the subject of a forthcoming paper.

#### ACKNOWLEDGEMENT

I would like to thank all those whose criticisms and comments contributed to this paper. In particular, I thank Mr. J. Doyle of Honeywell, Inc. and Mr. P. Van Dooren of the University of Southern California.

## APPENDIX

## Proof of Theorem 1

We begin by establishing a useful lemma.

Lemma Al: If  $Q \in \mathbb{C}^{n \times n}$  is a positive definite hermitian matrix and if  $\underline{B} \in \mathbb{C}^{r \times n}$  is a matrix of full rank  $r \le n$ , then the matrix  $\underline{Q} = (\underline{B}\underline{Q}^{-1}\underline{B}^*)^{-1}$  exists and has the following properties:

- i) Q B Q B is positive semi definite;
- ii) if  $\underline{S}$  is any matrix such that  $\underline{Q} \underline{B}^{*}\underline{S} \ \underline{B}$  is positive semi definite, then  $\overset{\circ}{Q} \underline{S}$  is positive semidefinite

iii) 
$$(\underline{B}^+)^*\underline{Q}\underline{B}^+ = (\underline{B}^+)^*\underline{B}\underline{Q}\underline{B}\underline{B}^+$$
 (A1)

<u>Proof:</u> For any positive definite matrix M and any positive integer m, let  $C_{\underline{M}}^{\underline{m}}$  denote the inner product space of complex m-vectors with inner product  $\langle \underline{z}_1, \underline{z}_2 \rangle \triangleq \underline{z}_1^* \, \underline{M} \, \underline{z}_1$ . Consider B as a linear mapping  $C_{\underline{Q}}^{\underline{n}}$  into  $C_{\underline{I}}^{\underline{r}}$ . Then the adjoint of  $\underline{B}$ , which we denote as  $\underline{B}^{\underline{a}}$ , is

$$\underline{\mathbf{B}}^{\mathbf{a}} = \underline{\mathbf{Q}}^{-1} \, \underline{\mathbf{B}}^{\star}$$

(recall  $\underline{B}^*$  denotes the complex-conjugate of  $\underline{B}^T$ ) and  $\underline{B}^+$  is the pseudo-inverse of  $\underline{B}$  [11, pp. 150-165]. Further,

$$\frac{\mathring{Q}}{\overset{\triangle}{Q}} \stackrel{\triangle}{=} (\underbrace{B} \overset{Q}{Q}^{-1} \overset{B}{B}^{*})^{-1} = (\underbrace{B} \overset{Q}{Q}^{-1} \overset{B}{B}^{*})^{-1} \overset{B}{=} \underbrace{Q}^{-1}) \overset{Q}{Q} (\underbrace{Q}^{-1} \overset{B}{B}^{*} (\underbrace{B} \overset{Q}{Q}^{-1} \overset{B}{B}^{*})^{-1})$$

$$= (\underbrace{B}^{+})^{*} \overset{Q}{Q} \overset{B}{B}^{+}. \tag{A3}$$

For any vector  $\underline{x} \in C_{\underline{Q}}^n$ , let  $\underline{x}_{\Pi(B)}$  and  $\underline{x}_{\Pi^\perp(B)}$  denote the respective projections of  $\underline{x}$  onto the nullspace of  $\underline{B}$  and the orthogonal complement of the nullspace of  $\underline{B}$ . Now, for any  $\underline{x} \in C_{\underline{Q}}^n$  and any  $\underline{y} \in C_{\underline{T}}^r$ 

$$\underline{B}^{+}\underline{B}\underline{\times} = \underline{\times}_{\Pi^{\perp}(B)} , \qquad (A4)$$

$$\underline{B} \ \underline{B}^{+} \underline{Y} = \underline{Y} . \tag{A5}$$

It follows that for all x

$$\underline{\mathbf{x}}^* (\underline{\mathbf{Q}} - \underline{\mathbf{B}}^* \underline{\underline{\mathbf{Q}}} \underline{\mathbf{B}}) \underline{\mathbf{x}} = \underline{\mathbf{x}}_{\Pi(\mathbf{B})} \underline{\underline{\mathbf{Q}}} \underline{\mathbf{x}}_{\Pi(\mathbf{B})} \geq 0$$

which establishes property (i). For any matrix S satisfying  $Q - B \le B \ge 0$  and any  $Y \in C_T^r$  we have

$$\underline{\underline{y}} \times \underline{\underline{S}} \underline{\underline{y}} = \underline{\underline{y}} \times (\underline{B}\underline{B}^{+}) \times \underline{\underline{S}} \times (\underline{B}\underline{B}^{+}) \underline{\underline{y}}$$

$$= (\underline{B}^{+}\underline{\underline{y}}) \times \underline{\underline{B}} \times \underline{\underline{S}} \times \underline{\underline{B}} \times (\underline{B}^{+}\underline{\underline{y}})$$

$$\leq (\underline{B}^{+}\underline{\underline{y}}) \times \underline{\underline{Q}} \times (\underline{B}^{+}\underline{\underline{y}})$$

$$= \underline{\underline{y}} \times \underline{\underline{\hat{Q}}} \underline{\underline{y}} , \qquad (A6)$$

which establishes property (ii). The identity of property (iii) follows by direct substitution of (A2) into (A1).

We now prove that, under the conditions of Theorem 1, equation (13) holds. We begin by noting the input-output relation  $y = T_u$  defined by (1) can be described equivalently by

$$\begin{bmatrix} \underline{v} \\ \underline{e} \end{bmatrix} = \underbrace{L}_{v} \begin{bmatrix} \underline{u} \\ \underline{v} \end{bmatrix} = \begin{bmatrix} (\underline{L}_{yu} \underline{u} + \underline{L}_{yv} \underline{v} \\ (\underline{L}_{eu} \underline{u} + \underline{L}_{ev} \underline{v}) \end{bmatrix}$$
(A7)

we take  $(\underline{u}, \underline{v}, e, \underline{f}, \underline{v})$  to be a solution of (1) and (A7). For any  $\underline{z} \in L_2$  and any  $L_2$ -stable operator A, we use the notation  $\hat{z}$  and  $\hat{z}$  to denote the Fourier transform of  $\underline{z}$  and frequency response of A respectively.

Suppose that (7) holds. Then  $(e, f) \in L_2$ -Cone (C, R, S) and hence

$$0 \ge \left| \left| \frac{1}{N_{C}} (\underline{f} - \underline{C} \underline{e}) \right| \right|_{L_{2}}^{2} - \left| \frac{1}{N_{C}} \underline{e} \right| \right|_{L_{2}}^{2}$$

$$= \langle \underbrace{S_{C}} \underline{f} - (\underbrace{S_{C}} \underline{C} + \underbrace{R_{C}}) \underline{e}, \underbrace{S_{C}} \underline{f} - (\underbrace{S_{C}} \underline{C} - \underbrace{R_{C}}) \underline{e} \rangle_{L_{2}}^{2}$$

$$= \langle (\underbrace{S_{C}} + \underbrace{R_{C}} \underline{L_{ev}}) \underline{v} + \underbrace{R_{C}} \underline{L_{eu}} \underline{u}, (\underbrace{S_{C}} - \underbrace{R_{C}} \underline{L_{ev}}) \underline{v} - \underbrace{R_{C}} \underline{L_{eu}} \underline{u} \rangle_{L_{2}}^{2}$$

$$= \langle (\underbrace{S_{C}} + \underbrace{R_{C}} \underline{L_{ev}}) \underline{v} + \underbrace{R_{C}} \underline{L_{eu}} \underline{u}, (\underbrace{S_{C}} - \underbrace{R_{C}} \underline{L_{ev}}) \underline{v} \rangle_{L_{2}}^{2}$$

$$= \langle (\underbrace{S_{C}} + \underbrace{R_{C}} \underline{L_{ev}}) \underline{v}, \underbrace{Q_{C}} \underline{v} - \underbrace{R_{C}} \underline{L_{ev}}) \underline{v} \rangle_{L_{2}}^{2}$$

$$= \langle (\underbrace{V} - \widehat{T_{V}} \underline{u}), \underbrace{Q_{V}} (\underbrace{V} - \widehat{T_{V}} \underline{u}) \rangle_{L_{2}}^{2} - \langle \underline{u}, \underbrace{P_{V}} \underline{u} \rangle_{L_{2}}^{2}$$

$$= \langle (\underbrace{V} - \widehat{T_{V}} \underline{u}), \underbrace{Q_{V}} (\underbrace{V} - \widehat{T_{V}} \underline{u}) \rangle_{L_{2}}^{2} - \langle \underline{u}, \underbrace{P_{V}} \underline{u} \rangle_{L_{2}}^{2}$$

$$= \langle (\underbrace{Q_{C} - \underline{T_{V}} \underline{u}}, \underbrace{Q_{C}} \underline{v}), \underbrace{Q_{C}} \underline{v} - \underbrace{Q_{C}} \underline{v} \rangle_{L_{2}}^{2} - \langle \underline{u}, \underbrace{Q_{C}} \underline{v} - \underline{u}, \underbrace{Q_{C}} \underline{v}) \rangle_{L_{2}}^{2}$$

$$= \langle (\underbrace{Q_{C} - \underline{T_{V}} \underline{u}}, \underbrace{Q_{C}} \underline{v}), \underbrace{Q_{C}} \underline{v} - \underbrace{Q_{C}} \underline{v} - \underbrace{Q_{C}} \underline{v}) \rangle_{L_{2}}^{2}$$

$$= \langle (\underbrace{Q_{C} - \underline{T_{V}} \underline{u}}, \underbrace{Q_{C}} \underline{v}), \underbrace{Q_{C}} \underline{v} - \underbrace{Q_{C}} \underline{v}) \rangle_{L_{2}}^{2} - \underbrace{Q_{C}} \underline{v} - \underbrace{Q_{C}} \underline{v} - \underbrace{Q_{C}} \underline{v}) \rangle_{L_{2}}^{2}$$

where Q, Z,  $\Theta$ ,  $T_{\rm v}$ , and  $P_{\rm v}$  are the (not necessarily causal) L<sub>2</sub>-stable operators specified in terms of their bilateral Laplace transform transfer functions by

$$\underline{\underline{Q}}_{\mathbf{V}}(s) \stackrel{\underline{\Lambda}}{=} \underline{\underline{S}}_{\mathbf{C}}^{\mathbf{T}}(-s) \underline{\underline{S}}_{\mathbf{C}}(s) - \underline{\underline{L}}_{\mathbf{eV}}^{\mathbf{T}}(-s)\underline{\underline{R}}_{\mathbf{C}}^{\mathbf{T}}(-s)\underline{\underline{R}}_{\mathbf{C}}(s)\underline{\underline{L}}_{\mathbf{eV}}(s)$$
(A10)

$$Z(s) \stackrel{\triangle}{=} L_{ev}^{T}(-s) R_{c}^{T}(-s) R_{c}(s) L_{eu}(s)$$
 (All)

$$\Theta(s) \stackrel{\Delta}{=} L_{eu}^{T}(-s) R_{c}^{T}(-s) R_{c}(s) L_{eu}(s)$$
(A12)

$$T_{v}(s) \stackrel{\Delta}{=} Q_{v}^{-1}(s) Z(s)$$
 (A13)

$$P_{V}(s) \stackrel{\Delta}{=} \Theta(s) + Z^{T}(-s) Q_{V}^{-1}(s) Z(s) = P_{T}(s)$$
 (A14)

where the latter equality in (A14) follows using the matrix identity

$$I + A (B - C A)^{-1} C = (I - A B^{-1} C)^{-1}$$
 (A15)

Thus, applying part (i) of Lemma Al, we have from (A9) that

$$0 \geq \langle \hat{L}_{yv} (\hat{v} - \hat{T}_{v} \hat{u}), (\hat{L}_{yv} \hat{Q}_{v}^{-1} \hat{L}_{yv}^{*})^{-1}$$

$$\hat{L}_{yv} (\hat{v} - \hat{T}_{v} \hat{u}) > L_{2} - \langle \hat{u}, \hat{P}_{T} \hat{u} \rangle_{L_{2}}$$

$$= \langle \hat{y} - \hat{T}_{nom} \hat{u}, \hat{Q}_{T} (\hat{y} - \hat{T}_{nom} \hat{u}) \rangle_{L_{2}}$$

$$- \langle \hat{u}, \hat{P}_{T} \hat{u} \rangle_{L_{2}}. \tag{A16}$$

Hence, from Parseval's theorem

$$||Q_{\text{T}}^{1/2}(y - \chi_{\text{nom}} \underline{u})||_{L_{2}} \le ||P_{\text{T}}^{1/2}\underline{u}||_{L_{2}}$$
 (A17)

from which (13) follows.

$$\hat{\mathbf{v}} = \hat{\mathbf{L}}_{\mathbf{y}\mathbf{v}}^{+} (\hat{\mathbf{y}} - \hat{\mathbf{L}}_{\mathbf{y}\mathbf{u}} \hat{\mathbf{u}}) + \hat{\mathbf{T}}_{\mathbf{v}} \hat{\mathbf{u}}$$
 (A18)

where

$$\hat{L}_{yv}^{+} \triangleq \hat{Q}_{v}^{-1} \hat{L}_{yv}^{*} (\hat{L}_{yv} \hat{Q}_{v}^{-1} \hat{L}_{yv}^{*})^{-1} . \tag{A19}$$

Then, (u, y, v) are consistant with (1) and (A7) and (using part (iii) of Lemma (A1) and Parseval's theorem) it follows that for all  $(\underline{u}, \underline{y}) \in L_2$ -Cone  $(T_{nom}, P_T^{1/2}, Q_T^{1/2})$ 

$$0 \geq ||\hat{Q}_{T}^{1/2}(\hat{y} - \hat{T}_{nom} \hat{u})||_{L_{2}}^{2} - ||\hat{P}_{T}^{1/2} \hat{u}||_{L_{2}}$$

$$= \langle (\hat{v} - \hat{T}_{v} \hat{u}), \hat{L}_{yv}^{*}(\hat{L}_{yv} \hat{Q}_{v}^{-1} \hat{L}_{yv}^{*})^{-1} \hat{L}_{yv}(\hat{v} - \hat{T}_{v} \hat{u}) \rangle_{L_{2}}$$

$$- \langle \hat{u}, \hat{P}_{T} \hat{u} \rangle_{L_{2}}$$

$$= ||\hat{S}_{C} (\mathbf{f} - C\mathbf{e})||_{L_{2}}^{2} - ||\hat{R}_{C} \mathbf{e}||_{L_{2}}^{2}$$
(A20)

where the latter equality follows as in (A9). Let  $\delta \mathcal{L}$  be the map defined by

$$\delta \mathcal{E} \underline{z} = |R_{c} \underline{e}|_{L_{2}}^{-2} \langle R_{c} \underline{e}, R_{c} \underline{z} \rangle_{L_{2}} \underline{v}. \tag{A21}$$

Using (A20) and the Schwartz inequality, one readily verifies that  $\delta C = v$  and that  $\delta C$  satisfies (7).

(End of proof)

#### REFERENCES

- [1] W. R. Evans, "Graphical Analysis of Control Systems," Trans. AIEE, Vol. 67, pp. 547-551, 1948.
- [2] H. M. James, N. B. Nichols, and R. S. Phillips, Theory of Servomechanisms. New York: McGraw-Hill, 1947.
- [3] R. C. Dorf, Modern Control Systems. Reading, Massachusetts: Addison-Wesley, 1973.
- [4] I. M. Horowitz and M. Sidi, "Synthesis of Feedback Systems with Large Plant Ignorance for Prescribed Time-Domain Tolerances," <u>Int. J. Control</u>, Vol. 16, pp. 287-309, 1972.
- [5] C. A. Descer and M. Vidyasagar, Feedback Systems: Input-Output Properties. New York: Academic Press, 1975.
- [6] M. G. Safonov and M. Athans, "A Multiloop Generalization of the Circle Stability Criterion," to appear in Proc. Twelfth Annual Asilomar Conference on Circuits, Systems, and Computers, Pacific Grove, California, November 6-8, 1978.
- [7] G. Forsythe and C. B. Moler, <u>Computer Solution of Linear Algebraic Systems</u>. Englewood Cliffs, New Jersey: Prentice-Hall, 1967.
- [8] D. C. Youla, "On the Factorization of Rational Transfer Function Matrices," <u>IRE Trans. on Information Theory</u>, pp. 172-182, July 1961.
- [9] M. G. Safonov and M. Athans, "On Stability Theory," to appear in Proc. IEEE Conf. on Decision and Control, San Diego, California, January 10-12, 1979.
- [10] M. G. Safonov, <u>Stability and Robustness of Multivariable Feedback Systems</u>. Cambridge, Massachusetts: The MIT Press, to appear 1979.
- [11] D. G. Luenberger, Optimization by Vector Space Methods, New York: Wiley, 1969.
- [12] I. M. Horowitz, Synthesis of Feedback Systems. New York: Academic Press, 1963.
- [13] G. Zames, "On the Input-Output Stability of Time-Varying Nonlinear Feedback Systems -- Part II: Conditions Involving Circles in the Frequency Plane and Sector Nonlinearities," IEEE Trans. on Automatic Control, Vol. AC-11, pp. 465-576, July 1966.

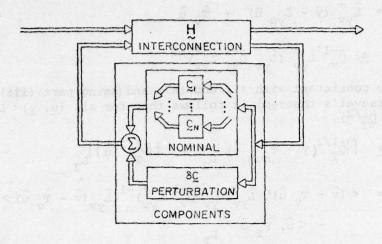


Figure 1. The system.

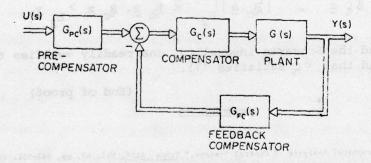


Figure 2(a). Multiloop 'two degree of freedom' feedback control system.

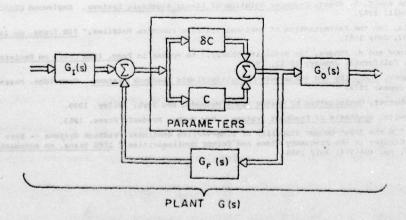


Figure 2(b). Internal structure of uncertain plant in Figure 2(a).

Foundations of Feedback Theory for Nonlinear Dynamical Systems

C. A. Desoer and Y. T. Wang

Department of Electrical Engineering and Computer Sciences and the Electronics Research Laboratory University of California, Berkeley, California 94720

## To Appear IEEE Tran IEEE CAS 1979

ABSTRACT

We study the fundamental properties of feedback for <u>nonlinear</u>, <u>time-varying</u>, <u>multi-input</u>, <u>multi-output</u>, <u>distributed</u> systems. The classical Black formula is generalized to the nonlinear case. Achievable advantages and limitations of feedback in <u>nonlinear</u> dynamical systems are classified and studied in five categories: desensitization, disturbance attenuation, linearizing effect, asymptotic tracking and disturbance rejection, stabilization. Conditions under which feedback is beneficial for <u>nonlinear</u> dynamical systems are derived. Our results show that if the appropriate linearized <u>inverse</u> return difference operator is small, then the nonlinear feedback system has advantages over the openloop system. Several examples are provided to illustrate the results.

Research sponsored by the National Science Foundation Grant ENG76-84522 and the Joint Services Electronics Program Contract F44620-76-C-0100.

#### I. INTRODUCTION

Feedback is one of the most important engineering inventions.

Historically [1], some third century B.C. water clocks may be viewed as primitive feedback devices. Some more definite feedback systems such as furnace temperature regulators, float regulators, windmills, etc. were invented between the 16th and 18th century. However, it is only at the turn of the 19th century, when James Watt invented the steam engine governor, that the concept of feedback began to be appreciated and used by engineers. Attempts to understand and to analyze the associated stability problems brought by feedback were then made by several pioneers, e.g. Airy, Maxwell, Lyapunov, Routh, Hurwitz, Vyschnegradskii, etc. Up to the 1920's, feedback devices were predominantly mechanical regulators whose primary objective was to reduce the regulated error to zero. The need of long distance telephony in the 1920's [2] resulted in the crucial invention of the negative feedback amplifier by H.S. Black [3,4]. Black's major invention was to conceive the benefits of feedback resulting from a high forward-path gain: he fed the output back to the input stage; he showed that by using a high gain in the forward path, one obtains an amplifier which is 1) more linear than the vacuum tubes in the forward path, 2) insensitive to variations in the vacuum tubes in the forward path, and 3) insensitive to noise injected at the output stage. Depending on the applications, the requirements on negative feedback amplifiers and on mechanical regulators may be quite different. Nevertheless, during World War II, the need of very accurate servomechanisms for anti-aircraft defense brought them together. It is our opinion that there is a unified underlying discipline of feedback: different applications emphasize different aspects of that discipline.

In practice, feedback is indispensable in many system designs because of 1) uncertainties: typically, incomplete knowledge of the plant due to plain ignorance or to the inordinate cost of measurements; unpredictable environmental effects; manufacturing tolerances; changes in the characteristics due to ageing, wearing, loading,...; etc., and 2) the use of inherently unstable plants, e.g. rockets, some chemical reactors, some nuclear reactors, some advanced design airplanes,..., etc. The effectiveness of feedback in coping with uncertainties was actually illustrated in the process of Black's invention of the negative feedback amplifier [4]: he realized that an "open-loop" cancellation scheme is impractical (because it requires the two "paths" track each other) and he eventually conceived the negative feedback amplifier. Moreover, Black's paper [3] exhibited many of the achievable advantages of feedback such as desensitization and disturbance attenuation.

Even though most of the existing expositions of the effects of feedback are essentially based on transfer functions calculations (thus necessarily restricted to the linear time-invariant case only), we believe that the benefits of feedback are the consequence of two facts: first, a topological structure - the loop; second, an order of magnitude relation (in the context of Black's classical paper [3], it reads  $|\beta\mu| >> 1$ ) which is independent of the linearity requirement. Pursuing this point of view, we derive below the basic properties of feedback in a much more general framework: we make full use of the recent developments in the input-output formulation of nonlinear, distributed, time-varying, multi-input, multi-output systems (see e.g. [5,6,7,8]). Such formulation allows for unstable, continuous-time as well as discrete-time subsystems; this is achieved by using causality and the technique of extended spaces,

- i.e. considering only the time interval [0,T], with T finite but arbitrary.

  The contents of this paper are as follows.
  - I. Introduction
    - I.1 Notation. I.2 General framework
- II. Black's formula generalized
- III. Advantages and limitations of feedback
  III.1 Densensitization. III.2 Disturbance attenuation.
  - III.3 Linearizing effect. III.4 Asymptotic tracking and disturbance rejection. III.5 Stabilization
- IV. Conclusion

References

Appendix

#### I.1 NOTATION

Let R ( $\mathbb C$ ) denote the field of real (complex, resp.) numbers. Let  $\mathbb N$  denote the set of non-negative integers. Let  $\mathbb Q_+$  denote the set of non-negative rational numbers. Let  $\mathbb R_+$  denote the non-negative real line  $[0,\infty)$ . Let  $\mathring{\mathbb C}_+$  denote the <u>open</u> right-half complex plane. Let R[s] (R(s)) be the set of all polynomials (rational functions, resp.) in s with real coefficients. Let  $R^{p\times q}$  ( $\mathbb C^{p\times q}$ ,  $R[s]^{p\times q}$ ,  $R(s)^{p\times q}$ ) denote the set of all  $p\times q$  matrices with elements in R ( $\mathbb C$ , R[s], R(s), resp.). Let  $\partial p(s)$  denote the degree of  $p(s) \in R[s]$ . Let  $\mathcal C \in \mathbb R_+$  be the set of time instants at which various signals of interest are defined: typically,  $\mathcal T = \mathbb R_+$  for the continuous-time case,  $\mathcal T = \mathbb N$  for the discrete time case. Let  $\mathcal T$  be a normed (seminormed) space of functions mapping  $\mathcal T$  into some vector space  $\mathcal V$ , (typically,  $\mathcal V = \mathbb R^n$ ,  $\mathcal M = \mathbb L^n_2$ ,  $\mathbb L^n_\infty$  or  $\mathbb L^n_2$ ,  $\mathbb L^n_\infty$ , etc.). Associated with the normed (seminormed) space  $\mathcal M$  is the extended normed

(seminormed) space  $\mathcal{M}_e$  defined by  $\mathcal{M}_e := \{f: \mathcal{T} \to \mathcal{V} | \forall T \in \mathcal{T}, |f|_T < \infty \}$ , where  $|f|_T := |f_T|$ ,  $f_T$  is obtained from f by a projection map  $\mathcal{P}_T$ , more

precisely,  $f_T := P_T f$  is defined by  $f_T(t) = \begin{cases} f(t), t \leq T \\ 0, t > T \end{cases}$ , for  $f_T \in \mathcal{T}$ . Let  $f_T \in \mathcal{T}$  denote the class  $\{P_T f | f \in \mathcal{T}_{e}\}$ . Let  $f_T \in \mathcal{T}_{e} \neq \mathcal{T}_{e}$  is said to be causal iff  $f_T \in \mathcal{T}_{e} = P_T \in \mathcal{T}_{e}$ ,  $f_T \in \mathcal{T}_{e} \neq \mathcal{T}_{e}$ . Nonlinear" means "not necessarily linear". ":=" means "is defined by". "u.t.c." means "under these conditions". Operators, i.e. maps from  $f_T \in \mathcal{T}_{e}$  are labelled by boldface symbols (e.g.  $f_T \in \mathcal{T}_{e}$ ). Let  $f_T \in \mathcal{T}_{e}$  denote the  $f_T \in \mathcal{T}_{e}$ . Let  $f_T \in \mathcal{T}_{e}$  denote the  $f_T \in \mathcal{T}_{e}$ . Let  $f_T \in \mathcal{T}_{e}$  denote the class of continuously differentiable maps [19, pp. 172]. We write a  $f_T \in \mathcal{T}_{e}$  to mean that a is very small compared to b.

#### 1.2 GENERAL FRAMEWORK

We will consider the nonlinear, feedback system S shown in Fig. I.1, where (1)

G: ue + ye,	is a	nonlinear,	causa1	operator	representing	(1.1)
the pla						

K: 
$$R_e \rightarrow U_e$$
, is a nonlinear, causal operator representing (I.2) the compensator,

F: 
$$\psi_e \rightarrow \mathcal{R}_e$$
, is a nonlinear, causal operator representing

the feedback,

$$r \in \mathcal{R}_{\rho}$$
, is the system input, (1.4)

$$u \in \mathcal{U}$$
, is the plant input, (1.5)

$$y \in \psi_e$$
, is the system output, (1.6)

$$e \in R_o$$
, is the error signal, (1.7)

$$R_e$$
,  $V_e$ ,  $V_e$  are extended normed spaces, unless otherwise (1.8) stated (hence  $P_T R_e$ , etc. are normed spaces with norm denoted by  $|\cdot|$ ).

We shall assume that

$$(I+FGK)^{-1}$$
 is a well-defined nonlinear, causal operator (1.9) mapping from  $R_{\rm e}$  into  $R_{\rm e}$ .

For specific conditions under which assumption (1.9) holds, see for example [7, sec. 2.8; 8, pp. 47]. Note that the closed-loop input-output map  $\mathbb{R}_{yr}$ :  $r \to y$  is given by  $GK(I+FGK)^{-1}$ .

#### II. BLACK'S FORMULA GENERALIZED

H.S. Black's invention of the negative feedback amplifier was based on the following analysis [3]: consider the feedback system S shown in Fig. I.1; let GK and F be specialized into the <u>scalar transfer functions</u>  $\mu$  and  $\beta$ , respectively, then the closed-loop input-output transfer function is (2)

$$h_{yr} := \frac{\mu}{1+\beta\mu} = \frac{1}{\beta} \cdot \frac{\beta\mu}{1+\beta\mu}$$

$$= \frac{1}{\beta} [1 - \frac{1}{1+\beta\mu}]$$

$$\approx \frac{1}{2}$$
(II.1)

for those frequencies where 
$$|\beta\mu| >> 1$$
. (II.3)

Black's crucial observation is that for those frequencies where  $|\beta\mu| >> 1$ , or equivalently  $|1+\beta\mu| >> 1$ , the output  $y \simeq \frac{1}{\beta} r$ , i.e., the closed-loop input-output transfer function is essentially independent of  $\mu$  and is essentially specified by  $\beta$ . So the recipe is:  $\beta$  is specified by the desired  $h_{yr}$  and the forward path gain  $\mu$  is made as large as possible to achieve (II.3).

Equations (II.1)-(II.3) summarize Black's fundamental observation.

We note that it is valid because 1) there is a loop structure, and 2) the

loop gain  $|\beta\mu|$  is large. This reasoning can be greatly generalized to the case of nonlinear system S shown in Fig. I.1. Note that in the linear, time-invariant case, we only have to consider the sinusoidal inputs within some frequency band of interest and the corresponding sinusoidal steady-state response. But in the <u>nonlinear</u> case, we have to formulate the condition in terms of <u>inputs of interest</u>, e.g., sinusoids of various frequencies and amplitudes, step, ramp, parabolas, etc.

## Theorem II.1: (Black's formula generalized: soft version)

Consider the nonlinear, feedback system S shown in Fig I.1 and described by Equations (I.1)-(I.9). Let  $R_{\rm d,e} \subseteq R_{\rm e}$  be the set of inputs of interest. U.t.c. if, for T sufficiently large,

$$\left| \left( \mathbf{I} + \mathbf{F} \mathbf{G} \mathbf{K} \right)^{-1} \mathbf{r} \right|_{\mathbf{T}} << \left| \mathbf{r} \right|_{\mathbf{T}}, \quad \forall \mathbf{r} \in \mathcal{R}_{\mathbf{d}, \mathbf{e}}$$
 (II.4)

then, asymptotically

$$\tilde{F} \stackrel{\text{H}}{\text{yr}} = \tilde{I} \quad \text{on} \quad \mathcal{R}_{d,e}$$
(II.5)

in the sense that, for  $T \in \mathcal{J}$  sufficiently large,

$$|\mathbf{r} - \mathbf{F} \underset{\sim}{\mathbb{H}}_{yr} \mathbf{r}|_{T} \ll |\mathbf{r}|_{T}, \quad \forall \mathbf{r} \in \mathcal{R}_{d,e}$$
 (II.6)

#### Proof:

Since F, G, K are nonlinear, we have

$$H_{vr} = CK(I+FCK)^{-1}$$
.

Apply the nonlinear operator F on the left to both sides of this equation:

Hence for all  $r \in R_e$ 

$$r - F H_{yr} r = (I + FGK)^{-1} r$$

Now let  $r \in R_{d,e} \subset R_e$  and let  $T \in \mathcal{J}$  be large, then, using (II.4),

the case of semilinear system & shown in Fig. 1.1. Note that in the

linear, bine-invariant cast, we only have to consider the sleuted

$$|\underline{r} - \underline{F} \underline{H}_{yr} r|_{T} = |(\underline{I} + \underline{F} \underline{G} \underline{K})^{-1} r|_{T} \ll |r|_{T}$$

and (II.5) follows.

Q.E.D.

Remarks II.1: a) (II.5) says that the feedback system  $H_{yr}$  followed by F behaves approximately like an identity operator as far as the inputs of interest are concerned. Equivalently, F is an approximate left-inverse of  $H_{yr}$  on  $R_{d,e}$ ; thus, on  $R_{d,e}$ ,  $H_{yr}$  is essentially independent of G and is essentially specified by F. (The left inverse is the one of interest because any operator P:  $\mathcal{U} \to \mathcal{V}$  has a right inverse Q in the sense that there always exists a Q such that  $PQ = I_{d}$  where  $I_{d}$  denotes the identity restricted to  $P(\mathcal{U})$ .

- b) Consider G perturbed into G; call H yr the resulting closed-loop input-output map. If G satisfies (II.4), then F H = I, on R is insensitive to the plant perturbations. This, however, does not assert that the relative change in H will be much less than that in G; it simply asserts that changes in G have little effect on H yr. The exact relation between the relative change in H and the relative change in G is given by Equation (III.7) below and discussed in Remarks III.1.
- c) (II.5) is a soft version of Black's formula (II.2). To obtain  $H_{yr} \simeq F^{-1}$  requires some additional assumptions. This is done in Theorems II.2 and II.3 below.

Note that eqn. (II.1) gives the exact relation

$$h_{yr} - \frac{1}{\beta} = -\frac{1}{\beta} \cdot \frac{1}{1 + \beta \mu} \tag{II.7}$$

As feedback designers know (see e.g. [9]), it is often advantageous to write this equation in terms of the "inverse loop-gain"

$$h_{yr} - \frac{1}{\beta} = -\frac{1}{\beta} \frac{(\beta \mu)^{-1}}{1 + (\beta \mu)^{-1}}$$
 (II.8)

Theorem II.2 below generalizes Black's result to the nonlinear case: an estimate of the difference  $\underset{\sim}{\text{H}}_{\text{yr}} = \underset{\sim}{\text{F}}^{-1} r$  is obtained under the condition that the "inverse loop-gain" is small for the class of inputs of interest. Note the similarity in form between the right-hand sides of eqn. (II.7) and eqn. (II.9) below.

## Theorem II.2 (Generalized Black formula)

Consider the nonlinear, feedback system S shown in Fig. I.1 and described by eqns. (I.1)-(I.9). Let  $R_{\rm d,e} \subseteq R_{\rm e}$  be the set of inputs of interest. Suppose that

- (a1)  $\forall T \in \mathcal{T}, \ P_T R_e$  is a Banach space;
- (a2)  $F^{-1}: \mathcal{R}_e \to \mathcal{Y}_e$  and  $(FGK)^{-1}: \mathcal{R}_e \to \mathcal{R}_e$  are well-defined nonlinear, causal maps;
- (a3)  $(FGK)^{-1}$  is continuous<sup>(3)</sup> on  $R_e$ , and for each  $r \in R_{d,e}$ ,  $z_{n+1} := r (FGK)^{-1}z_n \in \mathcal{N}(R_{d,e}) \subset R_e, \text{ where } z_0 = r, n \in \mathbb{N},$ and  $\mathcal{N}(R_{d,e})$  denotes a neighborhood of  $R_{d,e}$  in  $R_e$ .

U.t.c. if

(i) 
$$\lambda(\underline{F}^{-1}) := \sup_{\substack{r \in \mathcal{R}_{d,e}, \ r \in \mathcal{T} \\ e_T \neq 0}} \frac{\left|\underline{F}^{-1}(r-e)-\underline{F}^{-1}r\right|_{T}}{\left|e\right|_{T}} < \infty ;$$

(ii) for each T∈T,

$$\tilde{\gamma}_{T}[(FGK)^{-1}] := \sup_{\substack{r_{1}, r_{2} \in \mathcal{N}(R_{d,e}) \\ r_{1}, T}} \frac{\left| (FGK)^{-1} r_{1} - (FGK)^{-1} r_{2} \right|_{T}}{\left| r_{1} - r_{2} \right|_{T}} < 1,$$

then, for each T & T,

$$\left| \underset{\text{yr}}{\mathbb{H}} \mathbf{r} - \widetilde{\mathbf{r}}^{-1} \mathbf{r} \right|_{T} \leq \lambda \left( \widetilde{\mathbf{r}}^{-1} \right) \frac{\left| \left( \widetilde{\mathbf{F}} \mathsf{G} \mathsf{K} \right)^{-1} \mathbf{r} \right|_{T}}{1 - \widetilde{\gamma}_{T} \left[ \left( \widetilde{\mathbf{F}} \mathsf{G} \mathsf{K} \right)^{-1} \right]}, \ \forall \mathbf{r} \in \mathcal{R}_{d,e}$$
(II.9)

In particular, if for T∈T sufficiently large,

$$\tilde{\gamma}_{T}[(FGK)^{-1}] \ll 1$$
 (II.10)

and

$$\left| \left( \underbrace{FGK}_{T} \right)^{-1} r \right|_{T} \ll \frac{\left| \underbrace{F}^{-1} r \right|_{T}}{\lambda(F^{-1})}, \forall r \in \mathcal{R}_{d,e}, \qquad (II.11)$$

then asymptotically,

$$H_{\text{yr}} \simeq F^{-1} \text{ on } R_{d,e}$$
 (II.12)

in the sense that for  $T \in \mathcal{T}$  sufficiently large,

$$\left| \underset{\sim}{\mathbb{H}}_{yr} \mathbf{r} - \mathbf{r}^{-1} \mathbf{r} \right|_{T} \ll \left| \mathbf{r}^{-1} \mathbf{r} \right|_{T}, \ \forall \mathbf{r} \in \mathcal{R}_{d,e}. \tag{II.13}$$

Proof of Theorem II.2: see Appendix.

Remark II.2: Note that the classical Black condition that  $|\beta\mu| >> 1$  (which is achieved, in design, with  $|\mu| >> 1$ ) is a sufficient condition for the approximation (II.2). Thus one may want to pursue the idea of

small inverse forward path gain (large  $|\mu|$  in the single-input single-output case) as follows: assuming the existence of the required inverses, from

$$H_{\text{yr}} = GK(I+FGK)^{-1}$$
(II.14)

we obtain

$$H_{yr}^{-1} = (I + FGK) (GK)^{-1}$$

$$= F + (GK)^{-1}$$
(11.15)

This formula is the generalization to the <u>nonlinear</u> case of the well-known corresponding relation with matrix transfer functions [9, p. 121]. If we assume that  $\forall y \in \mathcal{Y}_{d,e}$ , the set of outputs of interest, and for  $T \in \mathcal{T}$  sufficiently large

$$\left| \left( \underbrace{\mathsf{GK}} \right)^{-1} \mathsf{y} \right|_{\mathsf{T}} << \left| \underbrace{\mathsf{F}} \mathsf{y} \right|_{\mathsf{T}} \tag{11.16}$$

then, asymptotically

$$H_{\text{vyr}}^{-1} \simeq F$$
, on  $\mathcal{Y}_{d,e}$  (II.17)

in the sense that for  $T \in \mathcal{T}$  sufficiently large,  $|\mathcal{H}_{yr}^{-1}y - \mathcal{F}y|_T << |\mathcal{F}y|_T$ ,  $\forall y \in \mathcal{Y}_{d,e}$ . Note, however, since  $\mathcal{F}$  and  $\mathcal{H}_{yr}$  are <u>nonlinear</u>, eqn. (II.17) does <u>not</u> imply that  $\mathcal{H}_{yr} \simeq \mathcal{F}^{-1}$ .

Going back to the Black formula (II.1), we note that the approximation (II.2),  $h_{yr} \simeq \frac{1}{\beta}$ , is valid as long as

$$\left|\frac{1}{\beta} \cdot \frac{1}{1+\beta u}\right| << \left|\frac{1}{\beta}\right| \tag{II.18}$$

Theorem II.3 below generalizes this condition to the nonlinear case:
eqn. (II.18) should be compared with the condition (ii) of Theorem II.3 below.

## Theorem II.3:

Consider the nonlinear, feedback system S shown in Fig. I.1 and described by eqns. (I.1)-(I.9). Let  $\mathcal{R}_{d,e} \subseteq \mathcal{R}_e$  be the set of inputs of interest. Suppose that  $F^{-1}: \mathcal{R}_e \to \mathcal{Y}_e$  is a well-defined nonlinear, causal map.

U.t.c. if

(i) 
$$\lambda(\tilde{F}^{-1}) := \sup_{\substack{r \in \mathcal{R}_{G,e}, \ T \in \mathcal{T} \\ e_{T} \neq 0}} \frac{\left|\tilde{F}^{-1}(r-e)-\tilde{F}^{-1}r\right|_{T}}{\left|\tilde{e}\right|_{T}} < \infty;$$

(ii) for T∈T sufficiently large,

$$\lambda(\underline{\mathbf{F}}^{-1}) \cdot |(\underline{\mathbf{I}} + \underline{\mathbf{F}} \underline{\mathbf{G}} \underline{\mathbf{K}})^{-1} \mathbf{r}|_{\mathbf{T}} \ll |\underline{\mathbf{F}}^{-1} \mathbf{r}|_{\mathbf{T}}, \ \mathbf{v} \mathbf{r} \in \mathcal{R}_{\mathbf{d}, \mathbf{e}},$$

then, asymptotically,

$$\frac{H}{vyr} \simeq F^{-1} \text{ on } R_{d,e}$$
 (II.19)

in the sense that for T∈T sufficiently large,

$$\left| \underset{\mathbf{v}_{\mathbf{T}}}{\mathbf{H}} \mathbf{r} - \mathbf{r}^{-1} \mathbf{r} \right|_{\mathbf{T}} << \left| \mathbf{r}^{-1} \mathbf{r} \right|_{\mathbf{T}}, \ \forall \mathbf{r} \in \mathcal{R}_{\mathbf{d}, \mathbf{e}}$$
 (II.20)

Proof of Theorem II. 3: see Appendix.

## Corollary II.3.1 (F linear)

Consider the nonlinear, feedback system S shown in Fig. I.1 and described by eqns. (I.1)-(I.9). Let F be linear. Let  $F^{-1}: \mathcal{K}_e \to \mathcal{Y}_e$  be a well-defined linear causal map. Let  $\mathcal{K}_{d,e} \subseteq \mathcal{K}_e$  be the set of inputs of interest. U.t.c. if for T sufficiently large and V  $y \in F^{-1} \mathcal{K}_{d,e}$ 

$$|(\underline{\mathbf{I}}+\underline{\mathbf{G}}\underline{\mathbf{K}}\underline{\mathbf{F}})^{-1}\mathbf{y}|_{\mathbf{T}} \ll |\mathbf{y}|_{\mathbf{T}}$$

then conclusions (II.19) and (II.20) hold.

Proof of Corollary II.3.1: see Appendix.

## Corollary II. 3.2 (Linear time-invariant case)

Consider the feedback system S shown in Fig. I.1 and described by eqns. (I.1)-(I.9). Let the operators G, K, and F be linear, time-invariant and represented by transfer function matrices G(s), K(s) and F(s), respectively. Let  $\mathcal{K}_{d,e} \subseteq \mathcal{K}_{e}$  consist of all sinusoidal inputs with frequencies in some interval  $\Omega \subseteq \mathbb{R}$ . Suppose that

- (al)  $\tilde{F}^{-1}$ :  $R_e + \gamma_e$  is a well-defined causal map;
- (a2) the closed-loop system is exp. stable, i.e. the impulse response of the transfer function  $H_{\gamma r}$ :  $r \mapsto y$  is bounded by a decaying exponential.

U.t.c., if  $\forall \omega \in \Omega$ ,  $\forall y \in range[F(j\omega)^{-1}] \subset c^{n_0}$ 

$$|[(I + GKF)(j\omega)]^{-1}y| <<|y|,$$
 (II.21)

then

$$H_{vr}(j\omega) \simeq F(j\omega)^{-1}, \forall \omega \in \Omega$$
 (II.22)

in the sense that  $\forall r \in \mathfrak{c}^n$ 

$$|H_{yr}(j\omega)r-F(j\omega)^{-1}r| \ll |F(j\omega)^{-1}r|, \forall \omega \in \Omega$$
 (II.23)

Proof of Corollary II.3.2: see Appendix

Remark II.3.2: If we use the  $\ell_2$ -norm in  $\mathfrak{C}^n$ , condition (II.21) is satisfied if the <u>largest singular value</u> (4) of  $[(I+GKF)(j\omega)]^{-1}$  is much smaller than 1, for all  $\omega \in \Omega$ .

## Comments on Theorems II.2 and II.3:

- (a) Theorems II.2 and II.3 conclude that, under suitable conditions, the output  $y = H_{yr}r$  is, asymptotically (i.e. for large T), approximately equal to  $F^{-1}r$  over the inputs of interest within a small <u>relative</u> error. Thus eqns. (II.12) and (II.19) are complete generalizations of the Black formula (II.2) to the nonlinear, time-varying, multi-input, multi-output, distributed systems S shown in Fig. I.1 and described by eqns. (I.1)-(I.9).
- (b) Typically,  $R_{d,e}$ , the set of inputs of interest, consists of sinusoids of various frequencies and amplitudes, or steps, ramps, parabolas, etc., of various magnitudes.
- (c) Note that the extended spaces framework allows us to treat the case where some of the operators G, K, F may be unstable and to state asymptotic conditions such as eqns. (II.10), (II.11).
- (d) It is the <u>nonlinearities</u> of the maps G, K, F which forces us to use the incremental gain (e.g.  $\tilde{\gamma}_T[(FGK)^{-1}]$  in theorem II.2), or Lipschitz constants (e.g.  $\lambda(F^{-1})$  in theorems II.2 and II.3), over appropriate sets, to obtain our estimates. In the linear case, one would use the induced norms of the corresponding maps over appropriate sets.
- (e) Theorems II.2 and II.3 have important design implications: Given a plant G, we first choose F such that, over the inputs of interest, F<sup>-1</sup> is asymptotically the desired input-output map. Next we choose the compensator K so that the conditions of theorem II.2 (or of theorem II.3) are satisfied. Then, asymptotically, the closed-loop input-output map H<sub>yr</sub> is close to F<sup>-1</sup> over the inputs of interest as we desired.
- (f) Note that  $F^{-1}$  can be <u>nonlinear</u>. A simple well-known example of realizing a nonlinear map by a feedback system (with large forward-path gain) is the logarithmic amplifier shown in Fig. II.1 Recall that node 2

is a virtual ground, and that the diode operates at currents much larger than its saturating current  $I_s$ , thus  $\tilde{F}^{-1}$ :  $i_D \mapsto v_0$  is given by  $v_0 = -v_D \approx -v_T \ln (i_D/I_s)$ . Hence  $v_0 \approx -v_T \ln [v_i/(R_iI_s)]$ .

## Examples:

To illustrate the implication of the generalized Black formula on nonlinear dynamical systems, we present the following two examples:

## Example II.1 (Nonlinear, single-input single-output dynamical system)

Consider the nonlinear, feedback system S shown in Fig. I.1, where G is characterized by a rational transfer function  $\frac{5\times 10^8}{(s+1)(s+10^3)(s+10^4)}$  followed by a nonlinear memoryless map  $\phi(\cdot)$  with  $\phi(\cdot)\in C^1$  described by

$$\phi(z) = \begin{cases} \frac{11}{30} + \sqrt{\left(\frac{11}{30}\right)^2 + \frac{z-3}{18.75}}, & z \ge 0.5 \\ 0.8z & , |z| \le 0.5 \\ 0.8e^{z+0.5} - 1.2 & , z \le -0.5 \end{cases}$$
(II.24)

K and F are characterized by constants k and 1, respectively. The closed-loop system and the characteristics of the nonlinearity  $\phi(\cdot)$  are shown in Fig. II.2 and Fig. II.3, respectively. By theorem II.2 (or theorem II.3), if k becomes large, then, asymptotically, the output y of the closed-loop system will be approximately equal to the reference signal  $r(\cdot)$  (since  $F^{-1} = 1$  in this case). Fig. II.4-Fig. II.6 show the system output  $y(\cdot)$ , the error signal  $e(\cdot)$ , and  $z(\cdot)$ , the input to the nonlinearity  $\phi(\cdot)$ , in the "steady state" for different values of k while the closed-loop system is driven by  $r(t) = \sin 10t$ . The effect due to high forward-path gain in a feedback system is clearly illustrated by Fig. II.4. Note that the high forward-path gain distorts  $z(\cdot)$ , the input to the nonlinearity  $\phi(\cdot)$ , so

that asymptotically, the output  $y(\cdot)$  is approximately equal to  $\sin 10t$ .

## Example II.2 (Nonlinear, multi-input, multi-output, dynamical system)

Consider the nonlinear, feedback system S shown in Fig. I.1, where G is characterized by a rational function matrix

$$L(s) = \begin{bmatrix} \frac{5 \times 10^8}{(s+1)(s+10^3)(s+10^4)} & \frac{1 \times 10^8}{(s+1)(s+10^3)(s+10^4)} \\ \frac{5 \times 10^7}{(s+1)(s+10^3)(s+10^4)} & \frac{5 \times 10^8}{(s+1)(s+10^3)(s+10^4)} \end{bmatrix}$$
(II.25)

followed by a nonlinear memoryless  $C^1$  map  $\Phi(\cdot)$  described by

$$\Phi\left(\begin{bmatrix} z_1 \\ z_2 \end{bmatrix}\right) = \begin{bmatrix} (1+0.2 \tanh z_2) \cdot v(z_1) \\ (1+0.2 \tanh z_1) \cdot v(z_2) \end{bmatrix}$$
(II.26)

with

$$v(z) := \begin{cases} z & , \text{ if } |z| \le 0.5 \\ \operatorname{sgn} z \cdot \left[\frac{3}{7} + \sqrt{\frac{|z| - 3/7}{14}}\right] & , \text{ if } |z| \ge 0.5 \end{cases}$$
(II.27)

K and F are represented by the constant matrices kI and I, resp., both in  $\mathbb{R}^{2\times 2}$ .

The closed-loop system, the characteristics of v(z), and the characteristics of 1+0.2 tanh z are shown in Fig. II.7, Fig. II.8, and Fig. II.9, respectively. By theorem II.2 (or theorem II.3), if k is sufficiently large, then, asymptotically, the output y of the closed-loop system will be approximately equal to the reference signal r (since  $\mathbf{F}^{-1} = \mathbf{I}$  in this case). Fig. II.10-Fig. II.13 show the system output components  $\mathbf{y}_1(\cdot)$ ,  $\mathbf{y}_2(\cdot)$  and the error signal components  $\mathbf{e}_1(\cdot)$ ,  $\mathbf{e}_2(\cdot)$ , respectively, for different values of  $\mathbf{k} \in \mathbb{R}$  while the closed-loop system is driven by the reference signal  $\mathbf{r} = \begin{bmatrix} \mathbf{r}_1 \\ \mathbf{r}_2 \end{bmatrix} = \begin{bmatrix} \sin 10\mathbf{t} \\ 0.8 \sin 15\mathbf{t} \end{bmatrix}$ . Fig. II.10 and Fig. II.11 show that as

we increase the compensator gain k, the system output (vector) function approaches to the reference signal r as if the closed-loop system was an identity map despite the complicated couplings in the nonlinear plant G. Fig. II.14 and II.15 show, for k = 40, a period of the steady-state trajectories of the system outputs,  $y(\cdot)$ , and of the nonlinearity inputs,  $z(\cdot)$ , on the y-plane and z-plane, respectively. Note that the greatly distorted trajectory of  $z(\cdot)$  (due to the coupling and saturation effects of  $\Phi(\cdot)$ ) produces a system output y(\*) very close to the reference signal sin 10t 0.8 sin 15t. Consider the three large irregular lobes on the z(\*) trajectory in the 2nd, 3rd and 4th quadrant of Fig. II.15 which reach their peaks at time instants t = 4.54, 4.90, 5.55 respectively. Observe that at those time instants, at least one of the desired plant output component  $(y_1^* = \sin 10t,$  $y_2^* = 0.8 \sin 15t$ ) reaches the peak of the negative cycle of sinusoidal waves (see Fig. II.10 and Fig. II.11). Further observe that  $y_1$  and  $z_1$ ,  $y_2$  and  $z_2$  are of same sign for all t since  $1+0.2 \tanh z > 0$  and v(z) is an odd function. Now at time t = 4.54, the desired plant output  $y_1^*(t) \approx .98$ ,  $y_2^*(t) \simeq -.70$ , thus  $v(z_1)$  ( $v(z_2)$ ) is required to operate in its positive (negative, resp.) "saturation" region. Due to the negative value of z2,  $1+0.2 \tanh z_2 \simeq 0.8$ . Consequently,  $(1+0.2 \tanh z_2) v(z_1)$  "saturates" earlier than  $v(z_1)$  itself and  $z_1$  is required to be a large positive number so that  $y_1 = (1+0.2 \tanh z_2) v(z_1)$  will be approximately equal to the desired value 0.98. This explains the large lobe on the trajectory of z(.) in the 4th quadrant. Similar reasoning explains the other two large lobes in the 2nd and 3rd quadrant.

## III. ADVANTAGES AND LIMITATIONS OF FEEDBACK

Consider the nonlinear, feedback system S shown in Fig. I.1 and described by eqns. (I.1)-(I.9) which satisfies the conditions stated in theorem II.2 (or theorem II.3), then asymptotically, the closed-loop system input-output map  $\mathbb{R}_{\text{vyr}}$  is approximately  $\mathbb{F}^{-1}$ . Thus we should expect that the closed-loop system input-output map is insensitive to the variations in the forward path map  $\mathbb{G}\mathbb{K}$  and that, if  $\mathbb{F}$  is linear, the closed-loop system is close to a linear system even though the forward path map  $\mathbb{G}\mathbb{K}$  is highly nonlinear.

In the following, we show the advantages and limitations of feedback for the nonlinear, feedback system S shown in Fig. I.1: section III.1 calculates the exact effect of plant perturbations on the closed-loop input-output map and demonstrates the relations between desensitization and i) the feedback structure, ii) the perturbation on the feedback map F, and iii) the closed-loop stability; section III.2 establishes the exact effect of various additive external disturbances on the closed-loop system output; section III.3 defines a nonlinearity measure and then shows precisely that feedback has a linearizing effect on a nonlinear plant; sections III.4 and III.5 briefly review the idea that feedback can achieve asymptotic tracking and disturbance rejection, and stabilize unstable systems.

#### III.1 DESENSITIZATION

One of the major reasons for using feedback in design is that feedback can reduce the effect of the plant perturbations on the input-output map. One way to <u>quantitatively</u> demonstrate the <u>desensitization</u> effect of feedback is to compare a feedback design with a corresponding open-loop design [10]: consider the nonlinear, feedback system S shown in Fig. I.1 and described by eqns. (I.1)-(I.9). Note that the closed-loop input-output map  $H_{yr}: r \mapsto y$  is given by  $GK(I+FGK)^{-1}$ . Also consider a <u>comparison open-loop system</u> (shown in Fig. III.1) consisting of the <u>same plant G preceded</u> by a compensator  $K_0$ . Thus the open-loop input-output map  $H_{y0}r: r \mapsto y_0$  is given by  $GK_0$ . Now if we select

$$K_0 = K(I+FGK)^{-1}, \qquad (III.1)$$

then for all system inputs r,  $y = y_0$ , i.e. the (nominal) open-loop inputoutput map  $H_{y_0}$ :  $r \mapsto y_0$  is identical to the (nominal) closed-loop inputoutput map  $H_{y_r}$ :  $r \mapsto y$ . Consider now an arbitrary, not necessarily small,
perturbation  $\Delta G$  on the plant G, then the plant G becomes  $G := G + \Delta G$ ; the
closed-loop (open-loop) system input-output map  $H_{y_r}$  ( $H_{y_0}$ ) becomes  $H_{y_r} := H_{y_r} + \Delta H_{y_r} = GK(I + FGK)^{-1}, (H_{y_0} = H_{y_0} + \Delta H_{y_0} = GK) = GK(I + FGK)^{-1},$ resp.). The perturbed closed-loop (open-loop) system is shown in Fig. III.2
(Fig. III.3, respectively).

Note that the changes of the closed-loop, and the open-loop system input-output maps due to the plant perturbation  $\Delta G$  are given by

$$\Delta_{\text{yr}}^{\text{H}} := \widetilde{H}_{\text{yr}} - H_{\text{yr}} = \widetilde{G}K(I + F\widetilde{G}K)^{-1} - GK(I + FGK)^{-1}$$
(III.2)

$$\Delta_{\mathbf{y}_{0}^{\mathbf{r}}}^{\mathbf{H}} := \tilde{\mathbf{H}}_{\mathbf{y}_{0}^{\mathbf{r}}} - \tilde{\mathbf{H}}_{\mathbf{y}_{0}^{\mathbf{r}}} = \tilde{\mathbf{G}}_{\mathbf{x}_{0}^{\mathbf{r}}}^{\mathbf{K}} - \tilde{\mathbf{G}}_{\mathbf{x}_{0}^{\mathbf{r}}}^{\mathbf{K}} - \tilde{\mathbf{G}}_{\mathbf{x}_{0}^{\mathbf{r}}}^{\mathbf{K}} = \Delta_{\mathbf{x}_{0}^{\mathbf{r}}}^{\mathbf{K}} = \Delta_{\mathbf{x}_{0}^{\mathbf{r}}}^{\mathbf{K}} (\mathbf{1} + \mathbf{F}_{\mathbf{G}}^{\mathbf{K}})^{-1}$$
(III.3)

respectively.

Theorem III.1 below generalizes some of the results in [10,11,12,46] and establishes the exact relation between  $\Delta H_{yr}$  and  $\Delta H_{y0}$ , and thus makes precise the desensitization effect of feedback for nonlinear systems.

## Theorem III.1 (Desensitization of plant perturbation by feedback)

Consider the nonlinear, feedback system S shown in Fig. I.1 and described by eqns. (I.1)-(I.9). Also consider the comparison open-loop system shown in Fig. III.1. Let  $\Delta H_{yr}$  and  $\Delta H_{yo}$  denote the changes of the closed-loop, and the open-loop system input-output maps due to the plant perturbation  $\Delta G$ , respectively. Assume that

(al) 
$$F: \mathcal{Y}_e \to \mathcal{R}_e$$
 is linear;

(a2) the perturbed plant  $\tilde{G}$  satisfies (I.9), i.e.  $(I+F\tilde{G}K)^{-1}$  is a well-defined nonlinear, causal map mapping  $R_e$  into  $R_e$ ;

(a3) 
$$\tilde{G}K: \mathcal{R}_e \rightarrow \mathcal{Y}_e \text{ and } (I+\tilde{G}KF)^{-1}: \mathcal{Y}_e \rightarrow \mathcal{Y}_e \text{ are } C^1 \text{ maps,}$$

then

$$\Delta H_{\text{vyr}} = \int_{0}^{1} \left[ \underbrace{\mathbf{I} + \mathbf{D} \left( \underbrace{\mathbf{G} \mathbf{K}}_{\text{c}} \right) \cdot \mathbf{F}}_{\text{c}} \right]^{-1} d\alpha \cdot \Delta H_{\text{c}}$$
, on  $\mathcal{R}_{\mathbf{e}}$  (III.4)

where the Fréchet derivative [13, p. 32]  $D(\tilde{G}K)$  is evaluated at  $(I+F\tilde{G}K)^{-1}(r+\alpha\Delta r)$  with  $\Delta r:=F\cdot\Delta H_{y_0}r(r)$ ,  $r\in\mathcal{R}_e$ , and  $\alpha\in[0,1]$ .

Proof of Theorem III.1: see Appendix.

When the map  $\widetilde{GK}$  is <u>linear</u>, theorem III.1 reduces to the following well-known result [10; 11, p. 24-26; 11 includes an extensive bibliography].

## Corollary III.1.1 (Linear case):

Under the conditions stated in theorem III.1, if in addition,  $\tilde{G}K$  is linear, then

$$\Delta H_{yr} = (I + \tilde{G}KF)^{-1} \cdot \Delta H_{y_0r}, \text{ on } \mathcal{R}_e$$
 (III.5)

Proof of Corollary III.1.1: Follows directly from the fact that  $D(\tilde{G}K) = \tilde{G}K$ , when  $\tilde{G}K$  is linear.

## Remarks III.1:

(a) Theorem III.1 indicates that for a class of plant perturbations  $\Delta G$ , if K and F are chosen such that  $\forall r \in \mathcal{R}_d$ ,  $(\subseteq \mathcal{R}_e)$ , the class of inputs of interest,

$$\left| \int_{0}^{1} \left[ \underbrace{\mathbf{I} + \mathbf{D} \left( \widetilde{\mathbf{G}} \mathbf{K} \right) \cdot \mathbf{F}}_{\mathbf{S}} \right]^{-1} d\alpha \cdot \Delta \mathbf{H}_{\mathbf{y}_{0} \mathbf{r}}(\mathbf{r}) \right| << \left| \Delta \mathbf{H}_{\mathbf{y}_{0} \mathbf{r}}(\mathbf{r}) \right|$$
 (III.6)

then, for such inputs  $r(\cdot)$ , the change of output  $(\Delta H_{yr}(r))$  in the feedback system S caused by the plant perturbation  $\Delta G$  is much smaller than the corresponding change in the open-loop system. Thus, with appropriate feedback design, the nonlinear closed-loop system can be made less vulnerable to the perturbations on the plant and hence performs more closely to the desired input-output map.

- (b) Equation (III.4) makes precise the concept (built upon linear cases) that if one makes the (linearized) inverse return difference small, then the closed-loop system is insensitive to the plant perturbations. Note that eqn. (III.4) states precisely where D(GK) has to be evaluated and along what path the linearized inverse return difference map should be integrated.
- (c) <u>Differential sensitivity</u>: suppose that G,  $H_{yr}$  are invertible, then eqn. (III.4) implies that, since  $\Delta H_{y0}^{r} = \Delta G \cdot G^{-1} \cdot GK(I + FGK)^{-1}$ ,

$$\Delta \mathbf{H}_{\mathbf{yr}} \cdot \mathbf{H}_{\mathbf{yr}}^{-1} = \int_{0}^{1} \left[ \mathbf{I} + \mathbf{D} \left( \widetilde{\mathbf{G}} \mathbf{K} \right) \cdot \mathbf{F} \right]^{-1} d\alpha \cdot \Delta \mathbf{G} \cdot \mathbf{G}^{-1}$$
(III.7)

For  $\Delta G$ , hence  $\Delta r$ , sufficiently small, (III.7) can be approximated by

The map [I+D(GK)·F]<sup>-1</sup> is thus a complete generalization of the classical differential sensitivity function (for linear time-invariant case, see, e.g. [14,15] for single-input single-output case, [10] for multi-input multi-output case; for some nonlinear case, see e.g. [11]).

(d) Consider the special case where G, K, F are represented by some transfer function matrices G(s), K(s), F(s), respectively. To achieve desensitization with respect to the given plant G(s) by feedback, one may design K(s) and F(s) so that the maximum singular value of the matrix  $[I+\widetilde{G}(j\omega)K(j\omega)F(j\omega)]^{-1}$  be much less than 1 over the frequency band of interest. Then, by Corollary III.1,  $|(\Delta H_{yr}r)(j\omega)|_2 << |(\Delta H_{y0}r)(j\omega)|_2$ , for any  $(\Delta H_{y0}r)(j\omega) \in \mathbb{C}^0$  over the frequency band of interest. Note that this requirement is not equivalent to the following: "over the frequency band of interest,  $|\lambda_i(j\omega)| >> 1$ ,  $\forall i$ , where  $\lambda_i(j\omega)$  is the i-th eigenvalue of  $I+\widetilde{G}(j\omega)K(j\omega)F(j\omega)$ ". Hence, in the linear, time-invariant, multi-input, multi-output case, plotting the eigenvalue loci of  $I+\widetilde{G}(j\omega)K(j\omega)F(j\omega)$  with  $\omega$  as a parameter, although useful for stability studies [16,17], does not have the same desensitization interpretation as in the single-input, single-output case (see e.g. [14; 15, Chap. 11]).

#### Discussion:

A. <u>Desensitization and Feedback Structure</u>: We note that one feedback structure is not necessarily superior to another one in terms of sensitivity with respect to the plant. We compare the nonlinear, feedback system S shown in Fig. I.1 and described by eqns. (I.1)-(I.9) with the nonlinear, multi-loop, feedback system shown in Fig. III.4 which consists of the

same plant G and nonlinear, causal operators  $K_1$ ,  $K_2$ ,  $K_1$  and  $K_2$ .

Suppose that the (nominal) closed-loop system input-output maps of these two nonlinear, feedback systems are identical, i.e.

$$\frac{GK(I+FGK)^{-1}}{GK(I+FGK)^{-1}} = \frac{GK_2(I+F_2GK_2)^{-1}K_1[I+F_1GK_2(I+F_2GK_2)^{-1}K_1]^{-1}}{GK(I+FGK)^{-1}}$$
(III.9)

Now we have the following result.

## Proposition III.2:

If GK, GK<sub>2</sub>, K<sub>1</sub> are <u>linear</u>, then eqn. (III.9) becomes

$$(I+GKF)^{-1}GK = [I+GK_2(F_2+K_1F_1)]^{-1} \cdot GK_2K_1$$
(III.10)

Proof of Proposition III.2: see Appendix.

With eqn. (III.10), the relation of the (differential) sensitivities of the two feedback structures shown in Fig. I.1 and Fig. III.4 is made clear in the following remarks.

#### Remarks III.2;

- (a) Suppose that, in addition, the maps F,  $F_1$  and  $F_2$  are also linear; then  $(I+GKF)^{-1}$  and  $[I+GK_2(F_2+K_1F_1)]^{-1}$  are the differential sensitivity functions (see equn. (III.8)) of the feedback systems shown in Fig. I.1 and Fig. III.4, respectively. Thus eqn. (III.10) exhibits a relation between these two differential sensitivity functions.
- (b) In the special case where G, K, F are represented by some scalar transfer functions, eqn. (III.10) reduces to

$$\frac{[1+g(s)k(s)f(s)]^{-1}}{[1+g(s)k_2(s)\cdot(f_2(s)+k_1(s)f_1(s))]^{-1}} = \frac{k_2(s)k_1(s)}{k(s)}$$
(III.11)

Hence, by appropriately designing k(s),  $k_1(s)$ ,  $k_2(s)$ , consistent with other requirements, we can make the feedback system shown in Fig. I.1 either more,

or less sensitive (to plant perturbations, over the frequency band of interest) than the one shown in Fig. 111.4.

(c) For a recent discussion of using local feedback to design an audio power amplifier, see [42].

## B. Desensitization and Feedback Perturbations

Proposition III.3 below derives the exact relation between the relative change in the closed-loop system input-output map (due to changes of the plant G and the feedback F) and the relative change in the feedback F, thus makes clear the tradeoff between the sensitivities of the closed-loop system with respect to the plant and to the feedback.

## Proposition III.3 (Desensitization and feedback perturbation)

Consider the <u>nonlinear</u>, feedback system S shown in Fig. I.1 and described by eqns. (I.1)-(I.9), where the plant G is perturbed and becomes  $\tilde{G}$ . Let the feedback map F be perturbed and become  $\tilde{F} := F + \Delta F$ . Let  $H_{yr} := \tilde{G}K(I + F\tilde{G}K)^{-1}$ :  $R_e + V_e$  and  $\tilde{H}_{yr} := \tilde{G}K(I + F\tilde{G}K)^{-1} = H_{yr} + \Delta H_{yr} : R_e + V_e$  be well-defined nonlinear, causal maps (thus  $\Delta H_{yr}$  includes the effect of plant and feedback perturbations). Suppose that

(a2) 
$$f^{-1}: R_e \rightarrow Y_e \text{ and } \tilde{H}_{yr}^{-1}: Y_e \rightarrow R_e \text{ are well-defined, causal maps;}$$

(a3) 
$$\tilde{G}K$$
 and  $(\tilde{I}+\tilde{F}\tilde{G}K)^{-1}$  are  $C^1$  maps.

Then

$$\Delta \mathbf{H}_{yr} \cdot \widetilde{\mathbf{H}}_{yr}^{-1} = \{ \int_{0}^{1} [\mathbf{I} + \mathbf{D}(\widetilde{\mathbf{G}}\mathbf{K}) \cdot \mathbf{F}]^{-1} d\alpha - \mathbf{I} \} \cdot \mathbf{F}^{-1} \cdot \Delta \mathbf{F}, \text{ on } \mathbf{Y}_{e}$$
 (III.12)

where the Fréchet derivative  $D(\widetilde{G}K)$  is evaluated at  $(I+F\widetilde{G}K)^{-1}(r+\alpha\Delta r)$  with  $\Delta r := -\Delta F \cdot \widetilde{H}_{yr} r$ ,  $r \in \mathcal{R}_e$  and  $\alpha \in [0,1]$ .

Proof of Proposition III.3: see Appendix.

## Remarks III.3:

- (a) Note that if we choose to desensitize the closed-loop system with respect to the plant G by making the inverse linearized return difference  $[I+D(\widetilde{GK})\cdot F]^{-1}$  "small" over some neighborhood of  $\mathcal{R}_{d,e}$ , the class of inputs of interest, as is suggested by eqn. (III.4), then  $\int_0^1 [I+D(\widetilde{GK})\cdot F]^{-1} d\alpha I \simeq -I$  and by eqn. (III.12),  $\Delta H_{yr} \cdot \widetilde{H}_{yr}^{-1} \simeq -F^{-1} \cdot \Delta F$  on  $\mathcal{U}_{d,e} := \widetilde{H}_{yr} \mathcal{R}_{d,e}$ . Thus, the relative change in  $H_{yr}$  is approximately equal to the relative change in the feedback F; consequently, the closed-loop system is insensitive to the plant perturbations but sensitive to the feedback perturbations.
- (b) In the special case where  $\tilde{\mathbb{G}}$ ,  $\tilde{\mathbb{K}}$ ,  $\tilde{\mathbb{F}}$  are represented by some scalar transfer functions, eqn. (III.12) reduces to the classical result: over the frequency band of interest, if  $|1+\tilde{\mathbb{E}}(j\omega)k(j\omega)f(j\omega)| >> 1$ , then  $\frac{\Delta h}{\Delta f/f} \simeq -1$ .
- (c) It is often advantageous to trade the insensitivity with respect to the feedback map F for the insensitivity with respect to the plant G, since the feedback F is usually operated at a low power level and hence can be built with inexpensive, high quality components.

## C. Desensitization and Instability

It is well-known (see e.g. [14, p. 141-143]) that, for most linear, time-invariant, single-input, single-output feedback systems, the closed-loop system stability requirement imposes an upper bound on the system loop gain, thus the stability requirement limits the achievable densitization of feedback.

We show below that such a constraint still holds for a large class of linear, time-invariant, multi-input multi-output systems.

Consider the feedback system S shown in Fig. I.1 where K, G and F are represented by kM  $\in \mathbb{R}$  ,  $G(s) \in \mathbb{R}(s)$  ,  $G(s) \in \mathbb{R}(s)$  ,  $G(s) \in \mathbb{R}(s)$  , respectively where g(s) , g(s)

achieve desensitization with respect to the given plant G(s) by feedback, we may choose  $k \in \mathbb{R}_+$  as large as possible so that the maximum singular value of the matrix  $[I+k\widetilde{G}(j\omega)M]^{-1}$  be much less than 1 over the frequency band of interest. However, stability considerations often impose an upper bound on the allowable k's. More precisely, we have the following proposition.

## Proposition III.4 (Desensitization and instability)

Consider the feedback system S shown in Fig. I.1, where K, G, F are represented by kM  $\in \mathbb{R}^{1 \times n_0}$ ,  $G(s) \in \mathbb{R}(s)^{n_0 \times n_1}$ ,  $I \in \mathbb{R}^{n_0 \times n_0}$ , respectively, with k > 0, and  $s \mapsto \det[I+k \ G(s)M]$  / constant. Assume that (6)  $\forall i = 1,2,\ldots,n_0$ , and  $\forall j = 1,2,\ldots,n_j$ ,

$$\partial[d_{ij}(s)] - \partial[n_{ij}(s)] \ge 3$$
 (III.14)

where  $\frac{n_{ij}}{d_{ij}}$  is the  $(i,j)^{th}$  element of  $G(s) \in \mathbb{R}(s)^{n \times n}$  and  $\partial[p(s)]$  denotes the degree of the polynomial p(s). Then, for  $k \in \mathbb{R}_+$  sufficiently large,  $\det[I+kG(s)\cdot M]$  has  $\mathring{C}_+$ -zeros with real parts which tends to  $+\infty$  as  $k + \infty$ .

Proof of Proposition III.4: see Appendix.

## Remarks III.4:

- (a) Since det[I+kG(s)M] is equal to the ratio of the closed-loop sytsem characteristic polynomial to the open-loop system characteristic polynomial (see e.g. [18]), Proposition III.4 states a condition under which the closed-loop system becomes unstable for k sufficiently large.
- (b) When  $n_i = n_o = 1$ , i.e., single-input single-output case, Proposition III.4 reduces to the classical result which can be easily proved by, e.g., the root locus method (see e.g. [14, p. 141-143]).

#### III.2 DISTURBANCE ATTENUATION

All physical systems operate in some environment where they are subjected to some "uncontrollable" disturbances. If we knew exactly these disturbances, then we could program (in advance) the system inputs such that the effect of these disturbances be cancelled out. However, in most real systems, there is either no complete knowledge of such disturbances (temperature, wind, wear, load changes, etc.) or the cost of measuring them and compensating for them is prohibitive; hence such "open-loop" design based on cancellation is not practical and we have to resort to feedback. The analysis below shows exactly what feedback can achieve for disturbances attenuation.

Consider the nonlinear, feedback system S shown in Fig. I.1 and described by eqns. (I.1)-(I.9) but subjected to some additive external disturbances as shown in Fig. III.5 where

- d<sub>i</sub>(\*) is the <u>system-input</u> <u>disturbance</u>,
- dg(.) is the plant-input disturbance,
- do(\*) is the system-output disturbance,
- df(.) is the feedback-path disturbance.

It is intuitively clear that, in general, an error-driven feedback system such as the one shown in Fig. III.5 cannot attenuate the input disturbances  $d_i(\cdot)$  and the feedback-path disturbance  $d_f(\cdot)$ , since such feedback systems cannot distinguish the system-input disturbance  $d_i(\cdot)$  from the system input  $r(\cdot)$  and the feedback path disturbance  $d_f(\cdot)$  from the system output  $y(\cdot)$ . Indeed, as seen from Fig. III.5, the error signal  $\tilde{e}(\cdot)$  is affected by the corrupting signals  $d_i$  and  $d_f$ ; hence  $\tilde{e}(\cdot)$  cannot drive the plant as desired (in some cases, judicious filtering may alleviate such problems). Nevertheless, we expect that feedback can reduce the effect of plant-input and system-output disturbances

on the system output; indeed such effects could be modeled by some appropriate plant perturbations, and their effect on the system output has been shown. in sec. III.1, to be reducible by feedback.

The propositions below <u>evaluate exactly</u> the effects of the disturbances  $d_1$ ,  $d_0$ ,  $d_f$ ,  $d_g$  on the system output  $y(\cdot)$ . Note that unlike the <u>linear</u> case, the effect of the disturbance  $d_{\alpha}$  ( $\alpha = i, o, f, g$ ) on the system output  $y(\cdot)$  is not given by  $H_{yd_{\alpha}}(d_{\alpha})$ , where  $H_{yd_{\alpha}}: d_{\alpha} \mapsto y$  is calculated when r and all the other disturbances are set to <u>zero</u>.

# Proposition III.5 (System-output disturbance, feedback-path disturbance and feedback)

Consider the nonlinear, feedback system shown in Fig. III.5 and described by eqns. (I.1)-(I.9). Let  $\tilde{Gu} := \tilde{Gu} + d_0$  and  $\tilde{Fy} := \tilde{F}(\tilde{y} + d_f)$ . Suppose that

(a1) 
$$F: \mathcal{Y}_e \to \mathcal{R}_p \text{ is } \underline{\text{linear}};$$

(a2) 
$$GK$$
 and  $(I+F\widetilde{G}K)^{-1}$  are  $C^1$  maps.

U.t.c.

(i) If 
$$d_0 \neq 0$$
 and  $d_1 = d_g = d_f = 0$ , then  $\forall r \in \mathcal{R}_e$ ,
$$\Delta y := \widetilde{G}K(I + \widetilde{F}\widetilde{G}K)^{-1}(r) - \widetilde{G}K(I + \widetilde{F}GK)^{-1}(r)$$

$$= \int_0^1 [I + D(GK) \cdot \widetilde{F}]^{-1} d\alpha \cdot d_0$$
(III.15)

where the Fréchet derivative D(GK) is evaluated at  $(I+FGK)^{-1}(r+\alpha\Delta r)$  with  $\Delta r = F \cdot d_{\Omega}$  and  $\alpha \in [0,1]$ .

(ii) if 
$$d_0 \neq 0$$
,  $d_f \neq 0$  and  $d_i = d_g = 0$ , then  $\forall r \in \mathcal{R}_e$ 

$$\Delta y := \widetilde{G}K(I + \widetilde{F}\widetilde{G}K)^{-1}(r) - \widetilde{G}K(I + \widetilde{F}\widetilde{G}K)^{-1}(r)$$

$$= \{\int_0^1 [I + D(GK) \cdot F]^{-1} d\alpha - I\} \cdot d_f \qquad (III.16)$$

where the Fréchet derivative D(GK) is evaluated at  $(I+FGK)^{-1}(r+\alpha\Delta r)$  with  $\Delta r = -F \cdot d$ , and  $\alpha \in [0,1]$ .

Proof of Proposition III.5: see Appendix.

## Proposition III.6: (Plant-input disturbance and feedback)

Consider the nonlinear, feedback system shown in Fig. III.5 and described by eqns. (I.1)-(I.9), where  $d_1=d_0=d_f=0$ . Let  $\widetilde{Gu}:=G(\widetilde{u}+d_g)$ . Suppose that

(a2) 
$$\tilde{C}K$$
,  $(\tilde{I}+\tilde{F}\tilde{G}K)^{-1}$  are  $C^1$  maps.

Then, ∀r ∈ R

$$\Delta y := \widetilde{G}K(I + F\widetilde{G}K)^{-1}(r) - GK(I + FGK)^{-1}(r)$$

$$= \{ \int_{0}^{1} [I + D(\widetilde{G}K) \cdot F]^{-1} d\alpha \} \cdot [\int_{0}^{1} DG(u + \beta d_{g}) d\beta \} \cdot d_{g}$$
(III.17)

where the Fréchet derivative  $D(\widetilde{GK})$  is evaluated at  $(I+F\widetilde{GK})^{-1}(r+\alpha\Delta r)$  with  $\Delta r = F[G(u+d_g)-G(u)]$ ,  $u := K(I+FGK)^{-1}r$ , and  $\alpha \in [0,1]$ .

Proof of Proposition III.6: see Appendix.

## Proposition III.7: (System-input disturbance and feedback)

Consider the nonlinear, feedback system shown in Fig. III.5 and described by eqns. (I.1)-(I.9), where  $d_g = d_o = d_f = 0$ . Suppose that F, GK and (I+FGK)<sup>-1</sup> are  $C^1$  maps, then  $\forall r \in \mathcal{R}_e$ ,

$$\Delta y := \frac{GK(I + FGK)^{-1}(r + d_{i}) - \frac{GK(I + FGK)^{-1}(r)}{GK(I + FGK)^{-1}(r)}$$

$$= \int_{0}^{I} D(GK) \left[ \frac{I + DF \cdot D(GK)}{I + DF \cdot D(GK)} \right]^{-1} d\alpha \cdot d_{i}$$
(III.18)

where the Fréchet derivative D(GK) is evaluated at  $(I+FGK)^{-1}(r+\alpha d_1)$  and DF is evaluated at  $GK[I+FGK]^{-1}(r+\alpha d_1)$  with  $\alpha \in [0,1]$ .

Proof of Proposition III.7: Follows directly from Taylor's expansion theorem [19, p. 190].

## Comments on Propositions III.5-III.7:

- (a) Eqns. (III.15)-(III.18) show exactly how feedback can reduce the effects of various external disturbances on the system output. Note that, by eqns. (III.15) and (III.16), simultaneous disturbance attenuation of  $d_0$  and  $d_1$  is, in general, impossible.
- (b) In the special case that G, K and F are linear, the effects of the disturbances  $d_0$ ,  $d_f$ ,  $d_g$ ,  $d_i$  on the system output reduce to  $(I+GKF)^{-1}d_0$ ,  $[(I+GKF)^{-1}-I]d_f$ ,  $(I+GKF)^{-1}Gd_g$  and  $GK(I+FGK)^{-1}d_i$ , respectively. Note that in this case, those disturbance-output maps are related by, with obvious notation

## III.3 LINEARIZING EFFECT [20] (7)

It is often required that the map from the system input to the system output is as linear as possible, e.g. HiFi amplifiers, telephone repeaters, measuring instruments, pen recorders, etc. How to design such a system which uses some inherently <u>nonlinear</u> plant is an important problem. From the discussion in section II, we know that if the feedback map F is <u>linear</u> and if the inverse loop gain is small, then the closed-loop system input-output map will be close to a linear map. Thus we expect that feedback has a linearizing effect on an otherwise nonlinear system. To make this idea precise, we first introduce the concept of <u>nonlinearity measure</u>.

## A Nonlinearity Measure

Let  $\mathcal{U}_e$  be an extended normed (input) space. Let  $\mathcal{V}_e$  be an extended semi-normed (output) space. Let  $\mathcal{N} = \{ \mathbb{N} \colon \mathcal{U}_e \to \mathcal{V}_e \mid , \mathbb{N} \text{ is causal, nonlinear} \}$ .

Let  $\mathcal{L} = \{\underline{L} \colon \mathcal{U}_e \to \mathcal{Y}_e | \underline{L} \text{ is causal, linear} \}$ . Now consider  $\underline{N} \in \mathcal{N} \text{ and } \mathcal{N} \subset \mathcal{U}_e$ , a set of inputs of interest. Intuitively, the degree of nonlinearity of  $\underline{N}$ , when  $\underline{N}$  is driven by  $\underline{u} \in \mathcal{V}$ , may be measured by the error  $|\underline{N}\underline{u} - \underline{L}\underline{u}|$  for  $\underline{u} \in \mathcal{V}$ , where  $\underline{L} \in \mathcal{L}$  is a "best" linear approximation of  $\underline{N}$  over  $\mathcal{V}$ . More precisely, we introduce the following definition.

## Definition III.8 (Nonlinearity measure)

Let  $N \in \mathcal{N}$ ,  $\mathcal{V} \subset \mathcal{U}_e$  and  $T \in \mathcal{T}$ . The <u>nonlinearity measure</u> of N over  $\mathcal{V}$  with respect to T is the non-negative real number defined by

$$\delta_{\mathbf{T}}(\mathbf{N}, \mathcal{O}) := \inf \sup_{\mathbf{I} \in \mathcal{L}} |\mathbf{N}\mathbf{u} - \mathbf{L}\mathbf{u}|_{\mathbf{T}}. \tag{III.20}$$

## Remarks III.8:

- (a)  $\underline{L}^* \in \mathcal{L}$  is thus said to be a <u>best linear approximation</u> of N over V iff  $\underline{L}^*$  is a minimizer of (III.20), i.e.,  $\delta_{\underline{T}}(N,Y) = \sup_{\underline{u} \in Y} |N\underline{u} \underline{L}^*\underline{u}|_{\underline{T}}$ .
- (b) In the case where  $V_e$  is a <u>seminormed</u> space, we then have the nonlinearity measure of N over V with respect to  $\sup \mathcal{T}$  (typically,  $\sup \mathcal{T} = \infty$ ) and eqn. (III.20) becomes  $\delta(N,V) = \inf \sup_{n \in \mathbb{N}} |Nu-Lu|$ .
- (c) The well-known describing function (see e.g. [21,22]) is the best linear approximation of a nonlinear operator with respect to our nonlinearity measure (III.20) provided that  $\mathcal{V}$ , the class of inputs, is suitably defined. Recall that the criterion which the describing function method uses to find a best linear approximation L of a nonlinear system N is to minimize the mean square error  $\lim_{T\to\infty} \frac{1}{T} \int_0^T [(\mathrm{Nu})(t) (\mathrm{Lu})(t)]^2 dt \text{ over a class of inputs u(·) (usually u(t) = a \sin \omega t, a > 0, \omega > 0, and thus L depends on the parameters a, \omega). To see the relation between the describing function and our nonlinearity measure, let a > 0, <math>\omega$  > 0 be given, let  $\mathcal{V}$  be the singleton (a sin  $\omega$ t) and  $\mathcal{U} = \{y(\cdot): \mathbb{R}_+ \to \mathbb{R}^{n_0} | y(\cdot) \text{ is asymptotically } \frac{2\pi}{\omega} \text{ periodic}^{(8)} \}$  be equipped with

the semi-norm  $|y|:=[\lim_{T\to\infty}\frac{1}{\tau}\int_0^\tau|y(t)|^2dt]^{1/2}$ , then a best linear approximation to the nonlinear system N according to our definition III.8 is a minimizer of  $\lim_{T\to\infty}\frac{1}{\tau}\int_0^\tau[(\mathrm{Nu})(t)-(\mathrm{Lu})(t)]^2dt$  which is precisely the describing function of N with respect to the inputs  $\mathrm{u}(t)=\mathrm{a}\sin\omega t$ . Note that in this case, the minimizer of (III.20) (i.e. the describing function of N with respect to  $\mathrm{u}(\cdot)$ ) is parametrized by a and  $\omega$ .

- (d) With the framework of extended spaces, we can discuss the nonlinearity measure of a nonlinear system over a bounded time interval, say, [0,T]. Note that a <u>nonlinear</u> system N may have its nonlinearity measure  $\delta_T(N,\mathcal{O}) = 0$ ,  $\forall T \leq T^* \in \mathcal{T}$ , but  $\delta_T(N,\mathcal{O}) \neq 0$  for  $T > T^*$ , simply because N is operating within the linear range of its characteristics before time  $T^*$ .
- (e) At the cost of some complication, the class of nonlinear operators under consideration can be extended to include the nonlinear dynamical relations.
- (f) Other nonlinearity measures may be defined, e.g., we can define  $\delta_T(\tilde{N}, \gamma) = \inf_{\tilde{L} \in \mathcal{L}} \sup_{u \in \gamma} \frac{\left| \tilde{N}u \tilde{L}u \right|_T}{\left| u \right|_T} \quad \text{Note that such nonlinearity measure does}$

satisfy all the remarks mentioned above and all the properties stated below. However, we have not been able to obtain results similar to the Theorem III.14 below.

## Properties of the Nonlinearity Measure $\delta_{T}(N, \mathcal{Y})$

#### Proposition III.9:

If 
$$N_2 = N_1 + L_1$$
 for some  $L_1 \in \mathcal{L}$ , then  $\delta_T(N_1, \mathcal{V}) = \delta_T(N_2, \mathcal{V})$ ,  $\forall T \in \mathcal{T}$ ,  $\forall \mathcal{V} \subset \mathcal{U}_e$ .

## Proposition III.10:

If 
$$\mathcal{V}_1 \subseteq \mathcal{V}_2 \subseteq \mathcal{U}_e$$
, then  $\delta_T(N,\mathcal{V}_1) \leq \delta_T(N,\mathcal{V}_2)$ ,  $\forall T \in \mathcal{T}$ .

## Proposition III.11:

Suppose that  $\forall T \in \mathcal{T}$ ,  $P_T \mathcal{Y}_e$  is a normed space and that N0 = 0. U.t.c. if N is Frechet differentiable (9) at 0, then  $\forall T \in \mathcal{T}$ ,

$$0 \leq \delta_{\mathbf{T}}(\tilde{\mathbf{N}}, \tilde{\mathbf{B}}_{\mathbf{T}}(0; \beta)) \leq \sup_{\mathbf{U} \in \tilde{\mathbf{B}}_{\mathbf{T}}(0; \beta)} |\underbrace{\mathbf{N}\mathbf{U} - \mathbf{D}\mathbf{N}(0) \cdot \mathbf{u}}_{\mathbf{T}}|_{\mathbf{T}} + 0, \text{ as } \beta + 0$$
 (III.21)

where  $\overline{B}_T(0;\beta) := \{u \in \mathcal{U}_e | |u|_T \le \beta\}$  and DN(0) denotes the Fréchet derivative of N at 0.

## Proposition III.12:

Let  $V \subset \mathcal{U}_e$  be the set of inputs of interest. If for some  $\underline{L} \in \mathcal{L}$ ,  $\underline{N}u = \underline{L}u$ ,  $\underline{V}u \in \mathcal{V}$ , then  $\delta_{\underline{T}}(\underline{N}, \mathcal{V}) = 0$ ,  $\underline{V}T \in \mathcal{T}$ . In particular, if  $\underline{N} \in \mathcal{L}$ , then  $\delta_{\underline{T}}(\underline{N}, \mathcal{V}) = 0$ ,  $\underline{V}T \in \mathcal{T}$ ,  $\underline{V}V \subset \mathcal{U}_e$ .

## Proposition III.13:

Let  $\mathcal{V} \subset \mathcal{U}_e$  be the set of inputs of interest. Let  $\mathcal{L}$  be specialized into the class of continuous,  $^{(10)}$  linear, causal operators mapping  $\mathcal{U}_e$  into  $\mathcal{Y}_e$ . Suppose that

- (al)  $v_T \in \mathcal{T}$ ,  $P_T v_e$  is a Banach space;
- (a2)  $\forall T \in \mathcal{T}, \ \mathcal{V} \subset \mathcal{U}_e \text{ is bounded, i.e. } \sup_{u \in \mathcal{V}} |u|_T < \infty;$
- (a3)  $\forall T \in \mathcal{T}, \ \exists \beta > 0 \ \text{ such that } \mathcal{V} \supset \widetilde{B}_{T}(0;\beta) := \{u \in \mathcal{U}_{e} \ \big| \ \big| \ u \big|_{T} \leq \beta \}.$

U.t.c. if for some  $T \in \mathcal{T}$ ,  $\delta_T(N,\mathcal{V}) = 0$ , then,  $\exists L^* \in \mathcal{L}$  such that

$$|\mathbf{N}\mathbf{u}-\mathbf{L}^{*}\mathbf{u}|_{\mathbf{T}}=0, \ \forall \mathbf{u}\in \mathcal{V}. \tag{III.22}$$

Proofs of Propositions III.9-III.13: see Appendix.

## Comments on Propositions III.9-III.13:

(a) Proposition III.9 states the obvious fact that if two nonlinear, causal

operators differ by a linear causal operator, then they must have the same nonlinearity measure. It is also intuitively clear, from a perturbational viewpoint, that if a linear, causal operator is subject to some nonlinear causal perturbation, then the nonlinearity measure of the perturbed nonlinear, causal operator must be the same as that of the nonlinear perturbation.

- (b) Proposition III.10 emphasizes the fact that the nonlinearity measure depends on the class of inputs we are considering: the larger the class of inputs we consider, the greater the nonlinearity measure of operator N.
- (c) Proposition III.11 is another way of stating the well-known fact that (since N0 = 0) the <u>best local linear approximation</u> of a Fréchet differentiable nonlinear operator N at the operating point 0 is the Fréchet derivative of N at 0. Note that by eqn. (III.21),  $\delta_{T}(N, \overline{\beta}_{T}(0; \beta)) \rightarrow 0$  as  $\beta \rightarrow 0$ , i.e. N behaves locally like a linear operator as we expected.
- (d) Proposition III.12 states that  $\delta_{T}(N,V)$  satisfies the natural requirement for a nonlinearity measure, namely, if N behaves as a linear causal operator over the class of inputs V in the time interval  $[0,T] \subseteq \mathcal{F}$ , then  $\delta_{T}(N,V) = 0$ .
- (e) With some mild technical assumptions, proposition III.13 establishes the following desirable property of  $\delta_{\mathbf{T}}(N,\mathcal{V})$ : if  $\delta_{\mathbf{T}}(N,\mathcal{V})=0$ , then N behaves like a linear, causal operator over  $\mathcal{V}$  in the time interval  $[0,T]\subset\mathcal{T}$ . Note that if  $\delta_{\mathbf{T}}(N,\mathcal{V})=0$ , then  $\delta_{\mathbf{T}}(N,\mathcal{V})=0$ , then  $\delta_{\mathbf{T}}(N,\mathcal{V})=0$ ,  $\nabla T$

# Linearizing Effect of Feedback

With the nonlinearity measure defined in eqn. (III.20), we now can make precise the idea that feedback has a linearizing effect on an otherwise nonlinear system.

Note that the nonlinearity measure defined in (III.20) allows us to compare nonlinear systems by their degree of nonlinearity. However, a meaningful

comparison requires careful choice of the sets of inputs since the nonlinearity measure depends on the set of inputs we are considering. From an engineering point of view, we are interested in comparing systems which produce
desired outputs (e.g., signals within certain frequency band or dynamical
range). Hence in the following discussion of the linearizing effect of
feedback, we shall compare the nonlinearity of measure of a nonlinear plant
and of a feedback system which includes such a plant; we shall choose a set
of inputs for each system so that both systems produce the same set of
desired outputs.

Consider the nonlinear feedback system S shown in Fig. I.l and described by eqns. (I.l)-(I.9), except now that

Let 
$$\mathcal{Y}_{d,e} \subset \mathcal{Y}_{e}$$
 be the set of desired outputs. Let  $\mathcal{R}_{d,e} \subset \mathcal{R}_{e}$  be the set of system-inputs  $r(\cdot)$  such that  $\mathcal{Y}_{yr} \mathcal{R}_{d,e} = \mathcal{Y}_{d,e}$ .

Let  $\mathcal{U}_{d,e} \subset \mathcal{U}_{e}$  be the set of plant-inputs  $u(\cdot)$  such that
$$\mathcal{C}\mathcal{U}_{d,e} = \mathcal{Y}_{d,e}.$$

(III.24)

Now we have the following theorem:

# Theorem III.14 (Linearizing effect of feedback)

Consider the nonlinear, feedback system S shown in Fig. I.1 and described by eqns. (I.1)-(I.9) and (III.23)-(III.24). For some  $T \in \mathcal{T}$ , let  $L_G^* \in \mathcal{L}$  be a best linear approximation to G, i.e.

$$\delta_{\mathbf{T}}(G, \mathcal{U}_{\mathbf{d}, \mathbf{e}}) = \sup_{\mathbf{u} \in \mathcal{U}_{\mathbf{d}, \mathbf{e}}} \frac{|G\mathbf{u} - \mathbf{L}_{\mathbf{G}}^*\mathbf{u}|}{\|\mathbf{u}\|_{\mathbf{d}, \mathbf{e}}}$$
(III.25)

Assume that  $f: \mathcal{Y}_e \to \mathcal{R}_e$  and  $K: \mathcal{R}_e \to \mathcal{U}_e$  are <u>linear</u>, causal and that the linear map  $(I+L_{G}^*KF)$  has a causal inverse, then

$$\delta_{\mathbf{T}}(\mathbf{H}_{\mathbf{yr}}, \mathcal{R}_{\mathbf{d}, \mathbf{e}}) \leq \rho \cdot \delta_{\mathbf{T}}(\mathbf{G}, \mathcal{U}_{\mathbf{d}, \mathbf{e}})$$
 (III.26)

where  $H_{yr} := GK(I+FGK)^{-1}$  is the closed-loop input-output map and

$$\rho := \sup_{\substack{y \in \tilde{Q}_{L} \\ y_{T} \neq 0}} \frac{\left| \left( 1 + L_{G}^{*} KF \right)^{-1} y \right|_{T}}{\left| y \right|_{T}}$$

$$(111.27)$$

with 
$$\tilde{Y}_e := (\tilde{G} \cdot L_{\tilde{G}}^*) u_{d,e}$$
.

Proof of Theorem ICI.14: see Appendix.

### Remarks III.14:

- (a) In a design problem, given some  $G \in \mathcal{H}$  together with its best linear approximation  $L_G^*$  over  $\mathcal{U}_{d,e}$  with respect to some  $T \in \mathcal{T}$ , if one designs K, F such that  $\rho$  be much less than 1, consistent with other requirements, then by eqn. (III.26),  $\delta_T(H_{yr}, \mathcal{R}_{d,e}) << \delta_T(G, \mathcal{U}_{d,e})$ , i.e. for the class of inputs under consideration and for the time interval of interest, the closed-loop system is much closer to a linear system than G itself. This result clearly exhibits the linearizing effect of feedback.
- (b) Note that  $\rho$  is defined via the inverse linearized return difference operator  $(I+L_G^*KF)^{-1}$  (when we break the loop after the plant G): since the nonlinear plant G can be thought as a linear plant  $L_G^*$  being subject to some nonlinear perturbation  $G-L_G^*$ , and we know that (see eqn. (III.8) or [43]) as a first order approximation, the effect of a nonlinear perturbation on the otherwise linear closed-loop system is reduced by the factor  $(I+L_G^*KF)^{-1}$  by feedback.

  (c) If  $L_G^*$ , K, F are linear and time-invariant, thus represented by transfer function matrices  $L_G^*(j\omega)$ ,  $K(j\omega)$ ,  $F(j\omega)$ , respectively), then  $\rho << 1$  if the maximum singular value of  $[I+L_G^*(j\omega)K(j\omega)F(j\omega)]^{-1}$  is small over the frequencies of interest.

# Example III.1 (Single-input single-output memoryless system)

Consider the nonlinear, feedback system S shown in Fig. I.1, where G is characterized by the piecewise-linear function shown in Fig. III.6, K and F are represented by constant gains 10 and 1, respectively. It is easy to show that the closed-loop input-output map H is characterized by the piecewise-linear function shown in Fig. III.7. Now let us consider the case where  $\mathcal{U}_{d,e} = \{y(\cdot): \mathbb{R}_+ \to \mathbb{R} | |y|_{\infty} \le 0.8 \}$ , then the corresponding  $\mathcal{U}_{d,e} = \{u(\cdot): d,e\}$  $\mathbb{R}_{+} \to \mathbb{R} ||\mathbf{u}|_{\infty} \le 1.2$  and  $\mathbb{R}_{d,e} = \{r: \mathbb{R}_{+} \to \mathbb{R} ||r|_{\infty} \le 0.92\}$ . A straightforward minmax calculation shows that the best linear approximation  $L_G^*$  of G is a constant gain of 0.6 and the nonlinearity measure of G is  $\delta_T(G,\mathcal{U}_{d,e}) = 0.12$ ,  $\forall T \in \mathcal{T}$ ; more precisely,  $\delta_{T}(\mathcal{C}, \mathcal{U}_{d,e}) = \sup_{\mathbf{u} \in \mathcal{U}_{d,e}} |\mathbf{Gu} - 0.6\mathbf{u}|_{\infty,T} = 0.12$ . Similarly,  $\delta_{T}(\mathbf{H}_{vyr}, \mathcal{R}_{d,e}) = \sup_{\mathbf{r} \in \mathcal{R}_{d,e}} |\mathbf{H}_{yr}\mathbf{r} - \frac{6}{7}\mathbf{r}|_{\infty,T} = \frac{0.12}{7}$ ,  $\mathbf{v}\mathbf{T} \in \mathcal{T}$ . Thus the nonlinearity measure of G has been reduced by 7 by feedback. Note that  $\rho = \frac{1}{1+0.6\times10} = \frac{1}{7}$ i.e. for this example, the equality holds in eqn. (III.26). The best linear approximations of G and H are shown, by the broken lines, in Fig. III.6 and Fig. III.7, respectively. To further illustrate the linearizing effect of feedback, we drive the nonlinear plant G with u = 1.2 sin wt and the closedloop system  $GK(I+FGK)^{-1}$  with  $r = 0.92 \sin \omega t$ . The corresponding (open-loop system) output  $y_0$  and the (closed-loop) output y are shown in Fig. III.8.

In general, it is quite difficult to calculate the nonlinearity measure  $\delta_{\rm T}$  of a nonlinear <u>dynamical</u> system and to obtain the best linear approximation of such a system. However, for a given nonlinear plant  ${\tt G}$ , we may illustrate the linearizing effect of feedback by computing the closed-loop system output with respect to several different compensator gains while the closed-loop system is driven by some test signals. Examples II.1 and II.2 in section II clearly exhibit the linearizing effect of feedback on nonlinear dynamical systems. Note that the higher the compensator gain is, the more linear the

closed-loop system appears to be as we expected from the result of theorem III.14 (since  $\rho$  defined in eqn. (III.27) decreases as the gain of K increases).

# III.4 ASYMPTOTIC TRACKING AND DISTURBANCE REJECTION

One important application of feedback in control is the servomechanism design which aims at asymptotic tracking and asymptotic disturbance rejection. Let us consider the asymptotic tracking problem. From the discussion of generalized Black's formula in sec. II, we know that if we let F = I in the nonlinear, feedback system S shown in Fig. I.1 and if we make the "forward-path gain" sufficiently large, then, asymptotically, the output  $y(\cdot)$  will be approximately equal to the system input  $r(\cdot)$ . Thus we might intuitively guess that we can obtain perfect asymptotic tracking, i.e. zero steady state error, by requiring the "forward-path gain" be infinite at the frequency of the system inputs. This turns out to be correct. Indeed in the classical servomechanism design [23], an integrator is required in the compensator in order that the system output track step signals with zero steady-state error. For multi-input, multi-output systems, such a design principle has also been proven to be correct for linear (see e.g. [24,25,26]) as well as nonlinear cases (see e.g. [27]).

# III.5 STABILIZATION

Stability is a primary concern of engineers since an unstable system is obviously useless. However, there are many inherently unstable systems such as rocket booster systems, nuclear reactors, some chemical reactors, etc. which are useful in practice and hence must be stabilized. Note that any open-loop stabilization scheme is doomed to failure in practice because it is based on some kind of cancellation which will eventually fail as a

result of changes in element characteristics, effects of environment, etc.

Hence feedback seems to be the only way out.

Many researchers have studied the use of feedback in stabilizing unstable systems. For lumped, linear, time-invariant systems, it has been shown that a constant state feedback (see e.g. [28,29]) or a dynamical output feedback (see e.g. [30]) can stabilize an unstable system; recently, Youla et. al. [31] gave a characterization of all stabilizing feedback controllers. For lumped, linear, time-varying systems, a time-varying state feedback can be obtained (see e.g. [32,38,39,40,41]) to stabilize an unstable system. For distributed, linear, time-invariant systems, state feedback can also stabilize unstable systems (see e.g. [33;34, chap. 14]). In contrast to linear cases, little is known about the nonlinear case except for some limiting cases. It should also be pointed out that little is known about how to proceed with the design of a, say, state feedback, stabilization scheme so that the resulting closed-loop system stability is very <u>robust</u> with respect to changes in the plant and/or the feedback map. In this aspect, for the linear timeinvariant case, singular value analysis has provided some valuable information (see e.g. [44]).

#### IV. CONCLUSION

This paper has treated the fundamental properties of feedback for nonlinear, time-varying, multi-input, multi-output, distributed systems. We observed that the classical Black formula does not depend on the linearity nor the time-invariance assumptions; we used the input-output description of nonlinear systems to actually generalize Black's formula to the nonlinear case (Theorems II.1 to II.3). Our analysis then established achievable advantages of feedback, familiar to feedback engineers, for nonlinear systems

tion, linearizing, asymptotic tracking and disturbance rejection by feedback

in nonlinear systems.

The benefits of feedback do not come without limitations or tradeoffs as propositions III.2-III.5 showed: proposition III.2 showed the relation between desensitization and feedback structure; proposition III.3 showed the tradeoff between the sensitivities of a nonlinear, feedback system with respect to the perturbations on the plant and on the feedback map; proposition III.4 showed that stability requirements restrict the achievable desensitization effect by feedback; proposition III.5 showed the tradeoff between the output disturbance attenuation and the feedback-path disturbance attenuation. Note that, due to the lack of appropriate language and tools, we did not discuss the tradeoff between the gain and bandwidth. Consequently, we did not explore the limitations on the benefits achievable by feedback imposed by the plant with fixed gain and and bandwidth (in the context of the Bode design method [45], the gain-bandwidth of a given active device imposes an upper bound on the return difference over a specified bandwidth).

Also note that we have only treated deterministic systems, i.e. no stochastic models were introduced for noise, perturbations, element variations, etc. Thus, in particular, we did not mention the well-known limitation on compensator gain caused by noise.

In clarifying the features of <u>nonlinear</u> systems that are required for feedback to be advantageous, this paper will help engineers obtain better understanding of nonlinear, feedback systems.

And There was a state what we had been the

#### REFERENCES

- [1] O. Mayr, The Origins of Feedback Control, Cambridge, MA: M.I.T. Press, 1970.
- [2] H. W. Bode, "Feedback—the history of an idea," Symposium on Active

  Networks and Feedback Systems, Polytechnic Institute of

  Brooklyn, Polytechnic Press, 1960, pp. 1-17.
- [3] H. S. Black, "Stabilized feedback amplifiers," The Bell System
  Technical Journal, Jan. 1934, pp. 1-18.
- [4] H. S. Black, "Inventing the negative feedback amplifier," <u>IEEE</u>

  Spectrum, Dec. 1977, pp. 55-60.
- [5] I. W. Sandberg, "Some results on the theory of physical systems governed by nonlinear functional equations," <u>The Bell System</u> <u>Technical Journal</u>, May 1965, pp. 871-898.
- [6] G. Zames, "On the input-output stability of time-varying nonlinear feedback systems, Parts I and II," <u>IEEE Trans. Aut. Contr.</u> Vol. AC-11, Nos. 2 & 3, 1966, pp. 228-238 and pp. 465-476.
- [7] J. C. Willems, <u>The Analysis of Feedback Systems</u>, Cambridge, MA:
  M.I.T. Press, 1971.
- [8] C. A. Desoer and M. Vidyasagar, <u>Feedback Systems: Input-Output</u>

  Properties, New York: Academic Press, 1975.
- [9] H. H. Rosenbrock, <u>Computer-Aided Control System Design</u>, New York:

  Academic Press, 1974.
- [10] J. B. Cruz and W. R. Perkins, "A new approach to the sensitivity problem in multivariable feedback system design," <u>IEEE Trans.</u>

  <u>Aut. Contr. Vol. AC-9</u>, July 1964, pp. 216-223.
- [11] W. R. Perkins, "Sensitivity Analysis," in <u>Feedback Systems</u> (ed. by J. B. Cruz), New York: McGraw-Hill, 1972, chap. 2.

- [12] C. A. Desoer, "Perturbation in the I/O map of a nonlinear feedback system caused by large plant perturbation," <u>Journal of the</u>

  Franklin Institute, Vol. 306, No. 3, pp. 225-237, Sept. 1978.
- [13] R. H. Martin, Nonlinear Operators and Differential Equations in
  Banach Spaces, New York: John Wiley and Sons, 1976.
- [14] I. M. Horowitz, <u>Synthesis of Feedback Systems</u>, New York: Academic Press, 1963.
- [15] E. S. Kuh and R. A. Rohrer, <u>Theory of Linear Active Networks</u>,

  San Francisco: Holden-Day Inc., 1967.
- [16] J. F. Barman and J. Katzenelson, "A generalized Nyquist-type stability criterion for multivariable feedback systems," <u>Int. J. Contr.</u> Vol. 20, No. 4, 1974, pp. 593-622.
- [17] A. G. J. MacFarlane and I. Postlethwaite, "The generalized stability criterion and multivariable root loci," <u>Int. J. Contr.</u>, Vol. 25, No. 1, 1977, pp. 81-127.
- [18] C. A. Desoer and W. S. Chan, "The feedback interconnection of lumped linear time-invariant systems," <u>Journal of the Franklin</u> <u>Institute</u>, Vol. 300, Nos. 5 and 6, Nov.-Dec. 1975, pp. 335-351.
- [19] J. Dieudonné, <u>Foundations of Modern Analysis</u>, New York: Academic Press, 1969.
- [20] C. A. Desoer, Y. T. Wang and A. N. Payne, "Linearizing effect of feedback on nonlinear dynamical systems," 16th Annual Allerton Conference on Communication, Control, and Computing, 1978, Oct. 4-6, pp. 521-528.
- [21] M. Vidyasagar, Nonlinear System Analysis, New Jersey: Prentice-Hall, 1978.

- [22] A. Gelb and W. E. Vander Velde, <u>Multi-Input Describing Functions and Nonlinear System Design</u>, New York: McGraw-Hill, 1968.
- [23] H. M. James, N. B. Nichols and R. S. Phillips, eds., <u>Theory of</u>

  Servomechanisms, New York: McGraw-Hill, 1947.
- [24] E. J. Davison, "The robust control of a servomechanism problem for linear time-invariant multivariable systems," <u>IEEE Trans. Aut.</u> Contr., Vol. AC-21, No. 1, 1976, pp. 25-34.
- [25] B. A. Francis, "The multivariable servomechanism problem from the input-output viewpoint," <u>IEEE Trans. Aut. Contr.</u>, Vol. AC-22, No. 3, 1977, pp. 322-328.
- [26] C. A. Desoer and Y. T. Wang, "Linear time-invariant robust servomechanism problem: a self-contained exposition," to appear in <u>Control and Dynamics</u>, Vol. XVI, ed. by C. T. Leondes, New York: Academic Press; also Electronics Research Lab/UC Berkeley, Memo ERL 77/50.
- [27] C. A. Desoer and Y. T. Wang, "The robust nonlinear servomechanism problem," to appear in <a href="Int.J. Contr.">Int. J. Contr.</a>, 17th IEEE Conference on Decision and Control, 1979; Jan. 10-12, pp. 7-11.
- [28] W. M. Wonham, "On pole assignment in multi-input controllable linear systems," <u>IEEE Trans. Aut. Contr.</u>, Vol. AC-12, No. 6, 1967, pp. 660-665.
- [29] B. D. O. Anderson and J. B. Moore, <u>Linear Optimal Control</u>, New Jersey: Prentice-Hall, 1971.
- [30] F. M. Brash Jr. and J. B. Pearson, "Pole placement using dynamic compensators," <u>IEEE Trans. Aut. Contr.</u>, Vol. AC-15, No. 1, 1970, pp. 34-43.
- [31] D. C. Youla, J. J. Bongiorno Jr. and H. A. Jabr, "Modern Wiener-Hopf design of optimal controller, Part 2: the multivariable case,"

  IEEE Trans. Aut. Contr., Vol. AC-21, No. 3, 1976, pp. 319-338.

- [32] J. C. Willems and S. K. Mitter, "Controllability, observability, pole allocation and state reconstruction," <u>IEEE Trans. Aut.</u> <u>Contr.</u>, Vol. AC-16, No. 6, 1971, pp. 582-595.
- [33] E. W. Kamen, "An operator theory of linear functional differential equations," J. of Diff. Eqn., Vol. 27, No. 2, 1978, pp. 274-297.
- [34] R. F. Curtain and A. J. Pritchard, <u>Functional Analysis in Modern</u>
  Applied Mathematics, New York: Academic Press, 1977.
- [35] E. Hille, Analytic Function Theory, Vol. 2, Boston, MA: Ginn & Co., 1962.
- [36] H. Kwakernaak, "Asymptotic root loci of multivariable linear optimal regulators," IEEE Trans. Aut. Contr., Vol. AC-21, No. 3, 1976, pp. 378-382.
- [37] T. E. Fortmann and K. L. Hitz, An Introduction to Linear Control

  Systems, New York: Marcel Dekker, 1977.
- [38] W. H. Kwon and A. E. Pearson, "A modified quadratic cost problem and feedback stabilization of a linear system," <u>IEEE Trans</u>. <u>Aut. Contr.</u>, Vol. AC-22, No. 5, 1977, pp. 838-842.
- [39] W. H. Kwon and A. E. Pearson, "On feedback stabilization of timevarying discrete linear systems," <u>IEEE Trans. Aut. Contr.</u>, Vol. AC-23, No. 3, 1978, pp. 479-481.
- [40] R. Conti, Linear Differential Equations and Control, London:
  Academic Press, 1976.
- [41] V. H. L. Cheng, "Stabilization of continuous-time and discrete-time linear time-varying systems," M.S. Thesis, U.C. Berkeley, 1978.
- [42] E. M. Cherry, "A new result in negative-feedback theory, and its application to audio power amplifiers," <u>Int. J. of Circuit Theory and Applications</u>, Vol. 6, No. 3, 1978, pp. 265-288.

- [43] J. B. Cruz, Jr., "Effect of feedback on signal distortion in nonlinear systems," in <u>Feedback Systems</u> (ed. by J. B. Cruz, Jr.), New York: McGraw Hill, 1972, Chap. 3.
- [44] J. C. Doyle, "Robustness of multiloop linear feedback systems,"
  17th IEEE Conference on Decision and Control, 1979, Jan. 10-12, pp. 12-18.
- [45] H. W. Bode, Network analysis and feedback amplifier design, Princeton, New Jersey: D. Van Nostrand Company, Inc., 1945.
- [46] G. Zames, "Functional analysis applied to nonlinear feedback systems," <u>IEEE Trans. Circuit Theory</u>, Vol. CT-10, pp. 392-404, Sept. 1963.

#### Proof of Theorem II. 2:

Note that

$$H_{yr} := \frac{GK(I+FGK)^{-1}}{FGK(I+FGK)^{-1}}$$
 (since F is invertible)
$$= \frac{F^{-1}FGK(I+FGK)^{-1}}{FGK(I+(FGK)^{-1})(FGK)}$$
 (since FGK is invertible)
$$= F^{-1}[I+(FGK)^{-1}]^{-1}$$
 (A.1)

To estimate  $\mathbb{F}_{yr}$  for  $r \in \mathbb{K}_{d,e}$ , we consider first  $z := [I+(FGK)^{-1}]^{-1}r$ . To obtain for any  $T \in \mathcal{T}$ ,  $z_T$ , note that  $r = [I+(FGK)^{-1}]z$ , hence  $z_T = r_T - (FGK)^{-1}z_T$ . Now the Lipschitz constant [13, p. 63] of the right hand side, over  $\mathcal{N}(\mathbb{K}_{d,e})$ , is  $\tilde{\gamma}_T[(FGK)^{-1}] < 1$ . By assumption (a3), the successive approximations starting with  $z_T = r$  remain in  $\mathcal{N}(\mathbb{K}_{d,e})$  forever; since the contraction constant is < 1, we have that

$$\left|z-r\right|_{T} \leq \frac{\left|\left(FGK\right)^{-1}r\right|_{T}}{1-\widetilde{\gamma}_{T}\left[\left(FGK\right)^{-1}\right]} \tag{A.2}$$

Thus, for each T∈T,

$$\begin{aligned} \left| \underbrace{\mathbb{E}_{yr} \mathbf{r} - \mathbf{F}^{-1} \mathbf{r}}_{T} \right|_{T} &= \left| \mathbf{F}^{-1} (\mathbf{r} - \mathbf{e}) - \mathbf{F}^{-1} \mathbf{r} \right|_{T} \\ &= \left| \mathbf{F}^{-1} \left[ \mathbf{I} + (\mathbf{F} \mathbf{G} \mathbf{K})^{-1} \right]^{-1} \mathbf{r} - \mathbf{F}^{-1} \mathbf{r} \right|_{T} \\ &\leq \lambda (\mathbf{F}^{-1}) \left| \left[ \mathbf{I} + (\mathbf{F} \mathbf{G} \mathbf{K})^{-1} \right]^{-1} \mathbf{r} - \mathbf{r} \right|_{T} \\ &\leq \lambda (\mathbf{F}^{-1}) \frac{\left| (\mathbf{F} \mathbf{G} \mathbf{K})^{-1} \mathbf{r} \right|_{T}}{1 - \tilde{\gamma}_{T} \left[ (\mathbf{F} \mathbf{G} \mathbf{K})^{-1} \right]} \end{aligned} \tag{by (A.2)}$$

In particular, if eqns. (II.10) and (II.11) hold, i.e. for  $T \in \mathcal{I}$  sufficiently large,

$$|(\widetilde{\text{FGK}})^{-1}r| \ll \frac{|\widetilde{r}^{-1}r|_{T}}{\lambda(\widetilde{r}^{-1})} \text{ and } \widetilde{\gamma}_{T}[(\widetilde{\text{FGK}})^{-1}] \ll 1,$$

then for  $T \in \mathcal{T}$  sufficiently large,

$$\left| \underset{\text{yr}}{\mathbb{E}} \mathbf{r} - \widetilde{\mathbf{r}}^{-1} \mathbf{r} \right|_{\mathbf{T}} \ll \frac{\left| \widetilde{\mathbf{r}}^{-1} \mathbf{r} \right|_{\mathbf{T}}}{1 - \widetilde{\gamma}_{\mathbf{T}} \left[ \left( \widetilde{\mathbf{r}} \mathbf{G} \mathbf{K} \right)^{-1} \right]} \simeq \left| \widetilde{\mathbf{r}}^{-1} \mathbf{r} \right|_{\mathbf{T}}, \ \forall \mathbf{r} \in \mathcal{R}_{d,e}.$$
 Q.E.D.

# Proof of Theorem II.3:

Since F is invertible, we have, from Fig. I.1,

$$y = H_{\sim yr} r = F^{-1}(r-e)$$

Hence, for  $T \in \mathcal{T}$  sufficiently large,  $\forall r \in \mathcal{R}_{d,e}$ ,

$$\begin{aligned} \left| \underbrace{\mathbb{H}_{yr} \mathbf{r} - \mathbf{F}^{-1} \mathbf{r}}_{\mathbf{T}} \right|_{\mathbf{T}} &= \left| \mathbf{F}^{-1} (\mathbf{r} - \mathbf{e}) - \mathbf{F}^{-1} \mathbf{r} \right|_{\mathbf{T}} \\ &\leq \lambda (\mathbf{F}^{-1}) \left| \mathbf{e} \right|_{\mathbf{T}} \qquad \text{(by assumption (i))} \\ &= \lambda (\mathbf{F}^{-1}) \left| (\mathbf{I} + \mathbf{F} \mathbf{G} \mathbf{K})^{-1} \mathbf{r} \right|_{\mathbf{T}} \\ &<< \left| \mathbf{F}^{-1} \mathbf{r} \right|_{\mathbf{T}} \qquad \text{(by assumption (ii))} \end{aligned} \quad Q.E.D. \end{aligned}$$

# Proof of Corollary II.3.1:

$$\frac{H}{\text{yr}} r - \overline{F}^{-1} r = \overline{F}^{-1} (r - e) - \overline{F}^{-1} r = - \overline{F}^{-1} e \qquad \text{(since } \overline{F}^{-1} \text{ is linear)}$$

$$= - \overline{F}^{-1} (\overline{I} + \overline{F} G \overline{K})^{-1} r$$

$$= - \left[ (\overline{I} + \overline{F} G \overline{K}) \overline{F} \right]^{-1} r$$

$$= - \left[ \overline{F} (\overline{I} + G \overline{K} \overline{F}) \right]^{-1} r$$
(since  $\overline{F}$  is linear)
$$= - (\overline{I} + G \overline{K} \overline{F})^{-1} \overline{F}^{-1} r$$

Hence for T∈ Sufficiently large,

$$\left| \underbrace{\mathbb{H}_{yr}}_{r} - \underbrace{\mathbb{F}^{-1}}_{r} \right|_{T} = \left| \left( \underbrace{\mathbb{I} + \mathbf{G} \mathbf{K} \mathbf{F}}_{r} \right)^{-1} \mathbf{F}^{-1} r \right|_{T}$$

$$<< \left| \mathbf{F}^{-1} \mathbf{r} \right|_{T}$$
(by assumption)
$$Q \cdot \mathbf{E} \cdot \mathbf{D}.$$

### Proof of Corollary II.3.2:

Consider the system S in the sinusoidal steady state (since the closed-loop system is exp. stable by assumption (a2)) with input  $r \cdot \exp(j\omega t) \text{ and error } e \cdot \exp(j\omega t), \text{ where } r, e \in \mathfrak{C}^n. \text{ Then, by linearity of } F(j\omega),$ 

$$H_{yr}(j\omega)r = F(j\omega)^{-1}(r-e) = F(j\omega)^{-1}r - F(j\omega)^{-1}e$$

Thus

$$H_{yr}(j\omega)r - F(j\omega)^{-1}r = -F(j\omega)^{-1}e$$

$$= -F(j\omega)^{-1}[(I+FGK)(j\omega)]^{-1}r$$

$$= -[(I+FGK)F](j\omega)^{-1}r$$

$$= -[F(j\omega)(I+GKF)(j\omega)]^{-1}r \qquad \text{(by linearity of } F(j\omega))$$

$$= -[(I+GKF)(j\omega)]^{-1}F(j\omega)^{-1}r$$

Hence

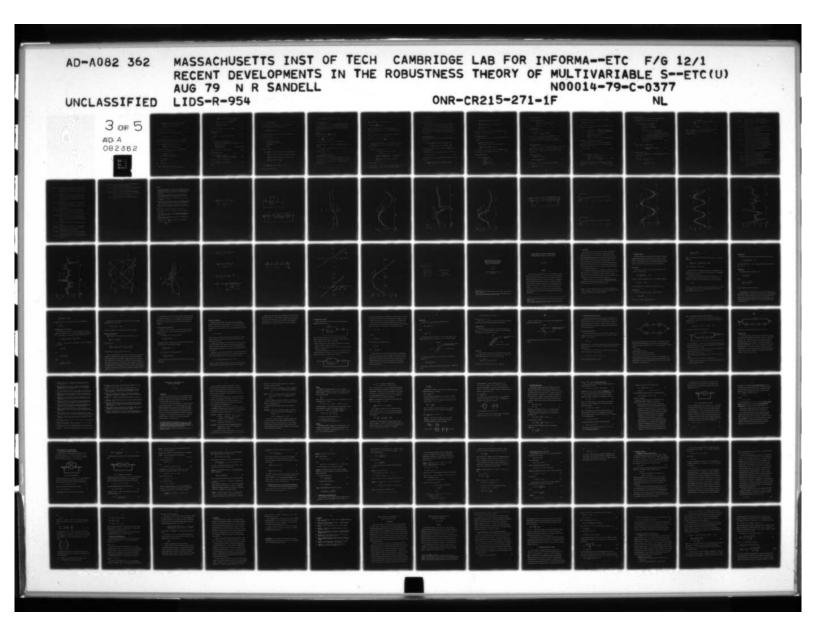
$$|H_{yr}(j\omega)r - F(j\omega)^{-1}r| = |[(I+GKF)(j\omega)]^{-1}F(j\omega)^{-1}r|$$

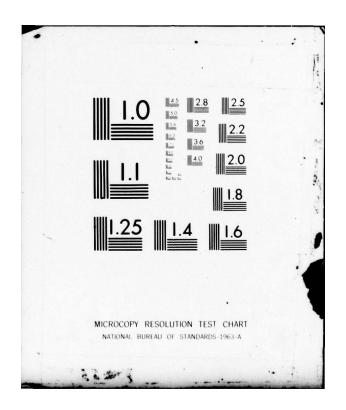
$$<< |F(j\omega)^{-1}r| \text{ (by assumption (II.21))} Q.E.D.$$

## Proof of Theorem III.1:

$$\Delta_{yr}^{H} := \widetilde{H}_{yr} - H_{yr}$$

$$= \widetilde{GK} (I + F\widetilde{GK})^{-1} - GK (I + FGK)^{-1}$$





$$= \widetilde{G}K(I+F\widetilde{G}K)^{-1} - \widetilde{G}K(I+FGK)^{-1} + \widetilde{G}K(I+FGK)^{-1} - GK(I+FGK)^{-1}$$

$$= \widetilde{G}K(I+F\widetilde{G}K)^{-1} - \widetilde{G}K(I+F\widetilde{G}K)^{-1}[I-F\cdot\Delta G\cdot K(I+F\widetilde{G}K)^{-1}]^{-1}$$

$$+ \Delta G\cdot K(I+FGK)^{-1} \text{ (since F is linear)} \tag{A.3}$$

Evaluating eqn. (A.3) at  $r \in \mathcal{R}_e$ , we have

$$\Delta_{yr}^{H}(r) = \widetilde{G}_{x}^{K} (\underline{I} + F\widetilde{G}_{x}^{K})^{-1}(r) - \widetilde{G}_{x}^{K} (\underline{I} + F\widetilde{G}_{x}^{K})^{-1}(r + \Delta r) + \Delta_{y_{0}}^{H} r(r)$$
(A.4)

where

$$r + \Delta r := \left[I - F \cdot \Delta G \cdot K \left(I + F \widetilde{G} K\right)^{-1}\right]^{-1} (r) \tag{A.5}$$

Since, by assumption,  $\tilde{H}_{yr} = \tilde{G}K(I+F\tilde{G}K)^{-1}$  is a  $C^1$  map, we can evaluate  $\Delta H_{yr}(r)$  by the Taylor's expansion theorem [19, p. 190] and obtain

$$\Delta_{yr}^{H}(r) = -\int_{0}^{1} D\left[\widetilde{G}K\left(I + F\widetilde{G}K\right)^{-1}\right] (r + \alpha \Delta r) \cdot \Delta r d\alpha + \Delta_{y_{0}r}^{H}(r)$$

$$= -\int_{0}^{1} D\left(\widetilde{G}K\right) \cdot \left[I + F \cdot D\left(\widetilde{G}K\right)\right]^{-1} \cdot \Delta r d\alpha + \Delta_{y_{0}r}^{H}(r)$$
(A.6)

where the Fréchet derivative  $D(\widetilde{G}K)$  is evaluated at  $(I+F\widetilde{G}K)^{-1}(r+\alpha\Delta r)$ .

Note that eqn. (A.5) implies that

$$\Delta \mathbf{r} = \{ [\mathbf{I} - \mathbf{F} \cdot \Delta \mathbf{G} \cdot \mathbf{K} (\mathbf{I} + \mathbf{F} \cdot \mathbf{G} \mathbf{K})^{-1}]^{-1} - \mathbf{I} \} (\mathbf{r})$$

$$= \mathbf{F} \cdot \Delta \mathbf{G} \cdot \mathbf{K} (\mathbf{I} + \mathbf{F} \cdot \mathbf{G} \mathbf{K})^{-1} [\mathbf{I} - \mathbf{F} \cdot \Delta \mathbf{G} \cdot \mathbf{K} (\mathbf{I} + \mathbf{F} \cdot \mathbf{G} \mathbf{K})^{-1}]^{-1} (\mathbf{r})$$

$$= \mathbf{F} \cdot \Delta \mathbf{G} \cdot \mathbf{K} \cdot (\mathbf{I} + \mathbf{F} \cdot \mathbf{G} \mathbf{K})^{-1} (\mathbf{r})$$

$$= \mathbf{F} \cdot \Delta \mathbf{H}_{\mathbf{y}_{0}} \mathbf{r} (\mathbf{r})$$

Thus eqn. (A.6) becomes

$$\Delta_{\mathbf{y}_{\mathbf{r}}}^{\mathbf{H}}(\mathbf{r}) = -\int_{0}^{1} D(\widetilde{\mathbf{g}}_{\mathbf{K}}) \cdot [\underbrace{\mathbf{I} + \mathbf{F} \cdot D(\widetilde{\mathbf{g}}_{\mathbf{K}})}_{-1}]^{-1} \cdot \underbrace{\mathbf{F} \cdot \Delta \mathbf{H}}_{-\mathbf{y}_{0}} \mathbf{r}(\mathbf{r}) d\alpha + \Delta \mathbf{H}_{-\mathbf{y}_{0}} \mathbf{r}(\mathbf{r})$$

$$= -\int_{0}^{1} D(\widetilde{G}K) \cdot F[I+D(\widetilde{G}K) \cdot F]^{-1} d\alpha \cdot \Delta H_{y_{0}} r(r) + \Delta H_{y_{0}} r(r)$$

$$= \int_{0}^{1} \{I-D(\widetilde{G}K) \cdot F[I+D(\widetilde{G}K) \cdot F]^{-1}\} d\alpha \cdot \Delta H_{y_{0}} r(r)$$

$$= \int_{0}^{1} [I+D(\widetilde{G}K) \cdot F]^{-1} d\alpha \cdot \Delta H_{y_{0}} r(r)$$

$$= \int_{0}^{1} [I+D(\widetilde{G}K) \cdot F]^{-1} d\alpha \cdot \Delta H_{y_{0}} r(r)$$
(A.7)

Eqn. (A.7) is true,  $\forall r \in \mathcal{R}_e$ , thus eqn. (III.4) follows. Q.E.D.

#### Proof of Proposition III.2:

Note that

$$GK(I+FGK)^{-1} = (I+GKF)^{-1}GK$$
 (since GK is linear)

and that

$$\begin{array}{l} & \underset{\sim}{\text{GK}}_{2} (\text{I} + \text{F}_{2} \text{GK}_{2})^{-1} \text{K}_{1} [\text{I} + \text{F}_{1} \text{GK}_{2} (\text{I} + \text{F}_{2} \text{GK}_{2})^{-1} \text{K}_{1}]^{-1} \\ & = \underset{\sim}{\text{GK}}_{2} (\text{I} + \text{F}_{2} \text{GK}_{2})^{-1} [\text{I} + \text{K}_{1} \text{F}_{1} \text{GK}_{2} (\text{I} + \text{F}_{2} \text{GK}_{2})^{-1}]^{-1} \text{K}_{1} \\ & = \underset{\sim}{\text{GK}}_{2} [\text{I} + (\text{F}_{2} + \text{K}_{1} \text{F}_{1}) \text{GK}_{2}]^{-1} \text{K}_{1} \\ & = [\text{I} + \text{GK}_{2} (\text{F}_{2} + \text{K}_{1} \text{F}_{1})]^{-1} \text{GK}_{2} \text{K}_{1} \\ & = [\text{I} + \text{GK}_{2} (\text{F}_{2} + \text{K}_{1} \text{F}_{1})]^{-1} \text{GK}_{2} \text{K}_{1} \\ \end{array} \qquad \text{(since } \underset{\sim}{\text{GK}}_{2} \text{ is linear)} \end{array}$$

Thus eqn. (III.10) follows from eqn. (III.9). Q.E.D.

### Proof of Proposition III.3:

$$\Delta H_{yr} := \widetilde{G}K(I + \widetilde{F}\widetilde{G}K)^{-1} - \widetilde{G}K(I + \widetilde{F}\widetilde{G}K)^{-1}$$

$$= \widetilde{G}K(I + \widetilde{F}\widetilde{G}K)^{-1}[I + \Delta F \cdot \widetilde{G}K(I + \widetilde{F}\widetilde{G}K)^{-1}]^{-1} - \widetilde{G}K(I + \widetilde{F}\widetilde{G}K)^{-1}$$
(A.8)

Evaluating eqn. (A.8) at  $r \in R_e$ , we have

$$\Delta H_{\text{yr}} r = \tilde{G}K (I + F\tilde{G}K)^{-1} (r + \Delta r) - \tilde{G}K (I + F\tilde{G}K)^{-1} (r)$$
(A.9)

where

$$\mathbf{r} + \Delta \mathbf{r} := \left[\mathbf{I} + \Delta \mathbf{F} \cdot \widetilde{\mathbf{G}} \mathbf{K} \left(\mathbf{I} + \mathbf{F} \widetilde{\mathbf{G}} \mathbf{K}\right)^{-1}\right]^{-1} \mathbf{r}$$
(A.10)

Since, by assumption (a3),  $\tilde{G}K(I+F\tilde{G}K)^{-1}$  is a  $C^1$  map, we can evaluate  $\Delta H$  r by the Taylor's expansion theorem and obtain

$$\Delta \mathbf{H}_{yr} \mathbf{r} = \int_{0}^{1} \mathbf{D}(\widetilde{\mathbf{G}}\mathbf{K}) \cdot [\mathbf{I} + \mathbf{F} \cdot \mathbf{D}(\widetilde{\mathbf{G}}\mathbf{K})]^{-1} d\alpha \cdot \Delta \mathbf{r}$$
(A.11)

where the Fréchet derivative  $D(\tilde{G}K)$  is evaluated at  $(\tilde{I}+\tilde{F}\tilde{G}K)^{-1}(r+\alpha\Delta r)$ , and DF=F since F is linear.

Note that eqn. (A.10) implies that

$$\Delta \mathbf{r} = \{ [\mathbf{I} + \Delta \mathbf{F} \cdot \mathbf{G} \mathbf{K} (\mathbf{I} + \mathbf{F} \mathbf{G} \mathbf{K})^{-1}]^{-1} - \mathbf{I} \} \mathbf{r}$$

$$= -\Delta \mathbf{F} \cdot \widetilde{\mathbf{G}} \mathbf{K} (\mathbf{I} + \mathbf{F} \widetilde{\mathbf{G}} \mathbf{K})^{-1} [\mathbf{I} + \Delta \mathbf{F} \cdot \widetilde{\mathbf{G}} \mathbf{K} (\mathbf{I} + \mathbf{F} \widetilde{\mathbf{G}} \mathbf{K})^{-1}]^{-1} \mathbf{r}$$

$$= -\Delta \mathbf{F} \cdot \widetilde{\mathbf{G}} \mathbf{K} (\mathbf{I} + \widetilde{\mathbf{F}} \widetilde{\mathbf{G}} \mathbf{K})^{-1} \mathbf{r}$$

$$= -\Delta \mathbf{F} \cdot \widetilde{\mathbf{H}}_{yr} \mathbf{r}$$

Thus eqn. (A.11) becomes

$$\begin{split} \Delta \mathbf{H}_{\mathbf{y}\mathbf{r}}\mathbf{r} &= -\int_{0}^{1} \mathbf{D}(\widetilde{\mathbf{G}}\mathbf{K}) \cdot \left[ \mathbf{I} + \mathbf{F} \cdot \mathbf{D}(\widetilde{\mathbf{G}}\mathbf{K}) \right]^{-1} d\alpha \cdot \Delta \mathbf{F} \cdot \widetilde{\mathbf{H}}_{\mathbf{y}\mathbf{r}}\mathbf{r} \quad (\text{since } \mathbf{F} \text{ is linear}) \quad (A.12) \\ &= -\int_{0}^{1} \mathbf{D}(\widetilde{\mathbf{G}}\mathbf{K}) \cdot \left[ \mathbf{I} + \mathbf{F} \cdot \mathbf{D}(\widetilde{\mathbf{G}}\mathbf{K}) \right]^{-1} \mathbf{F} d\alpha \cdot \mathbf{F}^{-1} \cdot \Delta \mathbf{F} \cdot \widetilde{\mathbf{H}}_{\mathbf{y}\mathbf{r}}\mathbf{r} \quad (\text{since } \mathbf{F} \text{ is invertible}) \\ &= -\int_{0}^{1} \mathbf{D}(\widetilde{\mathbf{G}}\mathbf{K}) \mathbf{F} \cdot \left[ \mathbf{I} + \mathbf{D}(\widetilde{\mathbf{G}}\mathbf{K}) \cdot \mathbf{F} \right]^{-1} d\alpha \cdot \mathbf{F}^{-1} \cdot \Delta \mathbf{F} \cdot \widetilde{\mathbf{H}}_{\mathbf{y}\mathbf{r}}\mathbf{r} \quad (\text{since } \mathbf{F} \text{ is linear}) \\ &= \left\{ \int_{0}^{1} \left[ \mathbf{I} + \mathbf{D}(\widetilde{\mathbf{G}}\mathbf{K}) \cdot \mathbf{F} \right]^{-1} d\alpha - \mathbf{I} \right\} \cdot \mathbf{F}^{-1} \cdot \Delta \mathbf{F} \cdot \widetilde{\mathbf{H}}_{\mathbf{y}\mathbf{r}}\mathbf{r} \end{split}$$

i.e.

$$\Delta \mathbf{H}_{yr} = \left\{ \int_{0}^{1} \left[ \mathbf{I} + \mathbf{D} \left( \widetilde{\mathbf{G}} \mathbf{K} \right) \widetilde{\mathbf{F}} \right]^{-1} d\alpha - \mathbf{I} \right\} \cdot \widetilde{\mathbf{F}}^{-1} \cdot \Delta \widetilde{\mathbf{F}} \cdot \widetilde{\mathbf{H}}_{yr} , \text{ on } \mathcal{R}_{e} \right\}$$

Since  $\tilde{H}_{yr}$  is invertible, we have

$$\Delta H_{yr} \cdot \widetilde{H}_{yr}^{-1} = \{ \int_{0}^{1} [1 + D(\widetilde{GK})F]^{-1} d\alpha - 1 \} \cdot F^{-1} \cdot \Delta F, \text{ on } Y_{e}$$
 Q.E.D.

# Proof of Proposition III.4:

For completeness, we first state an algorithm [36] which determines the <u>asymptotic behavior</u> of the zeros of a polynomial. This algorithm is a direct application of the Newton's diagram (or known as the method of Puiseux, see e.g. [35, p. 105]).

# Algorithm:

<u>Data</u>: Polynomial  $P(s,k) = \sum_{k=0}^{n} \alpha_{k}(k) s^{k} \in \mathbb{R}[s]$  where, for k = 0,1,2,...,n

$$\begin{split} &\alpha_{\ell}(\mathbf{k}) = \sum_{\mathbf{j}=0}^{m_{\ell}} \alpha_{\ell \, \mathbf{j}} \, \mathbf{k}^{\, \mathbf{j}} \ , \ \mathbf{k}, \ \alpha_{\ell \, \mathbf{j}} \, \mathbf{s} \in \mathbb{R} \\ &\alpha_{nm_{n}} \neq 0 \ , \ \text{and} \ \alpha_{\ell m_{\ell}} \neq 0 \ , \ \forall 0 \leq \ell \leq n-1 \ \text{such that} \ m_{\ell} > 0 \end{split}$$

Step 1: Find  $i \in \mathbb{N}$ , and  $\tau_p$ ,  $q_p \in \mathbb{Q}_+$ ,  $0 \le p \le i$ , where i,  $\tau_p$ 's,  $q_p$ 's are such that

- (i) i is the largest integer such that  $0 = \tau_0 < \tau_1 < \cdots < \tau_i$ ;
- (ii)  $q_0 = \max\{m_0, m_1, \dots, m_n\};$
- (iii) for  $0 \le p \le i$ ,

$$m_{\ell} \le q_p - \ell \cdot \tau_p$$
 ,  $\forall 0 \le \ell \le n$ 

with equality holds for at least two l's;

(iv) if  $\ell_p$  ( $\bar{\ell}_p$ ) is the smallest (largest)  $\ell_p$  such that  $m_{\ell} = q_p - \ell \cdot \tau_p$ , then  $\ell_{p+1} = \bar{\ell}_p$ , for  $p = 0, 1, \ldots, i-1$ . (The procedure of finding i,  $\tau_p$ 's,  $q_p$ 's can be best illustrated graphically by the modified Newton's diagram shown on Fig. A.1.)

Step 2: For each  $0 \le p \le i$ , form the polynomial

$$\phi_{\mathbf{p}}(\mathbf{z}) = \sum_{\ell \in \{\ell \mid \ell \tau_{\mathbf{p}} + m_{\ell} = q_{\mathbf{p}}\}} \alpha_{\ell m_{\ell}} \mathbf{z}^{\ell}$$
(A.13)

Step 3: Calculate the zeros of  $\phi_0$  and denote them by  $z_{0j}$ ,  $j=1,2,\ldots,n_0$ . Calculate the <u>nonzero</u> zeros of  $\phi_p$ ,  $1 \le p \le i$ , and denote them by  $z_{pj}$ ,  $j=1,2,\ldots,n_p$ .

Step 4: As  $|k| \rightarrow \infty$ , the n zeros of the polynomial P(s,k) behaves as

$$z_{pj}^{\tau}^{k}^{p}$$
,  $j = 1, 2, ..., n_{p}$ ,  $p = 0, 1, 2, ..., i$ 

where  $n_p \ge 1$ , for  $1 \le p \le i$ , and  $\sum_{p=0}^{i} n_p = n$ .

Now we can apply this algorithm to prove Proposition III.4. Without loss of generality, we only have to prove the case where  $n_0 = n_1$  and  $M = I_n$ . Note that

$$\begin{aligned} \det[I+kG] &= 1 + k[\operatorname{trace} \ G(s)] \\ &+ k^2[\Sigma \ \operatorname{principal} \ \operatorname{minors} \ \operatorname{of} \ G(s) \ \operatorname{of} \ \operatorname{order} \ 2] \\ &+ \cdots + k^m \det G \\ &= \frac{1}{\prod_{i,j}^d ij} \prod_{i,j}^d ij + k \sum_{i=1}^m n_{ii} (\prod_{j \neq i}^d ij) + \cdots + k^m \cdot \prod_{i,j}^d ij \cdot \det G] \\ &= \frac{1}{\prod_{i,j}^d ij} \prod_{i,j}^d ij + k\alpha_1(s) + k^2\alpha_2(s) + \cdots + k^m\alpha_m(s)] \end{aligned}$$

where  $\alpha_j(s) \in \mathbb{R}[s]$ , j = 1, 2, ..., m.

Let  $\partial [\prod d_{ij}] = n$ . Since, by assumption,  $\partial d_{ij} - \partial n_{ij} \ge 3$ ,  $\forall i,j = 1,2,...,m$ , we have that  $\partial [\alpha_j(s)] \le n-3j$ , j = 1,2,...,m. Hence with i defined in

Step 1 of the algorithm above,

$$\phi_i(z) = z^n + \alpha_{1\beta} z^{n-\beta} + \cdots, \quad \beta \ge 3$$
,

where  $\phi_i(z)$  is defined in (A.13).

Now we claim that  $\phi_{\bf i}(z)$  has  ${\stackrel{\circ}{\mathbb C}}_+$ -zeros. To see this, consider some  $\epsilon>0$  sufficiently small; apply the Routh test (see e.g. [37]) to the polynomial  $\phi_{\bf i}(z+\epsilon)$ . Since  $\beta\geq 3$ , the first column from the left in the Routh array contains some strictly negative numbers, thus  $\phi_{\bf i}(z)$  has some  ${\stackrel{\circ}{\mathbb C}}_+$ -zeros. Hence as  $k\to\infty$ , det [I+kG] has zero behaves as  $z_{\bf i}k^{\bf i}$  with  $z_{\bf i}\in{\stackrel{\circ}{\mathbb C}}_+$  and  $\tau_{\bf i}>0$ .

# Proof of Proposition III.5:

(i) By definition,  $\tilde{G}\tilde{u}:=\tilde{G}\tilde{u}+d_0$ . Then, by eqn. (III.4) (of Theorem III.1), we have that

$$\Delta y = \Delta H_{yr}(r) = \int_{0}^{1} [I + D(\tilde{G}K) \cdot \tilde{F}]^{-1} d\alpha \cdot d_{0} \quad (\text{since } \Delta H_{y_{0}r}(r) = d_{0})$$

$$= \int_{0}^{1} [I + D(\tilde{G}K) \cdot \tilde{F}]^{-1} d\alpha \cdot d_{0} \quad (\text{since } D(\tilde{G}K) = D(\tilde{G}K))$$

where the Fréchet derivative D(GK) is evaluated at  $(I+FGK)^{-1}(r+\alpha\Delta r)$  with  $\Delta r = F \cdot \Delta H_{xy_0} r(r) = F \cdot d_0$ .

(ii) By definition,  $\tilde{F}\tilde{y} := F(d_f + \tilde{y}) = Fd_f + F\tilde{y}$  (since F is linear). Then

$$\Delta_{\mathbf{F}} \cdot \widetilde{\mathbf{y}} = (\widetilde{\mathbf{F}} - \mathbf{F})\widetilde{\mathbf{y}} = \widetilde{\mathbf{F}} \cdot \mathbf{d}_{\mathbf{f}}$$
 (A.14)

Thus, following the proof of Proposition III.3, in particular, eqn. (A.12) we have that

$$\Delta y = -\int_0^1 D(GK) \left[ \underbrace{I + F \cdot D(GK)}_{\sim} \right]^{-1} d\alpha \cdot \Delta F \cdot \widetilde{y} \quad \text{(since } D(\widetilde{GK}) = D(GK))$$

$$= -\int_{0}^{1} D(\underline{GK}) [\underline{\mathbf{I}} + \mathbf{F} \cdot D(\underline{GK})]^{-1} \underline{\mathbf{F}} d\alpha \cdot \mathbf{d}_{f} \quad \text{(by eqn. (A.14))}$$

$$= -\int_{0}^{1} D(\underline{GK}) \cdot \underline{\mathbf{F}} [\underline{\mathbf{I}} + D(\underline{GK}) \cdot \underline{\mathbf{F}}]^{-1} d\alpha \cdot \mathbf{d}_{f} \quad \text{(since } \underline{\mathbf{F}} \text{ is linear)}$$

$$= \{ \int_{0}^{1} [\underline{\mathbf{I}} + D(\underline{GK}) \cdot \underline{\mathbf{F}}]^{-1} d\alpha - \underline{\mathbf{I}} \} \cdot \mathbf{d}_{f}$$

where the Fréchet derivative D(GK) is evaluated at  $(I+F\widetilde{G}K)^{-1}(r+\alpha\Delta r)$  with  $\Delta r = -\Delta F \cdot \widetilde{H}_{yr} r = -\Delta F \cdot \widetilde{y} = -Fd_f$  and  $\alpha \in \{0,1\}$ . Q.E.D.

# Proof of Proposition III.6:

By definition,  $\tilde{G}\tilde{u}:=\tilde{G}(\tilde{u}+d_g)$ . Then by eqn. (III.4) (of Theorem III.1) we have that

$$\Delta y = \int_{0}^{1} [I + D(\tilde{G}K) \cdot \tilde{F}]^{-1} d\alpha \cdot [G(u + d_{g}) - G(u)]$$

$$(\text{since } \Delta H_{y_{0}} r(r) \approx G(u + d_{g}) - G(u), \text{ where } u = K(I + FGK)^{-1} r)$$

$$= \{ \int_{0}^{1} [I + D(\tilde{G}K) \cdot \tilde{F}]^{-1} d\alpha \} \cdot \{ \int_{0}^{1} DG(u + \beta d_{g}) d\beta \} \cdot d_{g}$$

where the Fréchet derivative  $D(\widetilde{G}K)$  is evaluated at  $(I+F\widetilde{G}K)^{-1}(r+\alpha\Delta r)$  with  $\Delta r = F[G(u+d_g)-G(u)]$ ,  $u := K(I+FGK)^{-1}r$ , and  $\alpha \in [0,1]$ . Q.E.D.

#### Proof of Proposition III.9:

$$\begin{split} \delta_{\mathbf{T}}(N_2, \mathcal{V}) &:= \inf \sup_{\mathbf{L} \in \mathcal{L}} \sup_{\mathbf{u} \in \mathcal{V}} \left| \sum_{i=1}^{N} \mathbf{u}^{-i} \mathbf{L} \mathbf{u} \right|_{\mathbf{T}} \\ &= \inf \sup_{\mathbf{L} \in \mathcal{L}} \sup_{\mathbf{u} \in \mathcal{V}} \left| \sum_{i=1}^{N} \mathbf{u}^{-i} \mathbf{L} \mathbf{u} \right|_{\mathbf{T}} \\ &= \inf \sup_{\mathbf{L}' \in \mathcal{L}} \sup_{\mathbf{u} \in \mathcal{V}} \left| \sum_{i=1}^{N} \mathbf{u}^{-i} \mathbf{L}' \mathbf{u} \right|_{\mathbf{T}} \\ &= : \delta_{\mathbf{T}}(N_1, \mathcal{V}) , \quad \forall \mathbf{T} \in \mathcal{T}, \; \forall \mathcal{V} \subseteq \mathcal{U}_{\mathbf{C}} \;. \end{split}$$
 Q.E.D.

# Proof of Proposition III.10:

$$\begin{array}{lll} \delta_{\mathbf{T}}(\mathbf{N},\mathcal{V}_{\mathbf{1}}) &:= \inf_{\mathbf{L} \in \mathcal{L}} \sup_{\mathbf{u} \in \mathcal{V}_{\mathbf{1}}} \left\| \mathbf{N}\mathbf{u} - \mathbf{L}\mathbf{u} \right\|_{\mathbf{T}} \\ &\leq \inf_{\mathbf{L} \in \mathcal{L}} \sup_{\mathbf{u} \in \mathcal{V}_{\mathbf{2}}} \left\| \mathbf{N}\mathbf{u} - \mathbf{L}\mathbf{u} \right\|_{\mathbf{T}} \quad (\text{since } \mathcal{V}_{\mathbf{1}} \subset \mathcal{V}_{\mathbf{2}} \subset \mathcal{U}_{\mathbf{2}}) \\ &=: \delta_{\mathbf{T}}(\mathbf{N},\mathcal{V}_{\mathbf{2}}) \;\;, \quad \forall \mathbf{T} \in \mathcal{T} \;\;. \end{array}$$

# Proof of Proposition III.11:

Note that  $DN(0) \in \mathcal{L}$ . Hence

$$0 \leq \delta_{\mathbf{T}}(\mathbf{N}, \mathbf{B}_{\mathbf{T}}(0; \beta)) \leq \sup_{\mathbf{u} \in \mathbf{B}_{\mathbf{T}}(0; \beta)} |\mathbf{N}\mathbf{u} - \mathbf{D}\mathbf{N}(0)\mathbf{u}|_{\mathbf{T}}$$
(A.15)

By the definition of Fréchet derivative, we know that for any  $\epsilon > 0$ ,  $\exists \delta > 0 \quad \text{such that } \left| \underbrace{\text{Nu-DN}(0) \cdot \mathbf{u}}_{\mathbf{T}} \right|_{\mathbf{T}} \leq \epsilon \left| \mathbf{u} \right|_{\mathbf{T}}, \ \forall \left| \mathbf{u} \right|_{\mathbf{T}} \leq \delta. \quad \text{Hence as } \beta \to 0,$  the right-hand side of eqn. (A.15) tends to zero and  $\delta_{\mathbf{T}}(\mathbf{N}, \overline{\mathbf{B}}_{\mathbf{T}}(0; \beta)) \to 0.$  Q.E.D.

# Proof of Proposition III.12:

Let  $V \subset \mathcal{U}_e$ . If, for some  $L \in \mathcal{L}$ ,  $\mathbb{N}u = Lu$ ,  $\mathbb{V}u \in \mathcal{V}$ , then L is a minimizer of  $\sup_{\mathbf{v} \in \mathcal{V}} |\mathbb{N}u - Lu|_{\mathbf{T}}$ ,  $\mathbb{V}\mathbf{T} \in \mathcal{T}$ , and  $\delta_{\mathbf{T}}(\mathbb{N}, \mathcal{V}) = 0$ ,  $\mathbb{V}\mathbf{T} \in \mathcal{T}$ . In particular, if  $\mathbb{N} \in \mathcal{L}$ , then  $\mathbb{N}$  is a minimizer of  $\sup_{\mathbf{v} \in \mathcal{V}} |\mathbb{N}u - Lu|_{\mathbf{T}}$ ,  $\mathbb{V}\mathbf{T} \in \mathcal{T}$ ,  $\mathbb{V}\mathbf{V} \subset \mathcal{U}_e$ , hence  $\delta_{\mathbf{T}}(\mathbb{N}, \mathcal{V}) = 0$ ,  $\mathbb{V}\mathbf{T} \in \mathcal{T}$ ,  $\mathbb{V}\mathbf{V} \subset \mathcal{U}_e$ . Q.E.D.

# Proof of Proposition III.13:

By assumption, for some  $T \in \mathcal{T}$ ,

$$\delta_{\mathbf{T}}(\mathbf{N}, \mathbf{V}) := \inf \sup_{\mathbf{L} \in \mathbf{L}} |\mathbf{N}\mathbf{u} - \mathbf{L}\mathbf{u}|_{\mathbf{T}} = 0$$
(A.16)

Thus for this T, there exists a sequence  $(L_i)_{i=0}^{\infty} \subset \mathcal{I}$  such that

$$\sup_{\mathbf{x} \in \P} \left| \frac{\mathbf{N}\mathbf{u} - \mathbf{L}_{\mathbf{i}} \mathbf{u}}{\mathbf{T}} \right|_{\mathbf{T}} \to 0, \text{ as } \mathbf{i} \to \infty$$
 (A.17)

or equivalently, for any  $\varepsilon_1$  > 0, there exists  $\mathbf{m}_1$  > 0 such that

$$\sup_{\mathbf{v} \in \mathbf{V}} \left| \underset{\sim}{\operatorname{Nu-L_i}} \mathbf{u} \right|_{\mathbf{T}} < \varepsilon_1, \quad \forall i > m_1$$
 (A.18)

Now for any  $\varepsilon$  > 0, if we let  $\varepsilon_1 = \frac{\varepsilon}{2\beta}$  and choose the corresponding  $m_1$  > 0 such that (A.18) holds, then

$$\begin{aligned} \left| \begin{array}{c} L_{\mathbf{i}} - L_{\mathbf{j}} \right|_{T} &= \frac{1}{\beta} \sup_{\mathbf{u} \in \mathbf{V}} \left| \begin{array}{c} L_{\mathbf{i}} \mathbf{u} - L_{\mathbf{j}} \mathbf{u} \right|_{T} & \text{(by definition of the induced norm, with } \beta \text{ defined in assumption (a3))} \\ &\leq \frac{1}{\beta} \sup_{\mathbf{u} \in \mathbf{V}} \left| \begin{array}{c} L_{\mathbf{i}} \mathbf{u} - L_{\mathbf{j}} \mathbf{u} \right|_{T} & \text{(by assumption (a3))} \\ &\leq \frac{1}{\beta} [\sup_{\mathbf{u} \in \mathbf{V}} \left| \sum_{i=1}^{N} \mathbf{u} - L_{\mathbf{j}} \mathbf{u} \right|_{T} + \sup_{\mathbf{u} \in \mathbf{V}} \left| \sum_{i=1}^{N} \mathbf{u} - L_{\mathbf{j}} \mathbf{u} \right|_{T} \right| \\ &\leq \frac{1}{\beta} \cdot 2\varepsilon_{1} = \varepsilon \quad , \quad \forall \mathbf{i}, \mathbf{j} \geq m_{1} \quad \text{(by (A.18) and the choice of } m_{1} \text{)} \end{aligned}$$

Thus  $(L_i)_{i=0}^{\infty}$  is a Cauchy sequence in  $(P_T \mathcal{L}, |\cdot|_T)$ .

Note that for each  $T \in \mathcal{T}$ ,  $(P_T \mathcal{I}, |\cdot|_T)$  is a Banach space with the usual induced norm since, by assumption (a1),  $P_T \mathcal{I}_e$  is a Banach space. Hence there exists  $L^* \in \mathcal{I}$  such that

$$\begin{array}{ccc}
P_{T}L_{i} & \xrightarrow{|\cdot|_{T}} & P_{T}L^{*} \\
\sim T_{\sim}^{*} & & \end{array}$$
(A.19)

Note

$$\begin{split} \left| \underset{\sim}{\text{Nu-L}^{\star}} \mathbf{u} \right|_{T} &\leq \left| \underset{\sim}{\text{Nu-L}} \mathbf{u} \right|_{T} + \left| \underset{\sim}{\text{L}} \mathbf{u} - \underset{\sim}{\text{L}^{\star}} \mathbf{u} \right|_{T} \\ &\leq \sup_{\mathbf{u} \in \mathscr{V}} \left| \underset{\sim}{\text{Nu-L}} \mathbf{u} \right|_{T} + \sup_{\mathbf{u} \in \mathscr{V}} \left| \underset{\sim}{\text{L}} \mathbf{u} - \underset{\sim}{\text{L}^{\star}} \mathbf{u} \right|_{T} \\ &\leq \sup_{\mathbf{u} \in \mathscr{V}} \left| \underset{\sim}{\text{Nu-L}} \mathbf{u} \right|_{T} + \left| \underset{\sim}{\text{L}} - \underset{\sim}{\text{L}^{\star}} \right|_{T} \cdot \sup_{\mathbf{u} \in \mathscr{V}} \left| \mathbf{u} \right|_{T} , \quad \forall i \end{split} \tag{A.20}$$

By (A.18), (A.19) and the assumption (a2) that  $\sup_{\mathbf{u}\in\mathscr{U}}|\mathbf{u}|_{\mathbf{T}}<\infty$ , the right-hand side of eqn. (A.20) tends to zero as  $\mathbf{i}\to\infty$ . Hence  $|\mathbf{N}\mathbf{u}-\mathbf{L}^*\mathbf{u}|_{\mathbf{T}}=0$ ,  $\mathbf{v}\mathbf{u}\in\mathscr{U}$ .

#### Proof of Theorem III.14:

Let  $L_G$  be a linear, causal operator such that the linear operator  $L_{yr} := L_G K (I + F L_G K)^{-1}$  is well defined and causal. Then

$$\begin{split} & \underbrace{\mathbb{E}_{yr} \mathbf{r}} - \mathbb{E}_{yr} \mathbf{r} = \mathbf{G} \underbrace{\mathbb{K} (\mathbf{I} + \mathbf{F} \mathbf{G} \mathbf{K})}^{-1} \mathbf{r} - \mathbb{E}_{\mathbf{G}} \underbrace{\mathbb{K} (\mathbf{I} + \mathbf{F} \mathbf{G} \mathbf{K})}^{-1} \mathbf{r} \\ & = \mathbf{G} \underbrace{\mathbb{K} (\mathbf{I} + \mathbf{F} \mathbf{G} \mathbf{K})}^{-1} \mathbf{r} - \mathbb{E}_{\mathbf{G}} \underbrace{\mathbb{K} (\mathbf{I} + \mathbf{F} \mathbf{G} \mathbf{K})}^{-1} \mathbf{r} \\ & + \mathbb{E}_{\mathbf{G}} \underbrace{\mathbb{K} (\mathbf{I} + \mathbf{F} \mathbf{G} \mathbf{K})}^{-1} \mathbf{r} - \mathbb{E}_{\mathbf{G}} \underbrace{\mathbb{K} (\mathbf{I} + \mathbf{F} \mathbf{E}_{\mathbf{G}} \mathbf{K})}^{-1} \mathbf{r} \\ & = (\mathbf{G} - \mathbf{L}_{\mathbf{G}}) \mathbf{u} \\ & + \mathbb{E}_{\mathbf{G}} \underbrace{\mathbb{K} (\mathbf{I} + \mathbf{F} \mathbf{L}_{\mathbf{G}} \mathbf{K})}^{-1} [(\mathbf{I} + \mathbf{F} \mathbf{L}_{\mathbf{G}} \mathbf{K}) - (\mathbf{I} + \mathbf{F} \mathbf{G} \mathbf{K})] (\mathbf{I} + \mathbf{F} \mathbf{G} \mathbf{K})^{-1} \mathbf{r} \\ & = (\mathbf{G} - \mathbf{L}_{\mathbf{G}}) \mathbf{u} \\ & = (\mathbf{G} - \mathbf{L}_{\mathbf{G}}) \mathbf{u} + \mathbb{E}_{\mathbf{G}} \underbrace{\mathbb{K} (\mathbf{I} + \mathbf{F} \mathbf{L}_{\mathbf{G}} \mathbf{K})}^{-1} \mathbf{F} (\mathbf{L}_{\mathbf{G}} - \mathbf{G}) \underbrace{\mathbb{K} (\mathbf{I} + \mathbf{F} \mathbf{G} \mathbf{K})}^{-1} \mathbf{r}, (\text{since } \mathbf{F} \text{ is linear}) \\ & = (\mathbf{G} - \mathbf{L}_{\mathbf{G}}) \mathbf{u} - \mathbb{E}_{\mathbf{G}} \underbrace{\mathbb{K} (\mathbf{I} + \mathbf{F} \mathbf{L}_{\mathbf{G}} \mathbf{K})}^{-1} \mathbf{F} (\mathbf{G} - \mathbf{L}_{\mathbf{G}}) \mathbf{u}, (\text{since } \mathbf{F}, \mathbf{L}_{\mathbf{G}}, \mathbf{K} \text{ are linear}) \\ & = (\mathbf{G} - \mathbf{L}_{\mathbf{G}}) \mathbf{u} - \mathbb{E}_{\mathbf{G}} \underbrace{\mathbb{K} (\mathbf{I} + \mathbf{F} \mathbf{L}_{\mathbf{G}} \mathbf{K})}^{-1} \mathbf{F} (\mathbf{G} - \mathbf{L}_{\mathbf{G}}) \mathbf{u}, (\text{since } \mathbf{F}, \mathbf{L}_{\mathbf{G}}, \mathbf{K} \text{ are linear}) \\ & = (\mathbf{I} - \mathbf{L}_{\mathbf{G}} \mathbf{K} \mathbf{F})^{-1} (\mathbf{G} - \mathbf{L}_{\mathbf{G}}) \mathbf{u} \end{aligned} \tag{A.21}$$

Thus

$$\left| \underbrace{\mathbb{L}_{yr} \mathbf{r}} - \underbrace{\mathbb{L}_{yr} \mathbf{r}} \right|_{T} = \left| (\underbrace{\mathbb{I} + \mathbb{L}_{G} \mathbb{K} \mathbf{F}})^{-1} (\underbrace{\mathbf{G} - \mathbb{L}_{G}}) \mathbf{u} \right|_{T}$$

$$= \frac{\left| (\underbrace{\mathbb{I} + \mathbb{L}_{G} \mathbb{K} \mathbf{F}})^{-1} (\underbrace{\mathbf{G} - \mathbb{L}_{G}}) \mathbf{u} \right|_{T}}{\left| (\underbrace{\mathbf{G} - \mathbb{L}_{G}}) \mathbf{u} \right|_{T}} \quad \left| (\underbrace{\mathbf{G} - \mathbb{L}_{G}}) \mathbf{u} \right|_{T} \tag{A.22}$$

provided that  $P_T(\tilde{Q}-L_G)u \neq 0$ .

On letting  $L_{yr}^*$  : =  $L_{G}^*K(\underline{I}+\underline{F}L_{G}^*K)^{-1}$ , where  $L_{G}^*$  is defined in eqn. (III.25), we have, from eqn. (A.22)

$$\delta_{T}(\tilde{\mathbb{H}}_{yr}, \mathcal{R}_{d,e}) := \inf_{L \in \mathcal{L}} \sup_{r \in \mathcal{R}_{d,e}} |\tilde{\mathbb{H}}_{yr}r - \tilde{\mathbb{L}}r|_{T}$$

$$\leq \sup_{r \in \mathcal{R}_{d,e}} |\tilde{\mathbb{H}}_{yr}r - \tilde{\mathbb{L}}_{yr}^{*}r|_{T}$$

$$\leq \sup_{\mathbf{y} \in \mathbf{\hat{y}}_{e}} \frac{\left| (\mathbf{\hat{I}} + \mathbf{\hat{L}}_{G}^{*} \mathbf{\hat{K}} \mathbf{\hat{F}})^{-1} \mathbf{y} \right|_{\mathbf{T}}}{\left| \mathbf{y} \right|_{\mathbf{T}}} \sup_{\mathbf{u} \in \mathbf{\hat{u}}_{d,e}} \left| \mathbf{\hat{G}} \mathbf{u} - \mathbf{\hat{L}}_{G}^{*} \mathbf{u} \right|_{\mathbf{T}}$$

$$= \rho. \quad \delta_{\mathbf{T}}(\mathbf{\hat{G}}, \mathbf{\hat{u}}_{d,e}) \tag{A.23}$$

where  $\tilde{y}_e := (G-L_G^*)\mathcal{U}_{d,e}$  and  $\rho$  is defined in eqn. (III.27). Note the last inequality follows since when  $r \in \mathcal{R}_{d,e}$ , the corresponding  $u := K(I+FGK)^{-1}r \in \mathcal{U}_{d,e}.$  Q.E.D.

- Fig. I.1: Nonlinear, feedback system S under consideration.
- Fig. II.1: An example realizing a nonlinear input-output map using nonlinear feedback and a large forward-path gain: the logarithmic amplifier.
- Fig. II.2: A nonlinear, single-input, single-output, dynamical system illustrating the generalized Black result.
- Fig. II.3: Characteristics of the nonlinearity  $\phi(\cdot)$  in the nonlinear, feedback system shown in Fig. II.2.
- Fig. II.4: System outputs of the nonlinear, feedback system shown in Fig. II.2 when the system input is  $r(t) = \sin 10t$  and the compensator gain is k = 1, 10, 20 and 40, respectively.
- Fig. II.5: Error signals of the nonlinear, feedback system shown in Fig. II.2, when the system input is  $r(t) = \sin 10t$  and the compensator gains are k = 10, 20 and 40, respectively.
- Fig. II.6: The input to the nonlinearity  $\phi(\cdot)$  of the nonlinear, feedback system shown in Fig. II.2, when the system input is  $r(t) = \sin 10t$  and the compensator gains are k = 1, 10, 20 and 40, respectively.
- Fig. II.7: A nonlinear, multi-input, multi-output, dynamical system illustrating the generalized Black result.
- Fig. II.8: Characteristics of the odd function  $v(\cdot)$ .
- Fig. II.9: Characteristics of  $1+0.2 \tanh x$ ,  $x \ge 0$ .
- Fig. II.10: System output  $y_1(\cdot)$  of the nonlinear, feedback system shown in Fig. II.7 when the system inputs are  $r_1(t) = \sin 10t$ ,  $r_2(t) = 0.8 \sin 15t$  and the compensator gains are k = 1, 10, 20 and 40, respectively.

- Fig. II.11: System output  $y_2(\cdot)$  of the nonlinear, feedback system shown in Fig. II.7 when the system inputs are  $r_1(t) = \sin 10t$ ,  $r_2(t) = 0.8 \sin 15t$  and the compensator gains are k = 1, 10, 20 and 40, respectively.
- Fig. II.12: Error signal  $e_1(\cdot)$  of the nonlinear, feedback system shown in Fig. II.7 when the system inputs are  $r_1(t)$  = sin 10t,  $r_2(t)$  = 0.8 sin 15t and the compensator gains are k = 10, 20, and 40, respectively.
- Fig. II.13: Error signal  $e_2(\cdot)$  of the nonlinear, feedback system shown in Fig. II.7 when the system inputs are  $r_1(t) = \sin 10t$ ,  $r_2(t) = 0.8 \sin 15t$  and the compensator gains are k = 10, 20 and 40, respectively.
- Fig. II.14: One period of the steady state trajectory of the system output  $y(\cdot)$  of the nonlinear, feedback system shown in Fig. II.7 when  $r_1(t) = \sin 10t$ ,  $r_2(t) = 0.8 \sin 15t$  and k = 40.
- Fig. II.15: One period of the steady state trajectory of the input to the nonlinearity  $\Phi(\cdot)$  of the nonlinear, feedback system shown in Fig. II.7 when  $r_1(t) = \sin 10t$ ,  $r_2(t) = 0.8 \sin 15t$  and k = 40.
- Fig. III.1: A comparison open-loop system for (comparative) sensitivity .
  analysis.
- Fig. III.2: The perturbed closed-loop system: the plant G becomes G.
- Fig. III.3: The perturbed open-loop system: the plant G becomes  $\widetilde{G}$ , the precompensator  $K_{\widehat{O}}$  remains unchanged.
- Fig. III.4: The nonlinear, multi-loop feedback system for studying the relation between desensitization and feedback structure.
- Fig. III.5: Nonlinear, feedback system S subjected to additive external disturbances.

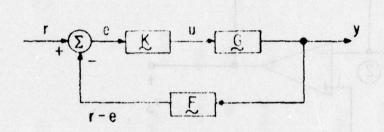
- Fig. III.6: Characterizations of the nonlinear plant G and its best linear approximation  $L_G^*$  (in broken lines).
- Fig. III.7: Characterizations of the closed-loop system H and its best linear approximation (in broken lines).
- Fig. III.8: Outputs of the nonlinear plant G,  $y_0$ , and the closed-loop system  $\lim_{x \to yr}$ , y, when the plant input  $u(t) = 1.2 \sin \omega t$  and the closed-loop system input  $r(t) = 0.92 \sin \omega t$ .

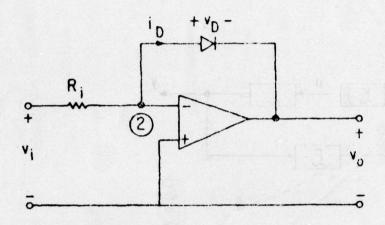
5 4 2 is got sent to the form to make the set select at the

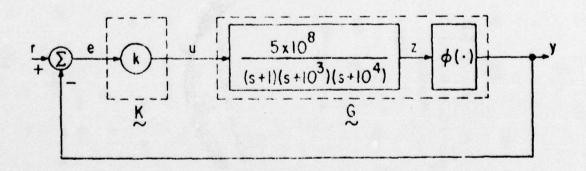
Fig. A.1: Modified Newton's diagram for finding the parameters i,  $\tau_p's, \ q_p's.$ 

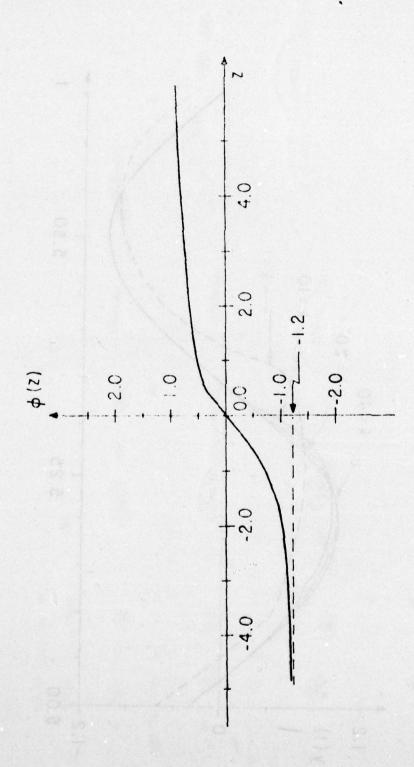
#### FOOTNOTES

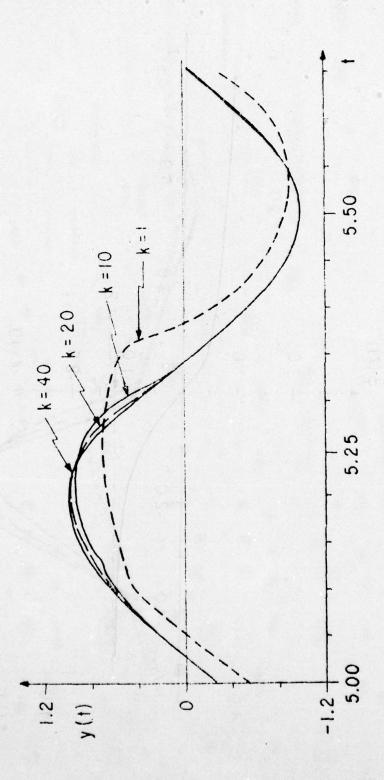
- (1) In describing the feedback system under consideration, we adopted the control terminology, i.e. the power stage of the amplifier is called the plant; the preamplifier is called the compensator; etc. We trust that this will cause no great inconvenience to feedback amplifier enthusiasts.
- (2) In the single-input single-output, linear, time-invariant case,  $\mu\beta = \beta\mu$ ; however, if any one of these three conditions fails, one must write  $\beta\mu$ . We do so to be self-consistent.
- (3) An operator N is continuous on an extended space  $R_e$  iff  $VT \in \mathcal{T}$ ,  $P_TN$  is continuous.
- (4) If  $A \in \mathbb{C}^{n \times n}$ , the largest singular value of A is the square root of the largest eigenvalue of A\*A, where A\* denotes the complex conjugate of A; it is also the  $\ell_2$ -induced norm of the linear map  $A: \mathbb{C}^n \to \mathbb{C}^n$ .
- Note that for any physical system,  $[I+\tilde{G}(j\omega)K(j\omega)F(j\omega)]^{-1} \rightarrow I$  as  $|\omega| \rightarrow \infty$ . Hence it is impossible to fulfill this requirement for all  $\omega \in \mathbb{R}$ .
- (6) Recall that if for some (i,j),  $n_{ij}(s) \equiv 0$ , then  $\partial n_{ij} : = -\infty$ .
- (7) The results of this section were obtained with the collaboration of A. N. Payne.
- (8) A function  $y(\cdot)$ :  $\mathbb{R}_+ \to \mathbb{R}^n$  is said to be <u>asymptotically T-periodic</u> iff  $y(\cdot) = y_T(\cdot) + y_O(\cdot)$ , where  $y_T(\cdot)$  is a T-periodic function and  $y_O(t)$  tends to  $\theta_n$  as  $t \to \infty$ .
- (9)  $N \in \mathcal{N}$  is said to be Fréchet differentiable at x iff  $\forall T \in \mathcal{T}$ ,  $P_TN$  is Frechet differentiable at x.
- (10)  $\underline{L} \in \mathcal{L}$  is said to be continuous iff  $\forall T \in \mathcal{T}$ ,  $\underline{P}_{T}\underline{L}$  is continuous, i.e.  $\forall T \in \mathcal{T}$ ,  $|\underline{L}|_{T} := \sup_{\underline{u} \in \mathcal{U}_{\underline{u}}} \frac{|\underline{L}\underline{u}|_{T}}{|\underline{u}|_{T}} < \infty$ .

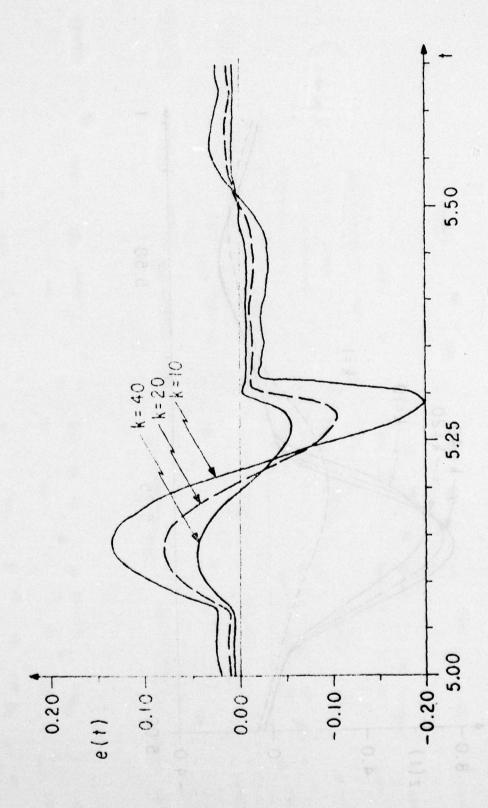


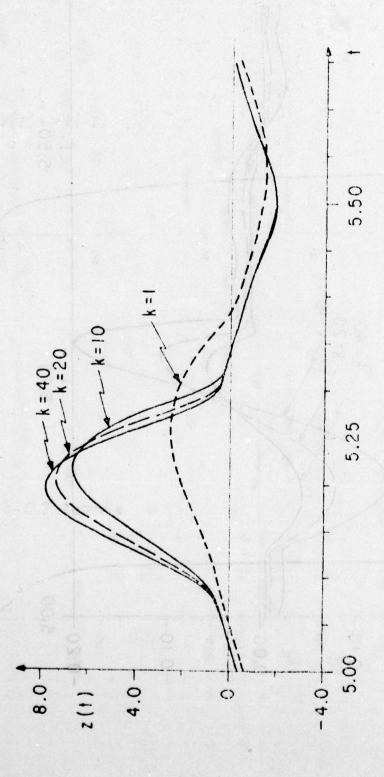


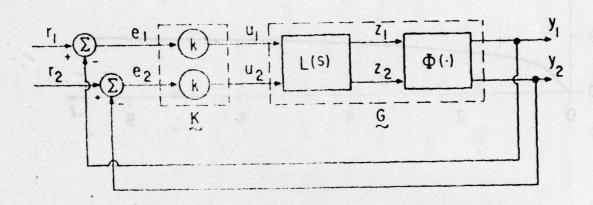


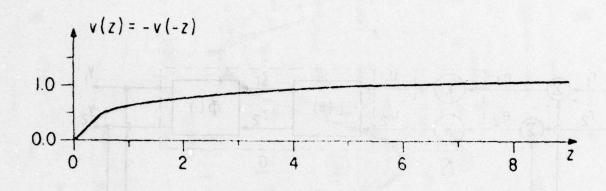


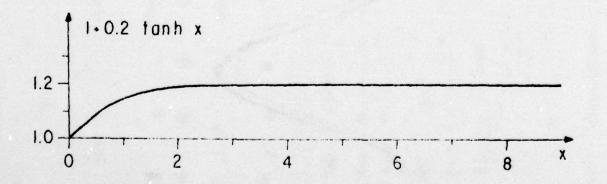


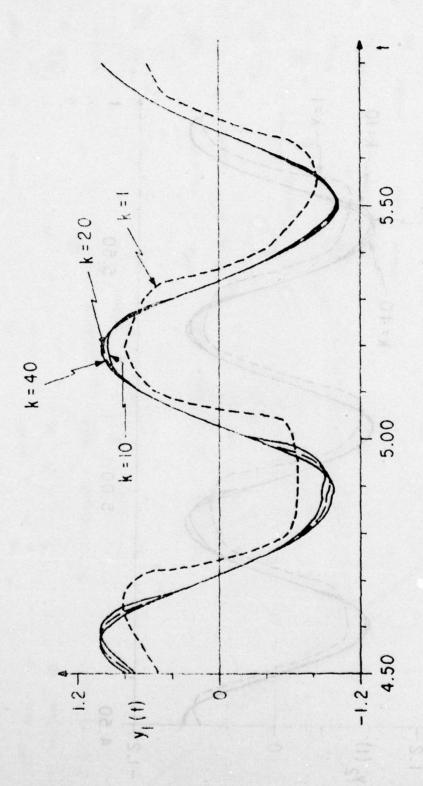


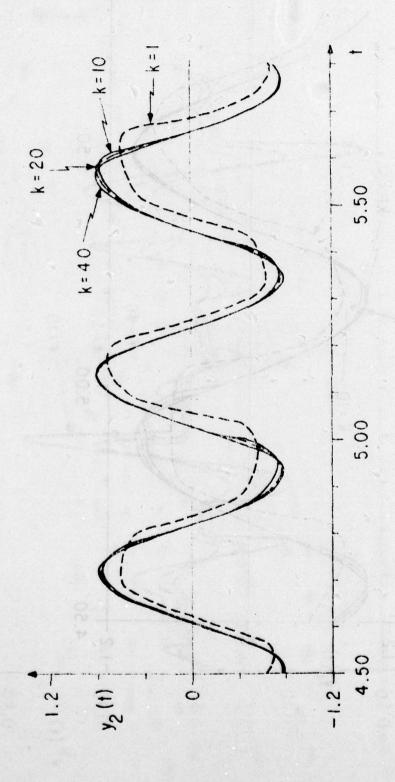


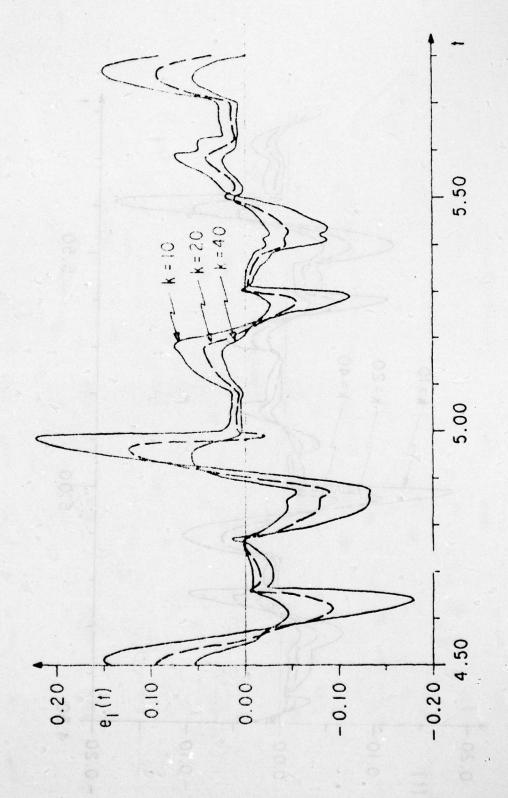


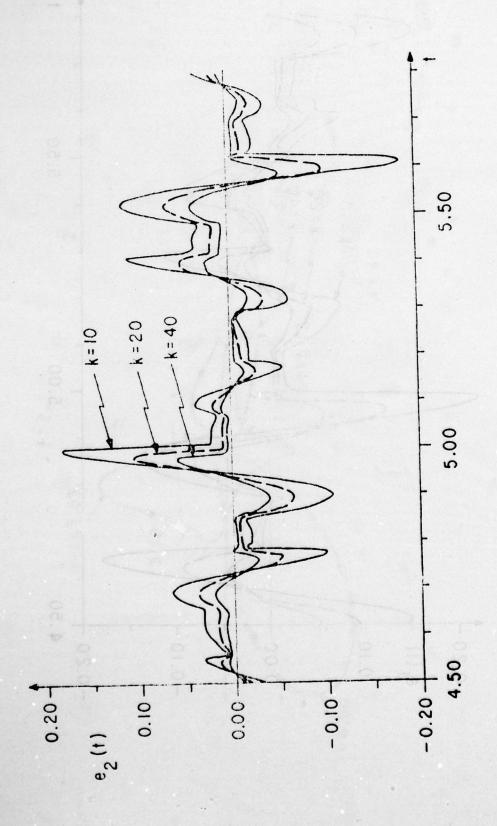


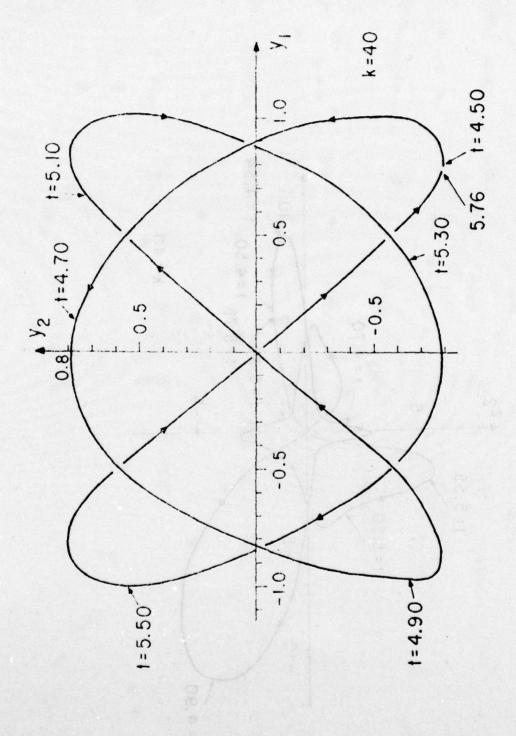


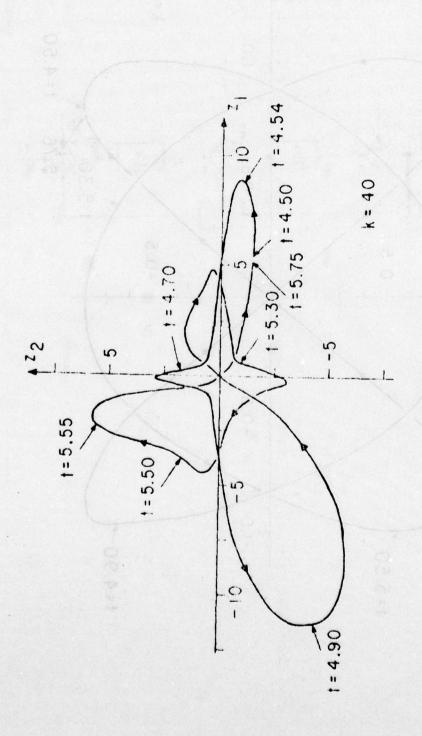


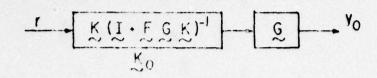


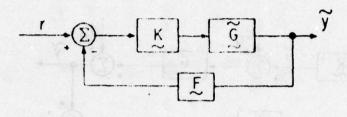


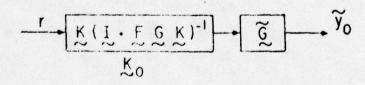


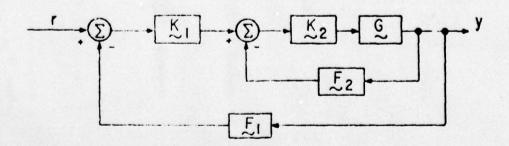


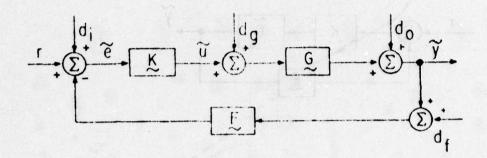




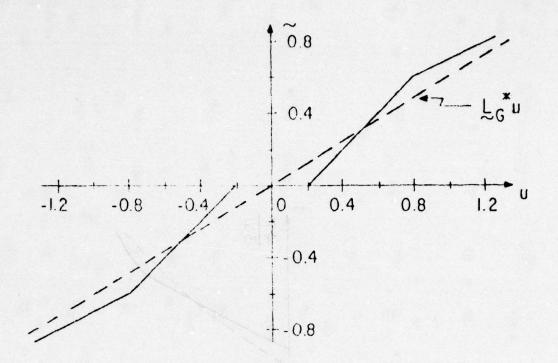


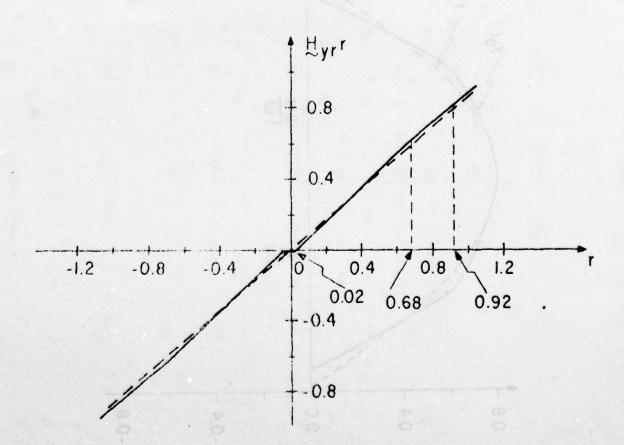


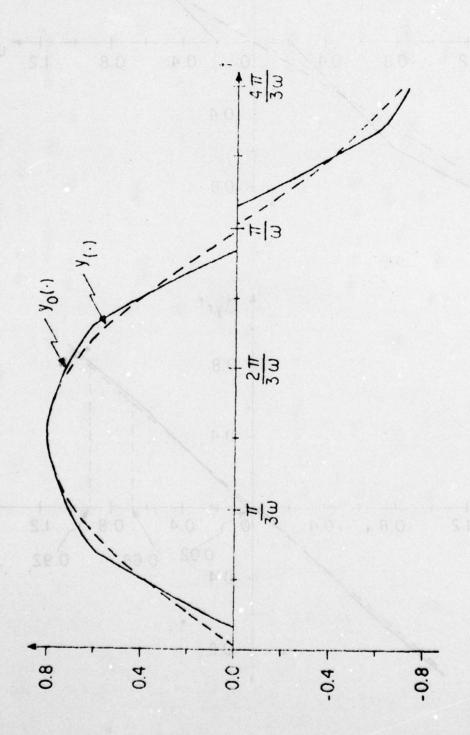


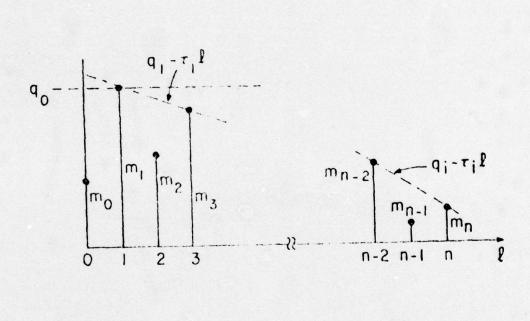


\* - 12 - [2] - [2] - [2] - [3] - [3]









# ON-LINE TUNING OF MULTIVARIABLE PI CONTROLLERS USING PRINCIPAL COMPONENT ANALYSIS: PRELIMINARY RESULTS

by

B.C. Moore

Systems Control Report No. 7905 April 1979

erg of before interest control over the control was interest and interest and interest and interest.

Mana and man Although value , daming a fluorer

Department of Electrical Engineering, University of Toronto, Toronto, Ontario, Canada. M5S 1A4

This research was supported by the Natural Sciences and Engineering Research Council of Canada, under operation grant No. A3925.

# ON-LINE TUNING OF MULTIVARIABLE PI CONTROLLERS USING PRINCIPAL COMPONENT ANALYSIS: PRELIMINARY RESULTS

by

B.C. Moore

#### **ABSTRACT**

There has been considerable interest lately in the application of singular value analysis in systems theory. The basic ideas, however, were developed in statistics (Hotelling introduced principal component analysis in 1933) and are currently used in numerical analysis and digital filtering. The fundamental results underlying principal component analysis are presented in this paper, and these results are applied to the problem of tuning multivariable proportional plus integral controllers. Although the tuning method proposed is preliminary, it is designed to avoid possible traps which would prevent "tight" tuning with conventional tuning of individual loops. When applied to non-interacting loops, the method reduces to conventional tuning of the loops simultaneously.

Department of Electrical Engineering, University of Toronto, Toronto, Ontario, Canada. M5S 1A4

This research was supported by the Natural Sciences and Engineering Research Council of Canada, under operating grant No. A3925.

#### I. INTRODUCTION

Although there has been considerable interest lately in the application of singular value analysis in systems theory, [1]-[9], the basic analysis techniques involved are at least 46 years old. Hotelling [10], [11], introduced principal component analysis in 1933, and the effectivenss of these techniques was enhanced substantially by the development of an algorithm (S.V.D.), [12], for efficient, accurate computation of the important objects. These techniques are currently used in the numerical analysis [13]-[15], and digital filtering [16]-[18]. Dempster [19] gives an excellent geometric treatment of principal component analysis as well as an overview of its history and relationship to least squares approximation.

In this paper the fundamental results underlying these analysis tools are presented (Section II), and a preliminary method (using these tools) for on-line tuning of multivariable proportional-plus-integral controllers is proposed (Sections III, IV). When the method is applied to a set of non-interacting loops, it reduces to a standard classical technique ([20], page 330).

Although the point will not be pursued here, <u>linearity does not play an</u>
essential role in principal component analysis. Preliminary ideas on the application of these tools to nonlinear problems are given in [21].

Notation:  $\mathbb{R}$ , ¢ will represent the fields of real and complex numbers. For a vector v and matrix M,  $v^T$ ,  $M^T$  represent the transpose,  $v^*$ ,  $M^*$  represent the complex conjugate and  $v^H$ ,  $M^H$  represent the conjugate transpose.

## II. FUNDAMENTAL RESULTS

The results given in this section form the foundation for the principal component analysis techniques to be discussed in later sections. The two propositions given below may be viewed as one result stated in two different contexts: the first involving discrete data samples; the second, continuous data. The constant K plays no role other than an aid for discussion.

#### Discrete Data:

For convenience the samples are organized into a sequence of vectors y(1),y(2),...,y(N) in  $C^n$ , with

$$W^{2} \stackrel{\Delta}{=} K \sum_{\ell=1}^{N} y(\ell) y^{H}(\ell). \qquad (K>0)$$

This matrix is positive semidefinite with a set of non-negative eigenvalues

$$\sigma_1^2 \geq \sigma_2^2 \geq \ldots \geq \sigma_n^2 \geq 0$$

and corresponding mutually orthogonal unit eigenvectors  $u_1, u_2, \ldots, u_n$ .

# Proposition 1A:

Let the scalar sequence  $y_i(1), y_i(2), \dots, y_i(N)$  be defined by

$$y_i(\ell) = u_i^H y(\ell)$$

for  $1 \le i \le n$ . Then  $y(\ell) = \sum_{i=1}^{n} u_i y_i(\ell)$ , where

$$\left[\kappa \sum_{\ell=1}^{N} |y_{i}(\ell)|^{2}\right]^{1/2} = \sigma_{i}$$

<u>Proof</u>: The first identity follows from the fact that  $U=(u_1,u_2,...,u_n)$  is unitary. Furthermore

$$K \sum_{\ell=1}^{N} ||y_{i}(\ell)||^{2} = K \sum_{\ell=1}^{N} u_{i}^{H} y(\ell) y(\ell)^{H} u_{i} = u_{i}^{H} w^{2} u_{i}^{H}$$

and the second identity follows trivially.

Stated in other words, Proposition 1A says that we can decompose the vector sequence into the vector sum of spacially orthogonal sequences (called <u>components</u>) ordered with respect to magnitude.

The important objects in Proposition 1A are the pairs  $(\sigma_i, u_i)$ , i=1,...,n, and these can be computed without first computing  $W^2$ . If a data matrix Y is constructed with N columns consisting of the vectors y(1), y(2),...,y(N), then

$$w^2 = yy^H$$

and  $(\sigma_i, u_i)$ ,  $1 \le i \le n$ , are the singular values and left singular vectors of Y. These may be computed directly using the well known algorithm (S.V.D.) developed by Golub and Reinsch [12] (see also [9]).

each a sourcement been arrive of season source values of court and cometruct a data

multis I whose column are the species . For X lerge, recompiler mirroximation

1

#### Continuous Data:

Now consider a piecewise continuous map  $f: C \to C^n$  defined by y=f(x), and let

$$w^2 = K \int_{x_1}^{x_2} f(x) r^H(x) dx$$
 (K>0)

with eigenvalues  $\sigma_1^2 \ge \sigma_2^2 \ge \ldots \ge \sigma_n^2 \ge 0$  and mutually orthogonal unit eigenvectors  $u_1, u_2, \ldots, u_n$ .

### Proposition 1B:

Let  $f_i: C \rightarrow C$  be defined by  $f_i(x) = u_i^H f(x)$ . Then

$$f(x) = \sum_{i=1}^{n} u_i f_i(x)$$

where

$$\left[K \int_{x_1}^{x_2} |f_i(x)|^2 dx\right]^{1/2} = \sigma_i$$

Proof: Similar to the proof of Proposition 1A.

Here we decompose the vector valued function into the sum of spacially orthogonal component functions ordered with respect to magnitude. The same computational tool, S.V.D., can be used to compute  $(\sigma_i, u_i)$  without actually computing  $W^2$ . To do this, divide  $[x_1, x_2]$  into N evenly spaced sample points and construct a data matrix Y whose columns are the samples. For N large, rectangular approximation of the integral gives

$$\int_{x_1}^{x_2} f(x) f^H(x) dx \approx (1/N) YY^H$$

To compute  $(\sigma_i, u_i)$ ,  $1 \le i \le n$ , one may apply S.V.D. to the scaled data matrix

$$(K/N)^{1/2}Y$$

# A Combined Result for Linear Systems

With linear systems, we shall often encounter a matrix F(x) which can be viewed as a set of maps  $f_1(x), f_2(x), \ldots, f_m(x)$ , one corresponding to each column of F. In this situation it is appropriate to combine Propositions 1A, 1B. Let

$$w^2 = K \sum_{i=1}^{m} \int_{x_1}^{x_2} f_i(x) f_i^H(x) dx = K \int_{x_1}^{x_2} F(x) F^H(x) dx.$$

If  $(\sigma_1^2, u_1), \dots, (\sigma_n^2, u_n)$  are the ordered eigenvalue, eigenvector (orthonormal) sets for  $W^2$ , and

$$F_i(x) \stackrel{\Delta}{=} u_i^H F(x)$$

then

$$F(x) = \sum_{i=1}^{n} u_i^H F_i(x)$$

where

$$\left\{ K \int_{x_{1}}^{x_{2}} \|F_{i}(x)\|^{2} dx \right\}^{1/2} = \sigma_{i}$$

To compute  $(\sigma_i, u_i)$  in this situation, divide  $[x_1, x_2]$  into N evenly spaced sample points  $s_1, s_2, \ldots, s_N$ , and let

$$Y = (F(s_1) F(s_2) \dots F(s_N)).$$

If there are m columns in F and N sample points, then Y has mN columns.

### Remarks about Perturbations:

Suppose the matrix F(x) is perturbed to give  $F_{\Delta}(x)=F(x)+\Delta F(x)$ . Then

$$u_{i}^{H}F_{\Delta}(x) = F_{i}(x) + u_{i}^{H}\Delta F(x)$$

and it follows that

$$\left\{ \int_{x_{1}}^{x_{2}} \|F_{i}(x) - u_{i}^{H} F_{\Delta}(x)\|^{2} dt \right\}^{1/2} \leq \left\{ \int_{x_{1}}^{x_{2}} \|\Delta F(x)\|^{2} dx \right\}^{1/2}$$

where the equality is achieved if  $\Delta F(x)$  is aligned with  $u_i$ .

This is a double edged sword. First, it gives a tool for coping with structural instability associated with many theoretical results. Theory says, for example, that if every column of F(x) is contained in a proper subspace S for all  $x_{\varepsilon}[x_1,x_2]$ , then we may project onto S to simplify the situation (by reducing dimensionality). Such a subspace S may, however, be structurally unstable: there may exist arbitrarily small admissable perturbations such that the columns of  $F(x)+\Delta F(x)$  are not contained in a proper subspace. We are guaranteed, however, that  $F_{\Delta}(x)$  will have weak components (assuming small perturbations) and that the strong components will define a subspace which is close to S.

The other edge of the sword gives us help in deciding roughly how accurate we can expect the components to be. If for example, there are components whose magnitudes are of the same order as the instrumentation precision, then they may be in error by ~100% and one can hardly use them (say for feedback) with confidence.

# General Comments about Applications:

The results of this section provide a strong tool for spacial analysis (possibly on-line in many situations) of multivariable signals in the time or frequency domains.

If, for example, f(t) is a vector of signals and

$$w^2 = K \int_{t_1}^{t_2} f(t) f^T(t) dt$$

then Proposition 1B gives a decomposition into components ordered with respect to their energy (K=1) or average power  $\left(K = \frac{1}{t_2 - t_1}\right)$ 

$$\left[K \int_{t_1}^{t_2} f_i^2(t) dt\right]^{1/2} = \sigma_i$$

For a vector f(jw) in the frequency domain, and

$$w^2 = \int_{w_1}^{w_2} f(jw) f^H(jw) dw,$$

one gets information about the spacial distribution of f(jw) over the frequency band  $[w_1, w_2]$ .

# Remarks about Computation:

Although one might be alarmed at the thought of using a minicomputer to compute the singular values and left singular vectors of a matrix Y with, say, 10 rows and 100 columns, it is quite reasonable. One can recursively (treating one column of data at a time) reduce Y to a unitarily equivalent matrix (see [14], p. 383)

The other edge of the sacrd gives on help in deciding

where  $\hat{Y}$  is 10×10; this process requires  $\approx 100(10^2)=10,000$  operations. Singular value decomposition of  $\hat{Y}$  requires  $\approx 6(10^3)=6000$  operations, giving a total of operation count of  $\approx 16,000$ .

At first it may seem simpler to find the components by computing the eigenvalues and eigenvectors of YY<sup>H</sup>. Experts recommend that this be avoided (by using S.V.D.) for the following reason (see [14], p. 382 for more discussion): This method <u>doubles</u> the demand for internal computer resolution associated with the algorithm.

Specifically, suppose one has invested money in 12 bit A-D converters and has interfaced these properly so that there is 12 bit resolution associated with the data. To get this same resolution on the span  $[0,\sigma_1]$ ; that is, to have

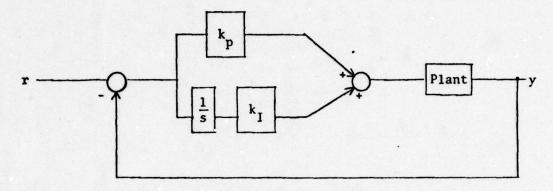
$$\sigma_{i} - 2^{-12}\sigma_{i} \le \{\text{computed value of } \sigma_{i}\} \le \sigma_{i} + 2^{-12}\sigma_{i}$$

requires at least 12 bit internal resolution using S.V.D., and at least 24 bit internal resolution using the "squared up" version where YYH is computed.

Stated in other words, possibly more to the point with current minicomputer hardware organization, it is highly probable (work needs to be done here) that one can get 12 bit resolution with 12 bit A-D converters and 16 bit operations if S.V.D. is used. It is impossible to do so with the other algorithm; one would probably need to carry out the computations using 32 bit arithmetic.

#### III. MULTIVARIABLE PI CONTROL

Consider the following PI (Proportional+Integral) control loop which is assumed to be open loop stable:

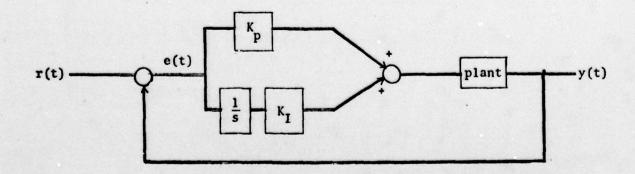


With a single isolated loop such as this, one can often follow a simple procedure to adjust the gains  $k_p$ ,  $k_I$ ; i.e. to "tune" the control loop. One classical method (see [20], p. 330) is the following:

with  $k_I$ =0 increase  $k_p$  (this improves response speed) until the step response is highly oscillatory. Reduce  $k_p$  by a factor of 2.

•increase  $k_{I}$  (this reduces offset) until the step response is highly oscillatory. Reduce  $k_{I}$  by a factor of 2.

With multiple interacting PI control loops, there are inherent "traps" associated with extending simple procedures such as this. To bring some of these problems into closer view, consider the system shown below



where  $K_p$ ,  $K_I$  are diagonal matrices of proportional and integral gains, respectively. Let's assume that each variable is scaled so that one unit corresponds to a fixed percentage of "full swing" and that we are free to sample e(t), the error vector.

Let E(t) be the matrix made up of error responses to unit steps; i.e. the i<sup>th</sup> column of E(t) is the error response to a unit step applied to the i<sup>th</sup> reference input. For a linear system, the response to an arbitrary vector of steps

projects significantly onto usek coord

$$r(t) = r \delta(t)$$

is given by

$$e(t) = E(t)r.$$

The steady state error (assuming stability) is

where 
$$E_{ss} \stackrel{\Delta}{=} \underset{t\to\infty}{\text{limit }} E(t)$$
.

A major trap follows from the fact that an operator sees only projections of the vector e(t) on the basis vectors of a <u>fixed</u> coordinate system associated with the physical arrangement of hardware (sensors). It is possible for rather simple mechanisms to appear complicated in this fixed coordinate system. The following paragraphs show that simple mechanisms involving the notions of settling time, oscillations, and steady state errors may be confusing when viewed through projections.

# Settling Time: Para a topmes for assat was assat bas to be t

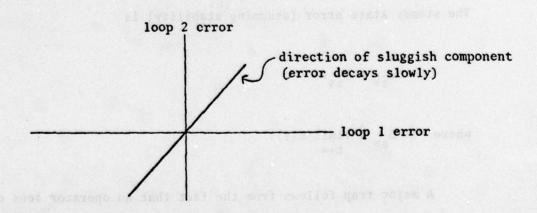
Let  $T(t) = E(t) - E_{ss}$  be the transient response map so that

$$e(t) = e_{tr}(t) + e_{ss}$$

where

$$e_{tr}(t) = T(t)r$$

It is certainly possible for the response to have one sluggish component which projects significantly onto each coordinate; i.e. all loops appear sluggish.



Actually for a system with n loops, one can define n settling times as follows: Let

$$W^{2}(t) = \int_{t}^{\infty} T(\tau)T^{T}(\tau)d\tau$$

with eigenvalue, eigenvector pairs  $(\sigma_1^2(t), u_1(t)), (\sigma_2^2(t), u_2(t)), \dots, (\sigma_n^2(t), u_n(t))$ .

Then

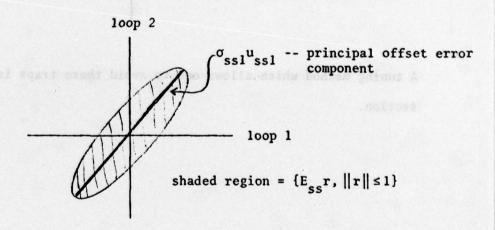
 $t_{si} \stackrel{\triangle}{=} minimum time such that <math>\sigma_i(t_{si}) < \epsilon$ .

Note that  $t_{s1} \ge t_{s2} \ge ... \ge t_{sn}$ .

Further on in this section we shall propose one procedure for "tightening" the response in the direction associated with sluggish components.

# Steady State Errors:

Consider  $W_{ss}^2 = E_{ss}E_{ss}^T$  with eigenvalue, eigenvector pairs  $(\sigma_{ss1}^2, u_{ss1}^2), \ldots, (\sigma_{ssn}^2, u_{ssn}^2)$ . It is entirely possible that there are only a few strong offset error components which project onto every loop



#### Oscillations:

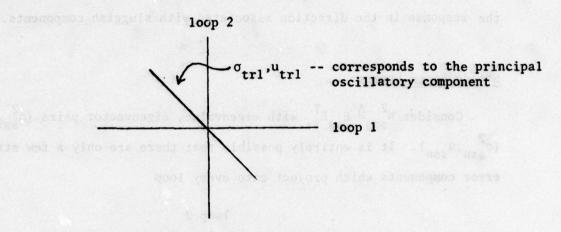
To avoid unnecessary complications, let's assume that there is a single lightly damped sinusoidal component observed in the loop error responses, and that the observed frequency is w. Let  $T_{av} = \int_{0}^{2\pi/w} T(t)dt$  and

$$w_{tr}^2 = \int_0^{2\pi/w} (T(t) - T_{av}) (T(t) - T_{av})^T dt$$

with eigenvalue, eigenvector pairs  $(\sigma_{trl}^2, u_{trl}^2), \dots, (\sigma_{trn}^2, u_{trn}^2)$ .

Again it is possible that there is one strong oscillatory component which projects onto a number of loops

D



A tuning method which allows one to avoid these traps is given in the next section.

# IV. A PRELIMINARY ON-LINE TUNING METHOD

These ideas are preliminary and essentially untested. Undoubtedly tests currently in progress will lead to better tuning methods than the rather vague one proposed in the following paragraphs. The tuning method is basically the classical technique (given in Section III) applied to principal components. If loops are noninteracting, the method reduces to the classical technique applied to all loops simultaneously.

# Part 1 Tightening the Response:

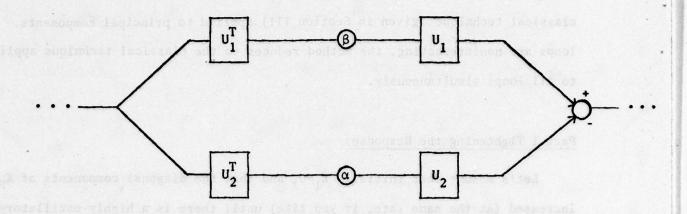
Let's assume that initially  $K_I$ =0, and that the diagonal components of  $K_p$  are increased (at the same rate, if you like) until there is a highly oscillatory component. If the components of

have magnitudes  $\sigma_{trl}, \ldots, \sigma_{trn}$  which are roughly equal, then this step is essentially complete; reduce the gains by a factor of two (to reduce the oscillations) and proceed to Part 2.

If there are some weak components, then increase gains in these directions. Specifically, suppose  $\sigma_{tk} >> \sigma_{trk+1}$ , and let

$$U_1 = (u_1 \ u_2 \ \dots \ u_k); \ U_2 = (u_{k+1} \ \dots \ u_n).$$

Then in the proportional branch, we insert



one proposed in the Sollaving rates realizable. The tuning method is bestcally

where  $\alpha, \beta$  are tuning parameters with  $\alpha=\beta=1$  initially. The parameter  $\alpha$  should be increased until oscillations appear in the lower branch; it may be necessary to reduce  $\beta$  in the process to maintain stability; i.e. to keep upper branch oscillations bounded.

This process

- •compute components of T(t)-Tav
- insert a Rotation-Tuning Gains-Rotation block
- ·adjust gains to get oscillations in weak branch

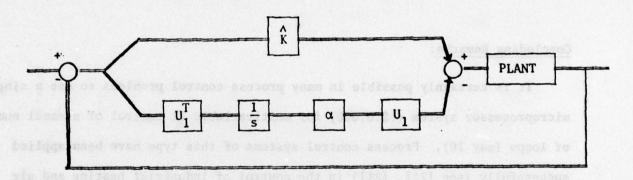
can be continued until the oscillations are "full" with no weak components. The resulting gain matrix  $\hat{K}_p$  in the proportional branch is the product of  $K_p$  and the inserted blocks. The elements of  $\hat{K}_p$  should be reduced by a factor of 2 to reduce oscillations. This completes Part 1.

# Part 2 -- Inserting integral gain to reduce offset errors:

At this point it may be necessary to insert integral action if there is significant offset. Here we shall use the components of  $E_{ss}$  (with controller K). If  $\sigma_{ss} k >> \sigma_{ss} k+1$ , let

$$U_1 = (u_{ss1} \ u_{ss2} \ \dots \ u_{ssk}); \ U_2 = (u_{ssk+1} \ \dots \ u_{ssn})$$

and configure the controller in the following way:

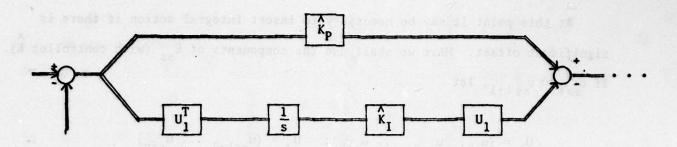


with this configuration,  $\alpha$  should be increased from zero until oscillations occur. If the oscillations are "full" in the space corresponding to the integral branch, reduce  $\alpha$  by a factor of two and stop.

If the oscillations in the integral branch are not full, we may proceed as follows iteratively until the oscillations are full.

- •compute components of  $U_1^T(T(t)-T_{av})U_1$
- •insert a Rotation-Tuning Gains-Rotation block (as in part 1) in the integral branch
- ·adjust gains to increase oscillation in weak integral branch

We are one step away from completion of the proposed tuning algorithm, with the following controller structure



The last step is to reduce the elements of  $\overset{\wedge}{K}_{I}$  by a factor of two.

# Concluding Remarks:

It is certainly possible in many process control problems to use a single microprocessor system (<\$10,000) for multivariable PI control of a small number of loops (say 10). Process control systems of this type have been applied successfully (see [22], [23]) in the control of industrial heating and air conditioning equipment (boilers, chillers, cooling towers, air handlers, etc.). The tuning method proposed in this section can be implemented with little or no additional hardware. The procedure is simple and consistent with classical tuning methods. With a well designed man-machine interface (say bar graphs for singular values and automatic generation of rotation blocks) the method would probably be acceptable to plant operators.

- [1] Moore, B.C. and A.J. Laub, "Computation of supremal (A,B)-invariant and controllability subspaces", IEEE Trans. on Auto. Control, vol. AC-23, no. 5, pp. 783-792.
- [2] Moore, B.C., "Singular value analysis of linear systems", Proceedings of the 1978 IEEE Conference on Decision and Control, Jan. 1979, pp. 66-73.

  Revised paper to appear in IEEE Trans. on Auto. Control, as "Principal Component Analysis in Linear Systems".
- [3] Doyle, J.C., "Robustness of multiloop linear feedback systems", Proceedings of the 1978 IEEE Conference on Decision and Control, Jan. 1979, pp. 12-17.
- [4] Stein, G. and J. Doyle, "Singular values and feedback: design examples", Proceedings of the 16th Annual Allerton Conference on Communication, Control, and Computing, Oct. 1978, pp. 461-470.
- [5] Sandell, N.R., "Robust stability of multivariable feedback systems", Proceedings of the 16th Annual Allerton Conference on Communication, Control, and Computing, Oct. 1978, pp. 471-479.
- [6] Safonov, M.G., "Tight bounds on the response of multivariable systems with component uncertainty", Proceedings of the 16th Annual Allerton Conference on Communication, Control, and Computing, Oct. 1978, pp. 451-459.
- [7] Laub, A.J., "Computational aspects of the singular value decomposition and some applications", Proceedings of the 16th Annual Allerton Conference on Communication, Control, and Computing, Oct. 1978, pp. 432-442.
- [8] Laub, A.J., "Linear multivariable control: numerical considerations", Electronic Systems Laboratory (Now Laboratory for Information and Decision Systems) report ESL-P-833, Massachusetts Institute for Technology, Cambridge, Mass. 02139.
- [9] Klema, V.C. and A.J. Laub, "The singular value decomposition: its computation and some applications", Laboratory for Information and Decision Systems, report LIDS-R-829, Massachusetts Institute of Technology, Cambridge, Mass. 02139
- [10] Hotelling, H., "Analysis of a complex of statistical variables into principal components", Journal of Educational Psychology, vol. 24 (1953), pp. 417-441, pp. 498-520.
- [11] Hotelling, H., "Simplified calculation of principal components", Psychometrika, vol. 1, (1936), pp. 27-35.
- [12] Golub, G.H. and C. Reinsch, "Singular value decomposition and least squares solutions", Numer. Math., 14 (197), pp. 403-420.
- [13] Forsythe, G.E. and C.B. Moler, Computer Solution of Linear Algebraic Systems, Prentice-Hall, Inc., Englewood Cliffs, N.J., 1967.
- [14] Stewart, G.W., Introduction to Matrix Computations, Academic Press, New York, 1973.

ins", itel Trans. on Auto. Concept, vol. AL-IN

- [15] Lawson, C.L. and R.J. Hanson, Solving Lieast Squares Problems, Prentice-Hall, Englewood Cliffs, N.J., 1974.
- [16] Andrews, H.C. and B.R. Hunt, Digital Image Restoration, Prentice-Hall, 1977.
- [17] Mullis, C.T. and R.A. Roberts, "Synthesis of minimum roundoff noise fixed point digital filters", <u>IEEE Trans. on Circuits and Systems</u>, vol. CAS-23, no. 9, pp. 551-562.
- [18] Mills, W.L., C.T. Mullis and R.A. Roberts, "Digital filter realizations without overflow oscillations", IEEE Trans. on Acoustics, Speech, and Signal Processing, vol. ASSP-26, no. 4, pp. 334-338.
- [19] Dempster, A.P., Elements of Continuous Multivariate Analysis, Addison-Wesley, 1969.
- [20] Luyben, W.L., Process Modelling, Simulation, and Control for Chemical Engineers, McGraw-Hill, 1973.
- [21] Moore, B.C., "Principal component analysis in nonlinear systems: preliminary results", University of Toronto Systems Control Report No. 7903, April 1979, Department of Electrical Engineering, University of Toronto, Toronto, Ontario, Canada. M5S 1A4.
- [22] Meals, M. and C.F. Moore, "Microprocessor based distributed control software organization", presented at the 1978 Conference on Computers, Electronics, and Control, Nov. 1978, Toronto, Ontario, Canada. M5S 1A4.
- [23] Jeffreys, J., R. Gaddis, and C.F. Moore, "Microprocessor based distributed control hardware organization", presented at the 1978 Conference on Computers, Electronics, and Control, Nov. 1978, Toronto, Ontario, Canada. M5S 1A4.

[11] Forsythe, C.E. and C.B. Moler, Computer Solution of Linear Algebraic Syst

### ROBUST STABILITY OF LINEAR SYSTEMS - SOME COMPUTATIONAL CONSIDERATIONS\*

by

Alan J. Laub\*\*

#### 1. INTRODUCTION

In this paper we shall concentrate on some of the computational issues which arise in studying the robust stability of linear systems. Insofar as possible, we shall use notation consistent with Stein's paper [1] and we shall make frequent reference to that work.

As we saw in [1] a basic stability question for a linear time-invariant system with transfer matrix G(s) is the following: given that a nominal closed-loop feedback system is stable, does the feedback system remain stable when subjected to perturbations and how large can those perturbations be? It turned out, through invocation of the Nyquist Criterion, that the size of the allowable perturbations was related to the "nearness to singularity" of the return difference matrix  $I + G(j\omega)$ . Closed-loop stability was said to be "robust" if G could tolerate considerable perturbation before I + G became singular.

Invited Paper presented at the Second Annual Workshop on the Information Linkage between Applied Mathematics and Industry held at Naval Postgraduate School, Monterey, California, Feb. 20-24, 1979; this research was partially supported by NASA under grant NGL-22-009-124 and the Department of Energy under grant ET-78-(01-3395).

<sup>\*\*</sup> Laboratory for Information and Decision Systems, Rm. 35-331, M.I.T., Cambridge, MA 02139.

We shall now indulge in a modicum of abstraction and attempt to formalize the notion of robustness. The definition will employ some jargon from algebraic geometry and will be applicable to a variety of situations. While no deep results from algebraic geometry need be employed, the exercise of formulating a precise definition is a useful one for clarifying one's thinking.

Let  $p \in \mathbb{R}^N$  be a vector of parameters from some problem being studied and suppose we are interested in some property  $\mathbb{R}$  of this data. The vector p may consist of the elements of various matrices, for example. If  $\mathbb{R}$  is true at some nominal parameter set  $p_0$  we are frequently concerned with whether  $\mathbb{R}$  remains true in a "neighborhood" of  $p_0$ .

For example,  $p_0$  may be the elements  $(a_{11}, \ldots, a_{1n}, a_{21}, \ldots, a_{nn})$  of a nonsingular nxn matrix  $A_0$  and we are interested in the nonsingularity of nearby matrices. We shall proceed to formalize the often-heard statement that "almost all nxn matrices are nonsingular". First, the jargon:

- Definition 1: A variety  $V = \{p \in \mathbb{R}^N : \psi_i(p_1, ..., p_N) = 0, i = 1, ..., k\}$ where  $\psi_i(x_1, ..., x_N) \in \mathbb{R}[x_1, ..., x_N]$  are polynomials. V is proper if  $V \neq \mathbb{R}^N$  and nontrivial if  $V \neq \emptyset$ .
- Definition 2: A property is a function  $\Pi: \mathbb{R}^N \to \{0, 1\}$ . The property  $\Pi$  holds if  $\Pi(p) = 1$  and fails if  $\Pi(p) = 0$ .
- Definition 3: If V is a proper variety,  $\overline{\mathbb{R}}$  is generic relative to V provided  $\overline{\mathbb{N}}(p) = 0$  only if  $p \in V$ . A property  $\overline{\mathbb{N}}$  is generic if such a V exists.

Our discussion to this point is purely algebraic. Now let us introduce a topology on  $\mathbb{R}^N$ , say the topology induced by some vector norm  $\|\cdot\|$ .

Furthermore, let V be any nontrivial, proper variety. Then we have the following topological definition.

- Definition 4: The property  $\Pi$  is <u>well-posed</u> at p  $\in V^{\mathbb{C}}$  (the complement of V) if  $\Pi$  also holds in a sufficiently small neighborhood of p.
- Lemma 1: The set S of points where a generic property is well-posed is open and dense. Moreover, the Lebesgue measure of S<sup>C</sup> is zero.

The proof of Lemma 1 is routine and is omitted. It is easy to see that a point p where a generic property holds is well-posed but that the converse is not necessarily true.

We now have sufficient framework to make a formal definition of robustness.

Definition 5: Given a point p with generic property  $\Pi$  (generic with respect to some proper variety V) well-posed at p, let  $d = \min_{v \in V} \| p - v \|.$ 

We say I is robust at p if d is "large".

The number d is frequently difficult to compute or estimate. When it can be determined, it gives valuable information about how much perturbation or uncertainty can be tolerated at p. For the situation of special interest in this paper, Example 2 below, we shall see that d can be explicitly calculated, at least theoretically. We now illustrate the above concepts with two examples.

#### Example 1

This example is chosen from Wonham [2] who uses the concepts of genericity and well-posedness in nontrivial ways for a variety of control-theoretic problems. In this trivial example, we seek solutions of the system of linear equations

where  $A \in \mathbb{R}^{m \times n}$  (i.e., A is an mxn matrix with real coefficients) and  $b \in \mathbb{R}^{m}$ .

Our parameter vector is p where

$$p^{T} = (a_{11}, ..., a_{1n}, ..., a_{mn}; b_{1}, ..., b_{m}) \in \mathbb{R}^{N}, N = mn + m$$

(T denotes transpose). If is the property of the equation having a solution which is equivalent, of course, to the statements that b @ Im A or rk[A, b] = rk A. For example, if  $A = \begin{pmatrix} 1 & 2 \\ 2 & 4 \end{pmatrix}$  and  $b = \begin{pmatrix} b_1 \\ b_2 \end{pmatrix}$  then  $II(1,2,2,4; b_1,b_2) = \begin{cases} 0 & \text{if } b_2 \neq 2b_1 \\ 1 & \text{if } b_2 = 2b_1 \end{cases}$ 

It is then easy to show the following: (see [2])

- 1.  $\Pi$  is generic if and only if  $m \le n$ .
- 2. It is well-posed at p if and only if rk A = m.

### Example 2

This example is similar to Example 1 in the special case m=n. We are given a nonsingular matrix  $A \in \mathbb{R}^{n \times n}$  and we are concerned with the nearness of A to singularity. Identifying A with  $p^T = (a_{11}, \ldots, a_{1n}, a_{21}, \ldots, a_{nn})$  we define the property II by

$$\Pi(p) = \begin{cases}
0 & \text{if p represents a singular matrix} \\
1 & \text{if p represents a nonsingular matrix}.
\end{cases}$$

Then it is easy to see that  $\Pi$  is a generic property and well-posed where it holds. This is the precise statement that "almost all nxn matrices are nonsingular". Formally writing down the determinant of A as a polynomial in  $a_{11}, \ldots, a_{nn}$  defines the necessary variety V. It turns out, in a theorem attributed by Kahan [3] to Gastinel, that the distance d from a point  $p \in V^C$  to V can be explicitly determined.

Theorem 1: A nonsingular matrix A differs from a singular matrix by no more in norm than  $\frac{1}{\|\mathbf{A}^{-1}\|}$ , i.e., given A,

$$\frac{1}{\|\mathbf{A}^{-1}\|} = \min\{\|\mathbf{E}\| : \mathbf{A} + \mathbf{E} \text{ is singular}\}.$$

Thus  $d = \frac{1}{\|A^{-1}\|}$  and we might say that A is robust with respect to invertibility if d is "large". To avoid certain scaling difficulties, it may be more desirable to work with a relative measure of distance,  $d^{rel}$ , defined by

$$d^{rel} = \frac{d}{\|A\|} = \frac{1}{\|A\| \cdot \|A^{-1}\|} = \frac{1}{\kappa(A)} .$$

The quantity  $\kappa(A)$  is recognizable as the condition number of A with respect to inversion. Of course, all the above quantities depend on the particular matrix norm used. To exhibit the specific dependence on the norm  $\|\cdot\|_q$  we shall append a subscript "q". For example,

$$\mathbf{d}_{\mathbf{q}} = \frac{1}{\left\|\mathbf{A}^{-1}\right\|_{\mathbf{q}}}$$

The minimizing E in Theorem 1 can be explicitly constructed for a number of standard matrix norms. For example:

1. 
$$\|\mathbf{A}\|_{2} = (\lambda_{\max}(\mathbf{A}^{\mathrm{T}}\mathbf{A}))^{1/2}$$
.

Let A have singular value decomposition  $A = USV^T$  where  $U, V \in \mathbb{R}^{n\times n}$  are orthogonal and  $S = diag\{\sigma_1, \ldots, \sigma_n\}$ . The  $\sigma_i$ 's,  $\sigma_1 \geq \ldots \geq \sigma_n > 0$ , are the singular values of A. The minimizing E is given by  $E = URV^T$  where  $R = diag\{0, \ldots, 0, -\sigma_n\}$ . Then

$$\|\mathbf{E}\|_2 = \sigma_{\mathbf{n}} = \frac{1}{\|\mathbf{A}^{-1}\|}$$

and A + E is singular. The singular direction, i.e., a nonzero vector z such that (A + E)z = 0, is given by the  $n + \frac{th}{c}$  column of V.

2. 
$$\|A\|_{\infty} = \max_{i \in \underline{n}} \{ \sum_{j=1}^{n} |a_{ij}| \}, \underline{n} = \{1, 2, ..., n \}$$
.

Suppose  $A^{-1} = [\alpha_{ij}]$  and  $||A^{-1}|| = \sum_{j=1}^{n} |\alpha_{kj}|$  for  $k \in \underline{n}$ . Then the minimizing E is a matrix all of whose elements are 0 except for the  $k^{\underline{th}}$  column which consists of the elements

$$\frac{-\operatorname{sgn} \alpha_{kl}}{\|\mathbf{a}^{-1}\|_{\infty}}, \dots, \frac{-\operatorname{sgn} \alpha_{kn}}{\|\mathbf{a}^{-1}\|_{\infty}}$$
In fact, letting  $\mathbf{z} = \operatorname{sgn} \begin{pmatrix} \alpha_{kl} \\ \vdots \\ \alpha_{kn} \end{pmatrix}$  and  $\mathbf{u} = \begin{pmatrix} 0 \\ \vdots \\ 1/\|\mathbf{a}^{-1}\|_{\infty} \end{pmatrix}$  with the only  $\vdots$ 

nonzero component of u being in the  $k^{\underline{th}}$  row, we have  $E = -zu^T$  and clearly  $\|E\|_{\infty} = \frac{1}{\|A^{-1}\|_{\infty}}$ . Now,  $(I + EA^{-1})z = (1 - u^TA^{-1}z)z = 0$  since the  $k^{\underline{th}}$  element of  $A^{-1}z$  is  $\sum_{j=1}^{k} |\alpha_{kj}| = \|A^{-1}\|_{\infty}$  so that  $u^TA^{-1}z = 1$ . Hence  $A + E = (I + EA^{-1})A$  is singular. Moreover, the singular direction is given by  $A^{-1}z$  since  $(A+E)A^{-1}z = 0$ .

3. 
$$\|\mathbf{a}\|_{1} = \max_{j \in \mathbf{n}} \{\sum_{i=1}^{n} |\mathbf{a}_{ij}|\}.$$

The results for this norm are analogous to  $\|\cdot\|_{\infty}$  and can be derived directly or by noticing that  $\|A\|_1 = \|A^T\|_{\infty}$ . For completeness we note that if  $\|A\|_1 = \sum\limits_{i=1}^n |\alpha_{ik}|$  for  $k \in \underline{n}$  and

$$z = sgn\begin{pmatrix} \alpha_{1k} \\ \vdots \\ \alpha_{nk} \end{pmatrix}, \qquad u = \begin{pmatrix} 0 \\ \vdots \\ 1/||A^{-1}||_{1} \\ \vdots \\ 0 \end{pmatrix}$$

then the minimizing E is given by  $E = -uz^{T}$ .

We shall see in Section 3 how the results in Example 2 can be applied in studying robustness of stability of linear systems.

There so is the spirit expensed at the bet not generally

#### 2. THE LINEAR SYSTEMS SETTING

In this section we shall provide a brief introduction to both the linear time-invariant systems setting and to the fundamental notion of feedback. This will serve a two-fold purpose: first, to set the stage for the basic stability results and second, to introduce the jargon and notation, especially for non-engineers. This material is standard and can be found in any of a number of standard textbooks on control systems.

We shall consider modelling physical systems by models which take
the form of a system of linear constant-coefficient ordinary differential
equations

$$\dot{\mathbf{x}}(\mathbf{t}) = \mathbf{A}\mathbf{x}(\mathbf{t}) + \mathbf{B}\mathbf{u}(\mathbf{t}) \tag{1}$$

$$y(t) = Cx(t) \tag{2}$$

The vector x is an n-vector of states, u is an m-vector of inputs or controls, and y is an r-vector of outputs or observed variables.

Starting from the initial condition x(0) the solution of (1) is well-known to be

$$\mathbf{x(t)} = \mathbf{e}^{tA}\mathbf{x(0)} + \int_{0}^{t} \mathbf{e}^{(t-\tau)A}\mathbf{B}\mathbf{u}(\tau)d\tau, \quad t \ge 0$$
 (3)

so that the output is given by

$$y(t) = Ce^{tA}x(0) + \int_{Ce}^{t} (t-\tau)^{A}Bu(\tau) d\tau, t \ge 0$$
 (4)

where e is the matrix exponential defined, but not generally computed, by

$$e^{tA}:=\sum_{k=0}^{+\infty}\frac{t^kA^k}{k!}.$$

The matrix Ce th is called the impulse response matrix.

Denoting (one-sided) Laplace transforms by upper case letters, take
Laplace transforms in (4) to get

$$Y(s) = CX(s) = C(sI - A)^{-1}x(0) + C(sI - A)^{-1}BU(s)$$
 (5)

The matrix G(s): =  $C(sI - A)^{-1}B$  is called the <u>transfer matrix</u>. Notice that G(s) is the Laplace transform of the impulse response matrix.

As will be seen in the sequel, it is of interest to study the response of the above linear system to sinusoidal inputs of the form

$$u(t) = e^{j\omega t}v, \quad t \ge 0 \tag{6}$$

where v is a constant m-vector,  $\omega$  is the frequency of the sinusoidal input, and  $j = \sqrt{-1}$ . The response of (1) to this input can then be shown to be of the form

$$x(t) = e^{tA}a + (j\omega I - A)^{-1}Bve^{j\omega t}, \qquad t \ge 0$$
 (7)

where a is a constant n-vector depending on initial conditions. Now, in the case where A is stable (i.e., its spectrum lies in the left-half of the complex plane) the quantity e A goes to zero as t approaches +\infty. The resulting output

$$y(t) = C(j\omega I - A)^{-1}Bve^{j\omega t}$$
 (8)

is called the steady-state frequency response and the matrix

$$G(j\omega):=C(j\omega I-A)^{-1}B, \qquad (9)$$

which turns out to be the transfer function evaluated at  $s = j\omega$ , is called the <u>frequency response matrix</u>.

Turning now to the case of a real signal given by

$$u_{k}(t) = v_{k} \sin(\omega t + \phi_{k}), \quad t \ge 0$$
 (10)  
 $u_{i}(t) = 0, \quad i = 1,..., m; i \ne k,$ 

we have steady-state frequency response of the 1th output given by

$$y_{\ell}(t) = |G_{\ell k}(j\omega)|v_{k} \sin(\omega t + \phi_{k} + \psi_{\ell k})$$
 (11)

where  $\psi_{l,k} = \arg(G_{l,k}(j\omega))$ .

Aside from its obvious importance in the above analysis, the frequency response matrix is important for two reasons:

- 1. Sinusoidal signals are readily available as test signals for a linear system so  $G(j\omega)$  can be experimentally determined.
- 2. Various plots or graphs associated with G(jω) can be used to analyze control systems, for example, with respect to stability. Plots such as those associated with the names of Bode, Nichols, and Nyquist are essentially different ways of graphically representing |G<sub>lk</sub>(jω)| and arg(G<sub>lk</sub>(jω)) as functions of ω. These plots are used extensively in the analysis of single-input single-output control systems where the robustness of stability, e.g., the amount of gain and phase margin available, is checked essentially visually. The appropriate techniques in the multiple-input multiple-output case are still being investigated and part of the motivation for the research in [1] and this paper is directed towards this end.

Turning now to the notion of feedback whose essential idea is to allow for stability of a system in the face of uncertainty (noise, model error, etc.), the diagram below illustrates the basic (unity) feedback control system:

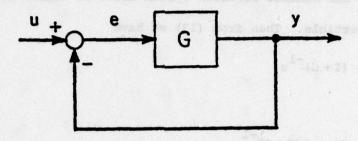


Fig. 1. Basic Feedback Control System

Here u is a reference input, y is the output, and e = u - y is the error or difference between the reference input and the output which we wish to be, ideally, zero. The plant, compensators, actuators, and sensors are all represented by G. There are much more elaborate and detailed feedback structures than that described above and the structure can be studied in a considerably more general function-space setting (see [4], for example) than the simple linear causal time-invariant setting we shall consider. However, the simple system is adequate to exhibit most of the key ideas in this paper. Now, in this system we have

$$e \neq u - y = u - Ge$$
 (12)  
or,  $(I+G)e = u$  (13)

The quantity I + G is called the return difference matrix. As in [1], the matrix G(jw) then provides sufficient data, via the Nyquist criterion, to test for stability of the closed-loop system. Henceforth, we shall assume that our nominal feedback system above is stable in which case I+G is invertible. Then from (13) we have

$$e = (I+G)^{-1}u$$
 (14)

so that

$$y = Ge = G(I + G)^{-1}u$$
 (15)

In (15), the quantity  $G(s)(I + G(s))^{-1}$  is called the <u>closed-loop transfer</u> matrix while  $G(j\omega)(I + G(j\omega))^{-1}$  is called the <u>closed-loop frequency</u> response matrix. We then pose the basic stability question:

Does the nominal feedback system remain stable when subjected to perturbations and how large can those perturbations be?

Let us observe at this point that there is nothing sacred about linearity in the above discussion and more general nonlinear treatments can be found in [4] and [5], for example. The question of "nearness to singularity" of (I+G), even in the nonlinear case, is naturally intimately related to a notion of condition number for nonlinear equations. The interested reader could readily adapt the ideas of Rheinboldt [6] to the particular application at hand here.

#### 3. BASIC STABILITY RESULTS AND RELATED TOPICS

#### a. ADDITIVE AND MULTIPLICATIVE PERTURBATIONS

We shall consider two fundamental types of perturbations in the basic feedback system of Fig. 1. Throughout this section,  $\|\cdot\|$  will denote any matrix norm with  $\|\mathbf{I}\| = 1$ . The first case to be considered is the case of additive perturbations to G, pictured below:

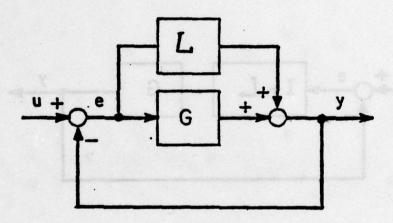


Fig. 2. Additive Perturbations

In other words, the nominal G is perturbed to G + L. Under the assumptions that both the nominal closed-loop system and the perturbation L are stable it can be seen from the Nyquist criterion and the identity

$$I + G + L \equiv (I + G) [I + (I + G)^{-1}L]$$
 (16)

that the perturbed closed-loop system remains stable if

$$\|(\mathbf{I} + \mathbf{G}(\mathbf{j}\omega))^{-1}\mathbf{L}(\mathbf{j}\omega)\| < 1, \quad \omega > 0$$
 (17)

A weaker condition than (17) but one which directly exposes L is

$$\|\mathbf{L}(j\omega)\| < \frac{1}{\|(\mathbf{I} + G(j\omega))^{-1}\|}, \quad \omega > 0$$
 (18)

The second case to be considered is that of multiplicative perturbations:

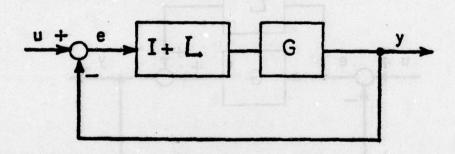


Fig. 3. Multiplicative Perturbations

In this case, the nominal G is perturbed to G(I+L). Under the assumptions that both the nominal closed-loop system and the perturbation L are stable it can be shown from the Nyquist criterion and the identity

$$I + G(I + L) \equiv (I + G) [I + (I + G^{-1})^{-1}L]$$
 (19)

that the perturbed closed-loop system remains stable if

$$\|(\mathbf{I} + \mathbf{G}^{-1}(j\omega))^{-1}\mathbf{L}(j\omega)\| < 1, \qquad \omega > 0$$
 (20)

(assuming G<sup>-1</sup> exists). Again, a weaker condition than (20) but one which directly exposes L is

$$\|\mathbf{L}(j\omega)\| < \frac{1}{\|(\mathbf{I} + \mathbf{G}^{-1}(j\omega))^{-1}\|}, \ \omega > 0.$$
 (21)

Remark 1: As we noted in Section 1, the above inequalities are tight,
i.e., the < cannot be replaced with < .</pre>

Remark 2: Where convenient we shall henceforth drop the "jw" arguments.

Remark 3: It must be stressed that the results based on

$$\|(\mathbf{I} + \mathbf{G}^{\pm 1})^{-1}\| \|\mathbf{L}\| < 1$$
 (18), (21)

are weaker than those based on

$$\|(\mathbf{I} + \mathbf{G}^{\pm 1})^{-1}\mathbf{L}\| < 1$$
 (17), (20)

since

$$\|(\mathbf{I} + \mathbf{G}^{\pm 1})^{-1}\mathbf{L}\| \leq \|(\mathbf{I} + \mathbf{G}^{\pm 1})^{-1}\| \cdot \|\mathbf{L}\|.$$
 (22)

For example, if  $L = c(I + G^{\pm 1})$  for some constant c, |c| < 1, the differences in the bounds are obvious. In (18), (21) we have

$$\|(\mathbf{I} + \mathbf{G}^{\pm 1})^{-1}\| \cdot \|\mathbf{L}\| = |\mathbf{c}| \cdot \kappa (\mathbf{I} + \mathbf{G}^{\pm 1})$$

while in (17), (20) we have

$$\|(\mathbf{I} + \mathbf{G}^{\pm 1})^{-1}\mathbf{L}\| = |c|$$

and it is possible to have

However, for random perturbations L, (22) is often approximately an equality. To see this, note that a random (dense) L will almost surely be invertible; recall Example 2. It is then easy to show that

$$\frac{\|(\mathbf{I}+\mathbf{G}^{\pm 1})^{-1}\|}{\|\mathbf{L}^{-1}\|} \leq \|(\mathbf{I}+\mathbf{G}^{\pm 1})^{-1}\mathbf{L}\| \leq \|(\mathbf{I}+\mathbf{G}^{\pm 1})^{-1}\| \cdot \|\mathbf{L}\|.$$

Again, since L is random, it will almost surely be well-conditioned (w.r.t. inversion) so that  $\|L^{-1}\| \approx \frac{1}{\|L\|}$ . Hence,

$$\|(\mathbf{I} + \mathbf{G}^{\pm 1})^{-1}\mathbf{L}\| \approx \|(\mathbf{I} + \mathbf{G}^{\pm 1})^{-1}\| \cdot \|\mathbf{L}\|$$
.

A related aspect, also worth noting, follows from the inequalities

$$\frac{\|(\mathbf{I} + \mathbf{G}^{\pm 1})^{-1}\| \cdot \|\mathbf{L}\|}{\kappa (\mathbf{I} + \mathbf{G}^{\pm 1})} \leq \|(\mathbf{I} + \mathbf{G}^{\pm 1})^{-1}\mathbf{L}\| \leq \|(\mathbf{I} + \mathbf{G}^{\pm 1})^{-1}\| \cdot \|\mathbf{L}\|.$$

If  $(I+G^{\pm 1})$  is reasonably well-conditioned  $(\kappa(I+G^{\pm 1})$  near 1), the majorization (22) will not be a bad overestimate.

Remark 4: By our discussion in Section 1, the appropriate measure of stability robustness is

$$d = \min_{\omega > 0} \frac{1}{\|(\mathbf{I} + \mathbf{G}^{\pm 1}(\mathbf{j}\omega))^{-1}\|}$$
 (23)

and in the sequel we shall consider methods of efficiently plotting  $\frac{1}{\|(\mathbf{I}+\mathbf{G}^{\pm 1})^{-1}\|} \text{ as a function of } \omega. \text{ This quantity is familiar from } \\ \text{classical sensitivity analysis where it is shown, in the single-input single-output case, that the change in the output of a closed-loop system, due to (additive) perturbations in G (scalar), is reduced by a factor of 1 + G compared with the open-loop effect.$ 

Remark 5: So far we have required nothing of our norm other than || I || = 1. Of course, a frequently occurring norm in much of the analysis of linear systems is the spectral norm  $|| \cdot ||_2$ . In that case

 $\frac{1}{\|(I+G^{\pm 1})^{-1}\|}$  is the smallest singular value of  $(I+G^{\pm 1})$ . Let

$$d_{q}(\omega) = \frac{1}{\|(\mathbf{I} + G^{\pm 1}(j\omega))^{-1}\|_{q}}$$
 (24)

We are interested in plotting  $d_q(\omega)$  versus  $\omega$  for large numbers of  $\omega$ 's. We shall see in the sequel that determining  $d_2(\omega)$  can be somewhat more expensive to determine than, say  $d_1(\omega)$  or  $d_\infty(\omega)$ . Moreover, note that

$$\frac{1}{\sqrt{m}} \|\mathbf{A}\|_{2} \leq \|\mathbf{A}\|_{1} \leq \sqrt{m} \|\mathbf{A}\|_{2} \tag{25}$$

and

$$\frac{1}{\sqrt{m}} \|\mathbf{A}\|_{2} \leq \|\mathbf{A}\|_{\infty} \leq \sqrt{m} \|\mathbf{A}\|_{2} \tag{26}$$

for A  $\in$   $\mathbb{C}^{m\times m}$ . Since we are usually most interested in order-of-magnitude estimates of  $d_q(\omega)$ ,  $d_2(\omega)$  will lie in a strip sufficiently close to  $d_1(\omega)$ , for example, to give the same qualitative information. The number m which is the number of inputs/outputs in the system is typically no more than about 10 and is frequently much less.

#### b. RELATIONSHIPS BETWEEN ADDITIVE AND MULTIPLICATIVE PERTURBATIONS

The following theorem relates additive and multiplicative perturbations. Again, the "j $\omega$ 's" will be omitted for convenience and all relations will be assumed to hold for all  $\omega$  > 0.

Theorem 2: 
$$\|(\mathbf{I} + \mathbf{G}^{-1})^{-1}\| - \|(\mathbf{I} + \mathbf{G})^{-1}\| \le 1$$

Proof: From the identity

$$(I+G^{-1})^{-1} + (I+G)^{-1} \equiv I$$
 (27)

we have

$$\left| \| (\mathbf{I} + \mathbf{G}^{-1})^{-1} \| - \| (\mathbf{I} + \mathbf{G})^{-1} \| \right| \leq \| (\mathbf{I} + \mathbf{G}^{-1})^{-1} + (\mathbf{I} + \mathbf{G})^{-1} \| = \| \mathbf{I} \| = 1.$$

We now get immediately the following useful corollary:

Corollary 1: Assuming that both the nominal closed-loop feedback system of Fig. 1 and the perturbation L are stable then the perturbed system is stable under:

(a) additive perturbations if

$$\|\mathbf{L}\| < \frac{1}{1 + \|(\mathbf{I} + \mathbf{G}^{-1})^{-1}\|}$$
 (28)

(b) multiplicative perturbations if

$$\|\mathbf{L}\| < \frac{1}{1 + \|(\mathbf{I} + \mathbf{G})^{-1}\|}$$
 (29)

Proof: Follows immediately from Theorem 2 noting that

$$\frac{1}{1 + \|(\mathbf{r} + \mathbf{g}^{\pm 1})^{-1}\|} \leq \frac{1}{\|(\mathbf{r} + \mathbf{g}^{\mp 1})^{-1}\|}.$$

#### C. SPECIAL RESULTS FOR THE SPECTRAL NORM

In this subsection we shall present some results related to those in subsections a. and b. but specialized to the  $\|\cdot\|_2$  - norm. For

a matrix H  $\in$   $\mathbb{C}^{m\times m}$  with singular values  $\sigma_1(H) \geq \ldots \geq \sigma_m(H) \geq 0$  we note that  $\|H\|_2 = \sigma_1(H)$ . If H is nonsingular,  $\|H^{-1}\|_2 = \frac{1}{\sigma_m(H)} > 0$ . In the  $\|\cdot\|_2$  - norm (28) becomes

$$\sigma_1(L) < \frac{\sigma_m(I + G^{-1})}{1 + \sigma_m(I + G^{-1})}$$

while (29) becomes

$$\sigma_1(L) < \frac{\sigma_m(I+G)}{1+\sigma_m(I+G)}$$
.

We shall make great use in the sequel of the following result of Fan [7].

Theorem 3: Let A,B e Cnxn. Then

(a) 
$$\sigma_{i+j-1}(A+B) \leq \sigma_i(A) + \sigma_j(B); \quad i \geq 1, \quad j \geq 1$$

(b) 
$$\sigma_{i+j-1}(AB) \leq \sigma_i(A)\sigma_j(B); \quad i \geq 1, \quad j \geq 1$$

Part (b) of Theorem 3 can be used to relate  $\sigma_{m}(I+G)$  and  $\sigma_{m}(I+G^{-1})$ .

Theorem 4: (a) 
$$\frac{1}{\|g^{-1}\|_2} \sigma_m(I + G^{-1}) \le \sigma_m(I + G) \le \|g\|_2 \sigma_m(I + G^{-1})$$

(b) 
$$\frac{1}{\|G\|_2} \sigma_m(I+G) \leq \sigma_m(I+G^{-1}) \leq \|G^{-1}\|_2 \sigma_m(I+G)$$

- 8 - 40 Z (0 + 11) 20 (d)

Proof: Follows immediately from Theorem 3 using

$$I + G^{-1} \equiv G^{-1}(I + G)$$
 and  $I + G \equiv G(I + G^{-1})$ .

For the rest of this subsection we shall let H denote either I+G or  $I+G^{-1}$  according to whether additive or multiplicative perturbations are appropriate. The next theorem will show how the singular values of H+L can be bounded in terms of  $\|L\|_2$  and the singular values of H.

Theorem 5: Suppose  $\sigma_k(H) \geq \alpha_k > 0$  for some k,  $1 \leq k \leq m$ , and  $\|L\|_2 \leq \beta$ . Suppose further that  $\beta < \alpha_k$ . Then:

(a) 
$$\sigma_{\mathbf{k}}(\mathbf{I} + \mathbf{H}^{-1}\mathbf{L}) \geq 1 - \frac{\beta}{\alpha_{\mathbf{k}}}$$

(b) 
$$\sigma_k(H + L) \geq \alpha_k - \beta$$
.

(Note: If  $k \neq m$ , H + L is not necessarily invertible if  $\beta$  is too large.)

Proof: (a) Use  $I \equiv I + H^{-1}L - H^{-1}L$  and  $A = I + H^{-1}L$ ,  $B = -H^{-1}L$ , i = k, j = m-k + 1 in Theorem 3(a) to get

$$\sigma_{m}(I) \leq \sigma_{k}(I + H^{-1}L) + \sigma_{m-k+1}(H^{-1}L)$$
.

Thus  $\sigma_{k}(I + H^{-1}L) \ge 1 - \sigma_{m-k+1}(H^{-1}L)$ 

$$\geq 1 - \|L\|_2 \cdot \sigma_{m-k+1}(H^{-1}) \text{ by Theorem 3(b)}$$

$$= 1 - \|L\|_2 \sigma_k(H)$$

$$\geq 1 - \frac{\beta}{\alpha_k}.$$

(b) Use H = H + L - L and A = H + L, B = -L, i = k, j = 1 in Theorem 3(a) to get

$$\sigma_{\mathbf{k}}(\mathbf{H} + \mathbf{L}) \geq \sigma_{\mathbf{k}}(\mathbf{H}) - \|\mathbf{L}\|_{2} \geq \alpha_{\mathbf{k}} - \beta$$
.

The case k = m is of special interest in Theorem 5 as it bears directly on our two basic inequalities (18) and (21) of the form

$$\|L\|_{2} < \frac{1}{\|H^{-1}\|_{2}}$$

which are sufficient to guarantee stability of a perturbed closed-loop system. Specifically, if  $\| H^{-1} \|_2 \le \frac{1}{\alpha}$  and  $\| L \| \le \beta$  with  $0 \le \beta < \alpha$ , then H+L is invertible and  $\| (H+L)^{-1} \|_2 \le \frac{1}{\alpha-\beta}$  or  $\sigma_m(H+L) \ge \alpha-\beta$ .

Note that Theorem 5 was expressed in terms of isolating  $\|L\|_2$ . By analogy with the inequalities (17) and (20) we can also have the following stronger, but perhaps less useful, theorem.

Theorem 6: Suppose  $\sigma_{m-k+1}(H^{-1}L) \leq 1 - \delta$  where  $0 < \delta < 1$  and  $1 \leq k \leq m$ . Then:

(a) 
$$\sigma_{\mathbf{k}}(\mathbf{I} + \mathbf{H}^{-1}\mathbf{L}) \geq \delta$$

(b) 
$$\sigma_{k}(H + L) \ge \frac{\delta}{\|H^{-1}\|_{2}}$$

Proof: (a) From the proof of Theorem 5 we have

$$\sigma_{k}(I + H^{-1}L) \ge 1 - \sigma_{m-k+1}(H^{-1}L) \ge \delta$$

(b) From  $I + H^{-1}L \equiv H^{-1}(H+L)$  and Theorem 3(b) we have

$$\sigma_{\mathbf{k}}(\mathbf{I} + \mathbf{H}^{-1}\mathbf{L}) \leq \sigma_{\mathbf{k}}(\mathbf{H} + \mathbf{L}) \cdot \|\mathbf{H}^{-1}\|_{2}$$

whence 
$$\sigma_k(H+L) \ge \frac{\delta}{\|H^{-1}\|_2}$$
.

## d. SPECIAL RESULTS WHEN $G(s) = C(sI - A)^{1}B$

In this subsection we shall make use of the fact that the frequency response matrix is of the form

$$G(j\omega) = C(j\omega I - A)^{-1}B$$

Let us further define

$$P(j\omega) = C(j\omega I - A + BC)^{-1}B$$
(30)

Recall the Sherman-Morrison-Woodbury formula:

$$(w + xyz)^{-1} \equiv w^{-1} - w^{-1}x(y^{-1} + zw^{-1}x)^{-1}zw^{-1}$$

assuming the indicated inverses exist. Then it is easy to verify that

$$(I + G(j\omega))^{-1} \equiv I - F(j\omega)$$
 (31)

and, from (27),

$$(\mathbf{I} + \mathbf{G}^{-1}(\mathbf{j}\omega))^{-1} \equiv \mathbf{F}(\mathbf{j}\omega) \tag{32}$$

Thus our results in the last section (for example, Theorems 4, 5, and 6) can all be cast in terms of F by noting that

$$\sigma_{\mathbf{k}}(\mathbf{I} + \mathbf{G}) = \frac{1}{\sigma_{\mathbf{m}-\mathbf{k}+\mathbf{1}}(\mathbf{I} - \mathbf{F})}$$
 (33)

and

$$\sigma_{\mathbf{k}}(\mathbf{I} + \mathbf{G}^{-1}) = \frac{1}{\sigma_{\mathbf{m} - \mathbf{k} + 1}(\mathbf{F})}$$
 (34)

Moreover,

$$\|(\mathbf{I} + \mathbf{G})^{-1}\| = \|\mathbf{I} - \mathbf{F}\|$$
 (35)

and

$$\|(\mathbf{I} + \mathbf{G}^{-1})^{-1}\| = \|\mathbf{F}\|$$
 (36)

for any of the norms we have been considering (in particular, k = m in (33) and (34)). Use of (31) and (32) results in an apparent savings in the number of linear systems to be solved (i.e., number of inversions) and we shall exploit this fact in the next section.

#### 4. COMPUTATIONAL PROBLEMS

#### a. COMPUTATION OF FREQUENCY RESPONSE MATRICES

As we have seen above, an object of considerable interest in studying the robustness of stability of linear systems is a graph of  $\frac{1}{\|(\mathbf{I}+\mathbf{G}^{\pm 1}(\mathbf{j}\omega))^{-1}\|}$  as a function of  $\omega$ . When  $G(\mathbf{j}\omega)=C(\mathbf{j}\omega\mathbf{I}-\mathbf{A})^{-1}B$  we saw that  $\|(\mathbf{I}+G(\mathbf{j}\omega))^{-1}\|=\|\mathbf{I}-\mathbf{F}(\mathbf{j}\omega)\|$  and  $\|(\mathbf{I}+\mathbf{G}^{-1}(\mathbf{j}\omega))^{-1}\|=\|\mathbf{F}(\mathbf{j}\omega)\|$  where  $\mathbf{F}(\mathbf{j}\omega)\approx C(\mathbf{j}\omega\mathbf{I}-\mathbf{A}+\mathbf{B}C)^{-1}B$ . Thus, regardless of the norm used, a quantity of the form

$$C(j\omega I - H)^{-1}B$$
 (37)

must first be computed. We shall assume throughout this and the next subsection that: (i)  $B \in \mathbb{R}^{n \times m}$ ,  $C \in \mathbb{R}^{m \times n}$ ,  $H \in \mathbb{R}^{n \times m}$  are given

(ii) n > m

(iii) (37) is to be evaluated for a large number, N, of values of  $\omega$ ; typically N >> n.

Rather than concentrate on exact operation counts, which may be fairly meaningless anyway, we shall give only order-of-magnitude estimates. It will be seen that the bulk of the computational load rests on evaluating matrices of the form (37) and so we shall focus initially on that problem.

If A  $\in \mathbb{R}^n$  is dense, the most efficient evaluation of  $C(j\omega I - A)^{-1}B$  by an LU factorization of A, solution of m triangular systems to get  $(j\omega I - A)^{-1}B$ , and finally a matrix multiplication, requires approximately  $\frac{1}{3}n^3 + \frac{1}{2}mn^2 + m^2$ n multiplications (and a like number of additions; we shall henceforth count only multiplications). This figure, when multiplied by N, represents a rather large amount of computation.

If A is initially transformed, however, the computational burden can be reduced quite considerably. If T is a similarity transformation on A we have

$$C(j\omega I - A)^{-1}B \equiv CT(j\omega I - T^{-1}AT)^{-1}T^{-1}B$$
.

Let us define

$$H = T^{-1}AT$$

and agree, for convenience to still label CT, T<sup>-1</sup>B the transformed C and B matrices, respectively, as C, B respectively. We now have the problem of evaluating

$$C(j\omega I - H)^{-1}B$$

where H may now be in such a form that  $(j\omega I - H)^{-1}$  can be computed in less than  $O(n^3)$  operations. For example, A can always be reduced to upper Hessenberg form by (stabilized) elementary transformations  $(\frac{5}{6} n^3)$  multiplications) or by orthogonal transformations  $(\frac{5}{3} n^3)$  multiplications). These transformations are very stable numerically and, while  $O(n^3)$ , are performed only once at the beginning of the calculations. The resulting linear system to be solved - for N different values of  $\omega$  — now has an upper Hessenberg coefficient matrix and can be solved in approximately  $\frac{1}{2}$  mm<sup>2</sup> multiplications. Moreover, Hessenberg systems can be solved very accurately with the growth factor in Gaussian elimination bounded above by n; see [8]. Computing  $C(j\omega I - H)^{-1}B$  still requires an additional m<sup>2</sup>n multiplications. Neglecting the initial transformation and determination of CT and T<sup>-1</sup>B, the Hessenberg method requires approximately

 $\frac{1}{2}$  mm<sup>2</sup> + m<sup>2</sup>n multiplications (for each value of  $\omega$ ), a considerable savings over the O(n<sup>3</sup>) algorithm if n >> m.

Of course, other transformations T are possible. One possibility is to reduce A to upper triangular (Schur) form by means of orthogonal similarities. This is considerably more expensive than reduction to upper Hessenberg but, again, need only be done once at the beginning. However, the resulting linear system to be solved at each step is upper triangular and so still requires O(mn2) multiplications. Because of potential difficulties with multiple eigenvalues of A there seems to be little real advantage gained by this procedure. Substantial savings could be gained though if the eigenstructure of A were such that it was diagonalizable by a reliably computable T. Since this involves consideration of the essentially open numerical problems associated with computing invariant subspaces we shall not pursue the details here. But assuming such a transformation were possible,  $C(j\omega I - D)^{-1}B$  with D diagonal, could be computed with approximately mn + m n multiplications for each value of  $\omega$ . Attractive as this appears, the potential for severe ill-conditioning of the eigenproblem associated with A render this latter method unreliable as a general-purpose approach. We shall subsequently consider only the Hessenberg method.

The analysis above has been done under the assumption that complex arithmetic was performed. We now outline how  $G = C(j\omega I - H)^{-1}B$  might be determined using only real arithmetic. The matrix H is assumed to be in upper Hessenberg form. We wish to solve first

Then

G = CZ .

Suppose Z = X + jY where X, Y  $\in \mathbb{R}^{n \times m}$ . Upon equating real and imaginary parts in (38) we get the following order 2n real system to determine X and Y:

$$\begin{pmatrix} -H & -\omega I \\ \omega I & -H \end{pmatrix} \begin{pmatrix} X \\ Y \end{pmatrix} = \begin{pmatrix} B \\ 0 \end{pmatrix}$$
 (39)

Thus  $X = \frac{1}{\omega} HY$  and  $Y = -\omega(\omega^2 I + H^2)^{-1}B$ . The matrix  $(\omega^2 I + H^2)$  will be invertible if  $(j\omega I - H)$  is invertible. Note that  $(\omega^2 I + H^2)$  is no longer upper Hessenberg but is almost in the sense of having two rather than one nonzero subdiagonal. Its shape is wholly typified for n = 5 by the matrix

Linear systems involving matrices of this type can be solved using approximately n<sup>2</sup> multiplications. We summarize the Hessenberg method using real arithmetic:

(i) Reduce A to upper Hessenberg form H, transform B and C, and compute H<sup>2</sup>; this step is done only once.

(ii) Solve 
$$(\omega^2 I + H^2)Y = -\omega B$$
 for Y.

(iii) Compute 
$$X = \frac{1}{\omega} HY$$
.

(iv) Compute 
$$G = (CX) + j(CY)$$
.

Step (ii) requires approximately mn<sup>2</sup> multiplications, step (iii) requires approximately  $\frac{1}{2}$  mn<sup>2</sup>, and step (iii) approximately m<sup>2</sup>n. The total number of multiplications is approximately  $\frac{3}{2}$  mn<sup>2</sup> + m<sup>2</sup>n.

Storage requirements for the Hessenberg method with real arithmetic are approximately double those for complex arithmetic.

#### b. COMPUTATION OF ROBUSTNESS MEASURES

We have seen above that quantities of the form (37) can be reliably evaluated in  $O(mn^2)$  operations. There then remains the problem of determining (35) or (36).

For (35), the singular value decomposition (SVD) of I + G(j $\omega$ ) can be computed for each value of  $\omega$ . Each SVD typically requires approximately 6m<sup>3</sup> multiplications. The smallest singular value is then the quantity of interest. For (36), inversion of G can be avoided by finding the SVD of F(j $\omega$ ), again in approximately 6m<sup>3</sup> multiplications. The inverse of the largest singular value of F is then the quantity of interest.

Use of either of these norms in (35) or (36) involves negligible computation as compared to Case 1, namely about m<sup>2</sup> additions and absolute

values and m-1 arithmetic comparisons.

In both cases, the additional work required is usually small compared with  $O(mn^2)$  especially if n >> m. However, if m is large relative to n, significant savings can be realized in using  $\|\cdot\|_1$  or  $\|\cdot\|_\infty$  rather than  $\|\cdot\|_2$ . In fact, using our previous approximate operation counts for the Hessenberg method and setting n = km, we have

$$\rho = \frac{\text{work per value of } \omega \text{ using } \| \cdot \|_2}{\text{work per value of } \omega \text{ using } \| \cdot \|_1 \text{ or } \| \cdot \|_{\infty}} \approx \frac{k^2 + 2k + 12}{k^2 + 2k}$$

Note though that  $\rho \approx \frac{k^2 + 2k + 24}{k^2 + 2k}$  if singular directions are also computed.

In the event A (or A - BC) can be successfully diagonalized as mentioned in Section 4.a. the potential savings in avoiding  $\|\cdot\|_2$  are somewhat greater. In fact, we then have

$$\rho \approx \frac{k+6}{k}$$

(or  $\rho \approx \frac{k+12}{k}$  if singular directions are also computed).

The above comparisons are only approximate and should in no way be construed as definitive statements. The purpose of this section is to merely introduce certain aspects of the numerical computations and suggest further avenues of exploration. A great deal of numerical experimentation remains to be done. Reliable software such as LINPACK [9] for linear systems will be of great benefit in this research.

and the S to S at a consent to smalle and at come of the transfer the

#### 5. CONCLUSIONS

We began this paper with an attempt at a "formal" definition of robustness. We then applied the definition to the problem of robustness of stability of linear systems as discussed in [1]. The cases of both additive and multiplicative perturbations were discussed and a number of relationships between the two cases were given. Finally, a number of computational aspects of the theory were discussed including a proposed new method for evaluating general transfer or frequency response matrices. The new method is numerically stable and efficient, requiring only  $O(mn^2)$  operations to update for new values of the frequency parameter rather than  $O(n^3)$ 

A number of interesting research areas suggest themselves in this work. One such area is that of constrained perturbations. For example, in our basic problem we were concerned with the nearness to singularity of a nonsingular matrix A @ C<sup>nxn</sup>. If the admissible perturbations E are somehow constrained for one reason or another, for example E upper triangular, the usual bound on ||E|| for which A + E is singular but E is "dense" may be overly pessimistic. Related to this is the fact that our bounds were derived for the "worst case". The size of perturbations allowed in a linear system to ensure continued closed-loop stability may very well be larger than we have derived if inputs to the system are constrained in certain directions.

We have concentrated in this paper on the analysis of linear control systems. There are many interesting — and difficult — synthesis problems, however. For example, can A, B, C be chosen to assign certain singular values of  $I + G^{\pm 1}$ ? What is the effect of changes in B or C on the

behavior of  $I + G^{\pm 1}$ ? Can a matrix K be determined so that  $I + (GK)^{\pm 1}$  has certain singular values?

On the computational side, more research needs to be done on updating parametric problems. That is, suppose we have a matrix (say,  $G(j\omega)$ ) which depends "in a rank m way" on a parameter  $\omega$ . When  $\omega$  changes how can various quantities be updated efficiently?

Finally, as mentioned in Section 4.b., a great deal of numerical experimentation is necessary to get a qualitative feel for the numbers in determining robustness measures.

Acknowledgment: It is a pleasure to acknowledge several stimulating conversations with Gunter Stein and Nils R. Sandell, Jr. which motivated much of the research reported in this paper.

#### 6. REFERENCES

- [1] Stein, G., Robust Stability of Linear Systems Engineering Motivation, these Proceedings.
- [2] Wonham, W.M., Linear Multivariable Control. A Geometric Approach, Springer-Verlag, Berlin, 1974.
- [3] Kahan, W., Numerical Linear Algebra, Can. Math. Bull., 9(1966), 757-801.
- [4] Willems, J.C., The Analysis of Feedback Systems, M.I.T. Press, Cambridge, MA, 1971.
- [5] Desoer, C.A., Perturbation in the I/O Map of a Non-Linear Feedback System Caused by Large Plant Perturbation, J. Franklin Institute, 306(1978), 225-235.
- [6] Rheinboldt, W.C., On Measures of Ill-Conditioning for Nonlinear Equations, Math. Comp., 30(1976), 104-111.
- [7] Fan, K., Maximum Properties and Inequalities for the Eigenvalues of Completely Continuous Operators, Proc. Nat. Acad. Sci., 37(1951), 760-766.
- [8] Wilkinson, J.H., Error Analysis of Direct Methods of Matrix Inversion, J. Assoc. Comput. Mach., 8(1961), 281-330.
- [9] Dongarra, J.J., C.B. Moler, J.R. Bunch, and G.W. Stewart, LINPACK User's Guide, SIAM, Philadelphia, 1979.

# QUANTITATIVE SYNTHESIS OF UNCERTAIN MULTIPLE. INPUT-OUTPUT FEEDBACK SYSTEMS

#### 1. INTRODUCTION

There is great interest in multiple input-output (mio) feedback systems, for obvious reasons. A great deal of significant work (too numerous to list but Wonham and Morse 1972, MacFarlane 1973, Wang and Davison 1973, Rosenbrock 1974, Porter and D'Azzo 1978 are representative and include bibliographies) has been done, primarily in the realization and properties of the closed-loop input-output relations, under the constraint of a feedback structure around the known, fixed mio "plant." There has been notable work done with uncertain inputs, but again only with fixed, known plants. Of course, plant uncertainty is always implicit, if only because of the usual approximations required to obtain a linear time-invariant (£ti) model.

In any case, there does not exist as yet any "quantitative synthesis" technique for the mio problem with significant plant uncertainty, even for the linear time-invariant case. By "quantitative synthesis" is meant that there are given quantitative bounds on the plant uncertainty, and quantitative tolerances on the acceptable closed-loop system response. The objective is to find compensation functions which guarantee that the performance tolerances are satisfied over the range of the plant uncertainty. In "quantitative design," one guarantees that the amount of feedback designed into the system is such as to obtain the desired tolerances, over the given uncertainty range. In other designs, the amount of feedback may be more or less than necessary—it is a matter of chance. The practical experienced designer may find the

# QUANTITATIVE SYNTHESIS OF UNCERTAIN MULTIPLE INPUT-OUTPUT FEEDBACK SYSTEM

Isaac Horowitz

#### **ABSTRACT**

There is given an n input, n output plant with a specified range of parameter uncertainty and specified tolerances on the n<sup>2</sup> system response to command functions and the n<sup>2</sup> response to disturbance functions. It is shown how Schauder's fixed point theorem may be used to generate a variety of synthesis techniques, for a large class of such plants. The design guarantees the specifications are satisfied over the range of parameter uncertainty. An attractive property is that design execution is that of successive single-loop designs, with no interaction between them and no iteration necessary. Stability over the range of parameter uncertainty is automatically included.

By an additional use of Schauder's theorem, these same synthesis

techniques can be rigorously used for quantitative design in the same sense
as above, for nxn uncertain nonlinear plants, even nonlinear time-varying
plants, in response to a finite number of inputs.

<sup>\*</sup> Cohen Professor/Applied Mathematics, Weizmann Institute of Science,
Rehovot, Israel and Professor of Electrical Engineering, University of Colorado,
Boulder. This research was supported in part by the U.S. Air Force Office of
Scientific Research, Grant No. AFOSR-76-2946B at the University of Colorado.

latter approach sufficient. However, a scientific theory of feedback should certainly include quantitative design techniques.

In this paper it is shown how Schauder's fixed point theorem can be used to generate a variety of precise quantitative mio synthesis techniques suitable for various problem classes. An outstanding feature of each synthesis procedure is that it consists of a succession of direct (no iterations necessary) single-loop design steps. Furthermore, by a second use of Schauder's theorem, the techniques are rigorously applicable to quantitative synthesis of nonlinear uncertain mio feedback systems. This paper concentrates on existence proofs but a 2 x 2 example is included.

## 1.1 Preliminary Statement of a Linear Time Invariant MIO Problem

In Fig. 1,  $P = [p_{ij}(s)]$  is a n x n matrix of the plant transfer functions in the form of rational functions, each with an excess  $e_{ij} > 0$  of poles over zeros, and with a bounded number of poles. The  $p_{ij}(s)$  are functions of q physical parameters, with m an ordered real q-tuple sample of their values.  $M = \{m\}$  is the class of all possible parameter combinations. The elements of the n x n lti compensation rational transfer function matrices  $F = [f_{ij}(s)]$ ,  $G = (g_{ij}(s)]$  are to be chosen practical (each with an excess of poles over zero). They must ensure that in response to command inputs the closed-loop transfer function matrix  $T = [t_{uv}(s)]$  (of c = Tr) in Fig. 1 where c, c are the n x 1 matrices (vectors) of system outputs and inputs, respectively, satisfy conditions of the form

$$0 < A_{uv}(\omega) \le |t_{uv}(j\omega)| \le B_{uv}(\omega), \forall m \in M$$
 (1)

If the  $t_{uv}(s)$  have no poles or zeros in the right half-plane (are stable and minimum-phase), then  $t_{uv}(s)$  is completely determined by  $|t_{uv}(j\omega)|$ , so (1) suffices (Bode 1945). It has been shown (Horowitz 1976) that time-domain tolerances of the form

$$u_1^{\nu}(t) \leq \frac{d^{\nu}\hat{c}(t)}{dt^{\nu}} \leq u_2^{\nu}(t)$$

 $\nu=0,1,\ldots,n_1$  any finite number, can be satisfied by means of tolerances like (1) on  $|c(j\omega)|$ , where  $c(s)=\int \hat{c}(t)$ . The writer finds it much more convenient to develop the synthesis theory in the frequency domain, and the above proves its sufficiency for time-domain synthesis.

This presentation concentrates on the command response problem, but the same ideas can be used to handle the quantitative disturbance response problem under plant uncertainty, as will be shown in Sec. 6. The constraints on the plant and the specifications are introduced as needed, in order to clarify the reasons for their need.

## 2. DERIVATION OF SYNTHESIS TECHNIQUE

In Fig. 1, there are available  $n^2$  loop transfer functions in L =  $[L_{ij}(s)] = PG$ , and  $n^2$   $f_{ij}$  in F for satisfying the tolerances (1) on the  $n^2$   $t_{ij}$ . But in the expansion of  $T = [t_{ij}(s)] = (I + L)^{-1}LF$ , each  $t_{ab}(s,m)$  (melt) is a function of all the  $L_{ij}(s,m)$  each uncertain, resulting in very complicated expressions for  $t_{ab}$  and making direct quantitative synthesis seemingly impossible—at least so far unsuccessful. The objective here is to convert each  $t_{ab}(s,m)$  design problem into an equivalent single—loop problem with uncertainty. This is done for each  $t_{ab}$ , by lumping all the other inter-

acting tij variables into an 'equivalent disturbance', as follows.

In Fig. 1, 
$$c = PG(Fr - c)$$
, so

$$(P^{-1} + G)c = GFr.$$
 (2)

Hence, the following restriction on P:

(P1):  $\Delta(s) \triangleq \text{determinant } P(s) \neq 0, \forall m \in M.$ 

Let  $r_v \neq 0$  and  $r_i \equiv 0$ ,  $i \neq v$ , so the resulting  $c_j(s) = t_{jv}(s)r_v$ . Let

$$P^{-1} = [P_{ij}(s)].$$
 (3)

The uth element of (2) is then

$$r_{v}(s) \sum_{i=1}^{n} (P_{ui} + g_{ui})t_{iv} = \sum_{i} g_{ui}f_{iv}.$$

To simplify the presentation, we take  $g_{ui} \equiv 0$  for  $u \neq i$  (although in practice it may be useful not to do so). Then letting  $r_v(s) = 1$ , the last equation can be written as

$$t_{uv} = \frac{\frac{1}{P_{uu}} g_{uu} f_{uv} - \frac{d_{uv}}{P_{uu}}}{1 + \frac{g_{uu}}{P_{uu}}} \stackrel{\Delta}{=} \tau_{uv} - \tau_{duv} d_{uv}$$
 (4a)

$$d_{uv} = \sum_{i \neq u} P_{ui} t_{iv}$$
 (4b)

This corresponds precisely to the single-loop problem of Fig. 2, with

 $P_{uve} = 1/P_{uu}$ . Of course, the  $t_{iv}$  in  $d_{uv}$  of (4b) are not known but the bounds (1) on  $|t_{iv}|$  are known generating a set  $D_{uv} = \{d_{uv}\}$ . We define the extreme  $d_{uv}$ 

$$|d_{uve}| = \sup_{M_{i\neq u}} |P_{ui}| |B_{iv}|, B_{iv} \text{ of (1)}$$
 (5)

Suppose we can find  $g_{uu}(s)$  and  $f_{uv}(s)$ , such that in the notation of (4,5)

$$0 < |\tau_{uv}| \pm |\tau_{duv}| |d_{uve}| \in [A_{uv}, B_{uv}], \forall m \in M$$
 (6)

Then the magnitude of the right side of (4a)  $\varepsilon[A_{uv}, B_{uv}]$  for all meM and for all possible combinations of  $t_{iv}$  (i  $\neq u$ ) which satisfy (1). Suppose this is so  $\forall u,v$  combinations, and the other Schauder conditions of Sec. 2.1 are satisfied. Then Schauder's fixed point theorem can be used to prove that these same n  $g_{uu}$  and  $n^2 f_{iv}$  are a solution to the synthesis problem (1).

## 2.1 Application of Schauder's Fixed Point Theorem

This theorem states that a continuous mapping of a convex, compact set of a Banach space into itself, has a fixed point (Kantorovich and Akilov 1964). We define the Banach space to be the  $n^2$   $C[0,\infty]$  product space denoted here by  $C(n^2)$ , with norm =  $\Sigma$  individual sup norms.  $C[0,\infty]$  is the Banach space of real continuous functions  $f(\omega)$ ,  $\omega \in [0,\infty]$  with  $||f|| = \sup_{\omega} |f(\omega)|$ . The convex compact set in each of the  $n^2$   $C[0,\infty]$  is taken as the acceptable set of  $|t_{uv}(j\omega)|$  satisfying (1), denoted by  $\{h_e(\omega)\} = H_{uv}$ . Additional constraints have to be assigned to the  $h_e(\omega)$  in order that each  $H_{uv}$  set is compact and convex in  $C[0,\infty]$ . These constraints have been justified in detail in (Horowitz 1975) and are therefore only summarized here. If each set is convex and compact in  $C[0,\infty]$ , their  $n^2$  product set denoted by  $H(n^2)$  is convex and compact in  $C(n^2)$ .

Constraints on  $H_{uv} = \{h(\omega)\}$  uv

- 1.  $\exists$  continuous functions  $A_{uv}(\omega)$ ,  $B_{uv}(\omega)$  with properties of (1) as bounds on  $h(\omega)$
- 2. h'(ω) is uniformly bounded: ∃ K, ∋ |h'(ω)| <K, Y h,ω

3.  $h(\omega) \rightarrow 0$  as  $\omega \rightarrow \infty$  in the form  $k/\omega^e$ , e a fixed finite number  $\geqslant 3$  to allow at least one excess of pole over zeros for the elements of F,G,P in Fig. 1. These constraints guarantee (Horowitz 1975) that  $h(\omega)$  can be taken as the magnitude of a function  $\hat{h}(s)_{s=j\omega}$  which has no zeros or poles in the interior of the right half-plane or on the  $j\omega$  axis. Arg  $\hat{h}(j\omega)$  is obtained from  $h(\omega)$  by anyone of a number of Bode integrals (Bode 1945).

An element of  $H(n^2)$  consists of  $n^2$  positive functions on  $[0,\infty]$ ,  $h_{ik}(\omega)$ . Using any appropriate Bode integral, find the associated phase function denoted here by  $\arg[h_{ik}(\omega)]$ , giving the minimum-phase stable function  $\hat{h}_{ik}(s)$ ,  $\hat{h}_{ik}(j\omega) = h_{ik}(\omega) + j \arg[h_{ik}(\omega)]$ . For future use, denote this sequence of operations whereby  $h(\omega)$  is transformed into  $\hat{h}(j\omega)$ , as the "Bode transformation"  $B(h(\omega))$ . Define  $\phi$  on  $H(n^2)$  by

$$\Phi = (\psi_{11}, \psi_{12}, \dots, \psi_{nn}) \colon H(n^{2}) \to H(n^{2}), \psi_{uv}(h_{11}, h_{12}, \dots, h_{nn})$$

$$= \left| \frac{g_{uu}f_{uv} - \sum_{i \neq u} P_{ui}B(h_{iv}(\omega))}{P_{uu}(1 + \frac{g_{uu}}{P_{uu}})} \right|$$
(7)

using for  $P_{ui}$ ,  $P_{uu}$  any specific fixed meM. (Note the similarity of (7) to (4a,b)). In Appendix 2, it is shown that  $g_{uu}$ ,  $f_{uv}$  can be found such that  $\Phi$  maps  $H(n^2)$  into itself. It is also necessary to prove  $\Phi$  is continuous, as follows.  $\Phi$  is a continuous mapping

 $\Phi$  is continuous if each of its  $n^2$  components is continuous. The first step in each mapping is  $B(h_{iv}(\omega)) = \hat{h}_{iv}(j\omega)$ . In (Horowitz 1975, Sec. III) it is proven that the step  $h_{iv}(\omega) \rightarrow arg \ h_{iv}(\omega) \triangleq \theta_{iv}(\omega)$  is continuous in the  $C[0,\infty)$  norm. Hence,

the mappings  $h_{iv}(\omega) \rightarrow h_{iv}(\omega) \cos\theta_{iv}(\omega) \stackrel{\Delta}{=} \mathcal{Q}_{iv}(\omega)$ ,  $h_{iv}(\omega) \rightarrow h_{iv}(\omega) \sin\theta_{iv}(\omega)$   $\stackrel{\Delta}{=} \chi_{iv}(\omega)$  are continuous. The denominator of (7) is a constant on  $H(n^2)$ , and so are  $g_{uv}$   $f_{uv}$  and the  $P_{ui}$  in the numerator. Thus, the numerator has the form

nts guarantee (Horowitz 1975) that h(w) can be taken as the magn⊈

Num. = 
$$|K_a + jK_b - \Sigma(C_j + jD_j)(Q_j(\omega) + jX_j(\omega)), j = \sqrt{-1}$$

all other terms real and only the  $R_i$ ,  $X_i$  mappings on  $H(n^2)$ . Infintesimal changes in  $R_i$ ,  $X_i$  clearly result in similar change in Num., so Num. is continuous on  $H(n^2)$  and so is each  $\psi_{uv}$  of (7) and hence  $\Phi$ . The conditions in Schauder's theorem are satisfied, so  $\Phi$  has a fixed point.

This means  $\exists$  a set of  $h_{ij}(\omega)$  denoted by  $h_{ij}^{*}(\omega)$ ,  $\ni$ 

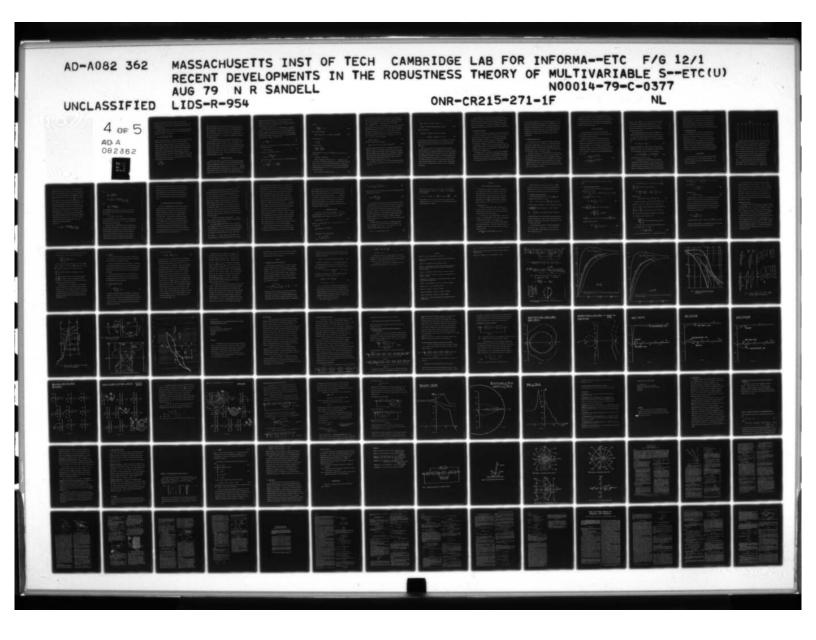
$$h_{uv}^{*}(\omega) = \left| \frac{g_{uu}f_{uv} - \sum_{i \neq u} P_{ui}\hat{h}_{iv}^{*}(j\omega)}{P_{uu}(1 + \frac{g_{uu}}{P_{uu}})} \right|$$
(8)

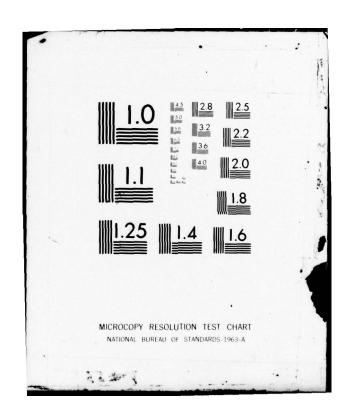
u, v = 1, ..., n, where  $\hat{h}_{iv}^{*}(j\omega) = B(h_{iv}^{*}(\omega))$ .

We would now like to deduce from (8), that

$$B(h_{uv}^{*}(\omega)) = h_{uv}^{*}(j\omega) = \frac{g_{uu}f_{uv} - \sum_{i \neq u} P_{ui}\hat{h}_{uv}^{*}(j\omega)}{P_{uu}(1 + \frac{g_{uu}}{P_{uu}})}$$
(9. ?)

For, if (9) is true, then by letting  $\hat{h}_{uv}^*(j\omega) = t_{uv}(j\omega)$ , we have recovered (4) and the  $n^2$   $\hat{h}_{uv}^*(j\omega)$  are a solution to the mio problem for that specific meM. The solution is unique if every building block in the mio system has a unique output for any given input, which is a very reasonable condition. This makes





it unnecessary to prove that there are no transitions from (8) to an expression similar to (9) but with right half plane poles and/or zeros. Since m is any element of M, this is true for all meM (of course with a different set of  $\hat{h}_{uv}^*$  for each m).

The step from (8) to (9) is a crucial one and must be justified with great care. Given an analytic function  $\phi(s)$ , there is an infinitude of  $\psi(s)$  such that  $|\phi(j\omega)| = |\psi(j\omega)|$ ,  $\omega \in [0,\infty]$ , e.g.

$$\psi(s) = \phi(s) \frac{(1 - \tau_1 s)}{(1 + \tau_1 s)} \frac{(1 + \tau_2 s)}{(1 - \tau_2 s)}$$

But  $\phi(s) \not\equiv \psi(s)$  even though  $|\phi(j\omega)| \equiv |\psi(j\omega)|$ . But suppose we know from other sources that  $\phi_1(s)$  has no right half plane zeros or poles, then given  $|\phi_1(j\omega)| \equiv M(\omega)$  a magnitude function which is Bode transformable, we can conclude that  $\phi_1(j\omega) \equiv B(M(\omega)) = \hat{M}(j\omega)$ . Hence, to justify (9) we must prove that the expression inside the vertical bars in (8) has no right half-plane zeros or poles. The pole part is easy, because  $1 + g_{uu}/P_{uu}$  is obviously designed to have no right half-plane zeros; certainly  $g_{uu}$ ,  $f_{uv}$  won't be assigned any such poles;  $\hat{h}_{iv}(s)$  doesn't have any by definition, and  $P_{ui}$  is not allowed any such poles--see Sec. 3.1. To prove the zero part, note that from (6) and Rouche's theorem, the number of zeros of the right side of (9) in the right half-plane, equals such number of

$$\frac{g_{uu}f_{uv}}{P_{uu}(1+\frac{g_{uu}}{P_{uu}})},$$

which is easily made zero in the single-loop synthesis steps (if P<sub>uu</sub> has no right half-plane poles, a condition necessary for other reasons--see Sec. 3.1). Thus, the expression inside the bars in (8) has no right half-plane poles or zeros, justifying (9). This is a very valuable result. The problem of stabilizing a highly uncertain n x n mio system is automatically disposed of in the synthesis procedure, which is furthermore one of designing n single-loop transmission functions.

It is worth noting that even if the above proof was not available, it would not be disastrous for this synthesis theory. It would only be necessary to guarantee that at one meM, the system is stable and minimum-phase. For then, this would be so meM, because by the continuity of the poles (and zeros) with respect to the parameters, the right side of (8) would have to be infinite (zero) at some w, in order that for some meM the system should be unstable (or have a right half-plane zero). However, the synthesis procedure by definition precludes this. And it is a relatively easy matter to guarantee the desired conditions at one meM.

## 3. CONSTRAINTS ON MIO PLANT

The above results hinge on our ability (a) to find  $g_{uu}$  and  $f_{uv}$  to satisfy (6)  $\forall \omega$ , all u,v pairs and all  $m \in M$  (b) that each equivalent single-loop design is stable and minimum-phase  $\forall m \in M$ . These lead to constraints on the mio plant, obtained by applying single-loop design theory to achieve (a,b). Appendix 1 gives an existence theorem for single-loop design. The first part of the design (see Appendix A3) gives bounds on the nominal loop transmission which is  $g_{uu}/P_{uuo}$  of (4a), where  $P_{uuo}$  is the 'nominal' associated with a nominal  $m_0 \in M$ .

These bounds must be satisfied in order that a specific system transfer function  $t_{uv}$  satisfy (1). Here  $g_{uu}/P_{uuo}$  is used for n  $t_{uv}$  (v=1,...,n) functions. It is proven in A3, that a  $g_{uu}/P_{uuo}$  can be found which satisfies the conditions for all n  $t_{uv}$  functions.

For example, consider  $t_{ul}$  at  $\omega = \omega_l$  and suppose  $A_{ul}(\omega_l) = .9$ ,  $B_{ul}(\omega_l) = 1.1$  in (1). We could split this range [.9, 1.1] into say [.95, 1.05] for  $\tau_{ul}$  and .05 for  $\tau_{dul}d_{ul}$  in (4), using  $d_{ul}e$  of (5) for  $d_{ul}$ . The technique in A3 or better (Horowitz and Sidi 1972), is then used to find a bound on  $g_{uu}(j\omega_l)$ . Here, we note a tough constraint. Sooner or later in  $\omega$ ,  $|g_{uu}(j\omega)|$  must become very small with  $1 + g_{uu}/P_{uu} \rightarrow 1$  and then in (4a)

$$t_{uv} \rightarrow \frac{g_{uu}f_{uv} - d_{uv}}{P_{uu}}$$
 (10)

and in (7),  $\psi_{uv} \rightarrow$  the numerator of its right side divided by  $P_{uu}$ . Now (4a, 5, 6) in general require that

$$|t_{uv}|_{max} > 2|\tau_{duv}d_{uve}| \tag{11}$$

But  $|t_{uv}|_{max} = B_{uv}$  and at high frequencies

$$|\tau_{duv}^{d} d_{uve}| \rightarrow \frac{\prod_{i \neq u}^{sup} |P_{ui}| |B_{iv}|}{|P_{uu}|}$$

To see what this leads to take, for example, n = 2 so that the above applied to v = 1, u = 1,2 gives

$$B_{11} > \frac{2|P_{12}|B_{21}}{|P_{11}|}, \quad B_{21} > \frac{2|P_{21}|B_{11}}{|P_{22}|},$$

Punctions of the province of the second second second second requiring

$$1 > \frac{4|P_{12}P_{21}|}{|P_{11}P_{22}|} \quad \text{as } \omega \to \infty$$
 (12)

Thus, a constraint on P is

$$(P_{2a}): \exists \omega_h, \ni \text{ for } \omega > \omega_h, |P_{11}P_{22}| > 4|P_{12}P_{21}| \forall meM.$$
 (13)

It is known that as  $s \rightarrow \infty$ ,

$$p_{ij} \rightarrow \frac{k_{ij}}{e_{ij}}$$
,

so the above becomes

$$\frac{|k_{11}k_{22}|}{e_{11}+e_{22}} > \frac{4|k_{12}k_{21}|}{e_{12}+e_{21}}.$$

If the uncertainties in the  $k_{ij}$  are independent and  $e_{11} + e_{22} = e_{12} + e_{21}$ , this becomes

$$k_{11\min}^{k} 22\min^{-3} {4k_{12\max}}^{k} 21\max^{-3}$$
 (14)

There is an important problem class for which he inequality is less harsh. This is the "basically noninteracting" class, where one ideally desires  $t_{ij} \equiv 0$  for  $i \neq j$ , but because of uncertainty accepts  $A_{ij} \equiv 0$ ,  $|t_{ij}| \leq B_{ij}$  for  $i \neq j$ , in (1). Also, one doesn't care if  $t_{ij}$  ( $i \neq j$ ) is nonminimum-phase. Condition (6) then applies only to  $u \equiv v$ . The  $f_{uv}$  ( $u \neq v$ ) are set equal to zero and (13) becomes

$$\exists \omega_{h}, \exists, |P_{11}P_{22}| > 2|P_{12}P_{21}| \text{ meM}, \omega > \omega_{h}.$$
 (15)

It is desirable to ease inequality (13) in the general case. Note that (6) can be satisfied over any finite  $\omega$  range by making  $|1 + g_{uu}/P_{uu}|$  large enough. Thus, as previously indicated, one can split the [Auv, Buv] tolerance so that  $|\tau_{uv}| > |\tau_{duv}| |d_{uve}|, \forall m \in M, e.g. assign |\tau_{uv}| \in [E - \epsilon, E + \epsilon]$  with  $E = (A_{uv} + B_{uv})/2$ ,  $2\varepsilon < B_{uv} - A_{uv}$  and the balance  $(B_{uv} - A_{uv} - 2\varepsilon)/2$  is assigned to  $\tau_{duv}d_{uv}$  of (4a). But  $|1 + g_{uu}/P_{uu}|$  must then be made large enough to satisfy the resulting requirements, and it can for any finite  $\omega$  range. The trouble is that  $g_{\mu\mu}$  must be allowed to  $\rightarrow$  zero as  $\omega \rightarrow \infty$ , leading to (13), etc., if we insist on (6). We could ignore (6) at large  $\omega$ , say for  $\omega > \omega_{\rm H}$ , with  $\omega_{\rm H}$  as large as desired but finite, letting  $|\tau_{uv}| \ll |\tau_{duv}| |d_{uve}|$  for  $\omega > \omega_H$ . Then for  $\omega > \omega_H$ , (11) is replaced by the weaker

$$|t_{uv}|_{M}^{max} > |\tau_{duv}^{d}|_{uve}|$$
and for n = 2, (13) is then replaced by

$$(P_{2b}): \exists \omega_h, \exists \text{ for } \omega > \omega_h, |P_{11}P_{22}| > |P_{12}P_{21}|, \forall m \in M$$
 (17a)

An important question is whether (17a) is an inherent basic constraint in the presence of uncertainty, no matter what design technique is used, or is due only to this specific design technique. The methods suggested in (Rosenbrock 1974, Owens 1978) to achieve diagonal dominance, may be helpful in satisfying (17a), but they would have to be extended to uncertain plants. Note that in Rosenbrock 1974, Owens 1978), diagonal dominance is desired  $\forall \omega \in [0,\infty)$ , whereas in  $(P_{2h})$  it is required only for  $\omega > \omega_H$ .

For the analog of (17a) at n = 3, it is found that diagonal row dominance of  $P^{-1}$  for  $\omega > \omega_H$ , is a sufficient condition. The necessary condition can be written as

$$\exists \omega_{H}, \ \ni \text{ for } \omega > \omega_{H} \ |P_{ii}P_{jj}| > |P_{ij}P_{ji}| \text{ and }$$

$$|P_{11}P_{33}| > (|P_{12}P_{23}| + |P_{13}P_{22}|)(|P_{22}P_{31}| + |P_{21}P_{32}|)$$

$$(17b)$$

which can be written as,

$$|P_{11}P_{22}P_{33}| > |P_{11}P_{23}P_{32}| + |P_{12}P_{21}P_{33}| + |P_{12}P_{23}P_{31}|$$

$$+ |P_{13}P_{22}P_{31}| + |P_{13}P_{21}P_{32}| \quad \text{for } \omega > \omega_{\text{H}} . \tag{17c}$$

The latter has the following interpretation. Array the matrix P<sup>-1</sup> in the usual manner, but twice-one under the other as in Fig. 3a. Then the terms on the right side of (17c) consist of the products of the entries crossed by the dashed lines.

However, if  $\omega_H$  is so used, it is no longer possible to use Rouche's theorem and thereby prove each  $t_{ij}$  is minimum-phase. But we can still design so that the nominal  $t_{ij}$  are minimum-phase and we know from (6) that  $t_{ij}(j\omega) \neq 0$  for  $\omega \in [0,\omega_H]$ . Therefore, from the continuity of the zeros of  $t_{ij}$  with respect to the parameters of the system, if  $t_{ij}$  has any right half-plane zeros, they must enter the right half-plane as shown in Fig. 3b. It is unlikely that such a zero which must migrate all the way up to  $j\omega_H$ , should move back into the significant control bandwith region A. The point is that if right half-plane zeros are "far-off", they have little effect and the system is "dominantly" minimum-phase.

Rouche's theorem can still be used if we can guarantee that (6) is satisfied for a semicircle consisting of the segment  $[-j\omega_H,j\omega_H]$  and the right half-plane half-circumference of the circle of radius  $\omega_H$ , centered at the origin. Then, there are definitely no right half-plane zeros of  $t_{ij}$  in this half-circle, and the system is "dominantly" minimum-phase. This is quite practical in the design technique of (Horowitz and Sidi 1972), discussed in A3.

## 3.1 Modification of mapping o

Note that for the "dominantly minimum-phase" and the "basically noninteracting" cases, the application of Schauder's theorem in (2.1), Eqs. (7-9), etc., needs modification, because nonminimum-phase  $t_{uv}(j\omega)$  cannot be uniquely derived from  $|t_{uv}(j\omega)|$ . Redefine  $h \in \mathbb{N}_{uv}$  of 2.1 to consist of an ordered pair:  $h(\omega)$  as before and  $q(\omega)$ , the imaginary part of  $\hat{h}_{uv}(j\omega)$  with  $h = |\hat{h}_{uv}(j\omega)|$ ;  $h \in H_{uv}$  the same as before but  $q(\omega) \in C$   $[0,\infty)$  with  $0 \le |q(\omega)| \le h(\omega)$ . Constraints 2,3 in 2.1 on  $h(\omega)$  also apply to  $q(\omega)$ . Let  $(HQ)_{uv} \subset C^2$   $[0,\infty)$  denote the set  $\{(h(\omega), q(\omega))\}$  with ||(h,q)|| = ||h|| + ||q||. Obviously,  $(HQ)_{uv}$  is compact and convex in  $C^2$   $[0,\infty)$ . The extension to the  $n^2$  product set is straightforward.

The mappings  $\psi_{uv}$  in (7) are redefined. Each  $\psi_{uv}$  is a pair of mappings, one the absolute value as before, the second the imaginary part with the absolute bars on the right removed. On the right side of (7),  $B(h_{iv}(\omega))$  is replaced by  $r_{iv}(\omega) + jq_{iv}(\omega)$ , with  $h_{iv}^2 = r_{iv}^2 + q_{iv}^2$ ,  $(h_{iv}, q_{iv}) \in (HQ)_{iv}$ . It is necessary to prove that  $\Phi$  maps each element of  $(HQ)_{uv}$  into itself.

The proof follows immediately from that for the minimum-phase case -- this is obvious from (6), the definition of  $d_{uve}$  in (5), and Appendices 1,2. The proof that  $\Phi$  is continuous is straightforward. Accordingly, the Schauder conditions are satisfied and there exists a fixed point which satisfies the specifications. Such specifications, by themselves, would not be good ones because they permit highly nonminimum-phase  $t_{uv}(s)$ . However, they are satisfactory if it is known from other sources that  $t_{uv}$  is "dominantly minimum-phase".

## 3.2 Additional Constraints on P

Constraints A1(1)-(3) in the Appendix, must be applied to the  $1|P_{uu}$ , since in Fig. (2)  $p_{uve} = \frac{1}{P_{uu}} = p$  of Appendix. Al.1 requires that there be no change in the excess of poles over zeros of  $\frac{1}{P_{uu}} = \frac{\Delta}{\Delta_{uu}}$  where  $\Delta = \det$ . P and  $\Delta_{uu}$  its uuth minor, as m ranges over M. Also, that for at least one meM, denoted by  $m_{uo}$ ,  $P_{uu}$  has all its poles and zeros in the interior of the left half-plane. The  $m_{uo}$  can be different for each u.

Al.2 requires that  $1/P_{uu}$  is minimum-phase  $\forall$  meM, and its zeros do not get arbitrarily close to the jw axis. Since  $1/P_{uu} = \Delta/\Delta_{uu}$ , this means  $\Delta$  must have no right half-plane zeros. Hence the  $P_{ij}$  in general have no right half-plane poles. (For those who wish it, P is restricted to be controllable and observable  $\forall$  meM, but these concepts are unnecessary if P is properly formulated in terms of physical uncertain parameters (Horowitz and Shaked 1975)). Since the  $p_{ij}$  in  $P = [p_{ij}]$  are finite rational functions, the latter part of Al.2 is automatically satisfied.

Al.3 for n=2 is the same as (17), which shows that (17) is a fundamental condition for linear time-invariant design, not an "extra" condition due to our design technique, at least for n=2. However, (13) is an "extra" condition. Note, the extension of single-loop design to disappearing poles and zeros in A6 may perhaps permit disappearing poles and zeros in the mio plant functions.

## 4. OTHER DESIGN EQUATIONS

The previous design equations constitute only one of many
design techniques derivable from Schauder's fixed point theorem. Only
two more will be briefly mentioned here.

Both are based on the use of a nominal diagonal loop transmission matrix. The design obligations on the loop transmission
elements are then independent of the way the plant input and output
terminals are numbered. If G is made diagonal, such numbering is
important and after one arbitrarily numbers the plant input terminals,
he should try to number the outputs such that the main effect of input i is on output i. Manipulation of (2) somewhat differently from
Sec. 2, gives

$$t_{11} = \frac{f_{11}\ell_{11}/\delta_{11} + \sum_{i \neq 1}^{\Sigma} v_{1i}t_{i1}/\delta_{11}}{1 + \ell_{11}/\delta_{11}}$$

$$t_{21} = \frac{f_{21}\ell_{22}/\delta_{22} + \sum_{i \neq 2}^{\Sigma} v_{2i}t_{i1}/\delta_{22}}{1 + \ell_{22}/\delta_{22}}, \text{ etc.}$$
(18)

where  $V = [V_{ij}] = I - P(P)^{-1}$ ,  $P_0$  is the 'nominal' plant matrix and therefore fixed, P is the general uncertain plant matrix,  $\delta_{ij} = 1 - V_{ij}$ . The  $L_{ij}$  are the nominal elements of the loop transmission matrix L. Eqs. (18) lend themselves to single-loop design and use of Schauder's theorem, pricely as did (4).

Another interesting set of design equations is obtained by designing to control the changes in  $t_{ij}$ , rather than  $t_{ij}$  directly. Let  $T_o = [t_{ijo}]$  be the 'nominal' system transfer matrix and  $T = [t_{ij}]$  the actual which is uncertain,  $\Delta T = [\Delta t_{ij}] = T - T_o$ . Then it can be shown that

$$\Delta T = (I+L)^{-1} VT, V = I-P_0 P^{-1}$$
 (19)

where  $P_0$ , P are likewise the 'nominal' and uncertain plant transfer matrices, and  $L = P_0G = [\ell_{ij}]$  is the <u>nominal</u> loop transmission matrix.

If L is taken diagonal, the result is (n = 2 for simplicity)

$$\Delta t_{11} = \frac{v_{11}t_{11} + v_{12}t_{21}}{1 + \ell_{11}}, \ \Delta t_{12} = \frac{v_{11}t_{12} + v_{12}t_{22}}{1 + \ell_{11}}$$
 (20)

and similar obvious ones for  $\Delta t_{21}$ ,  $\Delta t_{22}$ .

The design problem is now completely one of disturbance attenuation, with the disturbances  $d_{11} = v_{11}t_{11} + v_{12}t_{21}$ , etc., whose range is known. Schauder's theorem is applicable in the same manner as before. Note that V represents the 'normalized' plant variation matrix. Eqs. (20) appear to be much simpler to use for design (once

the At<sub>ij</sub> tolerances are formulated) than (4), and their use needs to be intensively researched. However, both for (18) and (20) the constraints considered in 3., leading to (11-15) must be found, and these may possibly be tougher than before. Also, both a nominal P and T must be chosen, which is not good, because the optimum pairing is not apriori known. However, the analogs of (14,17) may be more lenient.

#### 4.1 Bandwidth Minimization

An important criterion for comparison of design techniques is their "cost of feedback," which we take as the bandwidths of the loop transmission functions--because they determine the system sensitivity to sensor noise. Obviously, quantitative synthesis techniques must first be invented before one can turn to their optimization (for without such quantitative techniques comparison is possible at best, by analysis after a specific numerical design has been made). This approach via Schauder's theorem promises to generate a variety of such techniques, and the next step will be optimization.

### 5. DESIGN EXAMPLE

The 2 x 2 plant elements are  $p_{ij} = k_{ij}/(1+sA_{ij})$  with correlated uncertainties, giving a total of 9 parameter sets in Table 1. The design was performed to handle the convex combination generated by these 9 sets (Figure 6).

	Antonia a		TABLE	<u>l</u> 16 man				
No.	<u>k</u> 11	k <sub>22</sub>	k <sub>12</sub>	<u>k</u> 21	A <sub>11</sub>	A <sub>22</sub>	A <sub>12</sub>	A <sub>21</sub>
1.	en ad vem	2	.5	10	. 19v <b>1.</b> 59	2	2	3
2.	1	2.	.5	1	.5	1	1	2
3.	1	2	.5	1	.2	.4	.5	1 []
4.	4	5	1	2	1.	2	2	3
5.	4	5	1	2	.5	1	1	2
6.	4	5	60 LJ 00	2	.2	.4	.5	n roisna 1
7.	10	8	. 2	4	1. 13	2	2	2
8.	10	8	2	4	.5	1	1.	2
9.	10	8	2	4	.2	.4	.5	1

A "basically noninteracting" system is desired, with the off-diagonal transmissions specified in the  $\omega$ -domain  $|t_{12}(j\omega)|$ ,  $|t_{21}(j\omega)| < 0.1 \ V\omega$ . The diagonal  $t_{11}$ ,  $t_{22}$  bounds are identical and were originally in the time-domain in the form of tolerances on the unit step response shown in Fig. 4a, b (which also shows the design results for those of the 9 cases which were reasonably distinguishable). These time-domain bounds were translated into the "equivalent" bounds on  $|t_{ij}(j\omega)|$  shown in Fig. 5 (Horowitz and Sidi 1972, Krishnan and Cruickshank 1977).

Familiarity with quantitative single-loop design is assumed here. One can do a problem of this complexity by hand. The sets  $\{p_{iie}(j\omega)\}$ , called the plant templates, are obtained on the Nichols chart. Some of these templates of  $P_{11}^{-1} = \frac{\Delta}{P_{22}}$ ,  $P_{22}^{-1} = \frac{\Delta}{P_{11}}$ 

are shown in Fig. 6 at various  $\omega$  values. The larger the template, the greater uncertainty at that  $\omega$  value. The tolerances on  $t_{\mu\mu}$  of (4a) and Fig. 5 were divided between  $\tau_{uu}$  and  $\tau_{duu}^{d}_{uu}$  as discussed in Sec. 2. Each of these, in conjunction with the templates, leads to bounds on the nominal loop transmission  $\ell_{u\omega o} = \frac{g_{uu}}{P_{u\omega o}}$ . Some of these boulds on  $\ell_{iio}$ , due to  $\tau_{ll}$ , are shown as solid lines in Fig. 7, i.e., it is necessary for \$110 to lie above the indicated boundary. The tolerances on Tduuduu lead to the dashed line bounds on Lllo. No attempt was made to optimize the division of the tolerances between  $\tau_{11}$  and  $\tau_{d11}^{d}$  The composite bound on  $\ell_{110}$  must satisfy both. The  $\ell_{110}(j\omega)$  chosen is also shown in Fig. 7. There was no attempt made to optimize the l<sub>jio</sub>; the design was made by hand quickly, so the  $\ell_{ijo}(j\omega)$  are larger than need be, with the tolerances therefore satisfied better than necessary--as seen in Figs. 4a, b. Optimal  $\mathbf{L_{iio}}(\mathbf{j}\omega)$  would lie on their boundaries at each  $\omega$  , so in this example there is considerable overdesign.

Here we took

$$\ell_{110} = \frac{\Delta_0}{\rho_{220}} g_{11} = \frac{10}{s} \frac{(1+.007s)}{(1+.025s) \left[\frac{1+s}{400} + \frac{s^2}{(400)^2}\right]}$$

wi th

$$\frac{\Delta_0}{P_{220}} = \frac{.75 (1+3.66s)}{(1+s)(1+3s)};$$

$$\mathcal{L}_{220} = \frac{\Delta_0}{P_{110}} g_{22} = \frac{9}{s} \frac{(1+.02s)}{(1+.1s) \left[ \frac{1+s}{150} + \frac{s^2}{(150)^2} \right]}$$

are shown in Fig. 5 at wartons a values. The larger the template.

with

$$\frac{\Delta_0}{P_{110}} = \frac{1.5 (1+3.66s)}{(1+3s)(1+2s)}.$$

The requirements on  $f_{11}$ ,  $f_{22}$  ( $f_{12} = f_{21} = g_{12} = g_{21} = 0$  here) were found using single-loop design technique [15] as briefly explained here in A4, and

$$f_{11} = \frac{1}{1 + .5s}$$
,  $f_{22} = \frac{1}{1 + .33s}$ 

were found satisfactory. The system was simulated on the digital computer with the results shown in Figs. 4a, b. The  $t_{12}$ ,  $t_{21}$  tolerances were easily satisfied by the design.

While this is not a very challenging example of the design technique, nevertheless the uncertainty is very large and one should consider how quick, simple and straightforward was the design procedure, and also consider what alternatives are offered in the mio literature.

There are no other techniques available for systematic design to specifications in the presence of significant uncertainty, which guarantee design convergence and attainment of design tolerances.

Whatever present popular technique is used, it would be necessary to cut and try and endeavor to understand the relations between the cutting and the results as one continued to cut and try, because these techniques have no provision for significant uncertainty. In the above design, one sweep was known to be sufficient because the plant and the design tolerances ( $\omega$ -domain) satisfied constraints, P1 etc.

## 5. EXTENSION TO NONLINEAR UNCERTAIN MIO PLANTS

Once there is a quantitative design technique for linear time invariant mio uncertain plants, it appears at least conceptually possible to extend it to a significant class of nonlinear, even nonlinear time-varying, uncertain mio plants. The procedure is a generalization of that used (based also on Schauder's theorem) in (Horowitz 1976) for single loop uncertain nonlinear systems. The key feature is the replacement of the nonlinear plant matrix set (a set because of the uncertainty), by a linear time invariant plant set which is precisely equivalent to the original nonlinear set, with respect to the acceptable system output set. The procedure is briefly presented for the case where one wants the system with nonlinear uncertain plant to behave like a linear time-invariant system for a specified class of command input sets.

It is essential that the command input sets represent a good sampling of how the system will actually be used. For example, suppose n=3 and in actual use  $r_1$ ,  $r_2$  always exist simultaneously (with  $r_3=0$ ), and  $r_3$  appears by itself (with  $r_1=r_2=0$ ). Say there are ten typical  $r_1(t)$  inputs and for each typical  $r_1(t)$  there are five typical  $r_2(t)$ . This makes a subtotal of 50 input sets, to which is added the number of typical  $r_3(t)$  say 10, giving a class  $R=\{\bar{r}\}$  of 60 sets, of which 50 have the form  $\bar{r}=(r_1,r_2,0)$  and  $\bar{r}=(0,0,r_3)$  for the balance. Choose  $\bar{r}_1 \in R$ . The family of acceptable outputs for this input, is known from the tolerances on  $t_{ij}$ , giving for that one input vector a family  $f=\{\bar{h}\}$ ,  $\bar{h}=(h_1,h_2,h_3)$ . The mio plant is represented by a family (because of parameter uncertainty) W of nonlinear differential mappings

 $W = \{W\}, W = (w_1, w_2, w_3); c_1 = w_1(x_2, x_2, x_3, m), \dots, c_3 = w_3(x_1, x_2, x_3, m),$  where the  $x_2$  are the plant inputs,  $c_1$  the plant outputs, and m is the plant parameter vector  $m \in M$ .

Take a sample acceptable output triple  $\bar{h} = (h_1, h_2, h_3)$  and find the corresponding plant inputs at some specific meM (or in other words, pick a NeW) and let  $c_j = h_j$  and solve the nonlinear equations backwards. giving the input set  $(x_1, x_2, x_3)$ . Take the Laplace transforms  $\hat{x}_i(s)$  of  $x_i$ ,  $\hat{h}_j(s)$  of  $h_j$  giving the vectors  $\hat{x}[s] = (\hat{x}_1(s), \hat{x}_2(s), \hat{x}_3(s))$  fi[s] =  $(\hat{h}_1(s), \ldots, \hat{h}_3(s))$ . Repeat for other  $\bar{h}$  samples in the acceptable output set H, giving two paired families of  $\hat{x}[s]$ ,  $\hat{h}_j[s]$ .

Select any combination of three  $\hat{x}[s]$ , forming a 3 x 3 matrix  $\hat{X}$  and corresponding paired combination of three h[s], forming the matrix H. Set  $\hat{H} = \hat{P}\hat{X}$  and solve for  $P = \hat{H}(\hat{X})^{-1}$ . P is the linear-time-invariant equivalent of the specific WeW picked, with respect to the specific trio of acceptable output vectors picked. Repeat over different trios. Repeat the entire operation over different well, giving a class P<sub>1</sub> = {P} which is the linear-time-invariant equivalent of the W family, with respect to the class of acceptable outputs H for input vector  $\bar{r}_1$ . Repeat the entire operation for  $\bar{r}_2$ , ...,  $\bar{r}_{60}$  giving  $\{P_i\} = P_{total}$  which is the linear time equivalent for the nonlinear W, with respect to the tribe of 60 families of acceptable output sets. The equivalence is exact if the conditions for application of Schauder's theorem are satisfied. We now have a linear time-invariant uncertain mio problem, which let us presume we can solve. If and only if we can guarantee the solution of the latter, then the same compensation functions will work for the original nonlinear uncertain mio plant. Hence the importance of quantitative linear time invariant design techniques (over and above their intrinsic importance) -- for they enable the precise solution of nonlinear uncertainty problems.

The design effort in the above appears to be enormous but it is conceptually straightforward and easy. An ordinary control engineer can implement it and the digital computer is, of course, an essential

tool. Conceptually too, it appears possible to extend the method to obtain nonlinear relations between inputs and outputs within specified bounds, despite large plant uncertainty, even nonlinear time-varying, as can be done for the single input-output case. The prospect is fascinating. Imagine being able to work with the actual nonlinear equations of a jet engine, or a chemical process, etc., include uncertainties in the modelling, even uncertainty in system order (see Appendix), and designing to achieve outputs within specified tolerances over the given range of uncertainty.

#### 6. DISTURBANCE ATTENUATION

Let x in Fig. 1 be a nx1 matrix of distrubances. The resulting system output (with r = 0) is  $c = (I + PG)^{-1} Px \stackrel{\triangle}{=} Zx$ ,  $Z = [z_{ig}]$ , the nxn disturbance response matrix. Bounds on Z are given in the form

$$|z_{\mu\nu}(j\omega)| < b_{\mu\nu}(\omega)$$
,  $\forall m \in M$  (21)

Rewrite c = Zx in the form  $(P^{-1} + G)c = x$ . Let  $x_i \neq 0$  only for i = v, so  $c_i = z_{iv}x_v$ , and

$$\sum_{i=1}^{n} (P_{ui} + g_{ui})z_{iv} = \delta_{v}^{u} = (0, u \neq v),$$

$$(P_{uu} + g_{uu})z_{uv} = \delta_{v}^{u} - \sum_{i \neq u} (P_{ui} + g_{ui})z_{iv}$$
  
 $\delta_{u}^{u} - \sum_{i \neq u} (P_{ui} + g_{ui})z_{iv}$ 

$$z_{uv} = \frac{\delta_{v}^{u} - \sum_{i \neq u} (P_{ui} + g_{ui})z_{iv}}{a}$$

Let

$$x_{uve}(\omega) \stackrel{\Delta}{=} \sup_{\mathbf{i} \neq u} \sum_{\mathbf{i} \neq u} \left| \frac{P_{ui} + g_{ui}}{P_{uu}} \right| b_{iv}(\omega)$$
 (23)

The  $g_{ui}(\omega)$  ( $i\neq u$ ) can be chosen to minimize  $x_{uve}(\omega)$ , but for simplicity we shall assume them zero. From (22,23)

$$|z_{uv}(\omega)| < |\frac{\delta_{v}^{u}/P_{uu} + x_{uve}}{(1 + \frac{g_{uu}}{P_{uu}})}|$$
 (24)

If  $1/P_{uu}$  satisfies the constraints listed, then it is obviously possible to guarantee  $|z_{uv}(\omega)| <$  any finite number, no matter how small, at any finite  $\omega$ . Also it can be made zero at a finite number of  $\omega$  values by assigning poles to  $g_{uu}$  at these values. Assume that  $g_{uu}$  can be chosen to satisfy (21)  $\forall \ \omega \in [0,\infty)$ . Then one can set up the conditions for Schauder's theorem, precisely as was done in 2.1. The set  $b_{uv}(\omega)$  must have been formulated such that  $B(n^2)$ , the  $n^2$  product set of the  $b_{uv}(\omega)$ , is compact convex in  $C(n^2)$ , analogous to  $H(n^2)$  in 2.1. The analog of  $\Phi$  in (7) must be formulated with the modification of Sec. 3.1, inasmuch as we do not care if the  $z_{uv}(s)$  are nonminimum-phase.

Conditions analogous to (12-17) for n = 2, are obtained as follows. As  $\omega \to \infty$ ,  $g_{uu}/P_{uu} \to 0$  so in (24), the right side  $\to$  its numerator. But  $|z_{uv}(j\omega)| \le b_{uv}(\omega)$  of (21). Let u = 1, v = 2 and then u = 2, v = 1 and obtain the necessary condition (for  $g_{12} = g_{21} = 0$ ),

As 
$$\omega \to \infty$$
,  $p_{12}p_{21} < p_{11}p_{22}$ ,  $\forall m \in M$  (25)

similar to (17) but here only at  $\infty$ , because there is no concern with the minimum-phase property. Setting u = v = 1, and then u = v = 2 in (24), we get the conditions

As 
$$\omega \to \infty$$
,  $b_{11} > \left| \frac{1}{p_{11}} \right| = \left| p_{11} - \frac{p_{12}p_{21}}{p_{22}} \right|$ ,  $b_{22} > \left| p_{22} - \frac{p_{12}p_{21}}{p_{11}} \right|$  (26)

But in reality as  $\omega \to \infty$ ,  $c \to Px$  so  $Z \to P$  and  $z_{11} \to p_{11}$ ,  $z_{22} \to p_{22}$ . Hence, assignment of  $b_{ij}$  (as  $\omega \to \infty$ ) to satisfy (25) is no obstacle, because the  $b_{uv}(\omega)$  are upper bounds on the  $|z_{uv}(j\omega)|$ .

precisely as was done in 2.1. The set  $\mathfrak{d}_{ug}(\omega)$  must have been formulated such

that B(B), the B product set of the bowles is comment convex to C(B)

analogous to  $H(n^2)$  in 2.7. The analog of a  $\xi n$  (7) must be formulated

, which the necessary condition (for  $g_{12}=g_{21}=0$ ),

#### APPENDIX 1

### EXISTENCE THEOREM FOR SINGLE-LOOP DESIGN

The plant transfer function p(s) is uncertain, belonging to a set  $P = \{p(s)\}$  and is imbedded in a two-degree-of-freedom single-loop feedback structure, as in Fig. 2 (p in place of  $p_{uve}$ ). The rational functions f(s), g(s) (replacing  $f_{uv}$ ,  $g_{uu}$  in Fig. 2) are to be chosen to satisfy specified tolerances on the command frequency-response  $t(j\omega) = \frac{c(j\omega)}{r(j\omega)}$  and disturbance frequency response  $t_d(j\omega) = c(j\omega)/d(j\omega)$ , (r, d, c replacing  $r_v$ ,  $-d_{uv}$ ,  $c_u$  in Fig. 2).

### Al. Constraints on P

- 1. p(s) is a rational function with a fixed excess e > 1 of poles over zeros (this is relaxed later in A6, 7).  $\exists$  at least one peP one of which is designated as  $p_0$ , all of whose poles and zeros are in the interior of the left half-plane.
- 2. At each  $\omega \in [0,\infty)$ ,  $\exists \inf_{P} |p(j\omega)| \stackrel{\triangle}{=} b(\omega) > 0$ .  $\exists \inf_{I} b(\omega)$   $\stackrel{\triangle}{=} b_{I} > 0$  for any finite interval  $I = [0,\omega]$ . Also,  $|p_{0}|$  of Al(1) has a sup on each finite interval  $I = [0,\omega]$ , sup  $|p_{0}| = x_{0I}$ .
- 3. As s,  $p(s)+k_p/s^e$ ,  $k_p \epsilon [k_1, k_2]$  with  $\infty$   $k_2 > k_1 > 0$ , uniformly on P in the following sense: For any  $\epsilon > 0$ , no matter how small,  $\exists \ \omega_{\epsilon}$  (independent of p(s)), such that for each  $p \epsilon^P$  there is associated a  $k_p \epsilon [k_1, k_2]$  so that

 $\left|\mathbb{Q}_{n}\right| \frac{P}{k_{p}/\omega^{2}} \left| < \epsilon \text{ and Arg } |p(j\omega) + e^{\frac{\pi}{2}}| < \epsilon, \text{ for } \omega > \omega_{\epsilon}$ 

Note that Al(1) permits changes in plant order, e.g.,  $\frac{1+\alpha T_1 s}{1+T_1 s}$  with say  $\alpha \in [2, 5]$ ,  $T_1 \in [0, 3]$ . Al(2) dictates minimum-phase p(s) and that the jw axis is not a limit of any sequence of p(s) zeros. Al(3) requires a uniform bound on the poles and zeros of all peP.

## A2. Tolerances on $|t(j\omega)|$ and $|t_d(j\omega)|$

- (1)  $0 < A(\omega) \le |t(j\omega)| \le B(\omega)$  with A, B  $\in$  C  $[0, \infty)$ ,  $\frac{B(\omega)}{A(\omega)} \ge B(\omega) > 1$ .  $\exists \inf_{I} \beta(\omega) = \beta_{I} > 1$  on any finite  $I = [0, \omega]$ .
  - (2)  $\Rightarrow \lambda > 1.05$ ,  $\omega_{\lambda}$ ,  $\Rightarrow$  for  $\omega > \omega_{\lambda}$ ,  $\frac{B(\omega)}{A(\omega)} = \frac{\lambda k_2}{k_1}$ . This means that

in the high  $\boldsymbol{\omega}$  range, the feedback is allowed to increase the sensitivity

 $S = \frac{\partial t(j\omega)/t(j\omega)}{\partial p(j\omega)/p(j\omega)}, \text{ rather than decrease it. In fact, as noted by}$ 

Bode,  $\int_{0}^{\infty} \ln|S| d\omega = 0 \text{ in any practical system, so the decrease}$ 

in S(|S|<1) achieved in the control bandwidth range, must be balanced by |S|>1 in another range.  $\lambda$  can be a large number, because as  $\omega + \omega$ ,  $t(j\omega)+0$ , e.g., suppose  $k_2/k_1 = 10$ , who cares if  $|t(j\omega)| \epsilon [10^{-11}, 10^{-7}] (\lambda = 10^3)$  at very large  $\omega$ .

(3) The tolerances on  $t_d(j\omega)$  are in the form  $|t_d(j\omega)| \le Q(\omega) > 0$ . For any  $I = [0, \omega]$ ,  $\exists$  inf  $Q(\omega) = \beta_{dI}$ . Since  $t_d = P(1 + pg)^{-1} = pS$  of A2(2), |Q/p| > 1 at high frequencies, so  $\exists \omega_d$ ,  $\exists$  for  $\omega > \omega_d$ ,  $Q(\omega) = \beta_1(\omega)|p(j\omega|, \beta_1 > 1.05$ . stricted to the interior of the left half-plane \peP, and minimum-phase.

## A3. Choice of Compensation Functions

Let  $p_0(s)$  of Al(1) be the 'nominal' plant with  $k_0 \in [k_1, k_2]$  its associated  $k_p$  value of Al(3).

Let 
$$\mathcal{E} = .01 \frac{k_0}{k_2}$$
 in Al(3),  $\omega_t = \text{largest of } \{\omega_{\varepsilon}, \omega_{\lambda}, \omega_{d}\}$ ,  $I_t = [0, \omega_t]$ ,  $\mathcal{E} = \sup_{I_t} \frac{\left|p_0(j\omega)\right|}{b_{I_t}}$ , of Al(2). In Fig. 2,

$$t(s) = \frac{fgp}{1+gp} = \frac{f\ell_0}{\frac{p_0}{p} + \ell_0}, \ \ell_0 = g \ p_0.$$
 (A1)

We want  $\frac{P}{\inf_{P} |t(j\omega)|} \leqslant \frac{B(\omega)}{A(\omega)}$  of A2(1). This is achieved in

$$I_{t} \text{ if } \frac{\sup_{p} \left| \frac{p_{o}}{p} + \frac{\ell_{o}}{p} \right|}{\inf_{p} \left| \frac{p_{o}}{p} + \frac{\ell_{o}}{p} \right|} < \beta_{I_{t}} \text{ of A2(1)}.$$

to a to the right of the lines - o. satisfies A2(1. 2) in 1

Since  $\left|\frac{p_0}{p}\right| < \gamma_t$  in  $I_t$ , it suffices for  $I_t$ , if  $|l_0| > \gamma_t$  and  $\frac{|l_0| + \gamma_t}{|l_0| - \gamma_t} \le \beta_{I_t}$ ,

giving the sufficient condition

$$\frac{|\ell_0| \geqslant \gamma_t}{(\beta_{i_t} - 1)} \stackrel{\triangle}{=} |\ell_{ot}|, \text{ in } I_t.$$
(A2)

To satisfy A2(3) in  $I_t$ , it is necessary that  $|t_d| = \left| \frac{p}{1+gp} \right| = \left| \frac{p_0}{p_0} \right| < Q(\omega)$ , which is certainly achieved if

$$\frac{|\ell_0| > \frac{\sup |p_0|}{\beta_{dI_t}} + \frac{\sup |p_0|}{\inf |p_0|} = x_{oI_t} \left( \frac{1}{\beta_{dI_t}} + \frac{1}{b_{I_t}} \right) \stackrel{\Delta}{=} |\ell_{od}|.$$

Therefore, choose

$$|l_0(j\omega)| > \text{larger of } (|l_{ot}|, |l_{od}|)^{\frac{\Delta}{2}} |l_{ox}|, \text{ in } I_t.$$
 (A3)

Next, we find a bound on  $\ell_0$  in  $\bar{l}_t = [\omega_t, \infty)$  to satisfy A2 in  $\bar{l}_t$ . From A1(3), in  $\bar{l}_t = [\omega_t, \infty)$ ,  $\{\frac{-p_0}{p}\}$  lies in the narrow sliver V in Fig. A1,  $\leq .01 \frac{k_0}{k_2} \leq .01$  radians angular width, with magnitude bounds  $\left[.99 \frac{k_0}{k_2}, 1.01 \frac{k_0}{k_1}\right]$ . Let A in Fig. A1 be a trial value of  $\ell_0$ , so  $\frac{p_0}{p} + \ell_0$  is the vector originating at point  $\frac{p_0}{p}$  in V and terminating at A. Bounds on  $\ell_0$  may be obtained so that

$$\frac{\sup_{P} \left| \frac{P_0}{p} + \ell_0 \right|}{\inf_{P} \left| \frac{P_0}{p} + \ell_0 \right|} \quad \text{satisfies A2(1,2) and A2(3) in } \bar{I}_t = [\omega_t, \infty).$$

It is easily seen that a very conservative boundary for  $\mathbf{L}_0$  in  $\bar{\mathbf{I}}_t$  is the vertical line  $s=-\sigma$ , with

$$\sigma = \sigma_1 = \frac{k_0}{2} \left( \frac{.99\lambda - 1.01}{\lambda k_2 - k_1} \right) > 0 \tag{A4a}$$

i.e.,  $\ell_0$  on the right of the line  $s = -\sigma$ , satisfies A2(1, 2) in  $\bar{l}_t$ .

$$\left|\frac{p}{1+pq}\right| = \left|\frac{p_0}{\frac{p}{p}+\ell_0}\right| \le \beta_1|p|$$
, or  $\left|\frac{p_0/p}{\frac{p}{p}+\ell_0}\right| \le \beta_1$ . This is easily satis-

fied if the above

$$\sigma = \sigma_2 = .99 \frac{k_0}{k_2} (\beta_1 - 1)$$

$$\frac{2 \beta_1}{2 \beta_1}$$
(A4b)

Therefore, choose

$$\sigma = \text{smaller of } (\sigma_1, \sigma_2)$$
 (A4c)

Thus, the problem is to find  $\ell_0(s)$  such that  $|\ell_0(j\omega)|$  is outside the circle C in Fig. Al for  $\omega \leqslant \omega_t$  and to the right of the line  $s=-\sigma$  for  $\omega > \omega_t$ . It is obviously very easy to find such an  $\ell_0(s)$  which also has all its poles and zeros in the interior of the left half-plane, with any desired finite excess of poles over zeros, and which furthermore has the property shown in Fig. Al, i.e., lies on the right of  $s=-\sigma$ , for all  $\omega$ . For example, let

$$\ell_0 = \frac{2\ell_{ox}}{(1 + \frac{s}{\omega_t}) \prod_{i=1}^{e} (1 + \frac{s}{\omega_i})}$$

e any desired finite number,  $\omega_{i} = larger of (10\omega_{t}, \frac{2l_{ox}\omega_{t}}{\sigma}), \omega_{i+1} = 100\omega_{i}$ .

Note that it would be impossible to guarantee the existence of the desired  $\ell_0$  if  $\rho_0$  was nonminimum-phase (Horowitz and Sidi 1978).

It is conceivable that even though A2(1)-A2(3) are satisfied, A2(4) is not satisfied. Consider the zeros of  $1 + pg = 1 + l \frac{p}{o p_o}$  or of  $(\frac{p_c}{p} + l_o)$ . Recall that in  $[0, \omega_t], \{\frac{p_o}{p}\}$  lies in the circle of radius  $\gamma_t$  which is inside the circle C of Fig. A1, while  $l_o$  lies outside the larger circle C. In  $[\omega_t, \infty)$ ,  $l_o$  lies on the right of the line  $s=-\sigma$  while  $\{\frac{p_o}{p}\}$  is contained in V of Fig. A1. Also,  $l_o(j\omega)$  lies on the right of  $l_o(j\omega)$  lies on the origin clockwise (or alternatively  $l_o(j\omega)$  does not encircle the origin clockwise (or alternatively  $l_o(j\omega)$  does not so encircle  $l_o(j\omega)$ ,  $l_o(j\omega)$  and the system is stable.

### Application to mio system

In the mio system (4a), the loop function  $\ell_{uu} = g_{uu}/P_{uu}$  must handle the n  $t_{uv}$  problems  $v = 1, 2, \ldots, n$ . The bounds on  $\ell_{uuo}$  will be, in general, different for each v with its own  $\ell_{oxv}$ ,  $I_{tv}$  of (A3) and  $\sigma_v$  of (A4c). Let  $I_u = \max_v \ell_{oxv}$ ,  $\ell_{ou} = \max_v \ell_{oxv}$ ,  $\ell_{ou} = \min_v \sigma_v$  be the design parameters  $\ell_{uuo}$ . Obviously such a  $\ell_{uuo}$  is satisfactory for all n  $\ell_{uv}$  problems.

In Sec 3 (just before 3.1), there was noted the desirability of satisfying (6) on the boundary of a semicircle of radius  $\omega_H$  in the right half-plane. This requires, in addition to the previous, rewriting Sec A3, replacing jw by  $\omega_H e^{j\theta}$ ,  $\theta \epsilon$  [0,  $\pi/2$ ]. The development is easier if  $\omega_H$  is large enough so that each  $p_{ij} = k_{ij}/s^{e_{ij}}$  on  $s = \omega_H e^{j\theta}$ . Clearly, there will emerge bounds on  $\ell_{uuo}$  on  $s = \omega_H e^{j\theta}$ , which will have to be satisfied, in addition to those on  $s = j\omega$ . Obviously, such bounds can always be satisfied by suitable shaping of  $\ell_{uuo}$ , so that  $|\ell_{uuo}|$  is large enough on  $\omega_H e^{j\theta}$ .

There remains the design of f(s), inasmuch as  $\ell_0(s) = g(s) p_0(s)$  only determines g(s). Note that  $\ell_0(s)$  only guarantees that

$$\frac{\sup_{P} \left| \frac{P_0}{p} + \ell_0 \right|}{\inf_{P} \left| \frac{P_0}{p} + \ell_0 \right|} < \frac{B(\omega)}{A(\omega)} \text{ of A2(1)};$$

f(s) is chosen so that  $|t(j\omega)| \in [A(\omega), B(\omega)]$ . For example, suppose  $A(\omega_1) = .9$ ,  $B(\omega_1) = 1.04$ , and at  $\omega_1$ ,  $\sup_{M} \left| \frac{p_0}{P} + \ell_0 \right| = 100$ , while inf M  $\left| \frac{p_0}{P} + \ell_0 \right| = 90$  with  $|\ell_0(j\omega_1)| = 80$ . The range of  $|t(j\omega_1)| = \left| \frac{f\ell_0}{\frac{p_0}{P} + \ell_0} \right|$  is therefore  $[.8|f(j\omega_1)|, .889|f(j\omega_1)|]$ , so we need

 $.8|f(j\omega_1)|>.9$ ,  $.889|f(j\omega_1)|<1.04$ , giving the permissible range of  $\left[\frac{9}{8},\frac{1.04}{.889}\right]$  for  $|f(j\omega_1)|$ . In this way, the bounds on  $|f(j\omega)|$  are found and it is always possible to find an f(s) with left half-plane poles and zeros which satisfies such bounds.

The above procedure in all its details, is not recommended as a practical design procedure. Simplifications were made to make the proof easier, but the loop bandwidth is much larger than necessary. Its primary purpose is as an existence theorem. A practical optimum design procedure based on these ideas, but without the rigor, has been given in (Horowitz and Sidi 1972) and used a great deal with considerable success.

zeros?" For such a, a ony tolerances satisfying A2 but otherwi-

# A5. Extensions wante wind (a) A said sould (ale asmirrades wind

- (1) It is possible to have  $A(\omega) = B(\omega)$ ,  $Q(\omega) = 0$  in A2(1), (3) at a finite number of  $\omega$  values, by cheosing g infinite at these points. The sensitivity zeros can be single or multiple.
- (2) Some or all  $p \in P$  can have zerox on the  $j \omega$  axis. If these zeros are precisely known (unlikely), g(s) can be assigned poles there. Otherwise,  $t(j \omega)$  must be zero at these points for such p, requiring obviously much more careful statement of the tolerance on  $t(j \omega)$  and  $t_d(j \omega)$  near such points.
- (3) The most significant extension is that Constraint Al(1) can be relaxed. There can be uncertainty in the order of the plant due to disappearing poles and zeros--closely related to the problem of singular perturbations (Porter and Tsingas 1978).

## A6. Disappearing Poles and Zeros

Let

$$p = \frac{p_{1}^{m} (1+sa_{1})}{\frac{n}{m} (1+sb_{1})} = p_{1}^{\Psi}(s)$$
 (A5)

with  $a_i \in [0, a_{ix}]$ ,  $b_j \in [0, b_{jx}]$  and  $p_l \in P$  satisfying A1. The question of concern is: "For what m, n values can the loop transmission be arbitrarily large over an arbitrarily large bandwidth but still be practical, i.e., go to zero as  $\omega \to \infty$  with any desired finite excess of poles over zeros?" For such m, n any tolerances satisfying A2 but otherwise arbitrary, can be satisfied.

$$t(s) = \frac{fgp}{1 + gp} = \frac{fgp_1\Psi}{1 + gp_1\Psi} = \frac{f\varrho}{1 + \varrho}.$$
 (A6)

The question posed can be answered by referring to the logarithmic complex plane (Nichols chart) in Fig. A2. The intersections of the zero db line with the vertical lines (2n+1)  $180^{\circ}$ ,  $n = 0 \pm 1$ , . . . is the point -1. Because of uncertainty,  $\ell = gp_1 \forall$  is not a point but a set (2) denoted here as the template of 2,  $J_{\nu}(\omega)$  which occupies some region in the complex plane--Fig. A2. The shape of  $J_{i}$  is that of {p1 Y} because there is no uncertainty in g. The latter permits the translation (but not rotation of £) in the complex logarithmic plane, horizontally by arg g and vertically by |g| in For some finite  $\omega$  range, large  $|\mathfrak{l}|$  is needed so  $J_{\mathfrak{l}}$  lies above the zero db line, e.g.,  $J_{\ell}(\omega_1)$  in Fig. A3. At large enough  $\omega$ ,  $|\ell|$ must be very small ( $\rightarrow 0$  as $\omega \rightarrow \infty$ ) so  $\int$ , must be well below the zero db lines and continue downwards to  $-\infty$ . In the transition of  $J_2$  from above to below the zero db line, it must not interest -1, nor encircle it. Hence, the width of  $J_{\mu}$  must be restricted to <360° for some  $\omega$  interval in which  $\mathcal{J}_{\omega}$  can squeeze in between two -1 points on its way downward (Fig. A2). But we want arbitrary sensitivity reduction for arbitrary bandwidth. This requires  $\exists \omega_u$ ,  $\ni$  for  $\omega > \omega_H$  the width of  $J_{\ell}(\omega) < 360^{\circ}$ .

Consider now the shape of  $\mathcal{J}_{\ell}$  which is that of  $\mathcal{J}_{\text{pl}}$  which is that of  $\mathcal{J}_{\text{pl}}$  +  $\mathcal{J}_{\psi}$  in the Nichols chart. Constraint A1(3) assures that at large enough  $\omega$  the width of  $\mathcal{J}_{\text{pl}}$  + zero degrees, so it is entirely a question of the width of  $\mathcal{J}_{\psi}$ . Consider any factor of  $\Psi$ , e.g.,  $\frac{1}{1+j\omega b}$ , be  $\{0,m\}$ . At any specific  $\omega$ , the maximum width of the template is  $\tan^{-1}\omega b_{\max}=\tan^{-1}\omega m$ . For  $\omega m=20$ , the template is OAB in Fig. A3 (O at b=0, B at  $\omega b=20$ ); for  $\omega m=100$  it is OABU and for  $\omega m=1000$ , it is OABUV. For two such independent factors, it is easy to find the new template. This is done in Fig. A3 for  $\omega m_1=\omega m_2=20$ . Draw O"A"B" = OAB and position O" at points on OAB (because of the independent uncertainties). The result is ABEJDEFO =  $\mathcal{J}[(\frac{1}{1+j\omega b_1})(\frac{1}{1+j\omega b_2})]$ ,  $b_1$ ,  $b_2 \in [0, m]$ . The template of a zero factor (1+j $\omega$ a) is obtained by reflecting that of the pole if  $\{\omega a\}_{\max}=\{\omega b\}_{\max}$ , giving OA'B' in Fig. 3.

As  $\omega$  increases, the contribution of each factor (pole or zero)  $\rightarrow 90^{\circ}$  in width. Therefore, while theoretically four factors can be admitted between two-1 points, stability margins dictate a maximum of three. But this is only a necessary condition, because it must also be possible to decrease |L| from arbitrary large to small values. This basically means that over arbitrary large frequency range Arg L must be overwhelmingly negative. The extreme right side of  $\sqrt{1}$  must then lie on the left of the  $0^{\circ}$  line in Fig. A2. One disappearing pole or zero poses no problem, but two do because the left side of  $\sqrt{1}$  will then intersect -1

be made rigorous, of course.) Note that this is for the most demanding situation. If only stability is desired, then any finite number of disappearing poles or zeros can be handled.

### APPENDIX 2

## A7. CONDITIONS THAT & MAPS H(n2) INTO ITSELF

The constraints on  $H_{uv}$  were given in 2.1. The first is satisfied if (6) is. From Appendix 1, it is seen that at finite  $\omega$ , the only possible difficulty is, if in Fig. 2,  $d_{uv}(j\omega)$  is unbounded but  $g_{uu}p_{uv}e$  is bounded. If such unboundedness of  $d_{uv}$  is at a finite number of  $\omega$  values, it is possible to assign poles there to  $g_{uu}$ . Since  $d_{uv}$  is a function of the plant parameters (Eq. 4b), an infinite number of such poles is conceivable, in fact is so in practice if there is one, because of inevitable uncertainties. How can  $d_{uv}$  be unbounded while  $p_{uv}e$  is bounded? From (3,5)

$$d_{uv} = \frac{\sum_{i \neq u} (-1)^{iu} \Delta_{iu} t_{iv}}{\Delta = \sum_{i \neq u} (-1)^{iu} p_{iu} \Delta_{iu} + p_{uu} \Delta_{uu}}, \quad p_{uve} = \frac{\Delta}{\Delta_{uu}}$$

$$i \neq u$$
(A7)

Hence, such a situation is possible, if  $\Delta_{1u}$  has such a pole which is cancelled by a zero of  $p_{1u}$  and is not present in  $p_{uu}\Delta_{uu}$  e.g. n=2,  $p_{21}$  has a pole at  $\pm ja$ ,  $p_{12}$  has a zero there and  $p_{11}P_{22}$  does not have a pole there. Such situations are therefore not allowed. It can be argued that they are in practice impossible (Horowitz and Shaked 1975),

because p<sub>12</sub>, p<sub>21</sub> must involve different physical parameters and the uncertainties in each cannot be 100% correlated. Irrespective of this argument, the constraint is

$$|P_{ij}(j\omega)|$$
 is uniformly bounded on  $[0,\infty)$  and M,  $\forall i \neq j$  (A8)

The problem is more difficult as  $\omega \rightarrow \infty$  and is treated in Section 3.

To satisfy constraint (2) on  $H_{uv}$  in 2.1, note first that if  $z(j\omega) = z_1 + jz_2$  with  $z_1$ ,  $z_2$  real functions of  $\omega$ , then |z|' is bounded if z' is bounded. For

$$|z|' = (z_1^2 + z_2^1)' = \frac{z_1 z_1' + z_2 z_2^1}{z_1^2 + z_2^2}$$
. If  $z^1 = z_1^1 + j z_2^1$ 

is bounded, so are  $z_1^1$ ,  $z_2^1$  and |z|'. Consider separately  $\tau_{uv}'$   $(j\omega)$  and  $(\tau_{duv}^1 d_{uv}^1)'(j\omega)$  of (4). The former can be written

$$\tau' = \left(\frac{f\ell}{1+\ell}\right)' = f' \frac{\ell}{1+\ell} + \frac{f(gp' + g'p)}{(1+gp)^2}$$

$$\ell = gp, \quad p = p_{uve}, \quad g = g_{uu}$$
(A9)

of Fig. 2. Since  $f\ell/(1+\ell)$  is bounded by the appropriate  $B_{uv}$ , the first term on the right of (A9) needs only uniform boundedness of f', which is easy as f is chosen by the designer. Obviously, the only possible difficulties with the second term of (A9) are g', p' which can be infinite only at  $j\omega$  axis poles. However, at such poles, the denominator forces the second term to be bounded. At large  $\omega$  where gp, g',  $p' \rightarrow 0$ , there is obviously no problem.

Next, consider  $(\tau_{duv}^{d}_{uv})'(\omega)$  written as

$$y' = \left(\frac{dp}{1+gp}\right)' = \frac{d'p}{1+gp} + \frac{d(p'-g'p')}{(1+gp)^2}$$
 (A10)

g,p of (A9),  $d = d_{uv}$ .

From (A8), d and since d is a rational function d', are unitermly bounded on the j $\omega$  axis. From the previous discussion re p', g' etc. and Appendix 1, y' can be uniformly bounded on any finite  $\omega$  range by proper choice of g. At large  $\omega$  each of d, d', p, p' etc  $\rightarrow$  0.

It is easy to see that constraint (3) is satisfied, because it has been required that the elements of P, G, F all  $\rightarrow$  0 as s  $\rightarrow \infty$ .

Sect 7.9, 3.9, 6.14; 1976, 1976 trans, Aut. Control, 26, 464-464; 1938;

Pantorovich, L. V., and Akriov. C. R., 1964, Finetional Analysis in Normed

#### REFERENCES

Astrom, K. J., et al., 1977, Automatica, 13, 457-476.

Bode, H. W., 1945, Network Analysis and Feedback Amplifier Design (New York: Van Nostrand).

Davison, E. J., 1976, IEEE Trans. Aut. Control, 21, 35-47.

Horowitz, I., 1963, Synthesis of Feedback Systems (New York: Academic Press) Secs 7.9, 3.9, 6.14; 1975, IEEE Trans. Aut. Control, 20, 454-464; 1976, Proc. IEEE, 123-130.

Horowitz, I., and Shaked, U., 1975, IEEE Trans. Aut. Control, 20, 84-97.

Horowitz, I. and Sidi, M., 1972, Int. J. Control, 16, 287-309; 1978, Int. J. Control, 27, 361-386.

Kantorovich, L. V., and Akilov, G. P., 1964, Functional Analysis in Normed Spaced (New York: Pergamon Press).

Krishnan, K., and Cruickshank, A., 1977, Int. J. Control, 25, 609-620.

MacFarlane, A. G. J., 1973, Automatica 9, 273-277.

Owens, D. H., 1978, Int. J. Control, 27, 603-608.

Porter, B., and D'Azzo, J., 1978, Int. J. Control, 27, 487-492.

Porter, B. and Tsingas, A., 1978, Int. J. Control, 639-650.

Rosenbrock, H. H., 1974, Computer-Aided Control System Design (New York: Academic Press).

wang, S. H., and Davison, E. J., 19/3, IEEE Trans. Aut. Control, 18, 220-225.

Wonham, W. M., 1974, Multivariable Control Systems: A Geometric Approach (Springer Verlag).

Fig. 1 Highlight angular contents and the of-freedom feedback and  $r_{\rm eq}$  .  $r_{\rm eq}$ 

Wonham, W. M., and Morse, A. S., 1972, Automatica, 8, 93-100.

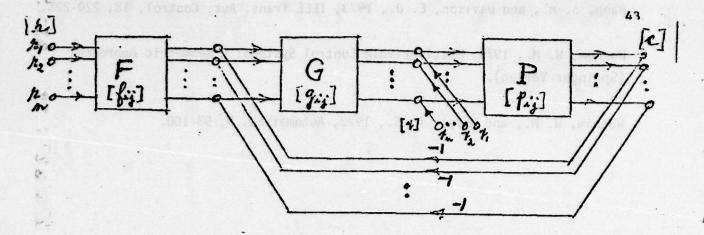


Fig. 1 Multiple input-output two matrix degree-of-freedom feedback structure c = Tr,  $T = [t_{ij}]$ ,  $c = [c_1 \dots c_n]'$ ,  $r = [r_1 \dots r_n]'$ .

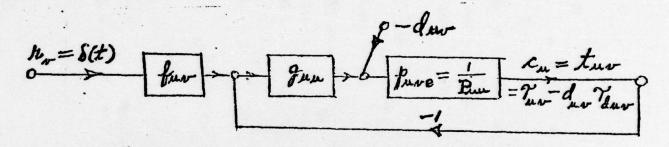


Fig. 2 Single-loop structure equivalent, for synthesis of  $t_{uv}$ ;  $d_{uv} = \sum_{i \neq u} P_{ui} t_{iv}, P^{-1} = [P_{ij}], \qquad P = [P_{ij}]$ 

$$\tau_{uv} = \frac{f_{uv}g_{uu}p_{uve}}{1 + g_{uu}p_{uve}}$$
,  $\tau_{duv} = \frac{p_{uve}}{1 + g_{uu}p_{uve}}$ .

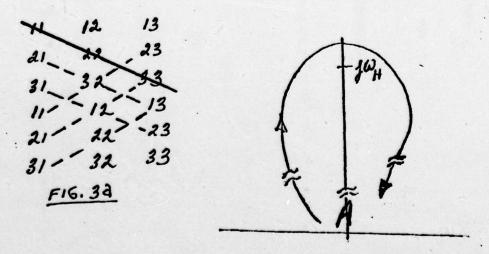
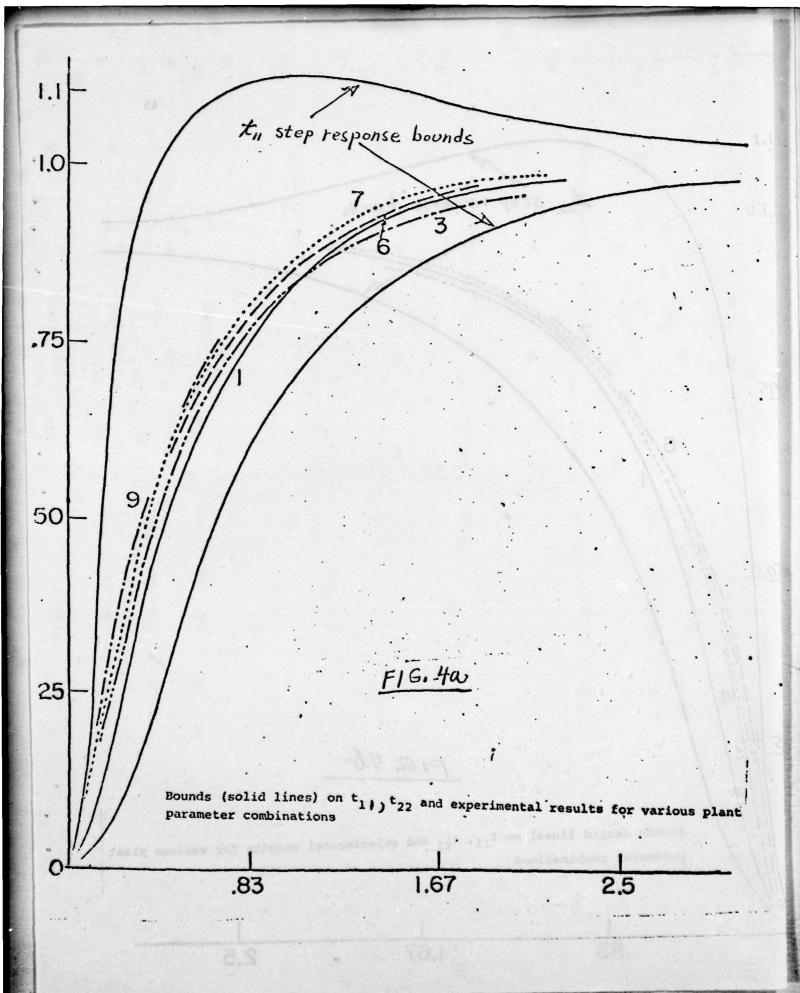


Fig. 3b To reach A in right half-plane, a zero must cross  $j_{\omega}$  axis above  $j_{\omega_H}$ .



taz step response bounds .1.0 75 F16.46 Bounds (solid lines) on  $t_{11}$ ,  $t_{22}$  and experimental results for various plant parameter combinations .83 1.67

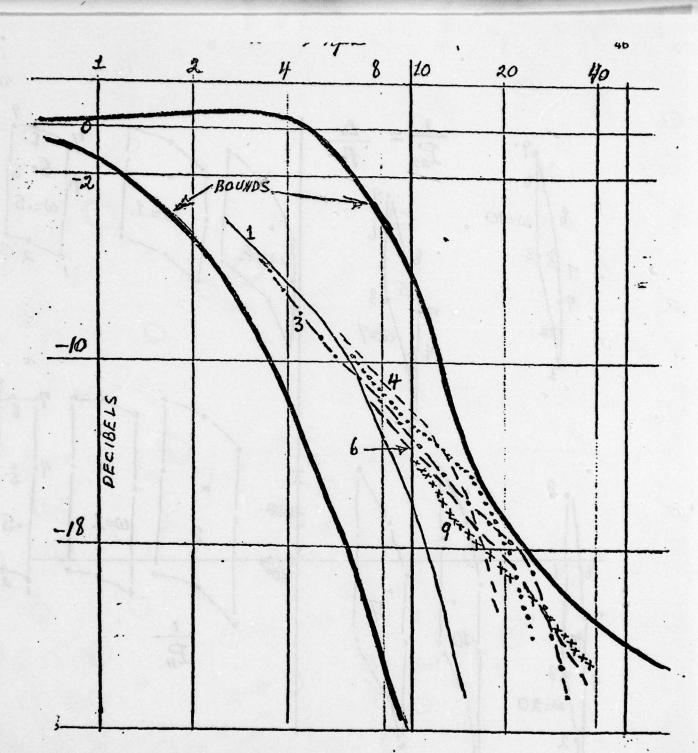


Fig. 5. "Equivalent" frequency domain bounds and experimental results for various plant parameter sets

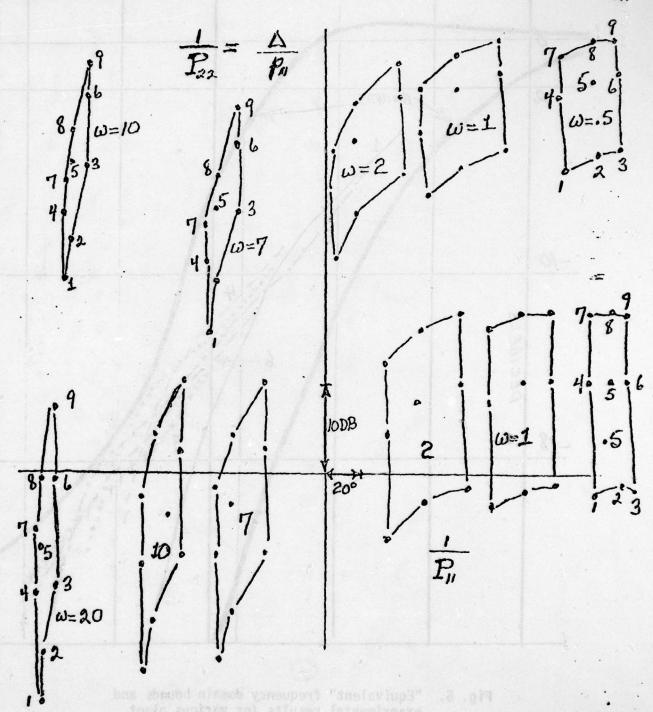


Fig. 6. Templates of  $P_{22}^{-1} = \Delta/P_{11}$ ,  $P_{11}^{-1} = \Delta/P_{22}$  at various frequencies, on Nichols Chart

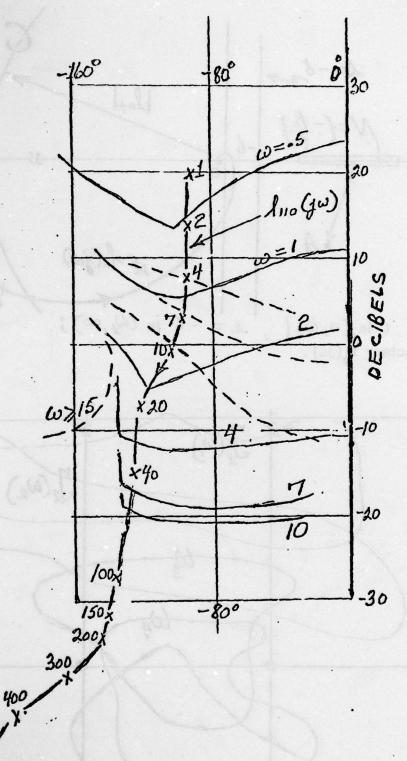


Fig. 7. Bounds on  $\ell_{110}(j\omega)$ . Solid lines are due to  $|\gamma_{il}|$ , broken lines due to  $|\gamma_{il}|$   $d_{line}|$ 

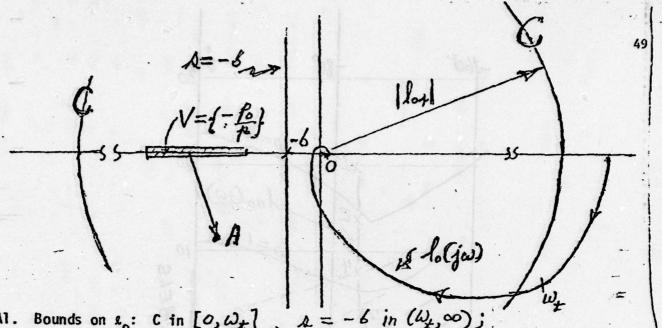


Fig. A1. Bounds on  $\ell_0$ : C in  $[0, \omega_{\pm}]$ ,  $\lambda = -6$  in  $(\omega_{\pm}, \infty)$ ; and a satisfactory  $\ell_0(j_{\omega})$ .

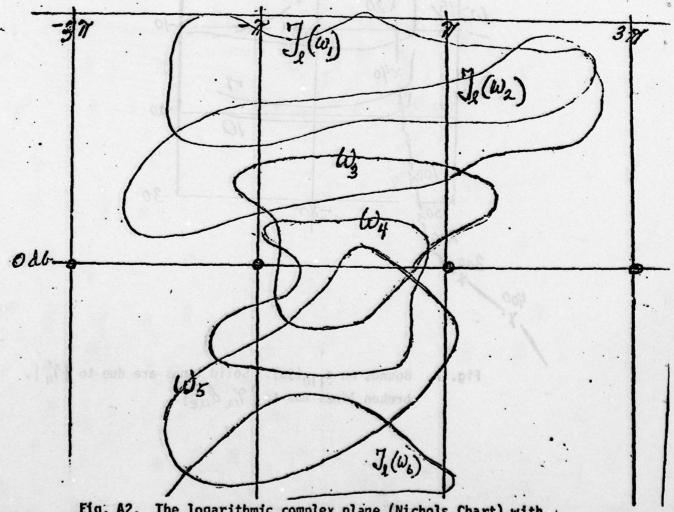


Fig. A2. The logarithmic complex plane (Nichols Chart) with

	1		
		······	
	j		
		the contract of the contract o	
	· · · · · · · · · · · · · · ·		
			1
		1	
			• • •
A CANADA CANADA MANADA			• • • • • •
	1 10		
	10		
	1 41		
	1 12		• • • • • • • • • •
	1 24		
	<b>Q</b>		
	( Pg		
	1		
	1 4		
	.0		
enter the second terms of the second contract			
	10	*************************	
with the contract of the second of the secon	18		
	2		
	2		
	1		
and the second s			
	U		
	10		
	110		
	63		
	l		
and the second of the second place of the second of the se			0
			Q
			<b>9</b>
	V		
80	10		
, ,			
	19	<del></del>	-1
			-1
			1
*	2	8	1
8	, ,		-1
	76		-1
	8		
	36-1		
	1		
	36	9	2
	<i>y</i> 6.	9	00
		9	2
	96	9	2
		9	2
		9	2
		9	2
		9	2
		9	2
		cAsE Wb=100	000
		cAsE wb= 100	WF = /000
		CASE 600	## = /000 - 1000
		cAsE = 100	WF = /000
		CASE 600	000/= 4m
		cAsE \wh= 100	000/= 4m
		CASE 00 = 100 -50	4- WA = 1000
		CASE 100	1 WF = (000
		CASE 100	1 WF = (000
		CASE 100	1 WF = (000
		CASE 100	V 1 4- WA = 1000
		CASE 00	000/= 4m - 1000
		CASE 00	V 1 4- WA = 1000
		CASE   00	000/= 477
		CASE 100	V 4 4 4 6000
		CASE 100	000/= 477
		CASE 100	000)= 4m - 1
		CASE 100	V 4 4 4 4 4 4 4 4 4 4 4 4 4 4 4 4 4 4 4
		CASE 100	V 4 4 4 4 4 4 4 4 4 4 4 4 4 4 4 4 4 4 4
		CASE 100	000)= 4m - 1
		CASE 100	000)=4m + (000)
		CASE 100	000/= 477
		CASE 100	000/= 477
		CASE 100	000/= 477
		CASE 100	000/= 477
		CASE 100	000/= 477
		CASE 100	000/= 477
		CASE 100	000/= 477
		CASE 100	000/= 477
		CASE 100	000

46 0700

STATE TO KIND TO THE INCHES KIND DESIGNATION OF THE STATE OF THE STATE

Methods for assessing the robustness properties of a linear multivariable feedback design.

open-look inverse hydring army dwith dermhydring direles)

Ian Postlethwaite,
Control and Management Systems Division,
University Engineering Department,
Mill Lane,
Cambridge,
England.

# 

On completing the design of amultivariable feedback system it is always desirable to be able to predict that under certain changes the system will remain stable. In these notes some methods are described for determining the robustness properties of a multivariable feedback system under

(i) simultaneous variation of sensor (or actuator) gains,

(ii) simultaneous nonlinear perturbations of loop gains, and

(iii) plant parameter uncertainty.

mercanetor uncertainty to discussed. In party ouler it is shown

multivariable feedback systems can be used to determine stabil

tow recent developments to the complex vertible analysis of

### 1. Introduction

In the inverse Nyquist array method for multivariable feedback design, the designer, having made the inverse of the open-loop system diagonally dominant, can by examination of the open-loop inverse Nyquist array (with Gershgorin circles) determine bounds on feedback gains for stability. The characteristic locus design method, although a procedure which does not require the constraint of diagonal dominance, only gives stability with respect to a single gain common to all the loops. But, since low interaction and accurate tracking are main objectives of this procedure the closed-loop transfer function will almost certainly be diagonally dominant, and in Section 2 it is shown how by looking at appropriate closed-loop Nyquist arrays bounds can be obtained on sensor or actuator changes for stability. This is a technique developed and implemented on the Cambridge multivariable design package by Dr. J.M. Edmunds.

In Section 3 the robustness of a multivariable feedback system is considered under simultaneous nonlinear perturbations of loop gains. A simple interpretation of work by Mees and Rapp 4 provides a bound on the nonlinear perturbations for stability in terms of principal gains 5.

In Section 4 the problem of stability under plant parameter uncertainty is discussed. In particular it is shown how recent developments in the complex variable analysis of multivariable feedback systems can be used to determine stability with respect to any system parameter.

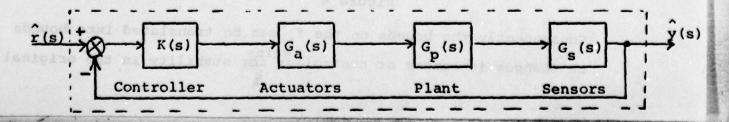
## 2. Closed-loop Nyquist arrays

The Nyquist array of a transfer function G(s) is formed by drawing the Nyquist diagrams of the individual elements of G(s). If G(s) describes an open-loop system then the array is called the open-loop Nyquist array; a similar diagram for  $G(s)^{-1}$  is called the inverse Nyquist array. If G(s)  $(G(s)^{-1})$  is diagonally dominant then the diagonal elements of the Nyquist (inverse Nyquist) array, with superposed Gershgorin circles<sup>1</sup>, give bounds on the simultaneous variation of loop gains for stability. This is a well known result due to Rosenbrock<sup>1</sup> and is a highly attractive consequence of the inverse Nyquist array design method.

The characteristic locus design method is atechnique which does not require the constraint of diagonal dominance but as such only gives stability with respect to a single gain common to all the loops. However, the main objective of this approach is to obtain a stable closed-loop system with low interaction and accurate tracking, and so the closed-loop transfer function R(s) will almost certainly be diagonally dominant. By forming a Nyquist array for R(s), called the closed-loop Nyquist array, and drawing Gershgorin circles on the diagonal-element diagrams, bounds can be obtained on simultaneous variation of sensor gains for stability. By looking at a similar closed-loop transfer function bounds can be determined for actuator variations. These methods are now described.

### 2.1 Closed-loop configuration

We will consider the configuration shown in figurel below.



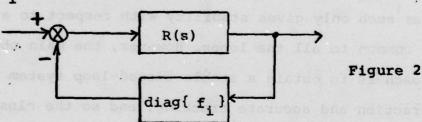
The closed-loop transfer function R(s) is given by

$$R(s) = \left[I_{m} + G_{s}(s)G_{p}(s)G_{a}(s)K(s)\right]^{-1}G_{s}(s)G_{p}(s)G_{a}(s)K(s)$$

and if K(s) has been designed successfully then R(s) will be diagonally dominant.

# 2.2 Stability under simultaneous changes in sensor or controller gains

Consider a situation where feedback is applied around the closed-loop system via a real diagonal operator  $F=diag\{f_i\}$ ; see figure 2. Then from the diagonal elements of the closed-loop Nyquist array the Gershgorin circles can be used to give bounds on the  $f_i$  for stability.



But the configuration of figure 2 is equivalent to figures 3

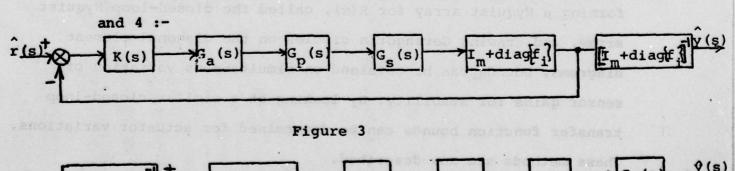


Figure 4

Consequently the bounds on the  $f_i$  can be translated into bounds on changes in sensor or controller for stability in the original

Remark 1. Note that the diagonal elements of the closed-loop Nyquist array (without Gershgorin circles) give exact information about system stability under changes in a single sensor assuming all other sensors remain unaltered. To see this, suppose that we are interested in varying the jth sensor gain, and let f<sub>i</sub>=0 for all i except i=j. Then we see from figure 3 that we have a single-input single-output problem described by the j,jth element of R(s). Stability with respect to f<sub>j</sub> can therefore be determined exactly using the Nyquist diagram of the j,jth element of R(s) which is the j,jth element of the closed-loop Nyquist array.

Remark 2. Note that the Gershgorin circles define bands within which the characteristic gain loci of R(s) must lie.

### 2.3 Stability under changes in actuator or plant gains

For the closed-loop system shown in figure 1 consider a new input and output between the actuators and plant as shown below in figure 5.

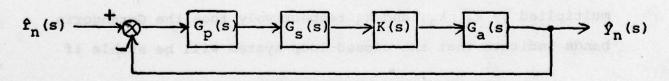


Figure 5

The closed-loop transfer function relating  $\hat{r}_n(s)$  and  $\hat{y}_n(s)$  is given by

$$R_n(s) = [I_m + G_a(s)K(s)G_s(s)G_p(s)]^{-1}G_a(s)K(s)G_s(s)G_p(s)$$

and following exactly the same procedure with  $R_n(s)$ , as with R(s) in the previous section, bounds can be obtained on changes

in actuator or controller gains for stability. These bounds will in general be more conservative than those obtained for sensor variations since there is no explicit objective in the design procedure which aims to make  $R_{\mathbf{n}}(\mathbf{s})$  diagonally dominant.

## 2.4 Example — PW F100 Jet Engine

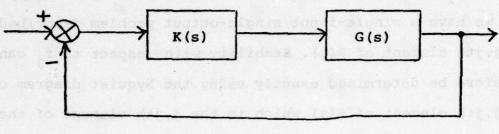


Figure 6

K(s) - controller obtained via characteristic locus design method

G(s) - actuator, plant and sensor dynamics combined

The characteristic gain loci and step responses are shown in figures 7-11, and the open-loop Nyquist array is shown in figure 12 from which it can be seen that the open loop system is not diagonally dominant. The closed-loop Nyquist array is shown in figure 13. If the three sensors have their gains multiplied by  $k_1$ ,  $k_2$ , and  $k_3$  respectively then the Gershgorin bands indicate that the closed-loop system will be stable if

$$k_1 < -0.48$$
 or  $0 < k_1$ ,  $k_2 < -0.43$  or  $0 < k_2$ , and  $0.33 < k_3 < 11$ .

If  $k_3 < -1.2$  then instability will definitely occur.

# CHARACTERISTIC GAIN LOCI

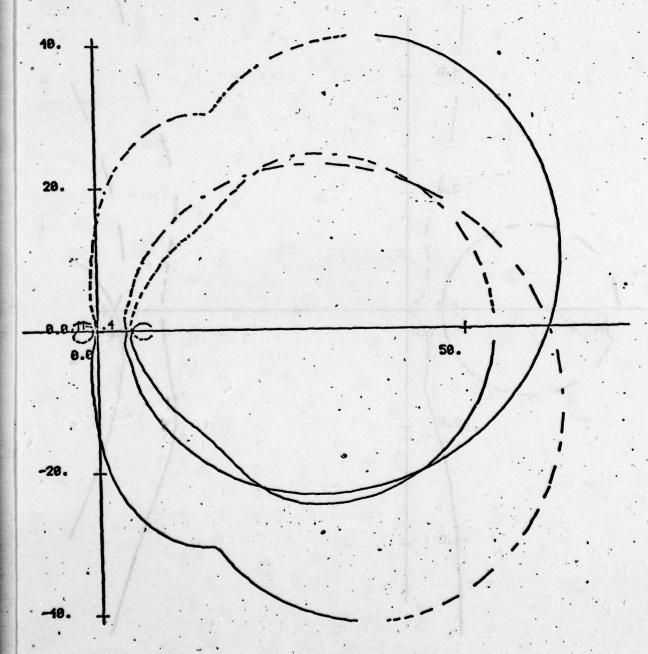
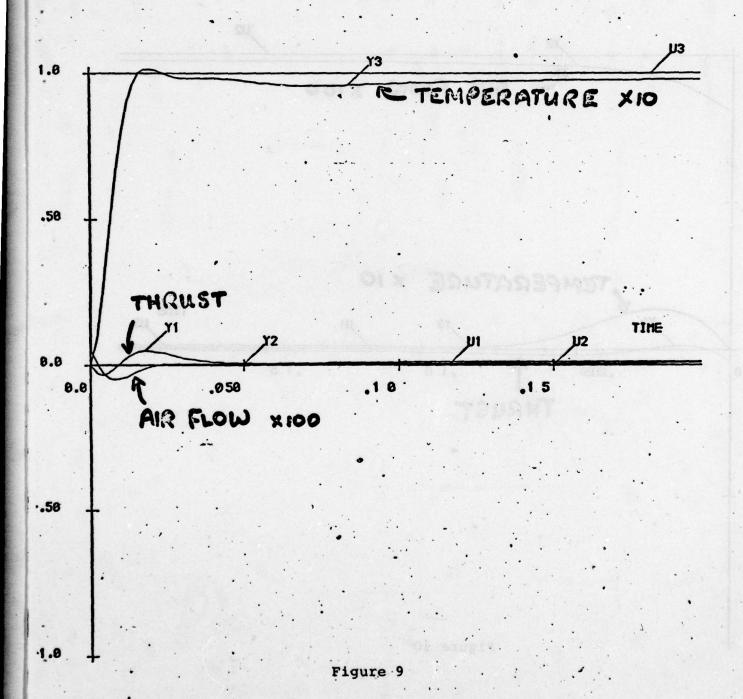


Figure 7

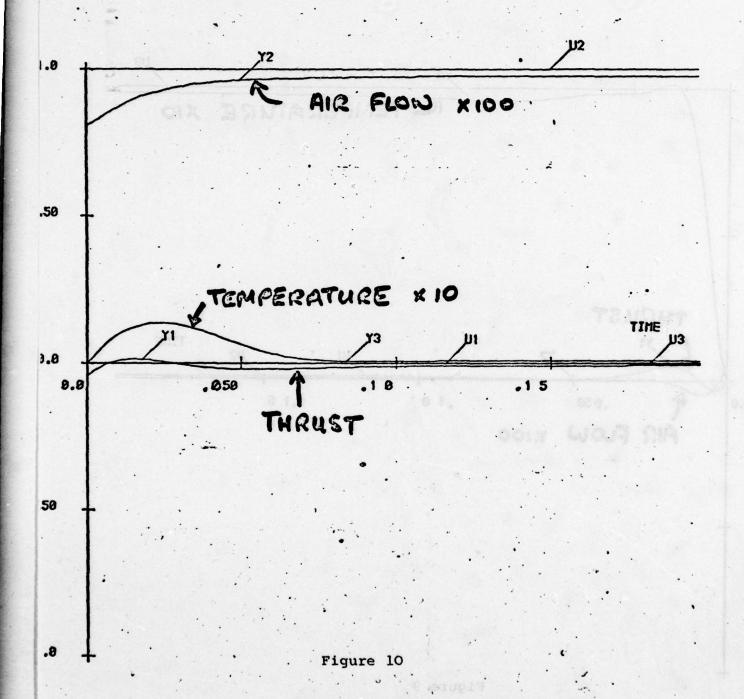
# CHARACTERISTIC GAIN LOCI about the F100 Engine 4.0

Figure 8

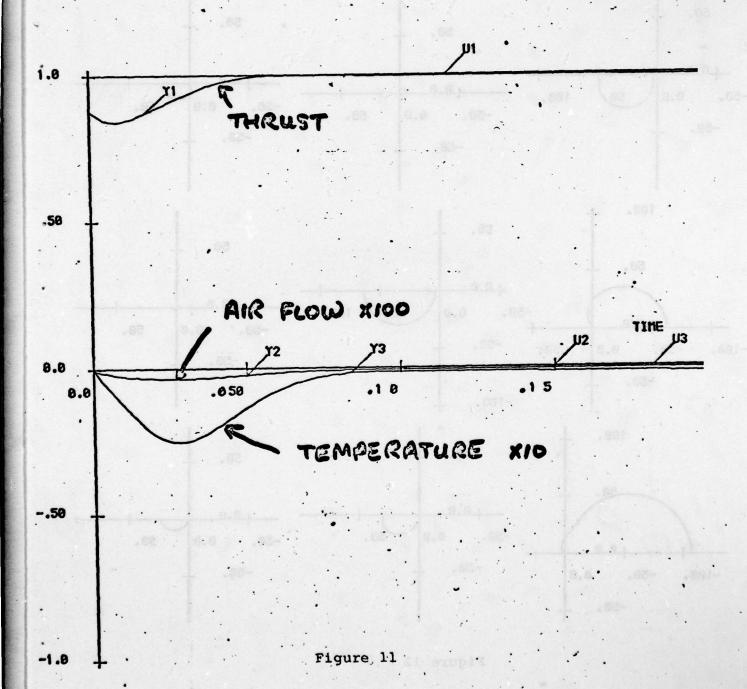
# STEP RESPONSE



# step response



# step restante



# Frod Engine

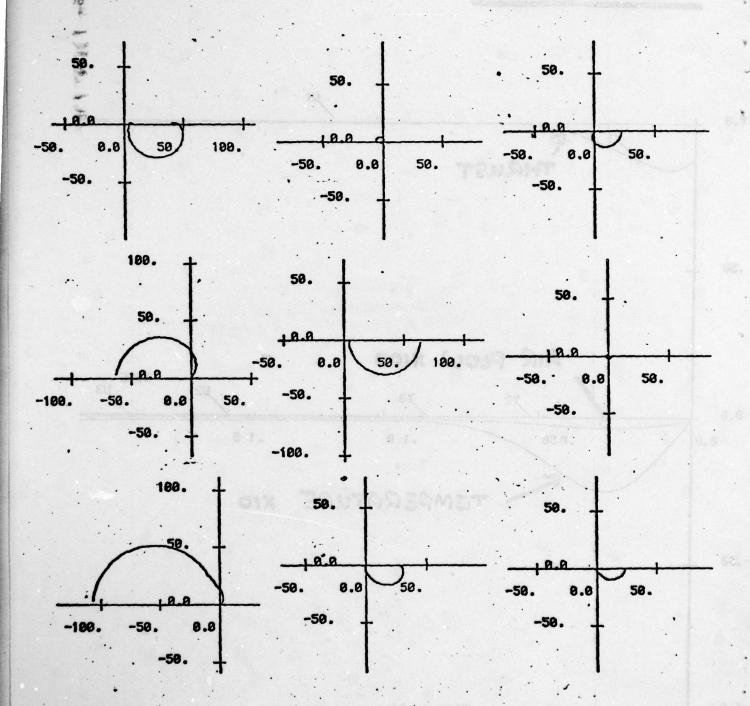


Figure 12

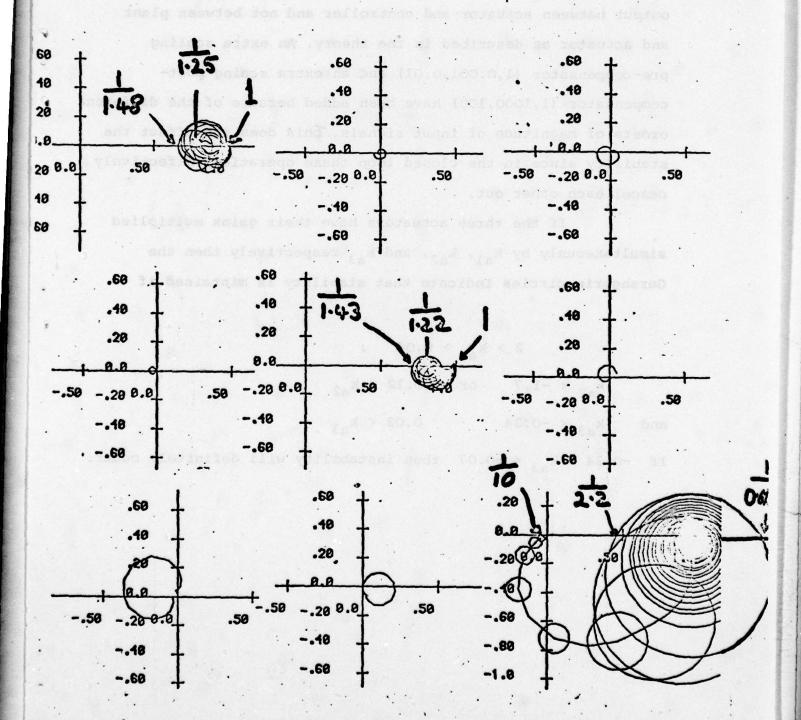


Figure 13

The closed-loop Nyquist array for actuator variations is shown in figure 14. Because the actuator dynamics is included for an G(s) the closed-loop transfer function is from an input and output between actuator and controller and not between plant and actuator as described in the theory. An extra scaling pre-compensator (1,0.001,0.01) and an extra scaling post-compensator (1,1000,100) have been added because of the different orders of magnitude of input signals. This does not affect the stability since in the closed loop these operations effectively cancel each other out.

If the three actuators have their gains multiplied simultaneously by  $k_{a1}$ ,  $k_{a2}$ , and  $k_{a3}$  respectively then the Gershgorin circles indicate that stability is maintained if

$$2 > k_{a1} > 0.04$$
 ,  $k_{a2} < -1.7$  or  $0.12 < k_{a2}$  , and  $k_{a3} < -0.24$   $0.02 < k_{a3}$  .

If  $-0.24 < k_{a3} < -0.07$  then instability will definitely occur.

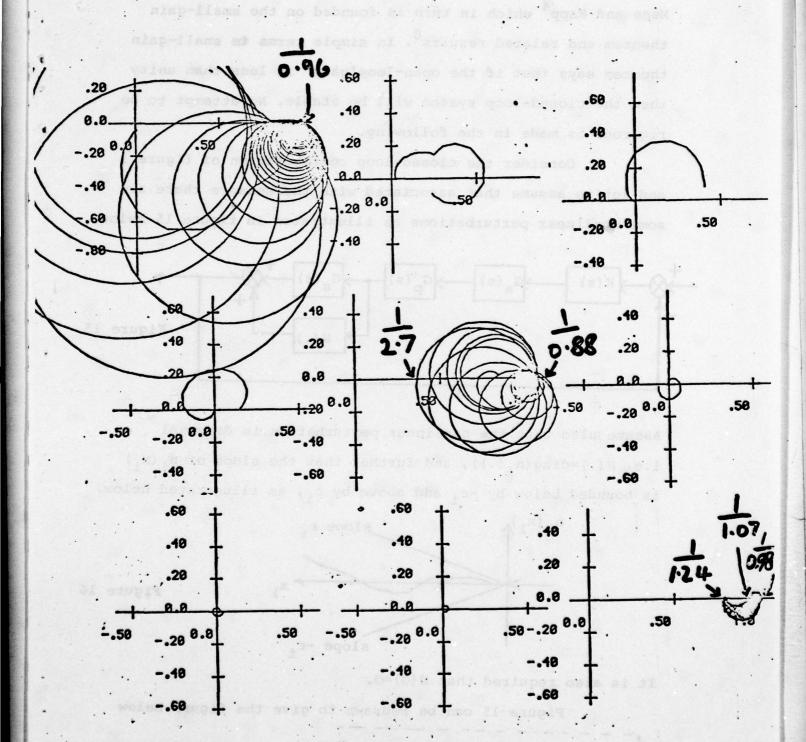
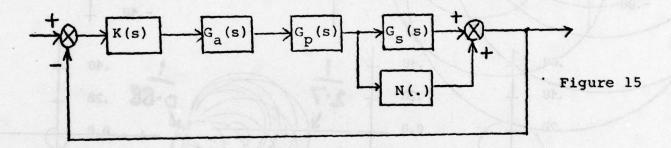


Figure 14

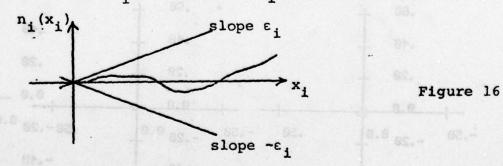
### 3. Stability with nonlinear perturbations

The results in this section are based on work by Mees and Rapp which in turn is founded on the small-gain theorem and related results. In simple terms to small-gain theorem says that if the open-loop gain is less than unity then the closed-loop system will be stable. No attempt to be rigorous is made in the following.

Consider the closed-loop configuration of figure 1 and let us assume that associated with the sensors there are some nonlinear perturbations as illustrated in figure 15 below.

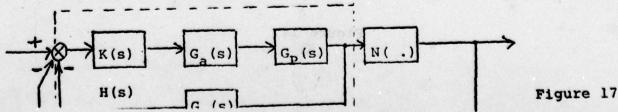


Assume also that the nonlinear perturbation is diagonal i.e.  $N(.)=\operatorname{diag}(n_i(.))$ , and further that the slope of  $n_i(x_i)$  is bounded below by  $-\varepsilon_i$  and above by  $\varepsilon_i$ , as illustrated below.



It is also required that N(O)=O,

Figure 15 can be redrawn to give the figure below



and applying the small-gain theorem to this we have that for stability H(s) must be stable, which it is by design, and the gain round the loop must be less than unity. To check this we must first give suitable definitions for the gains of the linear and nonlinear operators.

The gain of the linear part H(s) can be defined as

where  $||A|| = \sqrt{(\text{max. eigenvalue of A}^{\dagger}A)}$ 

and so is the maximum principal gain of H(s).

The gain of the nonlinear part will be taken as

$$\max_{i} \{ \epsilon_{i} \}$$

Consequently the inverse of the maximum principalgain of H(s) gives an upper bound to the slopes of the nonlinear perturbations for stability to be maintained.

By taking a slightly different definition for the gain of the linear operator H(s) a graphical test, analogous to the multivariable circle criteria, can be obtained. The resulting bound on the  $\varepsilon_i$  however is more conservative; this is now explained.

At a particular value of s

$$H = R\Lambda R^{-1}$$

R—matrix of eigenvectors A—diagonal matrix of eigenvalues

therefore 
$$\|H\| = \|R\Lambda R^{-1}\| \le \|R\| \|\Lambda\| \|R^{-1}\|$$

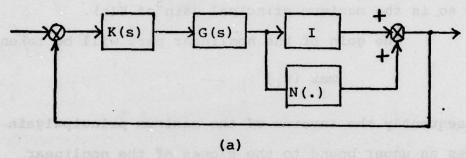
where  $\gamma = \|R\| \|R^{-1}\|$  is the square root of the largest to the smallest principal gain of R, and p is the largest eigenvalue of H. Since  $\gamma \rho$  is an upper bound on  $\|H\|$ , thegain of

H(s) can be taken as

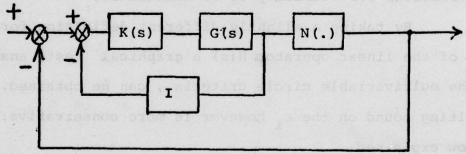
sup 
$$\gamma(jω)$$
 ρ $(jω)$  ω>0

Therefore if the eigenvalue-loci of  $H(j\omega)$  multiplied by  $\gamma(j\omega)$  all lie within a circle centre the origin radius  $\varepsilon_{max}^{-1}$  then the system remains stable. The radius of the circle which just touches these loci is therefore a maximum bound on the nonlinear perturbations.

## 3.1 Example — PW Floo Engine 7



which is equivalent to



Note H(s) =  $[I+G(s)K(s)]^{-1}G(s)K(s)$  (b)

Figure 18

The principal gains of H(s) are shown in figure 19. The maximum principal gain is 1.22 which gives an upper bound on the magnitude of the  $\varepsilon_i$  of 0.82.

The eigen-loci of  $H(j\omega)$  modified by  $\gamma(j\omega)$  are shown in figure 20, and  $\gamma(j\omega)$  is shown separately on figure 21. From figure 20 we see that the loci are completely enclosed by a circle

# PRINCIPAL GAINS

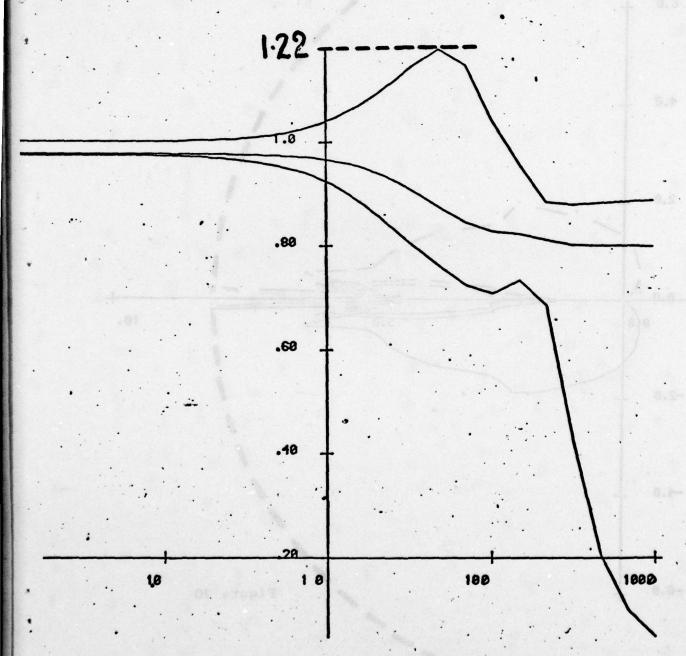
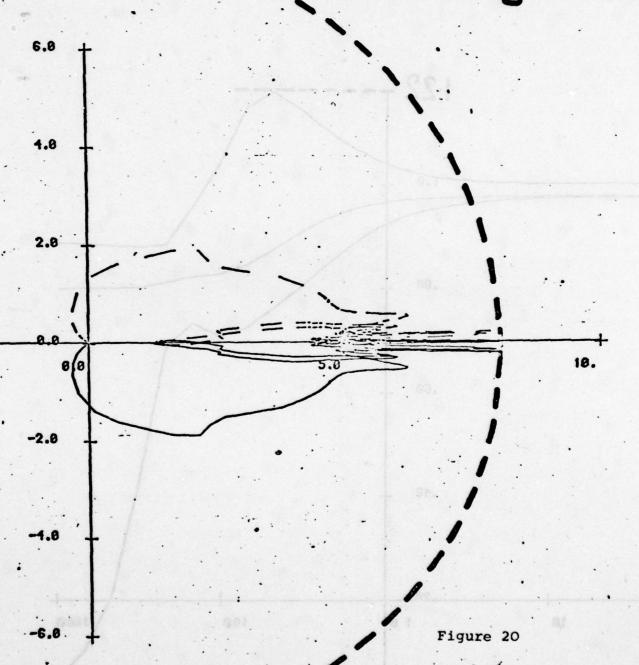
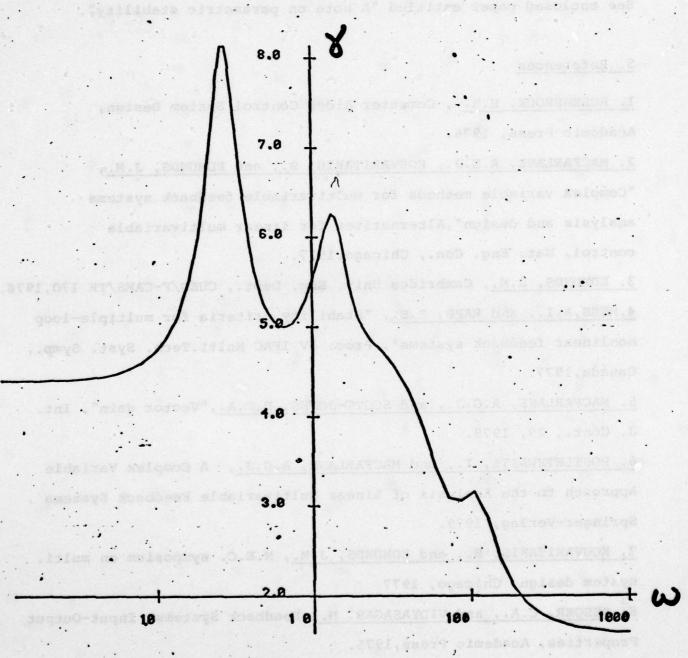


Figure 19

# Eigenvalus-loci of Hijw) modified by Jijw)



# Plot @ 2(10)



of radius 8 which wives as upper bound of 0.12% on the

Figure 21

of radius 8 which gives an upper bound of 0.125 on the magnitude of the  $\epsilon_i$ .

4. Stability under plant parameter uncertainty

See enclosed paper entitled "A note on parametric stability".

## 5. References

- 1. ROSENBROCK, H.H., Computer Aided Control System Design,
  Academic Press, 1976.
- 2. MACFARLANE, A.G.J., KOUVARITAKIS, B., and EDMUNDS, J.M.,
  "Complex variable methods for multivariable feedback systems
  analysis and design", Alternatives for linear multivariable
  control, Nat. Eng. Con., Chicago, 1977.
- 3. EDMUNDS, J.M., Cambridge Univ. Eng. Dept., CUED/F-CAMS/TR 170,1978.

  4.MEES,A.I., and RAPP, P.E., "Stability criteria for multiple-loop nonlinear feedback systems", Proc. IV IFAC Multi.Tech. Syst. Symp., Canada, 1977.
- 5. MACFARLANE, A.G.J., and SCOTT-JONES, D.F.A., "Vector gain", Int. J. Cont., 29, 1979.
- 6. POSTLETHWAITE, I., and MACFARLANE, A.G.J., A Complex Variable Approach to the Analysis of Linear Multivariable Feedback Systems, Springer-Verlag, 1979.
- 7. KOUVARITAKIS, B., and EDMUNDS, J.M., N.E.C. symposium on multi. system design, Chicago, 1977
- 8. DESOER, C.A., and VIDYASAGAR, M., Feedback Systems: Input-Output Properties, Academic Press, 1975.

# A NOTE ON PARAMETRIC STABILITY

I. postlethwaite
University Engineering Department
Control and Management Systems Division
Mill Lane
Cambridge

destrable, for economic reasons, to change a parameter

the relative stability of a system with respect to a given

recliniques for multiveriable feedback systems tol saupinthes

a single parameter, can be determined. To halp to assess

the degree of stability, generalizations of main and phase

by an example in section 4. In the concluding section

A dominant theme in redent research on complex varieble

## ABSTRACT TO THE STATE OF THE ST

This note shows how recent developments in the complex variable analysis of multivariable feedback systems can be used to determine stability with respect to a system parameter.

## 1. Introduction

A feedback system is said to be stable if all of its closed-loop poles are in the left half-plane. The stability of a control system is therefore dependent on its associated parameters. Sometimes in a control system the value of a parameter is uncertain perhaps due to ageing, deterioration, or damage; in other instances it may be desirable, for economic reasons, to change a parameter value. In both these cases a technique which predicts the relative stability of a system with respect to a given parameter would be extremely useful.

A dominant theme in recent research on complex variable techniques for multivariable feedback systems (MacFarlane and Postlethwaite 1977; MacFarlane, Kouvaritakis and Edmunds 1977; Postlethwaite 1978), has been the association of a system with two sets of algebraic functions: characteristic gain functions and characteristic frequency functions. In section 2 characteristic 'parameter' functions are introduced, and used to develop the ideas of 'parametric' root loci and 'parametric' Nyquist loci from which the relative stability of a system, with respect to a single parameter, can be determined. To help in assessing the degree of stability, generalizations of gain and phase margin are given in section 3. The ideas are demonstrated by an example in section 4. In the concluding section tentative proposals and suggestions for future research are made.

## (which for simplicity of exposition will be regarded as 2. Characteristic frequency and characteristic parameter functions

The feedback configuration considered is shown in figure 1, where  $A(k_2,k_3,...k_q)$ ,  $B(k_2,k_3,...,k_q)$ ,  $C(k_2,k_3,...,k_q)$  and  $D(k_2,k_3,...,k_q)$  are state-space matrices which are dependent on (q-1) real, time-invariant parameters and k<sub>1</sub> is a scalar, time-invariant gain parameter common to all the loops.

The branches of s(ki), for k, real, clearly define the variation of the closed-loop poles with respect to kg, and as such are termed parametric root loci. Alternatively, the parametric root loci can be viewed as the O phase contours of k (s) on the Riemann surface domain for k (s). known as the frequency surface for ki.

Dual to the parametric root loci are the parametric

Nyquist loci or characteristic parameter loci which are the

## Figure 1. Feedback configuration for parameter analysis

The closed-loop poles for this configuration are solutions viewed as the ±90° phase contours of s(k,) on the Riemann

surface domain for s(k), which will be called the parameter 
$$\det_{n} - s(k) = 0$$
 and surface for k, (2.1)

where

where

If a particular system has a set of nominal parameter 
$$(k_1, \dots, k_q) = (k_1, \dots, k_q) \cdot (k_1, \dots, k_q)$$

If a parameter surfaces of the parameters are sensitive.

is the closed-loop frequency matrix (Postlethwaite 1978). If numerical values for all the parameters except one, k, say, are substituted into equation (2.1) and k, considered as a complex variable, then the resulting algebraic equation

(which for simplicity of exposition will be regarded as irreducible) defines a pair of algebraic functions (Bliss 1966)  $s(k_j)$  and  $k_j(s)$ . The algebraic function  $s(k_j)$  is called the characteristic frequency function with respect to  $k_j$ , and the algebraic function  $k_j(s)$  is called the characteristic parameter function for  $k_j$ . (Note that the characteristic frequency function s(g) and the characteristic gain function g(s), introduced by MacFarlane and Postlethwaite (1977), are equivalent to  $s(-k_1^{-1})$  and  $-k_1(s)^{-1}$  respectively).

The branches of  $s(k_j)$ , for  $k_j$  real, clearly define the variation of the closed-loop poles with respect to  $k_j$ , and as such are termed <u>parametric root loci</u>. Alternatively, the parametric root loci can be viewed as the  $0^{\circ}$  phase contours of  $k_j$ (s) on the Riemann surface domain for  $k_j$ (s), known as the <u>frequency surface</u> for  $k_j$ .

Dual to the parametric root loci are the parametric Nyquist loci or characteristic parameter loci which are the branches of  $k_j$  (s) as s traverses the imaginary axis. Alternatively, the characteristic parameter loci can be viewed as the  $\pm 90^{\circ}$  phase contours of  $s(k_j)$  on the Riemann surface domain for  $s(k_j)$ , which will be called the parameter surface for  $k_j$ .

If a particular system has a set of nominal parameter values then it is possible from the set of parameter surfaces to determine which, if any, of the parameters are sensitive with respect to stability. To help in such an assessment the following generalizations of gain and phase margin are introduced.

## 3. Gain and phase margins

The  $\pm 90^{\circ}$  phase contours of  $s(k_{j})$  on the parameter surface for  $k_{j}$  trace out the boundary between stable and unstable closed-loop poles and therefore we can define parameter gain and phase margins for  $k_{j}$  about a stable operating point  $k_{j}$  which give a measure of the relative stability of the system with respect to  $k_{j}$ .

Parameter gain margin. Parameter gain margin is defined with respect to a stable operating point  $k_j$  as the smallest change in parameter gain about  $k_j$  needed to drive the system into instability. Let  $d_i$  be the shortest distance along the real axis from a stable operating point  $k_j$  to the stability boundary (characteristic parameter loci) on the ith sheet of the parameter surface for  $k_j$ . Then the parameter gain margin is defined as  $\min_{i} \{d_i: i=1,2,\ldots,n\}$ 

Parameter phase margin. On each of the n sheets of the parameter surface for  $k_j$  imagine that an arc is drawn, centre the origin, from a stable operating point  $k_j$  until it reaches the stability boundary (characteristic parameter loci). Let  $\phi_i$  be the angle subtended at the origin by the corresponding arc on the ith sheet. Then the parameter phase margin is defined as  $\min\{\phi_i\colon i=1,2,\ldots,n\}$ .

## 4. Example

In this section an inverted pendulum positioning system (see figure 2) is considered and its stability analysed with respect to one of its parameters, namely the mass of the carriage

## Figure 2. Inverted pendulum positioning system

for M. Lince out the boundary between stools and unstable

and phase margins for k -about a stable operating point k

which cive a measure of the relative stability of the system

respect to a stable operating moint k. as the smallest change

rual axis from a stable operating point | Kg to the stability

instability. Let d. be the shortest distance along the

This system has also been used by Kwakernaak and Sivan (1972), Cannon (1967), and Elgerd (1967). The system can be modelled by the following linearized state differential equation (Kwakernaak and Sivan 1972).

$$\dot{\mathbf{x}}(t) = \begin{bmatrix} 0 & 1 & 0 & 0 \\ 0 & \frac{F}{M} & 0 & 0 \\ 0 & 0 & 0 & 1 \\ -\frac{g}{L}, & 0 & \frac{g}{L}, & 0 \end{bmatrix} \mathbf{x}(t) + \begin{bmatrix} 0 \\ \frac{1}{M} \\ 0 \\ 0 \end{bmatrix} \mathbf{u}(t) \tag{4.1}$$

where u(t) is a force exerted on the carriage by a small motor;

M is the mass of the carriage; F is the friction coefficient

associated with the movement of the carriage; and L' is given

by

$$U = \frac{J + mL^2}{mL} = \text{algebra condy (area) independed} \qquad (4.2)$$

where m is the mass of the pendulum; L is the distance from the pivot to the centre of gravity of the pendulum; and J is the moment of inertia of the pendulum with respect to the centre of gravity.

The system is stabilizable using state feedback of the form

solely by left half-plane closed-loop poles whereas sheets

$$1001 \text{ rest } \mathbf{u}(t) = -Kx(t) \text{ satisfies and } \mathbf{u}(t) \text{ satisfies a finite of } \mathbf{u}(t)$$

and using the numerical values

from 
$$\frac{F}{M}$$
 = 1 s<sup>-1</sup> and on the new and of success  $\frac{1}{M}$  = 1 kg<sup>-1</sup> and obtained an inverse of the second (4.4)

1.1 of 
$$0$$
  $\frac{q}{L}$  = 11.65  $s^{-2}$  aldedal a and markly good-baselo

L' = 0.842m

it can be found (Kwakernaak and Sivan 1972) that

Postletiwatte 1977); from thacks I and I we find that the

$$K = [86.81, 12.21, -118.4, -33.44]$$
 (4.5)

stabilizes the linearized system placing the closed-loop poles at -4.706±j 1.382 and -1.902±j3.420 .

We will now look at the parameter surface for M to see how variations in the carriage mass, about an operating point of lkg, affect the stability of the system. The four sheets of the mass surface, characterized by constant phase and magnitude contours of s(M), are shown in figures 3-6, from which the following stability margins are obtained:

parameter (mass) gain margin = 1 kg
parameter (mass) phase margin = 60°

The gain margin of lkg corresponds to reducing the carriage mass to zero before instability occurs and the phase margin of 60° indicates adequate damping of the closed-loop system.

Sheets 3 and 4 of the mass surface are characterized solely by left half-plane closed-loop poles whereas sheets 1 and 2 have both stable and unstable closed-loop poles separated by the characteristic parameter loci. The crossings of the real mass axes by the characteristic parameter loci determine bounds on the mass for closed-loop stability analogous to the way in which the characteristic gain loci can be used to determine bounds on  $k_1$  (MacFarlane and Postlethwaite 1977); from sheets 1 and 2 we find that the closed-loop system has a 'stable mass interval' of 0 to 2.125 kg.

## 5. Conclusion

As indicated in this note recent developments in the complex variable analysis of multivariable feedback systems are not only applicable to gain and frequency but any system parameter and frequency. In particular it has been shown how stability with respect to a given parameter can be examined using characteristic parameter loci (generalized Nyquist loci) and characteristic frequency loci (generalized Evans' root loci) viewed on their appropriate Riemann surfaces. To obtain stability results in terms of more than one parameter variation seems to be a much more complicated problem but one with great practical significance. It is felt that such results might

complex variables.

It is also thought that the parameter surfaces may prove to be useful in the design of parameter-dependent controllers for systems in which a particular parameter suffers large variations during normal operation. For example, the controller of an aircraft engine needs to operate satisfactorily over a wide range of altitudes. A possible design scheme could be

- (i) to design real constant controllers at a number of altitudes,
- (ii) to obtain an altitude dependent controller by "matrix interpolation", and finally
- (iii) to analyse the stability of the system over the whole working range using an "altitude surface".

## ACKNOWLEDGMENT

This work was supported by the S.R.C. and Trinity Hall, Cambridge.

## References

BLISS, G.A., 1966 (reprint of 1933 original), Algebraic Functions (New York: Dover).

.usidsiyav xsiqmoo

Hall, Cambridge.

CANNON, R.H., Jr, 1967, Dynamics of Physical Systems (New York:

McGraw-Hill).

ELGERD, O.I., 1967, Control Systems Theory (New York: McGraw-Hill).

KWAKERNAAK, H., and SIVAN, R., 1972, Linear Opti al Control Systems

(New York: Wiley).

MACFARLANE, A.G.J., KOUVARITAKIS, B., and EDMUNDS, J.M., 1977,

International Forum on Alternatives for Multivariable

Control, Chicago.

MACFARLANE, A.G.J., and POSTLETHWAITE, I., 1977, Int. Journal Control, 26,265.

POSTLETHWAITE, I., 1978, Ph.D. Thesis, University of Cambridge.

(111) to sualyse the stability of the system over the whole

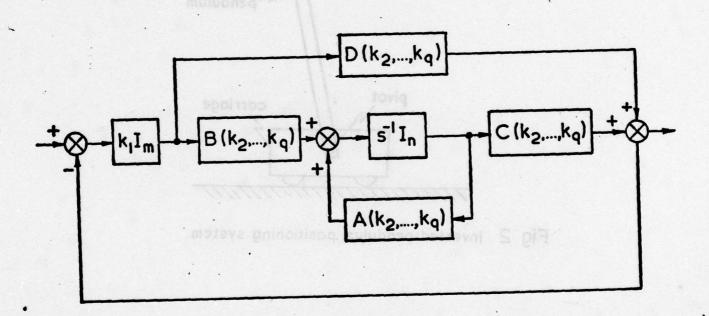


Fig. 1 Feedback configuration for parameter analysis

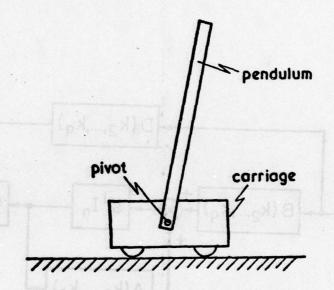


Fig. 1 Feedback configuration for parameter analysis

Fig 2 Inverted pendulum positioning system

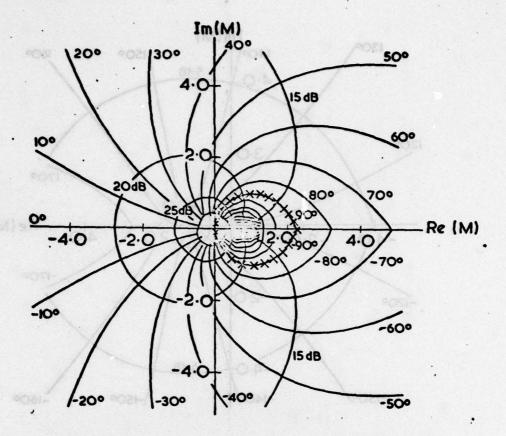


Fig. 3 Sheet 1 of parameter (mass) surface

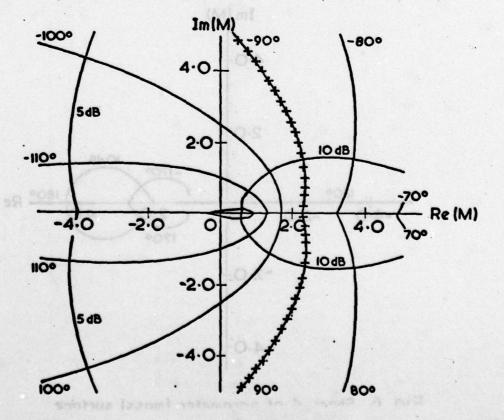


Fig. 4 Sheet 2 of parameter (mass) surface

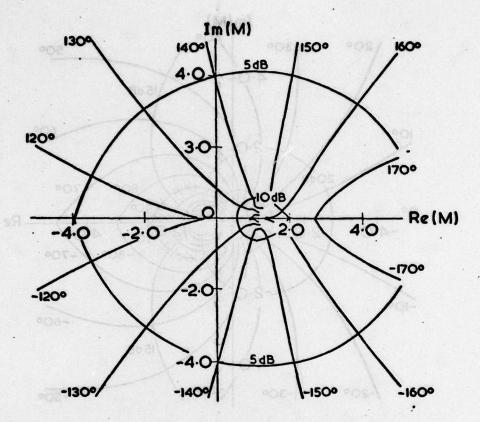
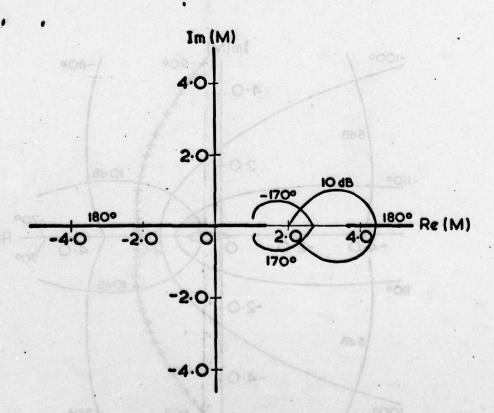


Fig. 5 Sheet 3 of parameter (mass) surface



Fin A Short A of norameter Imass) surface

#### A ROBUST CONTROL SYSTEM DESIGN\*

Juergen E. Ackermann
Coordinated Science Laboratory
University of Illinois, Urbana, Illinois 61801, USA

#### Abstract

A representation of controllable linear systems is introduced, which permits assigning poles or characteristic parameters to a state feedback system by a matrix multiplication. This is used as a link between state space and classical parameter plane methods. The system representation maps a point in a n/p dimensional parameter space  $\mathcal V$  of characteristic parameters into the nxp dimensional parameter space  $\mathcal V$  of state feedback gains, where p is the number of actuators. For p=1 the coordinates of the  $\mathcal V$  space are the coefficients of the closed loop characteristic rolynomial, for p>1 they are coefficients in a characteristic polynomial matrix and its determinant is the characteristic polynomial. By this computationally simple mapping procedure it becomes feasible to map not only a fixed set of eigenvalues but also regions in the s or 2 plane, in which the eigenvalues shall be located. This relaxation of the dynamic specifications permits satisfying other typical design specifications like robustness with respect to sensor and actuator failures, large parameter variations, finite wordlength implementation, and actuator constraints. All tradeoffs between such requirements can be made in the  $\mathcal V$  space. Three examples illustrate the variety of problems which can be tackled with this new tool.

#### 1. INTRODUCTION

Control system specifications are usually not given in terms of a quadratic cost function or a set of eigenvalues. These are mainly used as free parameters in trial and error design procedures aimed at good tradeoffs between the dynamics of the system and other design aspects, for example actuator limitations and robustness with respect to sensor or actuator failures or other large parameter variations. Three questions in this context:

- Quadruplex techniques (for example in aircraft control systems) are an expensive solution to the reliability problem. Is it not sufficient to guarantee that all unstable and insufficiently damped modes remain observable and controllable under all considered combinations of sensor and actuator failures?
- 2. Which system changes are so essential that they require adaptation of the control system by identification, failure detection etc.? Which range of such changes can be covered satisfactorily by fixed gain feedback or a few sets of gains and a simple switching criterion.
- 3. Is a given set of mixed specifications, e.g. on bandwidth and damping, actuator constraints, robustness requirements, etc., compatible within an assumed control system structure, or which of the specifications are conflicting, how far do we have to relax them?

This paper does not give a complete answer to these questions, however a method is proposed and some tools are provided to attack such questions under the following assumptions:

1. Only linear plants

 $\dot{\mathbf{x}} = \mathbf{A} \underline{\mathbf{x}} + \mathbf{B} \underline{\mathbf{u}} \quad \underline{\mathbf{x}} = [\mathbf{x}_1 \dots \mathbf{x}_n]', \ \underline{\mathbf{u}} = [\mathbf{u}_1 \dots \mathbf{u}_p]'$  (1) or  $\underline{\mathbf{x}}(\mathbf{k}+1) = \underline{\mathbf{A}} \underline{\mathbf{x}}(\mathbf{k}) + \underline{\mathbf{B}} \underline{\mathbf{u}}(\mathbf{k})$  are considered. It is assumed that eq. (1) is written in "sensor coordinates," i.e. all measured variables are state variables  $\mathbf{x}_1$ . Several pairs  $(\mathbf{A}_1, \mathbf{B}_1)$ ,  $(\mathbf{A}_2, \mathbf{B}_2)$ , etc. may be given, e.g. for different operating points of an underlying nonlinear system. It is assumed that all pairs  $(\mathbf{A}_1, \mathbf{B}_1)$  are controllable and have the same controllability indices.

The price of an actuator is assumed to increase with

$$\overline{u}_i = \max |u_i(t)|$$
 and/or (2)

$$u_i' = \max |\dot{u}_i(t)| \tag{3}$$

where the worst initial state within given limitations is considered.  $\overline{u}_i$  and/or  $u_i'$  should be kept "small."

3. A state feedback structure

$$\underline{\mathbf{u}} = -\underline{\mathbf{K}}'\underline{\mathbf{x}} \tag{4}$$

is assumed. The details and examples are worked out for single input plants with

$$u = -\underline{k}'\underline{x} = -[k_1 \ k_2 \ \dots \ k_n]\underline{x}.$$
 (5)

For multi-input plants the basic result is stated in the Appendix. The nxp elements of K are the free parameters of the proposed method. They are coordinates of a parameter space

called "state feedback gain space" or "%-space."

4. It is assumed that sensor and actuator failures occur in the form that the output of a failed element is not correlated to its input. Then the output is an external disturbance. Rejection of external disturbances is not considered in this paper. For the closed loop system

$$\dot{\mathbf{x}} = (\underline{\mathbf{A}} - \underline{\mathbf{B}} \, \underline{\mathbf{K}}') \underline{\mathbf{x}} \tag{6}$$

in sensor coordinates a failure of the ith sensor (actuator) is equivalent to a structural change by which the ith column (row) of K' becomes zero. Also in the case that a state variable is not measured, the corresponding column of K' is zero. It is part of the design to decide, which state variables are measured and for which of them redundancy must be provided for high system reliability. It is a goal to avoid failure detection and multiplexed components whenever possible.

5. It is assumed that the nominal dynamic behavior of the control system can be specified by a region in the eigenvalue plane - e.g. for a continuous time system in the s plane the region to the left of the boundary marked with ρ=1 in Fig. 1 - where all eigenvalues must be located for the nominal structure and parameter values. For failure situations a relaxed "emergency specification," e.g. the boundary ρ=0.5 or the

This research was supported by the Deutsche Forschungs-und Versuchsanstalt für Luft-und Raumfahrt and by the U. S. Air Force under Grant AFOSR 78-3633.

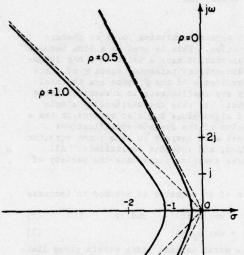


Fig. 1. A family of hyperbolic boundaries in s plane.

stability limit p=0 in Fig. 1 may be given. A specification is robust under a failure if no eigenvalue crosses the corresponding boundary due to the failure.

The proposed method is: Design in X-space. region  $X_1$  in the X-space is determined, such that all eigenvalues meet the specifications iff  $\underline{K}' \in \mathcal{K}_1$ . This may be the intersection of several such regions for different parameter values. Subsets of K1 with certain robustness properties can be found and tradeoffs with actuator constraints, bandwidth requirements, etc. can be made in the Xspace. The method also shows, whether a solution exists under the given assumptions and if not, which alternatives exist for relaxation of specifications such that a solution will exist.

Parameter space methods have a long tradition, mainly in Russia and Yugoslavia. Siljak [1] gives a historical review of the work by Vishnegradsky, Neimark, Mitrovic, and others. Siljak generalized these parameter mapping methods significantly. A typical procedure for a continuous time system is to assume a controller structure with two free parameters o and 3. Determine the closed-loop characteristic polynomial

 $P(s) = \sum_{i=0}^{n} P_{i}(\alpha, \beta) s^{i} = 0.$ (7)

Substitute s = \sigma+jw and separate eq. (7) into its real and imaginary parts: Re(σ,ω,α,β)=0,  $\operatorname{Im}(\sigma,\omega,\alpha,\beta)=0$ . Assume these nonlinear equations have a solution

$$\alpha = \alpha(\sigma, \omega), \quad \beta = \beta(\sigma, \omega).$$
 (8)

Equation (8) allows to map o,w pairs on the boundary into the o-B-plane. The image boundaries divide the a-8-plane into regions characterized by the number of eigenvalues inside and outside the s-plane region.

In the present paper the control system structure is restricted to state feedback. This permits simplifying the determination of eq. (8) by pole placement methods. Consider for example a second order single-input system with k1-0, k2-8 in eq. (5). In classical parameter plane methods  $P(s) = \det(s\underline{I} - \underline{A} + \underline{b} \underline{k}') = p(\alpha, \beta) + p_1(\alpha, \beta) s + s^2 = 0$  is determined and with  $s = \sigma + \underline{j} \omega$  solved for  $\alpha$  and  $\beta$ . In the method proposed in this paper the pi are expressed in

terms of o and w by  $P(s) = (s-\sigma+jw)(s-\sigma-jw) = s^2-2\sigma s+\sigma^2+w^2$  $= p_0(\sigma, \omega) + p_1(\sigma)s + s^2 = 0.$ 

Then by pole placement

$$k_1 = \alpha(p_0, p_1) = \alpha(\sigma, \omega)$$
  
 $k_2 = \beta(p_0, p_1) = \beta(\sigma, \omega).$  (10)

Thus the mapping equation (8) is obtained in a different way. More generally for an nth order single input system in both approaches an n dimensional parameter space @ with coordinates p, is introduced as an intermediate step between the set of eigenvalues  $\Lambda = \{\lambda_1 \dots \lambda_n\}$  and the X-space. The relation between A and X can be expressed in both directions:

- a) From  $\chi$  to  $\theta$  by the characteristic equation P(A)=det (A I-A+bk'), from @ to A by numerical factorization of  $P(\lambda)$ .
- From A to & by multiplication of elementary factors  $P(\lambda) = (\lambda - \lambda_1)(\lambda - \lambda_2) \cdots (\lambda - \lambda_n)$ , from  $\theta$  to \* by pole placement.

In the next section pole placement is formulated in a form which makes direction b) far more attractive than direction a). In Section 3 the use of such boundaries for the design of robust control systems in X-space is discussed. Section 4 shows the application to three examples.

#### BOUNDARY MAPPING

Pole-placement for single-input systems. The pole placement theorem is used in the form originally published in German in [2], available in English in [3]: Given an nth order monic polynomial P(A), an nxn matrix  $\underline{A}$  and an nxl vector  $\underline{b}$  such that det  $\underline{R} \neq 0$ ,  $\underline{R} = [\underline{b}, \underline{A}\underline{b} \dots \underline{A}^{n-1}\underline{b}]$ , the equation  $P(\lambda) = \det(\underline{\lambda} \underline{I} - \underline{A} + \underline{b} \underline{k}')$  has a unique solution and this solution is

$$\underline{\mathbf{k}}' = \underline{\mathbf{e}}' P(\underline{\mathbf{A}}) \tag{11}$$

where e' is the last row of  $R^{-1}$ .

With 
$$P(\lambda) = (\lambda - \lambda_1)(\lambda - \lambda_2) \dots (\lambda - \lambda_n)$$
 (12)  

$$= P_0 + P_1 \lambda + \dots + P_{n-1} \lambda^{n-1} + \lambda^n$$
 (13)

$$= p + p + \lambda + \cdots + p + \lambda^{n-1} + \lambda^n$$
 (13)

eq. (11) may be written as

$$\underline{\mathbf{k}}' = \underline{\mathbf{e}}' (\underline{\mathbf{A}} - \lambda_1 \underline{\mathbf{I}}) (\underline{\mathbf{A}} - \lambda_2 \underline{\mathbf{I}}) \dots (\underline{\mathbf{A}} - \lambda_n \underline{\mathbf{I}}) 
= \underline{\mathbf{e}}' (\mathbf{p}_0 \underline{\mathbf{I}} + \mathbf{p}_1 \underline{\mathbf{A}} + \dots + \mathbf{p}_{n-1} \underline{\mathbf{A}}^{n-1} + \underline{\mathbf{A}}^n).$$
(14)

$$= \underline{e}' (p_0 \underline{I} + p_1 \underline{A} + \dots + p_{n-1} \underline{A}^{n-1} + \underline{A}^n).$$
 (15)

For mapping from & space to X space it is more convenient to rewrite eq. (15) as

$$\underline{\mathbf{k}'} = \underline{\mathbf{p}'}\underline{\mathbf{E}}$$

$$\underline{\mathbf{p}'} = [\mathbf{p}_0 \ \mathbf{p}_1 \dots \mathbf{p}_{n-1} \ 1], \quad \underline{\mathbf{g}} = \begin{bmatrix} \underline{\mathbf{e}'}, \underline{\mathbf{A}} \\ \underline{\mathbf{e}'}, \underline{\mathbf{A}} \end{bmatrix}$$

$$(16)$$

E is an (n+1)xn matrix. If the inverse of eq. (16) is needed, it is convenient to express the last row of E by the Cayley-Hamilton theorem in terms of the previous rows. This however requires the evaluation of the characteristic polynomial  $\det (\lambda I - A) = a_0 + a_1 \lambda + \cdots + a_{n-1} \lambda^{n-1} + \lambda^n$ . The invertible form of eq. (16) is

$$\underline{\mathbf{k}'} = [\mathbf{p}_0 - \mathbf{a}_0 \quad \mathbf{p}_1 - \mathbf{a}_1 \quad \dots \quad \mathbf{p}_{n-1} - \mathbf{a}_{n-1}] \underline{\mathbf{w}}^{-1}, \quad \underline{\mathbf{w}}^{-1} = \begin{bmatrix} \underline{\mathbf{e}}' \\ \underline{\mathbf{e}}' \underline{\mathbf{A}} \\ \underline{\mathbf{e}}' \underline{\mathbf{A}}^{n-1} \end{bmatrix}$$

The columns of W can be evaluated recursively by Leverrier's algorithm, which also gives the ai [2].

The form (16) is most convenient for trial and error design procedures, graphical displays of cross-sections of the % space, etc. The plant description in the form of the matrix E is evaluated only once for a given pair  $(\underline{A},\underline{b})$ . The mapping of a trial design point in  $\partial$  space then requires  $n^2$  multiplications and  $n^2$  additions. This compares favorably with mapping a trial design point from the parameter space of quadratic criteria via the Riccati equation into % space. The generalization of eq. (16) to multiinput systems is given in the Appendix.

Sensitivities. The influence of a coefficient  $p_1$  of the characteristic polynomial on  $\underline{k}'$ , given the other  $p_j$ , follows from eq. (16) as  $\frac{dk'}{dn} = e' \underline{A}^{\underline{i}}.$ 

(18)dpi

The influence of an eigenvalue  $\lambda_i$  on k', given the other 1, follows from eq. (14) as  $\frac{d\underline{\mathbf{k}'}}{d\lambda_{-}} = -\underline{\mathbf{e}'}(\underline{\mathbf{A}} - \lambda_{1}\underline{\mathbf{I}}) \dots (\underline{\mathbf{A}} - \lambda_{1}-1\underline{\mathbf{I}})(\underline{\mathbf{A}} - \lambda_{1}+1\underline{\mathbf{I}}) \dots (\underline{\mathbf{A}} - \lambda_{n}\underline{\mathbf{I}})(19)$ 

For complex conjugate eigenvalues quadratic factors in P(s) are more convenient. Let P( $\lambda$ ) =  $(a+b)+h^2$ )Q( $\lambda$ ), then

$$\underline{\mathbf{k}}' = \underline{\mathbf{e}}' (\underline{\mathbf{a}}\underline{\mathbf{I}} + \underline{\mathbf{b}}\underline{\mathbf{A}} + \underline{\mathbf{A}}^2) \cdot Q(\underline{\mathbf{A}})$$
 (20)

$$\frac{d\mathbf{k'}}{d\mathbf{a}} = \underline{\mathbf{e}}' Q(\underline{\mathbf{A}}), \qquad \frac{d\underline{\mathbf{k'}}}{d\mathbf{b}} = \underline{\mathbf{e}}' \underline{\mathbf{A}} Q(\underline{\mathbf{A}}). \tag{21}$$

Regions in  $\lambda$  plane. Boundaries, symmetric with respect to the real axis, in the  $\lambda$  plane will be specified, which describe the desired eigenvalue locations. Two cases will be discussed: A real root crossing a boundary or a complex conjugate pair crossing a boundary. The third possible case of roots leaving the region through infinity can be avoided by closing the contour by an arc of a circle with large radius. Typically the region is a connected set and the boundary has two intersections with the real axis. In this case there are two real root boundaries and one complex root boundary in X space. However other boundaries are possible, e.g. separate boundaries for slow and fast modes, etc. For each intersection of a boundary in the  $\lambda$  plane with the real axis at  $\lambda = 0$ , a real root boundary in X space is obtained from  $P(A) = (A - \sigma)R(A), R(A) = r_0 + r_1 \lambda + \dots + r_{n-2} \lambda^{n-2} + \lambda^{n-1}$ By eqs. (16) and (22)

 $k_i = k_i (p_0 \dots p_{n-1}) = k_i (\sigma, r_0 \dots r_{n-2})$  i=1,2...n (23) where the ki depend linearly on o. Thus o can be eliminated by one of the ki's to give the linear boundary  $k_{j} = k_{j}(k_{1}, r_{0} \dots r_{n-1})$   $j=1,2,\dots,n, j\neq 1.$ 

This is a straight line in the k<sub>1</sub>-k<sub>1</sub> plane. Another part of the boundary is obtained if a complex pair of eigenvalues crosses the boundary at \ = o+jw. Then

 $P(\lambda) = (\lambda^2 - 2\sigma\lambda + \sigma^2 + \omega^2)Q(\lambda)$  $Q(\lambda) = q_0 + q_1 \lambda + \dots + q_{n-3} \lambda^{n-3} + \lambda^{n-2}$ (25)

and the type of boundary in X space depends on the form of the boundary  $w = w(\sigma)$  in the  $\lambda$  plane. For  $\sigma$  = const., i.e. a parallel to the imaginary axis, the  $k_1$  are linear in  $w^2$ . Thus for given  $q_1$  the image in the X space is a straight line.

Most commonly used boundaries are conic sections symmetric to the real axis, i.e.

$$w^2 = c_1 + c_1 \sigma + c_2 \sigma^2.$$
 (26)  
Special cases are

c, < 0 ellipse, of particular interest are circles c\_=-1, e.g. constant natural frequency curves in s plane, stability limit and other boundaries in z plane.

c2=0 parabola, or if also c1=0, c2>0 straight line parallel to the real axis.

 $c_2 > 0$  hyperbola, in particular 2 straight lines for  $\omega^2 = c_2 (\sigma - \sigma_o)^2$ ,  $c_2 > 0$ , e.g. constant damping lines in s-plane.

Figure 1 shows the family of hyperbolas
$$\omega^2 = -\rho^2 + \sigma^2/\rho^2. \tag{27}$$

For  $\rho\!-\!0$  this goes to the imaginary axis, for  $\rho\!=\!1$  the asymptotes are the  $1/\!\sqrt{2}$  damping lines. For a different scaling o may be replaced by o/d. Substituting eq. (26) into (25)

$$P(\lambda) = [\lambda^2 - 2\sigma\lambda + (1+c_2)\sigma^2 + c_1\sigma + c_0]Q(\lambda).$$
 (28)

This shows that the  $p_1$  and  $k_1$  depend linearly on  $\sigma$  for  $c_2$ =-1, i.e. for circular boundaries. Thus also in this case the boundaries in X space are straight lines if the eigenvalues in  $Q(\lambda)$  are fixed and a complex pair of poles moves along the circle. For c2 = -1 the functions

 $p_{i} = p_{i}(\sigma, q_{0} \cdots q_{n-3})$ (29)

are quadratic in o and by eq. (16) the same is true for

 $k_1 = k_1(\sigma, q_0 \dots q_{n-3}).$ (30)

One of these equations can be solved for  $\sigma^{\bullet\sigma}(k_i)$ , where only real roots o=y+6 are of interest. only the left half  $\lambda$  plane branch of the conic section is needed, then o=y-6 is selected and substituted into the other k; equations to give

 $k_j = k_j (k_1, q_0 \dots q_{n-3}), \quad i \neq j.$ Note that this is not the curve in the  $k_i$ - $k_j$ -cross-section of the  $\chi$  space, which would be obtained for  $k_n$ =const.,  $m^2i$ , j; eq. (31) gives the curve  $k_1(k_1)$  for constant  $q_0 \dots q_{n-3}$ . For the numerical determination of boundaries in crosssections of the X space the implicit form (30) is more useful. It gives o-values as a parameter along the boundary. Constant damping spirals in the z plane are not conic sections. Usually they are supplemented by a condition |z| < a, a < 1. The resulting regions can be reasonably well approximated by a family of nonintersecting circles

$$(v-v_0)^2 + w^2 = r^2$$
,  $z = v + jw$   
 $v_0(v_0-1) = 0.99r(r-1)$  ,  $v_0 < 0.5$ . (32)

It is shown in Fig. 2. For ral it is the unit circle, with decreasing r the center v of the circles moves to the right until it reaches 0.45 for r=0.5, it then goes back to zero, where v =r=0 is the deadbeat solution.

Regions in  $\chi$  space. Equations (22) and (25) show that the mapped boundaries in  $\chi$  space represent the conditions under which the number of eigenvalues inside and outside a  $\lambda$ -region can change. These Xboundaries partition the  $\tilde{X}$  space into regions; each of them corresponds to a fixed number of eigenvalues inside the  $\lambda$  region, and it must be decided, for which & region all eigenvalues are inside the \ region. For closed contours in the λ-plane the χ region is bounded, since by eq. (16) no ki can go to infinity. If there are several bounded regions, a simple test is to check the eigenvalues for an arbitrary K' in the considered \* region. An alternative are Siljak's "shading rules" for the

Consider a second order system and a circular  $\lambda$ region. Boundaries in the k1-k2-plane are three

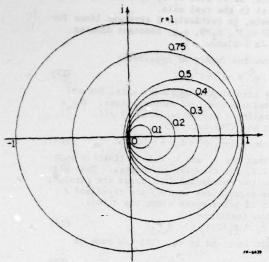


Fig. 2. A family of circular boundaries in z plane. straight lines obtained for the two real root cases  $\lambda=_1$  and  $\lambda=_2$  and one complex root case. They partition the  $\chi$  plane into seven regions with the properties: no pole outside the circle, one left, two left, one right, two right, one left and one right, complex outside. The only bounded region is the triangle, thus for  $k_1,k_2$  in the triangle,  $\lambda_1$  and  $\lambda_2$ are inside the circle. At the vertices of the transle both poles cross boundaries simultaneously. At the vertices of the tri-This is the case for 1) a double pole at  $\sigma_1$ , 2) a double pole at  $\sigma_2$ , and 3) one pole at  $\sigma_1$  and one at og. Thus the total mapping procedure consists of just three pole placements, i.e. twelve multiplications and twelve additions. This makes it easy to map the family of circles of Fig. 2. If the circle is deformed to a different closed contour with the same real axis intersections at  $\sigma_1$  and  $\sigma_2$ , then the three vertices and two edges of the triangle remain unchanged, the third edge, i.e. the complex root boundary, is replaced by a curve. For a third order system and a circular \u03b4-region the two real root boundaries are planes. The complex root boundary for a fixed real pole in a straight line. By moving the real pole the straight line moves and forms the third surface. The 4 vertices of the region are again obtained by pole placement of the four characteristic polynomials with zeros in the set  $\{\sigma_1, \sigma_2\}$ . For the corresponding region in  $\theta$ space, Fam and Meditch [4] have shown that the convex hull of the region is the tetrahedron with the above mentioned vertices. By the linearity of the mapping equation k'=p' this property does hold in the  $\chi$  space also. Similarly for arbitrary n from [4] follows: The convex hull of the  $\chi$  region, for which all eigenvalues are located inside a circle with center on the real axis and intersecting the real axis at  $\sigma_1, \sigma_2$ , is a polyhedron with n+1 vertices. They can be obtained by pole placement for the n+1 characteristic polynomials with zeros in the set  $\{\sigma_1, \sigma_2\}$ . The two real root hyperplanes are two of the surfaces of the polyhedron.

#### 3. DESIGN IN X SPACE

Robustness with respect to sensor failures. A specification is "Fi-robust" if it remains satisfied after a failure of sensor i, it is "Fi-robust" if the same holds after failures of both sensors i and j. Fig. 3 shows an example of

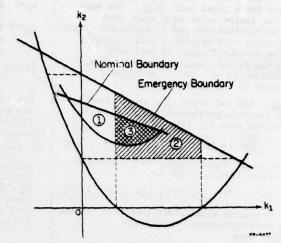


Fig. 3. Illustration of failure robustness and emergency boundaries.

boundaries in the  $k_1$ - $k_2$ -subspace. It is assumed, that all other feedback gains are fixed. The projection of point 1 on the  $k_1$  axis is outside the energency region, i.e. the emergency specification is not  $F_2$ -robust, it is however  $F_1$  robust. Points 2 and 3 are  $F_1$  and  $F_2$  robust. No point is  $F_{12}$  robust since the origin  $k_1^{-}k_2^{-}0$  lies outside the emergency region. Point 3 also meets the nominal specification and is a good candidate for a robust control system. Since the nominal boundary intersects the  $k_2$  axis, an alternative to the robust solution 3 is to eliminate the  $k_1$  sensor and to multiplex the  $k_2$  sensor. This would maintain the nominal specifications under a failure of one of the  $k_2$  sensors. However it requires failure detection with at least three  $k_2$  sensors and very likely is the more expensive solution.

Robustness with respect to actuator failures. Assume  $k_1$  and  $k_2$  in Fig. 3 are elements of different rows of the feedback matrix  $\underline{K}'$  in eq. (A.8). Then the same arguments as above apply for the robustness of specifications with respect to actuator failures.

Robustness with respect to large parameter variations. Assume that for different operating conditions different pairs  $(A_1,B_1)$ ,  $(A_2,B_2)$  etc. are given. One boundary in the eigenvalue plane now maps into different boundaries in  $\mathcal K$  space, and it must be tested, whether there exists an intersection of the admissible regions. If it does not exist, then at least a gain scheduling system can be designed, in which each gain covers as many operating conditions as possible. Robustness with respect to finite wordlength. The

Robustness with respect to finite wordlength. The feedback control law may be implemented approximately in a short wordlength microprocessor as

 $\underline{u+h}\underline{u} = (\underline{K}'+h\underline{K}')(\underline{x}+h\underline{x}) \approx \underline{K}'\underline{x}+h\underline{K}'\underline{x}+\underline{K}'\Delta\underline{x}. \tag{33}$  For small  $\underline{x}$  the dominant term in  $\Delta\underline{u}$  is  $\underline{K}'\Delta\underline{x}$ , i.e. the gains should be not too high. For large  $\underline{x}$  the dominant term is  $\Delta\underline{K}'\underline{x}$ . The maximally  $\Delta\underline{K}'$  robust solution is the center of the largest hypercube with edges parallel to the axes in the admissible K-region. Fig. 4 illustrates  $\Delta\underline{K}'$  robustness. Actuator constraints. Constraints on  $\overline{u}$ -max $[\underline{u}(t)]$  and  $\underline{u}$ -max $[\underline{u}(t)]$  can be treated in K space. For the regulator problem

 $|u(t)| = |\underline{k}'\underline{x}(t)| \le |\underline{k}| \cdot |\underline{x}(t)|$  (34) with equality for the worst case of  $\underline{x}(t)$  (e.g.,  $\underline{x}$ =ck for some c $\neq$ 0). Assuming that all state variables have been normalized to their maximum value,

the norm || k = Vk k (35) i.e., the distance from the origin in X space can be used as a measure for u-max u(t) . Similarly  $|\dot{u}(t)| = |\underline{k}'\dot{\underline{x}}(t)| = |\underline{k}'(\underline{A}-\underline{b}\,\underline{k}')\underline{x}(t)|$ and | k' (A-b k') | can be used as a measure.

#### EXAMPLES

The following three examples of second, third, and fourth order show various typical design aspects and solutions in X space using the tools introduced in this paper. All calculations were done on a programmable pocket calculator. Second order discrete system.

$$\underline{\mathbf{x}}(\mathbf{k}+1) = \underline{\mathbf{A}}\underline{\mathbf{x}}(\mathbf{k}) + \underline{\mathbf{b}}\mathbf{u}(\mathbf{k}), \quad \underline{\mathbf{A}} = \begin{bmatrix} 0 & -4 \\ 1 & 4 \end{bmatrix}, \quad \underline{\mathbf{b}} = \begin{bmatrix} 6/16 \\ -5/16 \end{bmatrix}$$
 (36)  
Find  $\mathbf{u} = -[\mathbf{k}_1 \ \mathbf{k}_2]\underline{\mathbf{x}}$  such that

i) stability is F1-robust and, if possible, also

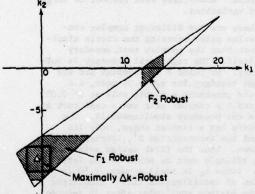
F2-robust,
ii) the system remains stable for u=-[k\_±\text{\Lambda},k\_2±\text{\Lambda}k]\_X with the maximum Ak.

$$\underline{k'} = \underline{p'}\underline{g} = [p_0 \ p_1 \ 1] \begin{bmatrix} 5 & 6 \\ 6 & 4 \\ 4 & -8 \end{bmatrix}$$
 (37)

The vertices of the stability triangle in the  $k_1$ - $k_2$ -plane are determined by 3 pole placements

1. 
$$P(z) = (z+1)^2 = z^2 + 2z + 1$$
,  $k' = [21 6]$   
2.  $P(z) = (z+1)(z-1) = z^2 - 1$ ,  $k' = [-1 -14]$   
3.  $P(z) = (z-1)^2 = z^2 - 2z + 1$ ,  $k' = [-3 -10]$ . (38)

In Fig. 4 it is seen that the requirements for F1 and F2 robustness are not compatible, the F1 robust region is chosen. ii) requires to place the largest square with sides parallel to the axes into the  $F_1$  robust region. It has the center  $\underline{k}'=[-0.454545 -10.727272]$  and permits  $\Delta k=1.454545$ . This k' places the eigenvalues at z1=0.132, z2=0.686.



Second order system: A circle maps into a triangle. Finite wordlength robustness. Fig. 4.

DC servo motor. State variables in sensor coordinates are  $x=[\alpha w i]'$  with  $\alpha = \text{shaft angle, } w = \text{angular velocity, } i = \text{armature current, input: volt-}$ voltage u. Assumptions: a) load torque M<sub>L</sub> = cw, b) all state variables normalized to their maximal values, c) simple numerical values

$$\frac{\dot{\mathbf{x}}}{\mathbf{x}} = \begin{bmatrix} 0 & 1 & 0 \\ 0 & -c & 1 \\ 0 & -1 & -1 \end{bmatrix} \mathbf{x} + \begin{bmatrix} 0 \\ 0 \\ 1 \end{bmatrix} \mathbf{u} \quad c > 0$$
(39)

d) state feedback u= k1 (r-x1)-k2x2-k3x3, which gives a zero stationary error lim(r-x1(t)) for a step reference input r, provided the system is stable. Find  $\underline{k}' = [k_1 \ k_2 \ k_3]$  such that

stability is F<sub>23</sub> robust for all loads c.
 For a load c=2 a complex pair of eigenvalues

with damping  $1/\sqrt{2}$  or more is required: Boundaries A and B in the s-plane of Fig. 5. This specification shall be F2, F3, and F23 robust.

iii) A tradeoff with the magnitude of u-max u and the maximum bandwidth is to be made. The observability analysis shows, that a cannot be observed by  $\omega$  or i, thus the  $\alpha$  sensor is essential, i.e. the reliability with respect to a failure of the  $\alpha$  sensor can be increased only by redundant  $\alpha$ sensors. The gain k1 will be determined first. F23 robustness of stability requires that  $P(s) = s^3 + (1+c)s^2 + (1+c)s+k_1$ , c>0, is Hurwitz, i.e.  $0 < k_1 < (1+c)^2$ . The worst case is c=0. For maximum bandwidth choose k1=1.

$$\underline{\mathbf{k}}' = \underline{\mathbf{p}}' \underline{\mathbf{g}} = [\mathbf{p}_0 \ \mathbf{p}_1 \ \mathbf{p}_2 \ 1] \begin{bmatrix} 1 & 0 & 0 \\ 0 & 1 & 0 \\ 0 & -\mathbf{c} & 1 \\ 0 & -1+\mathbf{c}^2 & -1-\mathbf{c} \end{bmatrix}$$
(41)

i.e.  $k_1 = p_0 = 1$ ,  $k_2 = p_1 - cp_2 - 1 + c^2$ ,  $k_3 = p_2 - 1 - c$ . By eq. (25)  $P(s) = (s^2 - 2\sigma s + \sigma^2 + w^2) (q + s) = q(\sigma^2 + w^2) + (\sigma^2 + w^2 - 2\sigma q)s + (q - 2\sigma)s^2 + s^3$ .  $p_0 = q(\sigma^2 + w^2) = 1$  guarantees q > 0, i.e. the real eigenvalue is stable. For c = 2 and boundary A, i.e.  $w^2 = \sigma^2$ ,  $p_0 = 2q\sigma^2$ ,  $p_1 = 2\sigma(\sigma - q)$ ,  $p_2 = q - 2\sigma$  and by eq. (41)  $k_1 = 2q\sigma^2 = 1$ ,  $k_2 = 2\sigma(\sigma + 2) - 2q(1 + \sigma) + 3$ ,  $k_3 = q - 2\sigma - 3$ . By  $k_1 = p_0 = 1$ ,  $q = 1/2\sigma^2$ , the product of eigenvalues is fixed and  $k_2 = 2\sigma(\sigma + 2) - (1 + \sigma)/\sigma^2 + 3$ ,  $k_3 = 1/2\sigma^2 - 2\sigma - 3$ . This is curve A in Fig. 5. A Bode plot shows

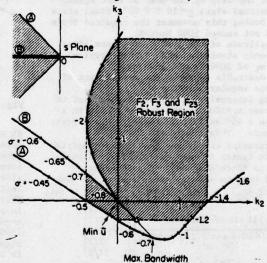


Fig. 5. Tradeoffs between tachometer (kg) and amperemeters (k3) feedback for a dc motor.

that the maximum bandwidth is obtained if real and complex poles have the same distance from the origin, i.e.  $q=1, \sigma=-1/\sqrt{2}$ , see Fig. 5. The minimum T is obtained at the point of curve A, which is closest to the origin.

For boundary B  $P(s)=(s-\sigma)^2(s+q)=q\sigma^2+\sigma(\sigma-2q)s+(q-2\sigma)s^2+s^3$ , and as before  $k_2=\sigma(\sigma+4)-2(1+\sigma)/\sigma^2+3$ ,  $k_3=1/\sigma^2-2\sigma-3$ . Points in the shaded region satisfy specifications ii). The point of maximum bandwidth on the A curve is not in the robust region, therefore damping  $> 1/\sqrt{2}$  is necessary. If q=1 is kept constant and the complex poles move along the unit circle, then k moves along a straight line in the  $k_2-k_3$ -plane. Two points of this line are  $k_2=k_3=0$  for a triple pole at s=-1 and the point  $\sigma=-1/\sqrt{2}$  on curve A. Thus a good first choice would be the point k2=0.3, k3=-0.3 indicated by the triangle in Fig. 5.

<u>Crane</u>. Consider a crane with the physical parameters  $m_{\rm C}$ =crab mass,  $m_{\rm L}$ =load mass, £=rope length. Its state variables are  $x_1$ =crab position,  $x_2$ =crab velocity,  $x_3$ =rope angle and  $x_4$ =rope angular velocity. For small rope angles the linearized state equations are

$$\underline{\dot{\mathbf{x}}} = \begin{bmatrix}
0 & \dot{\mathbf{1}} & 0 & 0 \\
0 & 0 & \mathbf{m}_{\mathbf{L}}\mathbf{g}/\mathbf{m}_{\mathbf{c}} & 0 \\
0 & 0 & 0 & 1 \\
0 & 0 & -\omega^{2} & 0
\end{bmatrix} \underline{\mathbf{x}} + \frac{1}{\mathbf{m}_{\mathbf{c}}} \begin{bmatrix}
0 \\
1 \\
0 \\
-1/\ell
\end{bmatrix} \mathbf{u} \tag{42}$$

with  $w^2 = (m_c + m_L) g/m_c l$ . Let  $g = 10 m/\sec^2$  for operation on earth. Input u is the force accelerating the crab. Eigenvalues are [0,0,jw,-jw]. The observability analysis shows that  $x_1$  is not observable by  $x_2$ ,  $x_3$  or  $x_4$ , thus the crab position sensor is essential. It was shown in [5] that  $x_2$  must be measured or estimated, without  $x_2$ -feedback a stabilization is impossible.

Given: mc=1000 kg, L=10 m, maximum load 3000 kg, design a sampled-data controller

$$u(kT) = -\underline{k}'\underline{x}(kT) \tag{43}$$

for the following specifications:

 Consider a typical movement: Pick up a load at rest and drop it 10m away at rest again, i.e. initial state x=[10 0 0 0]', final state x=0. During this movement the required force should not exceed 5000 Newton.

ii) The amplitude of the load oscillation after 10 seconds should be small for two typical loads m<sub>L</sub> of 3000 kg and 1000 kg.

iii) It is desirable to avoid the measurement of the rope angular velocity x<sub>4</sub>.

The sampling interval T was selected such that in the worst case  $m_L$ =3000 kg the complex poles in z-plane lie on a 45° angle with respect to the positive real axis. This results in  $T=\pi/8$ . The discretization and evaluation of the E matrix

The discretization and evaluation of the  $\underline{E}$  matrix were done in center of mass coordinates, in which the system is block diagonalized. The result transformed back to sensor coordinates  $\underline{x}$ , is then

$$\underline{\mathbf{E}} = [\underline{\mathbf{E}}_{1} \quad \underline{\mathbf{a}}\underline{\mathbf{E}}_{1} + \underline{\mathbf{E}}_{2}] \quad \mathbf{a} = \mathbf{m}_{L} \mathbf{L}/(\mathbf{m}_{c} + \mathbf{m}_{L})$$

$$\underline{\mathbf{E}}_{1} = \frac{(\mathbf{m}_{c} + \mathbf{m}_{L}) (2 \sin \omega \mathbf{T} - \sin 2\omega \mathbf{T})}{\mathbf{T}^{2} \cdot (5 \sin \omega \mathbf{T} - 4 \sin 2\omega \mathbf{T} + \sin 3\omega \mathbf{T})} \begin{bmatrix} 1 & -3\mathbf{T}/2 \\ 1 & -7/2 \\ 1 & \mathbf{T}/2 \\ 1 & 3\mathbf{T}/2 \\ 1 & 5\mathbf{T}/2 \end{bmatrix}$$

 $\frac{\mathbb{E}_{2}}{2} \frac{2 \sin \omega T / 2 \left(5 \sin \omega T - 4 \sin 2\omega T + \sin 3\omega T\right)^{2} \left(\frac{v_{0}v_{1}v_{2}v_{3}v_{4}}{v_{1}}\right)^{2}}{\left[\frac{\omega^{2} \left[\cos \left(1 - 1/2\right)\omega T - 2 \cos \left(1 - 3/2\right)\omega T + \cos \left(1 - 5/2\right)\omega T\right]}{\left[\omega \left[\sin \left(1 - 1/2\right)\omega T - 2 \sin \left(1 - 3/2\right)\omega T + \sin \left(1 - 5/2\right)\omega T\right]\right]}}{1 = 0, 1, 2, 3, 4.}$ 

Note that this form  $\underline{\underline{\mathbf{E}}} = \underline{\underline{\mathbf{E}}} (\mathbf{m}_{\underline{\mathbf{L}}}, \mathbf{m}_{\underline{\mathbf{c}}}, \boldsymbol{\ell}, T)$  could also be used to implement a gain scheduled control law  $\underline{\underline{\mathbf{k}}}' = \underline{\mathbf{p}}' \underline{\underline{\mathbf{E}}} = \underline{\mathbf{k}}' (\mathbf{m}_{\underline{\mathbf{L}}}, \mathbf{m}_{\underline{\mathbf{c}}}, \boldsymbol{\ell}, T)$ , which keeps the eigenvalues constant.

In the first design step a first guess for k' is determined for  $m_L$ =3000kg only. First a partial pole placement is made by eq. (14), which gives a  $1/\sqrt{2}$  damping to the pendulum motion without changing its natural frequency, i.e. a pole pair at  $z_1, 2^{=0}.4876\pm0.3026$ . For the initial condition  $\underline{x}(0)=[10\ 0\ 0\ 0]'$  the first control input is  $u(0)=10\ k_1$ , thus  $k_1\leq500\,(\text{Newton/m})$  is necessary to weet specification i). For a fast response  $k_1=500$  is chosen. After specifying two eigenvalues and one feedback gain there remains one free parameter, which is conveniently exhibited as a parameter on the root locus for the remaining two poles. Its complex part is a circle around z=1 with radius 0.1786, the intersection of this circle with the  $1/\sqrt{2}$  damping spiral at  $z_3\neq -0.8657\pm 0.1177$  is chosen. This results in k=100 1927 7867 -788].

The simulation shows that u(kT) does not exceed 5000 Newton. For the nominal load of 3000 kg the maximal amplitude after 10 seconds is 4.3% of the initial displacement. This first solution is however unsatisfactory for m<sub>1</sub>=1000 kg, with a maximal amplitude of 12.3% after 10 seconds.

In the second design step primarily the solution for  $m_L$ =1000 kg must be speeded up. From the first solution only the values  $k_1$ =500 and  $k_2$ =1927 are kept and  $k_3$  and  $k_4$  are the free parameters of the second step. The four eigenvalues move with  $k_3$  and  $k_4$ , they shall be kept however in the circle r=0.5 in Fig. 2. The circle maps into the 3000 kg boundary in the  $k_3$ - $k_4$  plane shown in Fig. 6.

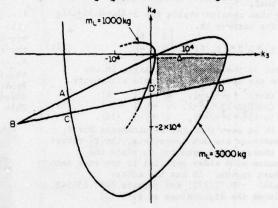


Fig. 6. A crane: Robustness with respect to large load variations.

At point A there are two different complex conjugate eigenvalue pairs crossing the circle simultaneously, such that the complex root boundary intersects itself. The right real boundary is outside the figure. At point B the complex and the left real root boundary for z1 =-0.05 meet, i.e. this k3, k4 pair generates a double pole at z=-0.05. In points C and D a complex pair and a real root at z=-0.05 cross the boundary simultaneously. 1000 kg boundary has a similar shape, only its right part and the intersection D', corresponding to D, are shown. Thus the first design point indicated by the triangle must be moved to the left; let k3=4000. Since k4 is small anyway, k4=0 is chosen in view of specification iii). Simulation shows that the maximum amplitudes after 10 seconds are 6.4% for 3000 kg and 3% for 1000 kg. The angle x3 remains small, such that this assumption for the linearization of the plant equation is satisfied. If necessary a third design step could follow in which k1=500 and k4=0 are fixed and k2 and k3 are varied.

#### 5. CONCLUSIONS

Classical parameter plane ideas have been combined with pole placement results to a design method in  $\mathcal K$  space. The crucial step is the introduction of a plant representation in the form of the matrix  $\mathbf E$  in eqs. (16) and (A.5). The linear mapping from  $\mathbf F$  space to  $\mathbf F$  space is performed by a multiplication with the matrix  $\mathbf E$  and is thus reduced to a computationally very simple step. In  $\mathbf F$  space typical design aspects such as actuator limitations and robustness with respect to sensor and actuator failures, large parameter variations and short wordlength implementation have elementary geometric interpretations, and several questions of practical interest can be treated in a clear and simple way

as is illustrated by three examples.

The examples are restricted so far to tradeoffs in two free parameters at a time, where a graphical interpretation in cross-sections of the X space is possible. This is already a practically applicable tool with apparent advantages over graphical one-parameter methods like root locus. For example in successively closing loops of a cascaded system it allows to make tradeoffs between two successive

The concept of the method is however not limited in the number of parameters. Due to the computational simplicity of the mapping it seems feasible to develop computer-aided design methods with displays visualizing three-dimensional surfaces and regions by moving point of view or moving cross-section. If the computer has to make the tradeoffs in problems with many parameters, difficulties arise, if there does not exist a point in X space satisfying all specifications. In this situation the concept of a moving boundary may be useful, which was used by Zakian and Al-Naib [6] in the numerical treatment of inequalities. In Figs. 1 and 2 this means that the parameter p or r is varied continuously until a solution is found.

6. REFERENCES
[1] Siljak, D. D., Nonlinear Systems, The Parameter Analysis and Design, J. Wiley, New York, 1969, Chapters I and 2.

[2] Ackermann, J., Abtastregelung (Sampled-data control), Springer, Berlin, 1972, pp. 310-312.
[3] Ackermann, J., "On the Synthesis of Linear

Control Systems with Specified Characteristics," Automatica 13, pp. 89-94 (1977).

[4] Fam, A. T. and Meditch, J. S., "A Canonical Parameter Space for Linear Systems Design, IEEE Trans. AC-23, pp. 454-458 (1978).

[5] Ackermann, J., "Entwurf durch Polvorgabe," (Design by Pole Placement), Regelungstechnik

25, pp. 173-179 and 209-215 (1977). [6] Zakian, V. and Al-Naib, U., 'Design of Dynamical and Control Systems by the Method of Inequalities," IEE Proc. 120, pp. 1421-1427 (1973).

[7] Popov, V. M., "Invariant Description of Linear Time-Invariant Controllable Systems," SIAM J. Control 10, pp. 252-264 (1972).

#### APPENDIX

The generalization of eq. (16), k'=p'E, to the multivariable case was published in [5] and is quoted here for easier reference: Given a controllable pair  $(\underline{A},\underline{B})$ , let  $\underline{B}=[\underline{b_1}\ldots\underline{b_p}]$  $r_{ik}$ =rank $[\underline{B}, \underline{A}\underline{B}...\underline{A}^{k-1}\underline{B}, \underline{A}^{k}\underline{b}_{1}...\underline{A}^{k}\underline{b}_{1}]$  i=1,2...p A controllability index  $\mu_1$ , i=1,2...p of the pair  $(\underline{A},\underline{B})$  is the smallest integer k such that  $r_{1k}=r_{1-1k}$ . Then  $\underline{A}$  b, is linearly dependent on the vectors left of it in the controllability matrix and can be expressed as  $\underline{\underline{A}^{\mu_1}}\underline{\underline{b}_1} = \{\underline{\underline{B}}\underline{\underline{A}}\underline{\underline{B}}...\underline{\underline{A}^{\mu_1}}\underline{\underline{B}}]\underline{\underline{\alpha}_1} = \{\underline{\underline{A}^{\mu_1}}\underline{\underline{b}_1}...\underline{\underline{A}^{\mu_1}}\underline{\underline{b}_{1-1}}]\underline{\underline{\beta}_1}. \quad (A.2)$ In order to make \$1 = [\$11...\$11-1]' unique, let Bij=0 if mishi. Let

$$\underline{\mathbf{M}}_{AB} = \begin{bmatrix}
1 & \beta_{21} & \cdots & \beta_{p1} \\
0 & 1 & & \vdots \\
& & \ddots & \beta_{pp-1} \\
0 & & 0 & 1
\end{bmatrix} .$$
(A.3)

Note that by Popov's theorem on feedback invariants [7],  $\underline{M}_{AB}$  is invariant under a transformation  $(\underline{A},\underline{B}) \to (\underline{T}(\underline{A}-\underline{B}\underline{K}')\underline{T}^{-1}\underline{T}\underline{B})$ , det  $\underline{T} \neq 0$ . Let

$$R = [\underline{b}_1 \dots \underline{A}^{\mu_1 - 1} \underline{b}_1, \underline{b}_2, \dots, \underline{A}^{\mu_p - 1} \underline{b}_p], \quad \underline{R}^{-1} = \begin{bmatrix} \underline{Q}_1 \\ \vdots \\ \underline{Q}_p \end{bmatrix} \quad (A.4)$$

and  $e_i$  the last row of the  $\mu_i \times n$  matrix  $Q_i$ .

$$\underline{\underline{\mathbf{E}}} = \begin{bmatrix} \underline{\underline{\mathbf{E}}}_1 \\ \vdots \\ \underline{\underline{\mathbf{E}}}_p \end{bmatrix} \qquad \underline{\underline{\mathbf{E}}}_1 = \begin{bmatrix} \underline{\underline{\mathbf{e}}}_1^{\top} \underline{\underline{\mathbf{A}}} \\ \vdots \\ \underline{\underline{\mathbf{e}}}_1^{\top} \underline{\underline{\mathbf{A}}} \end{bmatrix} \qquad (A.5)$$

Introduce nxp characteristic parameters in a pxp

$$\underline{\mathbf{p}}' = \begin{bmatrix} \mathbf{p}'_{11} & \cdots & \mathbf{p}'_{1p} \\ \vdots & \vdots & \ddots & \mathbf{p}'_{pp} \end{bmatrix}$$
(A.6)

with 
$$p'_{ii} = [p_{ii0} \ p_{ii1} \dots p_{iji_1-1} \ 1]$$
  
 $p'_{ij} = [p_{ij0} \ p_{ij1} \dots p_{iji_1-1} \ 0]$   $i \neq j$ 

 $\underline{P}'$  generalizes  $\underline{p}'$ , the vector of coefficients of the characteristic polynomial, its coefficients  $p_{\underline{i},\underline{j},\underline{k}}$  are the coordinates of an nxp dimensional para meter space Q. P' is related to the characteristic polynomial by

$$P(\lambda) = \det(\lambda \underline{I} - \underline{A} + \underline{B} \underline{K}') = \det[\underline{P}' \cdot \operatorname{diag}(\underline{\lambda}_{\underline{I}})],$$

$$\underline{\lambda}_{\underline{I}} = \{1 \quad \lambda \quad \dots \quad \lambda^{\mu \underline{I}}\}' \qquad (A.7)$$

and to the state feedback matrix by

$$\underline{\mathbf{K}}' = \underline{\mathbf{M}}_{\mathbf{A}\mathbf{B}}\underline{\mathbf{P}}'\underline{\mathbf{E}}$$
 (A.8)

Thus the system representation  $(E,M_{AB})$  may be considered as a mapping between two nxp dimensional parameter spaces  $\theta$  and  $\chi$ . Note that the n coefficients of any row of  $\underline{P}'$  enter linearly into the determinant in eq. (A.7), thus they can be expressed by the coefficients of P(A) and by the remaining mx (p-1) characteristic parameters in P', which parameterize the remaining degrees of freedom after pole placement. If the coefficients of the first row of P' are eliminated in this way, eq. (A.8) results in n.p equations relating the feedback gains to the n(p-1) free parameters. Due to the structure of MAB, n(p-1) of these equations are linear, only the equations for the elements of the first row of K are nonlinear in the free parameters.

The free parameters can now be chosen according to additional requirements, e.g. minimizing the maximal feedback gain in view of actuator limitations or to make certain columns of  $\underline{K}'$  equal to zero in order to save sensors.

#### Closed-Loop Structural Stability for **Linear-Quadratic Optimal Systems**

POH KAM WONG AND MICHAEL ATHANS, FELLOW, IEEE

Abstract-This paper contains an explicit parametrization of a subclass of linear constant gain feedback maps that will not destabilize an originally open-loop stable system. These results can then be used to obtain several new structural stability results for multiinput linear-quadratic feedback optimal designs.

#### I. INTRODUCTION AND MOTIVATION

This paper presents preliminary results which, in our opinion, represent a first necessary step in the systematic computer aided design of reliable control systems for multivariable control systems. A specific motivating example arises in the context of future high performance aircraft. It is widely recognized that advances in active control aircraft and control configured vehicles will require the automatic control of several actuators so as to be able to fly future aircraft characterized by reduced stability margins and additional flexure modes.

As a starting point for our motivation we must postulate that the design of future stability augmentation systems will have to be a multivariable design problem. As such, traditional single input-single output system design tools based on classical control theory cannot be effectively used, especially in a computer aided design context. Since modern

Manuscript received January 28, 1976; revised August 31, 1976. Paper recommended by J. B. Pearson, Chairman of the IEEE S-CS Linear Systems Committee. This work was supported in part by the NASA Ames Research Center under Grant NGL-22-009-124 and by the Air Force Office of Scientific Research under Grant AF-AF0SR-72-2273. The authors are with the Electronic Systems Laboratory, Department of Electrical Engineering and Computer Sciences, Massachusetts Institute of Technology, Cambridge, MA 02139.

Copyright © 1977 by The Institute of Electrical and Electronics Engineers, Inc. Printed in U.S.A. Annals No. 702AC017

control theory provides a conceptual theoretical and algorithmic tool for design, especially in the linear-quadratic-Gaussian (LQG) context (see Athans [1] for example), it deserves a special look as a starting point in the investigation.

In spite of the tremendous explosion of reported results in LQG multivariable design, the robustness properties have been neglected. Experience has shown that LQG designs "work" very well if the mathematical models upon which the design is based are somewhat accurate. There are several sensitivity studies involving "small parameter perturbations" associated with the LQG problem. We submit, however, that the general problem of sensitivity and even stability of multivariable LQG designs under large parametric and structural changes is an open research area.

It is useful to reflect upon the basic methodology in classical servomechanism theory which dealt with such large parameter changes. The overall sensitivity and stability considerations were captured in the definition of gain and phase margins. If a closed-loop system was characterized by reasonable gain and phase margins, then I) reasonable changes in the parameters of the open-loop transfer functions and 2) changes in the loop gains due, for example, to saturation and other nonlinearities could be accommodated with guaranteed stability and at the price of somewhat degraded performance.

Although LQG designs are time-domain oriented nonetheless their frequency-domain interpretations are important, although not universally appreciated. For example, for the case of single input-single output linear-quadratic (LQ) optimal designs Anderson and Moore [2] have shown that LQ-optimal designs are characterized by

- 1) an infinite gain margin property and
- 2) a phase margin of at least 60 degrees.

Such results are valuable because it can be readily appreciated that at least in the single input-single output case, modern control theory designs tend to have a good degree of robustness, as measured by the classical criteria of gain and phase margin.

Advances in the multiinput-multioutput case, however, have been scattered and certainly have not arrived at the cookbook design stage. Multivariable system design is extremely complex. To a certain extent the numerical solution of LQ-optimal problems is very easy, however, fundamental understanding of the structural interdependencies and its interactions with the weighting matrices is not a trivial matter. We believe that such fundamental understanding is crucial for robust designs as well as for reliable designs that involve a certain degree of redundancy in controls and sensors.

The recent thesis by Wong [3] represents a preliminary yet positive contribution in this area. In fact the technical portion of this paper represents a slight modification of some of the results reported in [3]. In particular we focus our attention on the stability properties of closedloop systems designed on the basis of LQ-optimal techniques when the system matrices and loop gains undergo large variations.

The main contributions reported in this paper are the eventual results of generalizing the concepts of gain margin and of performing large-perturbation sensitivity analysis for multivariable linear systems designed via the LQ approach. (For a corresponding generalization of the phase gain margin results to the multivariable problem see the paper by Safonov and Athans [7].)

We warn the reader that much additional theoretical and applied research is needed before the implications of these theoretical results can 1) be fully understood and 2) translated into systematic "cookbook" procedures that have the same value as the conventional results in classical servomechanism design.

This paper is organized as follows: in Section II we present an explicit parametrization of a subclass of linear constant feedback maps that never destabilize an originally open-loop stable system, and establish some of its properties. In Section III, we apply this construct to obtain several new closed-loop structural stability characterizations of multiinput LQ-optimal feedback maps. We conclude in Section IV with a brief discussion of the relevance of the results of this paper for computeraided iterative feedback design.

Notation

1) The linear time-invariant system

$$\dot{x}(t) = Ax(t) + Bu(t)$$

$$z(t) = H^{T}x(t)$$

x(1) = 97" x(·) state vector u(1)∈ 9.m u(·) control vector z(1)∈91' z(·) output vector

will be denoted by  $\Sigma(A, B, H^T)$ . Where  $H^T$  is irrelevant to the discussion, we will shorten the notation to  $\Sigma(A, B)$  and where the choice A, B is clear from the context, we will just use \(\Sigma\).

If the matrix A is stable (i.e., all eigenvalues of A have strictly negative real parts), we will refer to  $\Sigma(A, B, H^T)$  as a stable system.

- R(K) range space of K
- N(K) nullspace (kernel) of K
- Rk(K) rank of K.
- 3) Given the system  $\Sigma(A, B, H^T)$ ,

$$R(A,B) \stackrel{\triangle}{=}$$
 controllable subspace of the pair  $(A,B)$ 

$$\stackrel{\triangle}{=} R(B) + AR(B) + \cdots + A^{n-1}R(B)$$

 $N(H^T, A) \stackrel{\triangle}{=} \text{unobservable subspace of the pair } (H^T, A)$ 

$$\triangleq \bigcap_{i=1}^{n} N(H^{T}A^{i-1}).$$

4) If  $Q \in \mathbb{R}^{n \times n}$  is positive semidefinite, we will write

If Q is positive definite, we will write

- 5)  $[m_{ij}]$  denotes the matrix M whose (i,j) element is  $m_{ij}$ .
- II. PARAMETRIZATION OF NONDESTABILIZING FEEDBACK MAPS

We begin our discussion with Definition 1. Definition 1: Given the stable system  $\Sigma(A,B)$ , let

$$S(\Sigma) \triangleq \{G^T \in \Re^{m \times n} | (A + BG^T) \text{ is stable} \},$$

i.e.,  $S(\Sigma)$  is the set of all feedback maps that will not destabilize an originally open-loop stable system where

$$u(t) \triangleq G^T x(t)$$
.

Ideally, one would like to be able to explicitly parametrize  $S(\Sigma)$ , but as this is a well-known intractable problem our strategy here is to look for a simple parametrization of a (hopefully) sufficiently general subset of S(E)

We begin by first recalling some standard Lyapunov-type results. Lemma 1 (Wonham):

1) If A is stable, then the Lyapunov equation

<sup>&</sup>lt;sup>1</sup>Even the notion of what constitutes a "zero" of a multivariable transfer matrix was not fully appreciated until recently.

with Q > 0 has a unique solution P > 0. If, in addition,  $(Q^{1/2}, A)$  is observable, then P > 0.

2) If

$$P > 0$$
,  $Q > 0$  satisfy  $PA + A^TP + Q = 0$   
 $(Q^{1/2}, A)$  is detectable

then A is stable.

3) If Q > 0 and  $(Q^{1/2}, A)$  is observable (detectable), then for all p > 0, R > 0 and for all  $B, F^T$ , the pair  $(\sqrt{Q + P + FRF^T}, PA + BF^T)$  is observable (detectable).

*Proof:* For 1), see [4, p. 298]. For 2), see [4, p. 299]. For 3), see [4, p. 82].

To proceed, the following definition will be useful:

Definition 2: For any stable A, let

$$LP(A) \triangleq \{K > 0 | KA + A^{T}K < 0\}$$
  
$$LP^{+}(A) \triangleq \{K > 0 | KA + A^{T}K < 0\}.$$

Remark: LP(A) is, in general, a proper subset of the set of all positive-semidefinite matrices of dimension n.

Example: Suppose that

$$A = \begin{bmatrix} \lambda_1 & 0 \\ 0 & \lambda_2 \end{bmatrix}, \quad \lambda_1 < 0, \quad \lambda_2 < 0.$$

Then

$$LP(A) = \left\{ \begin{bmatrix} K_1 & K_{12} \\ K_{12} & K_2 \end{bmatrix} \middle|_{K_2 > 0}^{K_1 > 0}, K_1 K_2 > \left[ \frac{(\lambda_1 + \lambda_2)^2}{4\lambda_1 \lambda_2} \right] K_{12}^2 \right\}.$$

Note that  $\begin{bmatrix} K_1 & K_{12} \\ K_{12} & K_2 \end{bmatrix} > 0$  iff  $K_1 > 0$ ,  $K_2 > 0$ ,  $K_1 K_2 > K_{12}^2$  and that  $(\lambda_1 + \lambda_2)^2 / 4\lambda_1 \lambda_2 > 1$ , with equality iff  $\lambda_1 = \lambda_2$ .

Lemma 2:

1) LP(A) is a convex cone, i.e.,  $K_1, K_2 \in LP(A)$  implies  $\alpha_1 K_1 + \alpha_2 K_2 \in LP(A)$  for all  $\alpha_1 > 0$ ,  $\alpha_2 > 0$ ;

2)  $K \in LP(A_1) \cap LP(A_2)$  implies  $K \in LP(A_1 + A_2)$ ;

3)  $K \in LP(A)$  implies  $K \in LP(A + B(S - L)B^TK)$ ; for all S, L such that  $S = -S^T$ , L > 0, provided  $(A + B(S - L)B^TK)$  is stable.

Proof: Straightforward.

We are now ready to introduce our first crucial result.

Lemma 3: Let A be stable. Then (A + (N - M)K) is stable for all  $K \in LP(A)$  and for all M > 0,  $N = -N^T$  such that  $R(N) \subset R(M)$ . If  $K \in LP^+(A)$ , then the condition  $R(N) \subset R(M)$  can be omitted.

**Proof:** Let  $Q \triangleq -(KA + A^TK)$ . Since  $K \in LP(A)$ , we have Q > 0, and A stable implies  $(Q^{1/2}, A)$  is always detectable.

Now  $KA + A^TK + Q = 0$ , so  $K(A + (N - M)K) + (A + (N - M)K)^TK + 2KMK + Q - (KNK + KN^TK) = 0$  but  $KNK + KN^TK = 0$  since  $N = -N^T$ .

If  $K \in LP^+(A)$ , then Q > 0 so  $(\sqrt{Q+2KMK}, (A+(N-M)K))$  is observable, which implies (A+(N-M)K) is stable by Lemmas 1-2.

Otherwise, assume  $R(N) \subset R(M)$  which implies that there exists V such that N = VM or that (N - M)K = (V - I)MK.

By defining

$$B \triangleq (V - I)M^{1/2}$$

$$F^{\perp} \triangleq M^{1/2}K$$

$$P \triangleq 0$$

$$R \triangleq I$$

in Lemmas 1-3, we have that  $(\sqrt{Q+2KMK}, A+(N-M)K)$  is detectable. By Lemmas 1-2, we therefore have (A+(N-M)K) stable. Q.E.D.

Remark: A special case of Lemma 3 was established by Barnett and Storey in [5].

By specializing Lemma 3, we immediately obtain an explicit parametrization of a subclass of stabilizing feedback. First we introduce Definition 3.

Definition 3: Given the stable system  $\Sigma(A,B)$ , let

$$S_{\bullet}(\Sigma) \triangleq \{G^T \in \mathfrak{R}^{m \times n} | G^T = (S - L)B^T K, S = -S^T, L > 0.$$

and either  $K \in LP^+(A)$  or else  $K \in LP(A)$  with  $R(S) \subset R(L)$ .

We can now state our result as Theorem 1.

Theorem 1: Given the stable system  $\Sigma(A,B)$ , then 1)  $G^T \in S_1(\Sigma)$  implies  $(A+BG^T)$  is stable and 2)  $\int_0^\infty e^{A^T}Qe^{At} dt > \int_0^\infty e^{(A+BG^T)^T}Qe^{(A+BG^T)^2} dt$  where Q>0 is such that  $KA+A^TK+Q=0$  and  $G^T \triangleq (S-L)B^TK \in S_1(\Sigma)$ .

Proof.

1) Let  $M = BLB^T$ ,  $N = BSB^T$  in Lemma 3, and the result follows directly.

2) Let Q > 0 be such that

$$KA + A^TK + Q = 0. (1)$$

Then we have

$$K = \int_0^\infty e^{A^T i} Q e^{Ai} di.$$

Next rewrite (1) as

$$K(A+BG^{T})+(A^{+}BG^{T})^{T}K+(2KBLB^{T}K+Q)=0$$

where  $G^T \triangleq (S - L)B^T K \in S_1(\Sigma)$  which implies

$$K = \int_0^\infty e^{(A+BG^T)^T t} (2KBLB^T K + Q) e^{(A+BG^T) t} dt;$$

hence

$$\begin{split} \int_0^\infty e^{A^T i} Q e^{A i} \, di &= \int_0^\infty e^{(A + BG^T)^T i} Q e^{(A + BG^T) i} \, di \\ &+ 2 \int_0^\infty e^{(A + BG^T)^T i} KBLB^T K e^{(A + BG^T) i} \, di \end{split}$$

or

$$\int_0^\infty e^{A^T t} Q e^{At} dt > \int_0^\infty e^{(A+BG^T)^T t} Q e^{(A+BG^T) t} dt. \qquad \text{Q.E.D.}$$

Remark: It can be easily shown that all the eigenvalues of the feedback term  $B(S-L)B^TK$  have nonpositive real parts. This observation, and the content of Theorem 1-2), makes it convenient to interpret  $S_1(\Sigma)$  as a natural generalization of the concept of "negative" feedback to the multivariable and multiinput case.

The next two corollaries are easy consequences of Theorem 1.

Corollary 1.1: Let  $\Sigma(A, B)$  be a system with a single input, i.e., let B be a column  $(n \times 1)$  vector b. If  $\mathbf{g}_1^T, \dots, \mathbf{g}_t^T \in S_1(\Sigma(A, b))$ , then

$$\sum_{i=1}^{j} \alpha_i \mathbf{g}_i^T \in S_1(\Sigma), \quad \text{for all } \alpha_i > 0, i = 1, \dots, j.$$

**Proof:** Each  $\mathbf{g}_i^T$  is of the form  $-r_i \mathbf{b}^T \mathbf{K}_i$  for some admissible  $r_i > 0$ ,  $\mathbf{K}_i > 0$  so  $\sum_{i=1}^{r} \alpha_i \mathbf{g}_i^T = \sum_{i=1}^{r} -\alpha_i r_i \mathbf{b}^T \mathbf{K}_i = -\mathbf{b}^T (\sum_{i=1}^{r} \alpha_i r_i \mathbf{K}_i)$ .

But from Lemma 2-1)  $K_i \in LP(A)$  implies  $\sum_{i=1}^{j} \alpha_i r_i K_i \in LP(A)$  for all  $\alpha_i r_i > 0$ ; hence,  $\sum_{i=1}^{j} \alpha_i g_i^T \in LP(A)$  for all  $\alpha_i > 0$ . Q.E.D.

Corollary 1.2: Suppose there exists L > 0 such that  $BLB^T \in LP(A^T)$ . Then  $(A - BLB^T(K + N))$  is stable for all K > 0 and  $N = -N^T$  such that  $R(K) \supset R(N)$ .

If  $BLB^T \in LP^+(A^T)$  actually, then the condition  $R(K) \supset R(N)$  can be omitted.

**Proof:** Immediate from "taking the transpose" in Lemma 3. Q.E.D. Theorem 1 has illustrated the importance of LP(A). It is therefore useful to have an alternative characterization of LP(A).

Proposition 1: LP(A) is  $A^{T}$ -invariant, i.e., for all  $K \in LP(A)$ .

 $[A^TR(K)\subset R(K).]$ 

Proof:  $K \in LP(A)$  iff  $KA + A^TK + HH^T = 0$  for some H. We claim that  $N(K) = N(H^T, A) =$  unobservable subspace of  $T^TA$ , for  $K = \int_0^\infty e^{A^T} HH^T e^{At} dt$  so  $x \in N(H^T, A)$  implies  $H^T e^A x = 0$  for all  $t \in \mathbb{R}$ , which implies  $x \in N(K)$ . Conversely,  $x \in N(K)$  implies  $x^TKx = 0$  which

implies  $\int_0^\infty |H^T e^{At} x|^2 dt = 0$  or  $H^T e^{At} x = 0$  for all  $t \in \Re$ , i.e.,  $x \in N(H^T |A)$ .

To complete the proof, note that

$$R(K) = R(K^{T}) = N(K)^{\perp}$$

$$= N(H^{T}, A)^{\perp}$$

$$= R(A^{T}, H)$$

$$= \text{controllable subspace of } (A^{T}, H).$$

But any controllable subspace of  $A^T$  is necessarily an  $A^{T}$ -invariant subspace.

**Remark:** The significance of Proposition 1 is that it provides a systematic means for generating members of LP(A). For example, if A has distinct, real eigenvalues, then every  $K \in LP(A)$  is of the form

$$K = P^T M P$$

where the rows of P are left eigenvectors of A, i.e.,

$$PA = \Lambda P$$
,  $\Lambda = \text{diagonal}(\lambda_1, \dots, \lambda_n)$ 

and M > 0 is such that  $[-(\lambda_i + \lambda_j)m_{ij}] > 0$ , where  $M = [m_{ij}]$ .

Thus, all members of LP(A) can be generated once P is known.

While membership in  $S_1(\Sigma)$  is sufficient to guarantee closed-loop stability, it is of course not necessary, i.e.,  $S_1(\Sigma)$  is a strictly proper subset of  $S(\Sigma)$ . Intuitively, if the open-loop system is stable "enough" to begin with, it can tolerate a certain amount of "positive" feedback without leading to closed-loop instability. In other words, the poles of the open-loop system can be shifted to the right by feedback without destroying stability so long as none of them get shifted into the closed right-half plane. By allowing such additional nondestabilizing feedback, therefore, we ought to be able to "enlarge"  $S_1(\Sigma)$ . More precisely, we have Definition 4.

Definition 4: Given the stable system  $\Sigma(A,B)$  and any  $L>0, L\in \mathbb{R}^{m\times m}$ , let

$$LP(\Sigma,L) \triangleq \{K > 0 | KA + A^TK + 2KBLB^TK < 0\}$$
  
$$LP^+(\Sigma,L) \triangleq \{K > 0 | KA + A^TK + 2KBLB^TK < 0\}.$$

Definition 5: Given the stable system  $\Sigma(A, B)$ , let

$$S_2(\Sigma) \triangleq \left\{ G^T \in \mathfrak{R}^{m \times n} | G^T \right.$$

$$=(\hat{L}+S)B^TK, \hat{L}=\hat{L}^T, S=-S^T, L>0, L>\hat{L}$$

and either

$$K \in LP^+(\Sigma, L)$$

or else

$$K \in LP(\Sigma, L)$$

with

$$R(\hat{L}+S)\subset R(L-\hat{L})$$
.

Theorem 2: Given the stable system  $\Sigma(A, B)$ , then  $G^T \in S_2(\Sigma)$  implies  $(A + BG^T)$  is stable.

Proof: The proof follows by a straightforward extension of the proof of Lemma 3 and Theorem 1, and hence is omitted.

Q.E.D.

**Remark:** It can be easily seen that Theorem 1 is just a special case of Theorem 2 [with  $L \equiv 0$  and  $\hat{L} < 0$ ,  $S_2(\Sigma)$  will be reduced to  $S_1(\Sigma)$ ]. Note that in the general case covered by Theorem 2, no definiteness assumption is made of  $\hat{L}$ , and thus various "mixtures" of "positive" and "negative" feedbacks are allowed.

The next proposition provides further clarification on our parametrization scheme. First define

- note name and address of the a

$$F_2(B) \triangleq \{G^T \in \mathfrak{R}^{m \times n} | RK(G^T B) < RK(G^T)\}.$$

Proposition 2.

$$F_1(B) \cap F_2(B) = \phi$$

$$F_1(B) \cup F_2(B) = \Re^{m \times n},$$

i.e., any feedback map  $G^T \in \Re^{m \times n}$  is either in the set  $F_1(B)$  or else  $F_2(B)$ .

Proof: We need only to show that

$$F_1(B) = \{G^T \in \mathfrak{R}^{m \times n} | RK(G^TB) = RK(G^T)\}.$$

Necessity: Suppose  $G^T \in F_1(B)$ , i.e., there exists  $D \in \mathbb{R}^{m \times m}$  and  $K \in \mathbb{R}^{n \times n}$ , K > 0 such that  $G^T = DB^T K$ . Then

$$G^TBD^T = DB^TKBD^T > 0$$

so  $RK(G^TB) > RK(G^TBD^T) = RK(DB^TKBD^T) = RK(DB^TK) = RK(G^T)$ .

Sufficiency: Take  $D = G^T B$  and observe that the equation

$$G^T = G^T B B^T K$$

has a solution K > 0 if  $RK(G^TB) = RK(G^T)$ . Q.E.D.

We now relate the content of Proposition 2 to Theorem 2. Observe first that  $S_2(\Sigma) \subsetneq F_1(B)$ , and hence our parametrization scheme fails to capture any nondestabilizing feedback map  $\epsilon F_2(B)$ . That  $S(\Sigma) \cap F_2(B) \neq \emptyset$  is demonstrated by the following trivial example.

Example

$$\mathbf{A} = \begin{bmatrix} \lambda_1 & 0 \\ 0 & \lambda_2 \end{bmatrix}, \quad \lambda_1, \lambda_2 < 0$$

$$\mathbf{b} = \begin{bmatrix} 1 \\ 0 \end{bmatrix}, \quad \mathbf{g}^T = \begin{bmatrix} 0 & 1 \end{bmatrix} \in F_2(\mathbf{b})$$

and 
$$(\mathbf{A} + \mathbf{b}\mathbf{g}^T) = \begin{bmatrix} \lambda_1 & 1 \\ 0 & \lambda_2 \end{bmatrix}$$
 is stable.

Note, however, that if B is of full rank, then the set  $F_2(B)$  is NOT generic in  $\Re^{m \times n}$ .

The more interesting question: is  $S_2(\Sigma)$  generic (i.e., dense) in  $S(\Sigma) \cap F_1(B)$ ? is at present unsolved.

Our results so far have been on systems  $\Sigma(A,B)$  which are open-loop stable; the question next arises as to what the situation would be for systems which are NOT open-loop stable (i.e., A has unstable poles). For A unstable it is of course not possible to write down Lyapunov-type equations. One is reminded, however, of the algebraic Riccati equations; indeed, we have the following interpretation of the traditional LQ-optimization problem.

Definition 6: Given (A, B) a stabilizable pair, let

$$LQ(A,B) \triangleq \{K > 0 | K = K(A,B,R,H^T) \text{ for some } R > 0 \text{ and some } H^T$$

such that  $(H^T, A)$  is a detectable pair

where  $K(A,B,R,H^T)$  denotes the unique positive semidefinite solution to the algebraic Riccati equation

$$KA + A^TK - KBR^{-1}B^TK + HH^T = 0.$$

For R fixed, we will denote the corresponding set as LQ(A, B; R).

Definition 7:

$$S_3(\Sigma) \triangleq \{G^T \in \mathbb{R}^{m \times n} | G^T = -R^{-1}B^TK, R > 0, K \in LQ(A, B; R)\},$$

Proposition 3: Given any stabilizable system  $\Sigma(A,B)$ ,  $G^T \in S_3(\Sigma)$  implies  $(A+BG^T)$  is stable.

Remark: The above proposition merely summarizes the well-known "standard" results of LQ-optimal feedback theory (see, [1] and [4]). However, the interpretation here of the LQ-optimal feedback class  $(S_3(\Sigma))$  as a parametrization of a subclass of stabilizing feedback is

## III. STRUCTURAL STABILITY CHARACTERIZATION OF LINEAR QUADRATIC (LQ) OPTIMAL FEEDBACK MAPS

In this section we show how the parametrization scheme developed in the previous section can be applied to obtain characterization of closed-loop structural stability properties of systems under LQ-optimal feedback. More precisely, we establish an explicit parametrization of a general class of structural perturbations in the control feedback gains as well as in the control actuation matrix (B) that leave the closed-loop system stabilized. These new results, we believe, are the natural generalizations and nontrivial extensions of some earlier results of Anderson and Moore [2].

We begin by first recalling from Lemma 2-3) that for A stable,  $K \in LP(A)$  always implies  $K \in LP(A - BLB^TK)$ , however, for A unstable and K > 0 such that  $(A - BLB^TK)$  is stable, it need NOT be true that  $K \in LP(A - BLB^TK)$ . The following example underscores this unfortunate state of affairs.

Example:

$$A = \begin{bmatrix} 1 & 3 \\ 0 & 0 \end{bmatrix}, BLB^T = \begin{bmatrix} 2 & 0 \\ 0 & 1 \end{bmatrix}, K = \begin{bmatrix} 1 & 0 \\ 0 & 1 \end{bmatrix}.$$

Then

$$(A - BLB^TK) = \begin{bmatrix} -1 & 3 \\ 0 & -1 \end{bmatrix}$$

is stable, but

$$K(A-BLB^TK)+(A-BLB^TK)^TK=\begin{bmatrix} -2 & 3\\ 3 & -2 \end{bmatrix}<0.$$

However, we have an interesting observation in Lemma 4.

Lemma 4: If  $K \in LQ(A, B; R)$ , then  $K \in LP(A - BR^{-1}B^TK)$ .

Proof: Immediate from the Riccati equation. Q.E.D.

In other words, the above unfortunate state of affairs cannot occur if k is an LO-solution.

We are now ready to state our first main result of the section.

Theorem 3 (Infinite Gain Margin Property): Let  $K \in LQ(A, B; R)$ . Then  $(A - [B(S + L)B^T + B(N + M)B^T]K)$  is stable for all  $L > R^{-1}$ , M > 0,  $S = -S^T$ ,  $R(S) \subset R(L - R^{-1})$ ,  $N = -N^T$ ,  $R(N) \subset R(M)$ , B is arbitrary.

**Proof:** We have  $K \in LP(A - BR^{-1}B^TK)$ , so by Lemma 3,  $(A - BR^{-1}B^TK + (V - W)K)$  is stable for all W > 0,  $V = -V^T$  such that  $R(V) \subset R(W)$ . Take  $W = B(L - R^{-1})B^T + BMB^T$  and  $V = BSB^T + BNB^T$  and we are done. Q.E.D.

Remark: For  $B \approx 0$ , Theorem 3 is a generalization of the "infinite gain margin" property of LQ-optimal feedback for single-input systems first noted by Anderson and Moore [1], who showed that the feedback gain vector  $\mathbf{g}^T = -1/r\mathbf{b}^T \mathbf{K}$  can be multiplied by any scalar  $\alpha > 1$  without destroying stability; the proof they used involves classical Nyquist techniques. Theorem 3 not only generalizes this property to multiinput systems, but allows more complicated alterations of the feedback gain vectors; moreover, it makes the proof of this property much more transparent.

Remark: For  $B \neq 0$ , Theorem 3 allows for changes in the B matrix itself without destroying stability. One useful interpretation is the following

Suppose that the optimal feedback gain matrix has been computed for a nominal  $B_0$ , but that the actual value of B during system operation is changed to  $B = B_0 + B_1$ . Then the feedback term becomes  $(B_0 R^{-1} B_0^T K + B_1 R^{-1} B_0^T K)$ . As long as  $B_1 = B_0 (N + M) R$  for some  $N = -N^T M > 0$ , Theorem 3 will guarantee us that the system will remain stable. (For example,  $B_1 = \alpha B_0$ ,  $\alpha > 0$ .) More complicated cases are allowed.

Remark: Alternatively, the case  $B \neq 0$  can be interpreted as allowing for the possibility of adding extra controllers, and using these extra feedbacks to "fine-tune" the closed-loop behavior of the original system. (A more systematic exploitation of this idea will be dealt with in a future publication; see also [3].)

Theorem 3 has dealt with the case when the "negative" feedback gains, etc., are allowed to increase in magnitude; the converse situation, when the "negative" feedback gains are reduced in magnitude (or when

there is system structual parameter changes) is examined in the next proposition.

Theorem 4 (Gain Reduction and Robustness Property): Let K>0 be the Riccati solution to the LQ-problem (A,B,R,Q) where R>0 and  $(Q^{1/2},A)$  detectable. Then

1)  $(A - B(M + N)B^TK)$  is stable for all M > 0 such that  $M > \frac{1}{2}R^{-1}$ ,  $N = -N^T$ ;

2) if  $(\hat{Q}^{1/2}, A)$  is actually observable, then  $(A - B(M + N)B^TK + K^{-1}(\hat{Q} + \hat{N}))$  is stable where M, N are as above, and  $\hat{Q} = \hat{Q}^T$  is such that  $\hat{Q} < \frac{1}{2}Q$ ,  $R(\frac{1}{2}Q - \hat{Q}) \supset R(Q)$  and  $\hat{N} = -\hat{N}^T$  is such that  $R(\frac{1}{2}Q - \hat{Q}) \supset R(\hat{N})$ .

Proof: 1) Let  $\Sigma_c \triangleq \Sigma((A - BR^{-1}B^TK), B) = \Sigma(A_c, B)$ . Then we have  $K \in LP(\Sigma_c; \frac{1}{2}R^{-1})$  from the Riccati equation and so by Theorem 2.  $(A_c + B(\hat{M} - N)B^TK)$  is stable for all  $\hat{M} < \frac{1}{2}R^{-1}$ ,  $N = -N^T$  or  $(A - B(R^{-1} - \hat{M} + N)B^TK)$  is stable. Let  $M \triangleq R^{-1} - \hat{M} > \frac{1}{2}R^{-1}$ , and the proof is complete.

2) Let  $\hat{A}_c \triangleq (A - B(M + N)B^T K)$ . From the Riccati equation we have

$$KA_c + A_c^T K + KB(2M - R^{-1})B^T K + Q = 0.$$

Since  $(Q^{1/2}, A)$ -observable implies  $K > 0, K^{-1}$  exists, so we have

$$K(\hat{A}_c + K^{-1}(\hat{Q} + \hat{N})) + (\hat{A}_c + K^{-1}(\hat{Q} + \hat{N}))^T K + KB(2M - R^{-1})B^T K + (Q - 2\hat{Q}) \approx 0.$$

Hence, subject to the condition  $\frac{1}{2}Q > \hat{Q}$ ,  $R(\frac{1}{2}Q - \hat{Q}) \supset R(Q + \hat{N})$  it can be shown that  $(\sqrt{(Q-2\hat{Q}) + KB(2M-R^{-1})B^TK}, A_c + K^{-1}(\hat{Q} + \hat{N}))$  is observable. Thus, by Lemma 1-3),  $(\hat{A}_c + K^{-1}(\hat{Q} + \hat{N}))$  is stable.

Q.E.D.

Remark: Theorem 4-1) is a generalization of the known "gain reduction tolerance" property of LQ-optimal feedback. This interpretation is most transparent in the special case when  $R^{-1} = \operatorname{diag}(a_1, \dots, a_m)$  and  $M = \operatorname{diag}(\hat{a}_1, \dots, \hat{a}_m)$ ,  $N \equiv 0$ . Then the original individual feedback loops are of the form

$$u_i = -a_i b_i^T K$$
,  $i = 1, \cdots, m$ .

The theorem states that, in this special case, the system remains stable if the feedback gains are reduced to

$$u_i = -\hat{a}_i b_i^T K$$

so long as  $a_i > a_i$ .

More complicated cases are of course allowed.

Remark: By interpreting the additional term  $K^{-1}(\hat{Q} + \hat{N})$  as a model perturbation term  $\delta A$  of the open-loop matrix A, we can use Theorem 4-2) to perform finite perturbation sensitivity analysis.

The following simple example illustrates the usefulness of this approach.

Example: Let

$$A = \begin{bmatrix} 0.5 & 0 \\ 0 & -2 \end{bmatrix}, b = \begin{bmatrix} 1 \\ 1 \end{bmatrix}.$$

If we take

$$Q = \begin{bmatrix} 1 & 2 \\ 2 & 6 \end{bmatrix}, R = \frac{1}{2},$$

then we obtain the algebraic Riccati solution as

$$K = \begin{bmatrix} 1 & 0 \\ 0 & 1 \end{bmatrix}$$

and the feedback gain  $g^{\circ T} = -2[1 \quad 1]$ . For any

$$\delta A = \begin{bmatrix} \beta_1 & \beta_{12} + \gamma \\ \beta_{12} - \gamma & \beta_2 \end{bmatrix}$$

where

$$\gamma \in \mathfrak{R}. \quad \begin{bmatrix} \beta_1 & \beta_{12} \\ \beta_{12} & \beta_2 \end{bmatrix} < \begin{bmatrix} 0.5 & 1 \\ 1 & 3 \end{bmatrix}$$

we are assured by Theorem 4-2) that

$$\begin{bmatrix} 0.5 + \beta_1 & \beta_{12} + \gamma \\ \beta_{12} - \gamma & -2 + \beta_2 \end{bmatrix} + \alpha b g^{\bullet T}$$

is stable for all  $\alpha > \frac{1}{2}$ . Consider the following special cases:

a) 
$$\gamma = \beta_{12}, \quad \beta_1 = \beta_2 = 0.$$

we have

$$\begin{bmatrix} 0.5 & 2\beta_{12} \\ 0 & -2 \end{bmatrix} + \alpha b \mathbf{g}^{\bullet T}$$

stable for all  $\alpha > \frac{1}{2}$  and  $\beta_{12}$  such that

b) 
$$(1-\beta_{12})^2 < 1.5 \text{ or } 1-\sqrt{\frac{3}{2}} < \beta_{12} < 1+\sqrt{\frac{3}{2}}$$
.

We have

$$\begin{bmatrix} 0.5 + \beta_1 & 0 \\ 0 & -2 + \beta_2 \end{bmatrix} + \alpha b g^{\bullet T}$$

stable for all  $\alpha > \frac{1}{2}$  and  $\beta_1, \beta_2$  such that 1)  $\beta_1 < 0.5, \beta_2 < 3$  and 2) (0.5 –  $\beta_1)(3-\beta_2) > 1$ .

Thus, if  $\beta_1 = 0$ , the perturbed system is stable for all  $\beta_2 < 1$ . Other more general cases are of course allowed.

The above example thus shows that the combined effect of feedback gain reduction and perturbation or uncertainty of the open-loop system parameters (poles and coupling terms) can be tolerated by a linear quadratic design without leading to closed-loop instability. This robustness property of the LQ-feedback design deserves more attention.

#### IV. CONCLUDING REMARKS

Since further applications of the parametrization results established in this paper to reliable stabilization synthesis and decentralized stabilization coordination will be made in a future publication, we will reserve a fuller discussion of the implications of our approach until then. At this point, however, we would like to point out an important implication for practical design that is immediate: the ability to perform feedback "loop-shaping" analysis.

In any realistic synthesis problem (keeping a system stabilized, localizing particular disturbances, etc.) there is usually a large number of feasible solutions. While the use of cost-criterion optimization (e.g., LQ) in theory allows the designer to pick exactly one such solution, in practice, the difficulties of judging or fully incorporating the relevant cost considerations and their tradeoffs as well as the often gross model uncertainties and physical variabilities of the system and the controllers, necessitate further sensitivity analysis or trial-and-error "hedging" about the nominal solution. It is therefore very important in the computeraided design context that the "feasible solution space" structure be known in some details to facilitate and guide the conduct of iterative search. In this regard, a major merit of a "classical" design technique like root-locus is that it provides an explicit functional dependence of the closed-loop system structures (distribution of poles and zeros) on the control structure (feedback gain). However, such classical approaches become totally intractable when there is a multiple number of controllers, while modern "state-space" linear feedback design techniques like "pole-placement" algorithm and "dyadic-feedback" design suffer the serious drawback of providing little structural information about the solutions they generate, and moreover, such techniques are guided more by mathematical convenience than by physical interpretation.

From this perspective, the parametrization results established earlier appear to be promising in oroviding the basis for a new iterative design algorithm that will overcome the last-mentioned drawbacks.

Several wages and Darashenet ISI connected a fraguance damain

multiloop feedback design technique (the "inverse Nyquist array" method) which he motivated also as an attempt to overcome some of the above-mentioned drawbacks. His approach is in contrast with ours, which is a "time-domain" approach. It will be interesting to investigate the connection, if any, between the two approaches.

#### REFERENCES

- M. Athans, "The role and use of the stochastic linear-quadratic-Gaussian problem in control system design," *IEEE Trans. Automat. Contr.*, vol. AC-16, Dec. 1971.
   B. D. O. Anderson and J. B. Moore, *Linear Optimal Control*. Englewood Cliffs, NJ: Prentice-Hall, 1971.
- Prentice-rial, 1971.

  P. K. Wong, "On the interaction structure of linear multi-input feedback control systems," S. M. thesis, Dep. Elec. Eng. Comput. Sci., Massachusetts Inst. Technol., Cambridge, MA, 1975.

  W. M. Wonham, Linear Multivariable Control: A Geometric Approach. Berlin: Springer-Verlag, 1974.

- Springer-Verlag, 1974.

  O. Barnett, Matrices in Control Theory. New York: Van Nostrand, 1973.

  H. H. Rosenbrock, "Design of multivariable control systems using the inverse Nyquist array," Proc. Inst. Elec. Eng., vol. 116, pp. 1929–1936.

  M. G. Salonov and M. Athans, "Gain and phase margin for multiloop LQG regulators," in Proc. 1976 IEEE Conf. Decision and Control, Dec. 1976.

# Gain and Phase Margin for Multiloop LQG Regulators

MICHAEL G. SAFONOV, STUDENT MEMBER, IEEE, AND MICHAEL ATHANS, FELLOW, IEEE

Abstract—Multiloop linear-quadratic state-feedback (LQSF) regulators are shown to be robust against a variety of large dynamical linear time-invariant and memoryless nonlinear time-varying variations in open-loop dynamics. The results are interpreted in terms of the classical concepts of gain and phase margin, thus strengthening the link between classical and modern feedback theory.

#### I. INTRODUCTION

H ISTORICALLY, feedback has been used in control system engineering as a means for satisfying design constraints requiring

1) stabilization of insufficiently stable systems;

2) reduction of system response to noise;

 realization of a specific input/output relation (e.g., specified poles and zeros);

improvement of a system's robustness against variations in its open-loop dynamics.

Classical feedback synthesis techniques include procedures which ensure directly that each of these design constraints is satisfied [1], [2]. Unfortunately, the direct methods of classical feedback theory become overwhelmingly complicated for all but the simplest feedback configurations. In particular, the classical theory cannot cope simply and effectively with multiloop feedback.

Linear-quadratic-Gaussian (LQG) control theory has made the solution of many multiloop control synthesis problems relatively simple. The LQG technique [3] provides a straightforward means for synthesizing stable linear feedback systems which are insensitive to Gaussian white noise. Variations of the LQG technique have also been devised for the synthesis of feedback systems with specified poles [4, pp. 77-87], [5], [6]. Thus, the LQG technique is a valuable design aid for satisfying the first three of the aforementioned design constraints.

The results which follow show how the multivariable LQG design can satisfy constraints of the fourth type, i.e., constraints requiring a system to be robust against variations in open-loop dynamics. The linear-quadratic state-feedback regulator, which we refer to as the LQSF regulator, is considered. The robustness of LQSF regulator designs against variations in open-loop dynamics is

measured in terms of multiloop generalizations of the classical notions of gain and phase margin. Like classical gain and phase margin, the present results consider robustness as an input-output property characterizing variations in open-loop transfer functions which will not lead to closed-loop instability. Variations in system parameters (e.g., pole/zero locations) are considered by first determining how these variations map into variations in the open-loop frequency response matrix. It is shown that LQSF multivariable designs have the property of an infinite gain margin and at least  $\pm 60^{\circ}$  phase margin for each control channel. Similar results are derived for non-linear perturbations in the feedback loop.

Such robustness results may appear incorrect at first glance, especially to control engineers familiar with classical servomechanism design. It should be noted that in classical servomechanism design the nature of the compensators used (e.g., lead-lag networks) generally leads to excessive phase lag at high frequencies, so that one may never have the infinite gain margin property. However, it should be stressed that when one uses full state-variable feedback one, in effect, introduces a multitude of phase-lag-correcting zeros in the compensator without introducing corresponding lag-producing poles. It is this abundance of zeros together with the linear-quadratic optimal design procedure that results in the surprising robustness properties of LQSF designs.

Exploiting the mathematical duality between Kalman filters and linear-quadratic optimal feedback controllers, the authors have shown that the robustness results of this paper lead to conditions for the nondivergence of the estimates generated by nonlinear filters of the type considered by Gilman and Rhodes [33]; these dual results will be the topic of a future publication. In contrast to the results presented here, the dual nonlinear filtering results require the availability of an exact description of the system under consideration and hence have no comparable robustness interpretation. It can be shown that substituting the nondivergent state estimate from this type of filter for the true state in a nonlinear state feedback regulator will not destabilize the closed-loop system.

In order to provide a more detailed and realistic bridge between the classical and modern approaches, especially with respect to robustness issues, one has to examine the case in which not all state variables are available for feedback. In the modern control approach, one would then have to use a state reconstructor (Luenberger observer or constant gain Kalman filter). The overall robust-

Manuscript received April 5, 1976; revised October 21, 1976. Paper recommended by P. R. Belanger, Chairman of the IEEE S-CS Optimal Systems Committee. This work was conducted at the M.I.T. Electronic Systems Laboratory and supported in part by the NASA/AMES Research Center under Grant NGL-22-009-124 and by the AFOSR under Grant 72-2273.

The authors are with the Department of Electrical Engineering, Massachusetts Institute of Technology, Cambridge, MA 02139.

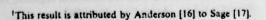
ness properties of such designs are not entirely settled as yet; they will be addressed in a future publication. Also there are interesting and as yet unresolved issues of the robustness properties of output (or limited-state) variable feedback designs using quadratic performance criteria [31].

#### II. PREVIOUS WORK

The fundamental work on the robustness of feedback systems is due to Bode [1, pp. 451-488]. Employing the Nyquist stability criterion, Bode showed how the notions of gain and phase margin can be exploited to arrive at a simple and useful means for characterizing the classes of variations in open-loop dynamics which will not destabilize single-input feedback systems. While Bode's concern was primarily with feedback amplifiers rather than control systems, his ideas have come to play a key role in the design of control systems. The control engineering implications of Bode's ideas are further developed by, for example, Horowitz [2]. Although the Nyquist criterion has been extended to multiloop feedback systems [7] and [8], there has as yet been only limited success in exploiting the multiloop version in the analysis of multiloop feedback system robustness [9]-[14].

Regarding the robustness properties specific to LQSF regulators, perhaps the most significant result is due to Anderson and Moore [4, pp. 70-76]. Exploiting the fact that single-input LQSF regulators have a return-difference greater than unity at all frequencies [15], these authors show that single-input LQSF regulator designs have ±60° phase margin, infinite gain margin, and 50 percent gain reduction tolerance. It has also been shown that the gain properties extend to memoryless nonlinear gains of the type shown in Fig. 1 ([16] and [4, pp. 96-98]). Related results by Barnett and Storey [18] and Wong [19], [35] parameterize a class of linear, constant perturbations in feedback gain which will not destabilize a multiloop LQSF regulator. A generalization of the latter result to multiloop nonlinearities in optimal nonlinear state-feedback regulators with quadratic performance index is incorrectly attributed to [16] by [20]. Insofar as the generalization stated in [20] applies to LQSF regulators, it is essentially equivalent to Theorem 1 of this paper.

Various other results have been produced which are more or less indirectly related to the question considered here. Issues related to the inverse problem of optimal control, i.e., the characterization of the properties of optimal systems, are considered by [15] and [20]-[24]. The question of sensitivity in LQSF regulators is considered by [10], [15], and [25]-[28]. The stability conditions of Zames [29], [30] involving loop gain, conicity, and positivity have many features in common with the results which are presented here.



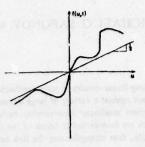


Fig. 1. Nondestabilizing nonlinear feedback gain.

#### III. DEFINITIONS AND NOTATION

The following conventions of notation and terminology are used:

- 1)  $A^{T}(x^{T})$  denotes the transpose of the matrix A (the vector x).
- 2)  $A^*$  denotes the adjoint of the matrix A (i.e., the complex-conjugate of  $A^T$ ).
- 3) We say that the function  $x:[0,\infty)\to R^n$  is square-integrable if

$$||x||^2 \equiv \int_0^\infty x^T(t)x(t)dt < \infty.$$

For all square-integrable x, the quantity ||x|| is called the norm of x.

- 4) The term operator is reserved for functions which map functions into functions. For example, a dynamical system may be viewed as an operator mapping input time-functions into output time-functions.
- 5) We say that an operator  $\mathcal{R}$  with  $\mathcal{R}0=0$  has finite gain if there exists a constant  $k < \infty$  such that

$$||\Re u|| < k||u||$$

for all square-integrable u.

6) We say that an operator mapping input time-functions into output time-functions is *nonanticipative* if the value assumed by the output function at any time  $t_0$  depends only on the values of the input-function at times  $t \le t_0$ .

7) If a function  $x:[0,\infty)\to R^n$  has the property that

$$\lim_{t\to\infty}x(t)=0,$$

then we say that x is asymptotically stable. A system of ordinary differential equations is asymptotically stable in the large if every solution is asymptotically stable.

8) If (S) denotes the system  $\dot{x}(t) = (\Im x)(t)$  where  $\Im 0 = 0$ , we say that the pair [H,S] is detectable if for each  $x:[0,\infty) \to R^n$  satisfying (S) with x not square-integrable, Hx is also not square-integrable. The significance of detectability is most apparent if we consider x(t) as a description of the internal dynamics of some physical system and (Hx)(t) as the observed output. Viewed in this manner, detectability means essentially that unstable behavior in the system's internal dynamics always results in

an output which is unstable. For example, if H is a nonsingular square matrix, then [H, S] will be detectable.

9) We say that an operator mapping time-functions into time-functions is *memoryless* if the value assumed by its output function at any instant  $t_0$  depends only upon  $t_0$  and the instantaneous value of the input function at time  $t_0$ .

10) A > 0 (A > 0) is used to indicate that the matrix A is positive definite (semidefinite).

11) We say that a rational transfer function P(s) is proper if P(s) has at least as many poles as zeros.

#### IV. PROBLEM FORMULATION

The linear-quadratic-state-feedback (LQSF) regulator problem can be formulated as follows:

$$\min_{\mathbf{n}} J(\mathbf{x}, \mathbf{u})$$
subject to
$$\dot{\mathbf{x}}(t) = A\mathbf{x}(t) + B\mathbf{u}(t), \quad \mathbf{x}(0) = \mathbf{x}_0$$

$$\mathbf{x}(t) \in \mathbb{R}^n, \mathbf{u}(t) \in \mathbb{R}^m, A \in \mathbb{R}^{n \times n}, B \in \mathbb{R}^{n \times m}$$

where the performance index J(x, u) is given by

$$J(x,u) = \int_0^\infty \left[ x^T(t) Q x(t) + u^T(t) R u(t) \right] dt$$

$$Q = Q^T > 0, \quad R = R^T > 0.$$
(2)

The optimal control  $u^*(t)$  and the associated optimal state-trajectory  $x^*(t)$  are given by

$$\dot{x}^*(t) = Ax^*(t) + Bu^*(t), \qquad x^*(0) = x_0 \\ u^*(t) = -Hx^*(t) \equiv -R^{-1}B^TKx^*(t)$$
 (\Sigma^\*)

where  $K = K^T > 0$  satisfies the Riccati equation

$$0 = KA + A^{T}K - KBR^{-1}B^{T}K + O.$$
 (3)

The minimal value of the performance index is

$$J(x^*, u^*) = x_0^T K x_0. (4)$$

The class of systems considered here are perturbed versions of  $(\Sigma^{\bullet})$  satisfying

$$\frac{d}{dt}\tilde{x}(t) = A\tilde{x}(t) + (B\tilde{\mathcal{M}}\tilde{u})(t), \qquad \tilde{x}(0) = x_0$$

$$\tilde{u}(t) = -H\tilde{x}(t)$$

$$\tilde{x}(0) = x_0$$

where A, B,  $x_0$ , and H are the same as in  $(\Sigma^*)$ . We assume that  $\mathfrak{N}$  is a finite-gain, nonanticipative operator with  $\mathfrak{N}0=0$  (see Fig. 2).<sup>2</sup>

<sup>2</sup>The condition NO=0 is not restrictive since we can always consider the dc or steady-state effects separately as is common engineering practice.

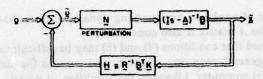


Fig. 2. Perturbed LQSF regulator  $(\tilde{\Sigma})$ .

#### V. RESULTS

The two theorems which follow quantitatively characterize the tolerance of  $(\bar{\Sigma})$  to perturbations  $\mathfrak{N}$ . It is noted that the significance of these results is not restricted to systems with perturbations originating only at the point shown in Fig. 2. Rather, it is only necessary that the system under consideration have open-loop input/output behavior which is the same as the open-loop behavior of  $(\bar{\Sigma})$ . Both of the theorems which follow have interpretations in terms of generalizations of the classical notions of gain and phase margin. The proofs are given in the Appendix.

Theorem 1 (LQSF Multiloop Nonlinear Gain Tolerance): Let the perturbation  $\mathfrak{N}$  of  $(\hat{\Sigma})$  be a memoryless, timevarying nonlinearity

$$(\mathfrak{R}\boldsymbol{u})(t) = f(\boldsymbol{u}(t), t). \tag{5}$$

If there exists a constant  $\beta > 0$  and a constant  $k < \infty$  such that

$$ku^{T}u > u^{T}f(R^{-1}u,t) > \frac{1+\beta}{2}u^{T}R^{-1}u$$
 (6)

for all  $u \in R^m$  and all  $t \in [0, \infty)$ , then

$$J(x^*, u^*) > \int_0^\infty \left[ \tilde{x}^T(t) Q \tilde{x}(t) + \beta \tilde{u}^T(t) R \tilde{u}(t) \right] dt \quad (7)$$

and if, additionally,  $[Q^{1/2}, \tilde{\Sigma}]$  is detectable then  $(\tilde{\Sigma})$  is asymptotically stable.

In Theorem 1, the least conservative stability result is obtained with  $\beta = 0$ . However, in this case, the bound (7) may be more conservative than necessary.

Theorem 2 (LQSF Multiloop Gain and Phase Margin): Let the perturbation  $\mathfrak R$  of  $(\tilde\Sigma)$  be a finite-gain, lineartime-invariant operator  $\mathfrak L$  with rational transfer function matrix L(s). If for all  $\omega$ 

$$L(j\omega)R^{-1} + R^{-1}L^{*}(j\omega) - R^{-1} > 0$$
 (8)

and if  $[Q^{1/2}, \tilde{\Sigma}]$  is detectable, then  $(\tilde{\Sigma})$  is asymptotically stable.

The results of Theorems 1 and 2 apply only in situations where the perturbation  $\mathfrak N$  is either memoryless or linear time-invariant. While this covers many interesting situations, these are not the most general results possible. In [34, Appendix B] it is shown that the stability conditions of Theorems 1 and 2 are actually special cases of a more abstract result concerning the input/output stability of a class of systems including  $(\Sigma)$  as a special case. The

possibility of nonlinear time-varying dynamical perturbations in the A-matrix is also considered.

It is noted that conditions (7) and (8) may be difficult to verify in general, requiring ingenuity and perhaps the aid of a digital computer. Likewise, the condition of detectability may not be easy to verify rigorously, though physical considerations may often make detectability a virtual certainty. In the next section, a special case is considered in which detectability is assured and (7) and (8) are relatively easy to verify.

#### VI. DISCUSSION

Theorems 1 and 2 characterize a wide class of variations in open-loop dynamics which can be tolerated by LQSF regulator designs. To appreciate the significance of these results and, in particular, their relation to classical gain and phase margin, it is instructive to consider the special case depicted in Fig. 3 in which

$$R = \operatorname{diag}(r_1, \dots, r_m) \equiv \begin{bmatrix} r_1 & 0 & \cdots & 0 \\ 0 & r_2 & \cdots & 0 \\ \vdots & \vdots & \ddots & \vdots \\ 0 & 0 & \cdots & r_m \end{bmatrix}$$
(10)

and the perturbation N satisfies

$$\mathfrak{N}_{\boldsymbol{u}} = \begin{bmatrix} \mathfrak{N}_{1} u_{1} \\ \vdots \\ \mathfrak{N}_{m} u_{m} \end{bmatrix}$$
 (11)

so that the perturbations in the various feedback loops are noninteracting. Condition (9) ensures that  $[Q^{1/2}, \tilde{\Sigma}]$  is detectable and (10) and (11) simplify the verification of conditions (7) and (8).

In this case Theorem 1 specializes to the following.

Corollary 3: If the perturbed system  $(\tilde{\Sigma})$  satisfies  $(\tilde{\Sigma})$ —(11), if each of the perturbations  $\mathcal{R}_i$  is memoryless with  $(\mathcal{R}_i u_i)(t) \equiv f_i(u_i(t), t)$ , and if for some  $k < \infty$ , some  $\beta > 0$ , and all  $t \in [0, \infty)$ ,

$$f_i(0,t) = 0$$
 (12a)

$$k > \frac{1}{u} f_i(u,t) > \frac{\beta+1}{2}$$
, for all  $u \neq 0$  (12b)

(see Fig. 1), then  $(\tilde{\Sigma})$  is asymptotically stable in the large and (7) holds.

Proof: This follows immediately from Theorem 1. 
If we consider the case in which the  $\Re$ ,'s of the system in Fig. 3 are linear time-invariant operators, then Theo-

rem 2 becomes Corollary 4.

Corollary 4: If the perturbed system  $(\tilde{\Sigma})$  satisfies (9)-(11) and if each of the perturbations  $\mathfrak{R}_i$  is linear-time-invariant with proper rational transfer function  $P_i(s)$ .

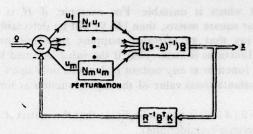


Fig. 3. LQSF regulator with noninteracting perturbations in each control loop.

**Proof:** The condition  $Re[s_j] < 0$  assures that  $\mathfrak{N}$  has finite gain. Taking  $L(s) = diag(P_i(s))$ , the result follows immediately from Theorem 2.

From Corollary 3, it is clear that the sufficient condition for stability

$$\frac{1}{u}f(u) > \frac{1}{2},\tag{13}$$

proved in [4, pp. 96-98] and [16] for single-input LQSF regulators, generalizes to multiloop systems when  $R = \text{diag}(r_1, \dots, r_m)$ .

From Corollary 4, the following two results follow directly.

Corollary 5 (LQSF  $\pm$  60° Multiloop Phase Margin): If Q and R satisfy (9) and (10), then a phase shift  $\phi_i$  with  $|\phi_i| \le 60^\circ$  in the respective feedback loops of each of the controls  $u_i$  will leave an LQSF regulator asymptotically stable in the large.

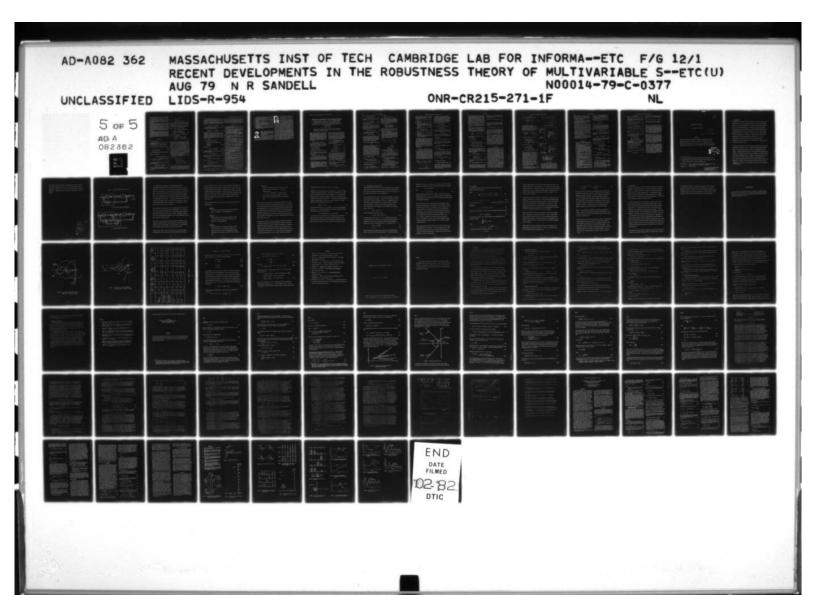
Proof: Take  $P_i(j\omega) = e^{j\phi_i(\omega)}$ . From Corollary 4, we require  $\cos\phi_i(\omega) > \frac{1}{2}$  or  $|\phi_i(\omega)| < \cos^{-1}(1/2) = 60^\circ$ .

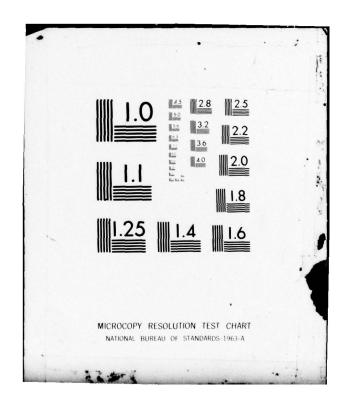
Corollary 6 (Multiloop LQSF Infinite Gain Margin and 50 Percent Gain Reduction Tolerance): If Q and R satisfy (9) and (10), then the insertion of linear constant gains  $a_i > \frac{1}{2}$  into the feedback loops of the respective controls  $u_i$  will leave an LQSF regulator asymptotically stable in the large.

Proof: Follows trivially from Corollary 4. 
Corollaries 5 and 6 are obvious multiloop generalizations of the previously established result [4, pp. 70-76] that single-input LQSF regulators have infinite gain margin, at least ±60° phase margin, and at least 50 percent gain reduction tolerance.

#### VII. CONCLUSIONS

Results have been generated which quantitatively characterize a wide class of variations in open-loop dynamics which will not destabilize LQSF regulators. A ±60° phase margin property of LQSF regulators has been established for multiloop systems (Corollary 5). The class of nondestabilizing linear feedback perturbations for multiloop LQSF regulators has been extended to include dynamical, transfer-function perturbations (Theorem 2). A nonlinearity tolerance property for LQSF regulators has been proved (Theorem 1). An upper bound on the performance





established [(7) of Theorem 1 and Corollary 3]. The latter result can be interpreted as a measure of the stability of a perturbed LQSF regulator in comparison with the unperturbed regulator. The process of generating these results has brought pertinent previous results [4, pp. 70-76, 96-98], [16], [18]-[20] together under a unified theoretical framework.

The results presented show that modern multiloop LQSF regulators have excellent robustness properties as measured by the classical criteria of gain and phase margin, thus strengthening the link between modern and classical feedback theory. Additionally, these results show that multiloop LQSF regulator designs can tolerate a good deal of nonlinearity. The quantitative nature of the results suggests that they may be useful in the synthesis of robust controllers.

Although the results presented all specify that the tolerable perturbations be measured with respect to a perfect state-measurement LQSF system, it is apparent that statements may also be made about the general LQG regulator if the effect of the Kalman filter on the system's open-loop dynamics is viewed as a component of the perturbation N.

#### APPENDIX

Proofs of Theorems 1 and 2

We begin by introducing the following notation to facilitate the proofs.

1) The inner-product space L," [0, ∞) is defined by

$$L_2^n[0,\infty) = \left\{ x | x : [0,\infty) \to R^n, \int_0^\infty x^T(t) x(t) dt < \infty \right\}$$
(A1a)

$$\langle x,y\rangle = \int_0^\infty x^T(t)y(t)dt.$$
 (Alb)

2) The extension  $L_{2}^{n}[0,\infty)$  of  $L_{2}^{n}[0,\infty)$  is defined by

$$L_{2a}^{n}[0,\infty) = \left\{ x | x : [0,\infty) \to R^{n}, \right.$$

$$\int_{0}^{\tau} x^{T}(t) x(t) dt < \infty \text{ for all } \tau \right\} \quad (A2a)$$

$$\langle x,y \rangle_{e} = \begin{cases} \langle x,y \rangle, & \text{if the integral (A1b) converges} \\ \infty, & \text{otherwise.} \end{cases}$$

(A2b)

3) The linear truncation operator  $\mathcal{P}_{\tau}: L_{2e}^{n}[0,\infty) \rightarrow L_{2}^{n}[0,\infty)$  is defined by

$$(\mathcal{T}, x)(t) = \begin{cases} x(t), & \text{if } t \in [0, \tau] \\ 0, & \text{otherwise.} \end{cases}$$
 (A3)

For brevity of notation we denote  $\mathcal{P}_{x}$  by  $x_{x}$ .

The key result in the proofs of Theorems 1 and 2 is the following.

for some  $\beta \ge 0$ 

$$(u,(2\Re -(1+\beta)I)R^{-1}u) > 0$$
 (A4)

.. .... perimination sees (-)

for all  $u \in I_{2}^{m}[0, \infty)$ , then 1)

$$x_0^T K x_0 > \langle \tilde{x}, Q \tilde{x} \rangle + \beta \langle \tilde{u}, R \tilde{u} \rangle$$
 (A5)

where  $\tilde{x}, \tilde{u}$  is the solution of  $(\tilde{\Sigma})$ , and 2) if, additionally,  $[Q^{1/2}, \tilde{\Sigma}]$  is detectable, then  $\tilde{x}$  is asymptotically stable and square-integrable.

**Proof:** For K the solution of (3) and  $\tilde{x}$  the solution of  $(\tilde{\Sigma})$  with  $\tilde{x}(0) = x_0$ , we have that for every  $\tau \in [0, \infty)$ 

$$x_0^T K x_0 = \tilde{x}^T(\tau) K \tilde{x}(\tau) - \int_0^{\tau} \frac{d}{dt} (\tilde{x}^T(t) K \tilde{x}(t)) dt$$

$$= \tilde{x}^T(\tau) K \tilde{x}(\tau) - 2 \langle K \tilde{x}_{\tau}, (A - B \mathcal{R} R^{-1} B^T K) \tilde{x}_{\tau} \rangle$$

$$> -2 \langle \tilde{x}_{\tau}, K (A - B \mathcal{R} R^{-1} B^T K) \tilde{x}_{\tau} \rangle$$

$$= \langle \tilde{x}_{\tau}, (KB(2 \mathcal{R} - I) R^{-1} B^T K + Q) \tilde{x}_{\tau} \rangle. \tag{A6}$$

Using (A4) and the fact that  $\tilde{u} = -R^{-1}B^TK\tilde{x}$ , we have

$$x_{0}Kx_{0} - \langle \tilde{\mathbf{x}}_{\tau}, Q\tilde{\mathbf{x}}_{\tau} \rangle - \beta \langle \tilde{\mathbf{u}}_{\tau}, R\tilde{\mathbf{u}}_{\tau} \rangle$$

$$> \langle \mathbf{x}_{\tau}, KB(2\mathfrak{N} - (1+\beta)I)R^{-1}B^{T}K\tilde{\mathbf{x}}_{\tau} \rangle$$

$$= \langle B^{T}K\tilde{\mathbf{x}}_{\tau}, (2\mathfrak{N} - (1+\beta)I)R^{-1}B^{T}K\tilde{\mathbf{x}}_{\tau} \rangle$$

$$> 0. \tag{A7}$$

Rearranging and taking the limit  $\tau \to \infty$ , (A5) follows. Now, suppose for the purpose of argument that  $\tilde{x}$  is not square-integrable. Since  $[Q^{1/2}, \tilde{\Sigma}]$  is detectable, this means  $(Q^{1/2}\tilde{x}_{\tau}, Q^{1/2}\tilde{x}_{\tau})$  increases without bound as  $\tau$  increases, contradicting (A5). Therefore,  $\tilde{x}$  is square-integrable. By hypothesis  $\mathfrak{N}$  and hence  $A - B \mathfrak{N} R^{-1} B^T K$  have finite gain. Thus,  $\tilde{x} = (A - B \mathfrak{N} R^{-1} B^T K) \tilde{x}$  is also square-integrable. Since both  $\tilde{x}$  and  $\tilde{x}$  are square-integrable, it follows (cf. [32, pp. 235-37]) that  $\tilde{x}$  is asymptotically stable.

Proof of Theorem 1: Equation (6) ensures that (A4) is satisfied. Since, for memoryless  $\mathfrak{N}$ ,  $\tilde{x}$  is the state of  $(\tilde{\Sigma})$  and since the initial time t=0 is not distinguished, the asymptotic stability in the large of  $(\tilde{\Sigma})$  is assured if  $\tilde{x}$  is asymptotically stable for every initial state  $\tilde{x}(0) = x_0$ . Theorem 1 follows from (4) and Theorem A1.

Proof of Theorem 2: From (8) and Parseval's theorem it follows that, for every  $u \in L_2[0,\infty)$ 

$$\langle u, (2\Re -I)R^{-1}u \rangle$$

$$= \langle u, (2\Re -I)R^{-1}u \rangle$$

$$= \frac{1}{2\pi} \int_{-\infty}^{\infty} \Re L^{*}(j\omega) (L(j\omega)R^{-1} + R^{-1}L^{*}(j\omega) - R^{-1}) \Re L(j\omega) d\omega$$

$$> 0$$
(A8)

where  $\mathfrak{A}(j\omega)$  is the Fourier transform of u. Thus, (A4) is satisfied with  $\beta = 0$ . Since  $[Q^{1/2}, \Sigma)$  is detectable, Theorem A1 implies that  $\tilde{x}$  is asymptotically stable, regardless of the value of  $x_0$ . It follows that the weighting pattern W(t)

(i.e., the response of  $(\Sigma)$  to an impulse  $I_n\delta(t)$  where  $\delta(t)$  is the Dirac delta function) is asymptotically stable. Thus, provided there are no unstable modes which are uncontrollable or unobservable, the closed-loop system is asymptotically stable in the large. Such modes correspond to "pole-zero cancellations" in the Laplace transform of W(t),

$$\mathscr{U}(s) = \left[ Is + A - BL(s)R^{-1}B^{T}K \right]^{-1}. \tag{A9}$$

The dynamics of  $(\tilde{\Sigma})$  are described (not necessarily minimally) by the differential equations

$$\begin{bmatrix} Is - A & -B \\ L_N(s)R^{-1}B^TK & L_D(s) \end{bmatrix} \begin{bmatrix} \tilde{x} \\ \tilde{u} \end{bmatrix} = 0$$
 (A10)

where s = d/dt,  $L_N(s)$  and  $L_D(s)$  are polynomial matrices satisfying  $L(s) = L_D^{-1}(s)L_M(s)$ , and the roots of det  $[L_D(s)]$ are the poles of L(s). For  $(\Sigma)$  to be asymptotically stable in the large, we require that the roots of the characteristic polynomial p(s) associated with (A10) all have negative real parts. Using a well-known matrix identity, we have from (A9) and (A10)

$$p(s) \equiv \det \begin{bmatrix} Is - A & -B \\ L_N(s)R^{-1}B^TK & L_D(s) \end{bmatrix}$$

$$= \det \begin{bmatrix} L_D(s) \end{bmatrix} \cdot \det \begin{bmatrix} Is - A + BL(s)R^{-1}B^TK \end{bmatrix}$$

$$= \frac{\det [L_D(s)]}{\det [\mathscr{M}(s)]}$$
(A11)

and therefore

$$\det\left[\mathcal{U}(s)\right] = \frac{\det\left[L_D(s)\right]}{p(s)}.$$
 (A12)

Now, from standard results on linear systems we have that W(t) is of the form

$$W(t) = \sum_{s_i \in \mathcal{C}(W)} C_i(t)e^{s_i t}$$
 (A13)

where  $C_i(t)$  are nonzero matrices of polynomials in t and the set  $\mathcal{C}(W)$  satisfies

$$P(W) - Z(W) \subseteq \mathcal{C}(W) \subseteq P(W)$$
where, in view of (A 12),
$$Z(W) \equiv \{s_i | \det [L_D(s_i)] = 0\}$$

$$P(W) \equiv \{s_i | p(s_i) = 0\}.$$
(A16)

[We call the members of Z(W) and P(W), respectively. the zeros and the poles of  $\mathfrak{A}(s)$ .] Since W(t) is square-integrable.

$$Re[s_i] < 0$$
, for all  $s_i \in \mathcal{C}(W)$ . (A15)

From (A12) and (A14) it follows that except for roots

that all the roots of  $det[L_D(s)]$  have negative real parts. Thus any cancellations in (A12) can involve only roots with negative real parts. We conclude that all the roots of the characteristic polynomial p(s) have negative real parts. and, hence, (\(\Sigma\) is asymptotically stable in the large.

#### REFERENCES

- H. W. Bode, Network Analysis and Feedback Amplifier Design. New York: Van Nostrand, 1945. [1]
- I. M. Horowitz, Synthesis of Feedback Systems. New York: [2]
- Academic, 1963.

  M. Athans, "The role and use of the stochastic linear-quadratic-Gaussian problem in control system design," IEEE Trans. Automat. Contr., vol. AC-16, pp. 529-552, Dec. 1971.

  B. D. O. Anderson and J. B. Moore, Linear Optimal Control Englewood Cliffs, NJ: Prentice-Hall, 1971.

  C. H. Houpis and C. T. Constantinides, "Relationship between
- conventional-control-theory figures of merit and quadratic performance index in optimal control theory for a single-input/single-output system," Proc. Inst. Elec. Eng., vol. 120, pp. 138-142, July 1973
- [6]
- 1973.

  M. A. Woodhead and B. Porter, "Optimal modal control," Trans. Inst. Meas. Contr., vol. 6, pp. 301-303, 1973.

  H. H. Rosenbrock, "Design of multivariable control systems using inverse Nyquist array," Proc. Inst. Elec. Eng., vol. 116, pp. 1929-1936, 1969.

  P. D. McMorran, "Extension of the inverse Nyquist method," Electron. Lett., vol. 6, pp. 800-801, 1970.

  J. J. Belletrutti and A. G. J. MacFarlane, "Characteristic loci techniques in multivariable-control-system design," Proc. Inst. Elec. Eng., vol. 118, pp. 1291-1296, 1971.

  A. G. J. MacFarlane, "Return-difference and return-ratio matrices and their use in the analysis and design of multivariable feedback

- and their use in the analysis and design of multivariable feedback control systems," Proc. Inst. Elec. Eng., vol. 117, pp. 2037-2049, Oct. 1970.
- [11] H. H. Rosenbrock, "Progress in the design of multivariable control systems," Trans. Inst. Meas. Contr., vol. 4, pp. 9-11, 1971.

  (A11) [12] A. G. J. MacFarlane, "A survey of some recent results in linear multivariable feedback theory," Automatica, vol. 8, pp. 455-492,

  - 1972.

    A. G. J. MacFarlane and J. J. Belletrutti, "The characteristic locus design method," Automatica, vol. 9, pp. 575-588, 1973.

    I. Horowtiz and M. Sidi, "Synthesis of cascaded multiple-loop feedback systems with large plant parameter ignorance," Automatica, vol. 9, pp. 589-600, Sept. 1973.

    R. E. Kalman, "When is a linear control system optimal," Trans. ASME (J. Basic Eng.), vol. 86, pp. 51-60, Mar. 1964.

    B. D. O. Anderson, "Stability results for optimal systems," Electron. Lett., vol. 5, p. 545, Oct. 1969.

    A. P. Sage, Optimum Systems Control. Englewood Cliffs, NJ: Prentice-Hall, 1968.

    S. Barnett and C. Storey. "Insensitivity of optimal linear control."
  - [15]
  - [16]

  - [18]
  - S. Barnett and C. Storey, "Insensitivity of optimal linear control systems to persistent changes in parameters," Int. J. Contr., vol. 4, pp. 179-184, 1966.

    P. K. Wong, "On the interaction structure of multi-input feedback control systems," M. S. thesis, Massachusetts Inst. Technol., Cambridge, MA, Sept. 1975.

  - [20] P. J. Moylan and B. D. O. Anderson, "Nonlinear regulator theory and an inverse optimal control problem," *IEEE Trans. Automat. Contr.*, AC-18, pp. 460-465, Oct. 1973.
    [21] B.D.O. Anderson, "The inverse problem of optimal control," Stanford Electron. Lab., Stanford, CA, Rep. SEL-66-038 (TR.)
- (A14) [22]
- Stanford Lab., Stanford, CA, Rep. SEL-60-038 (TR 6560-3), Apr. 1966.

  B. P. Molinari, "The stable regulator and its inverse," IEEE Trans. Automat. Contr., vol. AC-18, pp. 454-459, Oct. 1973.

  J. C. Willems, "Least squares optimal control and the algebraic Riccati equation," IEEE Trans. Automat. Contr., vol. AC-16, pp.
  - 621-634. Dec. 1971. R. Yokoyama and E. Kinnen, "The inverse problem of the optimal regulator," *IEEE Trans. Automat. Contr.*, vol. AC-17, pp. 497-504,
  - R. Yokoyama and E. Killien, regulator," IEEE Trans. Automat. Contr., vol. AC-17, pp. 497-504, Aug. 1972.

    W. R. Perkins and J. B. Cruz, "The parameter variation problem in state feedback control systems," Trans. ASME (J. Basic Eng.), vol. 87, pp. 120-124, Mar. 1965.

    —, "Feedback properties of linear regulators," IEEE Trans. Automat. Contr., vol. AC-16, pp. 659-664, Dec. 1971.

    J. B. Cruz, Ed., Feedback Systems. New York: McGraw-Hill, 1972.
  - 1261
  - [27]
  - System Sensitivity Analysis. Stroudsburg. PA: Dowden. [28]

---, "On the input-output stability of time-varying nonlinear feedback systems—Part II: Conditions involving circles in the frequency plane and sector nonlinearities," *IEEE Trans. Automat. Contr.*, vol. AC-11, pp. 465-476, July 1966.

[31] W. S. Levine and M. Athans, "On the determination of the optimal constant output-feedback gains for linear multivariable systems," *IEEE Trans. Automat. Contr.*, vol. AC-15, pp. 44-48, Ed. 1970.

[32] C. A. Desoer and M. Vidyasagar, Feedback Systems: Input-Output

[32] C. A. Descer and M. Vidyasagar, Peedodrk Systems: Input-Output Properties. New York: Academic, 1975.
[33] A. S. Gilman and I. S. Rhodes, "Cone-bounded nonlinearities and mean-square bounds—estimation upper bounds," IEEE Trans. Automat. Contr., vol. AC-18, pp. 260-265, June 1973.
[34] M. G. Salonov and M. Athans, "Gain and phase margin for multiloop LQG regulators," in Proc. 1976 IEEE Conf. Decision and Control. Dec. 1976.

Control, Dec. 1976.
P. K. Wong and M. Athans, "Closed-loop structural stability for linear-quadratic optimal systems," in Proc. 1976 IEEE Conf. Decision and Control, Dec. 1976; also IEEE Trans. Automat. Contr., vol. AC-22, pp. 94-99, Feb. 1977.



Michael G. Salonov (M'73-S'76) was born in Pasadena, CA, on Nov. 1, 1948. He received the B.S., M.S., and Engineer degrees in electrical engineering from the Massachusetts Institute of Technology, Cambridge, MA, in 1971, 1971, and 1976 respectively.

From 1972 to 1975 he was on active duty in the US Naval Reserve. Since 1975 he has been at the Massachusetts Institute of Technology where he is presently a Research Assistant and Ph.D. candidate. Currently he is working on

methods for the synthesis of robust multivariable feedback systems. Mr. Sasonov is a member of Tau Beta Pi, Eta Kappa Nu, and Sigma



Michael Athans (S'58-M'61-SM'69-F'73) was born in Drama, Greece, on May 3, 1937. He received the B.S., M.S., and Ph.D. degrees in electrical engineering from the University of California, Berkeley.

From 1961 to 1964 he was employed by the M.I.T. Lincoln Laboratory, Lexington, MA. In 1964 he joined the faculty of the Department of Electrical Engineering at the Massachusetts Institute of Technology where he currently has the rank of Professor and Director of the M.I.T.

Electronics Systems Laboratory. He has been a consultant to the M.I.T. Lincoln Laboratory; Bell Aerosystems, Buffalo, NY; Bolt, Beranek and Newman, Cambridge, MA; Hamilton-Standard, Windsor Locks, CT; Systems Control, Inc., Palo Alto, CA; the U.S. Army Material Command; and the Analytic Sciences Corporation, Reading, MA. His current research interests involve the theory and applications of optimal control and estimation techniques to aerospace, transportation, communications and socioeconomic systems. He is the co-author of more than 100 articles and co-author of the books Optimal Control (New York: McGraw-Hill, 1966), Systems, Networks and Computation: Basic Concepts (New York: McGraw-Hill, 1972), and Systems, Networks and Computation: Multivariable Methods (New York: McGraw-Hill, 1974).

Dr. Athans is a member of AAAS, Phi Beta Kappa, Eta Kappa Nu, and Sigma Xi. He was the recipient of the 1964 Donald P. Eckman Award. In 1969 he received the first Frederick Emmons Terman Award as the outstanding young electrical engineer educator, presented by the Electrical Engineering Division of the American Society for Engineering Education. He received honorable mention for a paper he co-authored for the 1971 Joint Automatic Control Conference. He has been Program Chairman of the 1968 Joint Automatic Control Conference and a member of several committees of AACC and the IEEE. From 1972 to 1974 he was the President of the IEEE Control Systems Society. At present he is Associate Editor of the IFAC journal Automatica and IEEE delegate to the American Automatic Control Council.

# Optimal Low-Sensitivity Linear Feedback Systems\*

Systèmes linéaires à réaction à sensibilité optimalement faible Optimale lineare Feedback systeme geringer Empfindlichkeit Линейные системы с обратной связью имеющие оптимальномалую чувствительность

#### H. KWAKERNAAK†

By choosing in the stochastic linear regulator problem the matrix which weights the input as the zero matrix, feedback filters may be obtained which make the closed-loop system insensitive in the sense of Cruz-Perkins.

Summary—The paper considers the stochastic linear regulator and tracking problem for multivariable time-invariant systems. It is shown that in the limiting case, where the matrix weighting the input in the quadratic criterion is the zero matrix, the closed-loop system is insensitive to parameter variations in the sense of Cruz-Perkins, provided that the system to be controlled is minimum-phase. The weighting matrix in the Cruz-Perkins sensitivity criterion turns out to be the inverse of the covariance matrix of the measurement noise. A simple example illustrates the decrease of sensitivity obtained for a system with two inputs and two outputs.

#### 1. INTRODUCTION AND MOTIVATION

KALMAN's optimal linear control and filtering theory (KALMAN [1], KALMAN and BUCY [2], WONHAM [3]) make it possible to design multivariable linear feedback systems which exhibit

- (a) Overall system stability;
- (b) Optimal transient behavior;
- (c) Optimal immunity against disturbances and noise.

It is the purpose of this paper to demonstrate that in addition to these a fourth objective may be achieved, namely

#### (d) Insensitivity to parameter variations.

In the literature a number of papers have appeared on the design of low-sensitivity linear feedback systems by state space techniques (ANDERSON [4], PORTER [5], HERNER [6], KAHNE [7], TUEL et al.

# 2. REVIEW OF STOCHASTIC LINEAR OPTIMAL CONTROL THEORY

Consider a linear time-invariant system described by the following equations

$$\dot{x}(t) = Ax(t) + Bu(t) + v(t) \tag{1}$$

$$z(t) = Dx(t) \tag{2}$$

$$y(t) = Cx(t) + w(t)$$
 (3)

$$E(v(t_1)v(t_2)') = N_v \delta(t_1 - t_2)$$
 (4)

$$E(w(t_1)w(t_2)') = N_w \delta(t_1 - t_2).$$
 (5)

Here x(t) is the state of the system; v(t) and w(t) are uncorrelated multidimensional white noise processes, with zero mean; A, B, C, D,  $N_v$  and  $N_w$  are constant matrices; the prime denotes the transpose. Furthermore z(t) indicates the output to be controlled; y(t) is the observed output.

It is well-known [3] that an optimal estimate  $\mathcal{L}(t)$  of the state may be obtained as follows

$$\dot{x}(t) = (A - PC'N_{w}^{-1}C) \qquad Bu(t) + PC'N_{w}^{-1}y(t) \quad (6)$$

where P is the asymptotic solution for  $t \rightarrow \infty$  of the matrix Riccati equation

$$\dot{P}(t) = -P(t)C'N_w^{-1}CP(t) + AP(t) + P(t)A' + N_v,$$

$$P(t_0) = 0,$$
(7)

<sup>[8],</sup> Rao et al. [9], and others). It seems not to have been noted, however, that by choosing the weighting matrix for the input in the quadratic criterion for the stochastic regulator problem very small, low-sensitivity controllers may be obtained for time-invariant minimum-phase systems. This idea is developed in this paper and an example is presented which shows how this property may be exploited.

<sup>\*</sup> Received 17 September 1968 and in revised form 23 December 1968. The original version of this paper was presented at the IFAC Symposium held in Dubrovnik, Yugoslavia in August 1968. It was recommended for publication by associate editor P. Kokotović.

<sup>†</sup> Department of Mathematics and Department of Applied Physics, University of Technology (Technische Hogeschool), Delft, Notherlands.

If the system is to be controlled such that

$$E[z(t)'z(t) + u(t)'Lu(t)]$$
 (8)

is minimal (L is a weighting matrix) the input must be chosen as

$$u(t) = -L^{-1}B'\bar{Q}\hat{x}(t) \tag{9}$$

where  $\overline{Q}$  is the asymptotic solution of another matrix Riccati equation [1].

In this paper the main interest is in feedback controller which is optimal for L=0. This may be found as follows. Suppose that r(t) is an external reference input for the controlled output z(t), and consider the criterion

$$E\{[z(t)-r(t)]'[z(t)-r(t)]\}. \tag{10}$$

It is not difficult to show that this is minimized if the system is controlled such that

$$\hat{z}(t) = r(t) \quad \text{for all } t \tag{11}$$

where  $\hat{z}(t)$  is the conditional expectation of z(t) given all past observations of the measured output. Since  $\hat{z}(t) = D\hat{x}(t)$  condition (11) may be expressed in terms of Laplace transforms by eliminating  $\hat{x}(t)$  from (6) after Laplace transformation. It follows, assuming zero initial conditions,

$$D(sI - A + \overline{P}C'N_w^{-1}C)^{-1}[BU(s) + \overline{P}C'N_w^{-1}Y(s)]$$
= R(s). (12)

Bold capitals indicate the Laplace transforms of the corresponding lower case time-functions.

One can solve U(s) from this equation if u(t), z(t) and r(t) have the same dimension. If the dimension of u(t) is smaller than that of z(t) and r(t), generally no solution exists which satisfies (12) for all s. If the dimension of u(t) is greater than that of z(t) and r(t) many solutions exist and the problem may be modified by increasing the number of outputs to be controlled. Assuming that u(t), z(t) and r(t) have the same dimension one finds

$$\mathbf{U}(s) = -\mathbf{G}(s)\mathbf{Y}(s) + H(s)\mathbf{R}(s) \tag{13}$$

where

$$G(s) = [D(sI - A + PC'N_{w}^{-1}C)^{-1}B]^{-1}$$

$$D(sI - A + PC'N_{w}^{-1}C)^{-1}PC'N_{w}^{-1}$$
 (14)

$$H(s) = [D(sI - A + \overline{P}C'N_w^{-1}C)^{-1}B]^{-1}.$$
 (15)

This solution is valid provided

$$[D(sI-A+PC'N_w^{-1}C)^{-1}B]^{-1}$$

exists (except at a finite number of values of s.)

This is the case if

$$\det[D(sI-A+\overline{P}C'N_w^{-1}C)^{-1}B]$$

does not vanish identically in s as indicated in BROCKETT and MESAROVIĆ [15]. For the case where C=D, where the observed output is precisely the controlled output, a condition for this may be found as follows. After some manipulations involving the relation (A.2) one obtains

$$\det[D(sI - A + PC'N_w^{-1}C)^{-1}B] = \frac{\det[D(sI - A)^{-1}B]\det(sI - A)}{\det(sI - A + PD'N_w^{-1}D)}.$$
 (15a)

It immediately follows that the inverse exists provided  $\det[D(sI-A)^{-1}B]$  does not vanish identically in s. If  $C \neq D$  it does not seem easy to find such an explicit condition.

The system arrangement is shown in Fig. 1. In section 3 it will be investigated under which conditions the feedback filter G(s) is indeed optimal and can be considered as the limit filter for  $L\rightarrow 0$ . In section 4 it will be shown that this filter possesses an interesting property with respect to the system sensitivity to parameter variations.

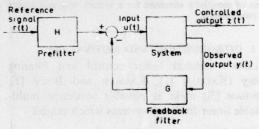


Fig. 1. Basic system configuration.

#### 3. STABILITY

For the feedback arrangement of Fig. 1 one can write for the input to the system

$$U(s) = -G(s)Y(s) + H(s)R(s) + U_0(s)$$
 (16)

where  $U_0(s)$  represents the combined effects of the initial conditions of feedback filter and prefilter. By Laplace transformation of (1) (2) and (3) one can derive

$$\mathbf{U} = (I + G\Phi)^{-1}H\mathbf{R} - (I + G\Phi)^{-1}G\Psi(\mathbf{V} + \mathbf{x_0})$$
$$-(I + G\Phi)^{-1}G\mathbf{W} + (I + G\Phi)^{-1}\mathbf{U_0}$$
(17)

$$Z = \Phi_{I}(I + G\Phi)^{-1}H\mathbf{R} + [\Psi_{I} - \Phi_{I}(I + G\Phi)^{-1}G\Psi](\mathbf{V} + \mathbf{x}_{0}) - \Phi_{I}(I + G\Phi)^{-1}G\mathbf{W} + \Phi_{I}(I + G\Phi)^{-1}\mathbf{U}_{0}$$
 (18)

where the Laplace variable s has been omitted,  $x_0$  is the initial state of the system, and

$$\Phi(s) = C(sI - A)^{-1}B$$
,  $\Psi(s) = C(sI - A)^{-1}$   
 $\Phi_1(s) = D(sI - A)^{-1}B$ ,  $\Psi_1(s) = D(sI - A)^{-1}$ . (19)

From these relations it is shown in Appendix A that the control system is stable if the following, sufficient, conditions are satisfied:

- (i) The system  $\dot{x} = Ax + Bu$  is completely controllable:
- (ii) The system  $\dot{x} = Ax$ , y = Cx is completely observable;
- (iii) One can write  $N_p = FN_0F'$ , where  $N_0$  is a constant positive-definite matrix and F, a constant but not necessarily square matrix, such that the system  $\dot{x} = Ax + Fu$  is completely controllable;
- (iv) The system  $\dot{x} = Ax + Bu$ , z = Dx is minimumphase, i.e.

$$\det[D(sI-A)^{-1}B] \tag{20}$$

has all of its zeroes in the left half complex plane;

- (v) The system  $\dot{x} = Ax$ , z = Dx is completely observable;
- (vi) A minimal realization [10] is used to implement the joint transfer matrix [-G(s), H(s)] of the prefilter and feedback filter.

The most restrictive of these requirements seems the minimum-phase property (iv). It is well-known [11] that the optimal feedback law (9) always yields a stable feedback system if the conditions (i), (ii), (iii) and (v) are satisfied. Therefore the minimum-phase property is the extra requirement which is needed to ensure that (14) is indeed the limiting feedback filter for  $L\rightarrow 0$  which results from the optimal control law (9) in conjunction with the optimal filter (6).

### 4. SENSITIVITY TO SYSTEM VARIATIONS

It is shown in this section that the feedback filter (14) makes the control system insensitive to parameter variations. The approach which is taken to sensitivity is that of CRUZ and PERKINS [12]. Feedback can only effectively reduce the sensitivity of the control system if the controlled output itself is fed back. Consider therefore the configuration of Fig. 2 and suppose that the system transfer matrix changes to  $\Phi(s) = \Phi(s) + \Delta \Phi(s)$ . Let  $\Delta Z_c(s)$  denote the corresponding change of the closed-loop

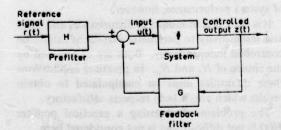


Fig. 2. System configuration for sensitivity study.

system response to a given command signal. Let  $\Delta Z_0(s)$  denote the corresponding change of response of an open-loop configuration consisting of a filter K(s) in series with the system such that the nominal overall transfer matrix  $K(s)\Phi(s)$  is precisely the nominal overall transfer matrix of the closed-loop system. Cruz and Perkins have demonstrated that  $\Delta Z_c(s)$  and  $\Delta Z_0(s)$  are related by

$$\Delta \mathbf{Z}_c(s) = S(s)\Delta \mathbf{Z}_0(s) \tag{21}$$

where the sensitivity matrix S(s) is given by

$$S(s) = [I + \tilde{\Phi}(s)G(s)]^{-1}$$
. (22)

To measure the difference in sensitivity of the closed-loop and the open-loop system the quantity

$$E[\Delta z(t)'R\Delta z(t)] \tag{23}$$

may be used, where R is some nonnegative-definite matrix. If  $\Delta z_0(t)$  is a stationary random process,

$$E[\Delta z_c(t)'R\Delta z_c(t)]$$

$$= tr \left\{ \int_{-\infty}^{\infty} [S(-j2\pi f)'RS(j2\pi f)] V_0(f) df \right\}$$
 (24)

where  $V_0(f)$  is the power spectral density matrix of  $\Delta z_0(t)$  and tr denotes the trace of a matrix. Similarly one finds

$$E[\Delta z_0(t)'R\Delta z_0(t)] = tr \left\{ \int_{-\infty}^{\infty} RV_0(f) df \right\}.$$
 (25)

Now suppose that

$$S(-j2\pi f)'RS(j2\pi f) \leq R$$
 for all  $f$  (26)

i.e. the matrix  $S(-j2\pi f)'RS(j2\pi f)-R$  is non-positive-definite for all frequencies. The spectral density matrix  $V_0(f)$  is Hermitian; by expanding it in terms of its eigenvectors it is not difficult to show that (26) implies

$$tr\{S(-j2\pi f)'RS(j2\pi f)V_0(f)\} \le tr\{RV_0(f)\}$$
  
for all f. (27)

This means that if (26) is satisfied

$$E[\Delta z_c(t)'R\Delta z_c(t)] \le E[\Delta z_0(t)'R\Delta z_0(t)]. \tag{28}$$

Thus relation (26) is a sufficient condition for the reduction of the sensitivity of the closed-loop system as compared to the open-loop system to variations in the system transfer matrix for all types of command signals.

It is known from the work of KALMAN [11] and KREINDLER [16] that the *deterministic* optimal linear regulator possesses excellent sensitivity characteristics in the sense that a criterion of the form (26) is satisfied. It is very easy to show by a counter-example, however, where a simple one-dimensional system suffices, that for the *stochastic* optimal regulator a condition of the form (26) does not generally hold for all frequencies. In the following it will be shown that a condition of the form (26) is satisfied for the proposed feedback filter of section 3 which has been obtained for the limiting case L=0.

To apply the Cruz-Perkins approach to the system of section 3, it is assumed that in the configuration of Fig. 1 the observed output includes the controlled output in the sense that the matrix C and correspondingly  $N_w$  can be partitioned as

$$C = \begin{pmatrix} D \\ M \end{pmatrix}, \qquad N_{\mathbf{w}} = \begin{pmatrix} N_{\mathbf{w}1} & 0 \\ 0 & N_{\mathbf{w}2} \end{pmatrix}. \tag{29}$$

Accordingly, the transfer matrix of the filter G(s) can be written as

$$G(s) = [G_1(s)G_2(s)]$$
 (30)

with

$$G_1(s) = [D(sI - A + \overline{P}C'N_w^{-1}C)^{-1}B]^{-1}$$

$$D(sI - A + \overline{P}C'N_w^{-1}C)^{-1}\overline{P}D'N_{w1}^{-1}$$
 (31)

$$G_2(s) = [D(sI - A + \overline{P}C'N_w^{-1}C)^{-1}B]^{-1}$$

$$D(sI - A + \overline{P}C'N_w^{-1}C)^{-1}\overline{P}M'N_{w2}^{-1}. (32)$$

The system has a main feedback loop with  $G_1(s)$  and a minor loop with  $G_2(s)$ . (Fig. 3) For the purpose of studying the sensitivity the minor combined with the plant to a block with overall loop is transfer matrix

$$\Phi_1(s)[I+G_2(s)\Phi_2(s)]^{-1}$$
 (33)

where

$$\Phi_1(s) = D(sI - A)^{-1}B,$$
  
 $\Phi_2(s) = M(sI - A)^{-1}B.$  (34)

The sensitivity matrix for this configuration thus has the form

$$S(s) = \{I + \Phi_1(s)[I + G_2(s)\Phi_2(s)]^{-1}G_1(s)\}^{-1}.$$
 (35)

The sensitivity matrix will be studied at the nominal value of the system transfer matrix rather than at the actual value on the basis of the assumption that the deviations from the nominal value are relatively small. It is shown in Appendix B that for the proposed  $G_1(s)$  and  $G_2(s)$  the sensitivity matrix takes the form

$$S(s) = [I + D(sI - A + \bar{P}M'N_{w2}^{-1}M)^{-1}\bar{P}D'N_{w1}^{-1}]^{-1}.$$
(36)

Starting from the Riccati equation (7) for the asymptotic variance matrix  $\vec{P}$ , it is also derived in Appendix B that the sensitivity matrix satisfies the inequality

$$S(-j2\pi f)'N_{w1}^{-1}S(j2\pi f) \le N_{w1}^{-1}$$
 for all  $f$ . (37)

This is a relation of the form (26), which demonstrates that if  $N_{w1}^{-1}$  is used as the weighting matrix in the sensitivity criterion, the feedback filter proposed in section 3 decreases the sensitivity of the control system to variations in the system transfer matrix.

The fact that the weighting matrix R should be chosen as  $N_{w1}^{-1}$  is not entirely surprising. If, for the sake of argument,  $N_{w1}$  is supposed to be diagonal, a small value of one of the diagonal elements means that the measurement errors at the corresponding output are small and consequently the admissible gain in the associated feedback loop will be high. The effects of system variations will therefore be smaller at this output than at other outputs. This is reflected in a correspondingly large weighting factor in the sensitivity criterion.

#### 5. DISCUSSION

In the preceding sections it has been shown that by letting the weighting matrix L go to zero, feedback filters may be obtained which reduce the sensitivity of the system, provided the system is minimum-phase. Since the feedback and feedforward filters (14) and (15) usually are differentiating filters, it is practical to use a feedback filter which is optimal for a suitably small L. Just how small L should be can be determined by considering the extra poles which are introduced into the feedback filter. Choosing L>0 will cause the sensitivity reduction criterion (26) to be violated, usually in the high frequency range, without a great loss of system performance, however.

It is clear that immunity to disturbances and noise and insensitivity to parameter variations cannot be controlled independently. Both are determined by the choice of  $N_{\nu}$  and  $N_{\nu}$ . In practical applications these quantities must be manipulated to obtain results which are in both respects satisfactory.

The problem of choosing a practical prefilter H(s) is not difficult and is not considered here.

#### 6. EXAMPLE

Consider a system with transfer matrix

$$\begin{bmatrix}
\frac{k_1 k_2}{s(s+1)} & \frac{k_2}{s+1} \\
\frac{k_1}{s} & 0
\end{bmatrix}$$
(38)

The nominal parameter values are  $k_1 = k_2 = 1$ . The disturbances are represented as white noise n with covariance matrix  $N_n$  which is added to the input u. For the calculations  $N_n$  was chosen as the identity matrix. Numerical solutions\* were obtained for the cases

$$N_{w} = \begin{pmatrix} 0.05 & 0 \\ 0 & 0.05 \end{pmatrix} \qquad N_{w} = \begin{pmatrix} 0.005 & 0 \\ 0 & 0.05 \end{pmatrix}.$$
 (case 2)

For the first case the solution was found to be

$$G(s) = \begin{pmatrix} 0.4881 & 4.445 \\ 3.662 & 0.4881 \end{pmatrix}$$

$$H(s) = \begin{pmatrix} 0.4881 & s + 4.445 \\ s + 4.662 & -0.5119 \end{pmatrix}. (40)$$

The solution of the second case is

$$G(s) = \begin{pmatrix} 2.354 & 4.410 \\ 13.32 & 0.2354 \end{pmatrix}$$

$$H(s) = \begin{pmatrix} 2.354 & s + 4.410 \\ s + 14.32 & -0.7646 \end{pmatrix}. \tag{41}$$

There is no need to introduce extra poles into the feedback filter since it does not contain any differentiating elements. The differentiating character of the prefilter can be eliminated by simply omitting the terms with s in the transfer matrix H(s); this is equivalent to introducing two far-off poles into the off-diagonal terms of the prefilter transfer matrix. Figure 4 shows the matrix of step responses for both cases for different values of the gains  $k_1$  and  $k_2$  as obtained by analog computer simulation. It is seen that the decrease in the 11-element of the matrix  $N_w$  effects a decrease of the sensitivity of the output  $z_1$  in agreement with the argument at the end of section 4.

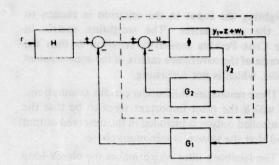
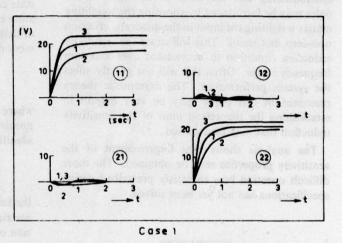


Fig. 3. Detailed system configuration.



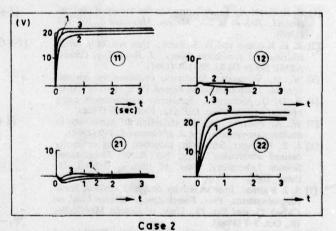


Fig. 4. Matrix of step responses of feedback system

Curve 1: Nominal gains,  $k_1=k_2=1$ Curve 2: Halved gains,  $k_1=k_2=0.5$ Curve 3: Doubled gains,  $k_1=k_2=2$ Command signal step amplitude 20 V.

### 7. CONCLUSIONS

The results of this paper show that for linear time-invariant systems a feedback filter may be found which renders the closed-loop system insensitive to parameter variations in the sense of Cruz-Perkins. This feedback filter follows from the stochastic linear regulator theory when the matrix

<sup>•</sup> The author is greatly indebted to Mr. R. C. W. Strijbos for writing and improving the programs which were developed for computing the optimal filters.

weighting the input in the criterion is chosen to be the zero matrix. The weighting matrix in the Cruz-Perkins sensitivity criterion is then the inverse of the covariance matrix of the measurement noise, which is not surprising.

These results are valid under certain assumptions, of which the most important seem to be that the controlled output is included in the observed output and that the system is minimum-phase.

The feedback filter which makes the closed-loop system insensitive often turns out to be violently differentiating and therefore unrealizable. Extra poles may be introduced by choosing the weighting matrix weighting the input in the quadratic criterion non-zero, but small. This will cause the sensitivity reduction condition to be violated over a certain frequency range. Often this will not greatly affect the system performance. The asymptotic theory presented in this paper may be very helpful in establishing the theoretical limit of the sensitivity reduction that may be achieved.

The analysis shows that improvement of the sensitivity properties may be obtained. The more difficult question how to satisfy prescribed design specifications has not yet been solved.

#### REFERENCES

- [1] R. E. KALMAN: Contributions to the theory of optimal control. Bol. de la Soc. Matem. Mexicana 5, 102-119 (1960).
- [2] R. E. KALMAN and R. S. BUCY: New results in linear filtering and prediction theory. J. Basic Eng. (Trans. ASME Series D) 83, 95-108 (1961).
- [3] W. M. WONHAM: Stochastic problems in optimal control. IEEE Convention Record, Pt. 2, 114-124 (1963).
- [4] B. D. O. ANDERSON: Sensitivity improvement using optimal design. Proc. IEE 113, 1084-1086 (1966).
  [5] W. A. PORTER: On the reduction of sensitivity in
- multivariate systems. Int. J. of Control 5, 1-9 (1967).
- [6] J. P. HERNER: Sensitivity reduction using optimally derived controllers. Rept. No. R.353, Coordinated Science Laboratory, Univ. of Illinois, Urbana, Ill. (May, 1967).
- [7] S. J. KAHNE: Low sensitivity design of optimal linear control systems. Proc. Fourth Annual Allerton Conf. on Circuit Th. and Sys. Th., Univ. of Illinois, Monticello, III., Oct. 5-7 (1966).
- [8] W. G. TUEL, I. LEE and P. M. DERUSSO: Synthesis of optimal control systems with sensitivity constraints. Proc. Third IFAC Congress, London (1966).
- [9] D. M. RAO, M. D. SRINATH and Y. Fu: Sensitivity in linear systems. Trans. Soc. Instr. Tech. 17, 150-154 (1965).
- [10] R. E. KALMAN: On structural properties of linear, constant, multivariable systems. Proc. Third IFAC
- Congress, London (1966).
  [11] R. E. KALMAN: When is a linear control system optimal? J. Basic Eng. (Trans. ASME Series D) 86, 51-60 (March 1964).
- [12] J. B. CRUZ and W. R. PERKINS: A new approach to the sensitivity problem in multivariable feedback system design. IEEE Trans. Aut. Control 9, 216-223 (July, 1964).
- [13] L. A. ZADEH and C. A. DESOER: Linear system theory: The state space approach, McGraw-Hill, N.Y. (1963).

- [14] M. K. SAIN: On the control application of a determinant equality related to eigenvalue computation. IEEE Trans. Aut. Control 11, 109-111 (1966).
- [15] R. W. BROCKETT and M. D. MESAROVIĆ: producibility of multivariable Systems. J. Math. Anal. Appl. 11, 548-563 (1965).
- E. KREINDLER: Closed-loop sensitivity reduction of linear optimal control systems. IEEE Trans. Aut. Control 13, 254-262 (1968).

### APPENDIX A

Stability of the control system

If a system is completely controllable any initial state can be reached instantaneously by the application of a suitable linear combination of derivatives of delta functions ([13], Ch. 11). Condition (vi) of section 3 therefore implies that one may write

$$U_0(s) = -G(s)q_1(s) + H(s)q_2(s)$$
 (A.1)

where  $q_1(s)$  and  $q_2(s)$  are suitable vector polynomials in s. By repeatedly using the matrix identity [14]

$$(I+AB)^{-1}=I-A(I+BA)^{-1}B$$
 (A.2)

the following expressions for the various transfer matrices occurring in (17) and (18) [after substitution of (A.1)] are obtained

$$(I+G\Phi)^{-1}H = [D(sI-A)^{-1}B]^{-1}$$
 (A.3)

$$(I+G\Phi)^{-1}G\Psi = [D(sI-A)^{-1}B]^{-1}$$

$$D(sI-A+PC'N_w^{-1}C)^{-1}$$

$$PC'N_w^{-1}C(sI-A)^{-1}$$
(A.4)

$$(I+G\Phi)^{-1}G = [D(sI-A)^{-1}B]^{-1}$$

$$D(sI-A+PC'N_w^{-1}C)^{-1}PC'N_w^{-1}$$
(A.5)

$$\Phi_{i}(I+G\Phi)^{-1}H=I \tag{A.6}$$

$$\Psi_{1} - \Phi_{1}(I + G\Phi)^{-1}G\Psi = D(sI - A + \overline{P}C'N_{w}^{-1}C)^{-1}$$
(A.7)

$$\Phi_{l}(I+G\Phi)^{-1}G = D(sI-A+PC'N_{w}^{-1}C)^{-1}PC'N_{w}^{-1}$$
(A.8)

Conditions (ii) and (iii) of section 3 imply that  $(sI - A + PC'N_w^{-1}C)^{-1}$  is stable [2]. This together with condition (i) and (iv) implies that all of the listed transfer matrices are stable.

Thus it has been shown that u and z have a stable response. Since by assumptions (v) and (vi) the system and the filters are completely observable also their states have a stable response.

#### APPENDIX B

Derivation of the sensitivity matrix and the sensitivity relation

After substitution of  $\Phi_1(s)$ ,  $\Phi_2(s)$ ,  $G_1(s)$  and  $G_2(s)$  into (35) one finds after some manipulations with the aid of (A.2)

$$S(s) = I - D(sI - A + \bar{P}C'N_w^{-1}C)^{-1}\bar{P}D'N_{w1}^{-1}.$$
 (B.1)

As a result of the partitioning of C and  $N_w$  one can write

$$C'N_{w}^{-1}C = D'N_{w1}^{-1}D + M'N_{w2}^{-1}M$$
. (B.2)

Using this again (A.2) can be invoked to show

$$S(s) = [I + D(sI - A + \overline{P}M'N_{w2}^{-1}M)^{-1}PD'N_{w1}^{-1}]^{-1}.$$
(B.3)

The asymptotic variance matrix  $\bar{P}$  satisfies the equation

$$0 = -\bar{P}C'N_{w}^{-1}C\bar{P} + A\bar{P} + \bar{P}A' + N_{u}. \tag{B.4}$$

One can employ (B.2) and add and subtract some extra terms to find after recording

$$0 = -(sI - A + \bar{P}M'N_{w2}^{-1}M)\bar{P}$$

$$-\bar{P}(-sI - A' + M'N_{w2}^{-1}M\bar{P})$$

$$+\bar{P}M'N_{w2}^{-1}M\bar{P} - \bar{P}D'N_{w1}^{-1}D\bar{P} + N_{g}. \quad (B.5)$$

Premultiplication by  $D(sI - A + \bar{P}M'N_{w2}^{-1}M)^{-1}$ , postmultiplication by  $(-sI - A' + M'N_{w2}^{-1}M\bar{P})^{-1}D'$  and further reordering result in the equality

$$\begin{split} & \big[ I + D(sI - A + \overline{P}M'N_{w2}^{-1}M)^{-1}\overline{P}D'N_{w1}^{-1} \big] \\ & N_{w1} \big[ I + N_{w1}^{-1}D\overline{P}(-sI - A' + M'N_{w2}^{-1}M\overline{P})^{-1}D' \big] \\ & = N_{w1} + D(sI - A + \overline{P}M'N_{w2}^{-1}M)^{-1} \\ & (N_v + \overline{P}M'N_{w2}^{-1}M\overline{P})(-sI - A' + M'N_{w2}^{-1}M\overline{P})^{-1}D' \,. \end{split}$$

$$(B.6)$$

The left-hand side of this expression can be recognized to be

$$S(s)^{-1}N_{w1}[S(-s)']^{-1}$$
. (B.7)

If s is replaced by  $j2\pi f$ , the right-hand side of (B.6) is the sum of  $N_{w1}$  and a nonnegative-definite matrix so that

$$S(j2\pi f)^{-1}N_{w1}(S(-j2\pi f)^{-1} \ge N_{w1}$$
 for all  $f$ . (B.8)

From this it may be shown, by simultaneous reduction to diagonal form, that (37) holds.

Résumé—L'article etudie le problème du régulateur et du servomécanisme linéaire stochastique pour des systèmes à variables multiples invariants dans le temps. Il est montré que dans le cas-limite, lorsque la matrice pondérant l'entrée dans le critère quadratique est la matrice zéro, le système en boucle fermé est insensible aux variations des paramètres dans le sens le Cruz-Perkins, à condition que la système à régler sort a dephasage minimale. La matrice de pondération dans le critère de sensibilité de Cruz-Perkins s'avère comme étant l'inverse de la matrice de covariance du bruit de mesure. Un exemple simple illustre la diminution de sensibilité obtenue avec un système à deux entrées et deux sorties.

Zusammenfassung—In der Arbeit wird der stochastische Regler und das Folge-Problem für mehrvariable zeitinvariante Systeme betrachtet. Gezeigt wird, daß in dem Grenzfall, wo die Matrix, die den Eingang in dem quadratischen Kriterium wertet, die Nullmatrix ist, das geschlossene System in Sinne von Cruz-Perkins unempfindlich ist für Parametervariationen, vorausgesetzt, daß das geregelte System minimalphasig ist. Die Gewichtsmatrix in Empfindlichkeitskriterium von Cruz-Perkins ist dann invers zur Kovarianzmatrix des Meßrauschens. Ein einfaches Beispiel illustriert die Abnahme der Empfindlichkeit für ein System mit zwei Eingängen und zwei Ausgängen.

Резюме—Статья рассматривает проблему линейного стохастического регулятора и сервомеханизма для инвариантных по времени многокоординатных систем. Показывается что в предельном сдучае, когда весовой матрицей входа в квадратическом критерии является нулевая матрица, система в замкнутом контуре нсчувствительна к изменениям параметров в смысле Круза-Перкинса, при условии что управляемая система имеет минимально-фазовый характер. Весовая матрица в критерии чувствительности Круза-Перкинёа оказывается обратной ковариантной матрице измерительного шума. Простой пример иллюстрирует уменъшение чувствительности полученное с системой обладающей двумя входами и двумя выходами.



### ROBUSTNESS WITH OBSERVERS

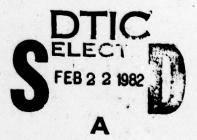
J. C. Doyle\* and G. Stein\*\*

31 aug 79

NO0014-79-C-0377

### **ABSTRACT**

This paper describes an adjustment procedure for observer-based linear control systems which asymptotically achieves the same loop transfer functions (and hence the same relative stability, robustness, and disturbance rejection properties) as full-state feedback control implementations.



<sup>\*</sup> Consultant, Honeywell Systems and Research Center, Minneapolis, MN.

Mailing Address: M.S. MN17-2367, Honeywell Systems & Research Center, 2600

Ridgway Parkway N.E., Minneapolis, MN 55413

Telephone No: (612)378-4254

This document has been approved for public release and sale; its distribution is unlimited.

<sup>\*\*</sup> Staff Engineer, Honeywell Systems and Research Center, Minneapolis, MN, and Adj. Professor, MIT, Dept. EECS, Cambridge, MA.

# I. Introduction

The trouble with observers is that they tempt us, through the expedient of state reconstruction, to assign undue generality to control results proven only for the full-state feedback case. An example is the recent robustness result of Safonov and Athans [1]. This result shows that multivarjable linear-quadratic optimal regulators have impressive robustness properties, including guaranteed classical gain margins of -6 db to + - db and phase margins of + 60 deg. in all channels. The result is only valid, however, for the full state case. If observers or Kalman filters are used in the implementation, no guaranteed robustness properties hold. In fact, a simple example has shown that legitimate LQG controller-filter combinations exist with arbitrarily small gain margins in both the positive and negative db direction [2].

In light of these observations, the robustness properties of control systems with filters or observers need to be separately evaluated for each design. Moreover, because such evaluations can come up with embarassingly small margins, a "design adjustment procedure" to improve robustness would be very desirable. The present paper provides such a procedure. We show that while the commonly suggested approach of "speeding-up" observer dynamics will not work in general, alternate procedures which drive some observer poles toward stable plant zeros and the rest toward infinity do achieve the desired objective. In effect, full-state robustness properties can be recovered asymptotically if the plant is minimum phase. This occurs at the expense of noise performance.

The principal results of the paper are summarized in Section II, where we introduce and interpret certain transfer function properties of observer-based control systems, and in Section III, where we develop the "adjustment procedure". A simple example which illustrates these results is given in Section IV.

Accession

NTIS GRAN

DTIC TAB

Unanneusced

Justification

By

Distribution/

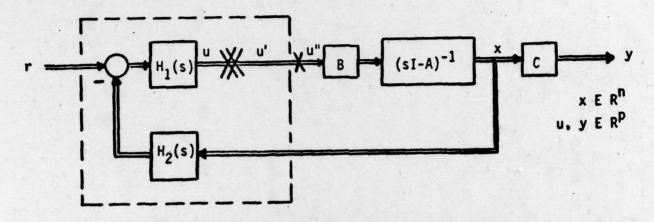
Availability Codes

Dist

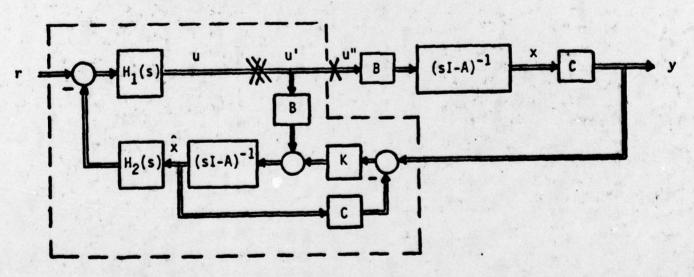
Availability Codes

Availability Codes

Figure 1. Linear Multivariable Control Loop



1A. Full-State Feedback Implementation



1B. Observer-Based Implementation

# II. Transfer Function Properties of Observer-Based Controllers

We consider the general multivariable control loop illustrated in Figure 1. The plant is an n-th order linear system, both observable and controllable, with m inputs, p=m outputs, and no transmission zeros [3] in the right half plane. The control law consists of two transfer function matrices H<sub>1</sub>(s) and H<sub>2</sub>(s). H<sub>2</sub> is driven either with full-state feedback (Fig. 1A) or with an n-th order "model-reference observer" [4] which reconstructs the state in the usual asymptotic sense (Fig. 1B). It is clear that this overall control loop includes linear-quadratic-gaussian controllers as special cases. It also allows dynamic elements such as integrators and lag elements which may be required in more realistic control situations.

This configuration also applies to nonsquare plants for which the number of controls, m, is not equal to the number of measurements, p. For the case, m<p, simply augment the original control vector with (p-m) more components which are not driven by the controllers (i.e.,  $\begin{bmatrix} H_1^T = H_{11}^T : 0 \end{bmatrix}$ ). Columns of the B matrix for these added components must, of course, be selected to introduce no unstable transmission zeros.

For the case, m>p, select any p- dimensional subset of controls for which there are no right half plane transmission zeros. Then the loop transfer properties which are established in this paper apply to this p-dimensional subset of control loops, with the remaining (m-p) loops closed.

A dashed line is shown in both Figure 1A and 1B in order to distinguish between elements of the loop which are part of the controller and those

which are part of the plant. Since we design and implement the controller, there is relatively little uncertainty associated with it, whereas there may be significant differences between the actual plant and its model. The loop transfer functions which we examine for robustness, below, are then taken with respect to the loop breaking point, X, at the control signal interface be ween these two sets of elements. Very misleading robustness results can be obtained for alternate loop breaking points, for example point XX. This is also shown below.

The following properties can be established for the above two control loop implementations:

# Property 1

The closed loop transfer function matrices from command r to state x are identical in both implementations.

# Property 2

The loop transfer function matrices from control signal u' to control signal u (loops broken at point XX) are identical in both implementations

# Property 3

The loop transfer function matrices from control signal u" to control signal u' (loops broken at point X) are generally different in the two implementations even when the observer's error dynamics are allowed to be arbitrarily fast.

# Property 4

The loop transfer function matrices from u" to u' are identical in both implementations if the observer dynamics satisfy

$$K \left[I + C \left(sI-A\right)^{-1}K\right]^{-1} = B\left[C(sI-A)^{-1}B\right]^{-1}$$
 (1) for all values of the complex variable s. The A, B, and C's above are plant matrices and K is the observer gain.

The first two of these properties are very well known [5,6]. They can be easily verified by noting that the transfer functions from u' to x and from u' to  $\hat{x}$  are identical because the nominal error dynamics of the observer are not controllable from u'. These two properties are also the source of much of the temptation surrounding observers, however. We see that input/output properties are the same and even certain loop transfer functions are the same. The latter promise equal relative stability properties, equal tolerance to uncertainties (robustness), and equal disturbance rejection properties. What more could we ask for?

The problem, of course, is that the loop transfer properties are the same at Point XX, inside our own control implementation where only masochists would insert significant uncertain elements or disturbances. According to Property 3, equal loop transfer characteristics are not obtained at the control signal interface to the plant, Point X, where Nature gets to insert uncertainties and disturbances. It is at this point that robustness properties must be measured, and, as seen in [2], it is here that observer-

based implementations can fall well short of our objectives.

Property 3 will be verified by means of example later. We now turn instead to the more interesting Property 4. This result is apparently not as well known, so a simple derivation is given in Appendix A. It is important because it offers a way to adjust observers so that full-state loop transfer characteristics are recovered at Point X. In particular, suppose the observer gains are parameterized as a function of a scalar variable q. Let this function, K(q), be selected such that as  $q \to \infty$ 

$$K(q) \rightarrow q BW$$
 (2)

for any nonsingular matrix W. Then equation (1) will be satisfied asymtotically as  $q \to \infty$ . The resulting observer error dynamics will have limiting poles given by roots of the polynominal

$$\chi(s) = \det(sI-A)\det \left[I + qC(sI-A)^{-1}BW\right]. \tag{3}$$

P of these roots will tend toward the P finite transmission zeros of the plant (stable by assumption) and the rest will tend to infinity. It is clear from this that the commonly suggested approach of making all roots of the error dynamics arbitrarily faster is generally the wrong thing to do.

# III. An Observer-Adjustment Procedure

Equation (2) defines the required limiting characteristics of an adjustment trajectory, K(q), which changes arbitrary initial nominal observer gains, K(0), with poor robustness properties into better gains asymptotically. We still need to define details of such trajectories.

A basic requirement for every point of an adjustment trajectory is stability of the observer error dynamics. Clearly, if we violate this requirement, overall closed loop stability is also lost. (Note that this does not mean that the net compensator within the dashed lines of Figure 1B needs to be stable.) One way to assure stable error dynamics is to restrict the observer to be a Kalman filter for some set of noise parameters. That is, let

$$K(q) = \Sigma(q) C^{\mathsf{T}} R^{-1}$$
 (4)

with  $\Sigma(q)$  defined by the Riccati equation

$$A\Sigma + \Sigma A^{\mathsf{T}} + Q(q) - \Sigma C^{\mathsf{T}} R^{-1} C\Sigma = 0$$
 (5)

As usual we take  $Q = Q^T >_{,0}$  and  $R = R^T >_{,0}$ . For Kalman filters, these matrices represent given process noise and measurement noise intensities, respectively. Here they are treated more freely as design parameters which we can select to suit broader purposes. In particular, let

$$Q(q) = Q_0 + q^2 B V B^T$$
 (6)

$$R = R_0 \tag{7}$$

where  $Q_o$  and  $R_o$  are noise intensities appropriate for the nominal plant, and V is any positive definite symmetric matrix. With these selections,

the observer gain for q = o corresponds to the nominal Kalman filter gain. However, as q approaches infinity, the gains are seen from (5) to satisfy,

$$K R K^{T} \longrightarrow q^{2} BVB^{T}$$

and

$$K \longrightarrow q B V_1 R_1^{-1},$$
 (8)

where  $V_1$  denotes some square root of V ( $V_1V_1^T = V$ ) and, similarly,  $R_1$  is some square root of R. Since (8) is a special case of (2), it follows that the adjustment procedure defined by (4)-(7) will achieve the desired robustness-improvement objective.

Note that the second term in equation (6) can be interpreted as extra process noise added directly to the control input of the plant. Within the constraints of Kalman filter mathematics, such "fictitious noise" is a natural mechanism to represent uncertainties at this point of the control loop. It is nice to know that the resulting filter design actually responds with a corresponding robustness improvement. Note, however, that arbitrary increases of the existing noise matrix (i.e.,  $Q = (1 + q^2) Q_0$ ) or addition of arbitrary full rank noise process (i.e.,  $Q = Q_0 + q^2 W$  with  $W = W^T > 0$ ) which are often suggested as other intuitive robustness improvement methods, will not in general produce the desired effect.

Finally, we note that the use of Kalman filter equations in the adjustment procedure is not fundamental. The filters merely provide a convenient way to assure stability along the entire adjustment trajectory. Any other procedure (pole placement, for example) with the same limiting properties (2) could be used as well.

### IV. An Example

To illustrate the observer properties and adjustment procedure above, consider the following example:

Plant:

$$\frac{dx}{dt} = \begin{bmatrix} 0 & 1 \\ -3 & -4 \end{bmatrix} \times + \begin{bmatrix} 0 \\ 1 \end{bmatrix} u + \begin{bmatrix} 35 \\ -61 \end{bmatrix} \xi \qquad (9)$$

$$y = \begin{bmatrix} 2 & 1 \end{bmatrix} x + \eta$$
 (10)  
with  $E(\xi) = E(\eta) = 0$ ; 
$$E[\xi(t)\xi(\tau)] = E[\eta(t)\eta(\tau)] = \delta(t-\tau)$$

Controller:

$$u = [-50 \ -10] \hat{x} + [50] r$$
 (11)

The plant in this example is a (harmless) stable system with transfer function.

$$\frac{y}{u}(s) = \frac{s+2}{(s+1)(s+3)} \tag{12}$$

The controller happens to be a linear-quadratic one, corresponding to the performance index

$$J = \int_0^\infty (x^T H^T H x + u^2) dt$$
 (13)

with

$$H = 4\sqrt{5} \qquad \boxed{\sqrt{35} \qquad 1}$$

It places the closed loop regulator poles at

$$s = -7.0 + j2.0$$

A Nyquist diagram (polar plot of the loop transfer function at Point X) for the full-state design is given in Figure 2. Gain margin is infinite in both directions and there is over  $85^{\circ}$  phase margin. The design is then implemented using a Kalman filter for the given noise parameters. The Nyquist plot for the resulting observer-based controller is also shown in Figure 2. Oops. . less than  $15^{\circ}$  phase margin.

In an effort to improve this margin, one adjustment to the filter that could be made is to speed it up. So, we can try moving the filter/observer poles to the left in a second-order Butterworth pattern. For the filter/observer poles at  $-22^{+}_{-}17.86$ j one gets the third Nyquist plot in Figure 2. As can be seen, the results are less than satisfactory. Not only are the margins disappearing (now less than 10 degrees) but the loop bandwidth has increased (crossover has gone from approximately 12. to 40. rad/sec).

Unless we're trying to design an explosive device, this is clearly undesirable. It gets worse as the filter gets faster. In fact, it can be shown that the margins go asymptotically to zero for large gains, while the loop bandwidth goes to infinity. The present example is not a pathological one, either. Similarly undesirable characteristics for fast filters are obtained with most systems.

When the observer adjustment procedure of Section III is applied to the same example, much more pleasing behavior is obtained. Following (6)-(7), we let the process noise covariance matrix be

$$Q = \begin{pmatrix} 35 \\ -61 \end{pmatrix} \quad (35 -61) + q^2 \begin{pmatrix} 0 \\ 1 \end{pmatrix} \quad (0 \quad 1)$$
 (14)

We then increase q from zero until a reasonable compromise between noise performance and robustness is achieved. Some results of this process are summarized in Figure 3 and Table 1. Figure 3 shows Nyquist diagrams for  $q^2 = 100$ , 500, 1000, and 10,000. Margins improved with essentially no change in bandwidth as the modified loop transfer function tends toward full state optimal. Noise performance is summarized in Table 1 for the same set of q values. As expected, the error covariance of the adjusted filter with respect to the original noise increases markedly with q. However, there was not the same deterioration in state covariance.

Table 1 also documents other parameters associated with these design points - - poles of the error dynamics, margins, and filter gains. Note in particular that the filter poles tend toward the plant zero and toward infinity, as required by (3).

This adjustment procedure was also successfully applied to reconstruction of measured outputs after sensor failures for the A7-D aircraft. [8] In this application the optimum Kalman filter produced an unstable system when tested in hybrid simulation over the A-7D flight envelope. After attempts with "ad hoc" fictitious noise adjustment procedures failed the method discussed here successfully stabilized the system. Also, the resulting error covariance properties remained closed to the optimum values.

# V. Conclusions

This paper illustrates some of the difficulties one can get into by relying on observers for state reconstruction. We have concentrated on robustness properties. In general, these will be poorer for observer-based implementations than for full-state implementations. For minimum-phase systems, however, full-state robustness can be recovered asymptotically provided it is done correctly. Fast observers are not in general correct. A "fictitious noise" adjustment procedure was suggested which is.

The apparent practical value of this procedure is that it gives a simple way of trading off between noise rejection and margin recovery. When q = 0, the filter will be optimal with respect to the "true" (as modelled) system noise. As q increases the filter will do a poorer job of noise rejection but the closed-loop stability margins will improve. Hopefully, a satisfactory compromise can be found through the adjustment of the single parameter q. We stress that margin recovery occurs at Point X in Figure 1 -- at the control signal interface to the outside world. Asymptotically, the full-state and observer-based implementations will have the same tolerance to disturbances and uncertain elements inserted at this point. While Point X is clearly a physically important one (more important than Point XX, certainly), engineers who may wish to test robustness at still other points in the control loop should recognize that the recovery results may not be applicable there.

The suggested adjustment procedure is essentially the dual of a sensitivity recovery method suggested by Kwakenaak [7]. The latter provides a method

for selecting the weights in the quadratic performance index so that fullstate sensitivity properties are achieved asymptotically as the control weight goes to zero. In this case, however, closed loop plant poles instead of observer poles are driven to the system zeros, which can result in unacceptable closed loop transfer function matrices for the final system.

# ACKNOWLEDGEMENTS

We would like to thank the Math Lab Group, Laboratory for Computer Sciences, MIT for use of their invaluable tool, MACSYMA, a large symbolic manipulation language. The Math Lab Group is supported by NASA under grant NSG 1323 and DOE under contract #E(11-1)-3070.

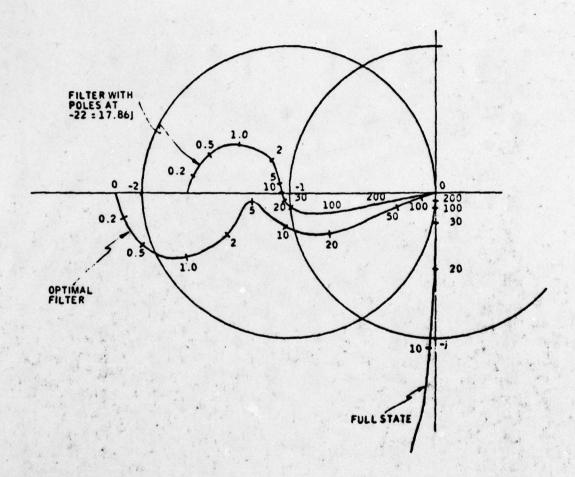


Figure 2. Loop Transfer Functions of Example:

"Fast Filter" Adjustment Procedure

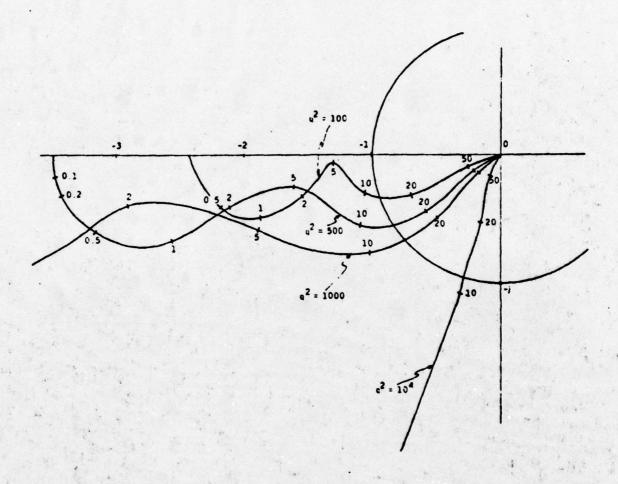


Figure 3. Loop Transfer Function of Example:
"Fictitious Noise" Adjustment Procedure

5	POLES	MARGIN	MARGIN	COVARIANCE $ (x-\hat{x})(x-\hat{x})$	COVARIANCE $\left[ (x-\hat{x})(x-\hat{x})^T \right]$	COVAR E(x	STATE COVARIANCE E(xx <sup>T</sup> )	FILTER
Optimal	-7-21	6.75	<u>.</u>	. 26	- 163	221	- 613	30
Lực Design				- 163	277	-613	2070	- 50
Fast Filter Adjust-	22+17 064	<b>8</b>	710	6284	-12224	130	- 613	720
ment Procedure	[00*/1-33-	3	,	-12224	23788	-613	8517	-1400
Fictitious Adjust-	-4.3	22 1 -	9	107	- 184	236	-613	26.8
q <sup>2</sup> = 100	-13.1			- 184	319	-613	1812	- 40.2
q <sup>2</sup> = 500	-2.9	-10 9	્રેર	163	- 301	268	-613	20.4
7 20	-24		3	-301	564	-613	1497	- 17.7
a <sup>2</sup> = 10 <sup>3</sup>	-2.5	13.0	CF CF	204	-385	285	-613	16.7
	-33		*	-385	743	-613	1360	- 1.9
q <sup>2</sup> = 10 <sup>4</sup>	-2.1	-37	7.4	290	-570	317	-613	6.9
	-100			-570	1169	-613	1198	84.6

TABLE 1. SUMMARY OF EXAMPLE

# APPENDIX A: Derivation of Property 4

Referring to Figure 1A, the loop transfer function from u" to u' of the full state implementation is obtained from the relationships

$$x = \phi(Bu'' + F_V) \tag{A.1}$$

$$u' = -H_1H_2x$$
, (A.2)

where

$$\Phi = (sI-A)^{1} \tag{A.3}$$

$$v = -G_1G_2x . (A.4)$$

The variables  $\vee$  above are now shown in Figure 1 for the sake of simplicity. They denote the (m-p) control components for which loops are not broken in the event that p < m. Matrices F,  $G_1$ , and  $G_2$  are to control input matrix and the feedback compensator matrices for these components, respectively. If the original plant is square or can be made square by augmenting (p-m) additional control variables, then  $\vee$ , F  $G_1$  and  $G_2$  are zero identically. For either situation, (A.1) - (A.4) define the following full-state loop transfew function:

$$u' = -H_1H_2 (I + \phi FG_1G_2)^{-1} \phi Bu''$$
 (A.5)

The corresponding relationships for observer-based implementations are (Fig. 1B).

$$\hat{x} = (\phi^{-1} + KC)^{-1} \{Bu' + Fv + KC\phi(Bu'' + Fv)\}$$

$$= (\phi^{-1} + KC)^{-1} \{Bu' + KC\phi Bu'' + (\phi^{-1} + KC) \phi Fv\}$$

$$= (\phi^{-1} + KC)^{-1} \{Bu' + KC\phi Bu''\} + \phi Fv$$
(A.6)

with

$$u' = -H_1H_2\hat{x}$$
  
 $v = -G_1G_2\hat{x}$  (A.7)

This gives

$$u' = -H_1H_2(I + \phi FG_1G_2)^{-1} (\phi^{-1} + KC)^{-1} \{Bu' + KC\phi Bu''\}.$$
 (A.8)

Now applying the Matrix inversion lemma to the  $(\phi^{-1} + KC)^{-1}$  term in this expression gives

$$u' = -H_1H_2(I + \phi FG_1G_2)^{-1} \left[ \phi - \phi K(I + C\phi K)^{-1}C\phi \right] \{Bu' + KC\phi Bu''\}$$

$$= -H_1H_2(I + \phi FG_1G_2)^{-1} \phi \left[ B - K(I + C\phi K)^{-1}C\phi B \right] u'$$

$$-H_1H_2(I + \phi FG_1G_2)^{-1} \phi K (I + C\phi K)^{-1}C\phi B u''. \tag{A.9}$$

From (A.9) it follows that if (1) is satisfied, then the u' term on the right hand side vanishes and the u" term is identical to (A.5). Since u" is arbitrary, this establishes the claimed equality of loop transfer functions.

### REFERENCES

- Safonov, M. G., and M. Athans, "Gain and Phase Margin of Multiloop
   LQG Regulators, "IEEE Trans. Auto. Control, April 1977.
- Doyle, J. C., "Guaranteed Margins for LQG Regulators," <u>IEEE Trans.</u>
   Auto. Control, August 1978.
- MacFarlane, A. G. J. and Karcanias, N., "Poles and Zeros of Linear Multivariable Systems: A Survey of Algebraic, Geometric, and Complex Variable Theory," Int. J. Control, July 1976, pp. 33-74.
- 4. Schweppe, F. C., Uncertain Dynamic Systems, Prentice-Hall, 1973.
- Kwakernaak, H. and Sivan, R., <u>Linear Optimal Control Systems</u>,
   Wiley-Interscience, 1972.
- Anderson, B. D. O. and Moore, J. B., <u>Linear Optimal Control</u>, Prentice-Hall, 1971.
- Kwakernaak, H., "Optimal Low-Sensitivity Linear Feedback Systems,"
   Automatica, Vol. 5, No. 3, May 1969, p. 279.
- 8. Cunningham, T. B., Doyle, J. C., and Shaner, D. A., "State Reconstruction For Flight Control Reversion Modes", 1977 IEEE Conference on Decision and Control, New Orleans, December 1977.

ROBUSTNESS RESULTS FOR STATE FEEDBACK REGULATORS

P. Molander\* and J. C. Willems\*\*

\* Dept. of Aut. Control, Lund Inst. of Technology, Lund, Sweden

\*\* Dept. of Mathematics, Univ. of Gronningen, Gronningen, The Netherlands

### Abstract

State feedback regulators are derived which have better robustness characteristics than the standard 60° phase margin and 50% gain reduction tolerance of standard linear- quadratic regulators. It is also shown how the Lyapunov equation can be used to design high-integrity regulators for open-loop stable systems.

### 1. Introduction

Any practical control system synthesis is subject to uncertainty. This uncertainty may appear as non-measurable disturbances on the input, or only partly known or time varying system parameters, to quote a few examples. The topic of the present paper is to study one example of such parameter uncertainty, namely large variations in the input channels.

The criterion chosen for our "acceptable" closed-loop system behavior is stability. This is, of course, far from sufficient for practical purposes, but such analysis may all the same produce some guidelines for the design of practical control systems. The step from a qualitative to a quantitative result is often a short one.

Since the discovery by Kalman [1] of the frequency domain inequality satisfied by linear-quadratic optimal regulators, a great deal of literature has been produced on the "robustness" of such regulators. In terms of classical control concepts, Kalman's inequality implies that they possess 60° phase margin, infinite gain margin, and 50% gain reduction tolerance. This result holds under the only assumption that the penalty matrix of the state variable in the performance index is positive semidefinitive.

Although  $60^{\circ}$  phase margin seems a lot, it may be insufficient in certain cases. Dynamics of the actuators  $x \rightarrow c$  and time delays may have been neglected in the model, for instance. Thus it is of interest to synthesize regulators with improved robustness characteristics.

As is easy to see from examples, the above results cannot be strengthened without further assumptions on the performance index or the plant. Assumptions used here are decreasing penalty on the control variables (cheap control) and stability of the open loop system, respectively.

### 2. Formulation of the Problem.

Consider the linear time invariant system described by

$$\dot{\mathbf{x}}(t) = \mathbf{A}\mathbf{x}(t) + \mathbf{B}\mathbf{u}(t)$$

$$\mathbf{x}(0) = \mathbf{x}_{0}.$$
(1)

x(t) and u(t) are n- and p-vectors, respectively. Assume that the desired input is given by the linear, constant state feedback

$$u(t) = -L^{T}x(t)$$
 (2)

but that the implementation is computed by some time varying nonlinearity  $\phi(\cdot,t)$ , i.e. the actual input u(t) is given by

$$u(t) = -\phi(L^{T}x(t),t)$$
 (2)'.

Here,  $\phi(\cdot,t)$  is a nonlinear function from  $R^P$  to  $R^P$  for each t, subject to the condition

The problem is to guarantee global asymptotic stability of the null solution of (1), (2)' subject to (3) for given  $K_1$ ,  $K_2$ .

Although the problem is formulated for the case of a memoryless non-linearity  $\phi(\cdot,t)$ , the results can easilty be generalized to dynamic disturbances using modern frequency domain stability theorems (see e.g. [2]). This has been exploited in [3], but will not be pursued here.

### 3. Results for Arbitrary Plants.

First a brief review of the result for linear-quadratic optimal controllers will be given. Associate with (1) the problem of optimizing, with respect to  $u(\cdot)$ , the performance index

$$J = \int_{0}^{\infty} (x(t)^{T} Q x(t) + u(t)^{T} R u(t)) dt.$$

It is well known that the solution is given by the linear constant feedback

$$u(t) = -R^{-1}B^{T}P \times (t)$$
 (4),

where P is the largest solution of the algebraic Riccati equation

For notational simplicity,  $R = I_p$  will be assumed in the sequel.

Standard manipulations of equation (5)lead to the frequency domain equality

$$(I + G^{T}(-i\omega))I_{p}(I + G(i\omega)) = I_{p} + B^{T}(-i\omega - A^{T})^{-1}Q(i\omega - A)^{-1}B$$
 (6),

where

$$G(s) = R^{-1}B^{T}P(sI - A)^{-1}B.$$

An alternative form of (6) for the closed-loop system is, with  $\tilde{G}(s) = G(s)(I+G(s))^{-1}$ .

$$(I - \tilde{G}^{T}(-i\omega))I_{p}(I - G(i\omega)) = I_{p} - B^{T}(-i\omega - A^{T})^{-1}Q(i\omega - A)^{-1}B$$
 (6).

If Q is positive semidefinite, the second term on the right-hand side is nonnegative, and the following inequality results:

$$(\mathbf{I} - \widetilde{\mathbf{G}}^{\mathbf{T}}(-i\omega)) \mathbf{I}_{\mathbf{p}} (\mathbf{I} - \widetilde{\mathbf{G}}(i\omega)) \leq \mathbf{I}_{\mathbf{p}}$$
 (7).

A straight-forward application of the circle criterion then implies the desired stability for

$$K_1 = \frac{1}{2}$$
,  $K_2 = \text{any finite } K$ .

It is obvious that the best possible lower bound K without restrictions on the plant is

$$K_1 > 0$$
 (8).

For certain high-gain regulators, (8) is in fact sufficient as will now be shown. Consider the performance index  $J_{\rho}$ , where the penalty on the input is modified via the scalar variable  $\rho$ :

$$J_{\rho} = \int_{0}^{\infty} (x(t)^{T} Qx(t) + \rho u(t)^{T} u(t)) dt.$$

Choosing  $\rho$  small means that very large control signals are permitted. It seems reasonable to conjecture that such a design should yield a controller with high integrity. This is indeed the case.

Theorem 1. Consider the control system (1), (2), with  $\phi(\cdot,t)$  subject to (3).

For any  $K_1$  >0 and any  $K_2$  <  $\infty$  there is a  $Q \ge 0$  such that the optimal controller relative to  $J_\rho$  quarantees asymptotic stability in the large of the null solution for all  $\rho$  >0 sufficiently small.

Proof: The Riccati equation pertaining to Jo is

$$A^{T}P_{\rho} + P_{\rho}A + Q - \rho^{-1}P_{\rho}B B^{T}P_{\rho} = 0$$
 (5).

Two reductions of the general case will be made. Firstly, it may assumed without loss of generality that

$$rank (Q) \leq rank (B) = p,$$

(see [4]). Thus Q can be factored as MMT, with

There are several M-matrices that generate the same feedback matrix, corresponding to various factorizations of

$$B^{T}(-sI - A^{T})^{-1}Q(sI - A)^{-1}B = B^{T}(-sI - A^{T})^{-1}MM^{T}(sI - A)^{-1}B.$$

If the M that makes

$$M(s) = M^{T}(sI - A)^{-1} B$$

minimum phase is chosen, the conditions are satisfied which ensure that ([5], [6])

$$\lim_{\rho \to 0} P_{\rho} = 0$$

Equivalently,

$$\lim_{\rho \to 0} \rho^{-1} P_{\rho} B B^{T} P_{\rho} = Q = M M^{T}$$
(9).

Starting from Riccati equation (5)' and using the same manipulations that lead to inequality (6)' then shows, inserting (9), that

$$\tilde{G}$$
 (s) =  $\rho^{-1}B^{T}P_{\rho}(sI - A + \rho^{-1}BB^{T}P_{\rho})^{-1}B$ 

satisfies

$$(\frac{1}{2}\mathbf{I} - \widetilde{G}_{\rho}^{\mathbf{T}}(-\mathbf{s}))\mathbf{I}_{p}(\frac{1}{2}\mathbf{I} - \widetilde{G}_{\rho}(\mathbf{s})) \leq \mathbf{I}_{\rho} + o(\rho^{-1}), \quad \rho + 0.$$

This proves the claim.

Remark: A weaker version of Theorem 1, corresponding to a  $\phi$  (°,t) that is

diagonal (i.e. no cross-couplings between the inputs), can be proved using the results of [7].

In classical terminology, this regulator possesses a phase margin arbitrary close to 90°, infinite gain margin, and a gain reduction tolerance arbitrarily close to 100%.

There is an alternative way of generating such controllers, which is almost trivial. The proof is left to the reader.

Theorem 2. Consider (1), (2)' with 
$$\phi(\cdot,t)$$
 subject to (3). If L is chosen as  $L = \varepsilon^{-1} L_0$ ,

where L is any optimal gain generated from a positive semidefinite Q, then the controller enjoys the same robustness properties when  $\varepsilon + 0$  as the controller of Theorem 1 when  $\rho + 0$ .

Theorems 1 and 2 must be used with some caution, since in applications the sector bounds  $K_1$  and  $K_2$  may depend on the nominal feedback gain L. An example is given in Section 5.

# 4. Results for Open-Loop Stable Plank

If the plant is open-loop stable, it should be possible to design controllers where the lower bound K<sub>1</sub> is zero. A complete characterization of such feedback matrices L is given in the following theorem.

Theorem 3. The feedback system (1), (2)' with  $\phi(\cdot,t)$  satisfying (3) has a globally asymptotically stable equilibrium solution for

$$K_1 = 0$$
,  $K_2 = any K > 0$ 

if there exist matrices  $K = K^{T} > 0$  and C, (C,A) being an observable pair, such that

$$\begin{cases} A^{T}K + KA = -CC^{T} \\ KB = L. \end{cases}$$
 (10)

Proof: This is a straight-forward application of the Kalman YakubovichPopov lemma in its multivariable form ([8]). Equation (10) provides a means
to design high-integrity controllers, namely by solving the (linear) Lyapunov
equation for K and then choosing the feedback gain L as (any positive multiple of)
KB. There remains the problem of choosing C and a positive gain, but this
problem is shared by the LQOC methodology. For single-input systems, equation (10)
is simplified further if it is translated into the frequency domain. Defining
p(s) as the open-loop characteristic polynomial and

$$\frac{q(s)}{p(s)} = L^{T}(sI - A)^{-1} B$$

$$\frac{r(s) \ r(-s)}{p(s) \ p(-s)} = B^{T}(-sI - A^{T})^{-1} CC^{T} (sI - A)^{-1} B$$

yields the equation

$$p(s) q(-s) + q(s) p(-s) = r(s) r(-s)$$
 (10)

This can be solved for q(s), which is turn gives the unique feedback gain L.

The condition of Theorem 3 is rather strong. In general an infinite gain margin is not required. The following theorem characterizes the feedback gains that retain stability for all gain drops.

Theorem 4. The claim of Theorem 3 remains valid for

$$K_1 = 0, K_2 = 1$$

if there exist matrices  $K = K^{T} > 0$ , C, and D, and an  $\varepsilon > 0$  such that

$$A^{T}K + KA = -CC^{T} - DD^{T}$$

$$KB = 1 - (\sqrt{2} - \varepsilon)D$$
(11)

<u>Proof.</u> This is again a direct application of the circle criterion in combination with the Kalman-Yakubovich-Popov lemma. Compared to equation (10), the use of equation (11) involves the extra problem of choosing D. Theorem 4 can of course

be generalized to any upper and lower bounds  $K_1$  and  $K_2$  (provided the system is open loop asymptotically stable if  $K_1 \leq 0 \leq K_2$ .

## 5. Discussion of the Results

The results presented above must be interpreted with some caution. It is quite clear that most actuator failures are such that no judicious choice of feedback gains can save the situation. This is even more true for the case of sensor failures (not treated here). Thus in general one will have to rely on external failure-handling routines.

The sharpening of previous results for arbitrary plants relies upon the use of high gains. This must be kept in mind if the nominal input influences the sector of  $\phi(\cdot,t)$ . For instance, if the gain drop of the regulator is caused by saturation, there is obviously no point in increasing the nominal gain.

With these reservations kept in mind, the theorems yet contribute to the general robustness picture of state feedback regulators. Theorem 3 is believed to yield a practicable design method for control systems where the input channel uncertainty is so great that it has to be accounted for in the synthesis.

## References

- Kalman, R.E., "When is a Linear Control System Optimal?" <u>Trans.ASME</u>,
   J. Basic Eng., Vol. 86, pp. 1-10, 1964.
- Zames, G. "One the Input-Output Stability of Time-Varying Nonlinear Feedback Systems", Part I & II, IEEE Trans. AC-11, pp. 228-238, 465 - 476, 1966.
- Safonov, M.G., Athans M. "Gain and Phase Margins for Multiloop LQG Regulators", IEEE Trans. AC-22, pp. 173-179, 1977.
- Popov, V.M., "Hyperstability and Optimality of Automatic Systems with Several Control Functions," <u>Rev. Roum. Sci.Tech.Ser.Electrotech.Energ.</u>, Vol. 9, pp. 629-690, 1964.
- Kwakernaak, H., Sivan R., "The Maximally Achievable Accuracy of Linear Optimal Regulators and Linear Optimal Filters", <u>IEEE Trans. AC-17</u>, pp. 79-86, 1972.
- 6. Molander, Per, "On the Design of High-Gain Feedback Regulators and Observers", to be published.
- Wong, P.K., Stein G., and Athans M., "Structural Reliability and Robustness Properties of Optimal Linear-Quadratic Multivariable Regulators". Preprints Helsinki IFAC Congress, pp. 1797-1805, 1978.
- Anderson B.D.O., "A System Theory Criterion for Positive Real Matrices", J.SIAM Control, Vol.5, pp. 171-182, 1967.

C.A. Harvey
Honeywell, Systems and Research Center
2600 Ridgway Parkway N.E.
Minneapolis, Minnesota 55413

# **ABSTRACT**

For systems that are open-loop stable, there is a class of feedback controllers that have the property that the closed loop system is stable and remains stable in case actuator outages occur. Properties of a special subclass of these controllers are discussed.

are stable. Such requisions may be contidered to possess interrity with

This work was supported by the Department of Energy under Contract ET-78-C-01-3391. The work was motivated by discussions with Mr. J.C. Doyle concerning the integrity property of controllers that have gains which are determined from Liapunov rather than Riccati equations.

INTRODUCTION: Consider the linear controllable system

$$\dot{x} = Ax + Bu \tag{1}$$

where A is stable, i.e., the eigenvalues of A have negative real parts. The class of state feedback regulators of the form

$$u = -B^{\mathsf{T}} \mathsf{P} \mathsf{x} \tag{2}$$

where P satisfies the Liapunov equation

$$PA + A^{T}P + Q = 0, Q \ge 0$$
 (3)

with (A,  $Q^{\frac{1}{2}}$ ) observable are of special interest because the closed loop systems with related regulators of the form

$$u = -LB^{\mathsf{T}} \mathsf{Px}, \quad L = L^{\mathsf{T}} \geq 0 \tag{4}$$

are stable. Such regulators may be considered to possess integrity with respect to loss of imputs, that is, stability of the closed loop system is maintained when one or more inputs is set to zero. This situation of loss of inputs can be represented by an admissible L in (4). For example, the loss of the first input may be represented by taking L to be

$$L = \begin{bmatrix} 0 & 0 \\ 0 & 1 \end{bmatrix} \tag{5}$$

The class of regulators defined by (2) and (3) is a subset of the class of optimal state feedback controllers. This fact and the proof of the stability for regulators of the form (4) are given below, followed by other results aimed at characterizing the class of regulators of interest.

Optimality of Regulators given by (2), (3) and (4): The regulator given by (2) and (3) is the optimal regulator for (1) with respect to the performance index

$$J = \int_0^\infty \{x^T (Q + PBB^T P) \ddot{x} + u^T u\} dt$$
 (6)

for P satisfying (3) and A being stable,  $P \ge 0$ , so that  $Q + PBB^TP \ge 0$ . The optimal regulator for (1) with respect to (6) is given by

$$u = -B^{T} \hat{P} x \tag{7}$$

with  $\hat{P}$  being the positive definite symmetric matrix solution to the Riccati equation

$$\hat{P}A + A^{T}\hat{P} + Q + PBB^{T}P - \hat{P}BB^{T}\hat{P} = 0$$
 (8)

Thus,  $\hat{P} = P$ , and the controls given by (2) and (7) are the same. Now conser the control given by (3) and (4). If L > 0, this control is optimal with respect to the performance index.

$$J = \int_0^{\infty} \{x^T(Q + PBLB^TP) \times u^TL^{-1}u\}dt$$
 (9)

since the optimal control is given by

$$u = -(L^{-1})^{-1} B^{T} P_{X} = -LB^{T} P_{X}$$
 (10)

where 
$$0 = PA + A^{T}P + (Q + PBLB^{T}P) - PB(L^{-1})^{-1}B^{T}P$$
  
=  $PA + A^{T}P + Q$  (11)

If L is singular, the control v = Tu is optimal with respect to

Stante Hight species also deconstrate that the set of controllers defined by

$$J = \int_0^\infty \{x^T (Q + PBLB^T P) \times v^T v\} dt$$
 (12)

for the system

$$\dot{x} = Ax + BLT^{T}y \tag{13}$$

Continuity of Regulators given by (2). (3) and (4): The regulator given

where 
$$T^{T}_{T} = L^{+}$$
 (the pseudo-inverse of L) (14)

since 
$$v = -(BLT^T)^T Px$$
 (15)

and 
$$O = PA + A^{T}P + (Q + PBLB^{T}P) - P(BLT^{T})(BLT^{T})^{T}P$$
  

$$= PA + A^{T}P + Q + PBLB^{T}P - PBLT^{T}TLB^{T}P$$

$$= PA + A^{T}P + Q$$
(16)

Thus, the closed loop system given by (13) and (15) is stable, i.e.

$$\dot{x} = (A - BLT^{T}(BLT^{T})^{T}P)x$$

$$= (A - BLT^{T}TLB^{T}P)x$$

$$= [A + B(-LB^{T}P]x$$
(17)

is stable. But (17) is the same closed loop system as that obtained using the control (4) in the system (1). This verifies the stability properties or integrity property of regulators of the special class of regulators described in the introduction.

Characterization of Regulators Defined by (2) and (3). A simple method of characterizing such regulators is to relate their closed loop parameters to the closed loop parameters of optimal linear regulators. This method can be applied to second order systems with a single input, but appears to be intractable for general systems. For the simple example with

$$A = \begin{bmatrix} 0 & 1 \\ -a & -b \end{bmatrix}, \quad B = \begin{bmatrix} 0 \\ 1 \end{bmatrix}, \quad a > 0, \quad b > 0$$
 (18)

Single input systems also demonstrate that the set of controllers defined by (2) and (3) is a conservative estimate of the set of controllers with integrity because all stabilizing controllers, for single input systems possess integrity with respect to input outages.

the closed loop characteristic polynomial is  $\hat{s}^2 + C_1\hat{s} + C_2$ . Consider the two control laws,  $u_L$  defined by (2) and (3), and  $u_R$  defined by

$$u_{R} = -B^{\mathsf{T}}P_{R}X \tag{19}$$

with  $P_R > 0$  satisfing the Riccati equation

$$P_{R}A + A^{T}P_{R} + Q_{R} - P_{R}BB^{T}P_{R} = 0$$
 (20)

The corresponding coefficients in the closed loop characteristic polynomial are:

$$C_{IL} = b + (q_{22}/2b) + (q_{11}/2ab), C_{2f} = a + (q_{11}/2a)$$
 (21)

$$c_{IR} = [b^2 + q_{22R} + 2(\sqrt{a^2 + q_{11R}} - a)^{\frac{1}{2}}, c_{2R} = \sqrt{a^2 + q_{11R}}]$$
 (22)

The sets of possible coefficients for these two control laws may be depicted in the  $(C_1,C_2)$  plane as shown in Figure 1. The set for  $u_L$  is a subset of the set for  $u_R$ . The lower boundaries of these two sets coincide (the line segment  $C_2 = a$ ,  $C_{1,2} > b$ ). The upper boundary for the  $u_R$  set is the segment of the parabola  $C_1^2 = b^2 + 2(C_2-a)$  with  $C_1^2 > b$ . The upper boundary for the  $u_L^2 > b$  set is the line segment,  $u_L^2 > b > b$  which is tangent to the upper boundary of the  $u_R^2 > b > b$ .

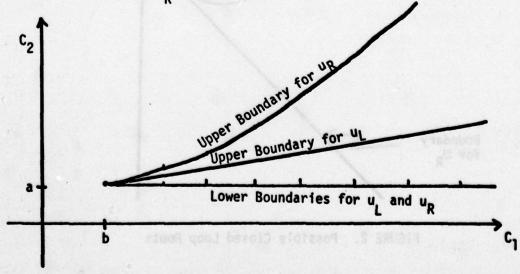


FIGURE 1. Possible Closed Loop Characteristic Polynomial Coefficients

The sets of possible closed loop roots may also be determined for this example. Figure 2 shows these sets for the case of a = b = 2. The negative real axis is contained in the possible sets for both  $u_L$  and  $u_R$ . The remaining set of possible roots for  $u_L$  is a small subset of the set of possible roots for  $u_R$ . Although these results appear to be impossible to generalize, let us note an interpretation of the sets of possible roots in this example that may be generalized. If we introduce

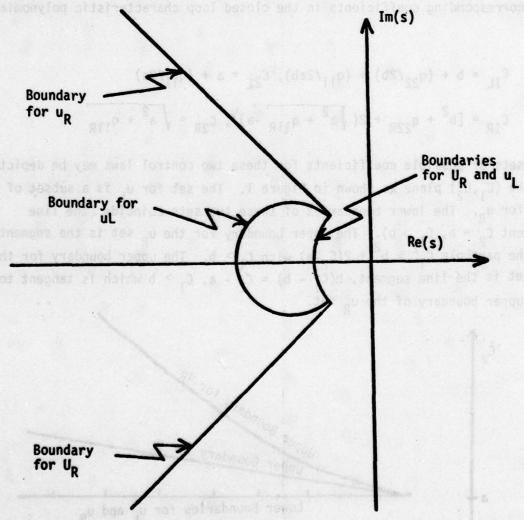


FIGURE 2. Possible Closed Loop Roots

a positive scalar parameter  $\alpha$  in the matrices Q and  $Q_R$ , say  $Q = \alpha \hat{Q}$  and  $Q_R = \alpha \hat{Q}_R$  and consider the loci of closed loop roots as  $\alpha$  tends to infinity.

these loci tend to zeros associated with  $\hat{Q}$  and  $\hat{Q}_R$ . For this example there is at most one such zero and it must be real and negative. In the optimal case, the zero is a transmission zero associated with  $\hat{Q}_R$  and its magnitude is arbitrary. In the case where  $u_L$  is obtained via (2) and (3) the magnitude of the zero associated with  $\hat{Q}$  is restricted to be less than b.

In this example the root locus of interest is the locus of roots of the polynomial

$$p(s,\alpha) = s^2 + 2[b + (\alpha/2ab)(\hat{q}_{11} + a\hat{q}_{22})] + a + (\alpha/2a)\hat{q}_{11}$$
 (23)

As ∝ tends to infinity, the polynomial may be factored as

$$p(s,\alpha) = [s + b\hat{q}_{11}/(\hat{q}_{11} + a\hat{q}_{22}) + O(\alpha^{-1})][s + (\alpha/2ab)(\hat{q}_{11} + a\hat{q}_{22}) + O(1)]$$
 (24)

so that one root tends to  $-b\hat{q}_{11}/(\hat{q}_{11}+a\hat{q}_{22}) \ge -b$  and the other root tends to infinity.

Let us now return to the general case for the system (1) and introduce the parameter,  $\alpha$ , into the control law, i.e.

$$u = -\alpha B^{\mathsf{T}} \mathsf{P} \mathsf{x}$$

with P given by (3). Such a system may be characterized by asymptotic properties as the parameter,  $\alpha$ , tends to infinity. The return difference matrix is

$$T(s) = I + \alpha B^{T} P(sI-A)^{-1} B$$
 (26)

Algebraic manipulation leads to the result that

$$T^{T}(-s) T(s) = I + \alpha B^{T}(-sI-A^{T})^{-1}Q(sI-A)^{-1}B + \alpha^{2} B^{T} (-sI-A^{T})^{-1} PBB^{T}P(sI-A)^{-1}B$$
(27)

Let the dimension of x be n and the dimension of u be m. For simplicity, let us assume that  $B^TPB$  has full rank. A generalization to the case in which the rank of  $B^TPB$  is less than m is of interest but is also somewhat more complicated. If we let  $s = \alpha \sigma$  in (27) and let  $\alpha$  tend to infinity, we obtain

$$T^{\mathsf{T}}(\neg \alpha \sigma) \ \mathsf{T}(\alpha \sigma) \rightarrow 1 \ -\alpha^{-1} \ \sigma^{-2} \ \mathsf{B}^{\mathsf{T}} \mathsf{QB} \ -\sigma^{-2} \mathsf{B}^{\mathsf{T}} \mathsf{PBB}^{\mathsf{T}} \mathsf{PB}$$

$$+\sigma^{-2} \left[\sigma^{2} \mathsf{I} \ -\mathsf{B}^{\mathsf{T}} \mathsf{PBB}^{\mathsf{T}} \mathsf{PB}\right] \tag{28}$$

We also note that

$$\phi_c(-s)\phi_c(s) = \phi_0(-s) \phi_0(s) \det [T^T(-s) T(s)]$$
 (29)

where  $\phi_{C}(s)$  denotes the closed loop characteristic polynomial and  $\phi_{0}(s)$  denotes the open loop characteristic polynomial. Since the closed loop system is stable for all  $\alpha \geq 0$ , we can deduce from (28) and (29) that m closed loop poles tend to infinity and are asymptotic to

$$s_{i}^{\infty} = -\alpha \sqrt{\lambda_{i}(B^{\mathsf{T}}PBB^{\mathsf{T}}PB)}, \quad i=1,2,...,m$$

$$= -\alpha \lambda_{i}(B^{\mathsf{T}}PB), \quad i=1,2,...,m$$
(30)

where  $\lambda(A)$  denotes an eigenvalue of the matrix A. The remaining n-m closed loop poles approach finite values which are the left half plane images of the zeros of the determinant of  $B^TP(sI-A)^{-1}B$ . Denote these left half plane finite zeros by  $s_i^0$ ,  $i=1,2,\ldots,n-m$ . The eigenvectors associated with the finite zeros are orthogonal to  $B^TP$  and are given by

$$X_i^0 = (s_i^0 I - A)^{-1} B \mu_i^0$$
,  $i = 1, 2, ..., n - m$  (31)

with the  $\mu_i^0$  determined by

$$B^{T}P(s_{i}^{0} I-A)^{-1} B \mu_{i}^{0} = 0, i=1,2,...,n-m$$
 (32)

The eigenvectors associated with the asymptotically infinite eigenvalues are given by

$$X_{i}^{\infty} = B^{\mu_{i}^{\infty}}, i=1,2,...,m$$
 (33)

with  $\mu_i^\infty$  determined by

$$\lambda_{i}(B^{T}PB)\mu_{i}^{\infty} = -B^{T}PB \mu_{i}^{\infty}, i=1,2,...,m$$
 (34)

These results are similar to those obtained for optimal regulators.  $^*$ For the optimal regulator, however, the asymptotic eigenvalues and eigenvectors are related to the weighting matrices  $Q_R$  and  $R_R$ . Here, unfortunately the relation is to P which is in turn related to Q, but a direct relationship to Q is not available.

In the special case for which  $B^T = \begin{bmatrix} 0 & B_1^T \end{bmatrix}$  with  $B_1$  an mxm nonsingular matrix, which would be the common representation for systems with actuator dynamics, we can proceed one step further. In this case, let  $v_1^{\infty} = B_1 u_1^{\infty}$ . Then from (33)

$$\chi_{\mathbf{j}}^{\infty} = \begin{bmatrix} 0 \\ B_{\mathbf{j}} \end{bmatrix} \psi_{\mathbf{j}}^{\infty} = \begin{bmatrix} 0 \\ v_{\mathbf{j}}^{\infty} \end{bmatrix}, i=1,2,\dots,m$$
 (35)

and from (34)

$$\lambda_{i} v_{i}^{\infty} = -B_{1}(B^{T}PB) B_{1}^{-1} v_{i}^{\infty} = -B_{1}B_{1}^{T} P_{4} v_{i}^{\infty}, i=1,2,...,m$$
 (36)

where  $P_4$  is the lower right mxm block of P. If we set  $N = [v_1^{\infty}, v_2^{\infty}, \dots, v_m^{\infty}]$  and  $A = diag(\lambda_i^{\infty})$ , then (36) may be written as

$$N\Lambda = -B_1 B_1^T P_4 N \tag{37}$$

Thus.

$$P_4 = -(B_1 B_1^T)^{-1} N \Lambda N^{-1}$$
 (38)

and the fact that  $P_4$  is symmetric implies constraints on N and A, which may be interpreted as constraints on actuator couplings and relative bandwidths.

<sup>\*&</sup>quot;Quadratic Weights for Asymptotic Regulator Properties", C.A. Harvey, G. Stein, IEEE Trans. on Auto. Control, Vol. AC-23, June 1978.

71

The fact that the finite zero,  $s_i^0$ , was constrained in the simple example is property that is common to the general case. Adding  $2s_i^0P$  to both sides of equation (3) and rearranging yields

$$P(s_{i}^{0}I-A) + (s_{i}^{0}I-A)^{T}P = Q + 2s_{i}^{0}P$$
 (39)

Multiplying equation (39) on the right by  $v_i^0 = (s_i^0 I - A)^{-1} B \mu_i^0$  and on the left by  $(v_i^0)^T$  yields

$$2(\mu_{i}^{0})^{\mathsf{T}}B^{\mathsf{T}}P \ v_{i}^{0} = (v_{i}^{0})^{\mathsf{T}} \ (Q + 2s_{i}^{0}P)v_{i}^{0} \tag{40}$$

But, 
$$B^{T}P \ v_{i}^{O} = B^{T}P(s_{i}^{O}I-A)^{-1} B_{\mu_{i}^{O}} = 0 \text{ from (32), so that}$$

$$-s_{i}^{O} = \frac{(v_{i}^{O})^{T} Q v_{i}^{O}}{2(v_{i}^{O})^{T} P v_{i}^{O}}$$
(41)

and it follows that

$$|s_i^0| \le \frac{\overline{\sigma}(Q)}{2\underline{\sigma}(P)}$$
 (42)

where  $\overline{\sigma}(Q)$  is the largest singular value of Q and  $\underline{\sigma}(P)$  is the smallest singular value of P. Thus, (42), shows that the magnitudes of the finite zeros are bounded, but the bound involves P and Q. Since P is a function of A and Q, the bound is an implicit function of A and Q. Unfortunately, the explicit dependence is not evident.

An alternate characterization of controllers defined by (2) and (3) can be derived by considering the optimal controllers for (1) with respect to the performance index

$$J = \int_0^\infty (\beta x^T Q x + u^T u) dt$$
 (43)

with  $\beta$  a small positive scalar parameter. In this case the optimal controller can be represented as

$$u = -B^{T}(\sum_{i=0}^{\infty} \beta^{i} P_{i})x$$
 (44)

where

$$(\sum_{i=0}^{\infty} \beta^{i} P_{i}) A + A^{T}(\sum_{i=0}^{\infty} \beta^{i} P_{i}) + \beta Q = (\sum_{i=0}^{\infty} \beta^{i} P_{i}) B B^{T}(\sum_{i=0}^{\infty} \beta^{i} P_{i})$$
 (45)

Equating terms of like powers of  $\beta$  in equation (45) yields

$$P_0A + A^TP_0 = P_0BB^TP_0$$
 (45a)

$$P_1A + A^TP_1 + Q = P_0B B^TP_1 + P_1B B^TP_0$$
 (45b)

etc.

With A being a stable matrix,  $P_0 = 0$ , so that the right hand side of (45b) is zero. Thus, the equation for  $P_1$  is the same as equation (3), and controllers defined by (2) and (3) may be viewed multiples of first order approximation to optimal controllers, i.e.

$$u = -B^{T} P_{1} x = -B^{T} \lim_{\beta \to 0} \left[ \frac{1}{\beta} \sum_{i=0}^{\infty} \beta^{i} P_{i} \right] x$$
 (46)

Another way of describing this characterization is to consider the controller given by (2) and (3) with Q in (3) replaced by  $\beta Q$ . Then this controller is the first order approximation to the controller given by (44) as  $\beta$  tends to zero. This implies that the closed loop root loci (parameterized with  $\beta$ ) associated with these controllers are tangent at  $\beta=0$  which corresponds to the open loop roots.

G. STEIN
Honeywell SRC
Minneapolis, MN. and
Massachusetts Institute of Technology
Cambridge, MA

J.C. DOYLE, Consultant Honeywell SRC Minneapolis, MN, and University of California Berkeley, CA

## ABSTRACT

Some control law design examples for the CH-47 helicopter are used to explore and illustrate the role of singular value analyses in multivariable design.

## 1.0 INTRODUCTION

Design techniques for linear multivariable control systems have long suffered from the lack of reliable measures of "robustness". By robustness, we mean an intentionally designed tolerance for differences between the nominal plant model used for design and the actual plant being controlled. Such differences arise as a result of parameter variations, neglected dynamics, approximated functional relationships, nonlinearities, etc. They are present to some extent in all physical systems. Critical closed loop properties such as stability must therefore be designed to remain intact in the face of these differences, and key performance variables should exhibit only weak dependence on them.

for single input single output systems, the degree to which such tolerance is achieved has been historically (and reliably) measured in terms of the minimum distance of a loop's Nyquist diagram from the so-called critical point (-1,0) in the complex plane [1]. The familiar concepts of phase margin and gain margin are measures of this distance and are often specified as explicit minimum robustness requirements of control loops [for example, 2].

Many attempts have been made to apply these measures of robustness to multivariable systems. A common engineering practice, for example, is to measure gain and phase margins of individual loops one at a time with other loops variously open or closed. More formal methods have been advocated by Rosenbrock [3], who applies these measures to the inverse Nyquist plots of diagonally dominant systems, and by MacFarlane et al. [4], who apply them to the eigenvalue (or characteristic loci) plots of multivariable systems. All of these approaches have been shown to be unrealistic in the sense that a lack of tolerance in certain directions goes undetected [5]. In effect, the methods can indicate that all is well with respect to robustness when dangerous sensitivities in fact exist.

The concept of singular values of matrix transfer functions has recently been applied to overcome this reliability problem. In [5], Doyle established a multivariable stability-robustness theorem which guarantees that a stable multivariable control system will remain stable in the face of multiplicative model perturbations whenever the singular values of these perturbations remain appropriately bounded. This result has since been shown by Sandell [6] to be a special case of a general invertability condition for stable perturbed operators. It is also implicit in the recent stability results of Safonov [7]. When it is combined with this work was supported by the Office of Naval Research under

Contract No. NO0014-75-C-0144.

efficient computational procedures for singular value decomposition and with tight bounding formulas for the magnitudes of model perturbations the result appears to provide a valuable new multivariable design tool.

It is the intent of this paper to explore and illustrate the role which singular value analyses might play in multivariable design. We do this by means of some trial control design examples for the longitudinal degrees of freedom of the CH-47 helicopter. In forward flight, this vehicle exhibits coupled pitch attitude and vertical motion dynamics which must be controlled by coordinated actuation of two inputs. This offers a realistic, yet manageable design example. We begin the discussions in Section II with a quick review of Doyle's stability-robustness result and of some bounding formulas for model perturbations recently developed by Safonov [8]. Specifics of the CH-47 design problem are given in Section III and IV, and various trial designs are discussed in Section V. Conclusions and some open research questions are given in Section VI. We caution all readers to consider the control laws presented as illustrative only. They are not, and are not intended to be, final "flight quality" designs.

# 2.0 MULTIVARIABLE ROBUSTNESS CONCEPTS

We consider finite dimensional, linear, time-invariant multivariable feedback loops represented in the frequency domain as shown in Figure  $1^*$ . The matrix  $G_{\rm c}(s)$  represents the nominal plant transfer function, and L(s) represents a multiplicative perturbation such that the actual plant is given by

 $G(s) = G_0(s) [1+L(s)].$  (1)

If L(s) and the nominal closed loop system,  $(I+G_0)^{-1}G_0$ , are both stable then the following result holds:

## Theorem

The perturbed closed loop system remains stable for all-perturbations L(s) such that

$$\bar{\sigma}[L(s)] < \sigma[1 + G_0^{-1}(s)]$$
 (2)

for all complex frequencies, s, on the classical Nyquist D-contour. \*\* Here the symbols  $\sigma[A]$  and  $\sigma[A]$  denote the maximum and minimum singular values of matrix A, respectively, with singular values being defined as the square roots of eigenvalues of A\*A. Equation (2) immediately suggests that the function  $\sigma[I+G_0^-(s)]$ , s(D) provides a reliable measure of multivariable robustness—the bigger  $\sigma$ , the better. Moreover, since this function is equal for s=tjw and tends to infinity on the infinite segment of the D-contour (at least for all physical systems), it suffices to look at the singular values for real positive frequencies only, i.e., the system remains stable if

$$\tilde{\mathfrak{o}}[L(jw)] < \underline{\mathfrak{o}}[I + G_0^{-1}(jw)]$$
for all  $0 \le \omega < \infty$ .

'More general systems can be treated with Sandell's [6] and Safonov's [7] generalizations.

\*\*The D-contour encloses the right half plane with three segments: 1) s=jw,  $0\le\omega<\infty$ ; 2) $s=Re^{j\theta}$ ,  $R\to\infty$ ,  $-\frac{\pi}{2}\le0\le\frac{\pi}{2}$ ; 3) s=jw  $-\infty<0\le0$ . It is usually indented to exclude singularities along this path.

(i.e., ō and q vs.ω) to measure system robustness. We will refer to these plots as sigma-plots for convenience.

In order to utilize equation (3), it is necessary to be able to calculate singular values efficiently and to be able to characterize realistic perturbations L(s) for complex systems. Numerical procedures for the first requirements are discussed by Laub in [9]. The second requirement is satisfied to substantial degree by the following composite sectoricity results due to Safonov [8]\*.

Consider the system diagram shown in Figure 2. The matrices  $G_0$ ,  $G_{yy}$ ,  $G_{eu}$  and  $G_{ey}$  are nominal transfer functions of our original plant with its block diagram redrawn such that the uncertainties of individual components are all collected into one perturbation matrix; dia  $[c_i(s) \mid i = 1, 2, ..., N]$ . The ci's are nominally zero and are assumed to have known individual bounds

$$|c_{i}(jw)| \leq |r_{i}(jw)| \tag{4}$$

where the r,'s are stable, minimum phase, rational transfer functions. R  $\triangleq \text{diag}(\textbf{r}_i)$  and let Let

- a) the nominal system be stable, and
- b) the matrix M  $\stackrel{\triangle}{=}$  I-G $_{\rm ev}^{\star}$  R\*RG $_{\rm ev}$  be uniformly positive for all  $\omega$ .

Then the perturbed system's transfer function matrix will belong to a "conic sector" (a circle in the frequency domain) defined by

$$\bar{O}[Q^{l_2}(jw)(G(jw)-G_C(jw))] P^{-l_2}(jw)] \le 1$$
 for all  $w$ 

with

$$Q = [G_{VV} M^{-1}G_{VV}^{*}]^{-1}$$
 (7)

$$P \stackrel{\triangle}{=} G_{eu}^{*} R^{*} [I - RG_{ev} G_{ev}^{*} - R^{*}] RG_{eu}$$
 (8)

Note that equations (5)-(8) provide a way to compute bounds for the total perturbation L(s) in Figure 1 from know bounds for individual component elements of the plant.

# III. THE EXAMPLE DESIGN PROBLEM

To examine the potential utility of the above concepts in multivariable system design, we will treat a longitudinal-axes design problem for the CH-47 helicopter. This vehicle is a tandem rotor machine whose physical characteristics and mathematical models are given in [10]. Control over vertical motions is achieved by simultaneous changes of blade angle-ofattack on both rotors (collective), while pitch and forward motions are controlled by changing blade angle differentially between the two rotors (differential-collective). These blade angle changes are transformed through rotor dynamics and aerodynamics into hub forces which then move the machine.

Our objectives will be to design a command augmentation control law which achieves tight, non-interacting control of the vertical velocity and pitch attitude responses. A small perturbation linearized aircraft model should prove adequate for this purpose and is available from [10]. The state vector consists of the vehicle's basic rigid body variables  $x = (V, z, q, \theta)$  (forward velocity, vertical velocity, pitch rate, pitch angle). Two integrators are appended to achieve integral control of the primary responses, and controls are the collective and differentialcollective inputs described avove, u.(c,dc). Hence, the design model is

$$\dot{x} = Ax + Bu \qquad A, B \text{ in [10]}$$

$$\dot{x}_5 = -\dot{z} + \dot{z}_{cmd} \tag{10}$$

$$\dot{x}_6 = -\theta + \theta_{cmd} \tag{11}$$

The major approximations associated with this model are due to neglected dynamics of the rotors, to neglected nonlinearities in the blade angle actuation hardware, and to variations of the A,B matrices with operating point (flight condition variations). We will treat modelling errors due to these approximations as sources of the perturbation L(s) in Figure 1 and will attempt to make controllers robust with respect to them.

# IV. CHARACTERIZATION OF L(s)

In view of the stability-robustness theorem cited earlier, it is not unjustified to consider nominal design models to be incomplete unless they are accompanied by estimates of the function  $\bar{\sigma}[L(s)]$ . (How else can a designer assure the required degree of robustness?) Such estimates are developed in this section for the model in equations (9)-(11).

# Perturbations Due to Rotor Dynamics

Elementary dynamic and aerodynamic analyses of rotating airfoils, hinged at the rotor hub, indicate that lift forces will not be transmitted to the hub instantaneously with collective changes in blade angle-of-attack but will appear only when the cone angle of the rotor has appropriately changed. The dynamics of the latter have been shown to be damped second order oscillations with natural frequency equal to rotor speed and damping determined by somewhat uncertain aerodynamic effects [11]. Hence, rotor dynamics can be crudely represented by second order transfer functions

$$g_{R}(s,\zeta) = \frac{\omega_{R}^{2}}{s^{2} + 2\zeta\omega_{R}s + \omega_{R}^{2}}$$
 (12)

with  $\omega_{\rm D}$ =25 and  $\tau$  conservatively confined to the range 0.1 <  $\tau$  < 1.0. Because collective and differential-collective inputs both involve coning motions of the rotors, one such transfer function will appear in each control channel. Since these dynamics are neglected in equation (9), it then follows that any perturbated transfer function matrix computed from Table 1 will have the form

$$G = G_0(I+L) = G_0 \text{ diag } (g_R),$$
 (13)

and hence,

$$L = diag (g_p-1)$$
 (14)

L = diag 
$$(g_R^{-1})$$
 (14)  
 $\bar{\alpha}[L]$  =  $\max_{\zeta} \left| \frac{s^2 + 2c\omega_R}{s^2 + 2c\omega_R s + \omega_R} \right|$  (15)

This function was evaluated for a range of s=jw values (with brute force maximization over () and is shown by the solid lines in Figure 3.

figure 3 also shows an alternate bound for o[L] developed from Safonov's formulas, equation (5)-(8). In this case, the rotor dynamics are redrawn as in figure 2, with nominal damping value, 50 = 0.55, plus an internal component perturbation, 8c, bounded by

$$|\delta\zeta| \leq |r|$$
 with r=0.45

$$\begin{bmatrix} G_o & G_{yv} \\ G_{eu} & G_{ev} \end{bmatrix} = \begin{bmatrix} \omega_R^2 & -2_{\omega R} \\ \omega_R^2 s & -2\omega_R s \end{bmatrix} / (s^2 + 2(\omega_R s + \omega_R^2))$$
(17)

and according to (5), the rotor dynamics at each frequency then belong to a circle in the complex plane with center,  $\tilde{g}_p$ , defined by (6) and radius,  $\tilde{g}_p$ , given by  $\sqrt{p/q}$  with scalars p and q defined by (7) and (8). Using this circle in (14)gives the bound

$$\tilde{\sigma} \left[ L \right] \leq \left[ \tilde{g}_{R}^{-1} \right] + \tilde{g}_{p}, \tag{18}$$

which is plotted in Figure 3. Note that this "Safonov bound" is slightly more conservative than equation (11) because it admits a larger class of damping perturbations—i.e.,  $\delta \zeta$  in (13) may itself be a dynamical operator.

# Perturbations Due to Rate Limits

In addition to the dynamics of rotors, each control channel of the CH-47 also exhibits various nonlinearities which are neglected in the nominal design model. Of these, the rate limit nonlinearity imposes the greatest dynamic constraint on performance, and we consider bounds only for this one effect.

An approximate model for rate limits on the CH-47 is given by

$$\dot{\mathbf{u}} = \mathbf{R}_{\ell \text{im}} \text{ SAT } \left[ 94(\mathbf{u}_{c} - \mathbf{u}) / \mathbf{R}_{\ell \text{im}} \right]$$
 (19)

where SAT() denotes the standard saturation nonlinearity, saturating at  $\pm$  1. Bounds for this model can be developed with Safonov's procedure by treating the SAT element as an uncertain component. For example, if we are prepared to restrict our system to functions  $\zeta(t)$  whose  $L_{\infty}$ -norms are less than some multiple of the limit, say

$$||\zeta||_{L_{\infty}} \le \eta, \qquad n \ge 1.0,$$
 (20)

then

SAT(
$$\zeta$$
) = (0.5 + 0.5/n) + ( $\delta c$ ) $\zeta$  with  $|\delta c| \le |r| = 0.5 - 0.5/n$  (21)

The &c perturbations are nonlinear, of course, and equation (5)-(8) do not apply to them as stated. Fortunately, reference [8] shows that the bounds are still valid for these and other more general perturbations. Hence, the rate limit nonlinearities belong to a conic sector and have a 5[L] bound analogous to (19). This bound is plotted in Figure 3 (dashed lines) for several values of the magnitude ratio  $\eta$ . Note that as  $\eta$  becomes large, the bound approaches unity at all frequencies. This is consistant with physical intuition, since the effective gain across rate limited nonlinearities will approach zero for large signal levels.

# Perturbations Due to Operating Point

The third major source of model uncertainty is the variation of A, B matrices with flight condition. Such "component" variation could again be translated into an overall bound for L(s) via Safonov's procedure. In this case, however, the result would be unduly conservative because coefficient variations tend to be highly correlated and are not arbitrary dynamical operators. A more direct way to compute the bound is to solve (1) for L(s) with known G(s) matrices and to maximize over a number of representative flight conditions, i.e.,

MARKET STREET, STREET,

Results of this process are shown by the dotted line in Figure 3. We see the (initially surprising result that  $\bar{\sigma}[L]$  becomes quite large at low frequencies. This happens because the basic helicopter's low frequency modes are stable at some flight conditions and unstable at others. (Theoretically,  $\bar{\sigma}(jw)$  will approach infinity for frequencies and flight conditions where these modes cross the jw-axis. This means that the perturbations exhibited by our plant are not necessarily stable and, hence, the stability-robustness theorem cited in Section II fails to apply. We will see later that stable controllers can still be obtained and that the ability to incorporate unstable L's in a generalized multivariable stability-robustness theory appears to be an important research topic. For the moment, however, our designs will be restricted to individual flight conditions for which the dotted L's in Figure 3 can be disregarded.

## V. TRIAL CONTROLLER DESIGNS

A bit of contemplation of equation (3) and the uncertainties given in Figure 3 shows that the stability-robustness theorem basically works by imposing a "multivariable bandwidth" limitation on the feedback loop. Magnitudes of L(jw) tend to be large (unity or greater) beyond certain frequencies, requiring  $G^{-1}$  to be large and consequently G to be small. This is most readily illustrated with a single loop example where plots of the function  $O[1+g^{-1}]$  reduce to the inverse closed loop frequency response, i.e.,

 $\underline{\sigma}[0+g^{-1}] = [\frac{1+g}{g}] = [\frac{1}{g}].$  (23)

The condition that  $a[1+g^{-1}]$  be large then translates directly into the high-frequency "roll-off" requirement commonly imposed on classical control loops [1]. We begin with such an example.

## Single Loop Pitch Attitude Control

The vertical velocity and pitch attitude motions of the nominal CH-47 model at hover uncouple naturally into two non-interacting channels--  $(z,x_{\rm f})$  controlled by (c), and  $(v,q,0,x_{\rm f})$  controlled by (dc). The hover flight condition thus offers an attractive single loop design case. Sigmaplots for several trail pitch-motion controllers for this case are shown in figure 4. These controllers were all designed with the linear-quadratic methodology (selected largely for convenience) and correspond to the following cost functional:

 $J = \int_{0}^{\infty} (57.3 \times_{6})^{2} + \rho(dc)^{2} dt$  (24)\*
with  $\rho = 900.$ , 9.0, 0.09, and 1.0, respectively, for the four trials. As

with f = 900., 9.0. 0.09, and 1.0, respectively, for the four trials. As expected, bandwidth of these controllers increases with decreasing  $\rho$  and eventually violates the stability-robustness constraint imposed by neglected rotor dynamics (for the moment we ignore rate limits and flight condition variations). That this violation actually produces instabilities was verified by computing closed loop roots of the trail controllers in the presence of the rotor. Irial 3 is unstable! Our options are therefore to restrict bandwidth to approximately Irial 2 or to provide additional roll-off beyond the maximum 20 db/decade attenuation inherent in LQ-designs [13]. The latter option is illustrated by Trial 4 which uses a  $\rho$ -value somewhat smaller than Irial 2 but includes a low-pass filter at

<sup>\*</sup>These weighting selections are motivated by the "asymptotic" procedure of Reference [12]. They achieve a single slow mode mean the origin for the remaining states.

loop frequency responses\* are well-shaped for all pure LQ-trials and that Trial 4 achieves extra bandwidth at the expense of slightly larger M-peaks.

Multi-Loop Designs

Maximizing Bandwidth--The beauty of singular values is that the above stability-robustness analyses carry over without change to multivariable systems. This is illustrated in Figure 5 with some trial two-channel designs at a 40 knot forward speed flight condition. These controllers are again of the LQ-type, this time using the cost function,

are again of the LQ-type, this time using the cost function,  $J = \int_{0}^{\infty} (x_5)^2 + (57.3 x_6)^2 + \rho_1(c)^2 + \rho_2(dc)^2 dt,$ with  $(\rho_1, \rho_2)^2 = (10000, 900), (9.0, 9.0), \text{ and } (1.0, 1.0) \text{ for the three}$ 

with  $(\rho_1,\rho_2)^*=(10000,900)$ , (9.0,9.0), and (1.0,1.0) for the three trials shown. The distinction between Figures 4 and 5 is that Figure 5 shows two sigma-plots for each trial, corresponding to the two singular values of  $(1+G^{-1})$ . For stability-robustness, the smaller of these values must fall above the sigma-plot of L at all frequencies. The larger value is unspecified. However, in order to maximize bandwidth "in all directions", it is reasonable to adjust the relative weights  $(\rho_1,\rho_2)$  such that the two singular values are approximately equal and then to push them jointly to as high a bandwidth as the  $\bar{\sigma}[L]$  plot permits. (For the moment, we again use only neglected rotor dynamics for L.) This design philosophy is incorporated in the three trials of Figure 5. The first trail has low bandwidth and substantial differences between the two singular values. These differences are reduced and bandwidth is increased in the next trial. The third trial serves to maximize bandwidth by using additional roll-off filters in each control channel.

Transient Response—As seen from these trials, singular value analyses appear to offer a convenient way to maximize multivariable bandwidth subject to stability-robustness limitations. The next design step is to achieve reasonable command responses from the resulting feedback loop. One way to do this is to place a command shaping filter ahead of the loop, as indicated by the dashed box in Figure 1. For feedback loops with integral control on the primary responses, such sophistication is often unnecessary because commands inserted at the integrators (as shown in equations (10) and (11)) produce good transients. This is the case here, as evidenced by the responses of Trail 3 to step attitude and step velocity commands shown in Figure 6. Note that the loops are tight, well damped, and non-interacting as desired.

Rate Limiting--So far we have ignored model uncertainties due to rate limits. This was done because there is no a priori way to select the parameter n for Figure 3, which is determined by the maximum magnitudes of signals in the closed loop. Clearly, for n sufficiently large all our trial designs would violate the resulting  $\sigma[L]$  bound. That such violations actually correspond to instabilities was verified by repeating the transient responses for Trail 3 with progressively larger attitude commands. Unstable behavior occurs for  $\theta_{\text{Cmd}} \geq 18$ . degrees, with  $n \geq 60$ .

In order to improve robustness with respect to rate limits, the following iterative procedure may be used:

1) Assume a signal level limit  $n \leq n_0$ 

2) Design ! +  $G_0^{-1}$  consistent with the resulting  $\tilde{\sigma}[L]$ 

<sup>\*</sup>According to (23), these are given by the sigma-plots of Figure 4 viewed "upside down".

- 3) Evaluate the actual maximum signal level, n<sub>1</sub>, by computing transient responses with worst case commands and/or initial conditions
- 4) If  $n_1$  and  $n_0$  are substantially different, return to step 1 with  $n_0 = n_0 + c(n_1 n_0)$ . Stop otherwise

An illustration of the first iteration of this procedure is given in Figure 5 where the assumed signal level  $n_{\rm c}=20$ . (the dashed  $\sigma[L]$ curve) yields a controller (Trial 2) whose actual signal level is  $n_1<0.6$ . The associated transient responses are slow but stable. To fine tune this design, a second iteration might be taken with  $n_0=5$ .

Flight Condition Variations—We noted earlier that  $\sigma[L]$  due to operating point changes becomes quite large at low frequencies because the helicopter's slow modes are not stable at all operating points. At intermediate and high frequency ranges, however, the uncertainty bounds are reasonably small (Fig. 3). This suggests that if the loop transfer matrix G(s) has sufficient low frequency gain to stabilize the slow modes under all conditions, then the design might well be stable even though the (sufficient) stability-robustness condition fails. This is in fact the case. Both trial design No. 2 and No. 3 remain stable at 8 representative flight conditions ranging from hover to 160 knot forward speed and from +2000 ft/min to -2000 ft/min ascent rates. The intuitive idea which underlies this result (sufficiently high low frequency gain) may well provide needed insight toward a generalized multivariable robustness theory for unstable perturbations.

## VI. CONCLUSIONS

This paper has presented several trial control law designs to explore and illustrate the role which singular value analyses might play in multivariable system design. The examples confirm that stability-robustness condition (2) provides a reliable measure of robustness, and they show that this condition offers a natural way to limit multivariable bandwidth during the design process. The bounding formulas (5)-(8) were seen to be very useful for bounding the functions a(1), although for some situations a(2), flight condition variation, they tend to be excessively conservative.

Major weaknesses displayed by the present singular value stabilityrobustness theory include its inability to handle unstable perturbations
and its implicit tendency to limit all loop bandwidths to be consistent
with the worst case L direction. Although such situations did not arise
with the helicopter, it is easy to imagine design problems where some
control directions have large L's at low frequencies, hence calling for
low bandwidth, while other direction have smaller L's, hence permitting
greater bandwidths. It is then unduly conservative to restrict all
direction to the slowest case. It is hoped that the examples presented
here will help to motivate further research to overcome these weaknesses.

<sup>\*</sup>ε is at the designers discretion

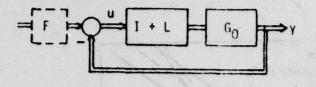


Fig. 1 Multivariable Feedback Loop

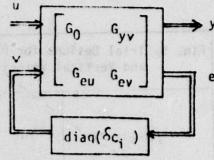
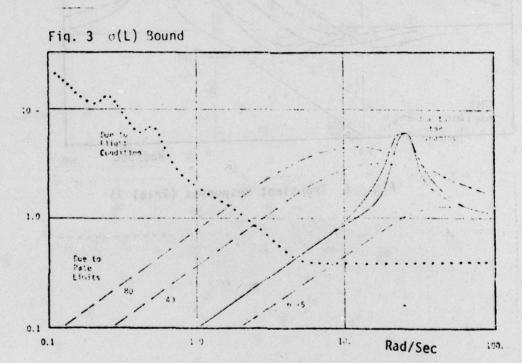
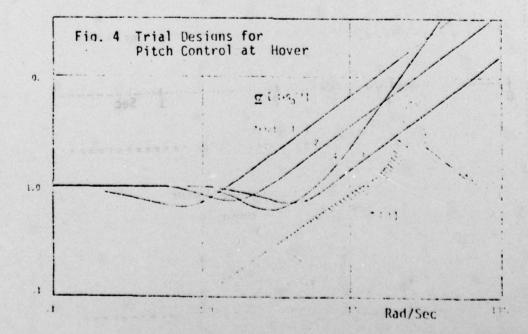
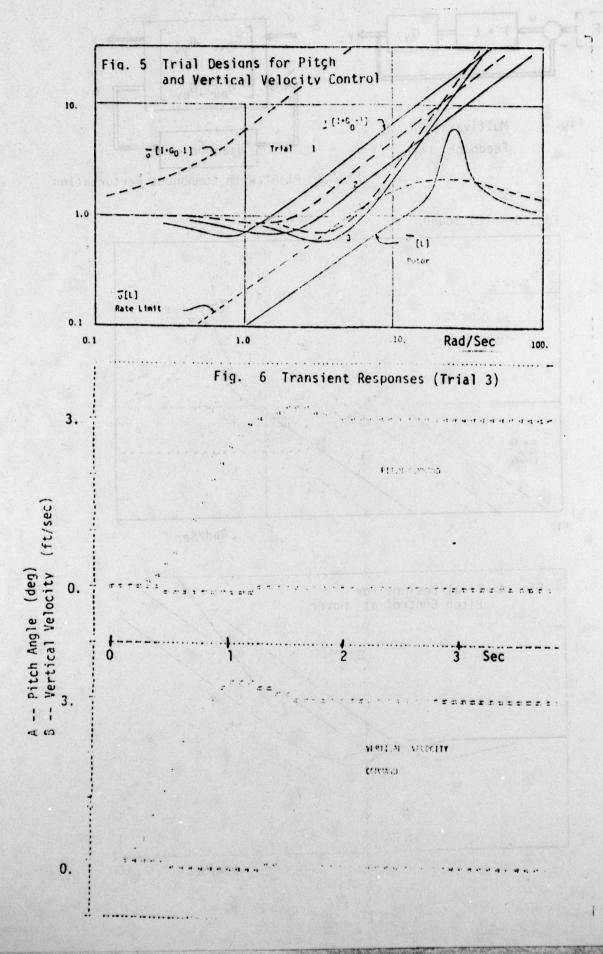


Fig. 2 Plant with Component Perturbation







- (For example) I.M. Horowitz, Synthesis of Feedback Systems, Academic Press, New York 1963.
- 2. Background Information and User Guide for MIL-F-94900, Air Force Flight Dynamics Laboratory, Report AFFDL-TR-24-116, Jan. 1975.
- H.H. Rosenbrock, Computer Aided Control System Design, Academic Press, 1974.
- 4. A.G.J. MacFarlane and B. Kouvaritakis, "A Design Technique for Linear Multivariable Feedback Systems", Int. J. Control, Vol. 23, No. 6, June 1977, pp. 837-874.
- J.C. Doyle, "Robustness of Multivariable Linear Feedback Systems", to be presented, Conference on Decision and Control, San Diego, Jan. 1979.
- 6. N. R. Sandell, "Singular Values and Robustness", 1978 Allerton Conference, this session.
- M.G. Safonov, "Robustness and Stability Aspects of Stochastic Multivariable Feedback Design" PhD Dissertation, MIT, Sept. 1977.
- 8. M.G. Safonov, "Tight Bounds on the Response of Multivariable Systems with Component Uncertainty," 1978 Allerton Conference, this session.
- 9. A.J. Laub, "Computational Aspects of Singular Value Decomposition," 1978 Allerton Conference, this session.
- A.J. Ostroff, D.R. Downing and W.J. Road, "A Technique using a nonlinear Helicopter Model for Determining Terms and Derivations", NASA Technical Note IN D-8159, NASA Langley Research -Center, May 1976.
- 11. R.H. Hoheuemser, and S. Yin, "Some Application of the Method of Multiblade Coordinates", J. Am. Helicopter Soc., July 1972.
- G. Stein, "Genralized Quadratic Weights for Asymptotic Regulator Properties," to Appear, IEEE Trans. Auto. Control.
- 13. R.E. Kalman, "When is a Linear System Optimal?" J. Basic Engrg., Vol. 86, pp. 51-60, 1964

by

N.A. Lehtomaki, S.M. Chan, N.R. Sandell, Jr., M. Athans, J. Carrig Laboratory for Information and Decision Systems Massachusetts Institute of Technology Cambridge, Massachusetts 02139

C.E. Grund, F. Nozari, R. Hauth Electric Utility Systems Engineering Department General Electric Company Schenectady, New York 12345

## INTRODUCTION

In the past two decades, dc power transmission has provided a viable alternative to ac in special applications such as long-distance, point-to-point transmission, asynchronous connection between power systems of different frequencies, and interconnection of systems via underground and undersea cables. Common to all these applications is the two-terminal dc link which consists of a rectifier and an inverter connected by a dc transmission line. The main advantage of dc transmission lies in its ability to transmit a large block of power, with very little loss, from one part of the network to another without the inherent synchronous and stability limitations of ac systems. Although most dc links to date are built for the purpose of bulk-power transmission, it was discovered recently that by modulating the dc current, a dc link can be used as an extremely effective control element for damping some of the inter-area, electromechanical oscillations in an integrated ac/dc system.

The successful application of two terminal dc links suggests that even greater flexibility in power dispatch and enhancement in stability can be realized by a multiterminal dc (MTDC) system embedded in an interconnected ac grid. Several utilities are looking into the possibility of building MTDC systems by adding new terminals to the existing dc links or by connecting dc links that are located in close proximity. It is quite conceivable that MTDC will become a major part of our energy delivery system by the end of this century.

A parallel connected MTDC system is envisaged as a network of n (n>2) inverters and rectifiers interconnected by dc transmission lines. In the steady state, n-1 converters are operated under a constant-current mode, and the nth converter with the lowest ac commutating voltage (voltage that is applied to the ac side of a converter) is operated under constant delayangle or constant extinction-angle mode and determines the voltage of the entire MTDC system. In a transient condition the terminals of an MTDC system can potentially be modulated in a coordinated manner to damp. out the inter-area electromechanical oscillations.

The design of the MTDC control system offers a unique challenge; since it involves a large-scale, multivariable system where the sensors and actuators are situated far apart, and the parameters of the system are difficult to estimate and may change abruptly due to failures such as short circuits or generators outages. A workable design for such a system must be sufficiently robust to tolerate actuator and sensor failures, unmodelled dynamics, and changes in system parameters. Moreover, economic and reliability considerations dictate that some form of decentralized feedback scheme be used, if possible.

The intent of this paper is to illustrate how the MTDC control problem can be analyzed from a physical viewpoint, and how the physical insights can be utilized to arrive at a reasonable, robust control design. The main emphasis is on robustness. Some of the latest results in robustness theory are used in the design stage as well as in analyzing the final design.

Although this paper presents a general design methodology for an MTDC system, a hypothetical, fiveterminal dc/ac system is used as an example to illustrate the steps of the design process. The model of this system is described in Section I, and a physical interpretation of the design model from a modal perspective is given in Section II. Section III shows how the physical insights can be used to construct a state penalty matrix for an IQ design, and the concept of gain observability is utilized to study the tradeoff between the LQ centralized design and other decentralized schemes. The robustness of the control design is studied in Section IV, after a brief review of a relevant theorem in robustness theory. Finally, some results of the open- and closed-loop systems are compared in Section V.

## I. MODELLING

The power system being studied consists of an nterminal MTDC system embedded in an ac system with m groups of coherent machines, each of which is represented by the classical constant-voltage-behindtransient-reactance generator model. For each generator the electrical angle 6 is governed by Newton's Second Law for a rotating mass:

$$J\ddot{\delta} + D\dot{\delta} = P_{\underline{a}} - P_{\underline{a}} \tag{1}$$

where

- J is a constant related to the inertia of the generator,
- P<sub>m</sub> is the mechanical power supplied by the prime mover,
- P is the electrical power injected into the power network, and
- D is a constant related to the damping of the machine.

It is further assumed that the mechanical power remains constant over the time period of interest.

The dynamics of the dc converter and the dc network are ignored, because they are much faster than the electromechanical dynamics being studied. If the dc terminals are viewed as actuators, this implies that the control action is equal to the command at all time.

<sup>\*</sup> Research supported by the U.S. Department of Energy under contract ET-78-C-01-3395

Under these assumptions, a linearized model is obtained by first solving for the steady-state solution of the ac/dc system, and then linearizing the equations about the steady-state point. The result is a linear time-invariant model of the form

$$\dot{x}(t) = Ax(t) + Bu(t) \tag{2}$$

where

 $\underline{x} \stackrel{\Delta}{=} (\Delta \delta_1, \delta \omega_1, \dots, \Delta \delta_n, \delta \omega_n)^T$  are the changes in electrical angle and frequency of the m generators,

 $\underline{\underline{u}} \stackrel{\Delta}{=} (\Delta I_2, \dots, \Delta I_n)^T$  are the changes in current injected by the dc terminals.

(The current injection of the first dc terminal is not a control variable). A and B are matrices of appropriate dimension.

In the subsequent discussion, the "A" symbol will be dropped, and all quantities are deviations from the steady-state solution unless otherwise specified. It is important to emphasize that the design model (2) does not take into account the dynamics associated with the excitation system, power-system stabilizer, shaft torsional vibrations, and a host of other physical phenomena which are significant at frequencies greater than 30 rad/sec; thus the design model (2) is valid only for low frequencies. This fact will be important when designing the feedback system.

important when designing the feedback system.

For the purpose of illustration, a hypothetical ac/dc system shown in Figure 1 is used throughout. A physical interpretation of the dynamics associated with this system will be given after a brief discussion on the methods of modal analysis.

# II. CONTROLLABILITY, OBSERVABILITY AND PHYSICAL INTERPRETATION OF MODES

Since the linearized model on which the control design is based has limitations, as all models do, it is important to be able to physically interpret the system modes in order that the control system design may be evaluated in part by how it affects them. It is also important to assess beforehand the inherent ability of the available control inputs to accomplish the performance objective using only information furnished by the available output measurements. This is done by computing the open-loop system eigenvalues the corresponding left and right eigenvectors, determining what each mode physically represents and then determining the controllability and observability of each mode.

## Modal Analysis

To facilitate the subsequent discussion on the physical interpretation of the system modes the role of the left and right eigenvectors of the system matrix A is reviewed. Consider the open-loop system

$$\dot{\underline{x}}(t) = \lambda \underline{x}(t) \; ; \quad \underline{x}(0) = \underline{x}_0 \tag{3}$$

where the eigenvalues of  $\lambda$ ,  $\lambda_1, \lambda_2, \ldots, \lambda_n$ , are assumed to be distinct. Let  $\underline{v}_i$  and  $\underline{w}_i^T$  be the right and left eigenvectors respectively of  $\lambda$  associated with the eigenvalue  $\lambda_i$  and define the matrices

$$\mathbf{v} \stackrel{\Delta}{=} (\underline{\mathbf{v}}_1,\underline{\mathbf{v}}_2,\ldots,\underline{\mathbf{v}}_n) \tag{4}$$

$$\mathbf{w} \triangleq (\underline{\mathbf{w}}_1, \underline{\mathbf{w}}_2, \dots, \underline{\mathbf{w}}_n)^{\mathrm{T}} = \mathbf{v}^{-1} . \tag{5}$$

The reason for the adjective "right" and "left" is obvious by noting that

where

$$\Lambda \stackrel{\triangle}{=} \operatorname{diag}[\lambda_1, \lambda_2, \dots, \lambda_n] . \tag{8}$$

Using the right and left eigenvectors, the matrices  ${\bf A}$  and  ${\bf e}^{{\bf A}{\bf t}}$  may be written as dyadic expansions:

$$\lambda = \sum_{i=1}^{n} \lambda_{i} \underline{\nu}_{i} \underline{\nu}_{i}^{T} \tag{9}$$

$$\bullet^{At} = \sum_{i=1}^{n} \bullet^{\lambda_i t} \underline{v_i} \underline{v_i^T}$$
 (10)

The unforced response of the system is now given by

$$\bar{x}(t) = \sum_{i=1}^{n} (e^{it} \bar{x}^i) (\bar{x}^i_{\perp} \bar{x}^0)$$
 (11)

which shows that  $\underline{x}(t)$  is simply a linear combination  $\lambda_1 t$  of n time-varying vectors,  $\mathbf{e} = \underline{\mathbf{v}}_1$ , or modes each weighted by the scalar  $\underline{\mathbf{w}}_1^T \underline{\mathbf{x}}_0$ . A physical interpretation of a right eigenvector,  $\underline{\mathbf{v}}_1$ , can best be illustrated graphically on an argand diagram where the components of  $\underline{\mathbf{v}}_1$  are plotted as vectors in the complex  $\lambda_1 t$  plane. The quantity  $\mathbf{e} = \underline{\mathbf{v}}_1$  can be visualized as rotating all components of  $\underline{\mathbf{v}}_1$  at the same rate  $\mathrm{Im}[\lambda_1]$  and simultaneously shrinking or expanding them  $\underline{\mathbf{x}}$  the rate  $\exp\{\mathrm{Re}[\lambda_1 t]\}$  depending on whether  $\lambda_1$  is stable or unstable. This is similar to the phasor representation of sinusoidal signals and is depicted in Figure 2.

The left eigenvectors, on the other hand, determine a linear combination of states that oscillate at the complex frequency equal to the corresponding eigenvalue since

$$\frac{d}{dt} \left\{ \underline{w}_{\underline{i}}^{T} \underline{x}(t) \right\} = \underline{w}_{\underline{i}}^{T} \underline{\lambda} \underline{x}(t) = \lambda_{\underline{i}} \left( \underline{w}_{\underline{i}}^{T} \underline{x}(t) \right) . \tag{12}$$

## Physical Interpretation of System Modes

The open-loop eigenvalues of the system are plotted in Figure 3. The Argand diagram associated with each of the four pairs of complex eigenvalues reveals that the frequencies of certain areas are approximately 180° out of phase with that of the other areas. This is interpreted as an electromechanical oscillation in which two coherent groups of areas for a given mode swing against each other. For example, in Figure 4 for the -.094+j3.80 modes, the areas 1 and 2 swing against areas 3,4 and 5 with areas 2 and 5 being dominant in the oscillation. The two remaining eigenvalues are real. For the eigenvalue at zero the right eigenvector is

$$\underline{y}_{0}^{T} = \{1,0,1,0,1,0,1,0,1,0\}$$
 (13)

where the 1's correspond to angle states and the 0's to frequency states. The physical interpretation is that an arbitrary phase reference exists for this

$$\lambda \underline{x} = \lambda (\underline{x} + \beta \underline{v}_0) \quad . \tag{14}$$

In other words, only the difference in angle states is important since any constant may be added to all the angle states without affecting the dynamic response of the system. The left eigenvector for the remaining mode at -.18 has the form

$$\underline{\mathbf{w}}^{\mathbf{T}} = \{0, \mathbf{H}_{1}, 0, \mathbf{H}_{2}, 0, \mathbf{H}_{3}, 0, \mathbf{H}_{4}, 0, \mathbf{H}_{5}\}$$
 (15)

where H<sub>i</sub> is the intertia of area i divided by the total system intertia. Equation (12) implies that

$$\overline{\omega}(t) = -.18\overline{\omega}(t) \tag{16}$$

where

$$\overline{\omega}(t) \stackrel{\Delta}{=} \underline{\mathbf{w}}_{\mathbf{a}}^{\mathbf{T}} \underline{\mathbf{x}}(t) = \sum_{i=1}^{5} \mathbf{R}_{i} \underline{\omega}_{i}$$
 (17)

is interpreted as the average frequency of the power system.

The foregoing analysis, clearly demonstrates the role of the left and right eigenvectors in determining the physical interpretation which may not be immediately apparent for some of the system eigenvalues. The left and right eigenvectors are also very useful in determining the controllability and observability of the modes.

## Modal Controllability and Observability

Consider the linear system with m inputs, p outputs and n states

$$\dot{x}(t) = Ax(t) + Bu(t), \quad x(0) = x_0$$
 (18)

$$y(t) = Cx(t) (19)$$

Using the variation of constants formula gives

$$\underline{x}(t) = e^{At}\underline{x}_0 + \int_0^t e^{A(t-\tau)}B\underline{u}(\tau)d\tau$$
 (20)

$$y(t) = Ce^{\lambda t}\underline{x}_0 + \int_0^t Ce^{\lambda(t-\tau)}B\underline{u}(\tau)d\tau . \qquad (21)$$

For linear operators  $L(\cdot)$  and  $H(\cdot)$  let R(L) denote the range of  $L(\cdot)$  and N(H) denote the nullspace of  $H(\cdot)$ . The system defined in (18) and (19) is completely controllable if and only if

$$R(L) = R^{n} \tag{22}$$

where

$$L(\underline{u}) \stackrel{\Delta}{=} \int_{0}^{\epsilon} e^{A(\epsilon-\tau)} B_{\underline{u}}(\tau) d\tau$$
 (23)

and is completely observable if and only if

$$N(H) = \{\underline{0}\} \tag{24}$$

where

$$H(\underline{x}_0) \stackrel{\Delta}{=} Ce^{At}\underline{x}_0$$
 (25)

solubia + (sega - con

if the state of the system can be driven anywhere in  $\mathbb{R}^n$  by some control  $\underline{u}(\tau)$  applied from  $\tau=0$  to t. Analogously, (24) implies that given the output  $\underline{v}(t)$  and the input  $\underline{u}(\tau)$  for  $0 \le \tau \le t$ , the initial state, and thus the state trajectory, can be determined or observed.

There are different ways of determining whether the conditions (22) and (24) are satisfied. However, the definitions of controllability and observability specified in these conditions are qualitative concepts and do not provide quantitative measures of how controllable or how observable a system may be; they can only say what part of the system is controllable or observable and what part is not. Part of the problem is that it is not immediately spparent what is meant by terms like "strongly controllable" or "almost observable", since it is possible to define them differently depending on their intended use.

One possible way to quantify controllability and observability is to measure the change with respect to perturbations in the nominal system model. In other words, if "small" perturbations in the nominal system change, the controllability of certain states, those states would be considered "weakly controllable" or "almost uncontrollable."

A different but not unrelated way of measuring the controllability and observability is based on the intuitive idea of how strongly the modes can be excited by the inputs and how strongly the modes appear at the outputs, respectively. This is made more precise by considering the original qualitative definitions of controllability and observability in terms of the modes of the system. Consider L(u) and  $H(\underline{x}_0)$  in terms of the dyadic expansion for  $\exp(At)$ :

$$L(\underline{u}) = \sum_{i=1}^{n} \begin{bmatrix} \lambda_{i}^{t} \\ \bullet & \underline{y}_{i} \end{bmatrix} \begin{bmatrix} \underline{u}_{i}^{T} \underline{b} \end{bmatrix} \int_{0}^{t} -\lambda_{i}^{T} \underline{u}(\tau) d\tau \quad (26)$$

$$H(\underline{x}_0) = \sum_{i=1}^n \left[ \underline{y}_i^T \ \underline{x}_0 \ e^{\lambda_i t} \right] \left[ \underline{c}\underline{y}_i \right] . \tag{27}$$

From (26) it is clear that if w B=0 for some i,

then  $L(\underline{u})$  is a linear combination of at most n-l eigenvectors for any  $\underline{u}$ ; hence dim R(L) < n and the system is not completely controllable. Similarly from (27), if  $C\underline{v}_1=0$  for some i, then  $R(\underline{v}_1)=0$  but  $\underline{v}_1\ne0$ ; hence dim N(H)>0 and the system is not completely observable. These facts are immediately obvious once  $\underline{\chi}(t)$  is written as

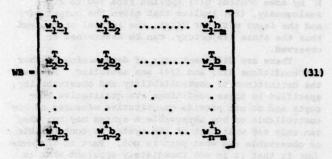
$$\chi(t) = \sum_{i=1}^{n} c_{\underline{y}_{i}} \left[ \underline{w}_{i}^{T} \underline{x}_{0}^{+} \underline{w}_{i}^{T} \mathbf{B} \int_{0}^{t} e^{-\lambda_{i} \tau} \underline{u}(\tau) d\tau \right] e^{\lambda_{i} t}. \quad (28)$$

If  $\underline{v_1}^TB=0$  then the input  $\underline{u}$  cannot excite the  $i\frac{th}{m}$  mode and if  $C\underline{v_1}=0$  the  $i\frac{th}{m}$  mode does not appear in the output  $\underline{v}(t)$ . In these cases the  $i\frac{th}{m}$  mode is said to be uncontrollable or unobservable respectively. If the matrices B and C are given by

$$\mathbf{z} = (\underline{b}_1, \underline{b}_2, \dots, \underline{b}_n) \tag{29}$$

$$C = (\underline{e}_1, \underline{e}_2, \dots, \underline{e}_p)^T$$
 (30)

where  $\underline{b}_{\underline{i}}$  is the  $i\frac{th}{c}$  column of B and  $\underline{c}_{\underline{i}}^{T}$  is the  $i\frac{th}{c}$  row of C then the matrices MB and CV given by



and

$$CV = \begin{bmatrix} \underline{c}_{1}^{T} \underline{v}_{1} & \underline{c}_{1}^{T} \underline{v}_{2} & \dots & \underline{c}_{1}^{T} \underline{v}_{n} \\ \underline{c}_{2}^{T} \underline{v}_{1} & \underline{c}_{2}^{T} \underline{v}_{2} & \dots & \underline{c}_{2}^{T} \underline{v}_{n} \\ \vdots & \vdots & \ddots & \vdots \\ \underline{c}_{p}^{T} \underline{v}_{1} & \underline{c}_{p}^{T} \underline{v}_{2} & \dots & \underline{c}_{p}^{T} \underline{v}_{n} \end{bmatrix}$$

$$(32)$$

have a nice interpretation: the magnitude of the entry  $\frac{\mathbf{T}}{\mathbf{U}_{i}}\mathbf{b}_{j}$  of WB measures how much the  $j\frac{\mathbf{t}h}{\mathbf{t}}$  input of  $\underline{\mathbf{U}}$  affects the  $i\frac{\mathbf{t}h}{\mathbf{t}}$  mode and the magnitude of the entry  $\mathbf{C}_{i}\frac{\mathbf{V}}{\mathbf{U}_{j}}$  of CV measures how much the  $j\frac{\mathbf{t}h}{\mathbf{t}}$  mode appears in the  $i\frac{\mathbf{t}h}{\mathbf{t}}$  output of  $\mathbf{v}(\mathbf{t})$ .

pears in the ith output of y(t).

If the rows of C and the columns of V are normalized to have unit euclidean length, the magnitude of c.v. represents the cosine of the angle between the vectors c, and v,. Thus when c, and v, are nearly orthogonal the k mode is unobservable from the ith output for some small perturbations of the nominal system.

In interpreting (31) and (32), it is important to keep in mind that the magnitude of  $\left| \left| \frac{\mathbf{v}}{2} \mathbf{b}_{j} \right| \right|$  and  $\left| \left| \frac{\mathbf{c}_{i}^{T} \mathbf{v}_{i}}{2} \right| \right|$  depends on the choice of units of the input

and output as well as the scaling of the eigenvectors. If the units of the input and output are considered fixed, the quantity  $||\mathbf{C}\mathbf{v}_{\perp}||$  can only be made large by making  $||\mathbf{w}_{\perp}^{T}\mathbf{B}||$  small, since V=W<sup>1</sup> and  $\mathbf{w}_{\perp}^{T}\mathbf{v}_{\perp} = \delta_{\perp 1}$ .

Thus it seems reasonable to balance the left and right eigenvectors corresponding to the same eigenvalue by making their norms equal. This ensures that a mode does not appear very observable but not very controllable or vice versa only because of the scaling chosen. It is also worth noting that the matrix products CV and WB are invariant under similarity transformations of the original system, and the terms  $\text{Cy}_{\underline{\mathbf{w}}_{1}^{T}\underline{\mathbf{x}}_{0}} \text{ and } \text{Cy}_{\underline{\mathbf{w}}_{1}^{T}}\underline{\mathbf{B}} \text{ in (28) are independent of the scaling of the right and left eigenvectors as long as$ 

scaling of the right and left eigenvectors as long-as N=V<sup>1</sup>. For the power system model, the matrices CV and WB (where the left and right eigenvectors are balanced), have the magnitudes of their elements plotted on bar graphs in Figures 5 and 6. The bars are plotted in pairs, the one on the left for the observability at the indicated output and the one on the right for the controllability at the indicated input. This is done for each mode of the system. In Figure 5 the heights of the bars in a given row have been scaled such that the most controllable and most chearently mode for the given input and output have

bars of unit height. In Figure 6 the bar heights have been scaled column-wise such that for a given mode the bars of the input and output from which the mode is most controllable and observable have unit height. Notice that the arbitrary phase reference mode is not observable from any frequency output but is controllable from every current input. From both Pigures 5 and 6 it is evident that the most observable oscillatory modes in each frequency output are also the most controllable from the input of the same area. This has important ramifications for the control system design in that the sensors and actuators may be colocated, obviating the need for expensive communication links.

## III. LINEAR QUADRATIC REGULATOR DESIGN

The basic design methodology adopted here is that of using a linear quadratic regulator to obtain a first iteration centralized design that moves the open loop poles of the system to an appropriate closed loop pole region. This region is determined approximately on engineering judgement by how large the closed loop bandwidth may be made without allowing unmodeled high frequency disturbances or dynamics to destabilize the system. The centralized design is done with an eye towards later decentralization which uses only the measurable frequency states. The decentralized control law then attempts to mimic the centralized control law by including only the important feedback gains from the centralized feedback gain matrix.

## Centralized Design

The optimal feedback control law that minimises the cost functional

$$J(\underline{u}) = \int_{0}^{1} \underline{x}^{T}(t) Q \underline{x}(t) + \underline{u}^{T}(t) R \underline{u}(t), \quad Q \ge 0, \quad R \ge 0 \quad (33)$$

is given by the familiar

$$\underline{u}^{*}(t) = -R^{-1}B^{T}KX(t)$$
 (34)

where

$$A^{T}K+KA+Q - KBR^{-1}BK = 0$$
 (35)

under the usual assumptions that  $[\lambda, 2^{1/2}]$  is detectable and [A,B] is stabilizable. The state weighting matrix Q is selected so that neither the real average frequency pole nor the arbitrary phase reference pole at zero are moved. It is not desirable to move the pole at zero since it is only observable from the angle states which are not measurable. The average frequency pole is not to be moved since the load frequency control loop is to control that mode. The only modes that are to be changed are the inter-area oscillatory modes since they require significant damp ing. There are at least two ways that the state weighting matrix Q may be selected to do this. The first method, a modal one, is more general than the second method which depends on the physical interpretation of the system.

## Modal Selection of Q Matrix

Consider the diagonalization of the system (18) by defining a model vector  $\underline{z}(t)$  given by

$$z(t) = Wx(t) \tag{36}$$

which results in

$$\underline{z}(t) = A\underline{z}(t) + WB\underline{u}(t) \tag{37}$$

only those components of z(t) in the cost that correspond to poles of the open-loop system that are to be moved. The rest of the modes of the system are made cost unobservable. Thus, if D is a diagonal matrix of weightings for each mode then (33) becomes

$$J(\underline{u}) = \int_{0}^{\pi} ||D\underline{z}(t)||^{2} + \underline{u}^{T}(t)R\underline{u}(t)dt$$
, (38)

Note that the term  $||Dz(t)||^2$  can be converted into  $x^T(t)Qx(t)$  with a real Q matrix in the following way. Define  $\Gamma$  as

$$\Gamma = DW = \Gamma_{p} + j\Gamma_{r} \tag{39}$$

then

$$||D_{\underline{x}}(t)||_{2}^{2} = \underline{x}^{T}(t)W^{H}D^{2}W\underline{x}(t) = \underline{x}^{T}(t)Q\underline{x}(t)$$
 (40)

where

$$Q = \Gamma_{R}^{T} \Gamma_{R} + \Gamma_{I}^{T} \Gamma_{I}$$
 (41)

There is a slight difficulty with this method, however, in that  $[\lambda, Q^{1/2}]$  may not be detectable. This is the case because the arbitrary phase reference mode at zero is made cost unobservable. One way around this problem is to use a reduced model that does not have this mode. An alternative way is to artificially stabilize the cost unobservable unstable modes leaving the other system modes fixed. This new system is essentially the same as the old system for the purposes of design of a feedback controller since the controller will not attempt to stabilize the unstable cost unobservable modes. This is accomplished utilizing the dyadic expansion of the A matrix in (9). Let A be the artificially stabilized system matrix which is defined by

$$\tilde{\lambda} = \sum_{i \in \Omega} \lambda_{i} \underline{v}_{i} \underline{v}_{i}^{T} - \varepsilon \sum_{i \in \Omega} \underline{v}_{i} \underline{v}_{i}^{T} ; \quad e>0 \quad (42)$$

where

$$\Omega = \{i: \lambda_i \text{ mode is unstable and cost}$$
unobservable \, (43)

Now the matrix  $\tilde{\mathbf{A}}$  has the same eigenvectors as  $\lambda$  and the same eigenvalues as  $\lambda$  except for those associated with the index set  $\Omega$ . This ensures that the old and new system will behave the similarly from the standpoint of controller design. A somewhat simpler variation of this approach, which works if  $\mathcal{E}$  is sufficiently small, is to define  $\tilde{\lambda}$  as  $\tilde{\lambda}=\lambda-\mathcal{E}I$ . Then  $\lambda$  has the same eigenvectors as  $\lambda$  and eigenvalues  $\tilde{\mathcal{E}}$ , away from those of  $\lambda$ .

# Average Frequency Deviation Selection of Q Matrix

The second method of selecting the state weighting matrix Q is to weight only each machine's or area's frequency deviation from the average frequency. Thus the state weighting is

$$\underline{x}^{T}(t)\underline{Q}\underline{x}(t) \stackrel{\Delta}{=} \sum_{i=1}^{5} \alpha_{i}(\omega_{i} - \overline{\omega})^{2}$$
 (44)

average frequency deviation weighting for the ith area. This Q only weights frequency variables so that the zero pole will not be moved and since only deviations from the average frequency are weighted the average frequency is used as a reference and hence the pole at -. 18 will not be moved. Using this method also requires the stabilization of the zero phase reference mode. Therefore in the centralized design, EI is subtracted from the system A matrix and is used as the system matrix when solving the Riccati equation (35); the resulting feedback control, however, is applied to the original unstabilized system. Both methods of selecting Q require only a few iterations of selecting modal weightings or frequency deviation weightings to obtain the approximate damping of the oscillatory modes required. It is interesting that both methods give approximately the same feedback gains. The centralized design that is used throughout the remainder of the paper is based on the weighting of deviations from average frequency. It should also be mentioned that the control weighting matrix R was selected as the identity matrix multiplied by a scalar to tradeoff state and control energy.

miere m an 3----- - --- min mi an ann attack-

## Peedback Structures

In order to describe several controllers that result from modifications of the centralized controller it is necessary to classify several different feedback structures. They are the following:

- (1) LQ Centralized full state feedback
- (2) LQ Full State without Angles frequency feedback only
- (3) IQ Major local area frequency and frequency of area 1 available for feedback (the major centralized gains)
- (4) IQ Decentralized only local areafrequency available for feedback.

In each case the feedback gain for the controller structure is obtained by simply setting the gains in the centralized gain matrix, that correspond to states not available for feedback, to zero. The closed-loop eigenvalues for cases 1,3 and 4 are given in Figure 7. To assess how closely each of the feedback controllers mimic the centralized feedback controller the concept of gain observability is introduced.

## Gain Observability

The ability to realize a centralized feedback law in a decentralized manner depends critically on the nature of the centralized feedback law. It may not even be possible if the centralized feedback law depends substantially on states not available for feedback. Thus only modes observable from the frequency outputs are moved in the centralized design. Eliminating gains in the centralized gain matrix that do not significantly affect the feedback is commonly done by setting the "small" gains to zero. What is considered "small" must be considered in reference to the expected size of the variations in the state. However, it is not always clear what the expected variare since, in general, some of the state variables may not be physical quantities. Also, while a particular gain may not by itself be insignificant, group of certain gains may collectively have very little effect on the feedback control signal implemented since cancellation of the contributions of different gain-state products may occur when summed. This later idea is made precise by the notion of gain observability. Gain observability merely determines

the modes being fedback in each control channel by using the gain matrix as an output measurement matrix and computing the matrix GV where G is the gain matrix and V, given by (4), is the matrix of right eigenvectors. By computing GV for different gain matrices G, the modes being fedback in each channel may be compared. This is done in Figure 8 for the four feedback structures previously described. From Figure 8 it is apparent that the LO Centralized and LO Full State without Angle feedback cases are practically identical indicating it is not important to try and measure the angle states. The LQ Major case is also quite similar to the 10 Centralized case while the IQ Decentralized case is somewhat less so. Thus gain observability indicates the dominant modes in each feedback channel and provides insight on how to construct a decentralized or limited state feedback controller that approximates a centralized controller.

As a matter of practical importance, each control signal in the real system is passed through a washout which washes out any constant frequency errors that may be generated. The washouts have a transfer function  $\frac{8}{s+.2}$  and are included in the subsequent analysis as part of the controllers.

## IV. ROBUSTNESS

In any control system design there is a degree of uncertainty about the model parameters and about the nature of the disturbances that act as exogenous inputs to the model. A well designed control system must be able to tolerate such uncertainty without destabilizing the system. Classically, a measure of robustness has been the notions of gain and phase margin for SISO feedback systems. In the multivariable version of the Nyquist stability theorem, the gain and phase margins do not provide an adequate measure of the robustness of the nominal feedback system since arbitrarily small simultaneous perturbations in the nominal system may cause instability of the closed-loop system even though there are good gain and phase margins in each feedback channel.

The multivariable Nyquist criterion counts the encirclements of the origin by the det(I+G(jw)) where G(s) is the loop transfer functions. In order to change the number of encirclements of the origin, det (I+G(jw)) must be zero for some w. Thus for nominally stable closed-loop systems the det(I+G) tries to measure the "distance" of I+G to the critical point but is not a good measure because det(I+G) may be very sensitive to small changes in G. In the scalar case det(I+G) becomes 1+g and small changes in g yield only small changes in the Nyquist diagram of 1+g or g so that this problem does not arise. Therefore, in the multivariable setting what is required is an insensitive measure of the "distance" of I+G to the origin. The minimum singular value of I+G is such a measure. It measures the minimum size of the additive perturbation, AG, required to make det(I+G+AG)=0 or I+G+AG exactly singular. The minimum and maximum singular values are denoted as o and o respectively and are defined by

$$\underline{\sigma}(A) \stackrel{\Delta}{=} \min_{x \neq 0} \frac{||Ax||_2}{||x||_2} = \frac{1}{||x^{-1}||_2}, \text{ if } A^{-1} \text{ exists}$$
 (45)

$$\overline{\sigma}(A) \stackrel{\Delta}{=} \max_{x \neq 0} \frac{\left|\left|A\underline{x}\right|\right|_{2}}{\left|\left|\underline{x}\right|\right|_{2}} \stackrel{\Delta}{=} \left|\left|A\right|\right|_{2}$$
(46)

Therefore if at some frequency  $\omega_0$ ,  $\underline{\sigma}(1+G(j\omega))$  is small, there exists a small perturbation in the

nominal system that will make the closed-loop system unstable. It has been known for some time that linear quadratic regulators for single input-single output systems have inherently good, guaranteed gain and phase margins, of namely infinite upward and 50% reduction gain margins and +60% phase margin [1]. This is because for LQ regulators |1+g(jw)|>1 \noting w so that the Nyquist diagram of g must avoid the unit disk centered at (-1,0). This is shown in Figure 9. For multivariable systems, Kalman's well-known inequality for LQ regulators [3,4] generalizes with R=I to

$$(I+G(-s))^{T}(I+G(s)) \ge I$$
 \(\frac{1}{2}\)

so that

$$\underline{\sigma}(I+G(j\omega)) \geq 1 \qquad \forall \omega$$
 (48)

is analogous to the scalar case where |1+g(jw)) |>1. It has more recently been shown [2] that for diagonal R>O and Q>O that the multivariable IQ regulators have the same gain and phase margins in each feedback channel simultaneously as in the single input-single output case. However, as is well known, the infinite gain margin is not a reality for the real world because the nominal model is only valid within a limited frequency range and furthermore a constant feedback gain at all frequencies is not realizable. Thus the bandwidth of the closed loop system must still be checked to ensure that the bandwidth is not excessive and that the loop is rolled off sufficiently where unmodelled dynamics might affect the closed loop stability of the system. The following robustness theorem checks this in a more formal way.

## Robustness Theorem [5,6]:

Let  $\widetilde{G}(s)$  be the transfer function matrix of a proper finite dimensional linear system. Let G(s) be its nominal (design) value, also proper and let  $\Delta G_{\widetilde{A}}(s)$  and  $\Delta G_{\widetilde{M}}(s)$ , defined by the relations,

$$\widetilde{G}(s) \stackrel{\Delta}{=} G(s) + \Delta G_{\alpha}(s)$$
 (49)

$$\tilde{G}(s) \stackrel{\Delta}{=} (I + \Delta G_M(s))G(s)$$
 (50)

be such that  $\widetilde{G}(s)$  and G(s) have the same number of open-loop poles in the closed right half plane. If the nominal feedback system

$$G(s)[I+G(s)]^{-1} = (I+G^{-1}(s))^{-1}$$
 (51)

is stable, then the perturbed system

$$\tilde{G}(s) (I+\tilde{G}(s))^{-1}$$
 (52)

is stable for all perturbations satisfying

$$\underline{\sigma}(\mathbf{I}+\mathbf{G}(\mathbf{j}\omega)) > \overline{\sigma}(\Delta G_{\mathbf{A}}(\mathbf{j}\omega)) \quad \forall \omega$$
 (53)

 $\underline{\sigma}(1+G^{-1}(j\omega)) > \overline{\sigma}(\Delta G_{\omega}(j\omega)) \quad \forall \omega$  (54)

Alternatively, the conditions (53) and (54) may be replaced by (55) and (56) respectively given as

$$||(I+G^{-1}(j\omega))^{-1}||^{-1}>||\Delta G_{\underline{w}}(j\omega)|| \quad \forall \omega$$
 (56)

where | | . | | denotes the 1 or \* matrix norms. O

subsequent discussion in place of the singular values[7]

To test the robustness of the modified LQ controller for the multiterminal dc system, several plots of the norms specified in conditions (55) and (56) have been computed with respect to different perturbed models. The nominal model consists of the open-loop system regulated by the LQ major controller modified as previously described, by passing the control inputs through washouts with transfer function

to eliminate response to constant frequency errors. The perturbed model is the same as the nominal except that it includes additional filtering of the control inputs by an approximately unity gain double pole filter at s=25 to simulate the additional phase lag of torsional filters in the real system. The plot for the multiplicative perturbation, Figure 11, shows that the perturbed system is stable and that the nominal system has a degree of robustness even beyond the perturbation. It is interesting to note that the additive perturbation, Figure 10, for the same perturbed model exceeds the nominal at the system resonances. This points out the fact that the conditions (55) and (56) are only sufficient but not necessary. Here in lies one of the major weaknesses of the singular value approach; it is sometimes unnecessarily conservative. In Figures 12 and 13 the LO Major controller is checked for robustness with respect to a perturbed system that includes an additional machine, with relatively small inertia, that is weakly coupled to the rest of the system to model intra-area dynamics. The resulting changes in the closed-loop system eigenvalues are insignificant even though the sufficient conditions indicate there does exist a perturbation of the same size as the additional intra-area dynamics that will destabilize the system. Notice also in the Figures 10 and 11 that  $||(I+G)^{-1}||^{-1}$  and  $||(I+G^{-1})^{-1}||^{-1}$  do not become small

at any frequency which is indicative of robustness. To make the connection with the classical SISO gain and phase margins, under the LQ major controller with washouts, one of the system feedback loops is broken. The margins for this channel are an infinite upward gain margin, a gain reduction margin of 100% and a phase margin of +100 degrees. This also gives an indication of how conservative the norm plots may be, since they take into account perturbations in the system that may not be reasonable. Other robustness norm-plots for the completely centralized decentralized case are similar in nature. The centralized case has the largest ||(I+G)<sup>-1</sup>||<sup>-1</sup>, as expected, and the decentralized the smallest.

Another method of evaluating the design is to break feedback loops simulating actuator or sensor failure or manual intervention and check the stability of the resulting system. If the system remains stable under the breaking of feedback loops the integrity of the system is said to be maintained. Even though a system is open-loop stable, this does not guarantee the the closed-loop will remain stable when feedback loops are broken. Thus it is important to check the integrity of the closed-loop system. For the LQ major feedback law with washouts added, the system integrity is maintained for all possible combinations of broken feedback loops. The same is true for the completely decentralized feedback law with washouts also.

Finally, a comparison between the open-and closed-loop bandwidths is made. In Figure 14  $||G(j\omega)||$ , the maximum open-loop frequency response, and  $||(I+G^{-1}(j\omega))^{-1}||$ , the

out the resonances in the open-loop system without affecting the rest of frequency response. Control energy is not wasted in modifying the open-loop system more than necessary. This is related to the performance of the control system which is discussed next.

## V. CONTROL SYSTEM PERFORMANCE

Evaluation of the closed-loop system performance is done by examining the system transient responses and feedback control inputs to the system generated by an initial condition corresponding to the state vector for the open-loop system after the clearing of a three-phase ground fault at area 4. Figure 15 shows the angle of area 4 using area 3 as a reference (i.e.  $\delta_4$ - $\delta_3$ ) for the open-loop, the LQ centralized, LQ major and LQ decentralized designs with the washouts in place. Figure 16 shows the corresponding frequency  $\omega_4$  for the same initial condition and controllers.

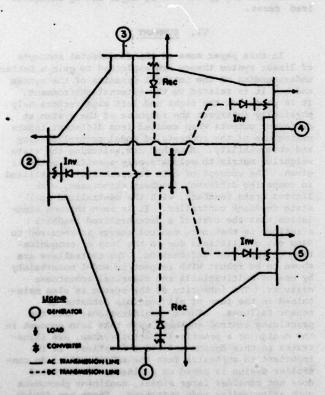
As can be seen from these figures, all the controllers give approximately the same performance in the transient responses. They significantly reduce the settling time of the inter-area oscillations. These responses are typical of all the angle and frequency transient responses. However, the control inputs for the various controllers are distinguishable. Figure 17 displays the control signal u<sub>2</sub> for the three different controllers, again with the washouts in place. As can be seen, the centralized feedback gain uses the least control energy indicating a coordinated control effort. The decentralized controller, as expected, use the most since it lacks information to yield a coordinated effort. The effect of the com munication of the frequency of area one to all other areas can be assessed in terms of the difference in the control energy for the LQ major and LQ decentralized cases.

## VI. SUMMARY

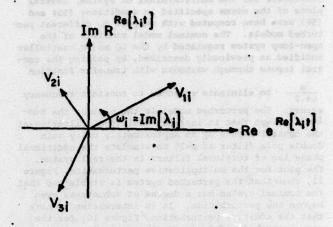
In this paper some of the fundamental concepts of linear system theory are exploited to gain a better understanding of the internal dynamics of the system and how it is related to the external environment. It is shown how the right and left eigenvectors help physically interpret the response of the system at different outputs when excited from different inputs making use of the concepts of modal controllability and observability. A method for selecting the state weighting matrix to relocate only specified modes is given. The concept of gain observability is utilized in comparing different feedback structures, with limited state feedback, with the centralized full state feedback controller. It is seen through simulation that the cost of a decentralized feedback structure is that more control energy is required to damp out oscillations due to the loss of communication of important information. The controllers are shown to be robust with respect to model uncertainty by use of multivariable and classical robustness measures. The integrity of the system is also maintained in the face of all possible actuator or sensor failures. These considerations, that the practicing control engineer must take into account in the design of a practical control system, are illustrated in this design and its evaluation. It is important to emphasize that the multiterminal dc controller design is based on a linearized model and does not consider large signal, nonlinear phenomena such as converter mode switching. These are topics for future research.

#### REFERENCES

- [1] Anderson, B.D.O. and Moore, J.B., Linear Optimal Control, Prentice-Hall, 1971.
- [2] Safonov, M.G., and M. Athans, "Gain and Phase Wargins for Multiloop LQG Regulators," IEEE Trans. <u>Auto. Control</u>, Vol. AC-22, pp. 173-179, April 1977.
- [3] Kalman, R.E., "When is a Linear System Optimal," J. Basic Eng., Trans. ASME, Ser, D. Vol. 86, pp. 51-60, 1964.
- [4] Anderson, B.D.O., "The Inverse Problem of Optimal Control," Fourth Annual Allerton Conference on Circuit and System Theory, Urbana, Ill., Oct. 1966.
- [5] Doyle, J.C., "Robustness of Multiloop Linear Feedback Systems," IEEE Conf. on Dec. and Control, San Diego, CA., Jan. 1979.
- [6] Sandell, Jr., N.R., "Robust Stability of Linear Dynamic Systems with Application to Singular Perturbation Theory," Laboratory for Information and Decision Systems, MIT, Report ESL-P-837, August 1978.
- [7] Laub, A.J., "Robust Stability of Linear Systems-Some Computational Considerations," Laboratory for Information and Decision Systems, MIT, Report LIDS-R-904, Peb. 1979.



<u>Pigure 1:</u> A Power System with 5 DC Terminals and 5 AC Nodes, each representing an Area or Group of Coherent Generators.



Pigure 2: Argand Diagram for ith Mode.

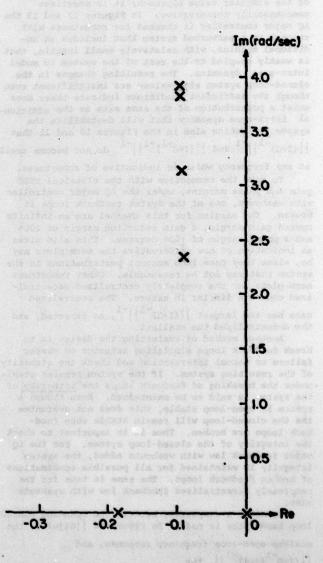
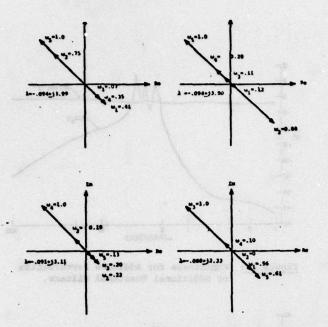
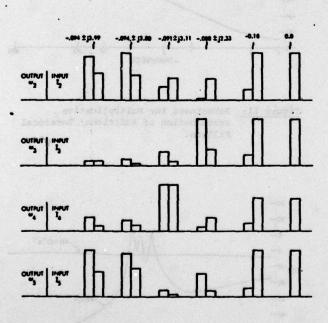


Figure 3: Open-Loop Eigenvalues with Monnegative Imaginary Parts.



Pigure 4: Argand Diagrams of Oscillatory Modes.



<u>Figure 5:</u> Model Observability and Controllability of Different Modes from a Specified Input or Output.

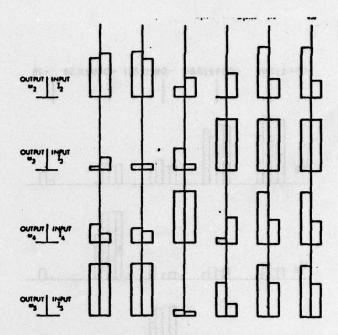


Figure 6: Modal Observability and Controllability of a Specified Mode from Different Inputs or Outputs.

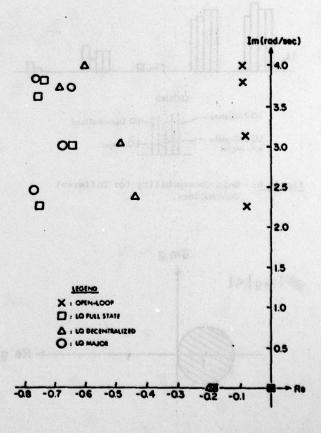
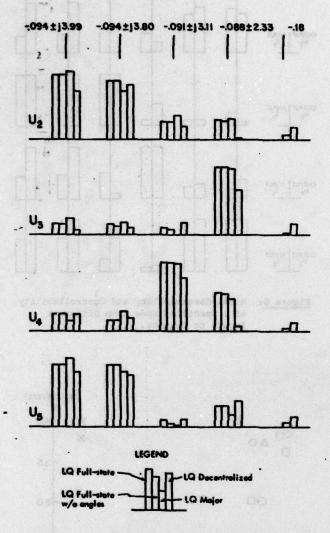
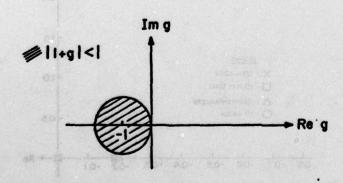


Figure 7: Closed-Loop Eigenvalues for Different Controllers.



Pigure 8: Gain Observability for Different Controllers.



Pigure 9: Disk that Nyquist Diagram for SISO 1Q Regulator must avoid.

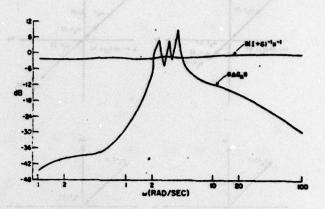


Figure 10: Robustness for Additive Perturbation of Additional Torsional Filters.

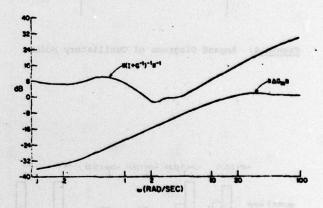


Figure 11: Robustness for Multiplicative .

Perturbation of Additional Torsional Filters.

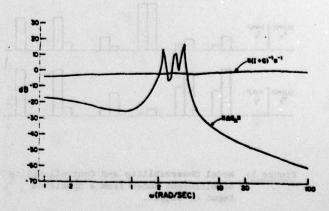
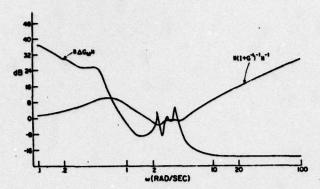


Figure 12: Robustness for Additive Perturbation of Additional Intra-Area Dynamics.



Pigure 13:
Robustness for Multiplicative
Perturbation of Additional Intra-Area
Dynamics.

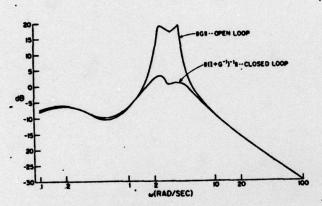
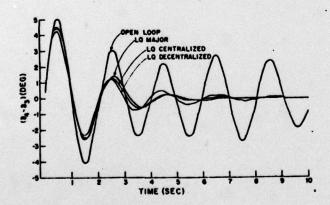


Figure 14: Maximum Open-Loop/Closed-Loop
Multivariable Frequency Response.



<u>Figure 15:</u> Comparison of  $(\delta_4 - \delta_3)$  Response for Different Controllers.

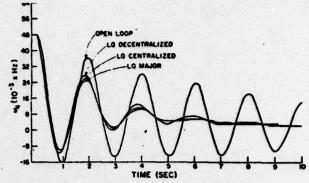


Figure 16: Comparison of w Response for Different Controllers.

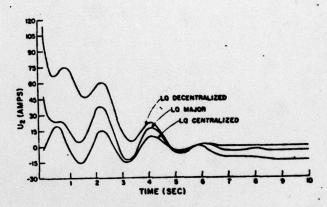


Figure 17: Comparison of u<sub>2</sub> Input for Different Controllers.

# DATE